Progress in
Respiratory Research
Editor: C.T. Bolliger
Vol. 37

Clinical Chest Ultrasound

From the ICU to the Bronchoscopy Suite

Editors
C.T. Bolliger
F.J.F. Herth
P.H. Mayo
T. Miyazawa
J.F. Beamis

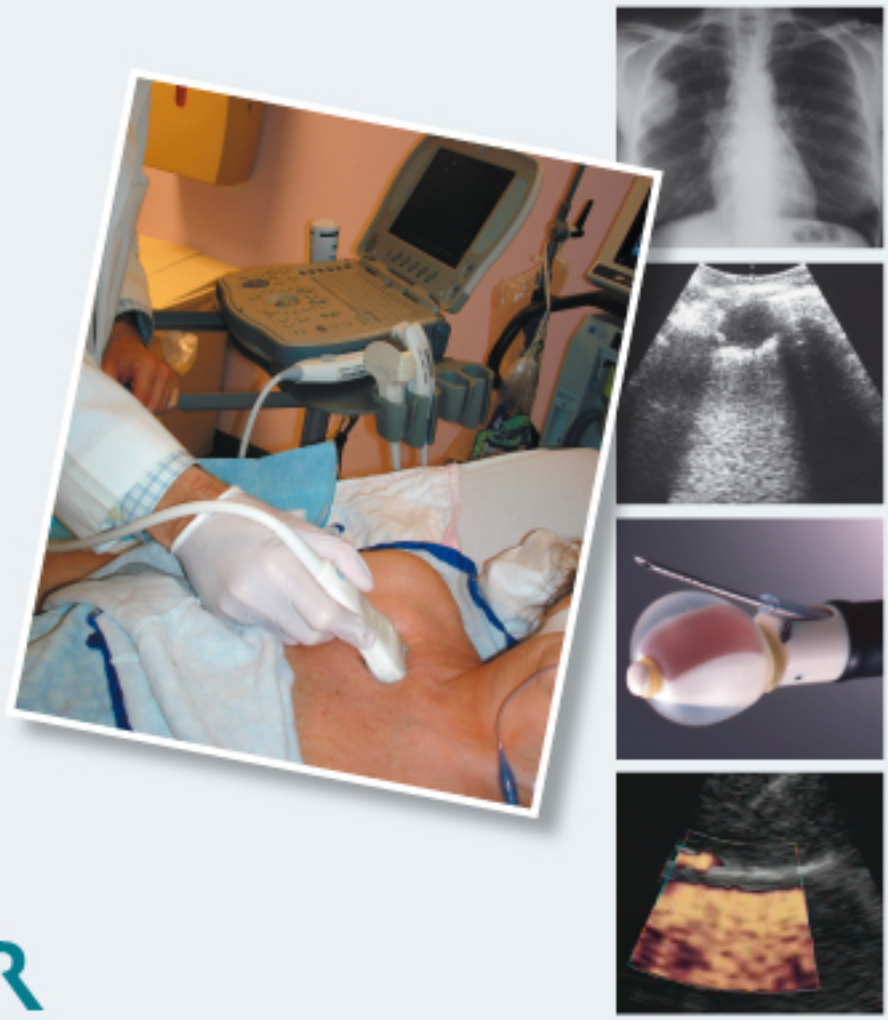

KARGER

Progress in Respiratory Research

Vol. 37

Series Editor

Chris T. Bolliger Cape Town

Clinical Chest Ultrasound

From the ICU to the Bronchoscopy Suite

Volume Editors

C.T. Bolliger Cape Town
F.J.F. Herth Heidelberg
P.H. Mayo New Hyde Park, N.Y.
T. Miyazawa Kawasaki
J.F. Beamis Burlington, Mass.

214 figures, 41 in color, 11 tables, and online supplementary material, 2009

KARGER

Basel · Freiburg · Paris · London · New York · Bangalore ·
Bangkok · Shanghai · Singapore · Tokyo · Sydney

Prof. Dr. Chris T. Bolliger
Department of Medicine
Faculty of Health Sciences
University of Stellenbosch
19063 Tygerberg 7505, Cape Town (South Africa)

Prof. Dr. Felix J.F. Herth
Department of Pneumology and Critical Care Medicine
Thoraxklinik, University of Heidelberg
Amalienstrasse 5
DE-69126 Heidelberg (Germany)

Dr. Paul H. Mayo
Long Island Jewish Medical Center
Division of Pulmonary, Critical Care, and Sleep Medicine
410 Lakeville Road
New Hyde Park, NY 11040 (USA)

Prof. Dr. Teruomi Miyazawa
Division of Respiratory and Infectious Diseases
Department of Internal Medicine
St. Marianna University School of Medicine
2-16-1 Sugao miyamae-ku
Kawasaki, Kanagawa 216-8511 (Japan)

Dr. John F. Beamis
Section Pulmonary and Critical Care Medicine
Lahey Clinic
41 Mall Road
Burlington, MA 01805 (USA)

Library of Congress Cataloging-in-Publication Data

Clinical chest ultrasound : from the ICU to the bronchoscopy suite / volume editors, C.T. Bolliger ... [et al.].
p. ; cm. -- (Progress in respiratory research ; v. 37)
Includes bibliographical references and index.
ISBN 978-3-8055-8642-9 (hard cover : alk. paper)
1. Chest--Ultrasonic imaging. I. Bolliger, C. T. (Christoph T.) II. Series: Progress in respiratory research ; v. 37.
[DNLM: 1. Thoracic Diseases--ultrasonography. 2. Thorax--ultrasonography. W1 PR681DM v.37 2009 / WF 975 C641 2009]
RC941.C647 2009
617.5'407543--dc22

2009000811

Bibliographic Indices. This publication is listed in bibliographic services, including Current Contents®.

www.karger.com
Printed in Switzerland on acid-free and non-aging paper (ISO 9706) by Reinhardt Druck, Basel
ISSN 1422–2140
ISBN 978–3–8055–8642–9
e-ISBN 978–3–8055–8643–6

Contents

Foreword

This current volume on *Clinical Chest Ultrasound: From the ICU to the Bronchoscopy Suite* is the 37th in the series, and the 10th since I took over as Editor-in-Chief. For this celebratory 10th volume I wanted to have an unusual topic, but one that would perfectly reflect the spirit of *Progress in Respiratory Research*. When talking to potential guest editors for the book John Beamis, a friend and well-known interventional pulmonologist from Boston, came up with the brilliant idea to choose ultrasound as the topic and to cover all aspects of its use in the chest that might be of interest to pulmonologists and intensivists. The above title was born. The next step was to find guest editors who would be willing to do this book together with me, and bring the necessary knowledge to cover every angle of this new imaging tool. I was delighted that we could get the support of John Beamis for the introductory section, Paul Mayo for the intensive care unit part, Felix Herth for the endoscopic ultrasound section, and Teruomi Miyazawa for the therapeutic procedures, while I covered the transthoracic applications.

A book on imagery tools should include as many illustrations as possible without overdoing it and becoming an atlas, which was clearly not our aim. We therefore made use of the electronic option to put a number of pictures and more importantly all video clips on a special on-line repository open to the purchaser of the book. We hope that this feature will be attractive to the reader especially since these illustrations can also be downloaded for personal use.

The final product should meet the very high standards of the book series, which — by the way — has seen two of its latest volumes receive a 'highly commended' award in the BMA Book Competition! In the future we will continue to produce about one book a year about any important aspect of chest medicine. But while waiting for upcoming volumes, get this one and enjoy it!

C.T. Bolliger
Cape Town

Preface

The use of ultrasound in medicine began during and shortly after the 2nd World War in various centres around the world. The work of Dr. Karl Theodore Dussik in Austria in 1942 on transmission ultrasound investigation of the brain is the first published work on medical ultrasonics.

From the mid-1960s onwards, the advent of commercially available systems allowed the wider dissemination of the art. Rapid technological advances in electronics and piezoelectric materials provided further improvements from bistable to greyscale images and from still images to real-time moving images. The technical advances at this time led to a rapid growth in the applications to which ultrasound could be put. The development of Doppler ultrasound had been progressing alongside the imaging technology but the fusing of the two technologies in Duplex scanning and the subsequent development of colour Doppler imaging provided even more scope for investigating the circulation and blood supply to organs, tumours, etc. The advent of the microchip in the 1970s and subsequent exponential increases in processing power have allowed faster and more powerful systems incorporating digital beamforming, more enhancement of the signal and new ways of interpreting and displaying data, such as power Doppler and 3-dimensional imaging.

Ultrasound has received increasing interest from chest physicians in recent years. Modern ultrasound devices are user-friendly, inexpensive, lightweight and portable, which makes them suitable for outpatient settings as well as bedside investigation of the severely ill.

In case of parabronchial lesions, for instance, the view during bronchoscopy is limited to the inner surface, whereas the addition of endobronchial ultrasound systems allows the inspection of structures surrounding the airways.

The various applications of chest ultrasound are set to become practical and essential tools for the pulmonologist in the near future.

However, the medical use of ultrasound remains highly operator dependent in spite of advances in technology, and the interests of the patient are best served by the provision of an ultrasound service which offers the maximum clinical benefit and optimal use of resources, i.e. with appropriately trained personnel using equipment of appropriate quality. Therefore, an adequate level of training in ultrasound is essential for the provision of a safe and effective ultrasound service.

Five different sections of the current volume in the *Progress in Respiratory Research* cover the basics of the technique, the indication and limitations of transthoracic ultrasound, the critical care applications, the endoscopic ultrasound applications, as well as the use of ultrasound in therapeutic procedures. One of the aims was to compile a book, covering all aspects of chest ultrasound ranging from important topics for a beginner to complex applications for the expert.

All chapters were written by leading experts in their respective field, and all have — true to the spirit of the book series — included the latest literature references. All chapters are richly illustrated: for most of them online video examples are available.

The Basics

Chapter 1

Bolliger CT, Herth FJF, Mayo PH, Miyazawa T, Beamis JF (eds): Clinical Chest Ultrasound: From the ICU to the Bronchoscopy Suite.
Prog Respir Res. Basel, Karger, 2009, vol 37, pp 2–10

Physics of Diagnostic Ultrasound

Creating the Image

Karen L. Reuter · Andrew Bogdan

Diagnostic Radiology, Lahey Clinic, Burlington, Mass., USA

Abstract

This chapter presents the physics of ultrasound, probe design, and some of the typicel artifacts present in pulmonological applications. Some of the techniques used for optimal imaging of chest anatomy are explained as well as the diagnostic questions that can be answered by a pulmonologist.

Diagnostic ultrasonography is the only clinical imaging technology currently in use that does not depend on electromagnetic radiation. This modality is based on the properties of sound waves, and hence the mechanical and acoustic properties of tissues.

Diagnostic ultrasound is mechanical energy that causes alternating compression and rarefaction of the conducting medium, traveling in the body as a wave usually at frequencies of 2–10 MHz, well beyond audible frequencies. In general it is assumed that the speed of sound in tissue is constant at 1,540 m/s [1]. By knowing the frequency and the speed of sound, one can determine its wavelength (similar to electromagnetic radiation) [2–4]:

$$\lambda(\text{wavelength}) = c(\text{speed})/f(\text{frequency}),$$

or using the assumed speed:

$$\lambda(\text{wavelength in mm}) = 1.54/f(\text{frequency in MHz}).$$

For example, at a frequency of 2 MHz (which is very close to the necessary frequency usually used to image deeply into the body compared to higher frequencies for more superficial structures) the wavelength is 0.77 mm. When a pulse of ultrasound energy is incident upon the body, it interacts with the tissue in a variety of ways which will be discussed. Some of the incident energy is directed back towards the source and is detected. The time delay between the energy going into the body and returning to the ultrasound probe determines the depth from which the signal arises, with longer times corresponding to greater depths (depth = velocity · time/2). This information is used in the creation of an image. Other factors that make the tissues distinguishable on a screen are their slightly different acoustical properties; one is known as the acoustic impedance defined as Z = density · speed of sound [2–4]. At the boundary between two different tissue types the sound waves can be: (1) reflected, like light off a mirror, this being the primary interaction of interest for diagnostic ultrasound, as it allows the major organ outlines to be seen; the diaphragm and pericardium are specular reflectors; (2) refracted, like light rays passing through a lens and hence having their directions altered; (3) scattered, like sunlight in the sky, sending sound waves off in different directions; this occurs when the ultrasound wave encounters a surface that is 'rough' [3, 4] or whose shape and density vary on a spatial scale which is small compared to the wavelength of the ultrasound, and (4) and attenuated or absorbed, as they lose energy, which is converted to heat in the tissue. These last 3 effects will, in general, cause the sound waves that are reflected back to the transducer from deeper tissues to be much weaker, causing the image to get increasingly noisy (too many echoes or small visible densities in the background compared with those of the desired image). The amount of attenuation that occurs as the sound wave passes through the tissue increases with higher frequency. However, for pulsed ultrasound the axial resolution (the ability to distinguish between adjacent dots in the direction of the sound wave) is improved at high frequencies. This difference in resolution produced comparing higher and lower frequency transducers is because for a given number of acoustic cycles, the pulse length is less at higher frequen-

Fig. 1. The time gain control adjustment panel on a typical ultrasound system.

cies. Thus, high frequency ultrasound would be preferred for better detail of anatomy closer to the surface.

Note that a time gain compensation control (fig. 1) which is adjustable by the operator of the ultrasound equipment can be used to boost the received signal intensity from increasing depths (which arrive at a later time) so that the image presented is more uniform in intensity and easier to interpret. Since attenuation varies with frequency, the time gain compensation is also adjusted depending on the frequency of the probe being used.

Doppler Ultrasound

Another useful physical effect which occurs in ultrasound is that the frequency of the reflected ultrasound wave is changed when it strikes a moving object, such as blood in a vessel. This alteration of the sound wave is known as the Doppler effect and can be used to determine blood flow velocity and the direction of the flow. The difference between the transmitted and received frequency is called the Doppler frequency shift [2–4].

$$\Delta F = Ft - Fr = 2 \times Ft \times \frac{V}{c} \times \cos\theta$$

where ΔF = Doppler frequency shift, Ft = transmitted frequency, Fr = received frequency, v = speed of moving target (blood flow velocity), c = speed of sound in soft tissue, θ = angle between the direction of blood flow and the direction of the transmitted sound phase.

The Doppler angle for imaging flow needs to be 60° or slightly less to the long axis of the vessel to obtain the correct velocity. The frequency shift is proportional to the velocity; the size of the waveform varies with the flow velocity.

Arterial waveforms are usually analyzed by the resistive index (RI):

$$RI = 1 - \frac{D}{S} = \frac{S - D}{S}$$

where S = peak systolic velocity (or frequency shift) and D = end-diastolic velocity (or frequency shift). RI increases with the increase in resistance to flow. Parenchymal organ arterial flow normally has an RI between 0.5 and 0.7.

Color Doppler sonography is sensitive to Doppler signals in a field of view. It provides a real-time image, tissue in gray scale and blood flow in color. Color Doppler sonography analyzes the phase information, frequency and amplitude of returning echoes. Signals from moving red blood cells are assigned a color (red or blue) based on the direction of the phase shift (direction of blood flow toward or away from the transducer, respectively). High frequency shifts are lighter [1]. Areas of abnormal slow flow can be seen rapidly. Color Doppler ultrasonography has been used to diagnose minimal or loculated pleural effusions by a color Doppler signal or 'fluid color' sign from respiratory or cardiac cycles [5]. This signal may help in guidance for aspiration of this fluid.

Power Doppler imaging estimates the power or strength of the Doppler signal rather than the mean frequency shift [1]. Power Doppler can pick up slower velocities of flow compared to the more commonly used frequency shift Doppler. This power Doppler single color image and hue relate to the moving blood volume but not the direction or velocity. Higher power gain settings can be used. Another distinguishing feature is that power Doppler is not affected by Doppler angle.

Diagnostic Ultrasound Equipment

Regarding diagnostic ultrasound equipment, ceramic crystals in the transducer deform and vibrate when electronically stimulated to produce the sound pulses [1–4]. Echoes that return to the transducer distort these crystal elements and produce an electric pulse, which is processed into an image. High-amplitude echoes create greater crystal deformation and produce a larger electronic voltage. These high amplitude echoes are displayed as brighter pixels, thus B-mode, or brightness mode, images.

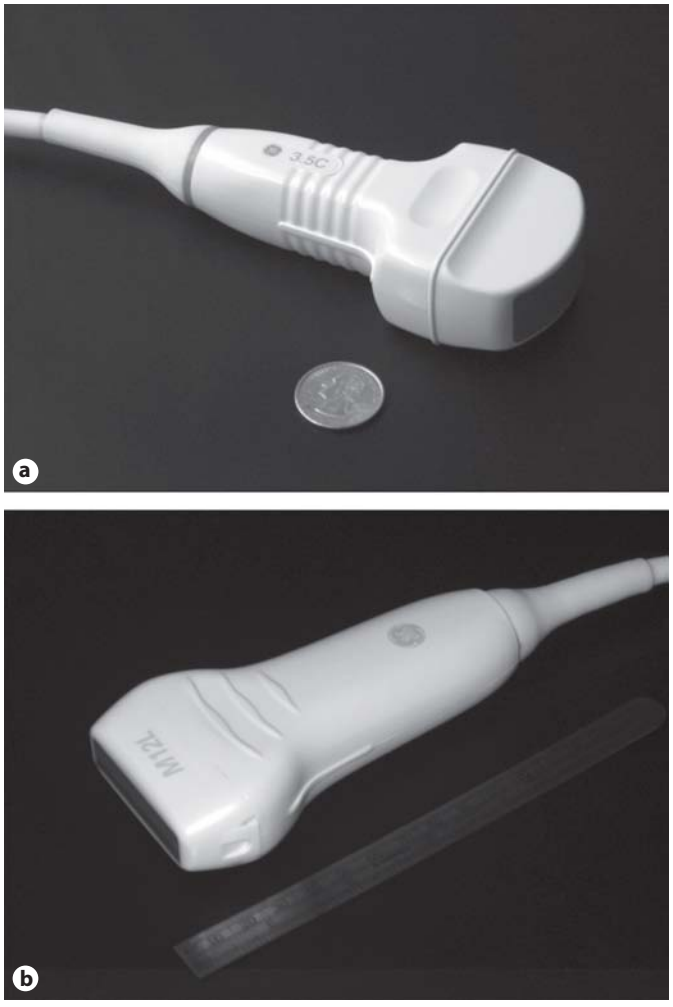

Fig. 2. **a** A 3.5C (bandwidth 2–5 MHz) convex phased array probe. This probe will show a larger anatomical cross section than the linear probe shown below. **b** An M12L linear array probe (bandwidth 5–13 MHz).

Resolution of an image is very important for diagnosing pathology. Resolution is determined by the frequency and duration of the transmitted sound pulse. Axial resolution refers to the ability to resolve objects within the imaging plane at different depths along the direction of the pulse, best with higher frequency probes with their shorter pulses. Lateral resolution is the ability to resolve objects in the imaging plane that are located side by side; the focal zone on the ultrasound console controls this.

The pulsed ultrasound energy is controlled by the system's electronics and emitted from the probe or transducer (fig. 2). The probe can have a single element or be composed of an array of many small elements that can be individually addressed and controlled. The latter is referred to as a phased array transducer. The elements are used both to transmit the ultrasound as well as to detect the energy directed back towards them. It should be noted that the individual elements cannot simultaneously transmit and receive – so following the emission of a pulse, an element in the probe or transducer starts listening for the echo. After a sufficient amount of time has passed, corresponding to a certain desired depth for acquiring information for an image, another pulse can be emitted. The size of the transmitted beam is related to both the size and number of elements that are used. By controlling the timing of transmission from individual (or groups of) elements, the ultrasound beam's direction and focusing can be controlled to obtain the image of the organ being studied.

Most transducers today are multielement probes called arrays. They contain groups of small crystal elements in a sequential linear fashion. By changing the timing and sequence of activation of the different arrayed elements, the pulse can be directed to different places and focused at specific depths depending on the organ being interrogated. In the phased array transducer each element in the array helps in the formation of each pulse. A sector image is created by this probe, which is small and can fit between ribs.

Curved-array transducers (fig. 2a) have a convex shape for a wider field of view. A 3.5-MHz curvilinear probe provides visualization of deeper structures, and the sector scan field allows a wider field of view through a small acoustic window. These transducers are required to image a thicker thoracic wall [1–4]. The chest wall, pleura, and lungs can be evaluated using this probe. The posterior chest is best imaged with the patient sitting upright, the anterior and lateral aspects of the chest in the lateral decubitus position. The suprasternal approach is the best way to view the upper anterior and middle mediastinum; the aorta and superior vena cava can be seen [6]. In abdominal and pelvic imaging curved-array transducers are used to image the general abdomen including the pelvis for obstetrical cases. Curved array transducers with a short radius can be used as intraluminal or endoluminal probes. These transducers are small and can be positioned close to the organ of interest, use higher frequencies, and thus obtain higher resolution for very detailed images. Not having to transmit sound through the abdominal wall minimizes the major degradation by adipose tissue.

With linear-array transducers (fig. 2b) a limited group of adjacent elements produce a pulse, which is perpendicular to the transducer face [1]. The image is rectangular. Linear-array transducers of high frequency are well-suited for patients with thin thoracic walls [7]. The major benefit of this large transducer is high resolution in the near field and a large superficial field of view.

The newer harmonic imaging uses higher integer multiples of the fundamental transmitted frequency. These sound waves progressively increase in intensity before they attenuate. A filter allows only the high-frequency harmonic signal to be processed into an image [1, 4]. Harmonic imaging sometimes provides a smoother-appearing image.

Three-dimensional (3D) sonography data are acquired as a stack of parallel cross sections with a 2D scanner or as a volume with a mechanical or electronic-array probe [1]. 3D images are used selectively to better appreciate the shape of a mass or organ and its relationship to surrounding structures.

Acoustic Shadowing and Artifacts

In biologic tissues the speed of the sound is lowest in gas, faster in fluid, and fastest in bone, where the molecules are more closely packed. There is no ionizing radiation. The sound pulses transmitted into the body can be reflected, scattered, refracted or absorbed as mentioned previously. Absorption, or attenuation, is the loss of acoustic energy from conversion to heat energy, more prevalent in bone than soft tissue, and more prevalent in soft tissue than in fluid. It is a key cause of acoustic shadowing (fig. 3b). Where there is a distinct loss of the echoes behind an imaged structure, the shadow has a relatively sharp border behind a bone.

Acoustic shadowing is so common in ultrasound images that it is only sometimes called an artifact. It is the result of the energy of transmitted sound being decreased by reflection and/or absorption. The shadowing behind gas is due to strong reflections at gas/tissue interfaces. The reflected pulse interacts with interfaces in front of the gas causing secondary reflections, which leads to low level echoes, causing 'dirty' images. However, the shadowing that occurs behind stones, calcifications and bones is reduced by sound absorption, resulting in only minimal secondary reflection, and therefore 'clean' images [1] with a distinctly bordered lack of echoes posterior to the calcified density.

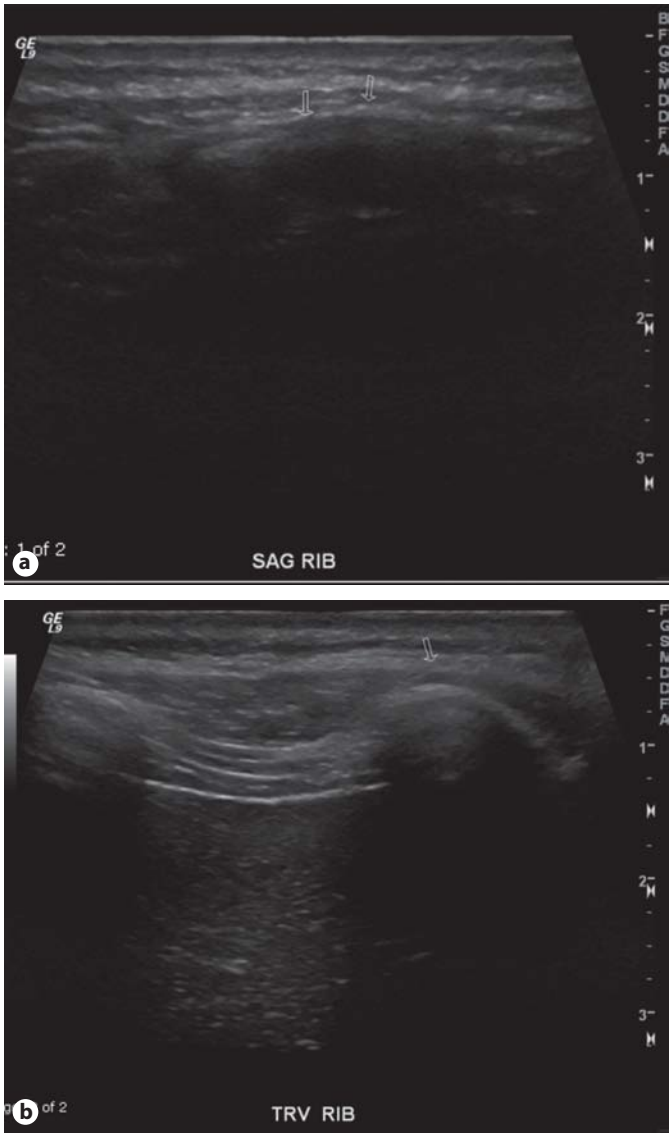

Fig. 3. **a** Sagittal rib view (see arrows). **b** Transverse rib view showing shadowing from behind rib (see arrow).

Ring-down artifacts [8] have been associated with gas collections in the body. These artifacts appear as a solid streak or series of parallel bands radiating away from the gas. They occur from a large mismatch or large difference in acoustic impedance between two kinds of tissues, such as air and water [9]. When struck by an ultrasound pulse, the fluid is excited to ring or vibrate. A soft tissue-gas interface produces strong artifacts. The interface reflects 99% of the sound beam and produces strong reverberation artifacts parallel to the transducer; the interface totally obscures the underlying lung tissue containing air. The interface generates vertical echoes projected into the underlying tissue. The large change in acoustic impedance at the pleura-lung interface results in horizontal artifacts, a series of echogenic parallel lines equidistant from one another below the pleural line. In healthy adults these artifacts usually only arise at the last intercostal space above the diaphragm [6]. While performing ultrasound images of a liver, one may see multiple, vertical, long, narrow bands or lines extending down from the posterior surface of the right hemidiaphragm [9]. These are ring-down artifacts. These findings have been noted to be most prevalent in patients with emphysema, idiopathic

interstitial pneumonia, bronchopneumonia and interstitial edema. It is speculated that the ring-down arises from thickened intralobular or interlobular septa filled with fluid touching the visceral pleural surface.

The comet tail artifact [10, 11] is a reverberation artifact; reverberation artifacts are strong reflections, in multiples, from the same surface. These artifacts look similar to ring-down. The comet tail artifact is an antishadow, a trail of dense continuous echoes simulating a comet tail. They are usually associated with foreign bodies, especially metallic objects such as surgical clips, and cholesterol foci [8]. The more the acoustic impedance of the object differs from the surroundings, the greater the number of reverberant echoes. The smaller the object is, the closer is the spacing between these echoes. If echo bands are strong and close together, they merge to produce the comet tail pattern. The reverberation is strongest when the object is perpendicular to the ultrasound beam [10]. In comparison to the ring-down artifact, the comet tail artifact tapers fast and is short.

Posterior enhancement occurs when fluid-containing structures attenuate the sound less than solid structures, the strength of the sound pulse increasing after passing through fluid compared to passing through a solid structure. This increase through transmission distinguishes cysts and fluid collections from solid masses.

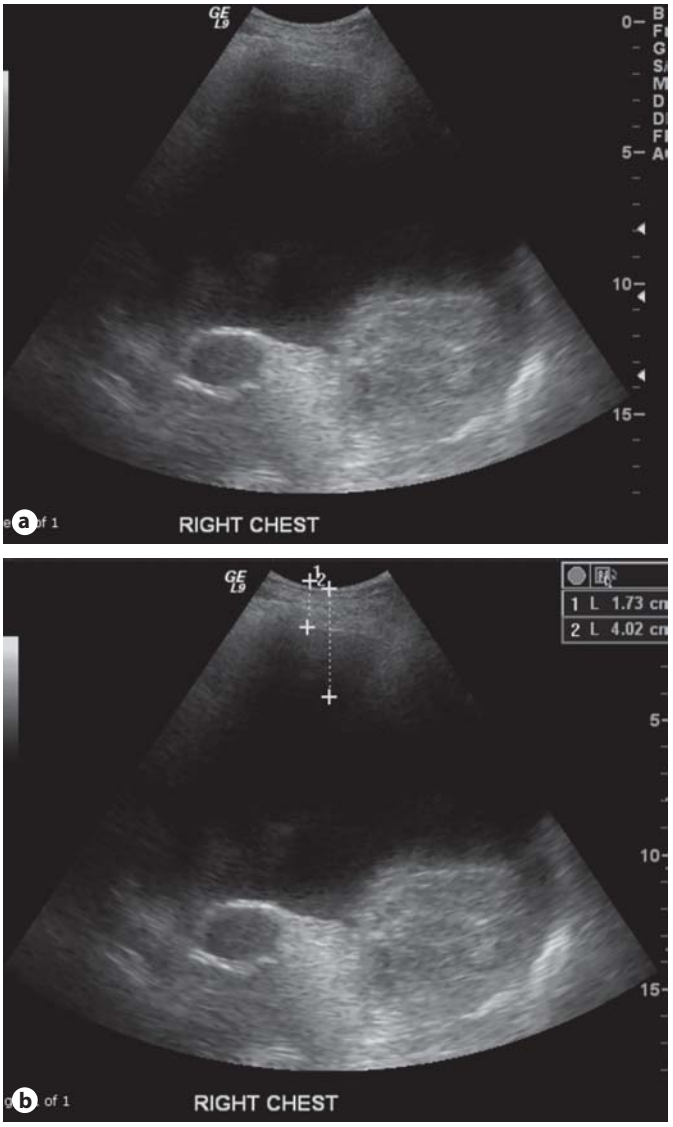

Fig. 4. **a** Sagittal image of the right pleural space showing a large anechoic right pleural effusion, **b** with the distance to reach the fluid 1.73 cm and the distance to quarter depth of the fluid 4.02 cm.

How Can Diagnostic Ultrasound Help the Pulmonologist?

Diagnostic ultrasonography is a very valuable tool for imaging the chest because it causes no clinically significant biological effects, is a real-time examination and has multiplanar imaging capability. In real time one can focus the study on a painful or palpable area. This modality of ultrasonography can be portable, very significant for the ICU and emergency room.

Transthoracic ultrasound can be used to evaluate peripheral parenchymal, pleural and chest wall diseases. The maximum visualization of the lung and pleural space is done by scanning along the intercostal spaces during quiet respiration for normal lung movement; and in suspended respiration when a lesion can be studied in detail. When color Doppler is used, the sensitivity of the Doppler should be set to low flow [6]. Ultrasound is used as guidance for interventions such as biopsies or intercostal chest drains or pleural fluid taps (fig. 4b, 5b).

The high degree of spatial resolution in B-mode and the flow imaging in the Doppler mode help diagnose lesions in the thoracic wall [7]. The modality of ultrasound can be used to distinguish a chest wall mass from a breast mass and can be used to guide a biopsy needle into the tissue [12]. The skin of the thoracic wall appears on ultrasound images as an echogenic layer 1–3 mm thick. Subcutaneous fat is just under the skin. The large muscles that comprise the middle layer of the chest wall are: the pectoralis, serratus, latissimus dorsi and trapezius. On ultrasound images skeletal muscle appears as uniform with multiple echogenic striae over a hypoechoic background on longitudinal scans, and multiple echogenic dots over a hypoechoic background on transverse images. Ultrasound has been used to illustrate the

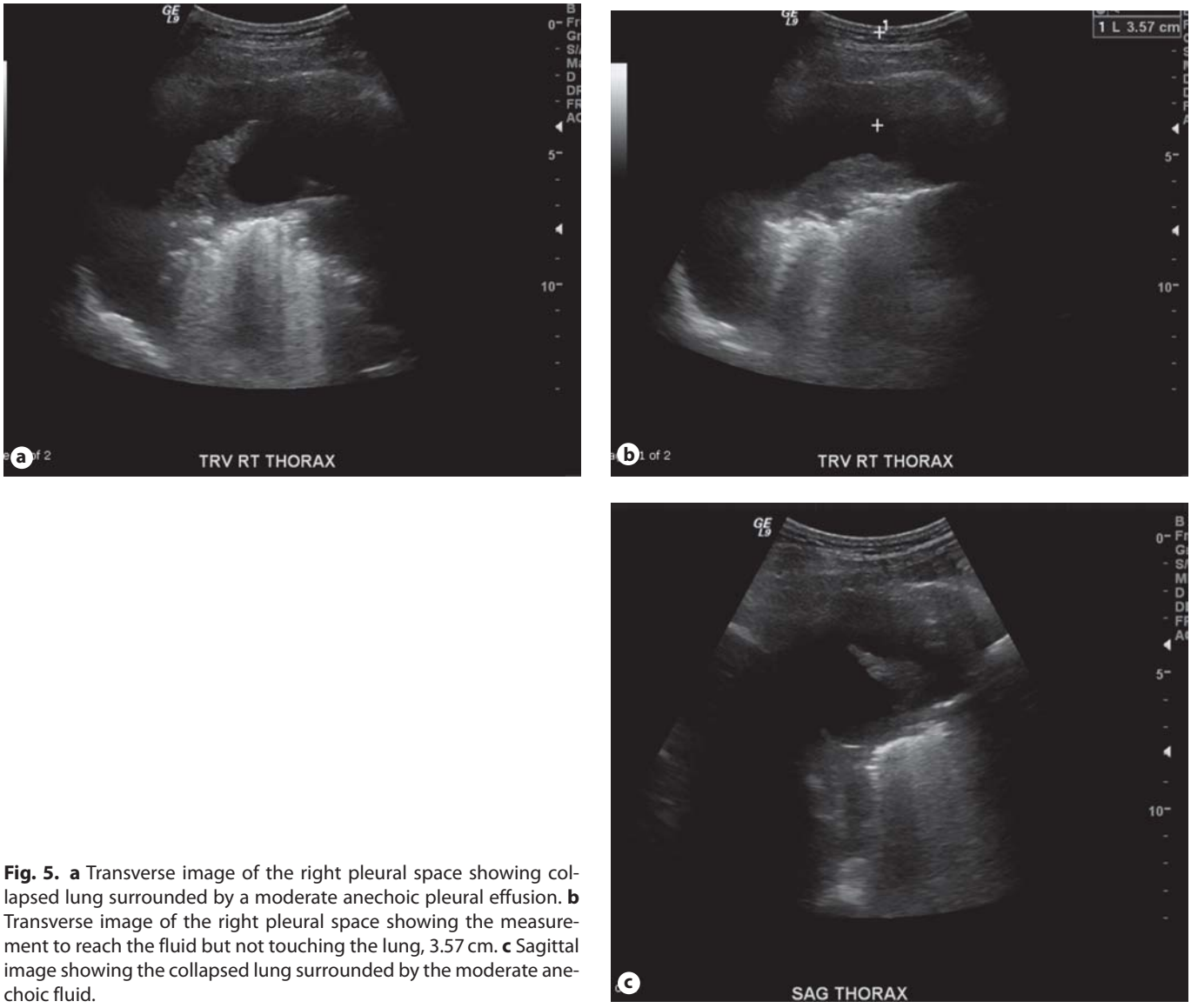

Fig. 5. **a** Transverse image of the right pleural space showing collapsed lung surrounded by a moderate anechoic pleural effusion. **b** Transverse image of the right pleural space showing the measurement to reach the fluid but not touching the lung, 3.57 cm. **c** Sagittal image showing the collapsed lung surrounded by the moderate anechoic fluid.

extent of an anomaly such as the absence of muscle in Poland's syndrome. The deepest layer of the thoracic wall is comprised of ribs (fig. 3), the intercostal musculature, and the parietal and visceral layers of the pleura. Usually only the superficial surface of the ribs can be seen on ultrasound images, appearing as a bright interface with a marked acoustic shadow (fig. 3b). With a high-resolution linear probe the visceral and parietal pleura are seen as two echogenic lines deep to the ribs. The visceral pleura usually appears thicker than the parietal [7]. These pleural surfaces slide over each other on real time; this is called the 'lung sliding' sign of normal movement of the lung related to the chest wall. The diaphragm is best imaged through the lower intercostal spaces, as an echogenic line, 1 mm thick [6]. Normal downward movement of the diaphragm should be seen on inspiration (fig. 6a).

The most salient application of pattern recognition in ultrasound is the differentiation between cysts or fluid collections and solid masses. Cystic structures have smooth well-delineated borders, low echogenicity of the liquid contents, no internal echoes and low attenuation (seen as signal enhancement distal to the cyst), described previously (see fig. 5 of the pleural effusion surrounding collapsed lung).

The classical appearance of a pleural effusion is an echo-free layer between the visceral and parietal pleura [6]

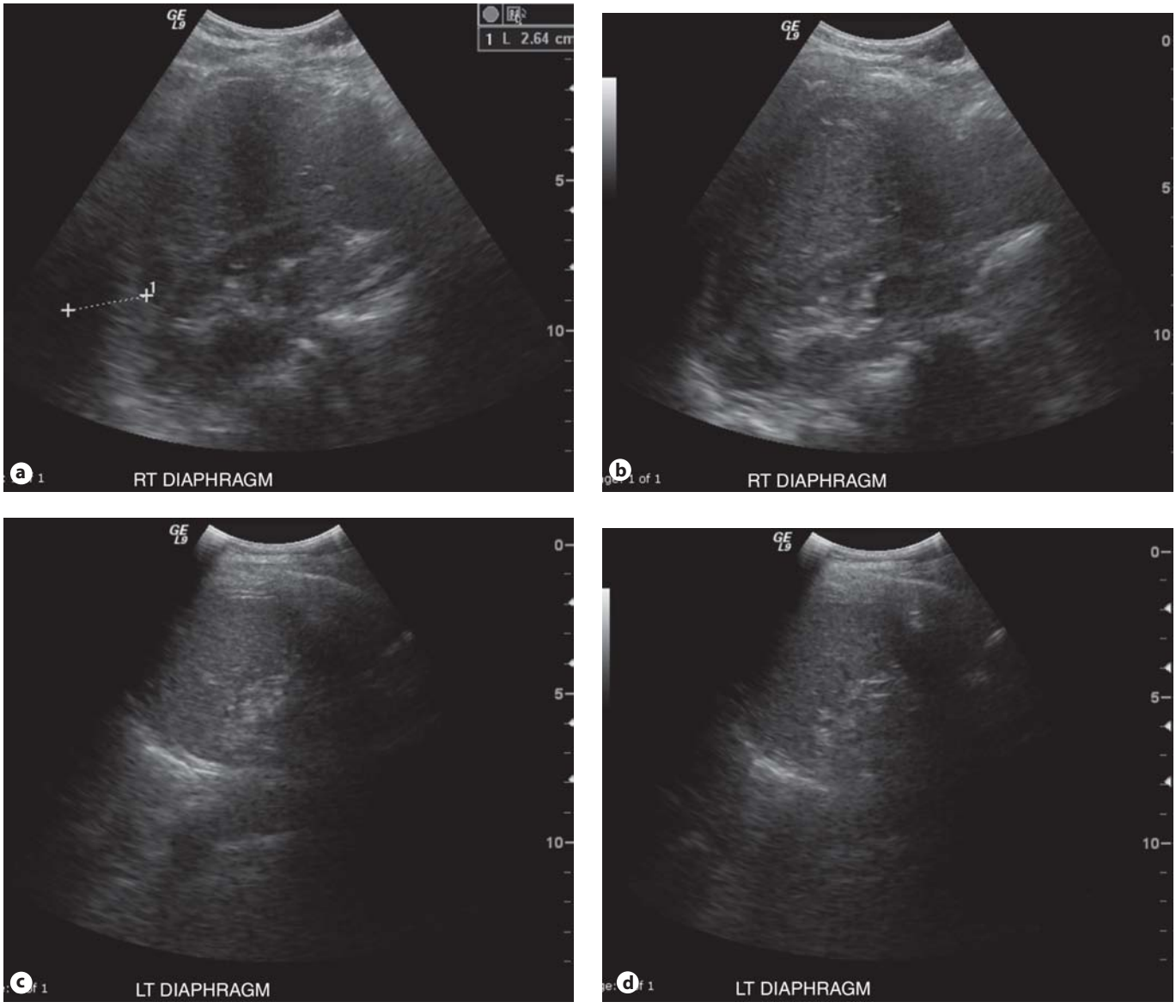

Fig. 6. **a** Sagittal images of the right upper quadrant showing the excursion of the diaphragm 2.64 cm moving appropriately inferiorly with inspiration. **b** Seen in real time. Expiration view is shown. **c**, **d** Sagittal images of the left upper quadrant showing a paralyzed left hemidiaphragm with no change in location between expiration and inspiration.

(fig. 4). Transudates are anechoic. Exudates may appear anechoic, complex or echoic. Doppler color signal within a pleural effusion ('fluid color' sign) can help differentiate a very small fluid collection from pleural thickening. This signal is from transmitted respiratory and cardiac movements [5, 6]. A hydropneumothorax can be diagnosed on ultrasound; the 'curtain sign' describes reverberation artifacts from the air within the pleura that obscures the underlying effusions on inspiration [5, 6].

Visualization of normal lung parenchyma is not possible by ultrasound because the large difference in acoustic impedance between the chest wall and air in the lung results in almost total reflection of the sound waves [9]. However, lobar pneumonia, segmental pneumonias affecting the pleura, and pleural-based consolidation can be seen on ultrasound images. Although pneumonia is the most common cause of lung consolidation, infarction, hemorrhage, vasculitis, lymphoma and endovascular carcinoma can appear the same.

Peripheral lung tumors appear as homogeneous, well-defined masses, usually hypoechoic with posterior acoustic enhancement. Color Doppler helps distinguish malignant from benign masses. Malignant masses have neovascularity with low-impedance flow. Solid tumors release substances which stimulate new vessel formation. The morphology of these tumor vessels is abnormal: these vessels lack vascular walls and therefore offer low resistance to flow, a low RI on waveform arterial tracings, and have a higher end diastolic velocity compared to benign tumors. A constant flow has a high correlation with malignancy; however, a pulsatile or triphasic pattern is seen in benign and malignant neoplasms [6].

Thoracic wall masses are easily interrogated with ultrasound. The most common tumor in the thoracic wall is a lipoma. It appears as a well-circumscribed mass, mildly hypo- or hyperechoic compared to surrounding fat. Few Doppler signals are detected in these neoplasms. Sebaceous cysts, hematomas and abscesses can also be seen [6, 7]. Desmoid tumors are frequently seen in the thoracic wall and appear poorly marginated and hypoechoic [7]. Primary malignant tumors of the thoracic wall are rare and include lymphoma, melanoma, malignant fibrous histiocytoma and sarcomas. They appear hypoechoic [6, 7].

Lymph nodes, especially within the axilla and supraclavicular fossa, are easily imaged on ultrasound. Reactive, inflammatory lymph nodes are oval or triangular with an echogenic fatty hilum. Malignant lymph nodes are plump, rounded, and hypoechoic, with loss of the fatty hilum [6].

Regarding trauma hematomas, muscle tears, rib fractures, and foreign bodies can be diagnosed by ultrasound. Acute hematomas appear as primarily homogeneous echogenic masses sometimes with fluid-filled levels. Chronic hematomas appear more heterogeneous and hypoechoic. To diagnose a rib fracture one sees a step-off instead of a straight bright line on longitudinal images [7]. Subtle crack fractures may show a small reverberation artifact called the 'light house phenomenon' or 'chimney phenomenon' [6]. Foreign bodies are usually recognized by a bright echogenic structure with distal acoustic shadowing or reverberation, such as the comet tail. Massive subcutaneous edema causes bright echoes in the superficial layers with reverberating echoes below, precluding the ultrasonographic imaging of underlying structures [7].

The utility of contrast agents, microbubble-based intravenous substances, in diagnostic ultrasound, is to improve image quality by introducing a change in the acoustic properties of tissue. Usually tissue contrast is improved by the increased reflectivity of selected tissues depending on the biodistribution of the agent. The bubbles increase the strength of the back-scattered signal from blood by several orders of magnitude. Therefore the Doppler signal of flowing blood is easier to detect after intravenous contrast agents have been given. Also, microbubbles oscillate when subjected to ultrasound waves, generating harmonic signals, mentioned previously, which are stronger than those usually generated by soft tissues. Thus, there is good visualization of blood flow and enhanced soft tissues. Ultrasound contrast agents [1] are currently used in certain academic medical centers, often as scholarly investigations under protocols for such goals as a more complete evaluation of masses in the liver.

Conclusion

In this chapter we reviewed some of the physical principles of ultrasound as well as its clinical use in pulmonology. Diagnostic ultrasound is a safe imaging modality which is based on the properties of sound waves and the mechanical and acoustic properties of tissue. Reflection of the sound beam from tissue back to the transducer produces a pulse which creates the image. The Doppler effect of ultrasound can be used to determine blood flow velocity and the RI. Images from diagnostic ultrasound, which can be viewed real time, and at the bedside, help the pulmonologist evaluate pleural effusions, pleural-based masses, chest wall collections, chest wall masses, peripheral lung masses and diaphragmatic movement. This ultrasound modality is also an excellent aid in guidance for biopsies and drainages.

References

1 Middleton WD, Kurtz AB, Hertzberg BS: Ultrasound, the Requisites, ed 2. Boston, Mosby, 2004, chap 1.
2 Hedrick WR, Hykes DL, Starchman DE: Ultrasound Physics and Instrumentation, ed 3. Boston, Mosby, 2004, chap 1.
3 McDicken WN: Diagnostic Ultrasonics. Principles and Use of Instruments, ed 3. New York, Churchill Livingstone, 1991.
4 Bushberg JT, Seibert JA: The Essential Physics of Medical Imaging, ed 2. New York, Lippincott Williams & Wilkins, 2002, chap 16.
5 Wu RG, Young PC, Kuo SH, Luh KT: 'Fluid color' sign – a useful indicator for discrimination between pleural thickening and pleural effusion. J Ultrasound Med 1995;14:767–769.
6 Koh DM, Burke S, Davis N, Padley SP: Transthoracic US of the chest: clinical uses and applications. Radiographics 2002;22:e1.
7 Meuwly JY, Gudinchet F: Sonography of the thoracic and abdominal walls. J Clin Ultrasound 2004;32:500–510.
8 Avruch L, Cooperberg PL: The ring-down artifact. J Ultrasound Med 1985;4:21–28.
9 Lim JH, Lee KS, Kim TS, Chung MP: Ring-down artifacts posterior to the right hemidiaphragm on abdominal sonography. J Ultrasound Med 1999;18:403–410.
10 Ziskin MC, Thickman DI, Goldenberg NJ, Lapayowker MS, Becker JM: The comet tail artifact. J Ultrasound Med 1982;1:1–7.
11 Lichtenstein D, Mexiere G, Biderman P, Gepner A, Barre O: The comet-tail artifact; an ultrasound sign of alveolar-interstitial syndrome. Am J Respir Crit Care Med 1997;156:1640–1646.
12 Lee JC, Banerjee S, King DM: Breast or chest? A diagnostic conundrum. Br J Radiol 2005;78:471–472.

Karen L. Reuter, MD
Diagnostic Radiology, Lahey Clinic
41 Mall Road
Burlington, MA 01805-0001 (USA)
Tel. +1 781 744 8170, Fax +1 781 744 5232, E-Mail Karen.L.Reuter@lahey.org

Chapter 2

Bolliger CT, Herth FJF, Mayo PH, Miyazawa T, Beamis JF (eds): Clinical Chest Ultrasound: From the ICU to the Bronchoscopy Suite.
Prog Respir Res. Basel, Karger, 2009, vol 37, pp 11–20

Thoracic Ultrasound Overview

Shaheen Islam[a] · Hermann Tonn[b]

[a]Division of Pulmonary, Allergy, Critical Care and Sleep Medicine, Ohio State University Medical Center, Columbus, Ohio, USA;
[b]Department of Pneumology and Internal Intensive Care Medicine, Oststadt-Heidehaus Hospital, Hannover, Germany

Abstract

Ultrasound examination is a valuable method in diagnosis of various thoracic conditions including pleural or pericardial effusion, empyema, pneumothorax, pulmonary embolism, pneumonia, and primary or metastatic lung cancer. Ultrasound guidance during thoracentesis or tube thoracostomy assures minimal complications. It can also assist with staging of lung cancer by defining the extension of thoracic wall invasion or by real-time ultrasound-guided biopsy of a supraclavicular lymph node. Invasive procedures such as mediastinoscopy can be spared with effective use of endoscopic or endobronchial ultrasound in cancer diagnosis. Intensivists are able to provide better bedside care efficiently with a focused examination in critically ill patients. Thoracic ultrasound is mostly used to locate a target organ or a disease-specific condition and is often used as a complement to other imaging such as chest radiograph, computed tomogram or magnetic resonance imaging. Advantages include portability permitting bedside examination even in the intensive care units. Specific focused skills can be easily learned with formal didactic lessons and supervised training.

Air is a poor medium for sound transmission. As lung contains air, ultrasound of the lung may seem counterintuitive. The interface between chest wall and normal lung with different acoustic densities reflects most of the ultrasound waves, preventing a direct examination of an otherwise healthy lung. In pathological conditions such as tumor invasion, consolidation or atelectasis, the alveoli are replaced with more dense tissue allowing better sound conduction. When the pleural space is occupied with fluid or the consolidated lung reaches the chest wall, it opens an acoustic window permitting ultrasound examination of the lung.

Although ultrasound is now being used in most intensive care units (ICU) for vascular access, the potential of ultrasound use by pulmonologists for other thoracic applications is still underestimated. The role of ultrasound examination in lung cancer staging is not mentioned in the current guidelines. Ultrasound is practiced in the emergency rooms throughout the world for focused assessment with sonography for trauma to determine rapid intervention for cardiac tamponade, severe intrathoracic or intra-abdominal bleeding or organ injury. Ultrasound is helpful to locate the best site for chest tube placement or the insertion of a trocar prior to thoracoscopy or to drain a complicated pleural effusion. It can be used to localize parenchymal consolidation, tumor, chest wall, pleural masses or lymph nodes. Intrathoracic invasion of tumor masses in addition to cardiac function may also be detected easily. At the Oststadt-Heidehaus Hospital in Germany, ultrasound is routinely used in cancer surveillance to scan pleura, chest wall, liver, adrenal glands, lymph nodes or bones. An enlarged supraclavicular lymph node detected during examination is aspirated at the same time with minimal additional preparation allowing diagnosis and cancer staging. Fine needle aspirate or histological specimen may be obtained under real-time guidance with minimal risk of pneumothorax from the chest wall or subpleural peripheral lung masses.

Ultrasound involves no ionizing radiation or nephrotoxic contrast dye exposure. As opposed to other imaging techniques such as computed tomogram (CT), magnetic resonance imaging (MRI) or even simple radiographs, ultrasound examination may be performed anywhere and on any critically ill patient as a preliminary examination or to further investigate an existing finding noted on other radiographic imaging.

In this chapter we will briefly describe the clinical applications of ultrasound in thoracic diseases involving chest wall, mediastinum, lung parenchyma, pleural fluid, lymph nodes, and diaphragm. We hope this discussion will

encourage nonradiologists to consider ultrasound as an attractive tool to aid with physical examination and interventional procedures.

Principles of Thoracic Ultrasound

Depending on the available transducers, a good examiner may be able to achieve best results even when the circumstances are not optimal. Frequently, the sonomorphological image may not be decisive because of limitations or artifacts. Lung patterns during examination are mostly dynamic and the thoracic ultrasound examination is largely based on the analysis of artifacts [1]. Familiarity with various common artifacts and adequate technical skills are the basic requirements for thoracic ultrasound.

Chest CTs are mostly done in supine position. Unlike CT or MRI, there is no standardized operator interface for image acquisition in ultrasound except for the marker on the screen that corresponds to the transducer orientation. The examination is dependent on the skills of the individual operator and the orientation of the probe. So, reproducibility of images is not as precise as with other imaging such as CT. An optimal image acquisition depends on the choice and placement of the appropriate probe with an adequate preset at the right spot at an optimal angle with the patient in the best possible position. Good thoracic ultrasound examination consists of not just the acquisition of static images but analysis of the dynamic sonomorphological changes associated with probe positioning or respiratory movement.

Echogenicity

Ultrasound images are displayed on a gray scale. The strongest echo appears white while it is black when no sound wave is reflected from the organs. Depending on the reflected wave amplitude, the following terms are used to define echogenicity. When no sound wave is reflected and the image appears black it is *anechoic* as in pleural effusion. It is *isoechoic* when the echoes are of comparable amplitude with the surrounding tissue as with kidneys or spleen. It is *hyperechoic* when echoes are stronger than the surrounding tissue as in diaphragm, and *hypoechoic* when it is weaker than that from the surrounding tissue.

Description of Probes

Tissue penetration of ultrasound decreases as frequency increases. Superficial organs are better visualized with higher frequency and deeper structures with lower frequency transducers. The gain and the power of the ultrasound need to be adjusted to obtain an adequate image. Most ultrasound equipments have preset modes for better imaging of specific organs of the body. For superficial imaging, a preset for the thyroid gland is useful. Otherwise most of the thoracic structures may be examined with abdominal preset.

The size of the probe is vital in real-time interventional procedures. A smaller probe will leave more room for needle insertion during real-time vascular access, thoracentesis, tube thoracostomy or percutaneous biopsy. There are primarily three types of transducers used in thoracic imaging, e.g. linear array, curvilinear array and a phased array.

Linear array transducers have piezoelectric crystals arranged in a linear sequence on the transducer head (fig. 1a). Parallel pulses are generated forming a line of sight perpendicular to the transducer face with a large footprint (part of transducer in contact with body surface). It produces a rectangular display. A linear array 7.5- to 10-MHz transducer with a thyroid preset is best to visualize superficial structures of the neck. This is also useful for vascular access or to determine pleural thickening, pleural masses or subpleural parenchymal lesions of lung. These high-frequency transducers provide an excellent high-resolution image of superficial structures but are not ideal for deeper tissue examination.

The curved array transducers consist of linear arrays shaped into convex curves that produce a large field of view with a large footprint (fig. 1b). These provide a pie-shaped image and are helpful to examine large pleural effusion, lung or abdominal structures or to view the lung from an abdominal approach.

In the phased array transducers, crystals located on the transducer head are pulsed as a group and the direction of the beam is continually changed in phases producing a pie-shaped image with a smaller footprint (fig. 1c). The benefit is a relatively smaller transducer with a large field of view at depth. A 2- to 5-MHz-phased array or a sector probe is good to visualize deeper structures such as atelectatic lung, complicated pleural effusion or heart through the intercostal space. They are also useful to visualize the pleural space from an abdominal approach through the liver.

Position of the Patient and Relationship with Other Organs

In the ultrasound nomenclature, a popular term used is the earth-sky axis. The thoracic organs are composed of water and air. Air rises and the water descends following the rules of gravity. Intrathoracic organs and pleural fluid shift with different patient positions. Successful examination depends on appropriate understanding of the anatomy in relation to patient position during image acquisition.

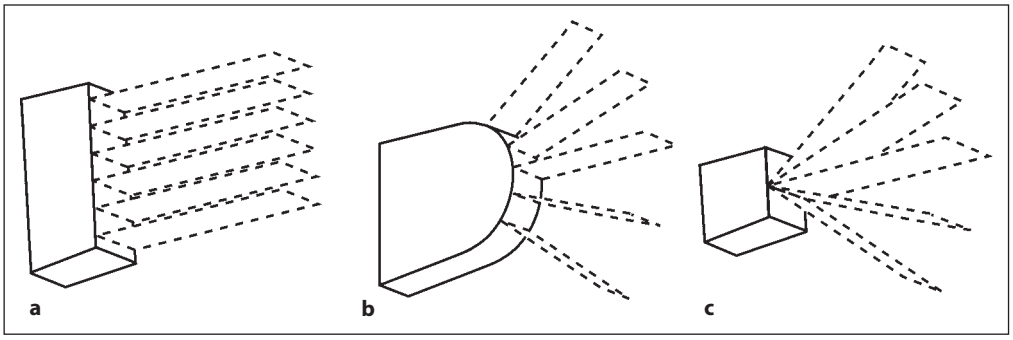

Fig. 1. **a** Linear array transducer. Parallel pulses are generated perpendicular to the transducer head. It provides a rectangular field of view. **b** Curvilinear transducer. Diverging pulses radiating from the convex transducer head. It generates a pie-shaped image with a larger footprint. **c** Phased array transducer. Alternating pulses radiating from the transducer head. It also generates a pie-shaped image but with a smaller footprint.

The lymph nodes or tumors of the anterior mediastinum that are not in contact with the chest wall in supine position may come against the chest wall when the patient is turned to a slightly prone left or right lateral decubitus position. A sitting position is ideal to localize very small pleural effusion, as most of the fluid is then collected in the costodiaphragmatic recess. The probe may need to be held close to the surface of the bed to locate pleural fluid in a supine patient in the ICU. Masses or lymph nodes in supraclavicular or the anterior mediastinum may be best visualized by turning the patient's head to the extreme right or left or in flexion or extension. Pleural space can be visualized better from a posterior approach in a sitting patient with the hand placed on the opposite shoulder or above the head.

Orientation of Transducers

The secret of the acquisition and interpretation of thoracic ultrasound images lies in the ability of the examiner to correlate the obtained images virtually with the patient anatomy. Although ultrasound provides a 2-dimensional image, by sliding or tilting the transducer or by observing respiratory movement, a 3-dimensional dynamic image may be reconstructed in the mind. Being able to see the 3-dimensional image of the pathological changes is a key factor in image interpretation. Depending on the location of the target organ, patient position, clinical complaints, chest radiograph or CT images, the examiner tries to orient the transducer to the best possible site. However, this requires experience.

Each transducer is marked with a probe indicator, signifying the direction of examination that corresponds to a marker on the display screen. Usually this marker is placed on the left upper corner of the display screen; however, most current ultrasound units allow customization of the screen. The probe indicator of the transducer is placed in the cephalad direction during sagittal scanning of the chest. The probe indicator should be placed as much cephalad as possible when scanning through the intercostal window along the rib axis. During transverse scanning, the probe indicator is directed toward the patient's right side. Transducer placement with operator and patient position to examine pleural cavity and mediastinal window are described in fig. 2.

Intrathoracic structures may be visualized better by holding the probe along the longitudinal or transverse axis over the rib spaces. It may take several attempts to find the best position and the correct angle to inspect a target structure. Anatomic landmarks are of assistance especially before any invasive procedure. Pleural surface on the right side is limited by the liver and the diaphragm, and on the left by the spleen with the diaphragm. The demonstration of kidneys on either side indicates structures below the diaphragm. The sonomorphological image of an empyema is very similar to a full stomach. Identification of these organs will assure a safe procedure and prevent needle puncture of liver, spleen or a full stomach.

Technical Skills

Good hand control is essential for successful scanning. By holding the probe comfortably, visualization can be maximized with a gentle rotating and rocking movement of the transducer. By sliding the transducer slowly over different rib spaces, a better window for visualization may be found. Using the thenar eminence to stabilize the hand against the

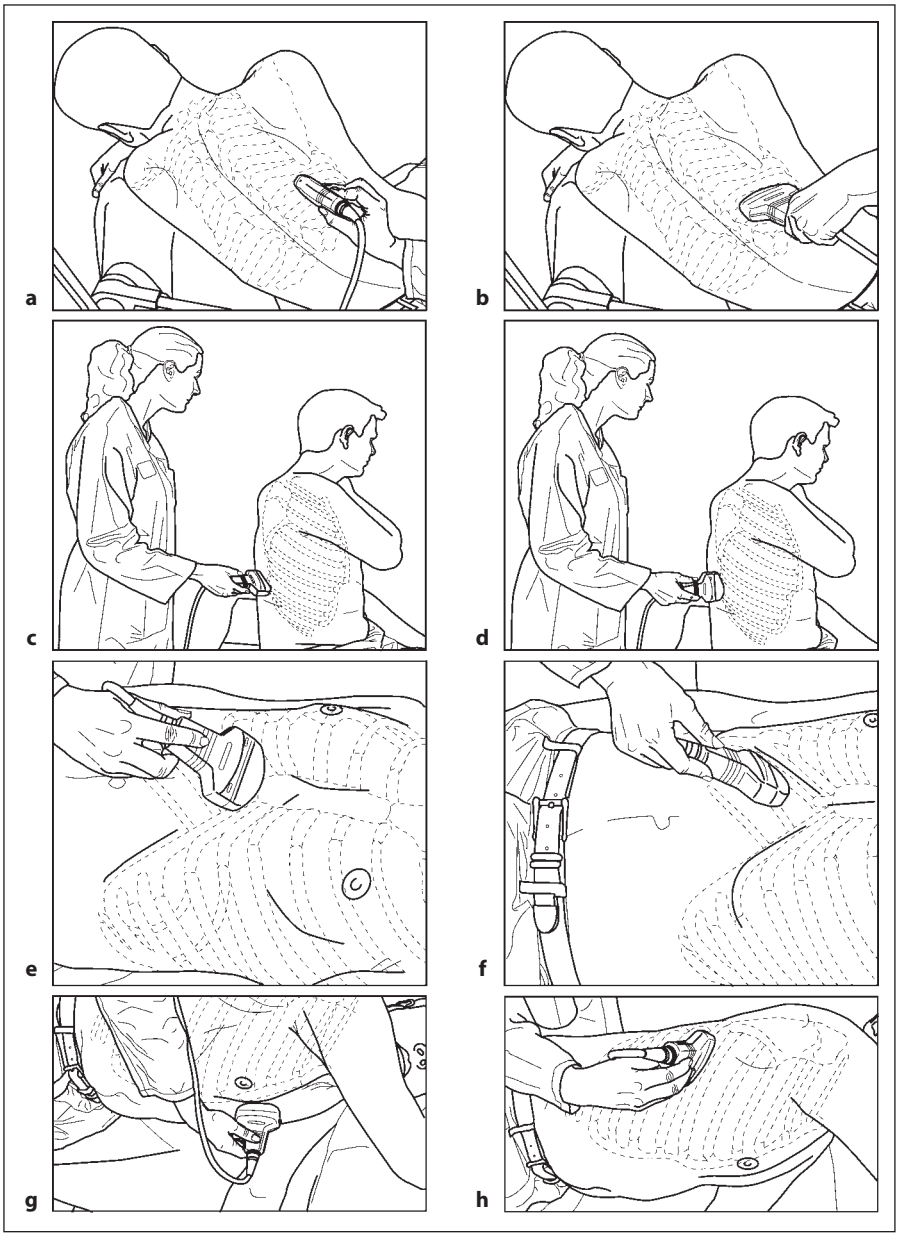

Fig. 2. Transducer orientation during thoracic ultrasound examination. **a** Examination of the posterior chest wall or pleural space in a supine patient in lateral decubitus position. Transducer placed longitudinally over rib spaces with the probe indicator in a cephalad direction. **b** Transducer placed transversely along rib spaces with the probe indicator directed towards the right side of the patient. **c** Examination of the posterolateral chest wall and pleural space in a sitting patient, transducer placed longitudinally with the probe indicator in the cephalad direction. **d** Transducer placed transversely with the probe indicator directed towards the right side of the patient. **e** Examination of the heart through the xiphisternal approach. Probe indicator directed towards the right side. **f** Transhepatic approach to visualize pleura, diaphragm or liver in a supine patient. **g** Examination of the mediastinum in a patient in left lateral decubitus position with the patient slightly pronated, so that the mediastinal structures are closer to the anterior chest wall. **h** Examination of the lateral chest wall, pleura in left lateral decubitus position.

chest wall during examination will prevent any unintentional sliding of the probe.

Examiner Position

In addition to appropriate positioning of patients and the transducers, the examiner needs to be flexible to complete an examination or ultrasound-guided procedure comfortably. A second monitor placed across the patient may be helpful in prolonged examination. An assistant available during interventional procedures to adjust the settings or to store images will assure a complete sterile technique. Some ultrasound units now have a foot paddle to allow image acquisition without compromising sterility.

Doppler Use in Thoracic Ultrasound

Doppler function has limited utility in the pleural examination but can be useful to detect vascularity of a chest wall, pleural or subpleural parenchymal mass. It can be useful

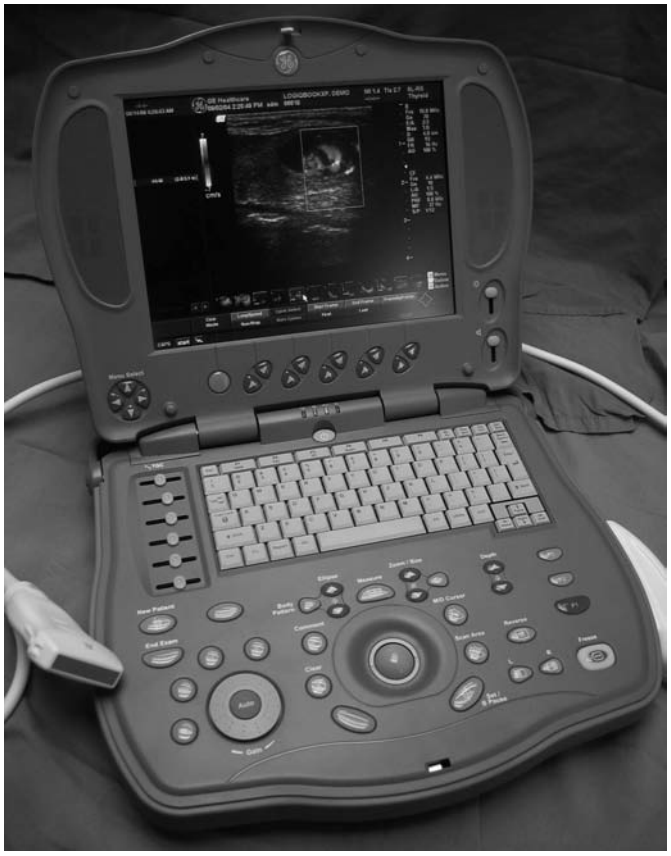

Fig. 3. Laptop-sized portable ultrasound (GE LOGIQ Book XP Enhanced; GE Healthcare, Wauwatosa, Wisc., USA).

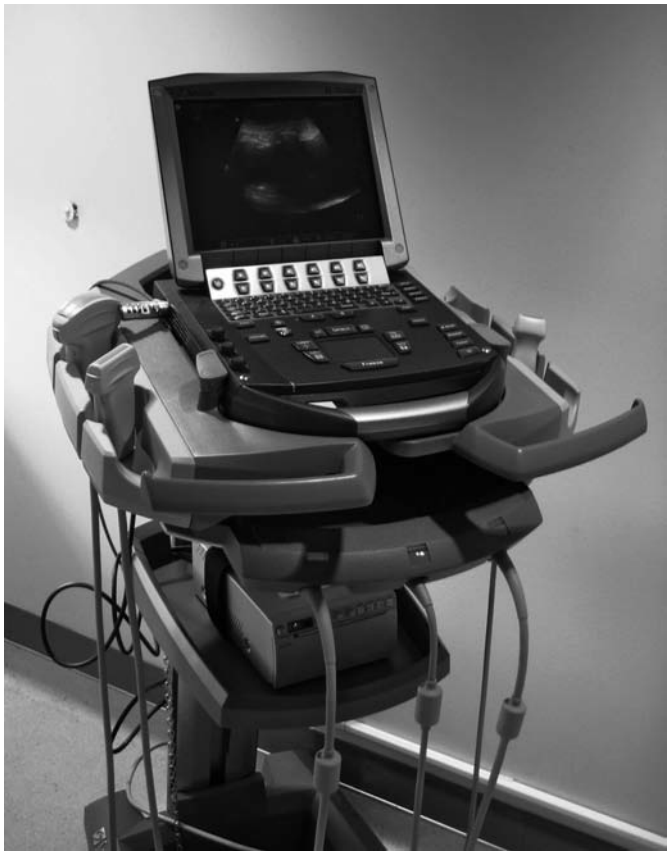

Fig. 4. Portable laptop-sized unit mounted on a pedestal (M-Turbo, SonoSite, Bothell, Wash., USA).

during vascular access, especially in hypotensive critically ill patients. Color flow Doppler needs to be used cautiously as it produces artifacts with respiratory movement and experience is needed to interpret it.

Normal Ultrasound Anatomy of the Chest

Normal chest wall consists of echogenic soft tissue layers representing layers of muscle and fascia. Ribs appear as smooth echogenic line below the soft tissue. Visceral and parietal pleura can be identified as two echogenic lines below the ribs with a 7.5- to 10-MHz high-resolution linear array probe. With real-time imaging, the sliding of the two pleural surfaces known as the 'gliding sign' can be seen. At the pleura-lung interface, air-filled lung prevents parenchymal examination.

Clinical Applications of Ultrasound

Ultrasound technology ranging from bulky machines to ultraportable pocket size equipments are now available (fig. 3–6). For critical care echocardiography or transthoracic ultrasound examination, we prefer a laptop-size instrument mounted on a cart with different probes (linear, curvilinear, phased array) available. A brief description of the clinical application in thoracic ultrasound follows. It is described in detail in other chapters of this book.

Pleural Pathology

Pleural effusion appears as an anechoic layer between the parietal and the visceral pleura. Movement of the atelectatic lung with respiratory cycle may be noticed through the pleural fluid. In supine position, pleural effusion is best witnessed from the lateral chest wall posterior to the midaxillary line with the probe pointed upwards. In the upright or sitting patient, it can be located easily from the posterior or lateral chest wall.

Transudates as a rule are anechoic, whereas exudates may appear anechoic or hyperechoic. Diffusely echogenic pleural effusion appearing as a 'snowstorm' usually represents empyema containing protein or tissue debris. Echogenic septations or loculations confirm a complex empyema and are much better identified with ultrasound than with the CT. The differentiation between lung abscess and empyema is sometimes difficult because a hypoechoic center may be found in both [2]. Hydropneumothorax can also be identified. A hemothorax may have hypoechoic or echogenic regions, occasionally with dependent layering of blood. Pleural thickening seen in fibrosis or empyema appears as a hypoechoic broadening of the pleura. Malignant effusions are usually anechoic but may become septated with repeated thoracentesis. Malignant pleural masses such as metastatic lesions or mesothelioma present as nodular pleural thickening and may accompany a pleural effusion.

Pneumothorax

Air localized within the pleural cavity collects in the nondependent part and is best identified in the supine position with the probe held perpendicularly on the anterior chest wall. The depth of the pneumothorax cannot be determined. A pneumothorax is usually diagnosed by the absence of normal pleural gliding sign (movement of parietal pleura on the visceral pleura) and comet tail appearance, and the presence of exaggerated reverberation artifact (an artifact produced by reflection of sound at the chest wall-air interface). M-mode is of additional help. Operator experience is crucial to analyze these artifacts.

Pneumonia

Consolidated lung in contact with chest wall or contained in pleural effusion may appear as echogenic. Similar findings may be seen with pulmonary hemorrhage, bronchoalveolar carcinoma or a lung infarct. Branching hyperechoic structures representing air bronchogram may be seen. Atelectatic lung is usually echogenic without any air bronchogram.

Primary or Metastatic Lung Cancer

Peripheral lung masses close to the pleura appear hypoechoic; however, it may become echogenic with bleeding. Diaphragmatic involvement can be detected through liver with an abdominal approach or with a transthoracic approach when pleural effusion is present.

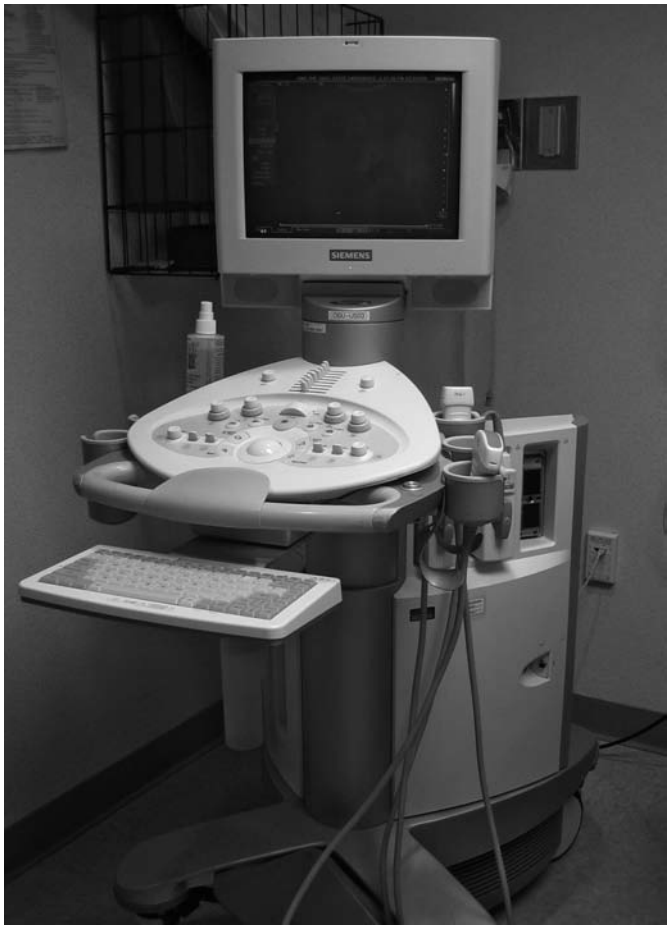

Fig. 5. A comprehensive full-size ultrasound system (SONOLINE Antares, Siemens Medical Systems, Issaquah, Wash., USA).

Chest Wall

Soft tissue invasion of the chest wall by a primary lung cancer or chest wall tumor is easily detected. Ultrasound provides a better image of the Pancoast tumor than CT [2]. Only MRI offers a good image of this complex anatomical location. Comparison of findings with the healthy normal side may be a clue to diagnosis. Bony invasion of tumors like plasmocytoma appear as hypoechoic lesions. The fracture of ribs or clavicle can be identified.

Lymph Nodes

Supraclavicular, cervical and axillary lymph nodes can be examined better with ultrasound. Reactive or malignant lymph nodes can be differentiated based on the consistency or vascularity.

Intrathoracic Tumor Extension
Malignant invasion of the aorta or pericardium from lung can be detected better with transesophageal echocardiogram compared to CT or MRI with up to 90% accuracy [3, 4].

Pulmonary Embolism
Pulmonary embolism can be diagnosed with ultrasound. It is described in detail in chapter 5, see pp. 43–50.

Cardiac Function
A focused cardiac examination can be done effectively by intensivists with the phased array probe to document pericardial tamponade, ventricular function, ejection fraction or contractility in critically ill patients. This is discussed in chapter 7, see pp. 60–68.

Fig. 6. The first smallest pocket-size ultrasound ACUSON P10 measuring 2.2 inches × 3.8 inches × 5.7 inches and weighing 1.6 lb (© 2008 Siemens Medical Solutions USA, all rights reserved; product photo provided courtesy of Siemens Medical Solutions USA).

Functional Tests

Diaphragm Function (Sniff Test)
Diaphragm paralysis or paresis can be diagnosed effectively with ultrasound. Pleural fluid-diaphragm interface makes the diaphragm hyperechoic. Without pleural effusion the diaphragm can be visualized only partially. However, by placing the probe in the subcostal location, the movement of both domes of the diaphragm may be compared to determine unilateral weakness. Bilateral weakness may be difficult to interpret. Ascites, when present, will push the diaphragm into the thoracic cage whereas in COPD, the diaphragm is flattened. With rupture of the diaphragm intra-abdominal organs may be seen within the thoracic cage.

Thoracic Tumor Localization
The gliding sign identifies structures at the interface of the parietal and visceral pleurae. A subpleural mass or lung mass will move with respiration against the parietal pleura; while pleural sliding seen deeper to a tumor or mass will confirm its location within the chest wall. Absence of any movement at a particular location will provide evidence that both lung and chest wall are involved.

Ultrasound-Guided Interventional Procedures

Vascular Access
Ultrasound-guided bedside central venous catheter placement is safer [5]. It is now a standard of care in most ICUs. A quick survey prior to placement may reveal a thrombosis of the central vein and help guide with the appropriate location. Use of ultrasound reduces failure rate and complications [6]. This is crucial in coagulopathic patients where successful cannulation can be obtained in a single attempt. Peripherally inserted central catheters (PICC) are nowadays placed in most hospitals in the US with ultrasound guidance.

Pleural Access
Ultrasound is an invaluable tool during thoracentesis to localize the deepest collection of pleural fluid. Although not completely eliminated, the incidence of pneumothorax is minimal with ultrasound-guided thoracentesis [7]. In very small pleural effusions sometimes the effusion is only visible when the patient is in sitting position. It can be used to guide chest tube in the pleural effusion and thereby prevent any subcutaneous placement, especially in obese patients. A chest tube cannot be guided in pneumothorax, as it will not be visible in the air within the pleural cavity.

We routinely use ultrasound prior to medical thoracoscopy or indwelling pleural catheter placement to locate the ideal site and to determine septations or loculations. The catheter is usually placed in the area of the largest collection.

Details on ultrasound use during thoracentesis and thoracoscopy are described in chapters 21 and 24, see pp. 182–188, 208–214.

Endoscopic and Endobronchial Ultrasound
Endobronchial ultrasound has proved to be a very effective tool to sample mediastinal lymph nodes. Combined endoscopic ultrasound and endobronchial ultrasound makes it possible to avoid mediastinoscopy completely. Details are described later.

Pericardiocentesis
Malignant pericardial effusion or traumatic effusion causing a tamponade can be drained safely with ultrasound guidance. An easier access under real-time ultrasound guidance is the parasternal approach rather than the traditional xiphosternal approach.

Paracentesis
A therapeutic or diagnostic paracentesis can be done safely in the ICU. A sector or curvilinear 3.5- or 5-MHz probe can be used to localize maximum fluid collection. A 7.5-MHz probe can then be used to localize vascular (inferior epigastric vein about 4–6 cm lateral to the midline) structures in the abdominal wall. The best area for paracentesis is about 2 cm below the umbilicus in the white line or 5 cm superomedial to the anterior superior iliac spine [8].

Percutaneous Tracheotomy
Because trachea contains air, only the anterior tracheal wall can be visualized with the transcervical approach. In obese patients or patients with difficult anatomy, laryngeal, cricoid and other tracheal cartilages can be identified with additional information on the depth of the trachea from the skin and the thickness of pretracheal fascia or tracheal deviation. An ultrasound examination is helpful to determine the size of the thyroid gland and the location of the isthmus. With Doppler flow imaging, nearby vascular structures can also be identified [9].

Ultrasound-Guided Biopsy
Subpleural peripheral lung, pleural-based or chest wall masses can be safely biopsied with ultrasound guidance. In Germany and some centers in the United States [10], pulmonologists perform needle aspiration or core biopsies. This technique largely depends on obtaining an image through an adequate acoustic window. A lung abscess reaching the chest wall may be percutaneously drained with ultrasound guidance. Mediastinal masses and lymph nodes in the anterior and superior mediastinum can also be accessed [2]. The best way to access these nodes is with the patient in the lateral decubitus position with a suprasternal or parasternal approach. Color flow Doppler may identify nearby vascular structures.

Supraclavicular and Cervical Lymph Node Biopsy
Supraclavicular lymph nodes that are not palpable can be detected easily by ultrasound and biopsied in real time. In malignant conditions, cytological diagnosis can assist with cancer staging [11]. Nonmalignant conditions such as sarcoidosis can also be diagnosed. It is superior to CT [12] and the sensitivity of detecting metastases is increased 3-fold [12, 13]. Even bronchoscopy or other invasive procedures may be avoided in about 15% of lung cancer patients if cervical ultrasound and biopsy are included early in the diagnostic workup [12].

Training

Radiologists, cardiologists and sonographers go through an intense training before they are credentialed to obtain or interpret ultrasound images. The use of ultrasound by nonradiologists is very focused and is usually limited to common examinations and procedures within their specialty. Therefore, limited training in focused areas may be adequate. Surgical residents are able to learn basic focused assessment with sonography for trauma examination after 8 h of formal training [14]. In emergency medicine, a 1- to 3-day training course is offered with follow-up mentoring [15]. Videotaped cases are also valuable in developing interpretation skills [16]. As with any other procedure, there is a learning curve for acquiring the technical skills.

At present, there are no guidelines on thoracic ultrasound examination. In Germany, a documentation of 100 cases of ultrasound examination is required to become an internist. Skills in focused thoracic ultrasound examination may be easily learned but being able to differentiate normal from abnormal structures and then to identify specific abnormal findings requires additional experience. When in question, available resources for comparison or referral for formal radiology evaluation may be necessary.

A successful thoracic ultrasound training program for nonsurgeons such as pulmonologists or medical and surgical intensivists should include a 1- to 2-day didactic session on basic ultrasound, practice on phantom and live models followed by supervised examinations where the images are recorded and reviewed with the mentors. Proficiency can be determined by a formal evaluation after about 5–15 cases depending on the scope of the examination. Although a required number of procedures is suggested by most authorities before an individual can practice independently, we are all aware that not everyone has the aptitude to learn or practice accurately even after completion of the required

numbers. A competency evaluation before credentialing is useful rather than the acquisition of a preset number. One must remember that it is a cumulative education and strict numerical requirements for each procedure may limit its use. The availability of dedicated and competent mentors for follow-up and ongoing supervision and posttraining evaluation is necessary as each examination is unique.

Most thoracic physicians or surgeons may use ultrasound as an adjunct to other imaging studies such as CT, chest radiograph or MRI. Localization of pleural fluid and ultrasound-guided thoracentesis is the easiest to learn second to vascular access. As most pulmonologists are proficient in thoracentesis, it may be considered as an ultrasound-assisted rather than an ultrasound-guided procedure. Pulmonary fellows at one institution in the US are credentialed to perform thoracentesis independently after watching a DVD on the technique [17]. Once basic skills in acquisition and interpretation of images of pleural effusion are achieved, ultrasound-guided thoracentesis, chest tube placement, peripheral lung mass or supraclavicular lymph node examination and biopsies can be done safely with some additional training.

Limitations

The examination may be limited in subcutaneous emphysema, massive peripheral edema, morbid obesity or when patients cannot be placed in an optimal position. Insufficient operator skills can be avoided with adequate training and proctored examinations. Familiarity with one or two transducers and appropriate placement and selection of the probe can minimize these limitations. A typical thoracic examination is possible with any simple ultrasound unit. Color flow Doppler interpretation needs experience.

Frequently, diagnosis cannot be made by a single imaging technique. Concomitant imaging of different organs of the body may lead to a diagnosis. For example, compression ultrasound of lower extremity, echocardiogram and transthoracic ultrasound examination may indicate pulmonary embolism when V-Q scan or CT angiogram cannot be done. Detection of a new pathological condition, for example, finding a tumor of the kidney during a routine ultrasound examination, is uncommon in thoracic ultrasound.

Conclusion

Ultrasound is no longer limited to the realm of the radiologists. Availability of newer, user-friendly, inexpensive, portable units has made them an excellent tool for nonradiologists such as emergency physicians, surgeons, intensivists or pulmonologists to provide superior care. In addition to a diagnosis, they provide a safe guidance for various bedside procedures, especially in critically ill patients where a detailed ultrasound examination may avoid transportation to the radiology suite. Cancer staging can be done by aspiration of an easily accessible lymph node or chest wall mass. Even though ultrasound has no significant physical risks, false-negative or false-positive diagnoses may have dire consequences. With adequate focused training, the same clinician can confirm a finding, provide necessary diagnostic or therapeutic intervention and deal with complications, if any, while the patient is still on the table, in a cost- and time-efficient manner.

Acknowledgment

We thank Tim Eubank, PhD for assistance with the drawings.

References

1 Lichtenstein D: Ultrasound in management of thoracic disease. Crit Care Med 2007;35:S250–S261.
2 Koh DM, Burke S, Davies N, Padley SP: Transthoracic ultrasound of the chest: clinical uses and applications. Radiographics 2002;22:e1.
3 Rankovic BS: Transesophageal ultrasound for identification of a lung cancer infiltration into great vessels. Chest 2001;120(suppl):318S.
4 Schröder C, Schönhofer B, Vogel B. Transesophageal echographic determination of aortic invasion by lung cancer. Chest 2005;127:438–442.
5 McGee W: Central venous catheterization: better and worse. J Intensive Care Med 2006;21:51–53.
6 Tan PL, Gibson M: Central venous catheters: the role of radiology. Clin Radiol 2006;61:13–22.
7 Grogan DR, Irwin RS, Channick R, Raptopoulos V, Curley FJ, Bartter T, Corwin RW: Complications associated with thoracentesis. A prospective, randomized study comparing three different methods. Arch Intern Med 1990;150:873–877.
8 Nicolaou S, Talsky A, Khashoggi K, Venu V: Ultrasound guided interventional radiology in critical care. Crit Care Med 2007;35(suppl):S186–197.
9 Kollig E, Heydenreich U, Roetman B, Hopf F, Muhr G: Ultrasound and bronchoscopic controlled percutaneous tracheostomy on trauma ICU. Injury 2000;31:663–668.
10 Doelken P, Strange C: Chest ultrasound for 'dummies'. Chest 2003;123:332–333.

11 Kumaran M, Benamore RE, Vaidhyanath R, Muller S, Richards CJ, Peake MD, Entwisle JJ: Ultrasound guided cytological aspiration of supraclavicular lymph nodes in patients with suspected lung cancer. Thorax 2005;60:229–233.
12 Prosch H, Strasser G, Sonka C, Oschatz E, Mashaal S, Mohn-Staudner A, Mostbeck GH: Cervical ultrasound (US) and US-guided lymph node biopsy as a routine procedure for staging of lung cancer. Ultraschall Med 2007;28:598–603.
13 van Overhagen H, Brakel K, Heijenbrok MW, van Kasteren JH, van de Moosdijk CN, Roldaan AC, van Gils AP, Hansen BE: Metastases in supraclavicular lymph nodes in lung cancer: assessment with palpation, US and CT. Radiology 2004;1:75–80.
14 Smith RS, Kern SJ, Fry WR, Helmer SD: Institutional learning curve of surgeon-performed trauma ultrasound. Arch Surg 1998;133:530–535.
15 Langlois Sle P: Focused ultrasound training for clinicians. Crit Care Med 2007;35(5 suppl):S144–S149.
16 Sisley AC, Johnson SB, Erickson W, Fortune JB: Use of an Objective Structured Clinical Examination (OSCE) for the assessment of physician performance in the ultrasound evaluation of trauma. J Trauma 1999;47:627–631.
17 Gilley SK, Doelken P: How to interpret floating lung and comet tails. Using ultrasonography in the diagnosis and management of pleural disease. J Respir Dis 2008;29:200–207.

Shaheen Islam, MD, MPH
Assistant Professor
Diector, Interventional Pulmonary
Division of Pulmonary, Allergy, Critical Care and Sleep Medicine
Ohio State University Medical Center
201 HLRI, 473 W 12th Avenue
Columbus, OH 43210 (USA)
Tel. +1 614 247 7707, Fax +1 614 293 4799
E-Mail shaheen.islam@osumc.edu

Transthoracic Ultrasound

Chapter 3

Bolliger CT, Herth FJF, Mayo PH, Miyazawa T, Beamis JF (eds): Clinical Chest Ultrasound: From the ICU to the Bronchoscopy Suite.
Prog Respir Res. Basel, Karger, 2009, vol 37, pp 22–33

Transthoracic Ultrasound for Chest Wall, Pleura, and the Peripheral Lung

Coenraad F.N. Koegelenberg · Andreas H. Diacon · Chris T. Bolliger

Division of Pulmonology, Department of Medicine, University of Stellenbosch and Tygerberg Academic Hospital, Tygerberg, Cape Town, South Africa

Abstract

Thoracic ultrasonography can be performed by means of the most basic ultrasound (US) equipment. In healthy individuals, US can visualize the chest wall, the diaphragm and the pleura but not the lung parenchyma. The main domain of thoracic US is the investigation of chest wall abnormalities, pleural thickening and pleural tumours, and the qualitative and quantitative description of pleural effusions. US can visualize lung tumours, pulmonary consolidations and other parenchymal pulmonary processes provided they abut the pleura. US is the ideal tool to assist with thoracentesis and drainage of effusions. US-assisted fine needle aspiration and cutting needle biopsy of lesions arising from the chest wall, pleura and peripheral lung are safe and have a high yield in the hands of chest physicians. US may also guide aspiration and biopsy of diffuse pulmonary infiltrates, consolidations and lung abscesses, provided the pleura is abutted. Advanced applications of transthoracic US include the diagnosis of a pneumothorax and pulmonary embolism.

Ultrasonography of the thorax remains an underutilized investigation. Although diagnostic sonography of the abdomen has been around for more than 60 years, its thoracic counterpart has lagged behind for many decades. The inability of ultrasound (US) to penetrate aerated tissue diverted clinicians from appreciating its excellent ability to visualize the chest wall, pleura and pathology of lung abutting the pleura [1]. The major advantages of thoracic US include its mobility, dynamic properties, low cost, lack of radiation, and short examination time [1–6]. Thoracic US is also increasingly being used to assist interventional procedures. The main aim of this chapter is to demystify ultrasonography for the clinician by reviewing the basic principles and recent advances from the perspective of the non-radiologist.

General Technical Aspects

Adequate thoracic ultrasonography can be performed by means of the most basic, entry-level, two-dimensional black-and-white US equipment. A low frequency probe (e.g. 3.5 MHz) with curvilinear shape for covering a large area is suitable for initial screening of superficial and deeper structures, while a high frequency probe (e.g. 8 MHz) with a linear shape is used for refined assessment of an abnormal chest wall or pleural area. Doppler and colour flow echo are not required for routine thoracic examination.

Optimal patient position for scanning is an underappreciated aspect. It is important to review a patient's chest radiograph and computed tomography (CT) scan prior to performing a thoracic US examination. This will not only identify the area of interest, but will also guide the positioning of the patient. The posterior chest is best scanned with the patient in the sitting position using a bedside table as an armrest (fig. 1), whereas the lateral and anterior chest wall can be examined with the patient in either the lateral decubitus or even supine position. Maximum visualization of the lung and pleura is achieved by examining along the intercostal spaces. Raising the arm above the patient's head increases the intercostal space distance and facilitates scanning in erect or recumbent positions. A patient can fold the arms across the chest in order to displace the scapulae when

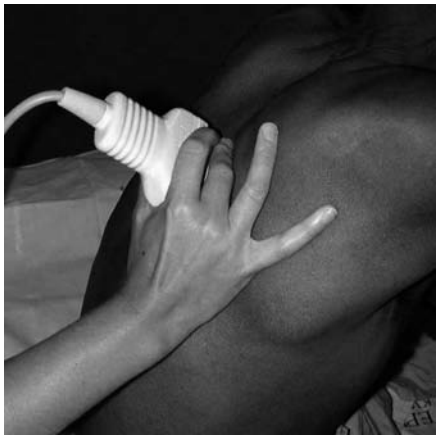

Fig. 1. Scanning position for thoracic US. The posterior chest is best scanned with the patient in the sitting position using a bedside table as an armrest. Note the way in which the probe is held. It is important to ask the patient to fold his arms across his chest when surveying the superior posterior chest. The lateral chest wall can be examined with the patient in the lateral decubitus position with the arm raised, and the anterior chest wall with the patient supine (not shown).

surveying the upper posterior thorax. Superior sulcus pathology can be visualized apically with the patient in the supine or sitting position.

Diagnostic Thoracic Ultrasonography

The Normal Thorax

A series of echogenic layers of muscles and fascia planes are seen during the initial surveillance of a normal chest with the low frequency probe (fig. 2a). Ribs appear as curvilinear structures on transverse scans, associated with posterior acoustic shadowing. When the ribs are scanned longitudinally, the anterior cortex appears as a continuous echogenic line.

The visceral and parietal pleura are normally displayed by a low-frequency probe as one highly echogenic line representing the pleura and pleuropulmonary surface. With a high-resolution linear probe, the visceral and parietal pleura can be seen as two distinct echogenic lines, with the latter seemingly thinner in appearance (online suppl. video 1). The two layers can be seen to slide over each other during in- and expiration. The respiratory movement of the lung relative to the chest wall is visible with both probes and is called the 'lung sliding' sign (online suppl. video 2). Its presence on real-time US is strong evidence against the presence of a pneumothorax [7].

The normal diaphragm is best seen through the lower intercostal spaces or via the liver or the spleen. It is seen as an echogenic 1- to 2-mm-thick line which contracts with inspiration.

The 'curtain sign' describes the variable obscuring of underlying structures by air-containing tissue. In normal subjects, the curtain sign is seen in the costophrenic angle. The upper abdominal organs are easily visible on expiration, but during inspiration the normal air-filled lung is moved downwards in front of the probe and temporarily obscures the sonographic window.

The parenchyma of normal aerated lungs is invisible by means of US. The large change in acoustic impedance at the pleura-lung interface causes horizontal artefacts that are seen as a series of echogenic parallel lines equidistant from one another below the pleura. These bright but formless lines are known as reverberation artefacts and diminish in intensity with increasing distance from the pleura. Vertical 'comet-tail' artefacts, caused by fluid-filled subpleural interlobular septa, can also be seen originating at the pleura-lung interface (fig. 2b).

Chest Wall Pathology

Soft-Tissue Masses and Lymph Nodes

Soft-tissue masses arising from the chest wall can readily be detected by high-frequency US. These include abscesses, lipomas and a plethora of other (mostly benign) lesions. Masses generally have variable echogenicity and US findings are too non-specific to differentiate between various aetiologies [1, 4].

Supraclavicular and axillary lymph nodes are accessible by means of US, and US may even aid in distinguishing reactive from malignant lymph nodes [4]. An echogenic fatty hilum and oval or triangular shapes are indicative of inflammatory lymph nodes, whereas lymph nodes with malignant infiltration usually show loss of the fatty hilum leading to a hypoechoic appearance [4, 8]. Malignant nodes also appear bulky, and extracapsular spread is suggested by irregular borders [9].

Skeletal Pathology

Sonography may sometimes detect bony metastases to the ribs, which appear as hypoechoic masses replacing the normal echogenicity of a rib and leading to the disruption of the cortical line [9]. US is also reported to be more sensitive than radiography in the detection of rib fracture [10], which appears as a breach or displacement of the cortex of the rib with or without a localized swelling or haematoma.

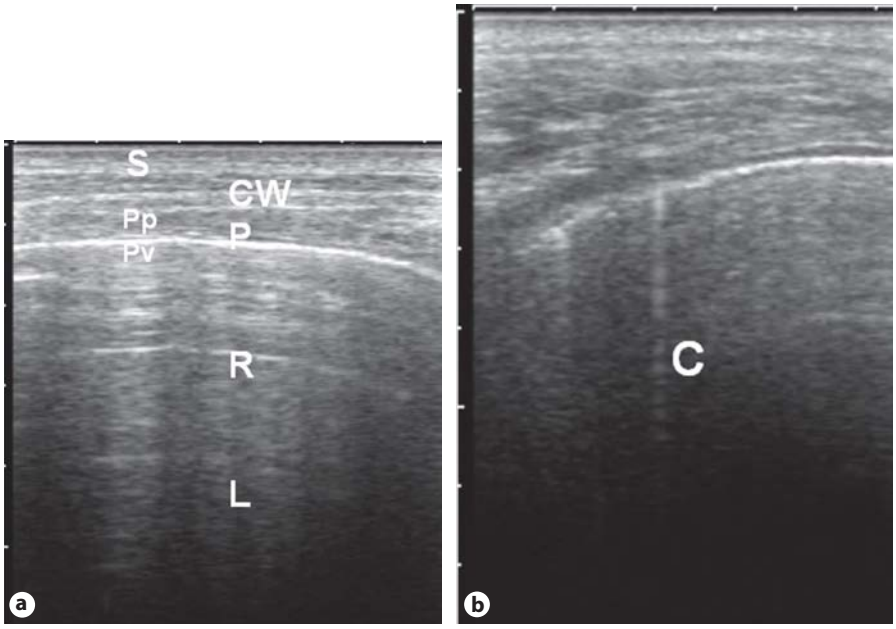

Fig. 2. **a** The typical appearance of a normal chest on US (transverse image through the intercostal space with high frequency probe). The chest wall is visualized as multiple layers of echogenicity representing muscles and fascia. The visceral and parietal pleura appear as echogenic bright lines that slide during respiration. Reverberation artefacts beneath the pleural lines imply an underlying air-filled lung. S = Skin; CW = chest wall; P = pleura; Pp = parietal pleura; Pv = visceral pleura; L = lung; R = reverberation artefact. **b** An example of a comet-tail artefact observed in an otherwise normal subject. C = Comet-tail artefact.

Diaphragmatic Abnormalities

Diaphragmatic movements are best assessed through solid upper abdominal viscera, i.e. the liver or the spleen [1]. A degree of asymmetry in the movement of the hemidiaphragms is considered normal [4]. Sonographic examination of a paralyzed diaphragm will yield paradoxical movement of the diaphragm with respiration [11]. This can be accentuated with forced inspiration ('sniff' test). Long-term paralysis causes muscle atrophy [11].

Pleural Pathology

Pleural Effusions

The value of sonography for the detection and quantification of pleural effusions remains uncontested. US is particularly useful in assessing the nature of localized or diffuse pleural opacities, and is more sensitive than decubitus expiratory films in identifying minimal or loculated effusions [12]. Sonographically, a pleural effusion appears as an anechoic, homogeneous space between parietal and visceral pleura (fig. 3). This space may change in shape with respiration, and the atelectatic lung inside a large effusion may appear as a tongue-like structure within the effusion. In inflammatory effusions, adhesions between the two pleural surfaces may result in the absence of lung motion above the effusion. If an abnormal elevation of a hemidiaphragm is noted on a chest radiograph, subpulmonary effusion can be differentiated from a subphrenic fluid collection and diaphragm paralysis [13].

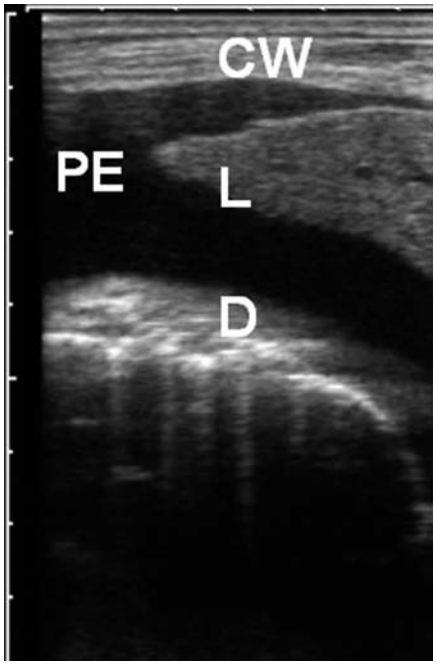

Fig. 3. A pleural effusion is presented as an echo-free space between the visceral and parietal pleura. Compressive atelectasis of the lung is seen on this high-frequency US. This is an example of an anechoic effusion. CW = Chest wall; PE = pleural effusion; L = lung; D = diaphragm.

The US appearance of a pleural effusion depends on its nature, cause and chronicity. Four appearances are recognized

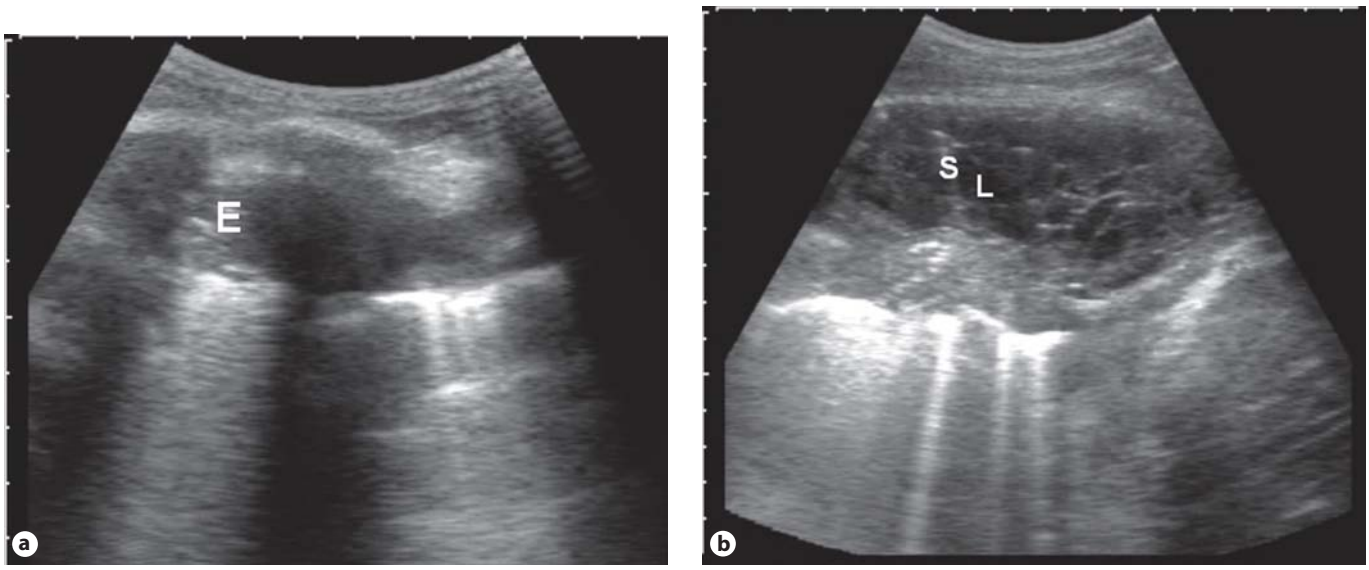

Fig. 4. More examples of pleural effusions. **a** A low-frequency US of a complex non-septated effusion showing movable echogenic shadows (E) within the effusion. **b** A low-frequency US of a complex septated effusion with thick septa (S) and loculations (L) (also see online suppl. video 3).

Video

based on the internal echogenicity: anechoic (fig. 3), complex but non-septated (fig. 4a), complex and septated (fig. 4b), and homogenously echogenic. Transudates are invariably anechoic, unseptated, and free flowing, whereas complex, septated or echogenic effusions are usually exudates [14, 15]. Malignant effusions are often anechoic. Nodular pleural thickening is apparent in the minority of malignant effusions, and echogenic swirling patterns have been linked to these effusions [16]. Inflammatory effusions are often associated with strands of echogenic material and septations (online suppl. video 3) which show more or less mobility with respiration and the cardiac cycle. The presence of septa has several implications. Chen et al. [17] demonstrated that patients with septated effusions needed longer chest tube drainage, longer hospital care, and were more likely to require fibrinolytic therapy or surgery compared with those with unseptated effusions. Tu et al. [18] confirmed some of these findings in medical intensive care unit patients.

Video

Several studies have shown reasonable correlation between the volume of an effusion estimated with planimetric measurements and its square dimensions [19–21]. Such geometric calculations are hampered by the uneven distribution of fluid in the presence of pleuropulmonary adhesions. Although not prospectively tested, we suggest the following practical way to classify the volume of an effusion: minimal, if the echo-free space is confined to the costophrenic angle; small, if the space is greater than the costophrenic angle but still within the range of the area covered with a 3.5-MHz curvilinear probe; moderate, if the space is greater than a one-probe range but within a two-probe range, and large, if the space is bigger than a two-probe range [1].

Distinguishing small effusions from pleural thickening can be challenging. Both may appear as hypoechoic on US. Furthermore, empyema may also cause a strongly echogenic effusion that may be mistaken for a solid pleural lesion. Mobility is an important sign for effusion. Marks et al. [22] found that if a lesion changed shape with respiratory excursion and if it contained movable strands or echo densities, the lesion was an effusion. If a colour Doppler is available, the fluid colour sign is the most sensitive and specific ultrasonographic evidence of a small effusion. The sign refers to the presence of a colour signal within the fluid collection that is believed to arise from transmitted motion during respiratory or cardiac cycles. This sign has a sensitivity of 89.2% and specificity of 100% in detecting minimal fluid collections [23].

Pleural Thickening

Pleural thickening can be defined as a focal lesion arising from the visceral or parietal pleura that is greater than 3 mm in width with or without an irregular margin (fig. 5). It appears as broadening of the pleura and does not exhibit a fluid colour sign or display movement relative to the chest wall (online suppl. video 4). Pleural thickening most often appears hypoechoic, but increased echogenicity with focal shadowing is sometimes observed and is indicative of calcification and chronicity.

Video

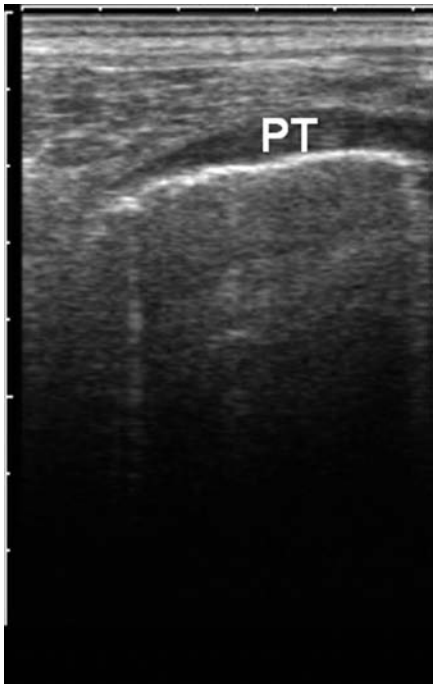

Fig. 5. Pleural thickening (PT). Note the hypoechoic appearance with distal enhancement (suggestive of chronicity). This patient was previously treated for tuberculous pleuritis (also see online suppl. video 4).

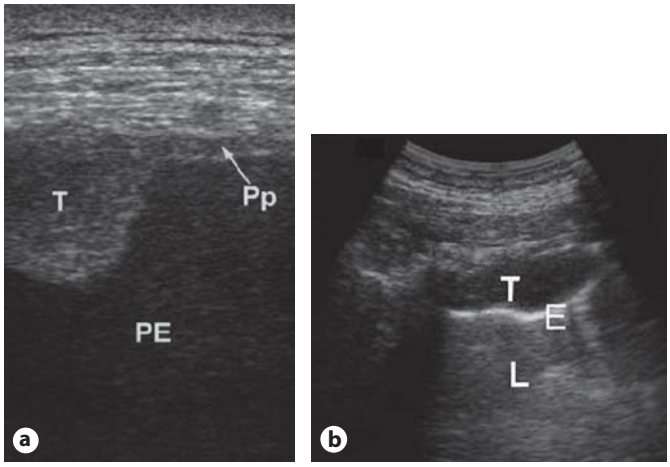

Fig. 6. Two examples of the sonographic appearance of pleural tumours, one with a large pleural effusion (**a**) and one without (**b**). Note the posterior echo enhancement (E). PE = Pleural effusion; T = pleural tumour; Pp = parietal pleura; L = lung [from 2, with permission].

Pneumothorax and Hydropneumothorax

The detection of a pneumothorax requires a higher level of skill and experience than the detection of pleural fluid. A pneumothorax (online suppl. video 5) can be diagnosed by means of the absence of normal lung sliding, exaggerated horizontal reverberation artefacts and the loss of comet-tail artefacts, provided that no diaphragmatic paralysis, prior pleurodesis, pleural adhesions or adult respiratory distress syndrome are present [24–27]. Ultrasonography is particularly useful in intensive care units and in other situations where radiographic equipment is unavailable. Herth et al. [26] showed that a pneumothorax following transbronchial biopsy can be reliably excluded with US (sensitivity 100%; specificity 83%). Soldati et al. [27] very recently found US to be superior to chest radiographs in diagnosing pneumothoraces in patients following blunt chest trauma. In their prospective study they were able to show that a rapid US performed by an experienced operator had a sensitivity of 92% (spiral CT was used as the gold standard). Only 52% of pneumothoraces in their study population were visible on routine chest radiographs.

Hydropneumothorax can also be identified with US by means of the visualization of air-fluid boundary [28], which can move with respiration. The sliding sign above the air-fluid level will be absent. The 'curtain sign' describes reverberation artefacts originating from the air within the pleura that obscures the underlying effusion during inspiration, allowing a confident diagnosis to be made.

Pleural Tumours

Benign pleural tumours are rare and appear on US as well-defined rounded masses of variable echogenicity (depending on their fat content) on either the parietal or visceral pleura. Both metastatic pleural tumours and malignant mesothelioma give rise to polypoid pleural nodules or irregular sheet-like pleural thickening [29], often with large pleural effusions (fig. 6).

Pulmonary Pathology

Neoplasms

A peripheral lung tumour will be detectable by US provided that pleural contact is present. These tumours most often appear hypoechoic with posterior acoustic enhancement [3] (fig. 7). Associated pulmonary collapse may cause fluid bronchograms. Visceral pleura or chest wall invasion has important implications for lung tumour staging (T2 or T3 staging, respectively). Although computer tomography is routinely used for determining the extent of invasion, high-resolution real-time US scanning has been found to be

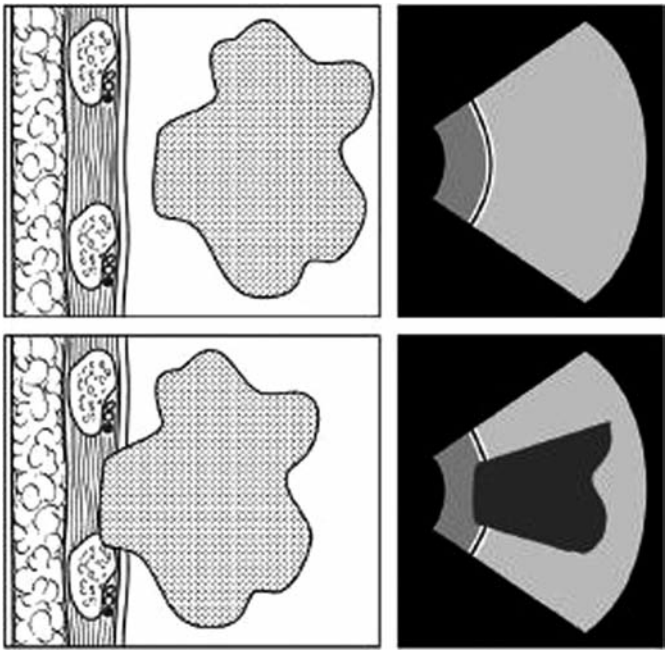

Fig. 7. A peripheral lung lesion is shown schematically without (top) and with (bottom) pleural contact. The corresponding sonar images recorded with a sector scanner are shown on the right. Only the lesion with pleural contact is visible on US. Note that the acoustic window is too narrow to demonstrate the whole circumference of the lesion, but it allows determining its full depth [from 3, with permission].

superior to routine chest CT in evaluating tumour invasion of the pleura and chest wall [30, 31]. When a tumour abutted to the chest wall is visualized with US, all layers of the chest wall, i.e. muscle, fascia, parietal pleura and visceral pleura, can be examined and the extent of tumour invasion can be accurately determined (fig. 8). Loss of movement of a visualized tumour with respiration suggests extension beyond the parietal pleura.

Colour Doppler US may aid in distinguishing malignant from benign pulmonary masses [32–34]. Almost two thirds of peripheral malignant masses will demonstrate a colour Doppler signal (low-impedance flow) due to neovascularity. A constant flow pattern correlates with malignancy, whereas a pulsatile or triphasic flow pattern is often observed in either malignant or benign masses [31]. At least one study has found that residual peripheral metastases showed diminished vascularity at colour Doppler imaging following chemotherapy [35].

Pneumonia and Lung Abscess

Apart from solid tumours, numerous pathological processes can replace the air within lung tissue and thereby become detectable with US, provided that the pleural contact is present. Pleural-based pneumonic consolidation is detectable by means of US, although the extent of disease appears smaller at US than on chest radiographs. In the early phase of consolidation, the lung appears diffusely echogenic, similar to the ultrasonographic texture of the liver. Air and fluid bronchograms appear as echogenic branches that vary with respiration. Fluid bronchograms appear as anechoic tubular structures, representing fluid-filled airways, and are typically seen in bronchial obstruction [9]. Fluid bronchograms should alert the clinician to the possibility of a postobstructive pneumonitis, secondary to a proximal tumour. US may also aid in distinguishing a central obstructive tumour (usually hypoechoic) from distal consolidation (more echogenic) [36]. Sonographically observed consolidation is not synonymous with infective pneumonia. Pulmonary infarction, haemorrhage and bronchoalveolar carcinoma are examples of noninfective causes of consolidations that are similar in appearance on US. US may guide transthoracic needle aspirations or biopsies of peripheral pulmonary infiltrates in cases with diagnostic uncertainty regarding the aetiology [37, 38].

A lung abscess abutting the pleura appears as a hypoechoic lesion with a well-defined or irregular wall (fig. 9) [38]. The centre of the abscess is most often anechoic, but may reveal septations and internal echoes. Abscesses containing air fluid levels are more inhomogeneous.

Pulmonary Oedema and other Alveolar-Interstitial Syndromes

In the setting of patients with acute dyspnoea it has been reported that the presence of bilateral, widespread comet-tail artefacts (fig. 10) is a reliable sign to differentiate patients with pulmonary oedema from those with chronic obstructive airway disease [39]. Lichtenstein et al. [40] reported that comet-tail artefacts were absent in 92% of patients with chronic obstructive airway disease, but detectable in 93% of patients with alveolar-interstitial syndromes.

Pulmonary Embolism

US can aid in the acute bedside assessment of patients presenting with possible pulmonary embolism [41]. Pulmonary infarction is recognized as a peripheral wedge-shaped hypoechoic region, often accompanied by a pleural effusion [42–44]. A central hyperechoic bronchiole and a congested pulmonary vessel can sometimes be

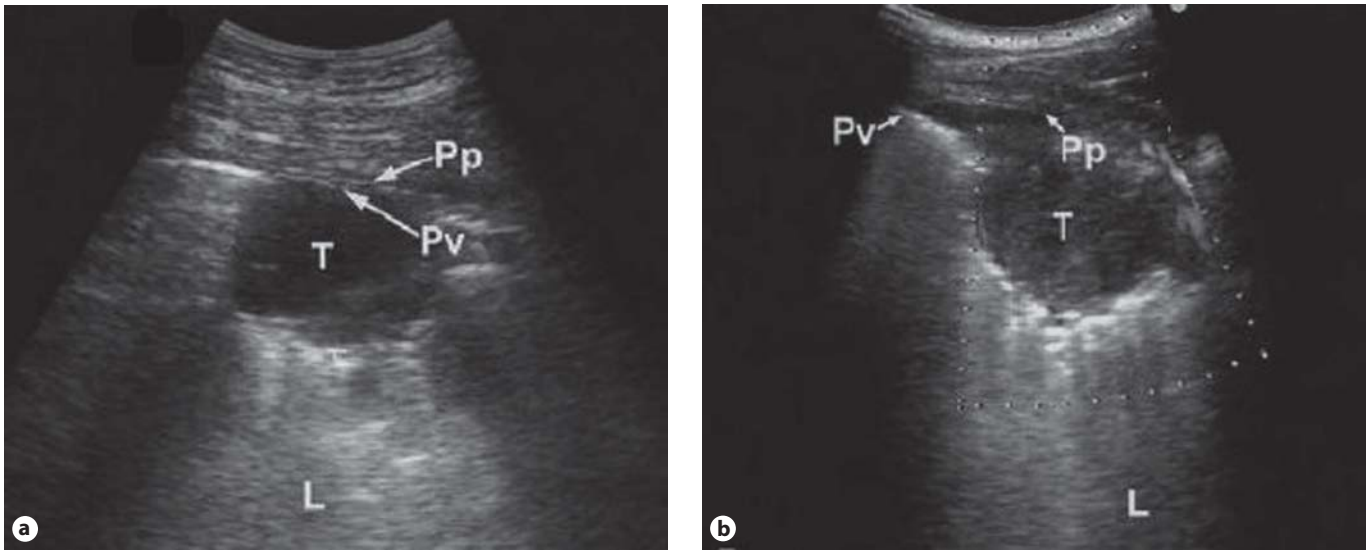

Fig. 8. **a** An US image showing a lung tumour with posterior echo enhancement. Note that both the visceral as well as the parietal pleural lines are intact. **b** This US shows tumour extension beyond the pleura. The visceral pleural line is interrupted, and the respiratory movement of the tumour is disturbed in real-time US. Invasion of the pleural cavity by the tumour is evident. L = Lung; T = tumour; Pv = visceral pleura; Pp = parietal pleura [from 2, with permission].

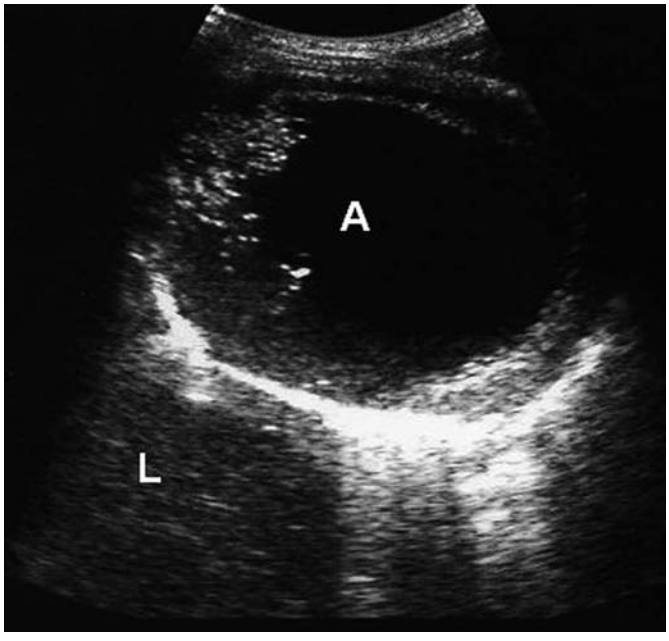

Fig. 9. A peripheral lung abscess. Note the hypoechoic centre and irregular wall. A = Abscess cavity; L = lung.

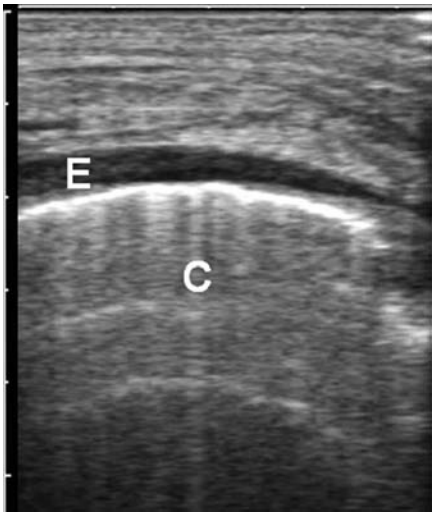

Fig. 10. A high-frequency US of a patient with pulmonary oedema showing widespread pronounced comet-tail artefacts (a reliable signs of interstitial pulmonary oedema). C = Comet-tail artefacts; E = pleural effusion.

observed [4]. The extent of pulmonary infarction is invariably underappreciated at US, as is the case for pneumonic consolidation. US is also useful in detecting the sequelae of thromboembolic disease such as right ventricular overload and dilated hepatic veins. In experienced hands, thoracic US has a sensitivity of 77–89% and specificity of 66–83% for pulmonary embolism [42–44]. However, sonographic detection of pulmonary emboli is currently still reserved for physicians with an interest in US, as pulmonary spiral CT angiography remains the investigation of choice.

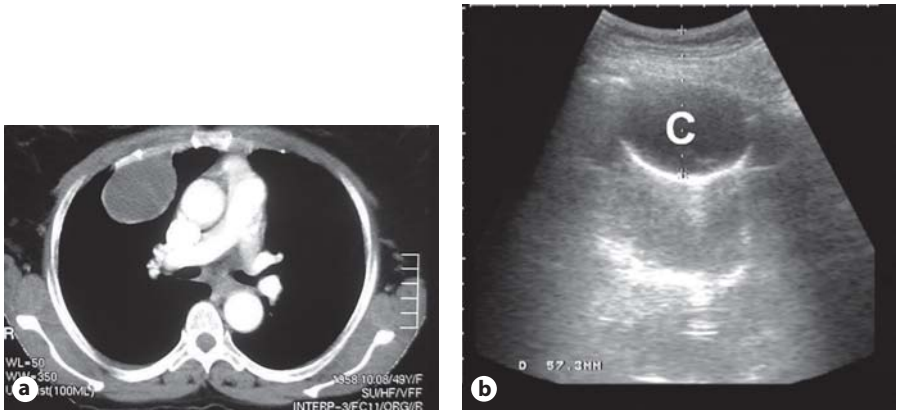

Fig. 11. This patient presented with a suspected hydatid cyst. Her CT chest showed cystic mass (pleural based) (**a**), and a FNA was safely performed with the assistance of low-frequency US (**b**). C = Cyst.

Other Pulmonary Pathology

Pleural-based cysts (e.g. echinococcus cysts) can be visualized as large anechoic (round) lesions (fig. 11). Pulmonary arteriovenous malformations may also be seen at US as these congenital abnormalities are often peripheral. Arteriovenous malformations appear as distinct hypoechoic lesions with posterior acoustic enhancement [45]. Lesions show high vascularity on Doppler with low-impedance flow.

Rounded atelectasis may give rise to a pleural-based mass with associated pleural thickening and extrapleural fat. The invaginated pleura may be seen as an echogenic line running from the pleura into the mass [46].

US-Guided Interventions

Principles

US is ideal for guiding chest wall, pleural and peripheral pulmonary interventions, including diagnostic thoracentesis, closed tube drainage, chest wall and pleural biopsies and biopsies of lung tumours abutting or invading the pleura. The use of US increases the success rate and minimises risk compared to blind procedures [1].

Specific reusable probes for real-time US guidance of needle biopsies are commercially available. Many experienced physicians, however, prefer the so-called 'freehand' technique. Following adequate patient positioning, the intended site of needle insertion is sonographically identified and marked, while the direction, the depth of interest and the safety range for the procedure are determined and memorized [1] (online suppl. video 6). It is essential that the subject must not change position in order to prevent a shift of the area of interest relative to the skin mark. It is occasionally even necessary to ask the patient to hold his breath for the duration of the aspiration. The practice of identifying a puncture site at a radiology department prior to transporting a patient elsewhere for thoracentesis should be discouraged, particularly in the case of small effusions, as both the fluid collection and the skin mark might shift considerably with minor changes in body position.

Video

Chest Wall Biopsy

Soft-tissue masses of indeterminate aetiology may be sampled by means of US-assisted fine needle aspirations (FNA) or biopsies [4]. US-guided procedures may also be used to detect chest wall invasion by pulmonary tumours. High-resolution US is superior to routine chest CT in evaluating tumour invasion of the pleura and chest wall [30, 31], and Nakano et al. [47] have even suggested US-assisted cutting needle biopsy (CNB) of the chest wall for the preoperative assessment of chest wall invasion by pulmonary neoplasms (specificity: 100%, diagnostic accuracy: 83%).

Pleural Fluid Aspiration

US is superior to chest radiographs for the documentation of the optimal site for diagnostic thoracentesis [48]. The most accessible area of fluid accumulation can be identified, and an aspiration can easily be performed by means of the 'freehand' technique (online suppl. video 7). The success rate of US-guided thoracentesis can be as high as 97% [49]. US-guided thoracocentesis improves the diagnostic yield and decreases the risk of complications in all patients, but is particularly helpful when a safe procedure is mandatory, e.g. in patients with bleeding diathesis.

Video

Intercostal Tube Drainage

Ultrasonography is ideal for identifying the optimal site for safe and effective pleural drainage (fig. 12). This is particu-

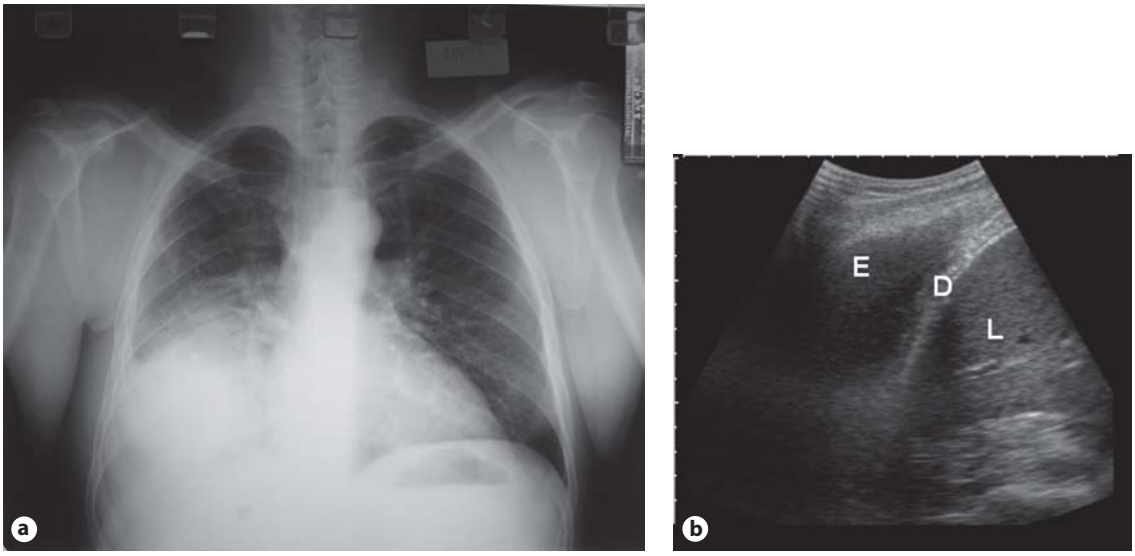

Fig. 12. A low-frequency US was used to guide a diagnostic aspiration and the insertion of an intercostal drain in this patient with empyema. **a** His chest radiograph was suggestive of a large loculated right-sided effusion. **b** US confirmed this, but also revealed a raised right hemidiaphragm. An optimal site for the aspiration and drain insertion was subsequently identified. E = Effusion; D = diaphragm; L = liver.

larly relevant in patients in an ICU setting and with loculated parapneumonic effusions, where thickened parietal pleura, adhesions or loculations often complicate insertion. Depending on operator experience, US may also guide further decisions regarding the need for subsequent intrapleural fibrinolytics, thoracoscopy or for surgical intervention in addition to tube drainage and antibiotics [50].

US-guided drains are most frequently inserted by means of the 'freehand' technique. As an alternative, effusions may also be accessed by means of an 18- or 16-gauge needle under direct (real-time) US visualization. This allows direct fluid aspiration followed by an insertion of a guide wire, which is used to guide dilatation of a tract and deployment of a small-bore catheter (8–14 french). These tubes are better tolerated than large bore (20–24 french) intercostal drains [51], although common sense suggests that smaller bore drains are more likely to fail in the presence of pus with a high viscosity. Some prospective studies have found that 8- to 12-french pigtail catheters or 10- to 14-french catheters inserted with the Seldinger technique under US or CT guidance were at least as effective as larger catheters inserted without imaging [51–53]. However, the positioning of the catheter tips with guidance is likely to be superior compared to a blind insertion, irrespective of drain size. Most of these studies also employed a strict rinsing schedule (often several times a day), which might be difficult to sustain in everyday clinical practice. Moreover, a recent study found a failure rate of 19% with small-bore catheters and concluded that the threshold for using fibrinolytics and large-bore catheters should be low in empyema [54].

Closed Pleural Biopsies

US is an extremely helpful guide for biopsies of the pleura. Focal pleural abnormalities can be identified with US, and biopsy can be aimed at areas of interest. Measuring the size of an associated effusion decreases the risk of visceral lacerations, which is particularly relevant in cases with small pleural effusion [1].

Closed pleural biopsies (e.g. with the Abrams needle) could conventionally only be performed in the presence of a sizeable pleural effusion or pneumothorax visible on chest radiography. Ultrasonography, however, can demonstrate small fluid collections and facilitate the use of devices that were not primarily designed for pleural biopsies in the absence of an effusion. Numerous studies have shown that US-assisted Tru-Cut needle biopsies have higher sensitivity and specificity in the diagnosis of pleural malignancy than unaided Abrams needle biopsies [55–59]. Chang et al. [55] found a sensitivity of up to 86% for pleural malignancies or tuberculosis, whereas Helio et al. [56] showed that US-assisted biopsies had a sensitivity of 77% and a positive predictive value of 100% for malignant mesothelioma. Diacon

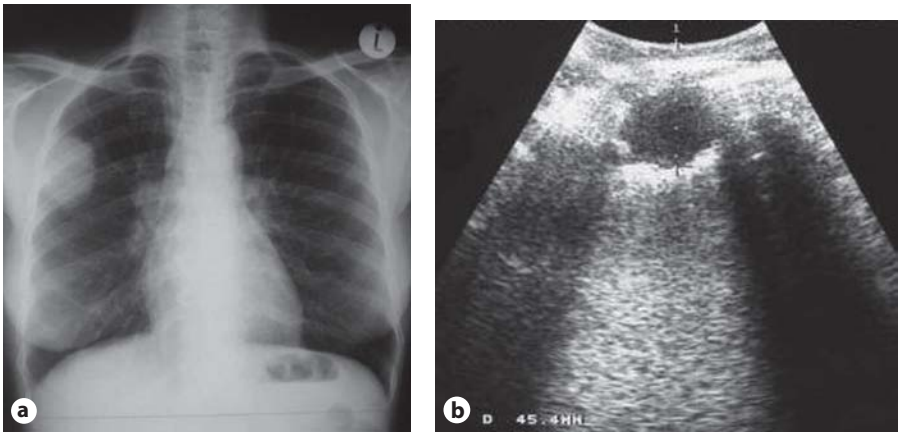

Fig. 13. An example of a case suitable for US-guided fine-needle aspiration and/or biopsy. **a** The chest radiograph showed a lesion in the peripheral right mid lung field. **b** The corresponding sonar image shows that good transthoracic access to the tumour is provided. An US-guided FNA and biopsy confirmed small cell lung cancer [from 3, with permission].

et al. [59] found that US-assisted biopsies had a sensitivity and specificity of 100% for mesothelioma provided the tumours were greater than 3 cm in diameter.

Transthoracic FNA and Needle Biopsies of Solid Tumours

Transthoracic FNA (TTFNA) and needle biopsies of solid tumours by means of US-assisted FNA or cutting biopsy performed under local anaesthesia and by non-radiologists are safe procedures and have high diagnostic yields [59]. Peripheral lung tumours that either abut or invade the pleura or chest wall and anterior mediastinal masses are ideally suited for these procedures (fig. 13). No aerated lung needs to be transversed with the biopsy device, and the risk of pneumothorax is therefore low. Furthermore, US-assisted biopsies can be readily performed outside a theatre, which offers advantages in immobile patients with advanced disease. TTFNA are performed under local anaesthesia, preferably with a 22-gauge injection-type or spinal needle (online suppl. video 8). CNB follow the same principles as TTFNA, but such devices are more invasive and carry the risk of vascular trauma if the anatomical locations of subclavian, brachial, intercostal and mammarian arteries are not respected.

Video

A prospective study by Diacon et al. [59] found that TTFNA and closed needle biopsies performed by pulmonologists corresponded well in the diagnosis of epithelial lung carcinoma and in the distinction of small cell and non-small cell bronchogenic carcinoma. They were able to show that US-guided 'free-hand' CNB of lung tumours abutting the chest wall had a diagnostic sensitivity of 85.5%. The same investigators also found that US-assisted TTFNA with rapid on-site evaluation by a cytopathologist of tumours abutting the chest wall were diagnostic in 82% [60]. Subanalyses of their data proved that US-guided TTFNA, compared to CNB, had a superior yield for bronchial carcinoma whereas CNB was superior in the minority of cases with non-carcinomatous tumours and non-malignant lesions [60]. CNB should therefore be performed in all cases where cytology is non-contributory and in cases where a diagnosis other than lung cancer is suspected. Both US-guided CNB and FNA had a low complication rate, with pneumothoraces observed in 4 and 1.3%, respectively [60].

US is not only used to assist transthoracic procedures, but also to exclude a pneumothorax post-TTFNA or biopsy. If the lesion remains visible and unchanged in location, shape and size, it implies that no free air is present between the sampled lesion and the visceral pleura, and that a clinically relevant pneumothorax is unlikely [1, 3].

TTFNA and/or Needle Biopsies of Diffuse Parenchymal Infiltrates, Consolidations and Lung Abscesses

The indications for US-assisted TTFNA and biopsies are not limited to solid tumours but can be helpful in other aetiologies of lung consolidation. Yang et al. [37] reported a diagnostic yield of as high as 93% with US-assisted biopsies of pulmonary consolidation of unknown aetiology. This procedure is particularly useful in the immunocompromised patient, given the extensive differential diagnosis. The same author was able to sonographically demonstrate abscess cavities in 94% of 35 patients with radiologically confirmed lung abscesses [61]. At US, lung abscesses were depicted as hypoechoic lesions with irregular outer margins and an abscess cavity that was manifested as a hyperechoic ring. More than 90% of all aspirates of these abscesses yielded pathogens, whereas less than 10% of patients had positive blood cultures.

Conclusion

The value of US for chest physicians is firmly established. Basic thoracic ultrasonography is an elegant and inexpensive investigation that extends the physicians' diagnostic and interventional potential at the bedside in peripheral lung, pleural, and chest wall disease. It has the potential to replace CT-guided FNA or biopsies of all lesions involving the pleura and chest wall as well as lung masses or consolidations abutting the pleura. Academic institutions should strive to have a basic training program in thoracic ultrasonography in place in order to ensure that all aspiring chest physicians are familiar with the basic aspects of chest ultrasonography.

References

1 Koegelenberg CF, Bolliger CT, Diacon AH: Pleural ultrasound; in Light RW, Lee YC (eds): Textbook of Pleural Disease, ed 2. London, Hodder & Stoughton, 2008, pp 271–283.
2 Tsai TH, Yang PC: Ultrasound in the diagnosis and management of pleural disease. Curr Opin Pulm Med 2003;9:282–290.
3 Diacon AH, Theron J, Bolliger CT: Transthoracic ultrasound for the pulmonologist. Curr Opin Pulm Med 2005;11:307–312.
4 Koh DM, Burke S, Davies N, Padley SP: Transthoracic US of the chest: clinical uses and applications. Radiographics 2002;22:E1. http://radiographics.rsnjnls.org/cgi/content/full/22/1/e1.
5 Mayo PH, Doelken P: Pleural ultrasonography. Clin Chest Med 2006;27:215–217.
6 Evans AL, Gleeson FV: Radiology in pleural disease: state of the art. Respirology 2004;9:300–312.
7 Lichtenstein DA, Menu Y: A bedside ultrasound sign ruling out pneumothorax in the critically ill. Chest 1995;108:1345–1348.
8 Bruneton JN, Caramella E, Hery M: Axillary lymph node metastases in breast cancer: preoperative detection with US. Radiology 1986;158:325–326.
9 Mathis G: Thoraxsonography. I. Chest and pleura. Ultrasound Med Biol 1997;23:1131–1139.
10 Bitschnau R, Gehmacher O, Kopf A, Scheier M, Mathis G: Ultrasound in the diagnosis of rib and sternal fracture. Ultraschall Med 1997;18:158–161.
11 Gottesman E, McCool MD: Ultrasound evaluation of the paralyzed diaphragm. Am J Respir Crit Care Med 1997;155:1570–1574.
12 Kocijancic I, Kocijancic K, Cufer T: Imaging of pleural fluid in healthy individuals. Clin Radiol 2004;59:826–829.
13 Ko JC, Yang PC, Chang DB: Ultrasonographic evaluation of peridiaphragmatic lesions: a prospective study. J Med Ultrasound 1994;2:84–92.
14 Yang PC, Luh KT, Chang DB: Value of sonography in determining the nature of pleural effusion: analysis of 320 cases. AJR Am J Roentgenol 1992;159:29–33.
15 Hirsch JH, Rogers JV, Mack LA: Real-time sonography of pleural opacities. AJR Am J Roentgenol 1981;136:297–301.
16 Chian CF, Su WL, Soh LH, et al: Echogenic swirling pattern as a predictor of malignant pleural effusions in patients with malignancies. Chest 2004;126:129–134.
17 Chen KY, Liaw YS, Wang HC, et al: Sonographic septation: a useful prognostic indicator of acute thoracic empyema. J Ultrasound Med 2000;19:837–843.
18 Tu CY, Hsu WH, Hsia TC, et al: Pleural effusions in febrile medical ICU patients: chest ultrasound study. Chest 2004;126:1274–1280.
19 Eibenberger KL, Dock WI, Ammann ME, et al: Quantification of pleural effusions: sonography versus radiography. Radiology 1994;191:681–684.
20 Lorenz J, Borner N, Nikolaus HP: Sonographic volumetry of pleural effusions. Ultraschall Med 1988;9:212–215.
21 Balik M, Plasil P, Waldauf P, et al: Ultrasound estimation of volume of pleural fluid in mechanically ventilated patients. Intensive Care Med 2006;32:318–321.
22 Marks WM, Filly RA, Callen PW: Real-time evaluation of pleural lesions: new observations regarding the probability of obtaining free fluid. Radiology 1982;142:163–164.
23 Wu RG, Yang PC, Kuo SH, Luh KT: 'Fluid color' sign: a useful indicator for discrimination between pleural thickening and pleural effusion. J Ultrasound Med 1995;14:767–769.
24 Chan SS: Emergency bedside ultrasound to detect pneumothorax. Acad Emerg Med 2003;10:91–94.
25 Chan SS: The comet tail artefact in the diagnosis of pneumothorax. J Ultrasound Med 2002;21:1060.
26 Herth FJ, Eberhardt R, Ernst A, et al: Diagnosis of pneumothorax by means of transthoracic ultrasound: a prospective trial. Eur Respir J 2004;24:S491.
27 Soldati G, Testa A, Sher S, Pignataro G, La Sala M, Silveri NG: Occult traumatic pneumothorax: diagnostic accuracy of lung ultrasonography in the emergency department. Chest 2008;133:204–211.
28 Targhetta R, Bourgeois JM, Chavagneux R, et al: Ultrasonographic approach to diagnosing hydropneumothorax. Chest 1992;101:931–934.
29 Gorg C, Restrepo I, Schwerk WB: Sonography of malignant pleural effusion. Eur Radiol 1997;7:1195–1198.
30 Sugama Y, Tamaki S, Kitamura S, et al: Ultrasonographic evaluation of pleural and chest wall invasion of lung cancer. Chest 1988;93:275–279.
31 Suzuki N, Saitoh T, Kitamura S: Tumor invasion of the chest wall in lung cancer: diagnosis with US. Radiology 1993;187:39–42.
32 Yuan A, Chang DB, Yu CJ, Kuo SH, Luh KT, Yang PC: Color Doppler sonography of benign and malignant pulmonary masses. AJR Am J Roentgenol 1994;163:545–549.
33 Hsu WH, Ikezoe J, Chen CY: Color Doppler ultrasound signals of thoracic lesions: correlation with resected histological specimens. Am J Respir Crit Care Med 1996;153:1938–1951.
34 Hsu WH, Chiang CD, Chen CY: Color Doppler ultrasound pulsatile flow signals of thoracic lesions: comparison of lung cancers and benign lesions. Ultrasound Med Biol 1998;24:1087–1095.
35 Liae YS, Yang PC, Yuan A: Ultrasonography and color Doppler imaging of metastatic pulmonary choriocarcinoma. Chest 1993;104:1600–1601.
36 Yang PC, Lee YC, Wu HD, Luh KT: Lung tumors associated with obstructive pneumonitis: US studies. Radiology 1990;174:717–720.
37 Yang PC, Chang DB, Yu CJ, Lee YC, Kuo SH, Luh KT: Ultrasound guided percutaneous cutting biopsy for the diagnosis of pulmonary consolidations of unknown aetiology. Thorax 1992;47:457–460.
38 Yang PC: Ultrasound-guided transthoracic biopsy of peripheral lung, pleural, and chest wall lesions. J Thorac Imaging 1997;12:272–284.
39 Lichtenstein D, Mézière G: A lung ultrasound sign allowing bedside distinction between pulmonary edema and COPD: the comet-tail artifact. Intensive Care Med 1998;24:1331–1334.
40 Lichtenstein D, Mézière G, Biderman P, Gepner A, Barré O: The comet-tail artifact: an ultrasound sign of alveolar-interstitial syndrome. Am J Respir Crit Care Med 1997;156:1640–1646.

41 Reissig A, Kroegel C: Transthoracic ultrasound of lung and pleura in the diagnosis of pulmonary embolism: a novel non-invasive bedside approach. Respiration 2003;70:441–452.
42 Mathis G, Metzler J, Fubenegger D: Sonographic observation of pulmonary infarction and early infarctions by pulmonary embolism. Eur Heart J 1993;14:804–808.
43 Mathis G: Ultrasound diagnosis of pulmonary embolism. Eur J Ultrasound 1996;3:153–160.
44 Lechleitner P, Raneburger W, Gamper G, Riedl B, Benedikt E, Theurl A: Lung sonographic findings in patients with suspected pulmonary embolism. Ultraschall Med 1998;19:78–82.
45 Wang HC, Kuo PH, Liaw YS: Diagnosis of pulmonary arteriovenous malformations by color Doppler ultrasound and amplitude ultrasound angiography. Thorax 1998;53:372–376.
46 Marchbank MD, Wilson AG, Joseph AE: Ultrasound features of folded lung. Clin Radiol 1996;51:433–437.
47 Nakano N, Yasumitsu T, Kotake Y, Morino H, Ikezoe J: Preoperative histological diagnosis of chest wall invasion by lung cancer using ultrasonically guided biopsy. J Thorac Cardiovasc Surg 1994;107:891–895.
48 Diacon AH, Brutsche MH, Soler M: Accuracy of pleural puncture sites: a prospective comparison of clinical examination with ultrasound. Chest 2003;123:436–441.
49 Yang PC, Kuo SH, Luh KT: Ultrasonography and ultrasound-guided needle biopsy of chest diseases: indications, techniques, diagnostic yields and complications. J Med Ultrasound 1993;1:53–63.
50 Chen KY, Liaw YS, Wang HC: Sonographic septation: a useful prognostic indicator of acute thoracic empyema. J Ultrasound Med 2000;19:837–843.
51 Tatersall DJ, Traill ZC, Gleeson FV: Chest drains: does size matter? Clin Radiol 2000;55:415–421.
52 Shankar S, Gulati M, Kang M, Gupta S, Suri S: Image-guided percutaneous drainage of thoracic empyema: can sonography predict the outcome? Eur Radiol 2000;10:495–499.
53 Ali I, Unruh H: Management of empyema thoracis. Ann Thorac Surg 1990;50:355–359.
54 Keeling AN, Leong S, Logan PM, Lee MJ: Empyema and effusion: outcome of image-guided small-bore catheter drainage. Cardiovasc Intervent Radiol 2008;31:135–141.
55 Chang DB, Yang PC, Luh KT, Kuo SH, Yu CJ: Ultrasound guided pleural biopsy with Tru-cut needle. Chest 1991;100:1328–1333.
56 Heilo A, Stenwig AE, Solheim OP: Malignant pleural mesothelioma: US-guided histologic core needle biopsy. Radiology 1999;211:657–659.
57 McLeod DT, Ternouth I, Nkanza N: Comparison of the Tru-cut biopsy needle with the Abrams punch for pleural biopsy. Thorax 1989;44:794–796.
58 Theron J, Diacon AH, Williams Z, Walzl G, Bolliger CT: Abrams versus TruCut needle in tuberculous pleuritis: a pilot study. Eur Respir J 2004;24:73s.
59 Diacon AH, Schuurmans MM, Theron J: Safety and yield of ultrasound assisted transthoracic biopsy performed by pulmonologists. Respiration 2004;71:519–522.
60 Diacon AH, Theron J, Schubert P: Ultrasound-assisted transthoracic biopsy: fine-needle aspiration or cutting-needle biopsy? Eur Respir J 2007;29:357–362.
61 Yang PC, Luh KT, Lee YC: Lung abscesses: US examination and US-guided transthoracic aspiration. Radiology 1991;180:171–175.

Dr. Coenraad F.N. Koegelenberg
Division of Pulmonology, Department of Medicine, University of Stellenbosch and Tygerberg Academic Hospital
PO Box 19063
Tygerberg 7505, Cape Town (South Africa)
Tel. +27 21 938 9423, Fax +27 21 933 3591, E-Mail coeniefn@sun.ac.za

Chapter 4

Bolliger CT, Herth FJF, Mayo PH, Miyazawa T, Beamis JF (eds): Clinical Chest Ultrasound: From the ICU to the Bronchoscopy Suite.
Prog Respir Res. Basel, Karger, 2009, vol 37, pp 34–42

Ultrasound of the Neck

Michael Kreuter[a] · Stefan Delorme[b] · Andreas Schuler[c] · Felix J.F. Herth[a]

[a]Department of Pneumology and Respiratory Critical Care Medicine, Thoraxklinik, University of Heidelberg and [b]Department of Radiology, German Cancer Research Centre, Heidelberg, and [c]Department of Internal Medicine, Helfensteinklinik, Geislingen, Germany

Abstract

Ultrasound is a highly valuable method for investigating organs and lesions of the head and neck region. Several diseases have a typical sonographic appearance, such as cysts, neurogenic tumors, or hemangiomas. However, the most common indication for sonography of this region is staging of cancer, supplemented by guided biopsy of suspicious lesions. In pneumology, ultrasound may be used in the assessment of lymph nodes for evaluation of sarcoidosis, tuberculosis and the staging of lung cancer.

Indications for Neck Ultrasound and Sonographic Technique

There are several indications for ultrasound of the neck:

- Local symptoms, such as pain, or local swelling or palpable tumors
- Dyspnea or signs of upper inflow congestion
- Abnormal thyroid or parathyroid function tests
- Staging and follow-up of lymphomas or solid tumors of the head and neck, lung, breast, or skin
- Sonographic guidance of biopsies of solid lesions

Scanning of the neck should be performed with transducers with a frequency of at least 5 MHz, preferably as high as 13 MHz. Generally, linear transducers with a width of 4 cm are used. However, in the parotid region or the floor of the mouth, where the access window is limited, curved array transducers or sector scanners may be helpful. Tissue harmonic imaging improves the contrast and reduces artifacts. Color Doppler can visualize vascularization of soft tissue lesions, may help differentiate thyroid gland diseases and is employed for evaluation of vascular disease, e.g. thrombosis or arteriosclerosis. The patient is placed in a supine position with the head turned slightly to the contralateral side. All parts of the posterior cervical triangle, the supraclavicular fossae, the perivascular space, the thyroid and the great salivary glands should be evaluated at least in two orthogonal sections [1, 2].

Lymph Nodes of the Neck

The strength of ultrasound is its potential to examine shape, margins, internal structure and abnormal vascularity of lymph nodes. Typically, they are oval with an outer hypoechoic parenchyma and an inner hyperechoic hilum, which represents a dense network of lymphatic cords and sinuses. With increasing age, fatty replacement resulting in node enlargement or degeneration is observed. Notably, the relation between echo-poor rim and hyperechogenic center depends on the region. Whereas in cervical lymph nodes the echogenic center may be thin or even hardly visible, it occupies almost the entire lymph node in the axilla or the groins. Vascularity is low and mainly perceived in the hilum, depending on the sensitivity of the unit and possible inflammatory changes (which are often asymptomatic). If visible, vessels are almost always arranged in a 'tree-like' fashion, originating from the hilum. Normal cervical lymph nodes are often detected in the submandibular, parotid, upper cervical regions and the posterior triangle (fig. 1) [2].

Cervical Lymphadenitis and Inflammatory Lymph Nodes

Cervical lymphadenitis is defined as enlarged, inflamed, and tender lymph node(s) of the neck resulting from an

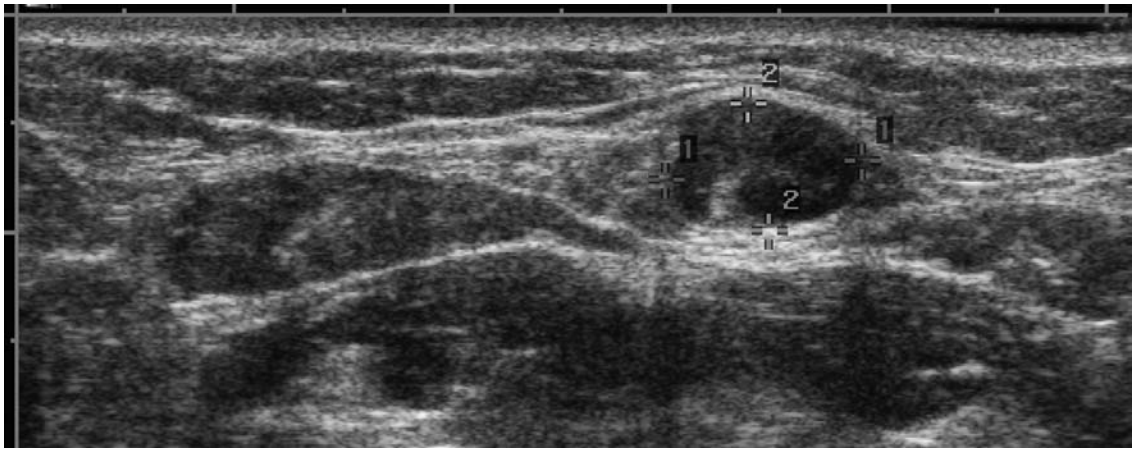

Fig. 1. Reactive submental lymph node. Note the subtle but distinct inner hyperechoic hilum.

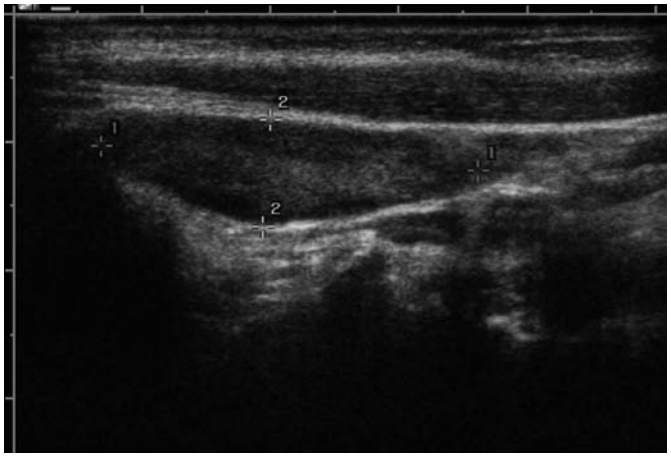

Fig. 2. Reactive lymph node of a noncancer patient. Besides the tender oval form the reduced echogenicity is striking, caused by hyperplastic follicles, thereby indicating benignancy.

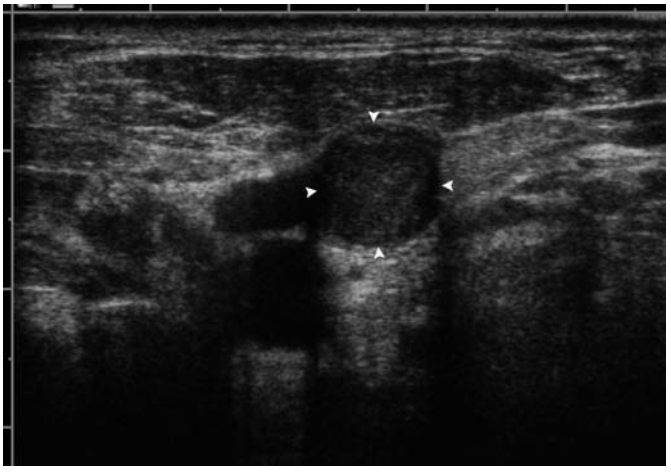

Fig. 3. Lymph node metastasis of a squamous cell carcinoma with inhomogeneous structure which is partially echo-rich.

infection in the head and neck region such as tonsillitis or pharyngitis, for example. By ultrasound, multiple enlarged, tender oval masses with reduced echogenicity and increased, branching vascularity can be detected. Necrosis of a lymph node shows a hypo- or anechoic center within a lymph node [1, 3, 4]. When scanning conditions are good, high-resolution ultrasound may disclose multiple, ill-defined or confluent, hypoechogenic spots along the periphery of the lymph node. These are neither necrosis nor signs of malignant involvement but hyperplastic follicles and thereby indicate that this node is rather benign (fig. 2).

Lymph Node Metastases

Most lymph node metastases are due to squamous cell carcinomas of the head and neck. Routine ultrasound evaluation of supraclavicular fossa may also be indicated for staging patients with lung cancer, who may have metastases in this region in advanced stages of their disease [5].

Typical features of cervical lymph node metastases are [1, 6, 7]:

- Round shape
- Inhomogeneous structure (fig. 3)
- Anechoic areas representing necrosis (fig. 4)
- Loss of the echogenic hilum (which as an isolated finding is unreliable, since the hilum may be only faint in normal lymph nodes)
- Unsharp borders and the invasion of surrounding structures

The roundness index (Solbiati index), which is the ratio of the longitudinal to transverse diameter, may help differentiate

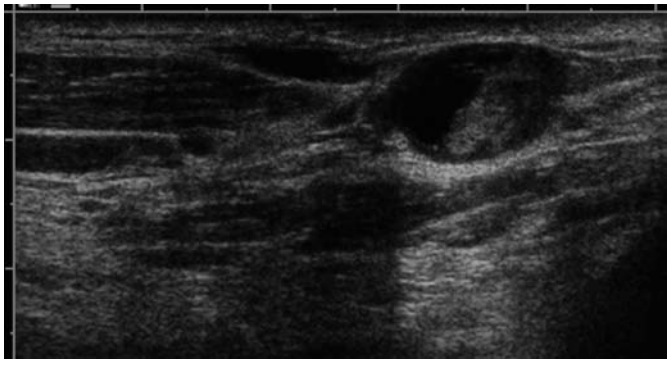

Fig. 4. Metastasis of a chordoma of the craniocervical junction. The metastasis shows an anechoic area representing necrosis.

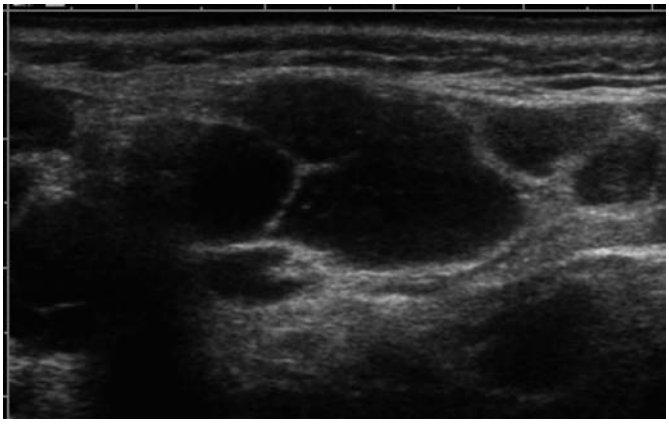

Fig. 5. A typical lymph node conglomerate of an aggressive lymphoma with several lymph nodes of low echogenicity. The sonographic examination shows the facet formation with lymph nodes abutting each other.

between inflammatory to metastatic lymph nodes. An index greater than 2 indicates inflammation in 84% while an index less than 1.5 implies malignancy in 71% [8]. Besides the above-mentioned grayscale criteria for malignant lymph nodes, also the use of color Doppler may help identify metastatic lymph nodes. According to Tschammler et al. [9] the following criteria might be used: a perfusion defect (which is only reliable if it can be discriminated from other, well-perfused parts of the same lymph node), subcapsular, peripheral vessels and vessel displacement as well as aberrant vessels. A chaotic network of vessels in a lymph node is suggestive of malignancy. Controversy exists regarding vascular resistance parameters. Peripheral vascular indices such as the resistivity index and the pulsatility index are based on flow velocities or Doppler frequency shifts derived from the Doppler spectrum and are independent of Doppler angle. Generally these indices are calculated using the maximum velocity/frequency envelope of the Doppler spectrum. A high resistivity index ($>$0.8) and pulsatility index ($>$1.5) were reported to be associated with malignancy while lower values may be found in inflammatory lymph nodes; however, several authors could not reproduce this association. Notably, these results were obtained in lymph nodes in which, according to their appearance in B-mode (size, shape), there was little doubt that they would be metastatic. Debate also exists on the role of contrast agents for the identification of malignant lymph nodes [2].

Lymphoma

In lymphoma, typically, several lymph nodes of one lymph node group are involved, frequently as lymph node conglomerates. Sonographic examination may show a facet formation because the lymph nodes abut each other. Their shape is round to spherical and they are mostly sharply delineated. Echogenicity is low and posterior acoustic enhancement may be found. Color Doppler reveals well-structured hypervascularity which is similar to inflammatory nodes [1, 2]. It may, therefore, be difficult to discriminate between lymphoma and reactive lymph nodes, but still ultrasound – at least of superficial lymph nodes – is more valid than are CT or MRI (fig. 5).

Sarcoidosis and Tuberculosis

Sarcoidosis, a multisystem granulomatous disorder of unknown origin, commonly affects the lung and intrathoracic lymph nodes. If peripheral lymph node enlargement is found, those of the head and neck region are regularly involved. However, ultrasound cannot differentiate between lymphoma and sarcoidosis. Further manifestations of sarcoidosis in the head and neck region are granulomatous inflammation of salivary and parotid glands. The ultrasound features of sarcoidosis in the glands are nonspecific. They may range from multiple hypoechoic foci to diffuse hypoechoic glandular enlargement and glands may be hypervascular on color Doppler flow studies (fig. 6) [1, 10, 11].

Sonographic features typical for lymph node tuberculosis are multiple, enlarged, conglomerating roundish and oval lymph nodes. They are hypoechoic, exhibit dorsal sound amplification and have sharp margins. With caseation, however, there may be blurred borders. As there is a trend for fistulas, hypoechogenic tracts might be visible. In the course of the disease, calcification can be found within the lymph nodes [12].

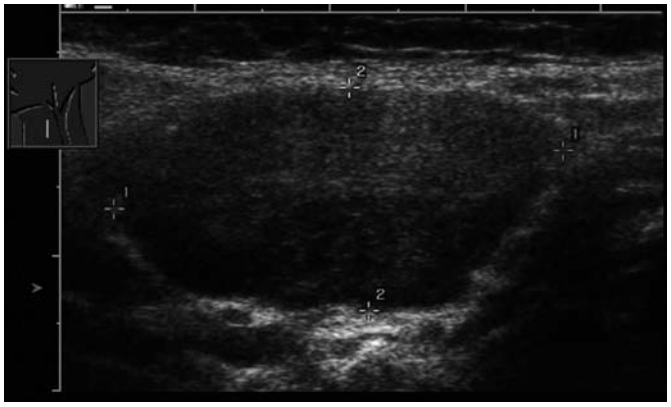

Fig. 6. Cervical lymph node of a patient with sarcoidosis with a diameter of 3.5 × 1.6 cm.

Salivary Glands

Sonography is an excellent tool for examining the superficial major salivary glands; only deep-seated parts of the parotid gland are occasionally difficult to assess. The normal structure of the glands is echogenic and homogeneous. Intraglandular ducts are hardly detectable.

Inflammatory diseases of the glands, such as sialoadenitis, lead to enlargement, convex borders, and decreased echogenicity. Ultrasound may help to identify abscesses or obstruction, as well as intraductal concrements. An abscess is typically hypoechogenic, and without perfusion in the liquefied center and hyperperfusion in the rim. Note that the echogenicity of an abscess depends on the composition of the pus. A newly developed abscess may contain echoes (occasionally moving ones) which gradually disappear as the detritus is degraded and the content becomes more and more liquid. A strong posterior sound enhancement (like with a cyst) is almost always present, even with highly echogenic pus, and may help to discriminate the abscess from more sinister lesions. In obstructive sialoadenitis, multiple intraglandular hypoechogenic tubular structures correspond to dilated ducts (fig. 7a). The sonographic feature of tuberculosis of the salivary glands resembles a malignant tumor with inhomogenicity and hypoechogenicity. Ultrasound in Sjögren's syndrome, an autoimmune disease with inflammation of glands, demonstrates an inhomogeneous gland. In advanced disease, multiple cystoid lesions and increased perfusion in Doppler sound are found. However, in atrophic glands vascularity diminishes. Lesions of more than 15 mm in a patient with Sjögren's syndrome should be suspected for secondary malignant lymphoma and be biopsied [13, 14].

Sialoadenosis, a nonneoplastic, noninflammatory enlargement of a salivary gland occurs mainly in the parotid. In ultrasound, glands are enlarged and their echogenicity is increased. Sialolithiasis refers to the formation of stones in the salivary glands most commonly found in the submandibular gland. Ultrasound is one of the most sensitive, noninvasive methods to find concrements with echogenic reflexes with dorsal shadowing and dilation of a duct. There may be no posterior shadowing with stones smaller than 2 mm (fig. 7b) [1, 15].

Tumors of salivary glands are rare, and occur mainly in the parotid gland. Most frequent are benign pleomorphic adenomas of the parotid which are sharply delineated, mostly homogeneous, and sometimes contain calcifications. Color Doppler shows enhanced vascularity compared to the origin gland (fig. 7c). Cystadenolymphoma is a sharply delineated ovoid, partly cystoid tumor. Malignant tumors, most commonly mucoepidermoid carcinoma, are hypoechogenic and inhomogeneous, with increased vascularity. Infiltration of the parapharyngeal space should be carefully evaluated, but the tumors are often not entirely accessible by ultrasound. However, sonography cannot accurately differentiate between malignant and benign salivary gland tumors [1, 14, 15].

Cystic Neck Lesions

The majority of cystic neck masses in children are congenital malformations and include thyroglossal duct cysts, branchial cleft cysts, epidermoid and dermoid cysts, and lymphatic malformations, whereas in adults cysts originating from the thyroid gland and an underlying malignancy should be considered [3].

Thyroglossal Duct and Branchial Cleft Cysts

Thyroglossal duct cysts, arising from a remnant of the thyroglossal duct, comprise about 70% of congenital neck masses (fig. 8). The cysts are found in the midline or near midline position of the neck and may be located at any level between the thyroid isthmus and the tongue base – about two thirds of them are infrahyoid. Sonographic examination shows a thin-walled, anechoic mass with posterior enhancement. By real-time ultrasound, synchronic movement of the cyst with the tongue is a typical feature. Infection should be suspected if mixed echogenicity is observed. Nevertheless, inhomogeneous echo structure should also arouse suspicion of papillary cancer within the cyst which shows additional perfusion within the lesion

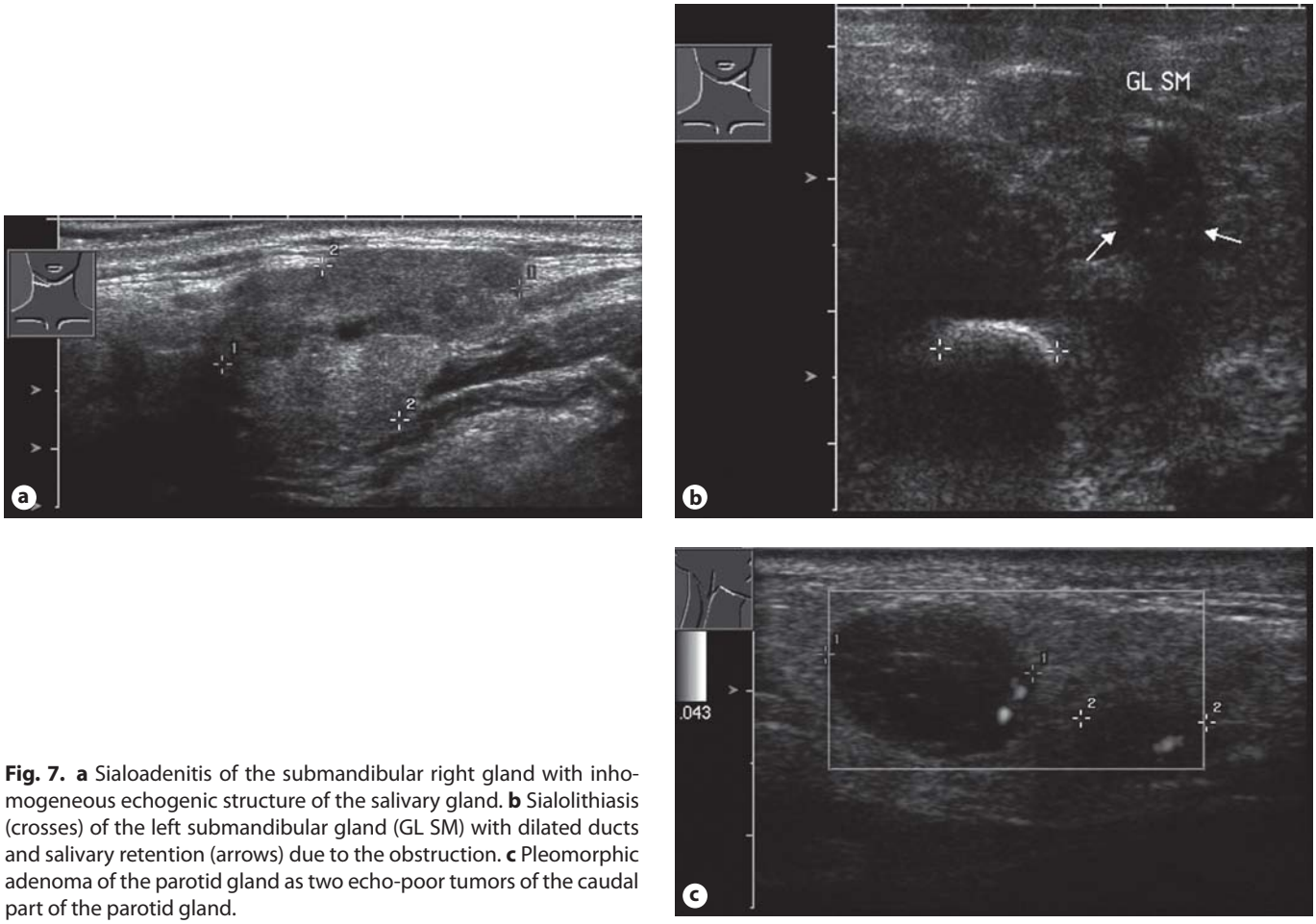

Fig. 7. **a** Sialoadenitis of the submandibular right gland with inhomogeneous echogenic structure of the salivary gland. **b** Sialolithiasis (crosses) of the left submandibular gland (GL SM) with dilated ducts and salivary retention (arrows) due to the obstruction. **c** Pleomorphic adenoma of the parotid gland as two echo-poor tumors of the caudal part of the parotid gland.

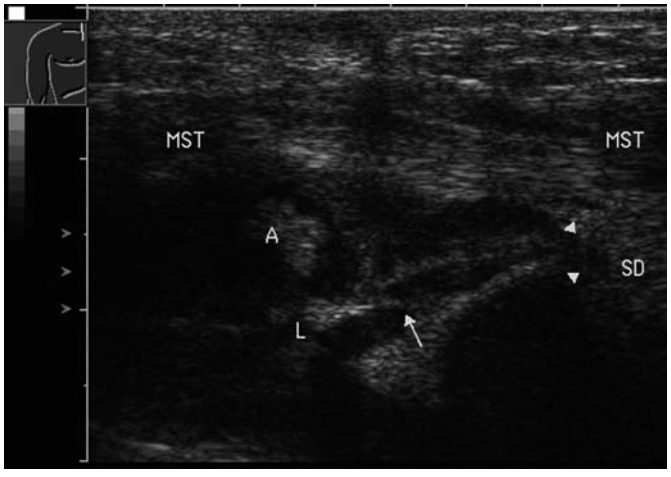

Fig. 8. 19-year-old male patient with relapsing cervical infections and abscesses. Persistent thyroglossal duct (arrow) ranging (arrowheads) from the thyroid (SD) to the larynx (L). MST = Sternocleidomastoid muscle; A = abscess formation.

[3, 16]. Branchial cleft cysts are congenital epithelial cysts, which arise in the lateral part of the neck mostly from a failure of the second branchial cleft to obliterate during embryonic development. With ultrasound, they mainly appear as a thin-walled, echo-free fluid-filled cyst, but their echogenicity varies. Most of the cysts have fine homogenous reflexes caused by cholesterol crystals. Sometimes, movement of these echoes can be found by intermittent pressure with the transducer (fig. 9) [1, 3, 15].

Epidermoid and Dermoid Cysts

Dermoid and epidermoid cysts are tumors composed of squamous epithelial cells. Epidermoids are devoid of skin appendages in their wall, while these are present in case of dermoids. They are often highly echogenic with internal echoes and a large amount of keratin debris may give the appearance of a solid mass [17].

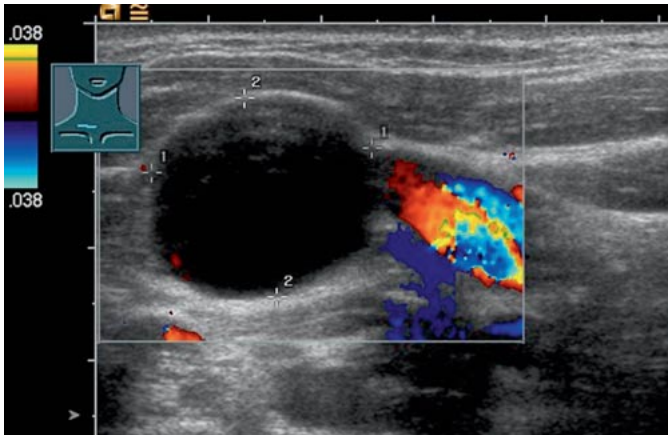

Fig. 9. Branchial cleft cyst (crosses, diameter of about 2 cm); echo-free structure lateral of the cervical vessels (color Doppler).

Laryngoceles

A laryngocele is usually a cystic dilatation of the laryngeal saccule. The external laryngocele is seen as a lateral swelling in the neck and passes superiorly through the gap of the thyrohyoid membrane from where the superior laryngeal nerve and vessels go by, whereas internal laryngoceles do not present as neck masses. The cystic laryngoceles can be depicted by sonography at the level of the thyrohoid membrane as anechoic lesions [1]. If they contain air, they present as a bright reflex with dorsal shadowing.

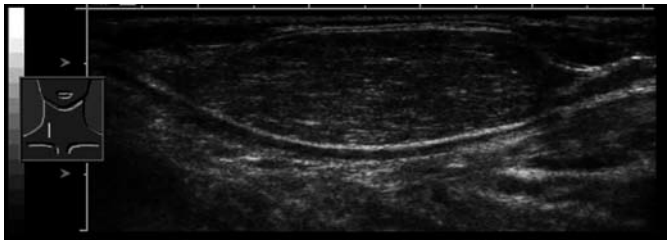

Fig. 10. Lipoma of the neck as an oval subcutaneous tumor with a typical striated feathery echo structure.

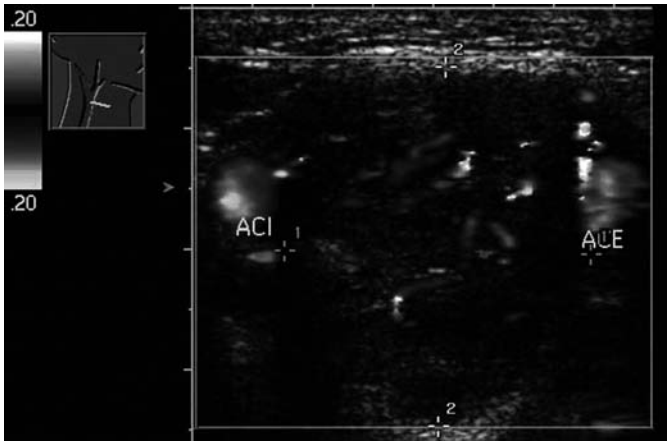

Fig. 11. Carotid paraganglioma (glomus tumor) in the carotid bifurcation which is highly vascularized. ACE = External carotid artery; ACI = internal carotid artery.

Soft Tissue Tumors of the Neck

Lipoma

Lipomas occur frequently in the neck region and are mostly localized in the subcutaneous space. Due to the relative distribution of fat and fibrous tissue, lipomas are relatively echogenic and show a typical striated, feathery echo structure. Color Doppler flow studies may reveal only sporadic vessels (fig. 10) [18].

Paragangliomas, Neurogenic Tumors and Neuroblastoma

Carotid paraganglioma is typically localized in the bifurcation of the carotid artery. The internal and external carotid artery are often displaced by a hypoechogenic, homogeneous solid tumor which is highly vascularized in color Doppler, often with low resistance flow due to arteriovenous shunts (fig. 11) [19]. Neurofibromas and schwannomas of the neck are mainly localized in the posterior cervical triangle. Ultrasound shows smoothly delineated hypoechogenic lesions with a spindle shape and occasionally necrotic areas. Skilful scanning may disclose a close continuity with a nerve. Vascularization in color Doppler is usually moderate to significant [1, 19]. Neuroblastoma, usually an adrenal tumor, may also arise in the cervical sympathetic chain, and then has a better prognosis. Sonography shows an echogenic mass which can appear homogeneous or heterogeneous showing sonographic signs of necrosis. Furthermore, calcification may be present [3].

Hemangioma and Lymphangioma

Infantile hemangiomas of the head and neck occur usually in children less than 6 months of age, grow rapidly until 10 months of age and tend to regress spontaneously within 10 years. Ultrasonographic studies show a mostly echogenic mass which is commonly highly compressible with septations that are vascular on color Doppler. Arteriovenous shunts with high diastolic flow may be present [3]. Lymphangioma is a rare, benign proliferation of lymph vessels and usually occurs in the head and neck region (75% of the cases). Sonography usually displays a multicystic compressible pattern, but no blood flow [1, 3].

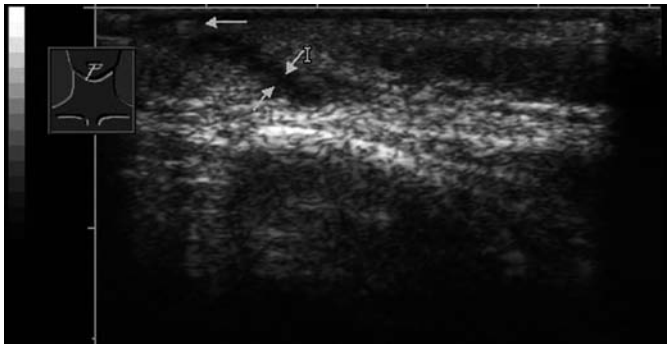

Fig. 12. 6-year-old girl after crashing through a glass door. Note the reflex of the glass (arrow to the left) with a hypoechogenic inflammation (I) in the submandibular region (arrows).

Ectopic Thymic Tissue and Fibromatosis Colli

Ectopic cervical thymic tissue is a rare finding in infants. Sonography shows an echogenic, soft and solid cervical lesion with echogenic strips and the same echogenicity as the children's thymus with marked vascularization [1]. Fibromatosis colli is a benign, firm, fibrotic mass in the sternocleidomastoid muscle, usually detected in infants around 2–8 weeks of age which spontaneously resolves between 6 and 12 months of age. Ultrasound shows an isoechoic or hypoechoid mass within the muscle which moves with the muscle [3].

Foreign Body, Granulomas and Abscesses

Foreign bodies and suture granulomas have a typical sonographic appearance as hypoechogenic lesions with a curved central echo complex caused by the retained material (fig. 12) [1]. An abscess most commonly appears as a hypoechoic or anechoic mass relative to adjacent structures, but may be echogenic when fresh. However, a strong posterior enhancement is constantly present and indicates that the content is rich in fluid. Scattered echoes may represent necrotic debris or tissue and abscess cavity may contain septa or gas, which shows small pockets of hyperechoic air within it. Color flow Doppler can show hyperemia adjacent to the abscess cavity and absence of flow within it. Once the abscess is identified, ultrasound can be used to drain it (fig. 8, 13) [3].

Brachial Plexus

The sonographic investigation of the supraclavicular region with high-resolution probes (5–13 MHz) allows the

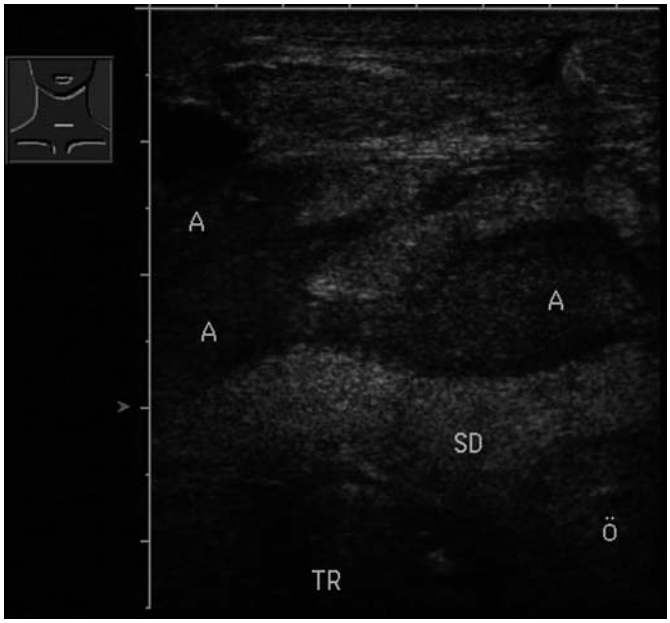

Fig. 13. Prethyroidal abscess (A) ventral of the isthmus of the thyroid gland (SD). TR = Trachea; Ö = esophagus.

inspection of the brachial plexus and the cervical nerve roots. Indications for ultrasound of this plexus are the examination of a possible infiltration of a Pancoast tumor, a traumatic lesion of the nerves or sonographically guided anesthesia of the plexus. Starting the sonographic assessment at the lateral base of the neck, the branches of the brachial plexus run lateral and downward between the scalenus anterior and medius muscle, reaching the axilla between the first rib and the clavicula [20]. The easiest way of identifying the cervicobrachial plexus is to first find the cervical nerve roots as they exit between the transverse vertebrae and then run downward. They are typically slightly echo-poor without visible internal structures and show a 'bulb-like' thickening at their origin.

Tumors of the Tongue, Floor of the Mouth, the Larynx and Hypopharynx

Ultrasound is useful for the evaluation of tumor infiltration. Compared with normal musculature, carcinomas are hypoechogenic and hypervascularized in Doppler sound (fig. 14a). Small tumors of the tongue and floor of the mouth can usually be delineated in total by sonography. However, advanced, infiltrative tumors often cannot be entirely examined by ultrasound; they belong to the realms of MRI or CT.

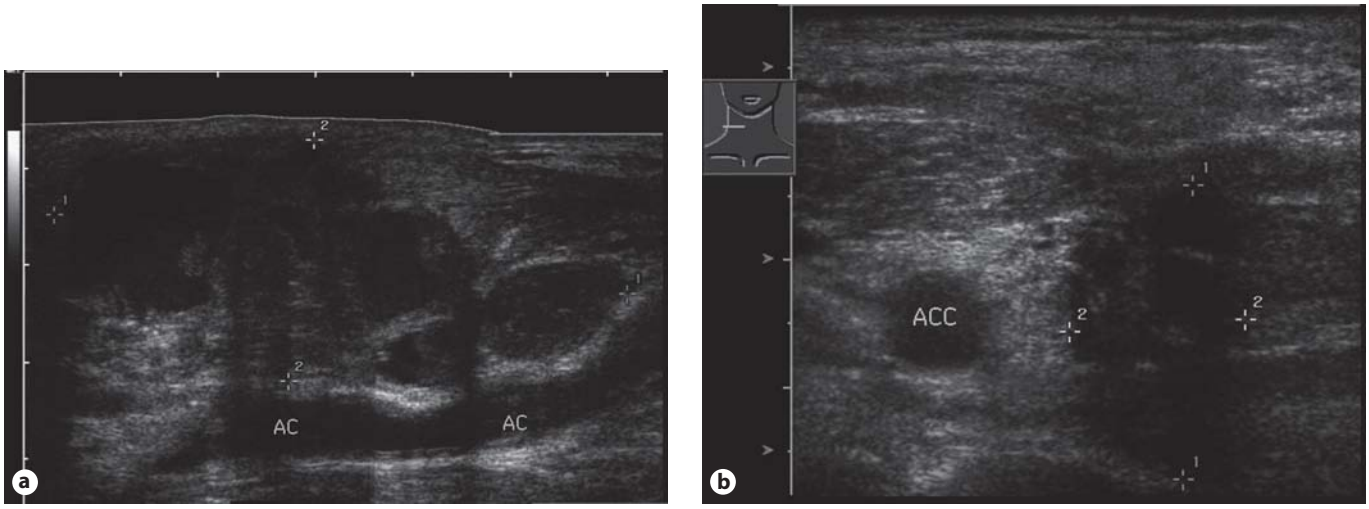

Fig. 14. **a** About 10-cm-sized echo-poor, partly cystic tumor (poorly differentiated sarcoma) of the right ventral neck with infiltration of the common carotid artery (AC). **b** Hypoechogenic-relapsed tumor (crosses) right cervical, medial of the cervical vessels (ACC = common carotid artery) of a patient with a laryngeal carcinoma after neck dissection and radiotherapy.

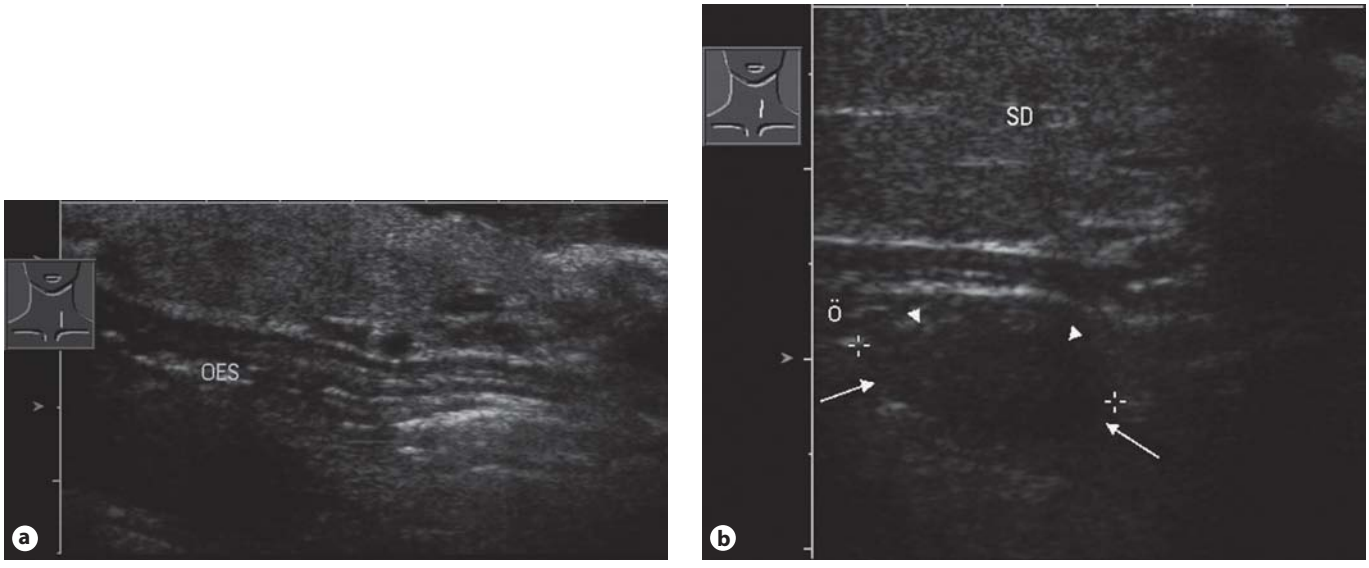

Fig. 15. **a** Cervical esophagus (OES) dorsal of the left thyroid with the typical sonographic wall structure of gastrointestinal organs of five discrete layers. **b** Echo-poor delineated tumor of the 2nd dorsal layer of the proximal esophagus (Ö). Histology revealed a leiomyoma. Arrowheads represent tumor borders in the second layer towards the esophageal lumen and arrows the distal tumor border. The crosses show the maximum diameter of the tumor. SD = Thyroid.

Many laryngeal tumors are difficult to examine by ultrasound due to calcified laryngeal cartilages (fig. 14b). Nevertheless, the preepiglottic space is well accessible for sonographic examination. By ultrasound, hypoechogenic tumors of the preepiglottic space as well as tumor infiltration of the anterior laryngeal or the thyroid cartilage can be depicted. By real-time sonography, it may be helpful to let the patient swallow to exclude tumor invasion [21, 22].

Disorders of the Cervical Esophagus

The cervical esophagus originates at the level of the larynx and shows the typical sonographic wall structure of gastrointestinal organs, i.e. five discrete layers. Not all of them are constantly visible, but it is almost always possible to see the inner, hypoechoic mucosa, the folded submucosa, which is echo-rich, and the muscularis, which is echo-poor

(fig. 15a). The esophagus usually protrudes to the left and can therefore be seen dorsomedially to the left lobe of the thyroid gland. Transcutaneous ultrasound allows detecting tumors of the upper esophagus and its passage into the hypopharynx showing hypoechogenic infiltration, destruction of the normal layer and enlargement of the wall (fig. 15b). Sonography may also be used for follow-up after stent implantation to document deglutition. Zenker's diverticulum can appear as an isoechoic or hypoechoic mass with internal or peripheral echogenic foci and a boundary hypoechoic zone at the posterior portion of the thyroid gland. Ultrasonographic evaluation for achalasia shows thickening of the esophageal wall with sustained layers and amotility of the upper esophagus [1, 15].

Ultrasound-Guided Biopsy of Head and Neck Masses

Ultrasound-guided biopsy of head and neck masses is a safe and reliable technique yielding the highest rates of accuracy in cervical lymph node metastases. Ultrasound-guided biopsy helps puncture the most suspicious area, which is most helpful in partial metastatic involvement of lymph nodes. Core needle biopsy lowers inadequate and false-negative results [2, 23].

References

1 Gritzmann N: Sonography of the neck: current potentials and limitations. Ultraschall Med 2005;26:185–196.
2 Esen G: Ultrasound of superficial lymph nodes. Eur J Radiol 2006;58:345–359.
3 Turkington JRA, Paterson A, Sweeney LE, Thornbury GD: Neck masses in children. Br J Radiol 2005;78:75–85.
4 Ying M, Ahuja AT, Evans R, King W, Metreweli C: Cervical lymphadenopathy: sonographic differentiation between tuberculous nodes and nodal metastases from non-head and neck carcinomas. J Clin Ultrasound 1998;26:383–389.
5 Prosch H, Strasser G, Sonka C, Oschatz Ä, Mashaal S, Mohn-Staudner A, Mostbeck GH: Cervical ultrasound and US-guided lymph node biopsy as a routine procedure for staging of lung cancer. Ultraschall Med 2007;28:598–603.
6 Solbiati L, Rizzatto G, Belotti E: High-resolution sonography of cervical lymph nodes in head and neck cancer: criteria for differentiation of reactive versus malignant nodes. Proceedings of the 74th Meeting of the Radiologic Society of North America, Chicago, 1988, p 113.
7 Vassallo P, Wernecke K, Roos N, Peters PE: Differentiation of benign from malignant superficial lymphadenopathy: the role of high-resolution US. Radiology 1992;183:215–220.
8 Gritzmann N, Hollerweger A, Macheiner P, Rettenbacher T: Sonography of soft tissue masses of the neck. J Clin Ultrasound 2002; 30:356–373.
9 Tschammler A, Ott G, Schang T, Seelbach-Goebel B, Schwager K, Hahn D: Lymphadenopathy: differentiation of benign from malignant disease – color Doppler US assessment of intranodal angioarchitecture. Radiology 1998;208:117–123.
10 Alyas F, Lewis K, Williams M, Moody AB, Wong KT, Ahuja AT, Howlett DC: Diseases of the submandibular gland as demonstrated using high resolution ultrasound. Br J Radiol 2005;78: 362–369.
11 Mori M, Sakamoto T, Murata K, Takahashi M, Aoki S, Furukawa A, Yamazaki M, Itoh R, Ohnaka Y, Koyama S, Okada Y, Morita R: Facet formation sign in sarcoidosis: a new sign in endoscopic ultrasonography. Eur Radiol 1992;2: 526–531.
12 Winkelbauer F, Denk DM, Ammann M, Karnel F: Ultrasound diagnosis of cervical lymph node tuberculosis. Ultraschall Med 1993;14:28–31.
13 Makula E, Pokorny G, Rajtár M, Kiss I, Kovács A, Kovács L: Parotid gland ultrasonography as a diagnostic tool in primary Sjögren's syndrome. Br J Rheumatol 1996;35:972–977.
14 Sakaguchi T, Arakawe A, Takahashi M: Appropriate use of ultrasonography in the neck. Semin Roentgenol 2000;1:54–62.
15 Braun B, Blank W: Sonography of the neck and superior mediastinum. Internist 2005;46: 1133–1146.
16 Ahuja AT, King AD, King W, Metreweli C: Thyroglossal duct cysts: sonographic appearances in adults. Am J Neuroradiol 1999;20: 579–582.
17 El-Silimy O, Corney C: The value of sonography in the management of cystic neck lesions. J Laryngol Otol 1993;107:245–251.
18 Ahuja AT, King AD, Kew J, King W, Metreweli C: Head and neck lipomas: sonographic appearance. Am J Neuroradiol 1998;19:505–508.
19 Gritzmann N, Herold C, Haller J, Karnel F, Schwaighofer B: Duplex sonography of tumors of the carotid body. Cardiovasc Intervent Radiol 1987;10:280–284.
20 Beckh S: Indications, technical prerequisites and investigation procedures; in Mathis G (ed): Chest Sonography. Springer, Berlin, 2008, pp 1–9.
21 Gritzmann N, Traxler M, Grasl M, Pavelka R: Advanced laryngeal cancer: sonographic assessment. Radiology 1989;171:171–175.
22 Fruehwald FX: Clinical examination, CT and US in tongue cancer staging. Eur J Radiol 1988;8: 236–241.
23 Pfeiffer J, Kayser G, Technau-Ihling K, Boedeker CC, Ridder GJ: Ultrasound-guided core-needle biopsy in the diagnosis of head and neck masses: indications, technique and results. Head Neck 2007;29:1033–1040.

Dr. Michael Kreuter
Department of Pneumology and Respiratory Critical Care Medicine, Thoraxklinik, University of Heidelberg
Amalienstrasse 5
DE–69126 Heidelberg (Germany)
Tel. +49 0 6221 396 1201, Fax +49 0 6221 396 1202, E-Mail michael.kreuter@thoraxklinik-heidelberg.de

Chapter 5

Bolliger CT, Herth FJF, Mayo PH, Miyazawa T, Beamis JF (eds): Clinical Chest Ultrasound: From the ICU to the Bronchoscopy Suite.
Prog Respir Res. Basel, Karger, 2009, vol 37, pp 43–50

Diagnosis of Pulmonary Embolism and Pneumonia Using Transthoracic Sonography

Angelika Reissig · Claus Kroegel

Pneumology and Allergology, Medical University Clinics I, Friedrich Schiller University, Jena, Germany

Abstract

Pulmonary embolism (PE) and pneumonia can be detected by transthoracic sonography (TS), if they extend up to the pleura. In about 70–80% central PE is accompanied by peripheral PE, which is detectable by TS. In patients with suspected PE, all intercostal spaces have to be investigated, especially those in the region of thoracic pain. Typical sonographic findings of peripheral PE are multiple (mean 2.3–2.6 lesions/patient), hypoechoic, pleural-based parenchymal lesions, mostly well-demarcated and either wedge shaped or rounded. A basal and/or localized pleural effusion is evident in 50–60% of the patients. The sensitivity, specificity and accuracy of TS for diagnosing PE is 74–80, 92–95 and 84%, respectively. Nevertheless, an inconspicuous TS does not exclude PE. Pneumonia characteristically demonstrates a hypoechoic area of varying size and shape featuring irregular and serrated margins and heterogeneous echotexture. Pneumonia typically reveals a bronchoaerogram and shows free breath-dependent motion. Occasionally, a positive fluid bronchogram may be detectable. Pleural effusion occurs in about 70% of the patients. By means of TS PE and pneumonia may be diagnosed and followed up over the course of the disease, and complications may be identified early. TS provides the basis for further diagnostic and treatment-related decisions.

Pulmonary Embolism

Introduction

Diagnosing pulmonary embolism (PE) continues to be a challenge for physicians. Clinical presentation is often nonspecific and may mimic various other cardiopulmonary conditions. In recent years, computed tomographic pulmonary angiography (CTPA) has become the method of choice for diagnosing PE. However, CTPA does not achieve sensitivity and specificity of 100%. Moreover, it may simply not be available for use. In addition, CT may fail to detect small peripheral emboli, and it is associated with potentially harmful radiation and application of contrast medium. In cases of renal failure, pregnancy or contrast agent allergy, sonographic imaging may be an alternative approach to CTPA. Ultrasound may also be the method of choice in an emergency setting, in intensive care units or in outpatients at home.

Detection of thromboembolic lesions of the lung using sonography was first described some 40 years ago [1, 2]. However, in recent years transthoracic sonography (TS) has become increasingly important for diagnosing PE [3–5].

In general, an intrapulmonary lesion is only detectable by TS provided that the following conditions are fulfilled: (1) the pulmonary lesion extends up to the pleura, (2) the pleural space contains no air (no pneumothorax), (3) there is no subcutaneous accumulation of air (no subcutaneous emphysema), and (4) the lesion is not hidden behind a bony structure.

Pathogenesis of PE

The pathogenesis of venous thromboembolism is associated with three main factors first described by Virchow over a 100 years ago: (1) hemodynamic imbalance (blood stasis), (2) endothelial vessel wall damage, and (3) a state of hypercoagulability.

Pathophysiology of PE

The pathophysiologic consequences of thrombotic vascular occlusion result from both the direct effects of arterial occlusion on cardiopulmonary function and from the preexisting comorbidity of the patient. They may be

divided into (1) complete infarction and (2) incomplete infarction.

A complete embolic occlusion of a pulmonary artery builds up increased pressure proximal to the thrombus and a decrease or even cessation of flow distal to it leading to a number of consequences including a breakdown of surfactant with consecutive packing of the alveolar lumen by erythrocytes containing exudates [6]. The alveolar filling combined with an evacuation of air from the affected lung tissue provides the basis for the sonographic detection of lesions extending up to the pleural surface thus making them accessible to TS.

An embolic occlusion of a pulmonary artery initially leads to intra-alveolar hemorrhage without necrosis on the first 2 days of PE [7]. This hemorrhage may subsequently result in a 'true' pulmonary infarction (complete infarction; in about 15% of all infarctions) with necrosis of the alveolar walls or more frequently in an incomplete pulmonary infarction. PE resulting in a 'true' infarction is often combined with passive congestion of the lungs in patients with preexisting cardiopulmonary conditions. Necrosis of the alveolar walls usually begins after 2 days and leads to complete infarction when occlusion persists. Complete infarction, which usually reflects a poor prognosis [8], results in a scar and persistent radiographic findings over the following weeks [7].

On the other hand, in healthy lungs, infarctions mostly remain incomplete and characteristically disappear completely within 2–4 days in accordance with the resolution of the intra-alveolar hemorrhage. However, both complete and incomplete infarctions are detectable and can be followed up using imaging techniques such as CT and TS.

Sonomorphology of PE

The sonographic appearance of peripheral PE may be categorized into the following criteria: (1) parenchymal, (2) pleural and (3) vascular criteria.

Parenchymal Criteria

Typical sonographic findings of peripheral PE are multiple, hypoechoic, pleural-based parenchymal lesions, mostly well demarcated from the surrounding tissue. Eighty-six percent of the lesions are wedge shaped, 11% are rounded and about 3.3% adopt a polygonal configuration [3]. Generally, a mean of 2.3–2.6 lesions/patient (range 1–9) [3, 5] is detectable with an average size of 13.8 × 10.6 mm [3] to 15.5 × 12.4 mm [5]. All parenchymal lesions associated with peripheral PE are hypoechoic and show free movement during respiration. In about 7% of the patients, a single echo typically localized at the center of the lesions (fig. 1) may be detected. The diagnosis of PE is confirmed if 2 or more typical triangular or rounded pleural-based subpleural lesions are identified. A single typical lesion with a corresponding pleural effusion points to a probable PE [5].

Using TS, 43% of the peripheral lesions were restricted to the right side, 27% to the left side, and in 30% both sides were affected simultaneously [9]. The lesions were located within the lower lobes in about 80% [3], and 66% of lesions were seen in the posterior basal segment of the lung [5].

Pleural Criteria

Characteristic signs of pleural involvement include:

- Widening of the pleural space corresponding to the parenchymal lesion due to local accumulation of fluid (localized effusion)
- Basal pleural effusion
- A thinned and/or fragmented hypoechoic visceral pleura line

In PE, localized effusion occurs in about 23%, basal effusion in 20% and both localized and basal effusion in 17% of the patients [3]. Data from a multicenter study revealed pleural effusions in 49%, basal effusions in 33% and focal effusion in 16% of the patients, respectively [5].

Vascular Criteria

Exploration of the peripheral lesions using color Doppler imaging may be helpful for the differential diagnosis of PE.

The vascularity of a lesion is defined by three methods: qualitative color Doppler sonography (CDS), spectral curve analysis and contrast-enhanced sonography (CES).

CDS: Generally, a pulmonary infarction does not show any flow signals; however, occasionally, a congested thromboembolic vessel ('vascular sign') may be visible [10, 11].

Spectral curve analysis may demonstrate a bronchial artery next to the pleura in certain cases [12].

CES shows no vascularity of the lesions or it presents a long time to enhancement and a clearly reduced extent of enhancement [12].

Course of the disease: Sonography allows monitoring the course of PE and the early detection of infarct-related complications, such as pneumonia. Sonographic features of end-stage postinfarct pneumonia may be indistinguishable from pneumonia of other causes.

As outlined above, incomplete pulmonary infarction will resolve without sequelae. Complete infarction results in a scar that is detectable by sonography as an echo-rich, well-demarcated peripheral lesion. Sometimes, comet tail artifacts due to local scarring may persist for many years.

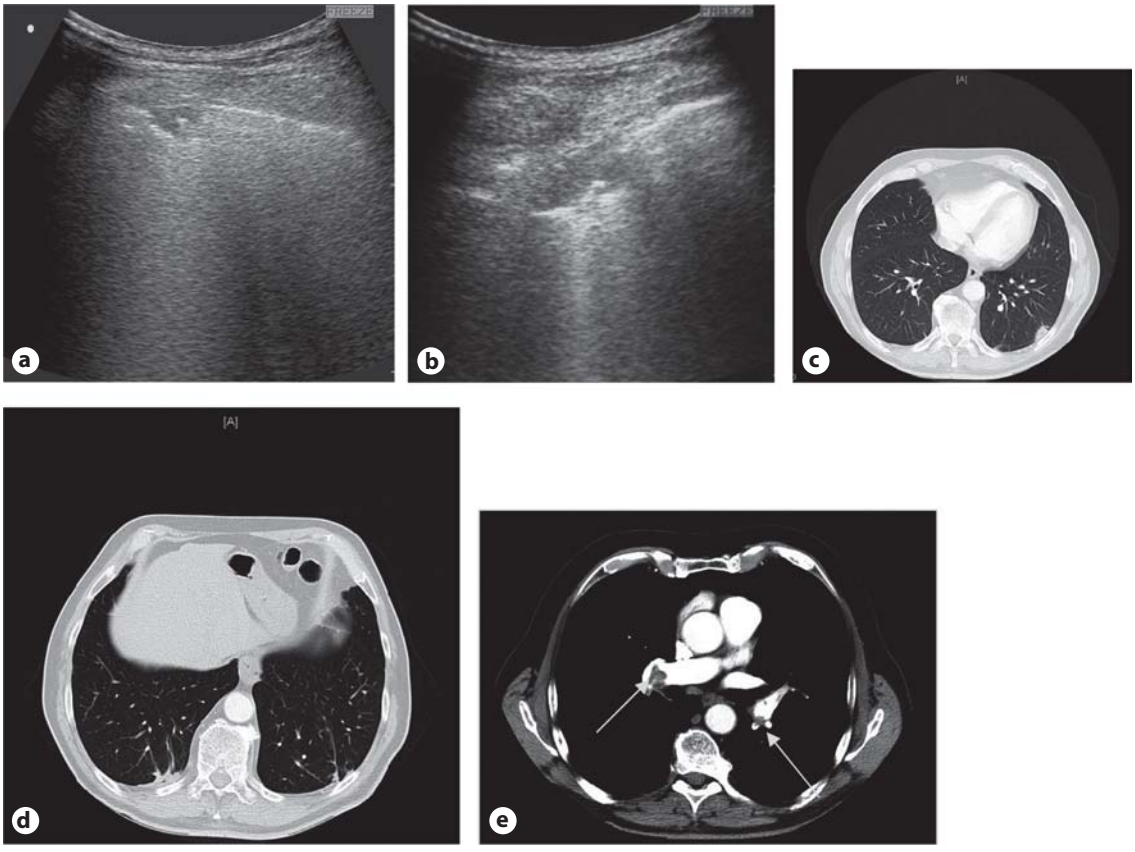

Fig. 1. PE: sonogram and corresponding computed tomogram. Seventy-year-old patient with CT-proven PE. The patient had been suffering from dyspnea on exertion, dizziness and tachycardia for 14 days. The sonogram depicts two triangular, hypoechoic, pleural-based parenchymal lesions with a single centrally located echo. One lesion was detected in the left (**a**) and the other in the right lower lobe (**b**) dorsally. On the corresponding CT the peripheral lesions are demonstrated on the left (**c**) as well as on the right side (**d**). They contain air inclusion. **e** Central PE on both sides of the lung (arrows).

Diagnostic Strategy for Acute PE

Multidetector CT angiography has been recommended as the reference standard for diagnosing acute PE since 2007, replacing pulmonary angiography [13]. The sensitivity of this technique for detecting PE varies between 83 and 100% whereas the specificity lies between 89 and 96%, respectively [14, 15]. However, CT scanning is associated with a few disadvantages, such as radiation exposure, the necessity of transporting the patient to the CT unit, as well as possible side effects (e.g. deterioration of renal function and allergy to iodinated contrast material). Therefore, sonographic imaging offers an attractive diagnostic approach in cases of suspected PE, particularly in children, pregnant women, patients with impaired renal function as well as in the critically ill. If available, ultrasound should be the initial method applied in all cases of suspected PE. Ultrasound imaging includes TS, venous ultrasound, transthoracic (or transesophageal) echocardiography and endobronchial sonography.

The diagnostic strategy for acute PE depends on the patients' clinical presentation. In cardiopulmonary-compromised patients either transthoracic (or transesophageal) echocardiography or endobronchial sonography [16] is the primary investigation to be carried out. In case of a negative or a nondiagnostic ultrasound, a CT scan should follow. On the other hand, in cardiopulmonary-stable patients, TS, venous ultrasound and transthoracic (or transesophageal) echocardiography should be carried out first. This may be followed by endobronchial sonography, if available. Only in case of a negative or a nondiagnostic ultrasound, should a CT scan be performed to establish PE. The sensitivity, specificity and accuracy of TS for diagnosing PE is 74–80, 92–95 and 84%, respectively [3, 5]. Approximately 66% of the peripheral lesions detected by TS are located in the

dorsobasal segments of the lung, which are well accessible to TS. This anatomical distribution closely reflects the anatomy of the pulmonary arteries.

The basic advantages of TS in diagnosing PE are:

- Immediate accessibility at bedside
- Ease of performance
- No ionizing radiation
- No contrast medium required
- Feasibility of repeated controls
- Identification of very small peripheral lesions
- Early detection of possible complications, such as postinfarction pneumonia

The disadvantages of TS in diagnosing PE comprise:

- Only lesions extending up to the lung periphery can be detected
- Approximately 66% of the peripheral lung areas are accessible to sonographic examination (although this is counterbalanced by the preferred localization of the lesions in the posterior basal segment of the lung)
- Strictly centrally localized emboli may not be detected
- Inconspicuous sonographic images do not exclude PE
- Operator-dependent investigation (experience of the investigator)

Pneumonia

Introduction

Pneumonia is classified into community-acquired pneumonia (CAP), hospital-acquired pneumonia and pneumonia associated with immunodeficiency.

CAP is commonly defined as an acute infection of the pulmonary parenchyma associated with some symptoms of acute infection, and accompanied by the presence of an acute infiltrate on a chest radiograph or auscultatory findings consistent with pneumonia in a patient not hospitalized for 4 weeks before onset of symptoms.

As the name suggests, hospital-acquired pneumonia develops during hospitalization, 48 h or more after admission, and is not present or incubating at the time of admission.

CAP affects about 2–3 million people/year in the USA. The estimated incidence of CAP in Germany is 1–11/1,000 and causes about 200,000 inpatient treatments/year. The overall mortality due to CAP is approximately 11%.

Pathophysiology of Pneumonia

Pneumonia, a disease of the peripheral lung tissue and distal bronchioles, is caused by an overwhelming inflammatory defense reaction of the host against pathogenic microorganisms. Flooding of the peripheral airways and alveoli by a neutrophil-rich exudate leading to air evacuation in the affected tissue is characteristic of pneumonia and provides accessibility to sonographic evaluation.

Sonomorphology of Pneumonia

The sonographic appearance of classical bacterial pneumonic lesions may be categorized into parenchymal, pleural and vascular criteria.

Parenchymal Criteria of Pneumonia

Parenchymal criteria of pneumonia may be divided into 'superficial fluid alveologram', bronchoaerogram, and fluid bronchogram.

Characteristically on sonography, pneumonia shows a hypoechoic area of varying size and shape with irregular and serrated margins and a heterogeneous echotexture. In most cases, the consolidated lung section adjacent to the scanner is visible as a small homogeneous subpleural area without air or fluid bronchograms and it refers to a so-called 'superficial fluid alveologram'. In addition, pneumonia typically reveals a bronchoaerogram (fig. 2) which has either multiple lentil-sized air inlets measuring a few millimeters in diameter or a tree-shaped echogenic structure. These hyperechoic signals are caused by the residual air within air-conducting airways. Occasionally, the breath-depending motion of the echoes can be demonstrated during real-time investigation.

Another typical sonographic feature of a pneumonic lesion is the fluid bronchogram (fig. 3). It is characterized by echo-free tubular structures along the airways and occurs less frequently than the bronchoaerogram. Color Doppler imaging may help to differentiate a fluid bronchogram from pulmonary vessels. The fluid bronchogram reflects exudate-packed conducting airways and may indicate poststenotic pneumonia.

Pleural Criteria of Pneumonia

The pleural criteria of pneumonia may be divided into pleural fragmentation, localized pleural effusion, and basal pleural effusion.

Pleural fragmentation refers to the 'pleural line' corresponding to the pneumonic lesion. The line is characterized by its interrupted, thin, mostly fragmented, and hypoechoic appearance when compared to pleura covering noninfected lung areas.

A localized pleural effusion designates a local extension of the pleural space corresponding to pneumonic lung section and can be detected in about 9% of the cases [17].

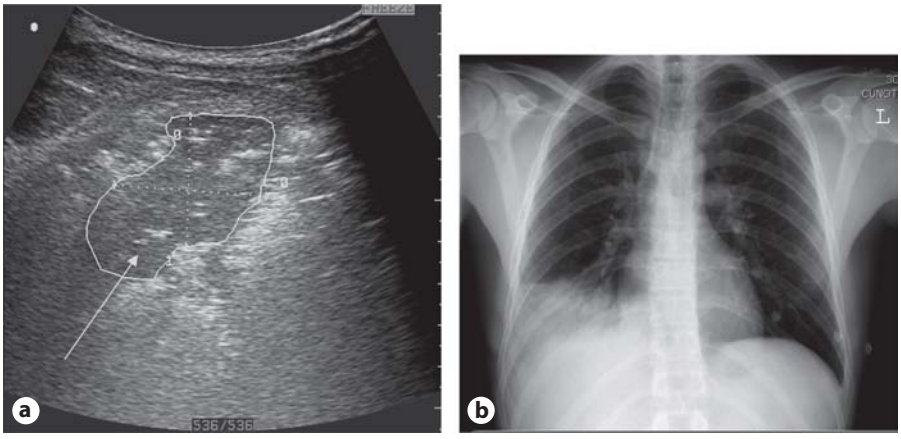

Fig. 2. Pneumonia: sonogram. A 32-year-old patient with fever, cough and purulent sputum. The pneumonia describes an area with irregular and serrated margins and an inhomogeneous echotexture caused by multiple lentil-sized hyperechoic reflexes indicating the presence of air within the lesion (bronchoaerogram, arrow) (**a**). Corresponding X-ray (**b**) reveals pneumonia in the right lower lobe.

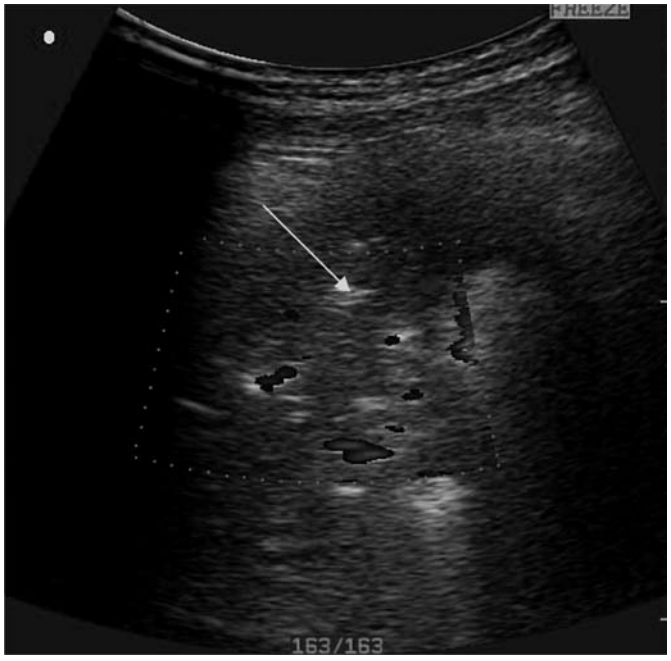

Fig. 3. Fluid bronchogram: sonogram. The fluid bronchogram reflects exudate-packed conducting airways and is characterized by echo-free tubular structures along the airways. In contrast to vessels, fluid bronchograms do not show any color Doppler flow signals (arrow).

Basal pleural effusion describes the pleural fluid accumulating in the costophrenic angle. It is seen in about 61% of pneumonia [17].

Vascular Criteria of Pneumonia

The third set of sonographic criteria for pneumonia refers to vascular alterations. Qualitative CDS resembles an enhanced, tree-like vascularity from the center to the periphery, which is typical of pneumonia.

The spectral curve analysis shows various vessels primarily representing pulmonary and bronchial arteries. By means of CES, the lesion can be defined in more detail. Lung lesions show a complex vascularity. Generally, pneumonia has a short time to enhancement and a marked extent of enhancement [12].

Even with vascular criteria differentiation between malignant and benign lesions is not possible. Color imaging strongly depends on the investigator's experience as well as on the localization, the size, and the breath-depending motion of the affected areas.

Course of the Disease

Pneumonia can follow different courses, which may be detectable by sonography: (1) noncomplicated pneumonia without sequelae, (2) necrotizing pneumonia, (3) complicated parapneumonic effusion, and (4) localized pleural thickening.

First, pneumonia may resolve completely without sequel. Irregularities of the pleural line causing comet tail artifacts may persist for some weeks or even months due to local scarring of the lung tissue.

Second, either necrotizing pneumonia or a pulmonary abscess may develop, particularly when the pathogens are anaerobic bacteria. A lung abscess is characterized as a hypoechoic area within the pneumonic lesion by sonography.

Third, a complicated parapneumonic effusion may develop. Without appropriate therapy, this will be followed by empyema. The sonographic appearance of a pleural empyema is characterized by an echo-rich effusion with spontaneous contrast and multiple echogenic structures,

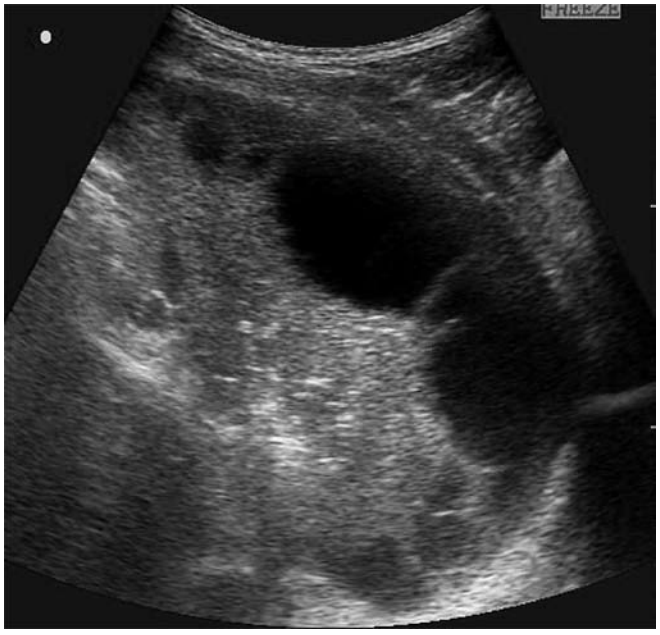

Fig. 4. Empyema: sonogram. As a complication of pneumonia, parapneumonic empyema developed in a 27-year-old patient with drug addiction. Pleural empyema is characterized by an echo-rich effusion, multiple echogenic structures within the effusion (resembles a net or Swiss cheese) and an absorbed lung.

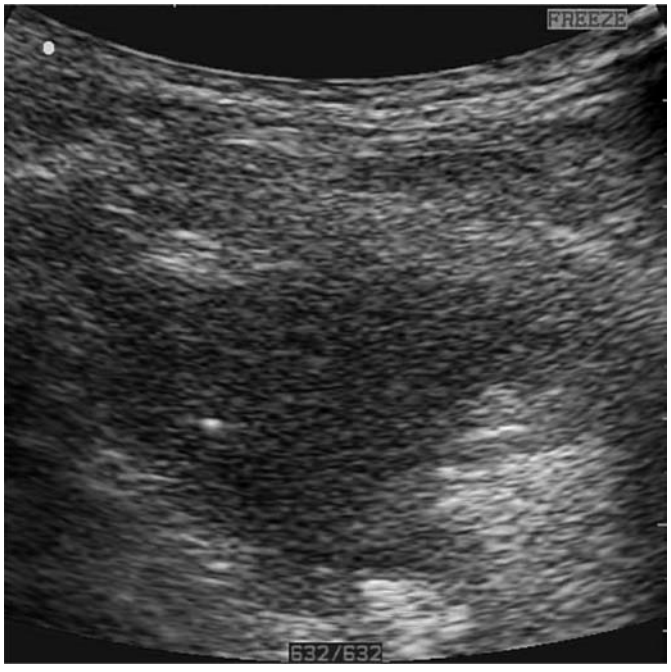

Fig. 5. Lung cancer: sonogram. An 81-year-old patient suffering from non-small cell lung carcinoma. The sonogram presents an echo-poor area with a polycyclic shape and an infiltrating growth within the thorax wall. The lesion does not exhibit a positive bronchogram.

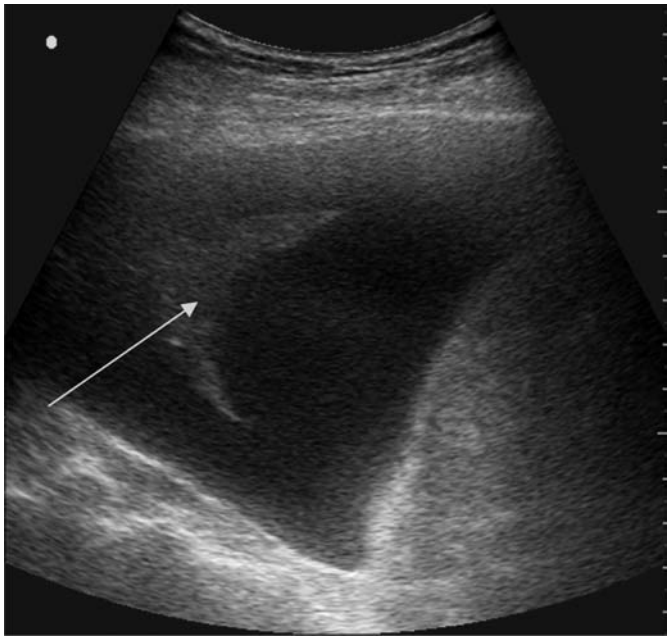

Fig. 6. Pleural effusion with compressive atelectasis: sonogram. A 78-year-old woman suffering from heart failure developed a large pleural effusion with consecutive compressive atelectasis (arrow). The atelectasis has sharp and smooth margins, is moderately echoic and has a concave shape (like a jelly bag cap). Under real-time conditions compressive atelectasis moves like a 'waving hand'.

resembling a net or a 'Swiss cheese' (fig. 4). In this case, a thoracocentesis or even surgical intervention is necessary.

Fourth, localized pleural thickening may become evident during the course of the disease.

Patients suffering from pneumonia can be diagnosed and monitored by means of TS. In this way exposure to radiation through X-ray will be reduced [17].

Interstitial Pneumonia

Interstitial pneumonia is another type of pneumonia caused by *Mycoplasma*, *Chlamydia*, *Legionella* and *Coxiella burnetti* as well as a number of viruses. These microorganisms influence the interstitial tissue and provide a different sonomorphologic picture involving multiple comet tail artifacts. Interstitial pneumonia may also predispose to bacterial superinfection resulting in an exudative filling of the alveoli. In this case, a positive bronchoaerogram is detectable, which may, however, be less pronounced than the bronchoaerogram found in typical pneumonia primarily caused by bacteria.

Differential Diagnosis of PE and Pneumonia

When sonographic features suggestive of PE and pneumonia are detected fundamentally important differential diagnoses,

Table 1. Differential diagnostic criteria of sonography for distinguishing between pneumonia, PE, bronchogenic carcinoma and compressive atelectasis [modified after 12, 18]

	Pneumonia	PE	Bronchogenic carcinoma	Compressive atelectasis
Echogenicity	hypoechoic	hypoechoic	hypoechoic	moderately echoic
Echotexture	nonhomogeneous	homogeneous	mostly homogeneous	mostly nonhomogeneous
Shape	irregular	triangular > round	rounded or polyclic	concave
Borders	serrated margins	well-demarcated	infiltrating growth	sharp and smooth
Bronchoaerogram	a regular feature	none	none	often
Characteristic features	fluid bronchgram may be visible	occasionally, a single central echo may be present	tissue necrosis may occur	associated with large effusion, reduced size following thoracocentesis
Vascularity CDS	enhanced, tree-like	no flow signals, 'vascular sign' possible	detectable	enhanced, tree-like
SCA	PA and BA	BA possible	ICA, TN	PA
CES	short TE, marked EE	no vascularity or delayed TE, reduced EE	delayed TE, variable EE	short TE, marked EE

SCA = Spectral curve analysis; PA = pulmonary artery; BA = bronchial artery; ICA = intercostal artery; TN = vessels of tumor neoangiogenesis; TE = time to enhancement; EE = extent of enhancement.

such as lung cancer, atelectasis (table 1) and bronchiolitis obliterans organizing pneumonia, have to be taken into account.

Lung Cancer

Lung carcinomas characteristically present as polycyclic-shaped echo-poor areas. Usually, they are not sharply demarcated and, occasionally, infiltrating growth into the adjacent tissue is visible. In case of carcinoma with tissue infiltration into the parietal pleura or the thorax wall (fig. 5) no breath-dependent motion can be detected. Occasionally, echo-free zones corresponding to central necrosis are observed. As a general rule, lung carcinomas do not show a positive bronchoaerogram, which is characteristic of pneumonia.

Vascularity may be detectable by means of qualitative CDS. The spectral curve analysis shows various vessels, which may primarily represent intercostal arteries or vessels of tumor neoangiogenesis. On CES, lung cancers have a delayed time to enhancement as well as a variable extent of enhancement [12].

Atelectasis

Atelectasis reflects nonventilated lung parenchyma. If atelectasis reaches up to the lung periphery, it may serve as an 'acoustic window' for a sonographic evaluation of the distant/central structures. Two different types of atelectasis can be distinguished: atelectasis following compression (compressive atelectasis) and atelectasis following central airway stenosis (resorption atelectasis).

Compressive Atelectasis

Compressive atelectasis is more common and is a regular consequence of space-occupying pleural effusion. This type of atelectasis usually has sharp and smooth margins, is moderately echoic and has a concave shape (like a 'jelly bag cap') (fig. 6). It reveals a breath- and heartbeat-dependent motion within the effusion. Occasionally, a breath-dependent reventilation of the atelectatic area may be visible. Compressive atelectasis decreases in size or even disappears after thoracocentesis. In CDS compressive atelectasis shows an enhanced, tree-like vascularity. Spectral curve analysis

predominantly presents pulmonary arteries, whereas in CES, a short time to enhancement and a marked extent of enhancement are depicted [12].

Resorption Atelectasis

The development of resorption atelectasis reflects a dynamic process. Therefore, resorption atelectasis characteristically appears as a homogeneous hypoechoic structure with an echogenicity comparable to that of the liver. This type of atelectasis has a large size in comparison to the extent of effusion. Its variable shape remains unchanged during cardiorespiratory cycles and after thoracocentesis. Occasionally, a fluid bronchogram may be detected due to obstruction of the airways such as due to retention of bronchial secretion or tumor obstruction.

In CDS, recent resorption atelectasis reveals an enhanced vascularity. Spectral curve analysis shows pulmonary and bronchial arteries. In CES, recent resorption atelectasis is characterized by a short time to enhancement and a marked extent of enhancement. By means of this technique metastasis or tumor necrosis within the atelectasis may be differentiated. In case of a long and persistent resorption atelectasis, reduced or absent vascularity as well as a long time to enhancement and a reduced extent of enhancement are present [12].

Bronchiolitis Obliterans Organizing Pneumonia

The sonographic appearance of bronchiolitis obliterans organizing pneumonia cannot be distinguished from pneumonia of other causes. For patients suffering from recurrent pneumonias of alternating localization and recurrent episodes of fever and malaise, bronchiolitis obliterans organizing pneumonia should be considered. Here, histology of tissue specimens obtained for instance by bronchoscopy are required to confirm the diagnosis.

References

1 Joyner C, Miller LD, Dudrick SJ, Eskin DJ, Knight GD: Reflected ultrasound in detection of pulmonary embolism. Trans Assoc Am Physicians 1966;79:262–277.
2 Miller LD, Joyner CR, Dudrick SJ, Eksin DJ: Clinical use of ultrasound in the detection of pulmonary embolism. Trans Assoc Am Physicians 1966;166:381–392.
3 Reissig A, Heyne J-P, Kroegel C: Sonography of lung and pleura in pulmonary embolism: sonomorphologic characterization and comparison with spiral CT scanning. Chest 2001;120:1977–1983.
4 Lechleitner P, Riedl B, Raneburger W, Gamper G, Theurl A, Lederer A: Chest sonography in the diagnosis of pulmonary embolism: a comparison with MRI angiography and ventilation perfusion scintigraphy. Ultraschall Med 2002;23:373–378.
5 Mathis G, Blank W, Reissig A, Lechleitner P, Reuss J, Schuler A, Beckh S: Thoracic ultrasound for diagnosing pulmonary embolism. A prospective multicenter study of 352 patients. Chest 2005;128:1531–1538.
6 Kroegel C, Reissig A: Principle mechanisms underlying venous thromboembolism: epidemiology, risk factors, pathophysiology and pathogenesis. Respiration 2003;70:7–30.
7 Hampton AO, Castleman B: Correlation of postmortem chest teleroentgenograms with autopsy findings. Am J Roentgenol Radium Ther 1940;43:305–326.
8 Dalen JE: Pulmonary embolism: what have we learned since Virchow? Natural history, pathophysiology, and diagnosis. Chest 2002;122:1440–1456.
9 Reissig A, Heyne JP, Kroegel C: Ancillary lung parenchymal findings at spiral CT scanning in pulmonary embolism. Relationship to chest sonography. Eur J Radiol 2004;49:250–257.
10 Mathis G, Dirschmid K: Pulmonary infarction: sonographic appearance with pathologic correlation. Eur J Radiol 1993;17:170–174.
11 Mathis G: Ultrasound diagnosis of pulmonary embolism. Eur J Ultrasound 1996;3:153–160.
12 Görg C, Bert T, Kring R, Dempfle A: Transcutaneous contrast enhanced sonography of the chest for evaluation of pleural based pulmonary lesions: experience in 137 patients. Ultraschall Med 2006;27:437–444.
13 Remy-Jardin M, Pistolesi M, Goodman LR, Gefter WB, Gottschalk A, Mayo JR, Sostman HD: Management of suspected acute pulmonary embolism in the era of CT angiography: a statement of the Fleischner Society. Radiology 2007;245:315–329.
14 Winer-Muram HT, Rydberg J, Johnson MS, Tarver RD, Williams MD, Shah H, Namyslowski J, Conces D, Jennings SG, Ying J, Trerotola SO, Kopecky KK: Suspected acute pulmonary embolism: evaluation with multi-detector row CT versus digital subtraction pulmonary angiography. Radiology 2004;233:806–815.
15 Stein PD, Fowler SE, Goodman LR, Gottschalk A, Hales CA, Hull RD, Leeper KV, Popovich J, Quinn DA, Sos TA, Sostman HD, Tapson VF, Wakefield TW, Weg JG, Woodard PK, PIOPED II Investigators: Multidetector computed tomography for acute pulmonary embolism. N Engl J Med 2006;354:2317–2327.
16 Aumiller J, Herth F, Krasnik M, Eberhardt R: Central pulmonary embolism diagnosed by real-time endobronchial ultrasound. Ultraschall Med 2007;28:S61.
17 Reissig A, Kroegel C: Sonographic diagnosis and follow-up of pneumonia: a prospective study. Respiration 2007;74:537–547.
18 Reissig A, Kroegel C: Ultrasound of the lung and pleura; in Gibson GJ, Geddes DM, Costabel U, Sterk PJ, Corrin B (eds): Respiratory Medicine, ed 3. London, Harcourt, 2002, pp 370–377.

Angelika Reissig, MD
Pneumology, Medical Clinic I, Friedrich Schiller University
Erlanger Allee 101
DE–07740 Jena (Germany)
Tel. +49 3641 932 4131, Fax +49 3641 932 4132, E-Mail angelika.reissig@med.uni-jena.de

Chapter 6

Bolliger CT, Herth FJF, Mayo PH, Miyazawa T, Beamis JF (eds): Clinical Chest Ultrasound: From the ICU to the Bronchoscopy Suite.
Prog Respir Res. Basel, Karger, 2009, vol 37, pp 51–58

The Mediastinum

Felix J.F. Herth

Department of Pneumology and Critical Care Medicine, Thoraxklinik, University of Heidelberg,
Heidelberg, Germany

Abstract

Mediastinal abnormalities are often discovered by radiological techniques. Clinical symptoms are usually unspecific; mediastinal lymphadenopathy, for example, is a frequent finding in inflammatory and neoplastic diseases. Both, acute and chronic inflammation of organs often leads to enlargement of adjacent lymph nodes. Apart from clinical and laboratory evaluations imaging techniques are the standard diagnostic tools. Mediastinal lymph node compartments can be evaluated by suprasternal and parasternal sonography. The value of mediastinal sonography as a routine diagnostic procedure has not yet been established. Mediastinal sonography allows sufficient access to the supra-aortic, paratracheal, prevascular, and pericardial regions as well as to the aortopulmonary window and, with less success, to the subcarinal region. High-resolution sonography is easy to perform and seems to be an effective diagnostic tool in evaluating the findings in the paratracheal region and aortopulmonary window. Occasionally lesions are also detectable in the subcarinal region. The lower detection rate in the subcarinal region may be a consequence of reduced sonographic visualization owing to the deep location of this region within the mediastinum or artifacts caused by heartbeats. However, transthoracic mediastinal sonography does have significant disadvantages. The procedure is strongly investigator-dependent and only reveals portions of the mediastinum compared with computed tomography. Moreover, the image quality is highly variable. But in the hands of a skilled ultrasonographist the technique is a helpful procedure, as it is repeatable, cheap and harmless for the patient.

Mediastinal structures can be visualized comprehensively by computed tomography as well as magnetic resonance tomography. Apart from echocardiography, transthoracic sonographic examination of the mediastinum has therefore not been widely applied until now.

Although an adequate view of the mediastinum is somewhat impaired by bone, ultrasonography (US) plays a useful role. In 1971, Goldberg [1] first described suprasternal US of the mediastinum. Cardiologists used this access to examine the aortic valve and thoracic aorta [2, 3]. In 1986, Wernecke et al. [4] described the diagnostic evaluation of mediastinal tumors utilizing suprasternal US. In 1990, they studied mediastinal sonography with an additional parasternal access [5]. They concluded that the sensitivity of US was similar to CT scanning for the supra-aortic, pericardial, prevascular, and paratracheal areas. CT scanning was superior to US for the aortopulmonary window, the subcarinal and paravertebral regions, and the posterior mediastinum. US contributes to the evaluation of the mediastinum despite limited view. Lesions of the anterior superior mediastinum may be identified clearly by US as solid or cystic [6].

US of the mediastinum has, however, several limitations. Successful examination requires considerable experience in visual interpretation, and a thorough knowledge of anatomic structures. Lesions that are located deeper in the mediastinum absorb more US energy and may not be identified against surrounding tissue. Patients with emphysema have reduced suprasternal, parasternal, and aortopulmonary windows that limit US evaluation. Endoscopic US using the flexible bronchoscope is another method with which to evaluate the mediastinal, paratracheal, and subcarinal lymph nodes [see chapters 13–20, pp. 110–179].

In the following paragraphs the technique will be described and the value of transthoracic US will be discussed.

Technique

Profound knowledge of anatomy is absolutely essential (fig. 1). The investigation procedure is based on Heinzmann's stratification [7] of the mediastinum into eight compartments, which correspond to the various lymph node

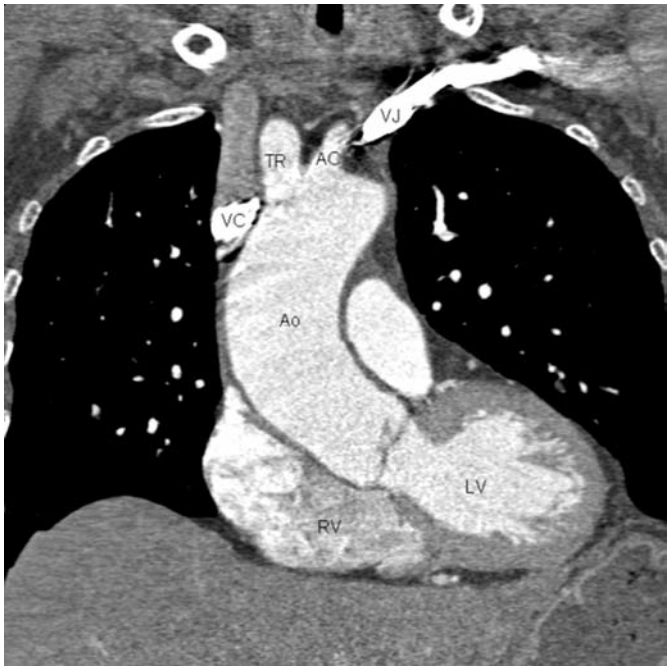

Fig. 1. Anatomy of the mediastinum on a computed tomography reconstruction of the coronary section level.

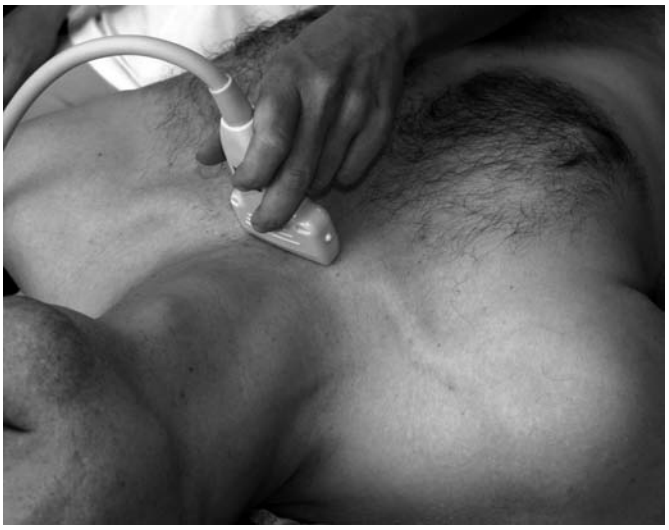

Fig. 2. Suprasternal ultrasound in the supine position; by moving the probe in different directions an adequate acoustic window can be obtained.

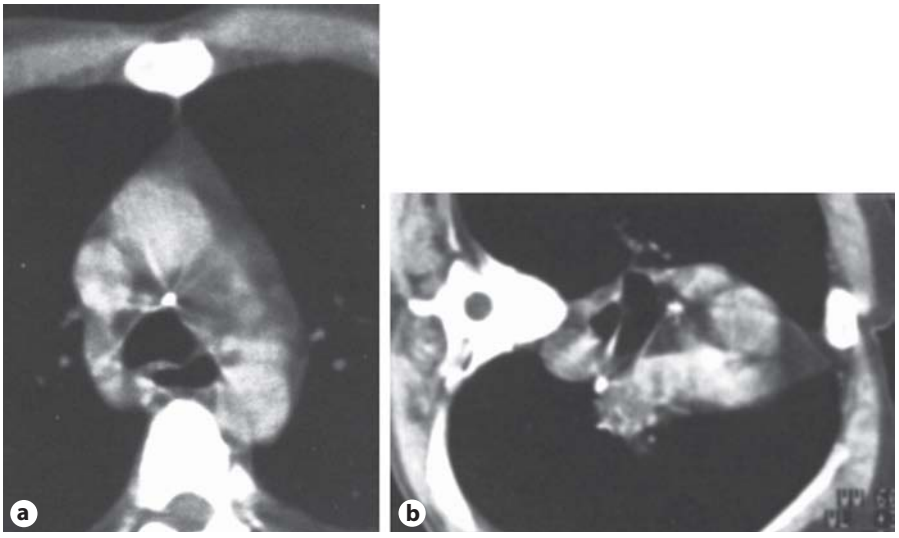

Fig. 3. Parasternal acoustic window in a supine (**a**) and a left-sided (**b**) position in expiration. Only in a left-sided position does the mediastinum reach the chest wall and an acoustic window is accessible.

groups. Because of the small sonic window, only 3.5- and 5-MHz sector, convex and vector transducers with small apertures are suitable for sonographic diagnosis. With sonography the mediastinum is accessed from the suprasternal and the parasternal regions, occasionally also from the infrasternal region [8]. The large vessels and their spatial relationship to the heart in the various planes serve as cardinal structures. The investigation from suprasternal is performed with the patient in the supine position, the parasternal view in a left- or right-sided position.

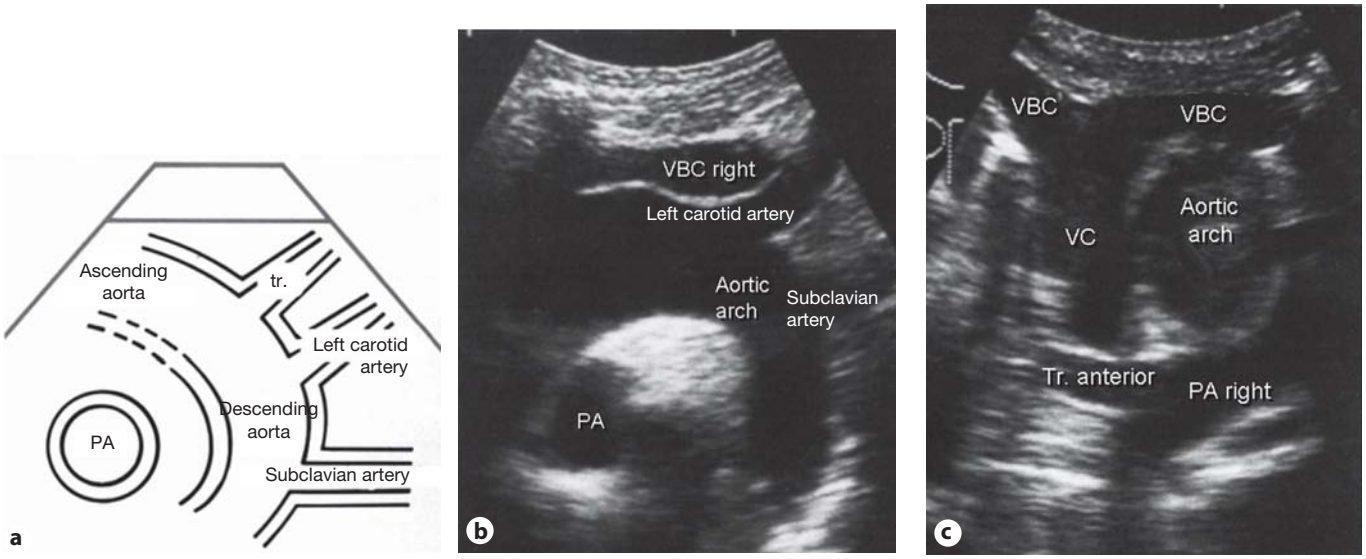

Fig. 4. a–c Suprasternal view [schematic view (**a**) and ultrasound (**b**)] of the aortopulmonary window and coronary view (**c**). PA = Pulmonary artery; Tr. anterior = anterior brachiocephalic trunk; VBC = brachiocephalic vein; VC = vena cava.

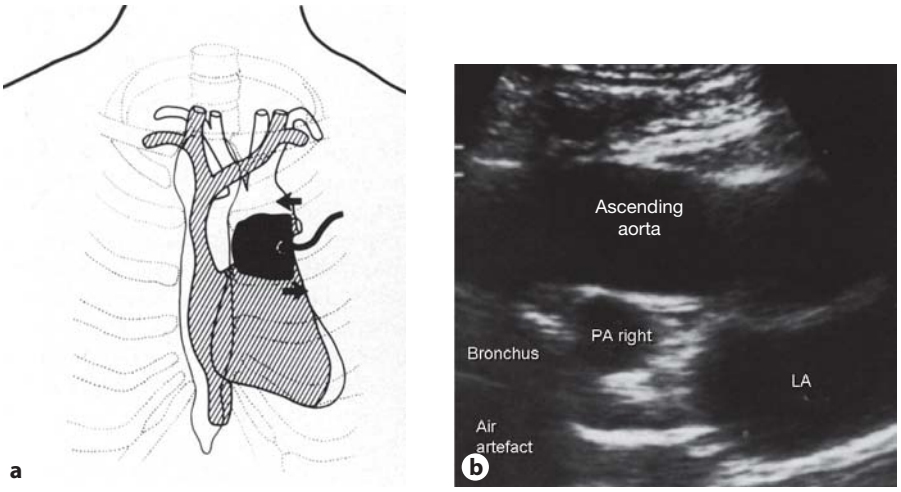

Fig. 5. a, b Parasternal examination in the left lateral position (**a**). **b** Left parasternal, sagittal section. The ascending aorta above the cross-sectional right pulmonary artery (PA right). In-between the bronchus and the left atrium (LA).

Viewing the upper mediastinum is facilitated by having the patient recline his/her head (fig. 2), ideally by cushioning the thoracic spine. Turning the head to the right and left is additionally helpful. In the right- and left-sided position described by Wernecke et al. [5] and by Brüggemann et al. [9] the mediastinum is shifted and the pulmonary cavity displaced, which permits better viewing of the mediastinum. It is easier to assess the mediastinum in expiration [10] (fig. 3a, b).

From suprasternal view the supra-aortic and paratracheal region and the aortopulmonary window can be imaged (fig. 4a–c). Here the vessels (brachiocephalic trunk, carotid artery, subclavian artery, aortic arch, superior vena cava, brachiocephalic veins, pulmonary trunk, aa. pulmonales) the thymus and the retrosternal space are visible.

From parasternal view the combined use of right-sided and left-sided lateral decubitus position permits evaluation of the anterior and mid mediastinum (fig. 5a, b, 6, 7a–c). For this purpose the transducer is placed adjacent to the sternum, cranially, and then moved caudad. Anatomical structures visualized through transverse and sagittal sections in angulated planes are again the vessels (superior vena cava, ascending aorta, right pulmonary artery, pulmonary veins, descending aorta, pulmonary trunk).

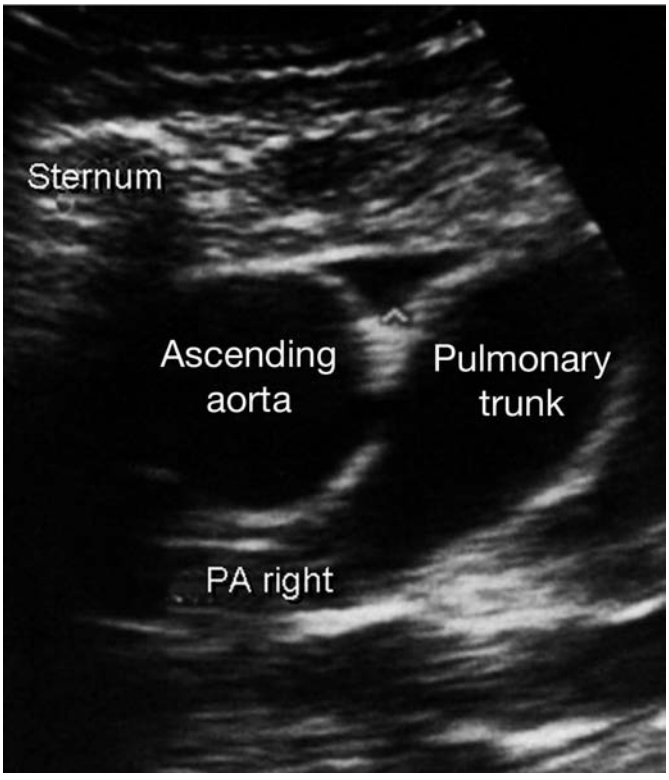

Fig. 6. Left parasternal, transversal section. The right pulmonary artery (PA right) winds around the cross-sectional ascending aorta.

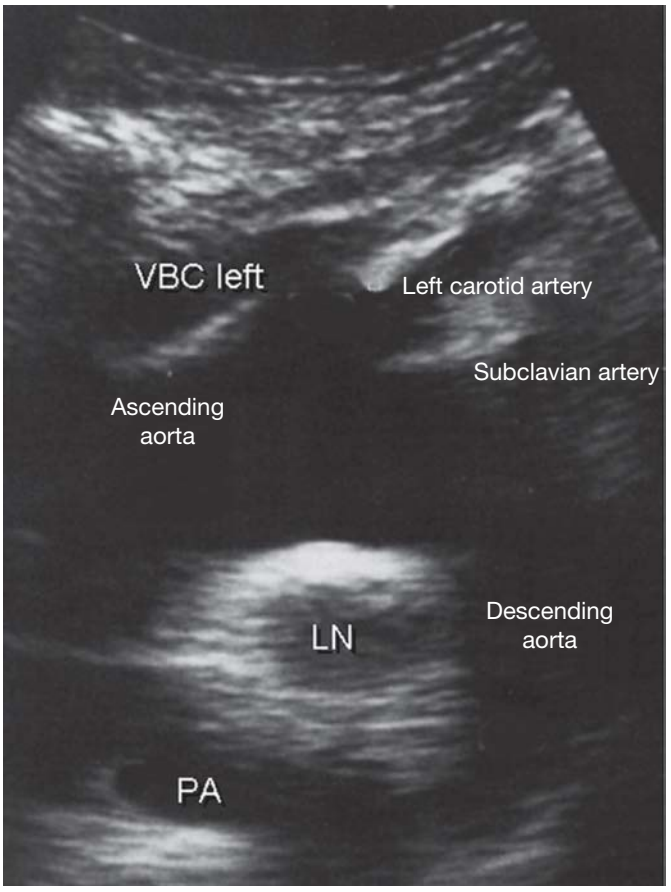

Fig. 8. Enlarged lymph node (LN) in the aortopulmonary window. VBC = Brachiocephalic vein; PA = pulmonary artery.

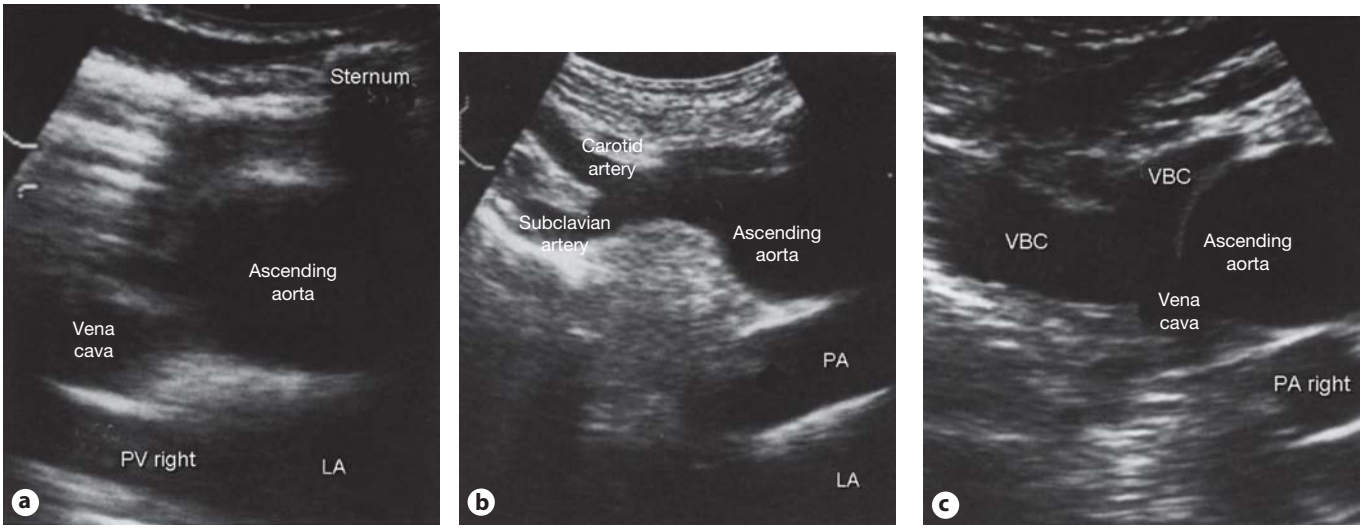

Fig. 7. a–c Parasternal examination in right lateral position. **a** Right parasternal transversel section. **b** Right parasternal half-sagittal section. The takeoff of the subclavian artery and common carotid artery is visible. **c** More caudal the brachiocephalic veins are visible. LA = Left atrium; PV right = upper lung vein; PA = pulmonary artery; VBC = brachiocephalic veins.

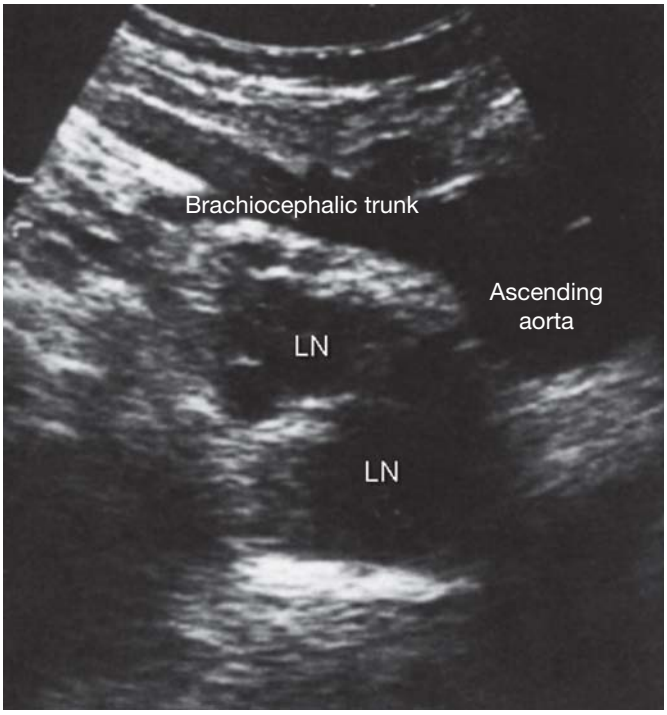

Fig. 9. Enlarged lymph nodes (LN) close to the brachiocephalic trunk in a right paratracheal half-sagittal view.

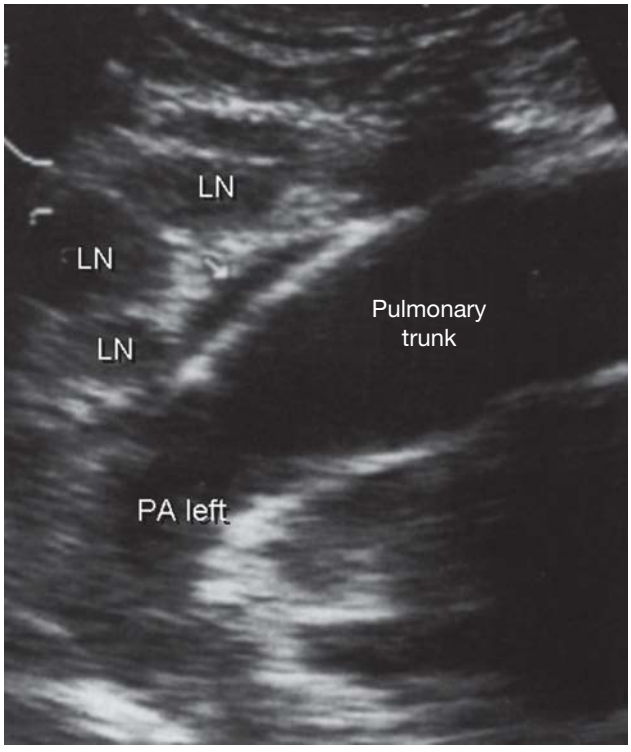

Fig. 10. Enlarged lymph nodes (LN) along the pulmonary trunk in a left paratracheal lateral view. PA left = Left pulmonary artery.

The infrasternal access only provides a limited view of caudal portions of the posterior mediastinum. The esophagus, aorta and vena cava are seen at the point where they pass through the diaphragm. Transverse and sagittal images in angulated planes are obtained through the left lobe of the liver [11].

The upper and mid mediastinum can be imaged well on sonography. The suprasternal access permits adequate evaluation in 90–95% of cases [7, 10]. The posterior mediastinum, paravertebral region, the hilum of the lung and the immediate retrosternal space, however, can only be partly assessed from a transthoracic approach. Transthoracic sonography may be severely hampered by obesity, pulmonary emphysema, mediastinal distortion as well as spinal deformities.

Indications

Sonographic investigation of the mediastinum is performed after chest radiographs have been obtained, when the findings of the latter are not distinct or if a mediastinal space-occupying mass is suspected. Sonography can be used as the first investigation procedure in cases of acute chest symptoms. The general indications for transthoracic sonography of the mediastinum are space-occupying masses in the mediastinum, tumor staging, monitoring the course of disease/therapy and punctures [12–14].

Lymph Nodes

Lymphomas account for approximately one quarter of all primary mediastinal tumors, whereas lymph node metastases of bronchial carcinomas, for instance, are more common [15].

On the basis of their hypoechoic transformation, inflamed and enlarged lymph nodes or lymph nodes invaded by tumor can be differentiated from the surrounding hyperechoic tissue (fig. 8–10).

Differentiation of the above-mentioned diseases of lymph nodes by sonography alone is not possible without biopsy.

Under treatment lymph nodes again become increasingly echogenic [4, 13]. Color Doppler sonography and, as

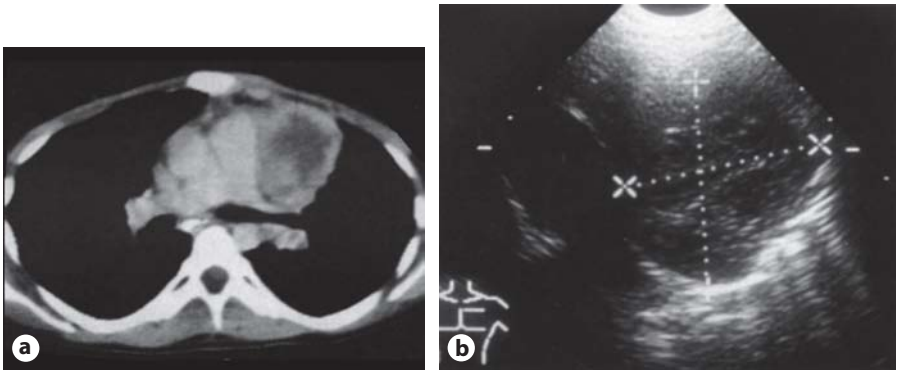

Fig. 11. Enlarged mediastinal mass in CT (**a**) and ultrasound (**b**) (marked by crosses). Areas of different echogenicity are distinguishable.

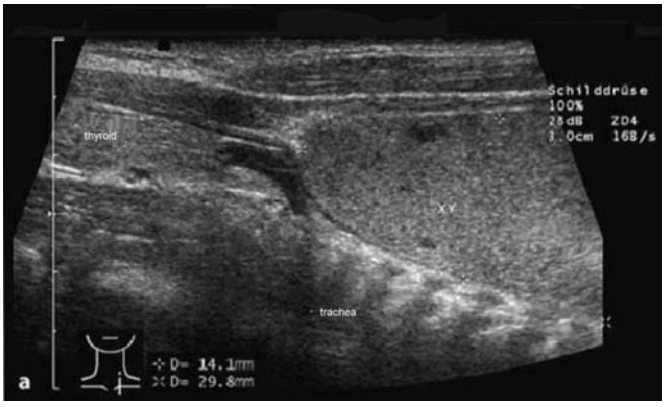

Fig. 12. Mediastinal process (marked by crosses) in a suprasternal sagittal section.

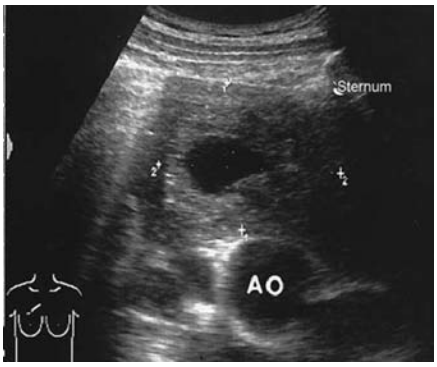

Fig. 13. Mass in parasternal, transversal section with central liquid area (margins of mass indicated by the 4). AO = Aorta.

an even more sensitive method that has recently been employed, contrast-enhanced sonography will reveal reduced blood circulation [12, 16]. With the use of high-resolution devices, normal mediastinal lymph nodes (hypoechoic) are also visualized (paratracheal, aortopulmonary window). A reliable differentiation of pathological processes, however, is not possible without obtaining bioptic material [13, 15].

Tumors

Depending on the localization in the mediastinum, different tumors are visible. The thymus is located in the anterior mediastinum, behind the sternum. In adults it cannot be distinguished from its hyperechoic surroundings. There are various malignant tumors; thymomas and lymphomas are the most common ones (more rarely, germ cell carcinoma, carcinoids and carcinomas) (fig. 11a, b). These entities can have characteristic sonographic features. The diagnosis is verified by performing a sonography-guided or computed tomography-guided biopsy [10].

Teratomas and seminomas are mostly situated in the ventral and middle part of the mediastinum, accounting for approximately 10% of primary mediastinal tumors. Teratomas usually occur in the second and third decades, grow slowly and only produce symptoms if they have grown to a large size (encroaching upon surrounding structures). These tumors are clearly delineated, contain cystic as well as epithelial structures and also tissue of mesenchymal origin (cartilage, bone, smooth muscle).

Value of Transthoracic Mediastinal US

Sonography is superior to survey radiographs of the chest in the assessment of nearly all portions of the mediastinum (with the exception of the paravertebral region). In the evaluation of supra-aortic, pericardial, prevascular and paratracheal regions, sonography has a sensitivity of 90–

100% and is nearly as reliable as computed tomography [10].

However, in the aortopulmonary window and the subcarinal region, sonography achieves a sensitivity of only 82–70% [4, 12, 13, 16]. Thus, sonography occupies an intermediary position between chest radiographs and computed tomography.

Conclusion

Mediastinal space-occupying masses are most frequently found in the anterior upper mediastinum. They can be evaluated with transthoracic sonography nearly as reliably as with computed tomography, and cytological/ histological material can usually be easily obtained by endosonography-guided puncture.

The disadvantages of sonography, however, are significant. The procedure is strongly investigator-dependent and only reveals portions of the mediastinum compared with computed tomography. Moreover, the image quality is highly variable. Some of these disadvantages can be balanced by the application of endoluminal transesophageal [see chapter 19, pp. 166–170] and endobronchial sonography [see chapter 17, pp. 153–159].

References

1 Goldberg BB: Suprasternal sonography. JAMA 1971;15:245–250.
2 Allen HD, Goldberg SJ, Sahn DJ, et al: Suprasternal notch echocardiography. Circulation 1977;55:605–612.
3 Goh TH, Venables AW: Scanning suprasternal echocardiography. Br Heart J 1980;43:148–158.
4 Wernecke K, Peters PE, Galanski M: Mediastinal tumors: evaluation with suprasternal sonography. Radiology 1986;159:405–409.
5 Wernecke K, Vassallo P, Potter R, et al: Mediastinal tumors: sensitivity of detection with sonography compared with CT and radiography. Radiology 1990;175:137–143.
6 Blank W, Schuler A, Wild K, et al: Transthoracic sonography of the mediastinum. Eur J Ultrasound 1996;3:179–190.
7 Heinzmann EK: The Mediastinum. Berlin, Springer, 1988.
8 Blank W, Braun B, Gekeler E: Ultraschalldiagnostik und Feinnadelpunktion pleuraler, pulmonaler und mediastinaler Prozesse; in Hansmann M (ed): Ultraschalldiagnostik. Berlin, Springer, 1986, pp 562–565.
9 Brüggemann A, Greie A, Lepsien G: Real-time sonography of the mediastinum in adults: a study in 100 healthy volunteers. Surg Endosc 1991;5:150–153.
10 Beckh S, Bolcskei PL, Lessnau KD: Real-time chest ultrasonography. A comprehensive review for the pulmonologist. Chest 2002;122:1759–1773.
11 Blank W, Schwaiger U, Wild K, Braun B: Die perkutane Sonographie zur Darstellung des cervicalen Ösophagus. Ultraschall Med 1998;1:4.
12 Braun B, Blank W: Sonographie von Hals und oberem Mediastinum. Internist 2005;46:1133–1145.
13 Dietrich CF, Chickakli M, Burgon I, Wehrmann T, Wiewrodt R, Buhl R, Caspary WF: Mediastinal lymph nodes demonstrated by mediastinal sonography: activity marker in patients with cystic fibrosis. J Clin Ultrasound 1999;27:9–14.
14 Herth FJF, Becker HD: Chest ultrasound; thoracic imaging; pleura mass; pleural effusion: ultrasound guidance. Respiration 2003;70:84–94.
15 Dietrich CF, Liesen M, Buhl R, Herrmann G, Kirchner I, Caspary WF, Wehrmann T: Detection of normal mediastinal lymph nodes by ultrasonography. Acta Radiol 1997;38:965–969.
16 Betsch B, Knopp MV, van Kaick G: Malignant tumors and lymphomas of the mediastinum: diagnosis and follow-up with color assisted doppler sonography. Eur J Cancer Res Clin Oncol 1992;118:107.

Prof. Felix J.F. Herth, MD, PhD, FCCP
Department of Pneumology and Critical Care Medicine
Thoraxklinik, University of Heidelberg
Amalienstrasse 5, DE–69126 Heidelberg (Germany)
Tel. +49 6221 396 1200, Fax +49 6221 396 1202, E-Mail Felix.Herth@thoraxklinik-heidelberg.de

Critical Care Applications

Chapter 7

Bolliger CT, Herth FJF, Mayo PH, Miyazawa T, Beamis JF (eds): Clinical Chest Ultrasound: From the ICU to the Bronchoscopy Suite.
Prog Respir Res. Basel, Karger, 2009, vol 37, pp 60–68

Critical Care Echocardiography

Paul H. Mayo

Division of Pulmonary, Critical Care, and Sleep Medicine, Long Island Jewish Medical Center, New Hyde Park, N.Y., USA

Abstract

Critical care echocardiography is performed and interpreted by the intensivist at the bedside in order to establish diagnosis and to guide therapy of the patient with cardiopulmonary failure. When echocardiography is used as a dynamic imaging modality, it is sufficiently different from standard echocardiography as performed by cardiologists that it warrants a separate designation: critical care echocardiography (CCE). This chapter will discuss the utility of CCE in the diagnosis and treatment of cardiopulmonary failure.

Cardiologists and intensivists deal with very different clinical challenges. Cardiology echocardiography reflects the practice interests and requirements of cardiologists. The cardiology echocardiogram is generally performed in a dedicated laboratory on an elective basis. The study is performed and interpreted as an isolated imaging event, and a report is issued by an offline reader who is often not directly involved with the clinical management of the case. This results in a double disassociation: a time delay as well as physical separation from the clinical reality at the bedside. This system works well for the challenges of clinical cardiology such as valvular heart disease, cardiomyopathy, and ischemic heart disease. In the United States, the disassociation of the physician from the patient has reached a logical endpoint; the majority of cardiology echocardiography is performed by highly skilled technicians with the physician cardiologist interpreting the scan. Because the scan is seen as a distinct complete imaging event, the cardiology approach to echocardiography will usually not include repeated echocardiography examinations performed in close sequence during a rapidly evolving clinical situation, it will not be performed at the bedside of the critically ill on an emergency basis, and it does not favor the concept of a limited or goal-directed echocardiogram.

The intensivist faces the challenge of caring for the patient with potentially life-threatening hemodynamic failure. The patient with severe cardiopulmonary failure requires immediate diagnosis and treatment. With critical care echocardiography (CCE), the approach is therefore different from that of cardiology. The scan is performed at the bedside of the patient by the clinician in immediate charge of the case. The results are interpreted and the management plan set up immediately. There is no disassociation effect. The echocardiogram is repeated as often as needed, and may be limited in scope. The concept that every study must be comprehensive is a cardiology concept; CCE favors a focused echocardiogram.

There will always be tension between the cardiology echocardiography approach and that of the intensivist performing CCE. This derives from the different clinical challenges of the two subspecialties. Cardiologists will utilize applications that relate to chronic heart disease. Intensivists will favor applications that relate to management of the patient with acute cardiopulmonary failure.

Technical Issues

CCE requires that the intensivist has immediate access to a capable echocardiography machine. For full advantage, the machine should be positioned in the intensive care unit (ICU) under complete operational control of the ICU team. Any other control option is suboptimal, as having to borrow the machine from another service is bound to cause problems and limit the utility of the technique. Fully capable cardiology echocardiography machines are large, expensive, and difficult to position at the crowded bedside of the unstable patient in the ICU. These high-end platforms are

designed for cardiology use, and have excellent 2-dimensional (2-D) image and Doppler capability. Until recently, they were the best option for the intensivist, as early-generation handheld ultrasound machines provided inadequate 2-D image and Doppler quality. This has changed with the availability of new-generation handheld units that have 2-D image quality and Doppler capability that is similar in quality to high-end cardiology machines. Some models may be equipped both for transthoracic echocardiography (TTE) and for transesophageal echocardiography (TEE). Not only are these portable units lower in cost, they are also much easier to set up at the bedside of the patient. Typically, they are mounted on a small cart, but they can be easily detached from the cart for use as a truly portable device. This allows the intensivist to carry them to the rapid response team or cardiac arrest situations outside of the ICU.

The physical principles of ultrasonography are similar regardless of the organ system under examination. The clinician must become proficient at optimizing machine settings and at transducer manipulation in order to acquire adequate images. Image acquisition requires knowledge of the physics of ultrasound and 2-D and Doppler image ultrasound artifacts; these are discussed elsewhere in this textbook. Echocardiography has special technical challenges that relate to the fact that the heart is positioned within the thorax and therefore surrounded by ribs and lung. This has relevance to TTE. Ribs block ultrasound waves. Cardiac transducers are therefore designed with a small footprint, the better to scan through the rib interspaces. If possible, the patient should be scanned with the left arm abducted, as this increases interspace size. Aerated lung blocks transmission of ultrasound, so that positioning the patient is important. The left lateral decubitus position will expose more of the heart, as it is moved out from behind the sternum and lung is shifted out of the scanning field. The supine position is favored for the subcostal view. Unfortunately, the critically ill patient may be difficult to position in an optimal scanning position. In addition, image quality may be poor in the muscular or obese patient. Patients on ventilatory support, particularly when on positive end-expiratory pressure or with emphysema, may have poor image quality due to lung hyperinflation. In this population the subcostal view is often the best image window. The presence of chest wounds, dressings, or subcutaneous air may make TTE difficult. TEE is an alternative in the difficult to image patient. Echocardiography has artifacts that relate to the fact that the heart is a highly mobile organ that is in constant motion within the thorax. Translational, torsional, and rotational movement of the heart may be misinterpreted as reflecting actual cardiac contractile function.

Levels of Competence in CCE

Competence in CCE can be separated into basic and advanced level. Basic CCE is performed as a goal-directed examination using TTE or TEE 2-D imaging. This allows the intensivist to identify characteristic echocardiographic findings and to answer specific clinical questions. Achieving competence in basic CCE is not difficult.

Competence in advanced CCE requires a high level of skill in all aspects of image acquisition and interpretation. Compared to basic CCE, advanced level competence requires extensive training. Advanced CCE allows a comprehensive evaluation of cardiac anatomy and function using TTE or TEE 2-D and Doppler echocardiography.

Basic CCE

Basic CCE has special utility in the bedside evaluation of shock. The intensivist frequently engages in an initial differential diagnosis of shock: hypovolemic, cardiogenic, obstructive, or distributive. Basic CCE allows the bedside clinician to distinguish between these primary causes of the shock state. The examination may be performed as often as mandated by the clinical situation, in order to guide therapy, to follow the evolution of disease, and to detect new problems. By definition, basic CCE is limited in scope, and therefore requires limited training. A key feature of basic CCE is that the examiner must understand their limitations. The approach requires the intensivist to assess a limited number of findings, and to seek consultation with an advanced echocardiographer when indicated. Basic CCE is often used as an initial emergency imaging modality followed by a more comprehensive examination.

The basic CCE examination includes the parasternal short axis view, the parasternal long axis view, the apical four-chamber view, the subcostal view, and the longitudinal view of the inferior vena cava (IVC) (fig. 1–5) (online suppl. videos 1–5). The examiner assesses left ventricular (LV) size Video and function, right ventricular (RV) size and function, and the presence of significant pericardial fluid (fig. 6) (online suppl. video 6). The size of the IVC is determined. Video Respiratory variation of IVC size is measured if the patient is on ventilatory support with passive ventilator patient interaction. The basic CCE examination includes inspec-

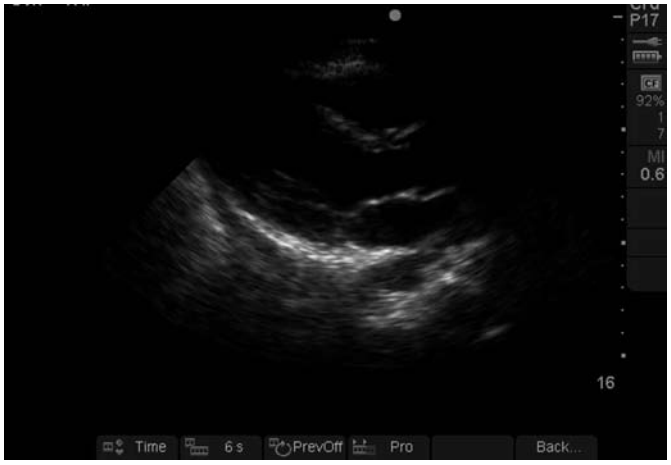

Fig. 1. Parasternal long axis view of the heart.

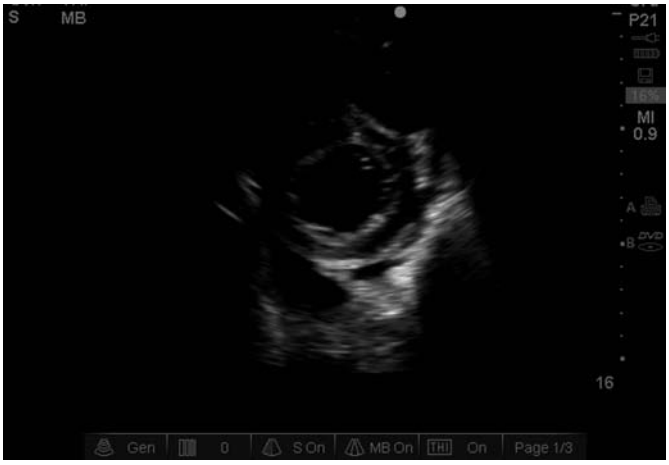

Fig. 2. Parasternal short axis view of the heart.

tion of the mitral (MV) and aortic valve (AV) (fig. 7) (online suppl. video 7) for gross anatomic abnormality. Color Doppler may be utilized to screen for severe aortic or mitral valvular regurgitation. However, the pitfalls of color Doppler may not be known to the basic level examiner (gain settings, wall jet effect, and angle effect), so that clinical suspicion of severe valvular failure requires advanced echocardiographic examination. Basic CCE does not include use of spectral Doppler. With focused basic CCE scanning approach, the examiner may quickly screen for the cause of the shock state and develop a logical management strategy. Follow-up examinations may determine the effect of therapeutic intervention and evolution of disease.

Video

Advanced CCE

Advanced CCE requires that the intensivist has a skill level that is similar to that of a cardiologist who is fully trained in echocardiography. In addition, the intensivist trained to advanced level has proficiency in ICU applications that are not commonly used by and therefore not familiar to many cardiologists.

The advanced CCE examination includes the standard 2-D views of the traditional cardiology echocardiogram [1]. These are performed in methodical sequence and include the following views: the parasternal long axis; the RV inflow and outflow; the parasternal short axis at the AV including examination of the pulmonary artery, MV and midventricular level; the apical four-, five-, two- and three-chamber view, and the subcostal long and short axis view. The suprasternal and modified subcostal pulmonary artery view may be performed if indicated. TEE is useful for imaging the aorta and posterior cardiac structures, and in any situation where TTE image quality is suboptimal. The complete 2-D study aims to assess LV and RV size and function, segmental wall function, wall thickness, valvular anatomy, the pericardial space, and other disease processes such as vegetation, thrombus, cardiac mass, or congenital heart disease. Using Simpson's method, the 2-D examination allows for quantitative measurement of stroke volume (SV) and ejection fraction.

The advanced CCE examination includes comprehensive Doppler evaluation using color, pulse wave, tissue, and continuous wave technique. Doppler analysis allows for accurate analysis of intracardiac pressures, SV, and diastolic function. Doppler study relies on the measurement of blood flow velocity in the heart and adjacent blood vessels. Through application of the simplified Bernoulli equation, blood flow velocity across valves and through cardiac chambers permits calculation of pressure gradients. Doppler measurements allow a large variety of qualitative and quantitative hemodynamic measurements to be made with both TEE and TTE. Some Doppler measurements that are of special interest to the intensivist utilizing CCE are as follows.

Quantitative SV: Measurement of SV allows calculation of indexed SV, cardiac output, and other standard derived values. It is a key aspect of determination of preload sensitivity (discussed below).

Qualitative estimate of pulmonary artery occlusion pressure (PAOP): Doppler analysis of MV and pulmonary venous inflow in combination with tissue Doppler of the mitral annulus yields estimated PAOP [2, 3].

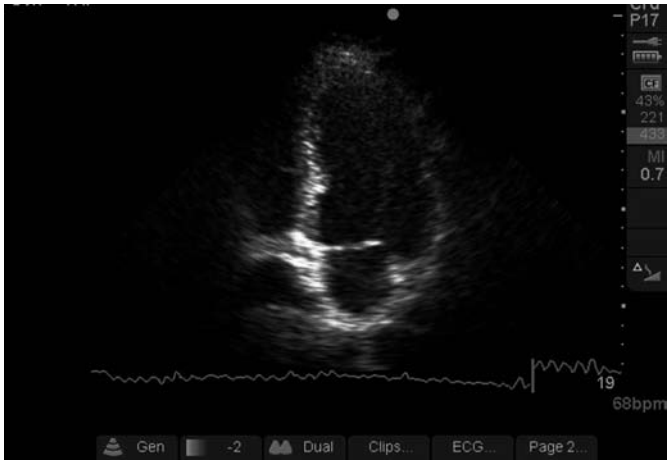

Fig. 3. Apical four-chamber view of the heart.

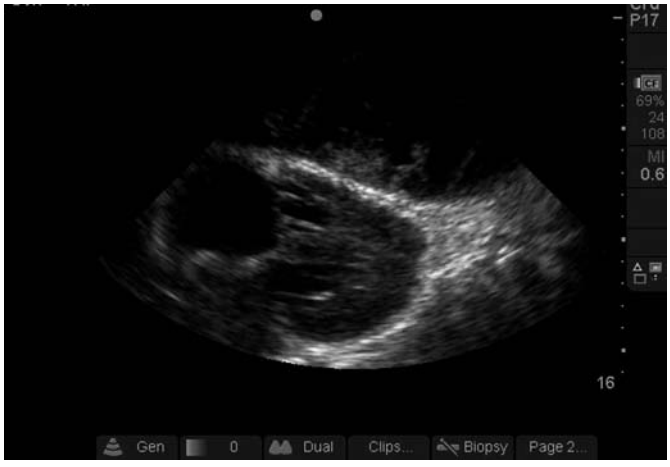

Fig. 4. Subcostal long axis view of the heart. Ascites is present.

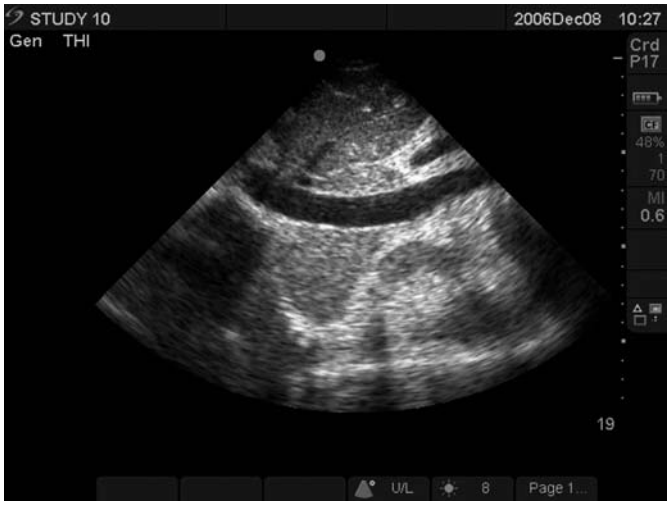

Fig. 5. Longitudinal view of the IVC.

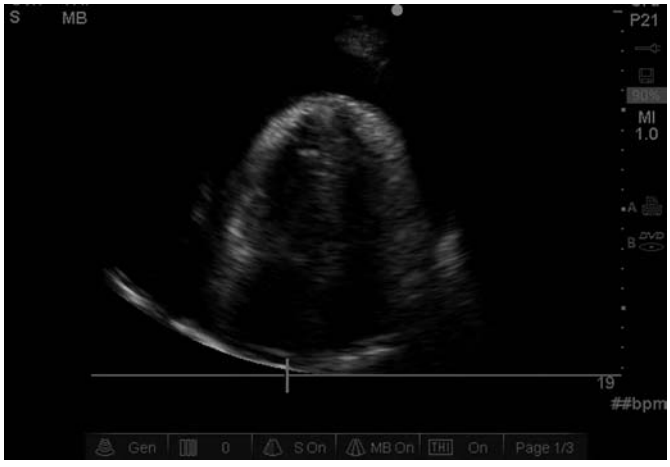

Fig. 6. Apical four-chamber view of the heart. There is a large pericardial effusion.

Quantitative measurement of valvular regurgitation and stenosis: Measurement of vena contracta, application of the continuity principle, and use of the proximal isovelocity method are standard advanced CCE techniques that allow the intensivist to quantitate valvular dysfunction.

Measurement of diastolic dysfunction: Both LV and RV diastolic function may be assessed by analysis of MV and pulmonary venous and tricuspid and hepatic venous inflow, respectively. These measurements may be complemented by tissue Doppler of the relevant annulus [4, 5].

Measurement of intracardiac pressures: The presence of even a small degree of valvular regurgitation or stenosis allows measurement of a transvalvular gradient using the simplified Bernoulli equation. This principle is useful in measurement of many intracardiac pressures such as measurement of pulmonary artery systolic pressure.

Identification of LV outflow obstruction: Doppler examination, showing a late peaking high velocity outflow pattern, may confirm what is suspected on 2-D examination.

Measurement of RV and LV Dp/Dt if tricuspid or mitral regurgitation is present [6, 7].

Diagnosis of pericardial constriction and tamponade: Analysis of mitral, pulmonary venous, tricuspid, and hepatic venous inflow patterns permits diagnosis of these problems.

The intensivist with advanced CCE training has, by definition, capability to perform a sophisticated assessment of cardiac function at the same level as the cardiology echocardiographer. Should a complete echocardiogram

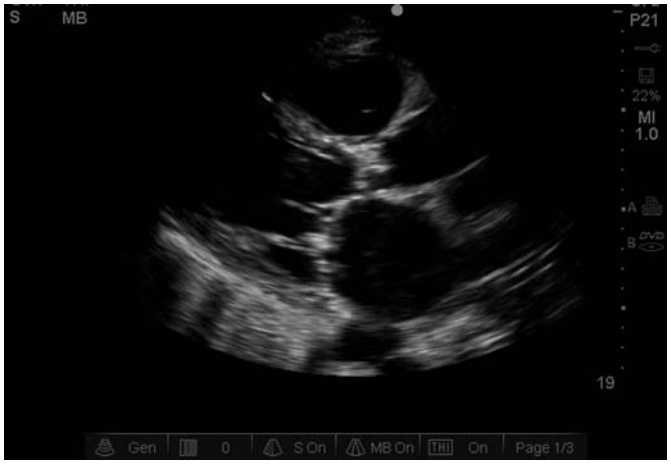

Fig. 7. Parasternal long axis view of the heart. The AV is heavily calcified consistent with aortic stenosis.

constitute every examination? Training in advanced CCE encourages a flexible approach. When clinically indicated, a complete examination may be required. A limited goal-directed examination may be all that is needed or practical. Advanced CCE capability gives the intensivist both options.

Training in CCE

In the United States, there is no clearly defined training pathway that is specific to CCE. Advanced CCE requires extensive training. At present, the best approach is for the intensivist to fulfill requirements for level 2 competence as defined by the American College of Cardiology/American College of Cardiology (ACC/AHA) Clinical Competence Statement on Echocardiography [8]. The National Board of Echocardiography (NBE) has defined an alternative pathway that is not open to intensivists, unless they have completed cardiology fellowship training. The NBE has developed a board-type examination that is a requirement to obtain NBE certification. The examination is open to any licensed physician, and is not a requirement for level 2 competence by ACC/AHA standard. It is therefore optional for the intensivist who wishes to follow ACC/AHA recommendations. Many cardiologists choose not to take the examination. Precisely because it is optional, the motivated intensivist demonstrates a serious commitment to the field by taking the examination.

In contrast to the United States, the French critical care community has developed a comprehensive training sequence that results in specific certification in advanced CCE. This requires the intensivist to undergo training in echocardiography during fellowship training over a 2-year period. The first year of training is shared with cardiology fellows, whereas the second year takes place in fellowship training programs that are specifically certified to provide training in advanced CCE. Training includes both TTE and TEE. Performance of 220 TTE is required. The trainee must then pass a board style examination that is specific to CCE in order to be certified in advanced CCE. The French system is an excellent model that will need to be emulated in other countries. There is serious effort being made in the United States to develop training in CCE that will lead to formal certification. Any result is still several years away.

For training in basic level CCE, there is no widely accepted standard to follow. The ACC/AHA statement defines a level 1 competence, but this does not address the requirements of basic level CCE. Level 1 competence occurs on a continuum that will eventually result in level 2 competence in echocardiography so that it includes training in aspects of Doppler and 2-D imaging that is not required for basic level CCE.

Specific Suggestions for Training in Advanced CCE

The knowledge base required for advanced CCE is large and requires a major time commitment. I strongly recommend two entry level English language textbooks [9, 10]. It is also useful to review a more comprehensive text of recent publication [11]. Programmed problem-orientated texts are useful for Doppler training. A good quality anatomic heart model is helpful as well (Denoyer-Geppert, Chicago, Ill., USA). An existing comprehensive DVD-based training program is an excellent basis for training in basic CCE, and is also useful for some elements of advanced CCE training [12].

The trainee needs to personally perform a large number of echocardiographic examinations, as a high level of skill in image acquisition is an essential component of advanced CCE. Unlike cardiologists, the intensivist must be skilled in all aspects of bedside imaging so that the number of examinations required by the ACC/AHA statement to achieve level 2 competence (150 TTE) should be regarded as minimal standard for the clinician training in advanced CCE.

Proficiency in image interpretation requires reviewing a large number of studies under the direct supervision of a capable teaching echocardiographer. Cardiology fellows spend many hours of attendance in the echocardiogram

reading room with a senior reader to guide their training. The intensivist must do the same. The skill is not amenable to an autodidactic approach. From a practical point of view, training is best achieved during the fellowship period. In the United States, this can be accomplished by the fellow during elective periods. Goodwill being present, the fellow who is interested in advanced CCE can arrange to enter the same echocardiology training sequence as followed by cardiology fellows at their institution.

An important question is whether every intensivist should seek training in advanced CCE. Competence in basic CCE should be a required component of general critical care ultrasonography, given its clinical utility and ease of training. It is also clear that advanced level training is not required for most intensivists. The decision to pursue training in advanced training will be predicated upon the interest level and practice requirements of the clinician. For a large group of full-time intensivists providing service to a busy ICU service, there is strong logic to having a few team members with training to advanced level, while having all team members proficient in basic CCE.

Clinical Applications of CCE

Assessment of Preload Responsiveness

Whether to give volume resuscitation to the patient in shock is a regular question in the ICU. It may benefit some patients (sepsis [13], hypovolemia of other types), but may be harmful to others (acute cor pulmonale, dilated cardiomyopathy). In addition, once the decision has been made to proceed with volume resuscitation, it is important to know when adequate volume has been given to the patient. Fluid accumulation is associated with poor outcome in the ICU [14, 15]. CCE allows determination of preload sensitivity before the volume challenge is given to the patient as well as of answering the question as to whether the system requires continued volume resuscitation.

Basic CCE has some limited ability to identify the patient with hemodynamic failure who is preload sensitive. Lacking Doppler skills, the examiner is limited to measurement of respiratory variation of IVC size in the patient who is completely passive while on ventilatory support. Preload sensitivity may be tested in patients who are on mechanical ventilatory support providing the patient is not making any respiratory effort in several ways. An inspiratory to expiratory variation of IVC variation $>12\%$ (maximum diameter – minimum diameter divided by their mean) correlates with volume responsiveness [16]. Qualitatively, an IVC <1 cm in a hypotensive patient generally indicates preload responsiveness [Slama, pers. commun.]. Respiratory variation of superior vena cava size is also a valuable method of determining preload sensitivity with TEE but is limited by the same constraints [17]; greater than 36% change in superior vena cava diameter between inspiration and expiration indicates a high probability of response in cardiac output to volume infusion.

Advanced CCE methods permit more sophisticated methods for determination of preload sensitivity in patients who are breathing spontaneously, triggering the ventilator, or while passive on the ventilator. Initial studies examined the effect of ventilator cycling on beat by measurement of SV measured by analysis of Doppler flow in the descending aorta [18], or at the level of the LV outflow. The method is limited to patients who are fully adapted to the mechanical ventilator and is related conceptually to measurement of the variation in pulse pressure measured with an arterial line. The results indicate that variation in SV of $<12\%$ is strongly correlated with volume preload sensitivity. Several recent studies have reported on passive leg raising as a prompt but reversible internal volume challenge while measuring SV and cardiac output using Doppler technique [19–22]. These studies report that an increase in cardiac output of $<10\%$ following passive leg raising is strongly correlated with volume responsiveness. This is a particularly interesting result as it works with patients who are breathing spontaneously, triggering the ventilator, or with atrial fibrillation. All previous methods have been limited to patients who are in sinus rhythm and passive in their interaction with the ventilator.

Normal individuals are preload sensitive. All of the tests of volume sensitivity are only clinically relevant if the patient is in shock. It is obvious that the patient with normal perfusion status who is preload sensitive by echocardiographic criteria should not receive volume resuscitation.

Diagnosis of Shock

Basic CCE has utility in identifying the category of shock by assessing the size and function of the LV and RV, the pericardial space, and preload responsiveness. Based on straightforward echocardiographic findings, the clinician may decide on volume resuscitation, pressors, inotropes, treatment directed at acute cor pulmonale, or pericardial drainage. Serial studies permit assessment of the effect of therapy and further management decision. Limited, goal-directed TTE and TEE have been reported to have clinical utility [23, 24].

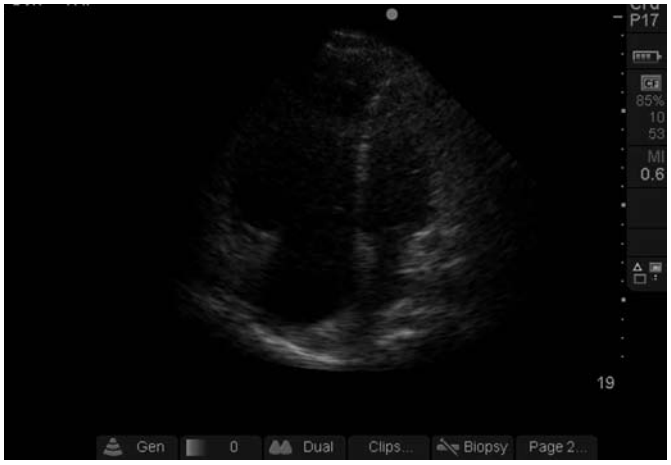

Fig. 8. Apical four-chamber view of the heart. The right ventricle is dilated.

Advanced CCE allows more complete assessment and differentiation of the cause of shock. A pericardial effusion with diastolic collapse of the right ventricle, systolic collapse of the right atrium, and <25% inspiration decrement of MV inflow (in spontaneously breathing patients only) suggests tamponade physiology [25–27]. A dilated heart with decreased LV systolic function in a hypotensive patient is consistent with the diagnosis of cardiogenic shock (online suppl. video 8). Myocardial ischemia results in segmental wall motion abnormality with involvement of specific segments corresponding to specific coronary arteries. Valvular abnormalities may cause shock. Severe AV or MV stenosis may complicate hemodynamic failure from other cause, or result in shock as a primary event. Mitral apparatus failure (ruptured chordae or papillary muscle resulting in a flail leaflet) (online suppl. video 9) or severe damage to the AV (online suppl. video 10) are both associated with severe valvular regurgitation. Quantitative measurement of valve function is a routine matter for the pulmonary critical care medicine (PCCM) clinician trained in advanced level CCE. Acute cor pulmonale may be caused by acute pulmonary embolism or acute respiratory distress syndrome, and is diagnosed by the presence of dilatation (RV end-diastolic area/LV end-diastolic area >1) and dyskinesia of the interventricular septum [28] (fig. 8) (online suppl. video 11). An RV myocardial infarction causes RV dilatation with decreased endomyocardial thickening of the RV free wall and the inferior wall of the LV. Depending on preload conditions and contractile function, vasodilatory shock is associated with an LV of normal, decreased or enlarged size with varying contractile function. Severe LV outflow obstruction may cause shock. Echocardiographic findings include a late peaking dagger-shaped intracavitary spectral Doppler signal that is often measured in midventricle in conjunction with a hyperdynamic LV function.

Monitoring

Echocardiography is a useful monitoring tool. Following the initial diagnostic examination, the intensivist may use it in serial fashion to observe response to therapy and to follow evolution of disease. Follow-up examinations are often limited in scope. Following initiation of volume resuscitation or inotropic support, repeat study is useful to check for effect and to guide continued therapy. LV dysfunction often occurs with sepsis. This warrants serial echocardiography in order to guide the use of inotropic agents and volume resuscitation, as well as to observe for improvement during the course of the illness. An echocardiogram demonstrating severe LV dysfunction in a patient with sepsis may label the patient with this diagnosis indefinitely. A repeat study may show complete recovery of LV function following treatment of the sepsis. Serial echocardiography is useful with acute cor pulmonale, in order to assess response to treatment. Preload responsiveness does not need to be based on a single assessment; echocardiography may be repeated to assess for continued need for volume resuscitation.

Acute Respiratory Failure

Echocardiography allows assessment of the causes of respiratory failure that are related to cardiac dysfunction. Cardiac dysfunction causing hydrostatic pulmonary edema must always be considered in the patient with respiratory failure. Cardiogenic pulmonary edema may occur with normal systolic function (diastolic dysfunction pattern). Both TTE and TEE allow Doppler measurements of MV inflow, pulmonary venous inflow, and annular function that yield qualitative estimates of PAOP [29–32]. This may be helpful in determining whether respiratory failure is related to hydrostatic pulmonary edema.

Code Team and Rapid Response Team Function

Recent generation portable hand-carried ultrasound units now have very high-quality 2-D image and Doppler capability. Both basic and advanced CCE echocardiography may now be performed immediately by the ultrasound equipped rapid response team. Likewise, echocardiography may be integrated into cardiac arrest team function. For example, a subcostal view is possible with minimal interruption of chest compressions. Other views may be obtained very rapidly, in

the immediate postresuscitation period. A limited echo examination can change management during cardiopulmonary resuscitation: a large pericardial effusion, an intracavitary thrombus, an acute cor pulmonale pattern, a flail leaflet, or continued cardiac contractions with absent pulse or blood pressure are diagnoses that have a potentially lifesaving therapeutic response. Echocardiography also may identify patients where continued cardiopulmonary resuscitation will not be successful [33] (online suppl. video 12).

Video

Procedural Guidance

Echocardiography allows for safe drainage of pericardial effusion [34]. It may be useful to guide insertion of transvenous pacermaker or pulmonary artery catheter.

TEE

Many groups have reported on the clinical utility and safety of TEE in critically ill patients [35–44]. Proficiency in TEE is therefore a desirable component of advanced CCE. In the United States, it is still uncommon for intensivists to have access and therefore competence with TEE. In some countries in Europe, this is not the case. In general, TEE is useful when TTE image quality is inadequate to answer the clinical question. This may occur predictably in certain patient populations such as the massively obese, those with chest wounds or dressings, and patients on high levels of positive end-expiratory pressure. Posterior structures of the heart are particularly well imaged with TEE. The use of TEE is mandatory in situations where a detailed view of posterior structures is required. The left atrium and its appendage, the pulmonary veins, the intra-atrial septum, the proximal pulmonary arteries, and the descending aorta are all well visualized with TEE. Reliable evaluation for endocarditis may require TEE. Pulmonary embolism may be visualized in the proximal pulmonary arteries [45–47]. Typically, the intensivist will perform TEE in patients who are already on ventilatory support, so that the risk of the procedure is low. The transducer is easy to introduce, particularly if done under direct visualization using a standard intubation laryngoscope. Transducer manipulation, image acquisition, and image interpretation are straightforward and are in some ways less challenging than TTE. North American intensivists are encouraged to acquire TEE skills.

Conclusion

Echocardiography has major application in the ICU. It allows rapid diagnosis and management of the critically ill patient with cardiopulmonary failure. The frontline intensivist is best positioned to acquire and interpret the images at the bedside of the patient and to immediately integrate this information into the overall management strategy. Whether the intensivist chooses to develop proficiency in basic or advanced level CCE depends on their practice needs. Either way, competence in CCE gives the intensivist a powerful and flexible tool of great utility in the ICU.

References

1 Henry WL, DeMaria A, Gramiak R, King DL, et al: Report of the American Society of Echocardiography Committee on the nomenclature and standards in two-dimensional echocardiography.1980. http://asecho.org/Guidelines_Documents/body_guidelines_and _documents.php (accessed March 8, 2004).

2 Ommen SR, Nishimura RA, Appleton CP, Miller FA, et al: Clinical utility of Doppler echocardiography and tissue Doppler imaging in the estimation of left ventricular filling pressures: a comparative simultaneous Doppler-catheterization study. Circulation 2000;102:1788–1794.

3 Appleton CP, Galloway JM, Gonzalez MS, Gaballa M, et al: Estimation of left ventricular filling pressures using two-dimensional and Doppler echocardiography in adult patients with cardiac disease: additional value of analyzing left atrial size, left atrial ejection fraction and the difference in duration of pulmonary venous and mitral flow velocity at atrial contraction. J Am Coll Cardiol 1993;22:1972–1982.

4 Khouri SJ, Maly GT, Suh DD, Walsh TE: A practical approach to the echocardiographic evaluation of diastolic function. J Am Soc Echocardiogr 2004;17:290–297.

5 Garcia MJ, Thomas JD, Klein AL: New Doppler echocardiographic applications for the study of diastolic function. J Am Coll Cardiol 1998;32:865–875.

6 Imanishi T, Nakatani S, Yamada S, Nakanishi N, et al: Validation of continuous wave Doppler-determined right ventricular peak positive and negative dP/dt: effect of right atrial pressure on measurement. J Am Coll Cardiol 1994;23:1638–1643.

7 Chung N, Nishimura RA, Holmes DR Jr, Tajik AJ: Measurement of left ventricular dp/dt by simultaneous Doppler echocardiography and cardiac catheterization. J Am Soc Echocardiogr 1992;5:147–152.

8 Quinones MA, Douglas PS, Foster E, Gorcsan J 3rd, et al: ACC/AHA clinical competence statement on echocardiography. J Am Coll Cardiol 2003;41:687–708.

9 Oh JK, Seward JB, Tajik JA: The Echo Manual, ed 3. Philadelphia, Lippincott Williams & Wilkins, 2007.

10 Otto CM: Textbook of Clinical Echocardiography, ed 3. Philadelphia, Saunders, 2004.

11 Feigenbaum H, Armstrong WF, Ryan T: Echocardiography, ed 6. Philadelphia, Lippincott Williams & Wilkins, 2007.

12 Beaulieu Y: The focused cardiac ultrasound study. Beaulieu Y, producer. Ontario, ICU Imaging Inc., 2008. 6 DVD, 8 hours, sound, color, DVD format.

13 Rivers E, Nguyen B, Havstad S, Ressler J, Muzzin A, Knoblich B, Peterson E, Tomlanovich M: Early goal-directed therapy in the treatment of severe sepsis and septic shock. N Engl J Med 2001;345:1368–1373.

14 National Heart, Lung, and Blood Institute Acute Respiratory Distress Syndrome (ARDS) Clinical Trials Network: Comparison of two fluid-management strategies in acute lung injury. N Engl J Med 2006;354:2564–2575.

15 Durairaj L, Schmidt GA: Fluid therapy in resuscitated sepsis: less is more. Chest 2008;133:252–263.
16 Barbier C, Loubières Y, Schmit C, Hayon J, Ricôme JL, Jardin F, et al: Respiratory changes in inferior vena cava diameter are helpful in predicting fluid responsiveness in ventilated septic patients. Intensive Care Med 2004;30:1740–1746.
17 Vieillard-Baron A, Chergui K, Rabiller A, Peyrouset O, Page B, Beauchet A, Jardin F: Superior vena caval collapsibility as a gauge of volume status in ventilated septic patients. Intensive Care Med 2004;30:1734–1739.
18 Feissel M, Michard F, Mangin I, Ruyer O, Faller JP, Teboul JL: Respiratory changes in aortic blood velocity as an indicator of fluid responsiveness in ventilated patients with septic shock. Chest 2001;119:867–873.
19 Monnet X, Rienzo M, Osman D, Anguel N, Richard C, Pinsky MR, et al: Passive leg raising predicts fluid responsiveness in the critically ill. Crit Care Med 2006;34:1402–1477.
20 Lafanechère A, Pène F, Goulenok C, Delahaye A, Mallet V, Choukroun G, et al: Changes in aortic blood flow induced by passive leg raising predict fluid responsiveness in critically ill patients. Crit Care 2006;10:R132.
21 Lamia B, Ochagavia A, Monnet X, Chemla D, Richard C, Teboul JL: Echocardiographic prediction of volume responsiveness in critically ill patients with spontaneously breathing activity. Intensive Care Med 2007;33:1125–1132.
22 Maizel J, Airapetian N, Lorne E, Tribouilloy C, Massy Z, Slama M: Diagnosis of central hypovolemia by using passive leg raising. Intensive Care Med 2007;33:1133–1138.
23 Benjamin E, Griffin K, Leibowitz AB, Manasia A, Oropello JM, et al: Goal-directed transesophageal echocardiography performed by intensivists to assess left ventricular function: comparison with pulmonary artery catheterization. J Cardiothorac Vasc Anesth 1998;12:10–15.
24 Manasia AR, Nagaraj HM, Kodali RB, Croft LB, Oropello JM, Kohli-Seth R, Leibowitz AB, DelGiudice R, Hufanda JF, Benjamin E, Goldman ME: Feasibility and potential clinical utility of goal-directed transthoracic echocardiography performed by noncardiologist intensivists using a small hand-carried device (SonoHeart) in critically ill patients. J Cardiothorac Vasc Anesth 2005;19:155–159.
25 Armstrong WF, Schilt BF, Helper DJ, Dillon JC, Feigenbaum H: Diastolic collapse of the right ventricle with cardiac tamponade: an echocardiographic study. Circulation 1982;65:1491–1496.
26 Gillam LD, Guyer DE, Gibson TC, King ME, Marshall JE, Weyman AE: Hydrodynamic compression of the right atrium: a new echocardiographic sign of cardiac tamponade. Circulation 1983;68:294–301.
27 Appleton CP, Hatle LK, Popp RL: Cardiac tamponade and pericardial effusion: respiratory variation in transvalvular flow velocities studied by Doppler echocardiography. J Am Coll Cardiol 1988;11:1020–1030.
28 Vieillard-Baron A, Prin S, Chergui K, Dubourg O, et al: Echo-Doppler demonstration of acute cor pulmonale at the bedside in the medical intensive care unit. Am J Respir Crit Care Med 2002;166:1310–1319.
29 Giannuzzi P, Imparato A, Temporelli PL, De Vito F, Silva PL, Scapellato F, et al: Doppler-derived mitral deceleration time of early filling as a strong predictor of pulmonary capillary wedge pressure in postinfarction patients with left ventricular systolic dysfunction. J Am Coll Cardiol 1994;23:1630–1637.
30 Boussuges A, Blanc P, Molenat F, Burnet H, Habib G, Sainty JM: Evaluation of left ventricular filling pressure by transthoracic Doppler echocardiography in the intensive care unit. Crit Care Med 2002;30:362–367.
31 Rossvoll O, Hatle LK: Pulmonary venous flow velocities recorded by transthoracic Doppler ultrasound: relation to left ventricular diastolic pressures. J Am Coll Cardiol 1993;21:1687–1696.
32 Vargas F, Gruson D, Valentino R, Bui HN, Salmi LR, Gilleron V, et al: Transesophageal pulsed Doppler echocardiography of pulmonary venous flow to assess left ventricular filling pressure in ventilated patients with acute respiratory distress syndrome. J Crit Care 2004;19:187–197.
33 Shoenberger JM, Massopust K, Henderson SO: The use of bedside ultrasound in cardiac arrest. Western J Emerg Med 2007;2:246–250.
34 Tsang TM, Enriquez-Sarano M, Freeman WK, Barnes ME, Sinak LJ, Gersh BJ, Bailey KR, Seward JB: Consecutive 1127 therapeutic echocardiographically guided pericardiocenteses: clinical profile, practice patterns, and outcomes spanning 21 years. Mayo Clin Proc 2002;77:429–436.
35 Pearson AC, Castello R, Labovitz AJ: Safety and utility of transesophageal echocardiography in the critically ill patient. Am Heart J 1990;119:1083–1089.
36 Pavlides GS, Hauser AM, Stewart JR, O'Neill WW, et al: Contribution of transesophageal echocardiography to patient diagnosis and treatment: a prospective analysis. Am Heart J 1990;120:910–914.
37 Foster E, Schiller NB: The role of transesophageal echocardiography in critical care: UCSF experience. J Am Soc Echocardiogr 1992;5:368–374.
38 Hwang JJ, Shyu KG, Chen JJ, Tseng YZ, Kuan P, et al: Usefulness of transesophageal echocardiography in the treatment of critically ill patients. Chest 1993;104:861–866.
39 Vignon P, Mentec H, Terre S, Herve G, et al: Diagnostic accuracy and therapeutic impact of transthoracic and transesophageal echocardiography in the mechanically ventilated patients in the ICU. Chest 1994;106:1820–1834.
40 Khoury AF, Afridi I, Quinones MA, Zoghbi WA: Transesophageal echocardiography in critically ill patients: feasibility, safety, and impact on management. Am Heart J 1994;127:1363–1371.
41 Alam M: Transesophageal echocardiography in critical care units: Henry Ford Hospital experience and review of the literature. Prog Cardiovasc Dis 1996;38:315–328.
42 Slama MA, Novara A, Van de Putte P, Diebold B, et al: Diagnostic and therapeutic implications of transesophageal echocardiography in medical ICU patients with unexplained shock, hypoxemia, or suspected endocarditis. Intensive Care Med 1996;22:916–922.
43 Poelaert J, Schmidt C, Colardyn F: Transoesophageal echocardiography in the critically ill. Anaesthesia 1998;53:55–68.
44 Colreavy FB, Donovan K, Lee KY, Weekes J: Transesophageal echocardiography in critically ill patients. Crit Care Med 2002;30:989–996.
45 Liebson PR: Transesophageal echocardiography in critically ill patients: what is the intensivist's role? Crit Care Med 2002;30:1165–1166.
46 Pruszcyk P, Torbicki A, Pacho R, Maciej C, et al: Noninvasive diagnosis of suspected severe pulmonary embolism: transesophageal echocardiography vs spiral CT. Chest 1997;112:722–728.
47 Vieillard-Baron A, Qanadli SD, Antakly Y, Fourme T, et al: Transesophageal echocardiography for the diagnosis of pulmonary embolism with acute cor pulmonale: a comparison with radiological procedures. Intensive Care Med 1998;24:429–433.

Paul H. Mayo, MD
Long Island Jewish Medical Center
Division of Pulmonary, Critical Care, and Sleep Medicine
410 Lakeville Road
New Hyde Park, NY 11040 (USA)
Tel. +1 718 470 7827
E-Mail mayosono@gmail.com

Chapter 8

Bolliger CT, Herth FJF, Mayo PH, Miyazawa T, Beamis JF (eds): Clinical Chest Ultrasound: From the ICU to the Bronchoscopy Suite.
Prog Respir Res. Basel, Karger, 2009, vol 37, pp 69–75

Use of Ultrasound for Central Venous Access

Brian Garibaldi · David Feller-Kopman

Division of Pulmonary and Critical Care Medicine, The Johns Hopkins Hospital, Baltimore, Md., USA

Abstract

The use of ultrasound to guide central venous access has been suggested as one of the most important measures we can incorporate into our daily practice to improve patient safety. Though many physicians have embraced this recommendation, up to 41% do not agree that ultrasound guidance should be the standard of care for placement of central venous catheters in the internal jugular vein. This likely stems from a lack of knowledge of the relevant data as well as unfamiliarity with the technique. This chapter will review the evidence supporting ultrasound guidance for central venous access, review the technique, and suggest a program to allow for sufficient training.

Central venous catheterization is an essential component of the care of hospitalized patients. There are a number of indications for central line placement including hemodynamic monitoring, frequent blood draws, difficult peripheral access, urgent hemodialysis, parenteral nutrition, vasopressor support and long-term chemotherapy or antibiotic administration. More than 5 million central venous catheters (CVCs) are placed in the USA each year with an estimated complication rate of >15% [1, 2]. Mechanical complications such as pneumothorax or arterial puncture have been reported to be as high as 21%, and in some series more than 35% of attempts are unsuccessful [3, 4]. Factors that affect the complication and success rate include operator experience, urgency of placement and patient factors such as body habitus, prior difficult cannulation or coagulopathy [4–6].

Recent evidence suggests that placement of CVCs under ultrasound (US) guidance increases 1st-pass and overall success rate while decreasing complications. In the adult literature, there have been nine randomized trials (table 1) [7–15] as well as two meta-analyses [16, 17] that support the use of US guidance for the placement of internal jugular (IJ) CVCs. These data led both the Agency for Healthcare Research and Quality in the USA, and the National Institute of Clinical Excellence in the UK, to recommend the use of US guidance for CVC insertion [18, 19]. Many health care professionals consider US guidance for CVC insertion the standard of care, especially when used for the IJ vein position.

This chapter will review the technique of US central venous catheterization as it pertains to the IJ, subclavian (SC) and femoral vein sites. We will also provide recommendations for incorporating US training and use into daily clinical practice. The use of US for peripheral vein cannulation or for peripherally inserted central catheters is beyond the scope of this review.

Basic Physics of US Imaging

'Ultrasound' refers to sound with a frequency greater than 20 kHz (i.e. above the range of audible sound for humans). For the purposes of medical imaging the frequency used is generally between 3 and 20 MHz. There are several reviews describing the basic physics of US imaging. Briefly, an US pulse is generated by applying a voltage to piezoelectric crystals in the probe. The pulse is then directed into the tissue which reflects the sound back towards the probe. The reflected sound waves are then processed as an audio or visual signal. Doppler US transforms the sound waves from a moving object (i.e. red blood cells) into an amplified audio signal. The venous waveform is sufficiently distinct from the arterial waveform to allow localization of the central veins from arteries. For vascular access, Doppler US has been shown associated with a longer learning curve, takes

Table 1. Placement of CVCs under US guidance: nine randomized trials

Authors	n	Success, %		1st attempt, %		Time, s		Carotid puncture, %	
		US	landmark	US	landmark	US	landmark	US	landmark
Mallory et al., 1990 [7]	29	100	65	58	41				
Troianos et al., 1991 [8]	160	100	96	73	54	61	117	1	8
Denys et al., 1993 [9]	1,230	100	88	78	38	9.8	44.5	2	8
Slama et al., 1997 [10]	79	100	76	43	26	95	235	14	12
Teichgraber et al., 1997 [11]	100			96	52	15	51	0	12
Nadig et al., 1998 [12]	65	100	65		204	288	0	0	
Hayashi and Amano, 2002 [13]	188 (RVD)	97	96	86	84				
	52 (no RVD)	100	78	86	30			0	13
Leung et al., 2006 [15]	130	94	79	82	71				
Karakitsos et al., 2006 [14]	900	100	94			17	44	1.1	10.6

RVD = Respiratory venodilation.

longer to use for CVC insertion and is associated with a higher cost. As a result, Doppler guidance has been abandoned in favor of B-mode imaging. B-mode US (brightness mode) converts the reflected sound waves into a real-time grey scale image. Fluid (i.e. blood) is hypoechoic, and appears dark on the screen, while tissue is more isoechoic and appears grey. Unless otherwise stated the term US will refer to B-mode for the remainder of this chapter.

Technique

Even when using the direct method, the intended site for insertion should always be examined with US prior to creating a sterile field. This allows for the assessment of clot and the degree of overlap of the target vein on the associated artery. Preprocedure US visualization can also help identify possible vascular abnormalities that may impact on the success of the CVC insertion. In one study of hemodialysis patients, US abnormalities such as total occlusion, nonocclusive thrombus, stenosis and anatomic variation were found in 35% of patients prior to hemodialysis catheter insertion in the IJ vein. This led to a change in site selection in 75% of these patients [20].

There are two potential ways to use US to guide CVC insertion: the indirect method and the direct method. The indirect method involves visualizing the relationship between the artery and vein and planning the best angle of approach prior to creating a sterile field. US is not used during the actual CVC insertion. The direct method uses US to visualize the needle in real time as it enters the target vessel. One study comparing the direct to the both the indirect and landmark methods for CVC insertion showed that while use of either method improved outcomes when compared to the landmark technique, direct US visualization was the best method in terms of 1st-pass and overall success rate [21]. Furthermore, since even minor changes in position can greatly alter the relationship between the target vessel and its surrounding structures, we advocate the use of direct US guidance for CVC insertion.

In general, veins can usually be distinguished from arteries since they are compressible, nonpulsatile, and distend with the Trendelenburg position or Valsalva maneuver (online suppl. video 1). If the suspected vein is not compressible, it may signify that there is an intraluminal thrombus which may or may not be seen directly by US. The IJ vein is typically anterior and lateral to the artery although significant anatomic variation exists, and it is crucial to note the effects of contralateral head rotation on the degree of overlap of the carotid by the IJ. The SC vein is usually inferior and anterior to the artery.

Video

Once the appropriate vein is selected, the site is prepped and draped as per standard technique with full barrier precautions. The US probe is then placed in a sterile sheath. The probe is placed vertically on a stand, or the assistant holds the US probe vertically and conducting gel is applied to the probe. The operator then inserts a hand into the sterile sheath, takes hold of the probe and inverts the sheath over the probe to make both the probe and cable sterile. Additional sterile gel is then placed on the outside of the sheath to ensure adequate coupling. If an assistant is not available, and one does not have a stand with the US unit, the operator may hang the US probe

from an IV pole, place sterile gel inside the sheath, and then grasp the probe from the pole, inverting the sheath as before to make the probe and cable sterile.

Once the US probe is inside the sterile sheath, it can be placed safely on the sterile field to allow the operator time to prepare the CVC insertion kit. Before beginning, it is important to make sure that the US screen is at a comfortable distance from the operator, and when possible, in the same line of vision as the desired insertion site. This will allow the operator to look back and forth from the US screen to the insertion site with minimal effort.

There are two possible methods for direct US-guided CVC insertion: the 'one-handed' method or the 'three-handed' method. In the one-handed method, the operator holds the US probe in the nondominant hand and the needle in the dominant hand. The 'three-handed' method requires an assistant in full sterile barrier precautions to hold the US probe while the operator directs the needle into the target vessel. While the 'three-handed' method may be easier for inexperienced operators learning how to place CVCs initially, the 'one-handed' method has been shown to improve 1st-pass success and overall procedural success when compared to the 'three-handed' method [21]. It also has the benefit of not requiring another operator in sterile precautions, and eliminates the need for communication between the primary operator and the assistant for proper positioning of the US probe. This is especially valid when using the transverse view as it is important to follow the needle tip into the vessel. With two operators, the operator controlling the US probe may see a hyperechoic dot that represents the middle of the needle as opposed to its tip. The 'one-handed' technique is the preferred method of US-guided CVC placement at our institution. As mentioned previously, using the US to mark the skin and proceed without real-time guidance is not recommended since many factors may alter the original position of the target vessel and its surrounding structures.

Once the desired method has been chosen, the target vein and associated artery are identified with US and centered on the screen. It is important at this time to pay careful attention to other objects on the US screen since in addition to minimizing arterial overlap, a path should be chosen that avoids any adjacent lymph nodes or muscle tissue. In order to help minimize this risk, the operator should use standard anatomic landmarks as the initial starting point of US probe placement and adjust the position accordingly to obtain the best view of the target vessel. It is thus important to remember the relationship of the US probe to the US screen. For this reason, all US probes have a groove or other mark that corresponds to a dot (or other mark) on the US screen. Prior to needle insertion (for the transverse approach) the operator should orient the probe such that the left of the probe is the left of the screen.

After an appropriate site has been identified, the lidocaine needle is inserted through the skin directly anterior to the vessel, and the wheal of subcutaneous lidocaine is visualized with the US as an enlarging hypoechoic area in the center of the screen. After allowing the topical anesthetic to take effect, the introducer needle is inserted into the same location. A 'finder' needle is not necessary as the target vein puncture will occur with real-time guidance. If using the 'one-handed' method, the operator may need to put the US probe down in order to pull the skin taut to allow the introducer needle to penetrate the skin. Once the introducer needle is through the skin, the probe is picked up with the nondominant hand and used to guide the needle into the vessel. The introducer needle will indent the anterior vein wall and may even penetrate the posterior wall, resulting in a flash of venous blood upon withdrawal of the needle. This 'double-wall' puncture occurs about 15–20% of the time and is directly related to the diameter of the target vessel [22]. This underscores the importance of choosing a site, head position, and angle of needle insertion that minimizes arterial-venous overlap.

Passage of the introducer needle into the IJ vein can be performed either with a transverse (short axis) view or a longitudinal (long axis) view (fig. 1). The transverse view has been associated with a shorter learning curve and can more easily identify smaller vessels. The longitudinal view provides better visualization of the advancing needle tip and may reduce the risk of posterior vessel wall perforation or injury. If using the transverse view, it is critical to follow the advancing needle tip with the US, making sure the plane of the US is not too proximal or distal (fig. 2). If using the longitudinal view, one needs to keep the US and needle in the same plane.

A needle guide is also available to assist with insertion of the introducer needle. This is a piece of plastic that attaches to the US probe over the sterile sheath. It is designed to angle the needle so that it will intersect with the center of the US beam at a given depth. There are different needle guides for different depths. Needle guides have been shown to improve 1st- and 2nd-pass success rates, but have not been shown to decrease the number of arterial sticks when compared to US guidance without the use of a guide. We generally find needle guides to be cumbersome, and an added step that is generally not required for more experienced operators.

Once the target vein is entered with the introducer needle, the US probe is placed on the field and the typical mod-

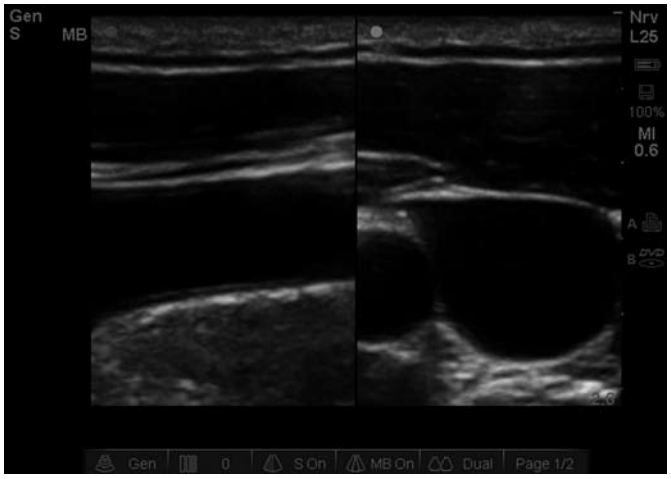

Fig. 1. Longitudinal and transverse view of right IJ and carotid (see online suppl video 2).

ified Seldinger technique is used to place the CVC. If there is any doubt as to whether or not the wire has been passed into the vein or artery, the US can be used to confirm wire placement in the target vessel prior to dilation.

Site-Specific Issues

IJ Vein

Most of the available evidence for the utility of US-guided CVC placement comes from studies that looked at the IJ vein site as the primary location [7–13, 16, 17, 23]. One possible reason for the beneficial effects of US in the IJ vein location is that the landmark technique does not allow for evaluation of arterial-venous overlap. In a prospective study of 1,136 patients, 54% of patients had more than 75% overlap of the carotid artery and IJ vein when the proposed path of the needle by landmark technique was examined by US [24]. It has been shown that contralateral head rotation increases the degree of overlap of the carotid by the IJ. As a result, if there is significant overlap of the IJ vein and carotid artery under US examination, the head should be returned to the neutral position and the relationship reexamined at varying degrees of head rotation before attempting US-guided cannulation.

US also allows for evaluation of IJ symmetry prior to choosing the ideal side of the body for attempted CVC insertion. There is considerable anatomic variation between patients, with more than 60% having a 2-fold difference in the size of the left and right IJ. Since vessel diameter is related to risk of posterior wall puncture [22] and likely overall success, US guidance allows the operator to choose both the optimal side and neck position prior to attempted IJ vein CVC insertion.

SC Vein

Some authors have suggested that given the more reliable anatomic position of the SC vein and the interference of the clavicle with obtaining a high quality image, the use of US guidance may actually hinder the placement of SC vein CVCs [1]. Unfortunately, there are limited data available to assess the efficacy of US for SC vein CVC insertion. One study in inexperienced operators showed that success rate improved from 44% with the landmark technique to 92% with US guidance while decreasing complication rate and number of needle sticks. Furthermore, failed landmark attempts could be converted to successful CVC placements with US 'salvage' 80% of the time [25]. Other studies that failed to show a benefit of US relied on Doppler and thus may not be applicable to the current B-mode US machines that most operators use. Some authors have advocated using US to enter the axillary vein more laterally in the infraclavicular position. However, since anatomic landmarks are not as reliable in this position, it is difficult to extrapolate these results to the more traditional landmark SC vein approach. At our institution we typically attempt SC vein cannulation using the landmark technique and use US guidance only as a 'salvage' strategy. Further work needs to be done to better evaluate the role of US in the insertion of SC vein CVCs.

Femoral Vein

As with the SC vein there is minimal evidence for the effect of US guidance on the placement of femoral vein catheters. In one randomized study of hemodialysis patients, US guidance was shown to improve 1st-pass success rate and overall procedural success, while reducing the number of femoral artery sticks, hematomas and the total length of the procedure [26]. Since femoral veins CVCs are known to have a higher incidence of both infectious and mechanical complications, most notably catheter-related bloodstream infections and deep venous thrombosis [2], the placement of femoral catheters is strongly discouraged at our institution, especially in critically ill patients. As a result, most femoral vein CVCs are placed in emergency situations where US guidance may or may not be readily available. These results suggest that if femoral vein CVC insertion needs to be undertaken for emergency reasons, it should be attempted with US guidance if the US device, and an operator trained to use it, are readily available. For an elective, but unavoidable, femoral vein CVC insertion we recommend the routine use of US guidance.

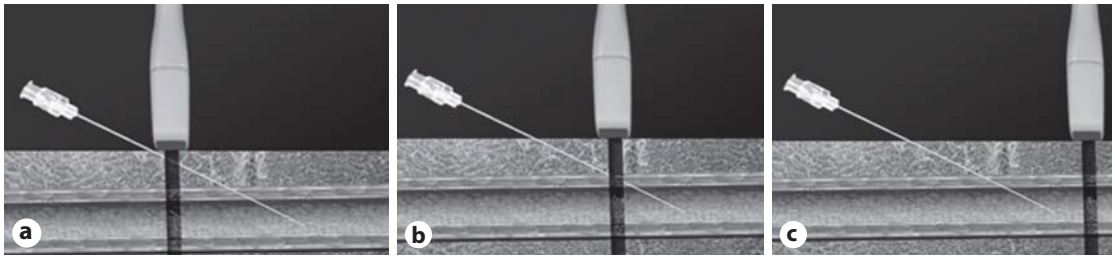

Fig. 2. Transverse US showing relationship of US plane to advancing needle tip (see online suppl video 3). Video

Confirming Line Placement

In addition to placement of CVCs, there is some evidence to suggest that US examination may be helpful in assessing for mechanical complications such as catheter tip malposition or pneumothorax. In one study of 85 CVC insertions, 10 misplacements and 1 pneumothorax were observed. The pneumothorax and all but one of the misplacements were detected by bedside US after the procedure. The time to obtain US confirmation was on the order of minutes, while radiographic confirmation routinely took longer than 1 h [27]. Another study looked at real-time US to assess for abnormal catheter or guidewire position in the ipsalateral IJ vein during SC vein CVC insertion. Using this approach, 42 of 49 (86%) malpositioned catheters were detected during the procedure and 81% were able to be repositioned at the time of detection [28]. The benefits of US confirmation are readily apparent – decreased time until the line can be used, decreased radiation exposure to the patient, and in some cases, real-time correction of aberrant placement that might decrease the time, risk and cost of the procedure. The use of US confirmation of CVC insertion may become more commonplace in the future as more physicians are trained in the use of bedside US. However, it has still not supplanted radiography as the standard of care in assessing for mechanical complications.

US Machine Requirements

US units have become smaller and more portable in recent years, making them well-suited for the ICU environment. For vascular access, a 7.5- to 10-MHz linear array transducer provides the best resolution and sufficient depth of visualization. There are a number of machines available, some designed specifically for vascular access, others with broader US applications. In addition to the US unit and transducer, sterile sheaths and sterile US gel are a necessary investment. A conservative estimate for the initial outlay required to perform US-guided CVC insertion is USD 25,000–40,000.

Cost Effectiveness

Given the initial expense and the fact that experienced operators are able to safely place CVCs with the landmark technique, it is reasonable to ask whether or not US-guided CVC insertion is cost-effective. A conservative analysis of US guidance in the National Health Service in the UK found that US use added only GBP £10/procedure, while potentially saving GBP £2,000 for every 1,000 procedures performed (assuming 90 prevented complications/1,000 procedures) [29]. It appears, at least in this analysis, that the use of US ultimately saved the health system money by avoiding potentially costly complications.

Implications for Training Programs

The use of US as both a diagnostic and procedural tool is not limited to radiologists. It is the responsibility of individual programs and hospitals to develop training and credentialing guidelines and to then incorporate them into our daily practice and fellowship training programs. A comprehensive approach to developing a formal training program for US-guided CVC insertion has been presented elsewhere [30].

Procedural skill requires integration of a knowledge base and psychomotor skill sets. In general, the learning curve for US vascular access is much steeper than other US procedures such as echocardiography and abdominal trauma exams. There are, however, no prospective data examining the appropriate amount of training and experience required to become proficient at US-guided CVC insertion. For the

landmark technique, operators who have performed more than 50 insertions have half the complication rate of operators who have performed less than 50 [4]. For the operator who is already an expert at landmark CVC insertion we suggest 2–3 h of didactics, 2–4 h of lab training, and 5–10 proctored examinations as a minimum to ensure competency in US-guided CVC insertion, recognizing that certain operators may require more or less experience to become proficient. Lab training should include exposure to a variety of US units that the operator may encounter in clinical practice, examination of normal vascular anatomy on healthy volunteers as well as hands-on simulation with vascular access models. If possible, lab training should also include visualization of abnormal anatomy such as intraluminal thrombus, significant arterial-venous overlap or even anatomy in obese patients, since these factors all decrease the rate of success in landmark-based attempts. The proctored examinations should include US evaluation of normal anatomy followed by CVC insertion attempts on vascular models or simulators. Following this initial training, operators should undergo a knowledge assessment of the basics of US-guided CVC insertion to ensure that they have a firm grasp of the fundamental issues and techniques of US use. For the physician who is already experienced in CVC placement, we would recommend 2 proctored exams on real patients followed by a review of the next 5 US-guided CVCs.

Quality improvement measures need to be in place to ensure a comprehensive review of all complications. Skill maintenance is critical as well – at least 10 US-guided CVCs should be performed each year in order to maintain an acceptable level of proficiency.

Barriers to the Use of US for CVC Insertion

Despite the growing evidence that US guidance improves both success rate and safety of CVC insertion, especially in the IJ vein site, there has been some delay in adopting US into daily clinical practice. A survey of 250 anesthetists in the UK found that 41% disagreed with the recommendation that US imaging should be the preferred method for insertion of a CVC into the IJ vein [31]. In addition to the initial financial investment required to establish a program for US-guided CVC insertion, there are other barriers to its widespread use. One such barrier is the lack of knowledge among practitioners that US improves outcomes, a factor that has been directly related to the frequency of its use.

Limitations of US

It is important to recognize that while the current data suggest improved success rate and decreased risk of arterial puncture with US guidance, there are no prospective data linking US use to long-term outcomes such as mortality, length of stay, catheter-related bloodstream infections or catheter-related thrombosis. As mentioned previously, while the evidence is compelling for the IJ vein position, there is a relative paucity of information regarding US in other central venous access sites.

Conclusion

US has become an integral part of the examination and care of hospitalized patients. US-guided CVC insertion is relatively easy to learn and has been shown to decrease complications while improving both 1st-pass and overall success. For many physicians it has already become the standard of care. We strongly recommend the use of US guidance for CVC insertion in the IJ vein. We encourage US use for femoral vein CVC insertions where possible. We also advocate the use of US in SC vein insertion attempts, especially when anatomic landmarks are difficult to appreciate or the landmark approach has been previously unsuccessful.

References

1 McGee DC, Gould MK: Preventing complications of central venous catheterization. N Engl J Med 2003;348:1123–1133.

2 Merrer J, De Jonghe B, Golliot F, Lefrant JY, Raffy B, Barre E, Rigaud JP, Casciani D, Misset B, Bosquet C, Outin H, Brun-Buisson C, Nitenberg G: Complications of femoral and subclavian venous catheterization in critically ill patients: a randomized controlled trial. JAMA 2001;286:700–707.

3 Bernard RW, Stahl WM: Subclavian vein catheterizations: a prospective study. I. Non-infectious complications. Ann Surg 1971;173:184–190.

4 Sznajder JI, Zveibil FR, Bitterman H, Weiner P, Bursztein S: Central vein catheterization. Failure and complication rates by three percutaneous approaches. Arch Intern Med 1986;146:259–261.

5 Goldfarb G, Lebrec D: Percutaneous cannulation of the internal jugular vein in patients with coagulopathies: an experience based on 1,000 attempts. Anesthesiology 1982;56:321–323.

6 Mansfield PF, Hohn DC, Fornage BD, Gregurich MA, Ota DM: Complications and failures of subclavian-vein catheterization. N Engl J Med 1994;331:1735–1738.

7 Mallory DL, McGee WT, Shawker TH, Brenner M, Bailey KR, Evans RG, Parker MM, Farmer JC, Parillo JE: Ultrasound guidance improves the success rate of internal jugular vein cannulation. A prospective, randomized trial. Chest 1990;98:157–160.
8 Troianos CA, Jobes DR, Ellison N: Ultrasound-guided cannulation of the internal jugular vein. A prospective, randomized study. Anesth Analg 1991;72:823–826.
9 Denys BG, Uretsky BF, Reddy PS: Ultrasound-assisted cannulation of the internal jugular vein. A prospective comparison to the external landmark-guided technique. Circulation 1993;87: 1557–1562.
10 Slama M, Novara A, Safavian A, Ossart M, Safar M, Fagon JY: Improvement of internal jugular vein cannulation using an ultrasound-guided technique. Intensive Care Med 1997;23:916–919.
11 Teichgraber UK, Benter T, Gebel M, Manns MP: A sonographically guided technique for central venous access. AJR Am J Roentgenol 1997; 169:731–733.
12 Nadig C, Leidig M, Schmiedeke T, Hoffken B: The use of ultrasound for the placement of dialysis catheters. Nephrol Dial Transplant 1998;13: 978–981.
13 Hayashi H, Amano M: Does ultrasound imaging before puncture facilitate internal jugular vein cannulation? Prospective randomized comparison with landmark-guided puncture in ventilated patients. J Cardiothorac Vasc Anesth 2002;16:572–575.
14 Karakitsos D, Labropoulos N, De Groot E, Patrianakos AP, Kouraklis G, Poularas J, Samonis G, Tsoutsos DA, Konstadoulakis MM, Karabinis A: Real-time ultrasound guided catheterization of the internal jugular vein: a prospective comparison to the landmark technique in critical care patients. Crit Care 2006;10:R162.
15 Leung J, Duffy M, Finckh A: Real-time ultrasonographically-guided internal jugular vein catheterization in the emergency department increases success rates and reduces complications: a randomized, prospective study. Ann Emerg Med 2006;48:540–547.
16 Randolph AG, Cook DJ, Gonzales CA, Pribble CG: Ultrasound guidance for placement of central venous catheters: a meta-analysis of the literature. Crit Care Med 1996;24:2053–2058.
17 Hind D, Calvert N, McWilliams R, Davidson A, Paisley S, Beverley C, Thomas S: Ultrasonic locating devices for central venous cannulation: meta-analysis. BMJ 2003;327:361.
18 Calvert N, Hind D, McWilliams RG, Thomas SM, Beverley C, Davidson A: The effectiveness and cost-effectiveness of ultrasound locating devices for central venous access: a systematic review and economic evaluation. Health Technol Assess 2003;7:1–84.
19 Rothschild JM: Ultrasound guidance of central vein catheterization. AHRQ, 2001, 3-15-0006. http://www.ahrq.gov/clinic/ptsafety/chap21.htm
20 Forauer AR, Glockner JF: Importance of US findings in access planning during jugular vein hemodialysis catheter placements. J Vasc Interv Radiol 2000;11:233–238.
21 Milling TJ Jr, Rose J, Briggs WM, Birkhahn R, Gaeta TJ, Bove JJ, Melniker LA: Randomized, controlled clinical trial of point-of-care limited ultrasonography assistance of central venous cannulation: the Third Sonography Outcomes Assessment Program (SOAP-3) Trial. Crit Care Med 2005;33:1764–1769.
22 Gordon AC, Saliken JC, Johns D, Owen R, Gray RR: US-guided puncture of the internal jugular vein: complications and anatomic considerations. J Vasc Interv Radiol 1998;9:333–338.
23 Wigmore TJ, Smythe JF, Hacking MB, Raobaikady R, Maccallum NS: Effect of the implementation of NICE guidelines for ultrasound guidance on the complication rates associated with central venous catheter placement in patients presenting for routine surgery in a tertiary referral centre. Br J Anaesth 2007;99:662–665.
24 Troianos CA, Kuwik RJ, Pasqual JR, Lim AJ, Odasso DP: Internal jugular vein and carotid artery anatomic relation as determined by ultrasonography. Anesthesiology 1996;85:43–48.
25 Gualtieri E, Deppe SA, Sipperly ME, Thompson DR: Subclavian venous catheterization: greater success rate for less experienced operators using ultrasound guidance. Crit Care Med 1995;23: 692–697.
26 Kwon TH, Kim YL, Cho DK: Ultrasound-guided cannulation of the femoral vein for acute haemodialysis access. Nephrol Dial Transplant 1997;12:1009–1012.
27 Maury E, Guglielminotti J, Alzieu M, Guidet B, Offenstadt G: Ultrasonic examination: an alternative to chest radiography after central venous catheter insertion? Am J Respir Crit Care Med 2001;164:403–405.
28 Ledonne J: Detecting and fixing errant central venous catheters without radiography. J Am Coll Surg 2006;202:554–555.
29 Calvert N, Hind D, McWilliams R, Davidson A, Beverley CA, Thomas SM: Ultrasound for central venous cannulation: economic evaluation of cost-effectiveness. Anaesthesia 2004;59: 1116–1120.
30 Feller-Kopman D: Ultrasound-guided internal jugular access: a proposed standardized approach and implications for training and practice. Chest 2007;132:302–309.
31 Howard S: A survey measuring the impact of NICE guidance 49: the use of ultrasound locating devices for placing central venous catheters. NICE. http://www.nice.org.uk/niceMedia/pdf/Final_CVC_placement_survey_report.pdf, 2004 (accessed January 15, 2008).

David Feller-Kopman, MD, Director
Interventional Pulmonology
The Johns Hopkins Hospital, 1830 East Monument Street, 5th Floor
Baltimore, MD 21205 (USA)
Tel. +1 410 502 2533, Fax +1 410 955 0036, E-Mail dfellerk@jhmi.edu

Chapter 9

Bolliger CT, Herth FJF, Mayo PH, Miyazawa T, Beamis JF (eds): Clinical Chest Ultrasound: From the ICU to the Bronchoscopy Suite.
Prog Respir Res. Basel, Karger, 2009, vol 37, pp 76–81

Ultrasound Evaluation of the Lung

C. Pellecchia[a] · P.H. Mayo[b]

[a]Beth Israel Medical Center, New York, N.Y., [b]Long Island Jewish Medical Center, New Hyde Park, N.Y., USA

Abstract

Lung ultrasonography is a useful tool in the intensive care unit. It is superior in many respects to standard supine chest radiography, and its immediate availability allows the intensivist to rapidly assess the patient with acute respiratory failure at the bedside. It is easy to learn and straightforward in its bedside application; therefore, the intensivist ultrasonographer should consider it as a key component of their skill set.

Lung ultrasonography is easy to perform, simple to learn, and has excellent clinical utility for the critical care clinician. This chapter will review applications of lung ultrasonography that are specific to critical care practice. A complete discussion of lung ultrasonography as related to pulmonary medicine may be found in chapter 3, see pp. 22–33.

Historical Perspective

Lung ultrasonography in the intensive care unit (ICU) is a bedside technique. It is not conducive to static image analysis, but rather lends itself to dynamic bedside scanning. As a result, traditional radiologists were not instrumental in the development of the field. A frontline intensivist, Dr. Daniel Lichtenstein, has been largely responsible for developing the field of critical care lung ultrasonography. In the 1990s, he published a series of definitive reports that established the basis for the field. He is responsible for the standard semiology of lung ultrasonography. Based upon this original work, other groups have published reports that have expanded and validated these techniques.

The Physics of Lung Ultrasonography

The difference in velocity of ultrasound and acoustic impedance between air and tissue is large, leading to reflection of the ultrasound wave at any tissue-air interface. In addition, air has an unfavorable attenuation coefficient. This leads to the homogeneous amorphic grayness that occupies the ultrasound screen beyond a tissue-air interface. This blocks any attempt to scan through air to deeper body structures. For the same reason, structures that are surrounded by air are not discernable to the ultrasonographer.

As lung parenchyma is normally filled with air, the lung is not visible as a discreet structural entity with ultrasonography. However, when air is displaced from the lung by a disease process, ultrasound findings change in a predictable fashion. The findings of lung ultrasonography relate to the ratio of air to fluid within the lung. Edematous lung, though still aerated, has air artifact patterns that are different than normally aerated lung. Likewise, lung that is consolidated from pneumonia or atelectasis (i.e. airless) appears as a well-defined hyperechoic structure. While aerated lung will block ultrasonographic visualization of an abnormality deep within the lung, most lung processes that are of interest to the intensivist (e.g. pneumonia, hydrostatic pulmonary edema, lesional edema) extend to the periphery of the lung.

Machine Requirements

Lung ultrasonography may be performed with practically any ultrasound machine with 2-dimensional (2-D) scanning capability. A 3.5- to 5.0-MHz transducer of microconvex sector design works well as it fits between the intercostal spaces. Vascular transducers of higher frequency

may also give acceptable images, though they have limited penetration in patients with a thick chest wall. Cardiac transducers are useful, as they can also be used for general critical care ultrasonography (e.g. cardiac, pleural, abdominal). Linear transducers, however, may be difficult to fit between the rib spaces when scanning in a longitudinal orientation in the slender individual. Expensive newer generation ultrasound machines may yield inferior lung ultrasound images. They often contain sophisticated image smoothing software that is appropriate for echocardiography but degrades near-field resolution and visualization of air artifact, which is critical in lung ultrasonography. All the important features of lung ultrasonography were described by Lichtenstein using a simple 2-D machine manufactured in the early 1990s. The intensivist should always test the machine for its intended application before any purchase. Some machines permit override of image smoothing technology in order to obtain basic or fundamental image quality. Doppler capability is not required for critical care lung ultrasonography.

How to Perform Lung Ultrasonography

Unlike chest radiography or chest computed tomography (CT) where the radiologist and intensivist interpret a static image, lung ultrasonography relies on dynamic image acquisition performed by the intensivist at the bedside of the critically ill patient. Compared to the ambulatory patient, lung ultrasonography is often more difficult in the ICU, as the patient is frequently supine. Generally, the transducer is held in a longitudinal orientation and perpendicular to the skin surface. By moving the transducer along a series of longitudinal scan lines while imaging through adjacent interspaces, the examiner can perform a complete lung examination in an efficient manner while constructing a 3-dimensional image of the thorax. It is helpful to examine the thorax using an organized section approach, so that results can be referenced to a particular area. The chest is divided into an anterior and lateral zone. The former is bordered by the sternum and the anterior axillary line, while the latter lies between the anterior and posterior axillary lines. Typically, the anterior chest is examined first, followed by the lateral thorax. In examining the lateral thorax in the longitudinal scanning plane, it is essential that the intensivist first identifies the hemidiaphragm. The diaphragm is a curvilinear, hyperechoic structure that separates the abdominal compartment from the thorax. The posterior region lies behind the posterior axillary line. This is frequently an important area to image, as pleural effusions and posterior consolidations are found in the dependent thorax. To image these areas, the transducer may have to be pressed into the patient's mattress and angled towards the center of the body. In order to completely examine the posterior lung in the supine patient, the patient may be placed in the lateral decubitus position. As with the anterior and lateral exam, lung ultrasonography is then performed by applying the transducer at multiple interspaces on the back.

Important Findings of Lung Ultrasonography

Lung ultrasonography is superior to standard supine radiography and similar to chest CT in detecting many findings that are important to the intensivist. It is able to detect lung consolidation, alveolar-interstitial fluid accumulation, normal aeration pattern, pneumothorax and pleural fluid [1]. The important findings of critical care lung ultrasonography are as follows.

Lung Sliding

A lung image obtained with a 3.5-MHz transducer is shown in video 1 (online suppl. video 1). The depth has been adjusted to examine the pleural interface. The transducer is held perpendicular to the skin surface in a longitudinal orientation and centered between an intercostal space. The rib shadows are present on either side of the image and the pleural line appears as a horizontally orientated hyperechoic line approximately 0.5 cm deep to the origin of the rib shadows. The pleural line represents the interface of the visceral and parietal pleural surfaces. Normally, the two pleural surfaces move across each other during the respiratory cycle. This causes the finding of lung sliding, which is seen as movement of the pleural line in synchrony with the respiratory cycle (online suppl. videos 2 and 3). The chest wall is immobile and separated from the underlying lung aeration pattern by the mobile pleural line. In addition to lung sliding that occurs with the respiratory cycle, the pleural line may move in synchrony with cardiac pulsation. This movement, termed lung pulse, is caused by the force of the cardiac pulsation being transmitted to the lung and hence to the visceral pleura (online suppl. videos 4 and 5). Real-time 2-D scanning is required to detect lung pulse and sliding lung. Like lung sliding, lung pulse indicates that the visceral and parietal pleural surfaces are apposed at the site of transducer application.

Lung sliding (and/or lung pulse) is a key finding of lung ultrasonography as it rules out pneumothorax at the point of transducer application with a very high level of certainty [2]. Multiple sites may be quickly examined for sliding lung in order to exclude pneumothorax. As a loculated pneumothorax is very uncommon, pleural air will generally distribute anteriorly in the supine patient. Therefore, the presence of sliding lung on the anterior chest allows the intensivist to exclude pneumothorax with confidence. Several groups have reported on the superiority of ultrasonography to rule out pneumothorax when compared to supine chest radiography [3–6].

Video The absence of sliding lung (online suppl. video 6 and online suppl. video 5b, chapter 3) may be caused by pneumothorax, but it has other causes as well. For example, apnea ablates sliding lung. Selective mainstem bronchial intubation with blockage of the contralateral mainstem by the endotracheal tube cuff [7], as well as any other cause for mainstem occlusion (e.g. mucous plug, tumor, blood clot, foreign body), will cause loss of lung sliding on the side of the blockage. Lung pulse will remain on the effected side indicating full lung inflation. Furthermore, pulmonary diseases that reduce lung inflation such as severe ARDS or pneumonia can cause loss of lung sliding. Pleural symphysis from any cause will result in loss of lung sliding. Therefore, the *presence* of lung sliding indicates that there is no pneumothorax, while the *absence* of lung sliding only indicates that there *may* be one. [8].

Lung Point

The finding of lung point is diagnostic for the presence of pneumothorax. The lung point is found at the site where partially collapsed lung is still apposed to the inside of the chest wall. Some pneumothoraces are total (i.e. the lung is completely collapsed), but most are partial with some remaining apposition of the visceral and parietal pleura. With careful technique, the examiner searches for the site at which the two pleural surfaces periodically meet. It appears as intermittent lung sliding, because the collapsed lung to some extent still inflates synchronously with the respiratory

Video cycle (online suppl. video 7). Designated as the lung point, this finding is diagnostic of pneumothorax [9]. Unfortunately, while 100% specific for pneumothorax, it is relatively insensitive and related to operator experience. Detection of lung sliding is an entry-level skill, while lung point requires more experience.

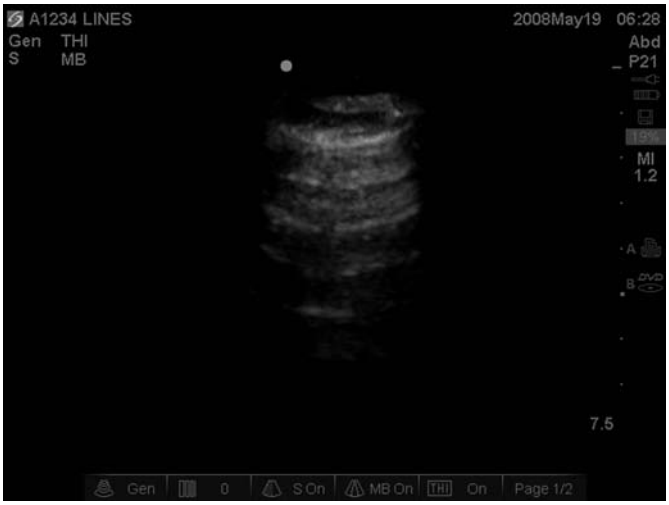

Fig. 1. Standard lung ultrasound image with 3.5-MHz transducer in longitudinal plane showing rib shadow artifacts, the pleural line, and A lines.

A Lines

Lung that is normally aerated has a characteristic pattern of air artifact designated as A lines. A lines are horizontally orientated lines seen deep to the pleural line (fig. 1) (online suppl. videos 1–3). They represent reverberation artifacts Video from ultrasound reflection between the pleural surface and the outer surface of the chest wall. Therefore, their depth is a multiplicative of the distance between the skin surface and the pleural line. If lung sliding is present, A lines are consistent with normal aeration pattern. A lines correlate strongly with a normal aeration pattern on CT scan [1]. They are, however, also found when a pneumothorax is present, and in the situation where there is no pneumothorax and absent lung sliding (see above). When evaluating findings such as A lines or B lines (see below), the depth setting on the machine should be set to image deeper structures. When examining for sliding lung, the depth setting should be set for imaging near structures.

B Lines

Lung that is edematous has a characteristic pattern of air artifact designated as B lines (fig. 2) (online suppl. video 8). Video B lines are strictly defined as one or more mobile vertically orientated lines that originate at the pleural interface. They must efface A lines where the two intersect. They always extend in a ray-like fashion to the bottom of the viewing screen, and they generally move synchronously with lung sliding. They may, however, be immobile in the absence of

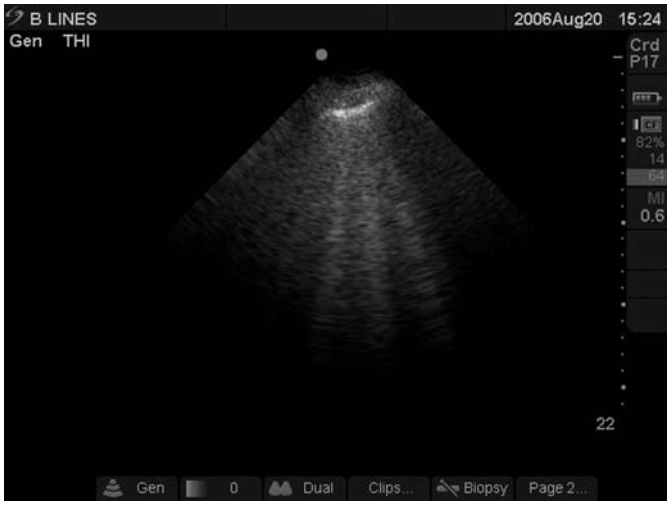

Fig. 2. Standard lung ultrasound image with 3.5-MHz transducer in longitudinal plane showing B lines.

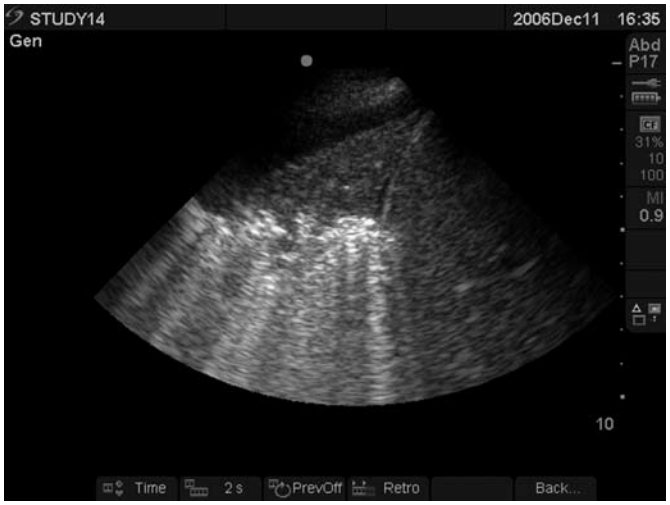

Fig. 3. Standard lung ultrasound image with 3.5-MHz transducer in longitudinal plane showing alveolar consolidation and a small pleural effusion. There are some B lines at the interface of the lung consolidation and the aerated lung.

pleural movement. B lines are also called comet tails or lung rockets.

B lines are caused by ring-down artifact derived from small subpleural fluid collections or tissue densities. Their presence excludes pneumothorax [10]. B lines are strongly correlated with an alveolar/interstitial pattern abnormality seen on CT scan (ground glass or reticular pattern abnormality) [1], and are characteristic of lung edema [11–15]. Any process that involves the interstitium of the lung such as inflammation, neoplasm, or scarring may also result in B lines. B lines may occur both focally or diffusely. Normal individuals may have a few B lines in the lower lateral chest. Multiple B lines over the anterior chest strongly suggest the presence of significant pulmonary edema. Anecdotally, lesional pulmonary edema (e.g. ARDS) results in a nonhomogeneous distribution of B lines, whereas hydrostatic pulmonary edema results in a homogeneous pattern.

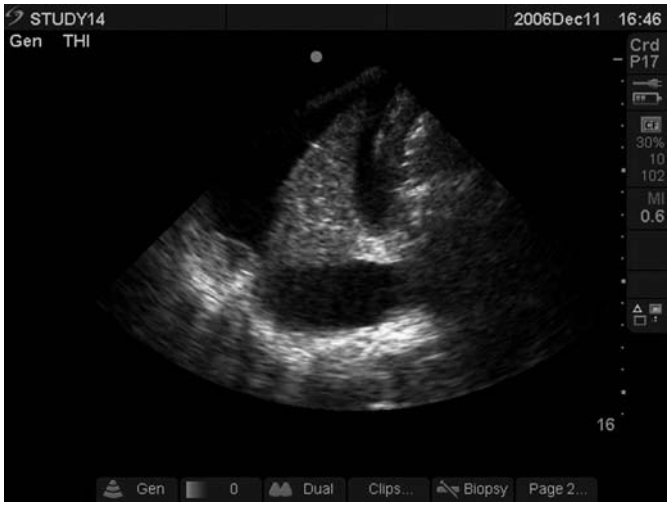

Fig. 4. Standard lung ultrasound image with 3.5-MHz transducer in longitudinal plane showing alveolar consolidation with a large pleural effusion. The consolidated lung is atelectatic. See similar situation in chapter 3, figure 3, p. 24.

Consolidation

Lung that is consolidated takes on the appearance of tissue density under ultrasound [16]. Consolidated lung has echogenicity that is similar to that of the liver, hence the term sonographic hepatization of the lung. With scanning depth set to examine deeper structures, areas of lung consolidation may be readily identified. A skilled examiner can identify focal areas of ultrasonographic lung consolidation down to the segmental level (fig. 3, 4) (online suppl. videos 9–11). Consolidated lung may have within it hyperechoic foci that are caused by small amounts of air in the bronchi. These represent sonographic air bronchograms and suggest that the bronchus supplying the effected area is patent. The hyperechoic foci may be mobile, which represents movement of air within the bronchus during the respiratory cycle. Consolidation found with lung ultrasonography is strongly correlated with its presence on chest CT [1]. The finding of lung consolidation on ultrasonographic examination does not imply any particular diagnosis. Pneumonia may result in lung consolidation pattern, but lung atelectasis of any cause,

Video

severe ARDS with dependent distribution, or an infiltrative tumor (e.g. broncoalveolar carcinoma) may all result in a consolidation pattern on ultrasound. Consolidation on lung ultrasonography is similar to the finding of consolidation on chest radiography or CT scanning; the clinician must determine the cause.

The Clinical Utility of Lung Ultrasonography

A simple application of lung ultrasonography is in assessing the patient for procedure-related pneumothorax following thoracentesis or central line access. If the sliding lung is documented *before* the procedure, and is then determined to be present *after* the procedure, no pneumothorax has occurred. If, on the other hand, sliding lung is absent following the procedure, the probability of procedure-related pneumothorax is very high. If the clinician uses ultrasonography for procedural guidance, checking for sliding lung should become a routine part of the procedure. This is particularly useful in patients who are on mechanical ventilatory support. In this population, a pneumothorax is particularly dangerous, as it may be under tension. Lung ultrasonography is a very rapid means of ruling out postprocedure pneumothorax in the patient on a mechanical ventilator. In addition, it is useful in the emergency evaluation for pneumothorax in cases of thoracic trauma [3, 4, 6].

Chest radiography in the critically ill patient is often difficult to interpret. Rotation, penetration, and projection artifact are common problems. The radiograph often shows nonspecific radiodensity due to summation artifact. Lung ultrasonography is an excellent means of clarifying the results of an ambiguous chest radiograph in the ICU.

The immediate bedside availability of lung ultrasonography makes it useful for rapid evaluation of acute desaturation of the patient on mechanical ventilatory support. The supine chest radiography is unreliable in ruling out pneumothorax [5], and there is often delay in obtaining a chest radiograph in what is a potentially life-threatening situation. Ultrasonography can be used to rule out pneumothorax and mainstem bronchial block (endotracheal tube movement or mucous plugging), as well as to evaluate for acute pulmonary embolism or pulmonary edema [1].

A major application of lung ultrasonography is for the rapid evaluation of acute respiratory failure. Lung ultrasonography allows prompt identification of the cause for acute respiratory failure in rapid response team events, the emergency department, and at the bedside of the acutely decompensating patient in the ICU. The limitations of chest radiography in the ill patient are clear. Chest CT has time delay, risk of transport of the unstable patient, and major radiation exposure [17]. The clinician who is equipped with a portable ultrasound unit can bring to the bedside a device that yields more accurate imaging than standard chest radiography. In a recent study, Lichtenstein and Mezière [8] report on the strong utility of lung ultrasonography for the assessment of acute respiratory failure. They describe a straightforward algorithm for evaluating the patient with acute dyspnea using lung ultrasonography that is of interest to the intensivist ultrasonographer.

Conclusion

Lung ultrasonography has excellent clinical utility in the ICU. It is superior to supine chest radiography in the ICU. Competence in lung ultrasonography helps the frontline intensivist to promptly recognize postprocedure pneumothorax, to clarify the ambiguous chest radiograph, and to rapidly evaluate the patient with acute respiratory failure.

References

1 Lichtenstein D, Goldstein I, Mourgeon E, Cluzel P, Grenier P, Rouby JJ: Comparative diagnostic performances of auscultation, chest radiography, and lung ultrasonography in acute respiratory distress syndrome. Anesthesiology 2004;100:9–15.

2 Lichtenstein DA, Menu Y: A bedside ultrasound sign ruling out pneumothorax in the critically ill. Lung sliding. Chest 1995;108:1345–1348.

3 Kirkpatrick AW, Sirois M, Laupland KB, Liu D, Rowan K, Ball CG, Hameed SM, Brown R, Simons R, Dulchavsky SA, Hamiilton DR, Nicolaou S: Hand-held thoracic sonography for detecting post-traumatic pneumothoraces: the Extended Focused Assessment with Sonography for Trauma (EFAST). J Trauma 2004;57:288–295.

4 Blaivas M, Lyon M, Duggal SA: Prospective comparison of supine chest radiography and bedside ultrasound for the diagnosis of traumatic pneumothorax. Acad Emerg Med 2005;12:844–849.

5 Lichtenstein DA, Mezière G, Lascols N, Biderman P, Courret JP, Gepner A, Goldstein I, Tenoudji-Cohen M: Ultrasound diagnosis of occult pneumothorax. Crit Care Med 2005;33: 1231–1238.

6 Soldati G, Testa A, Sher S, Pignataro G, La Sala M, Silveri NG: Occult traumatic pneumothorax: diagnostic accuracy of lung ultrasonography in the emergency department. Chest 2008;133:204–211.

7 Lichtenstein DA, Lascols N, Prin S, Mezière G: The 'lung pulse': an early ultrasound sign of complete atelectasis. Intensive Care Med 2003;29:2187–2192.

8 Lichtenstein DA, Mezière GA: Relevance of ultrasound in the diagnosis of acute respiratory failure. Chest 2008;134:117–125.
9 Lichtenstein D, Mezière G, Biderman P, Gepner A: The 'lung point': an ultrasound sign specific to pneumothorax. Intensive Care Med 2000;26:1434–1440.
10 Lichtenstein D, Mezière G, Biderman P, Gepner A: The comet-tail artifact: an ultrasound sign ruling out pneumothorax. Intensive Care Med 1999;25:383–388.
11 Lichtenstein D, Mézière G, Biderman P, Gepner A, Barré O: The comet-tail artifact. An ultrasound sign of alveolar-interstitial syndrome. Am J Respir Crit Care Med 1997;156:1640–1646.
12 Lichtenstein D, Mezière G: A lung ultrasound sign allowing bedside distinction between pulmonary edema and COPD: the comet-tail artifact. Intensive Care Med 1998;24:1331–1334.
13 Jambrik Z, Monti S, Coppola V, et al: Usefulness of ultrasound lung comets as a nonradiologic sign of extravascular lung water. Am J Cardiol 2004;93:1265–1270.
14 Agricola E, Bove T, Oppizzi M, Marino G, Zangrillo A, Margonato A, Picano E: 'Ultrasound comet-tail images': a marker of pulmonary edema: a comparative study with wedge pressure and extravascular lung water. Chest 2005;127:1690–1695.
15 Agricola E, Picano E, Oppizzi M, Pisani M, Meris A, Fragasso G, Margonato A: Assessment of stress-induced pulmonary interstitial edema by chest ultrasound during exercise echocardiography and its correlation with left ventricular function. J Am Soc Echocardiogr 2006;19:457–463.
16 Lichtenstein DA, Lascols N, Mezière G, Gepner A: Ultrasound diagnosis of alveolar consolidation in the critically ill. Intensive Care Med 2004;30:276–281.
17 Brenner DJ, Hall EJ: Computed tomography – an increasing source of radiation exposure. N Engl J Med 2007;357:2277–2284.

Paul H. Mayo, MD
Long Island Jewish Medical Center
Division of Pulmonary, Critical Care, and Sleep Medicine
410 Lakeville Road
New Hyde Park, N.Y. 11040 (USA)
Tel. +1 718 470 7827
E-Mail mayosono@gmail.com

Chapter 10

Bolliger CT, Herth FJF, Mayo PH, Miyazawa T, Beamis JF (eds): Clinical Chest Ultrasound: From the ICU to the Bronchoscopy Suite.
Prog Respir Res. Basel, Karger, 2009, vol 37, pp 82–88

Pleural Ultrasonography in the Intensive Care Unit

Jessica S. Wang · Peter Doelken

Division of Pulmonary, Critical Care, Allergy and Sleep Medicine, Medical University of South Carolina, Charleston, S.C., USA

Abstract

Physician-performed pleural ultrasonography has assumed a prominent role in the evaluation and management of pleural disease in the intensive care unit (ICU). Sonography can be used to rapidly diagnose pneumothorax, to evaluate pleural effusions, and to differentiate parenchymal lung disease from pleural disease. Interpretation of the images obtained by ultrasonograpy is based on the understanding of artifact to visualize normal and abnormal lung and pleura as well as to identify the surrounding structures. Pleural sonography may decrease the need for CT imaging, especially for guidance of drainage procedures, thus decreasing risk inherent to the transport of the critically ill. Among the numerous applications of sonography in the ICU, pleural sonography is distinguished by its relative simplicity and is therefore a natural choice as the first foray into the field by a beginning sonographer.

Pleural ultrasonography is a standard imaging modality in the management of pleural disease in the intensive care unit (ICU). Pleural disease in the ICU is generally encountered as a pleural effusion or as a pneumothorax. Not only is sonography superior in the detection and characterization of pleural effusion than standard chest radiography, it is also indispensable for the guidance of pleural interventions at the bedside. Furthermore, pleural sonography allows differentiation of pulmonary pathology from pleural disease far better than physical examination and standard chest radiography. Pneumothorax in the ICU is usually encountered as a complication of central line placement, of thoracentesis, or as a complication during mechanical ventilation, i.e. barotrauma. In these situations, sonography can provide instant information regarding the presence or absence of pneumothorax. While ultrasonography is the most useful bedside imaging modality in the ICU as far as pleural disease is concerned, computed tomography (CT) remains superior for complete imaging of the pleural space. However, the role of CT imaging, and especially CT guidance for procedures, clearly changes with the introduction of physician-performed pleural sonography. The use of pleural sonography in the critically ill allows earlier and more frequent assessment as well as more accurate characterization of pleural disease than standard chest radiography combined with physical examination, and eliminates in many cases the transport risk associated with off-site CT of the chest.

The advantage of ultrasonography in the ICU is the rapid bedside diagnosis of various conditions including pleural effusion, pneumothorax, atelectasis, consolidation, and pulmonary edema. While pleural sonography often results in anatomically correct imaging, the presence of air in the chest, physiologically as aerated lung or as pneumothorax, requires the physician sonographer to be familiar with air and other imaging artifacts. One might say that the dynamic nature of sonographic imaging and the proper recognition and interpretation of imaging artifact is the fundamental difference between pleural sonography and traditional radiographic modalities.

Hardware for Pleural Sonography

Simple two-dimensional ultrasound machines are suitable for pleural ultrasonography. Transducers with frequencies between 3 and 5 MHz and a small footprint, such as sector scanning or convex array transducers, are preferred due to the necessity of imaging between ribs and the acceptable compromise between near field resolution and penetration. In contrast to echocardiography, good near field resolution

is a requirement in pleural sonography in order to accurately determine depth of needle penetration during thoracentesis. As a consequence, some echocardiography machines are suboptimal for pleural sonography.

Imaging

Image acquisition in pleural sonography is straightforward and simpler in concept than many other ultrasound applications. By convention, the mark on the ultrasound transducer is directed cranially and the corresponding mark on the screen is placed in the left upper corner. Thus the orientation of a typical pleural sonography image is with the head to the left and the feet to the right. During interventional real-time imaging, other than standard orientations are used in order to align the image plane with the hardware to be imaged. Sufficient coupling medium must be used in order to minimize artifacts and improve image quality. The transducer is placed on the lower chest and moved circumferentially around the chest at various levels. Any abnormality found is examined further as appropriate. In the critically ill, supine patient, this technique needs to be adapted as needed, and a helper may be needed to complete the examination.

In most cases, ultrasonography of the pleura is goal directed and is used to further characterize an opacity seen on the standard chest radiograph or CT. Such focused use of pleural sonography significantly decreases examination time and need to change patient positioning.

Artifacts

Ultrasonography in general and chest ultrasonography in particular are beset by image artifacts. Although artifacts occur in pleural sonography, it is also true that artifacts are useful in many instances, and their correct interpretation is key in the successful clinical application of pleural sonography. The most common artifacts in pleural sonography are rib shadows and air artifact which are present to some degree in almost every pleural ultrasonographic image. Rib shadows are mainly an impediment to imaging and should not be misinterpreted as anechoic fluid. Alternately, air artifacts such as B lines, the curtain sign, and indirect air artifacts such as the reverberation lines in pneumothorax are put to good use in pleural ultrasonography (see below). Another more onerous artifact is the general image degradation caused by obesity or edema, which makes accurate assessment of echogenicity of underlying structures difficult. Subcutaneous emphysema may make the ultrasound examination impossible [1]. Many artifacts do not move with the underlying structures and may disappear or be attenuated with small changes in transducer angle, and will not interfere with the interpretation of images once some experience has been gained.

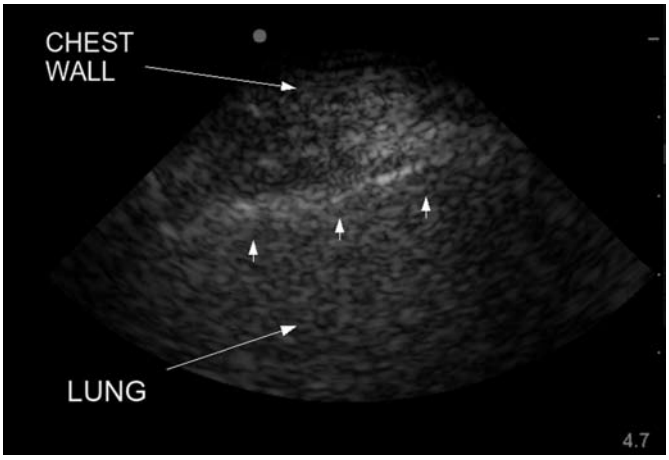

Fig. 1. The normal pleural reflection is seen as a bright line interposed between the chest wall and the lung. The apparent thickness of the pleural reflection is not the actual thickness of the pleura but is rather a reflection artifact.

The Normal Pleura

The normal pleura appears as a highly echogenic line between the chest wall and the aerated lung (fig. 1). With 3- to 5-MHz transducers as used in pleural sonography, the visceral and parietal pleural layers cannot be distinguished due to their thickness of only 0.2–0.4 mm [2, 3]. However, this inability to visualize the pleural layers is not clinically relevant. One clinically relevant finding related to normal pleura is lung sliding, which is a respirophasic to and fro movement of the lung and visceral pleura relative to the parietal pleura (see below). Lung sliding in the spontaneously breathing patient is most prominent in areas with most displacement during respiration, i.e. the lower chest (online suppl. video 5, chapter 3). The other dynamic finding is the lung pulse which is caused by cardiac action and is consequently most prominent close to the heart [4]. The mediastinal and most of the diaphragmatic pleura cannot be visualized in the normal condition because of the interposition of aerated lung. In the presence of pleural effusion, examination of these areas is often possible.

Video

Pleural Effusion

Pleural effusions are common in the ICU setting but most are small, typically due to edematous states or ARDS, and do not require further evaluation and treatment. Large effusions or effusions suspected as sites of infection require further diagnostic evaluation. On the chest radiograph, a minimum of 175 ml fluid must be present for traditional signs of pleural effusion, such as blunting of the costophrenic angle, to be evident [5]. Lateral decubitus films are more sensitive but are impractical in the critically ill. In comparison, ultrasound of the chest can detect all effusions that are ≥100 ml and can even demonstrate an effusion as small as 3–5 ml emphasizing the superiority of ultrasound [6]. Additionally, standard supine chest radiographs result in dependent fluid accumulation posteriorly, which creates indeterminate opacifications that may be a summation of pleural effusion, compressed lung, and parenchymal lung disease. Unlike chest radiography alone, ultrasound can distinguish between these abnormalities. In a study of 32 patients who underwent ultrasonography, Lichtenstein et al. [7] reported diagnostic accuracy of 93% for pleural effusion, 97% for alveolar consolidation, and 95% for alveolar-interstitial syndrome when compared to the standard of CT scan of the chest (table 1).

The detection of a pleural effusion by ultrasonography is based on three key findings: identification of the structures that define the boundaries of the effusion, the relatively echo-free characteristic of the effusion, and the dynamic changes characteristic of pleural effusion.

The borders of a pleural effusion are the diaphragm, lung, liver, spleen, kidney, heart/pericardium, spinal column, aorta, and inferior vena cava. With the imaging plane oriented in the craniocaudal axis and the transducer placed between two ribs, the upper rib shadow will be on the left and the lower rib on the right of the screen with the parietal pleura noted about 5 mm below the origin of the rib shadows. The diaphragm is the curvilinear structure which moves with the respiratory cycle. The liver or spleen is seen in a subdiaphragmatic location. Care must be taken not to confuse the curvilinear line of Morrison's pouch between spleen and left kidney for the diaphragm.

The dynamic changes of the fluid are characterized by various signs. The airless lung caused by compression floats in the pleural effusion and is termed floating lung (or lung flapping). This motion is also called the jellyfish sign. Consolidated lung may have similar echogenicity as the liver and this has been termed sonographic hepatization of lung. In smaller effusions which cause less lung atelectasis, the aerated lung does not show this undulating motion, but it may move into the scanning field with inspiration in a motion called the curtain sign. On M-mode, the lower border (the visceral pleura) will move toward the parietal pleura during respiration creating the sinusoid sign [2]. These movements that change the ultrasonographic image with respiration are termed respirophasic movements.

Ultrasound can aid in determining the volume of the effusion. No particular rules apply to assess the volume of a pleural effusion in a semiquantitative manner and the assessment is usually reported as an effusion of small, moderate, or large size. Eibenberger et al. [8] reported a correlation between the thickness of the effusion measured on ultrasound and the actual volume of effusion. In their study of 51 patients, a sonographic effusion width of 20 mm yielded a mean volume of 380 ± 130 ml of pleural fluid and a width of 40 mm yielded a mean volume of 1,000 ± 330 ml. This correlation was not perfect, but it was better than chest radiography in determining effusion volume. The correlation of the thickness of the effusion to the volume of pleural fluid also depends on the placement of the transducer. Vignon et al. [9] found that when the interpleural distance at the lung base was measured, a larger distance correlated with a larger effusion. There are other more complicated methods requiring geometric measurements that can be used to estimate the volume [10].

Pleural effusions are typically echo-free, but the characterization of the fluid can help with the etiology of the fluid. Transudates are generally anechoic, meaning they are uniformly black in appearance, but anechoic effusions can be transudates or exudates (fig. 2). Transudates do not have ultrasound reflectors within it, thus the fluid is typically anechoic. Pleural effusions may have swirling echoes, strands, fronds, or septations which describe a heterogeneously echogenic or complex effusion (fig. 3). The swirling within the effusion suggests cellular debris which can be seen in all types of exudates. In patients with known malignancy, this finding is associated with malignant pleural effusion in more than 80% of cases [11]. An effusion may also be described as homogenously echogenic which has diffuse internal echoes with a grey uniform appearance and may be isoechoic with the liver or spleen parenchyma. In an analysis of 320 patients, Yang et al. [12] found that this homogeneous pattern was only seen in hemorrhagic effusion or empyema. Rarely, cellular components may settle in the dependent parts of the pleural space in a pattern called the hematocrit sign.

In critically ill patients, the finding of a complex pleural effusion in the absence of malignancy should lead to

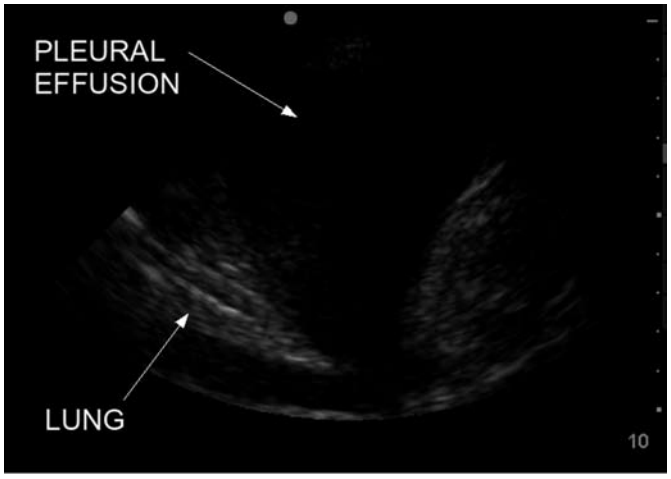

Fig. 2. A large anechoic effusion, atelectatic lung, and the diaphragm are seen on this image.

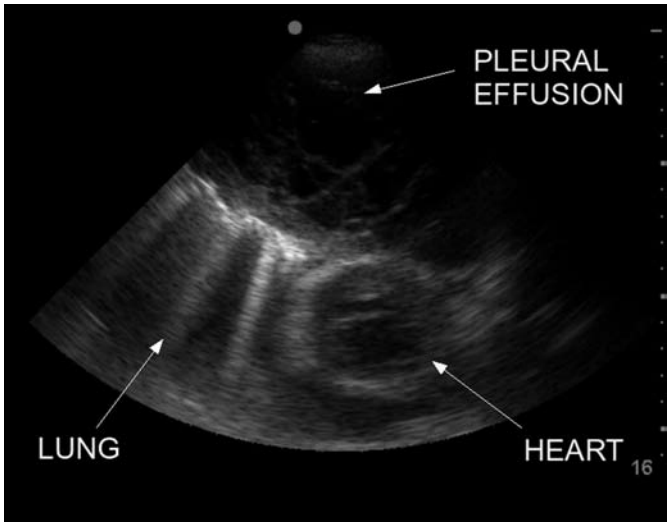

Fig. 3. A complex septate effusion bordered by the heart and aerated lung is seen on this image. Several B lines are also seen.

suspicion of complicated parapneumonic effusion or empyema. Tu et al. [13] evaluated 94 febrile medical ICU patients with pleural effusion, and 15 had empyema. All empyemas were characterized as complex nonseptated, complex septated, or homogenously echogenic effusions. No empyema was found when the effusion was anechoic or complex nonseptated and nonhyperechoic. For complex effusions, pleural ultrasonography is superior to chest CT scan even with contrast enhancement because CT is unable to clearly define the stranding and septations [14].

Pneumothorax

Rapid identification of pneumothorax in the critically ill patient is essential, particularly in the patient on mechanical ventilation. Ultrasonography can be used at bedside to quickly exclude pneumothorax. Scanning the chest with the ultrasound probe before and after invasive procedures that have a risk of iatrogenic pneumothorax, such as thoracentesis, subclavian/internal jugular central line placement, and transbronchial biopsy, should allow immediate confirmation or exclusion of pneumothorax after such procedures.

Determination of presence or absence of pneumothorax relies on the correct interpretation of air artifacts. Lung sliding is the respirophasic movement of the pleural interface relative to the chest wall, and the significance of evaluating for this sign is that the presence of lung sliding reliably excludes pneumothorax. In their study of 43 patients, Lichtenstein and Menu [15] found a negative predictive value of 100% for absence of pneumothorax in all patients with lung sliding. The ultrasound in lung sliding depicts the interaction between the lung and the chest wall during respiration; the presence of even a minute amount of air between the two pleural surfaces prevents this interaction leading to the loss of lung sliding. Lung sliding can also be rapidly assessed over a wide area of the thorax. Although the presence of lung sliding excludes pneumothorax, the absence of lung sliding only has a sensitivity of 95.3% with a specificity of 91.1% for pneumothorax, meaning that the absence of lung sliding cannot confirm pneumothorax. In critically ill patients, lung sliding is impaired in about 21% of patients which may be related to the loss of lung compliance. In those patients with absent lung sliding but without pneumothorax, B lines may be seen [16]. Other conditions associated with absence of lung sliding are pleural symphysis, emphysema or inadequate imaging.

B lines, also called comet tail artifacts, erase horizontal artifacts, are roughly horizontal and parallel lines that lie below the pleura. B lines are well defined, and move with lung sliding. B lines originate in the interstitium immediately below the visceral pleura and disappear with air interposed between visceral and parietal pleura, i.e. pneumothorax (fig. 4). Lichtenstein et al. [17] reported that the presence of B lines excludes pneumothorax. Their study in 73 critically ill patients found that the absence of lung sliding combined with the presence of horizontal lines had a sensitivity of 100% for diagnosing pneumothorax. Further importance of comet-tail artifact is described below.

The absence or presence of pneumothorax can be documented using M-mode sonography. The seashore sign is the

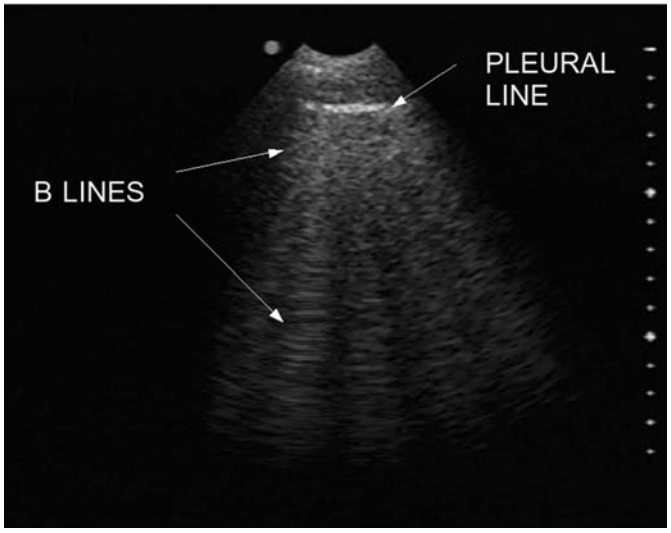

Fig. 4. B lines originate immediately below the bright pleural reflection and extend to the outer limits of the image.

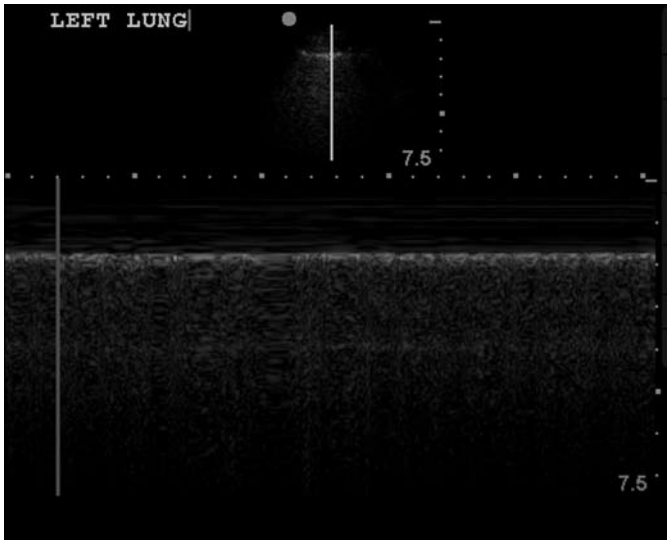

Fig. 5. Typical appearance of the seashore sign (see text).

equivalent of lung sliding in 2D mode, and the stratosphere sign is the equivalent of absent lung sliding and reverberation artifact in 2D mode imaging in the presence of pneumothorax. The seashore sign describes the granular pattern that underlies the horizontal motionless layers of the chest wall on M-mode. The straight motionless aspect depicts the stationary chest wall ('waves') that lies above the granular layer ('beach') which is indicative of the respirophasic movement of the lung (fig. 5). This sign is absent in the presence

Table 1. Evaluation of pleural effusions

1	Identify pleural fluid boundaries Chest wall, diaphragm with underlying liver or spleen, lung, heart, spinal column
2	Identify dynamic signs Floating lung, curtain sign, sinusoid sign, swirling particles, undulating fronds or strands
3	Assess echogenicity Anechoic, homogeneously echogenic, heterogeneously echogenic (complex) particles, strands, fronds, septations
4	Semiquantitative assessment of effusion volume

Table 2. Evaluation for pneumothorax

1	Exclude pneumothorax Lung sliding, B lines, seashore sign
2	Consistent with pneumothorax Stratosphere sign, lung point (confirms pneumothorax)

of pneumothorax because air prevents the visualization of movement of the underlying lung [4] (table 2).

When the ultrasound probe is placed slightly anterior and/or superior to the lung level, the lung point may be identified. The lung point indicates the area in which the lung intermittently comes in contact with the chest wall during respiration. The lung point confirms pneumothorax with a sensitivity of 79%, but a specificity of 100% [16].

Early identification of pneumothorax is also essential in the trauma patient. Small pneumothoraces in trauma patients can be missed initially on physical exam or chest radiograph but eventually may lead to tension pneumothorax and hemodynamic instability. Bedside ultrasound was compared to supine portable chest radiography in 176 trauma patients by Blaivas et al. [18]. Ultrasound was more sensitive (98.1%) than chest radiography (75.5%) for detecting pneumothorax. These lesions included small pneumothoraces which were confirmed by CT scan. Ultrasound allows for the differentiation of small, medium, and large pneumothoraces based on how far posterior the absence of lung sliding is noted. However, subcutaneous emphysema, large lung contusions, or bullous emphysema may result in absence of lung sliding as well and may lead to a false diagnosis of pneumothorax in the trauma population.

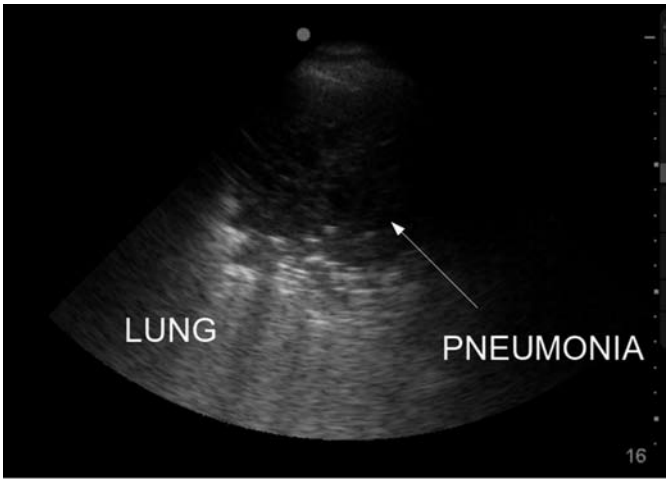

Fig. 6. This image of a necrotizing pneumonia shows hypoechoic areas in the lung parenchyma. This should not be confused with a complex septate pleural effusion. The irregular border of the consolidation contrasts briskly with the aerated lung.

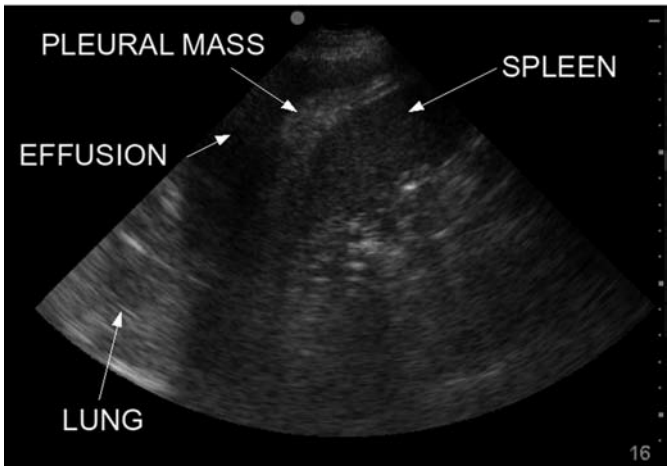

Fig. 7. A mass attached to the diaphragmatic pleura is seen within a pleural effusion. The spleen is seen below the diaphragm. This represents metastatic disease in the pleural space.

Miscellaneous Findings in Pleural Sonography

The pleural sonographer must be familiar with basic lung sonography in order to be able to positively identify abnormalities in the chest which do not constitute pleural effusion or are unrelated but clinically significant findings. After all, a major role of pleural sonography is the confirmation or exclusion of pleural effusion which is suspected on the basis of nonspecific opacities on the standard chest radiograph. Familiarity with basic lung sonography will prevent the inadvertent puncture of the lung during ill-advised drainage attempts. One of the most common questions in pleural sonography in the ICU is the differentiation between pleural effusion and alveolar consolidation or atelectasis. Lung consolidation refers to areas of fluid, infection, or blood collecting within the alveoli. It arises below the pleural line, above the diaphragm, and within the thorax. This tissue-like pattern is a real image, not an artifact. These findings must differentiated by the diaphragm from the underlying liver or spleen. Additionally, the sinusoid sign, which is described above and seen on M-mode, is absent indicating the lack of associated pleural effusion. The normal lung sliding with movement of the parietal and visceral pleura may also be impaired with this process. Lichtenstein et al. [19] correlated these various findings on lung ultrasonography with CT chest images and determined 90% sensitivity (56 of 62 cases) for alveolar consolidation. Another important consideration in pleural sonography is the distinction between necrotizing pneumonia and a complex pleural effusion. The liquefied content of necrotic areas in the lung may be hypoechoic and could be confused with pleural fluid (fig. 6). In these cases, careful dynamic imaging can usually locate the fluid collections in the lung and not the pleural space. On occasion, solid lesions other than particles, stranding, or septations are observed in the pleural space. Most commonly, the patient has a known malignancy and a pleural effusion coexists. In these cases, nodules or masses are visualized in a pleural effusion (fig. 7). Other solid lesions may mimic pleural effusion due to their hypoechoic character, although no fluid is present. Dynamic signs are uniformly absent in these cases. Pleural mesothelioma, lymphoma, but also pleural fibrosis are examples of such hypoechoic lesions. Peripheral tumors of the lung may also be visualized during pleural sonography. Absence of respirophasic movement of these lesions has been associated with direct parietal pleural involvement [20].

How to Get Started in Pleural Sonography

Pleural ultrasonography is a straightforward application of sonography, and proficiency can easily be achieved. Pleural sonography, together with vascular access sonography, may be recommended as the first step in becoming

Table 3. The pleural sonographer needs to be familiar with the following concepts and findings

1	Identify anatomic boundaries – diaphragm, chest wall, ribs, visceral pleura, lung (normal, consolidated, or atelectatic)
2	Identify other structures – liver, spleen, kidney, heart, spinal column, aorta, inferior vena cava
3	Identify characteristic dynamic changes – diaphragmatic motion, floating lung, lung point, respirophasic shape changes (sinusoid sign)
4	Characterize the pleural effusion – echogenicity, presence of strands/debris/septation
5	Identify miscellaneous findings – pleural-based lesions, masses or thickening
6	Semiquantitative assessment of fluid volume
7	Recognize the limits of pleural ultrasonography – inadequate image quality due to technical limitations, hemothorax, echodense purulent fluid, mimicking of effusion
8	Know the significance of lung sliding, B lines, seashore sign, lung point, stratosphere sign for evaluation of pneumothorax

an accomplished critical care ultrasonographer. The limited number of findings, the ease of image acquisition, and the immediate usefulness for procedure guidance are some aspects of pleural sonography making it attractive to the beginner. While learning under the supervision of a trained operator is ideal, this opportunity may not exist for many intensivists. In addition, some findings in pleural ultrasonography are rare and may not be encountered in a reasonable amount of time spent in training. In our fellowship program, we require review of commented videotaped cases before ultrasonography may be used independently by our fellows. In this way we overcome the shortcomings of static images in textbooks. In our experience, learning is much accelerated using this approach [21]. Table 3 summarizes key competencies of the pleural sonographer.

References

1 Lichtenstein DA: The ultrasound equipment; in General Ultrasound in the Critically Ill. Berlin, Springer, 2005, pp 9–12.
2 Lichtenstein DA: Pleural effusion and introduction to lung ultrasound; in General Ultrasound in the Critically Ill. Berlin, Springer, 2005, pp 96–104.
3 Reuss J: The pleura; in Mathis G, Lessnau KD (eds): Atlas of Chest Sonography. Berlin, Springer, 2003, pp 17–35.
4 Lichtenstein DA, Lascols N, Prin S, Meziere G: The 'lung pulse': an early ultrasound sign of complete atelectasis. Intensive Care Med 2003;29:2187–2192.
5 Colins JD, Burwell D, Furmanski S, Lorber P, Steckel RJ: Minimal detectable pleural effusions. A roentgen pathology model. Radiology 1972;105:51–53.
6 Gryminski J, Krakowka P, Lypacewicz G: The diagnosis of pleural effusion by ultrasonic and radiologic techniques. Chest 1976;70:33–37.
7 Lichtenstein D, Goldstein I, Mourgeon E, Cluzel P, Grenier P, Rouby JJ: Comparative diagnostic performances of auscultation, chest radiography, and lung ultrasonography in acute respiratory distress syndrome. Anesthesiology 2004;100:9–15.
8 Eibenberger KL, Dock WI, Ammann ME, Dorffner R, Hormann MF, Grabenwoger F: Quantification of pleural effusions: sonography versus radiography. Radiology 1994;191: 681–684.
9 Vignon P, Chastagner C, Berkane V, Chardac E, Francois B, Normand S, Bonnivard M, Clavel M, Pichon N, Preux PM, Maubon A, Gastinne H: Quantitative assessment of pleural effusion in critically ill patients by means of ultrasonography. Crit Care Med 2005;33:1757–1763.
10 Roch A, Bojan M, Michelet P, Romain F, Bregeon F, Papazian L, Auffray JP: Usefulness of ultrasonography in predicting pleural effusions > 500 mL in patients receiving mechanical ventilation. Chest 2005;127:224–232.
11 Chian CF, Su WL, Soh LH, Yan HC, Perng WC, Wu CP: Echogenic swirling pattern as a predictor of malignant pleural effusions in patients with malignancies. Chest 2004;126:129–134.
12 Yang PC, Luh KT, Chang DB, Wu HD, Yu CJ, Kuo SH: Value of sonography in determining the nature of pleural effusion: analysis of 320 cases. AJR Am J Roentgenol 1992;159:29–33.
13 Tu CY, Hsu WH, Hsia TC, Chen HJ, Tsai KD, Hung CW, Shih CM: Pleural effusions in febrile medical ICU patients: chest ultrasound study. Chest 2004;126:1274–1280.
14 McLoud TC, Flower CD: Imaging the pleura: sonography, CT, and MR imaging. AJR Am J Roentgenol 1991;156:1145–1153.
15 Lichtenstein DA, Menu Y: A bedside ultrasound sign ruling out pneumothorax in the critically ill. Lung sliding. Chest 1995;108:1345–1348.
16 Lichtenstein DA, Meziere G, Lascols N, Biderman P, Courret JP, Gepner A, Goldstein I, Tenoudji-Cohen M: Ultrasound diagnosis of occult pneumothorax. Crit Care Med 2005;33:1231–1238.
17 Lichtenstein D, Meziere G, Biderman P, Gepner A: The comet-tail artifact: an ultrasound sign ruling out pneumothorax. Intensive Care Med 1999;25:383–388.
18 Blaivas M, Lyon M, Duggal S: A prospective comparison of supine chest radiography and bedside ultrasound for the diagnosis of traumatic pneumothorax. Acad Emerg Med 2005;12:844–849.
19 Lichtenstein DA, Lascols N, Meziere G, Gepner A: Ultrasound diagnosis of alveolar consolidation in the critically ill. Intensive Care Med 2004;30:276–281.
20 Bandi V, Lunn W, Ernst A, Eberhardt R, Hoffmann H, Herth FJ: Ultrasound vs. computed tomography in detecting chest wall invasion by tumor: a prospective study. Chest 2008;133:881–886.
21 Doelken P, Mayo P: Ultrasonography of Pleural Effusion. Charleston, DM&C Electronic Publishing, 2003.

Jessica S. Wang, MD
Division of Pulmonary, Critical Care, Allergy and Sleep Medicine
96 Jonathan Lucas Street, Suite 812 – CSB, PO Box 250630
Charleston, SC 29425 (USA)
Tel. +1 843 792 3161, Fax +1 843 792 0732, E-Mail wanjs@musc.edu

Chapter 11

Bolliger CT, Herth FJF, Mayo PH, Miyazawa T, Beamis JF (eds): Clinical Chest Ultrasound: From the ICU to the Bronchoscopy Suite.
Prog Respir Res. Basel, Karger, 2009, vol 37, pp 89–95

Abdominal Ultrasonography as Related to Problems of the Chest

S. Beckh · K. Kirchpfening

Department of Internal and Pulmonary Medicine, Klinikum Nürnberg, Nürnberg, Germany

Abstract

Abdominal sonography represents one of the basic imaging procedures in diagnosing internal diseases. Thanks to bedside equipment examinations can be done in critically ill patients easily and quickly. Abdominal organs such as liver or spleen serve as acoustic windows for imaging of chest diseases. The diaphragm, the pleura and the lower parts of the lung are visible from the abdominal view. The view from the epigastrium towards the chest allows gaining information about the central blood vessels, the mediastinum and the heart. The examination of the abdominal organs gives diagnostic hints of chest diseases. In case of pleural effusion disorders of liver, kidneys or pancreas help to find out the nature of pleural affection. Metastasis in the abdomen may be present in thoracic carcinoma. In case of pulmonary metastasis the primary tumor may be localized in liver, pancreas or kidney. The hereditary hemorrhagic telangiectasia shows characteristic vascular malformations in liver and spleen explaining the findings of pathologic pulmonary vessels. In sarcoidosis granulomas may be found in liver and spleen. Calcifications of the spleen are a residue after miliary tuberculosis. In cystic fibrosis sonography reveals parenchymal disease of the pancreas. Peritoneal fluid with floating structures is a special finding in peritoneal tuberculosis.

In recent years bedside sonography has become an important imaging procedure for critically ill or bedridden patients. A lot of questions may be answered at once, though conditions for the examination might not be ideal [1–3]. In case of surgery, trauma, drains or bandages access for the ultrasound transducer may be limited. Thus it is a challenge in daily practice to manage examination of the chest from the abdominal view. Vice versa many findings in abdominal ultrasound examination are of diagnostic value in chest diseases. In the following the technique of abdominal ultrasound examination is described. The landmarks for sonographic orientation are outlined and examples of different pathologic findings are given.

Practice of Examination and Technical Equipment

For imaging deeper situated regions in the body a convex transducer with 3–5 MHz is recommended. To examine the right chest from the abdominal view the transducer is held in transverse position under the ribs and tilted towards the right shoulder. The ultrasound beam first passes the liver, which serves as an acoustic window for displaying the right diaphragm (fig. 1). The lateral part of the diaphragm and the right recess are best depicted in a lateral longitudinal view along the axillary lines (fig. 2).

On the left side the spleen serves as an acoustic window. In case of a normal-sized spleen only half of the left diaphragm can be seen. In the longitudinal section in axillary lines the lateral part of diaphragm and the left recess are to be examined.

In the epigastrium the transducer is positioned in longitudinal and transverse sections for receiving the crucial images. From this point of view structures of the lower anterior mediastinum are visible, such as the esophagus, cardia, aorta, caval vein and heart.

The abdomen is examined in longitudinal and transverse sections starting with liver, epigastrium and spleen, followed by kidneys, retroperitoneum, bowels and the lower abdominal region.

Pitfalls and Artifacts

The diaphragm appears as a strong reflector. On the right side the reflected ultrasound beams produce a virtual image of the liver above the diaphragm, on the left side the spleen may be mirrored [4]. Another important artifact is the simulation of a gap in the diaphragm [4]. Ultrasound

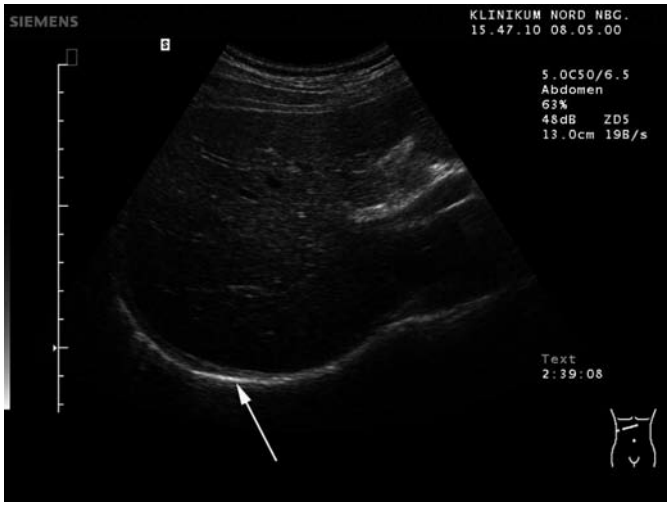

Fig. 1. Subcostal view through the liver. The echogenic line (arrow) represents the diaphragm.

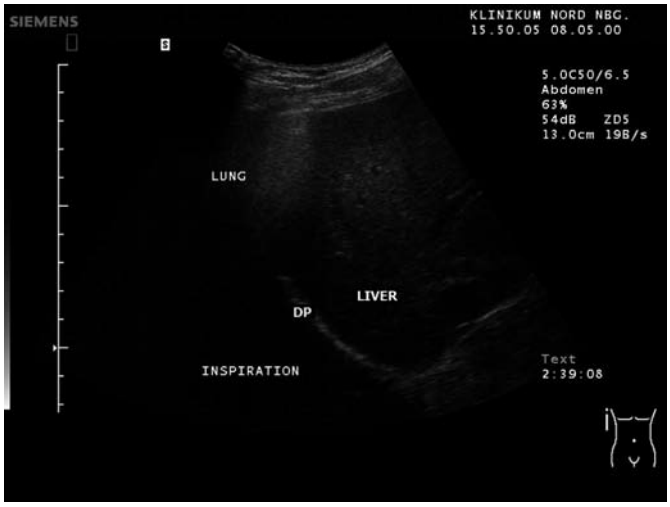

Fig. 2. View of the right recess in the middle axillary line. In inspiration the aerated lung fills the recess. DP = Diaphragm.

beams parallel to structures of the diaphragm will not be reflected and thus they produce no echo signal. The lack of reflection results in black dots in the gray-scale sonographic image and mimics an interruption of the diaphragm. Changing the transducer's position will remove the artifacts.

Liver and Spleen as an Acoustic Window for Sonography of the Chest

Diaphragm

The normal diaphragm contrasts as an echogenic line against the liver parenchyma (fig. 1). The movements as a result of respiration can be visualized in longitudinal sections from the axillary lines (fig. 2). Usually in inspiration the diaphragm extends at least 5–7 cm into the abdominal space. In case of paralysis the diaphragm moves paradoxically. In paresis, in severe lung emphysema and in pleural fibrosis excursions are decreased.

Traumatic ruptures of the diaphragm may be diagnosed by a displacement of abdominal organs into the thoracic space [5, 6]. Further signs of a rupture of the diaphragm are the absence of the echogenic reflected line or fluid with floating pieces [7].

Pleural effusion serves as an excellent acoustic window for imaging solid lesions of the diaphragm (fig. 3) [8]. The abdominal view is the best way for imaging tumors which infiltrate from the thoracic space into the diaphragm (online suppl. video 1). The medium part of the diaphragm has afferent innervation from the cervical roots C3 and C4; pain therefore may be projected into the shoulder or neck. The lateral part of the diaphragm has afferent innervation from the thoracic spine roots Th7–12. Pain will occur in the upper abdomen sometimes radiating into the back and into the epigastrium mimicking the symptoms of pancreatitis or cholecystitis. In case of mesothelioma tumor nodes destroy and interrupt the diaphragmal pleura.

Video

Pleura

Ultrasound shows even a minimal amount of fluid in the pleural space. From the abdominal view through liver or spleen basal pleural fluid can be seen (fig. 4a). Another access to the lower pleural space is from the lateral aspect. Even in the lying patient small amounts of fluid can be detected in the lateral pleural recess (fig. 4b). Sonography has proved to be much superior to supine chest radiography in measuring the quantity of pleural effusion in critically ill patients [9]. Some definite sonographic patterns of pleural effusion such as echogenicity and septations help to distinguish between effusion and empyema. Sonographic examination serves as a useful tool for the rapid adjusted therapy [10]. With additional color Doppler vessels in pleural strands and in thickened pleura can be imagined. Pleural fluid serves as an acoustic window to show irregular formations of the parietal or visceral pleura [11]. By ultrasound the criteria for the development of a pleural effusion into a

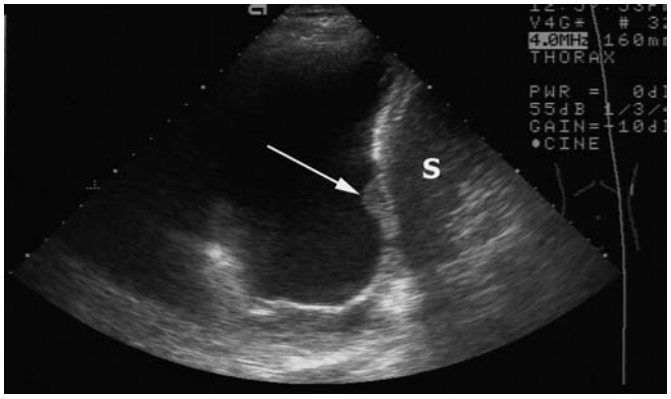

Fig. 3. Small tumor node (arrow) in the diaphragmatic pleura; large pleural effusion. S = Spleen.

Video pleural empyema can be observed (online suppl. video 2a–c).

Occasionally a pneumothorax may be diagnosed by a subpulmonic pleural displacement and the lack of 'lung sliding' [12].

Lung

From the abdominal view especially the lower lung lobes are visible. In case of effusion the atelectatic or compressed lung contrasts against the pleural fluid (fig. 4a). The form of an atelectasis in the pleural fluid gives hints of the inflammatory or tumorous nature of pulmonary consolidations. In case of pneumonia the non- or poorly aerated parts of the lung are to be detected by ultrasound. Inflammatory processes may lead to an adherence of the basal lung structures to the diaphragmal pleura.

Tumorous lesions of the lung sometimes result in complex formations. Ultrasound can distinguish between effusion, atelectatic lung and tumorous infiltration.

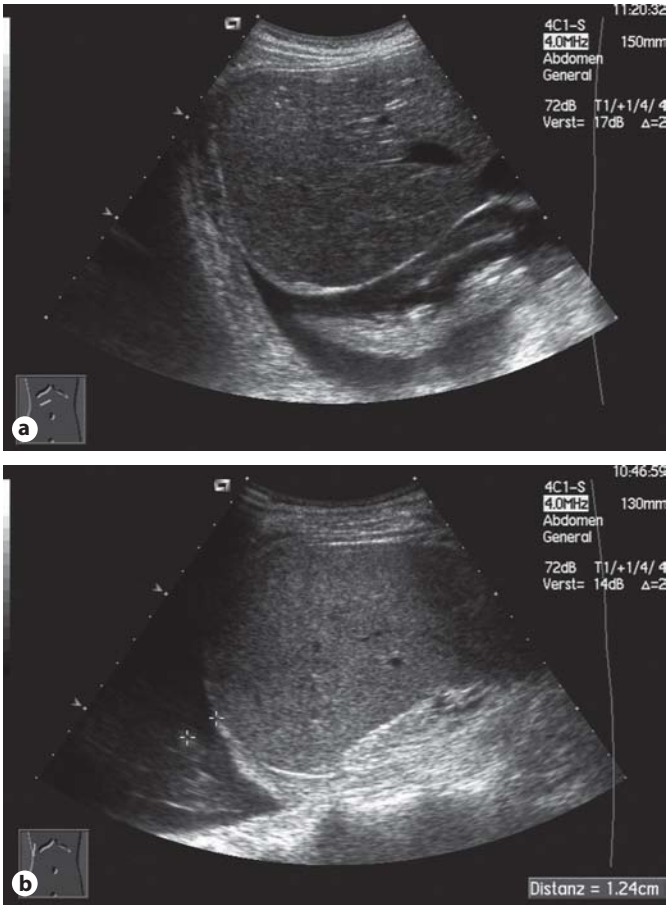

Fig. 4. **a** Small basal pleural effusion seen through the liver; in the effusion the atelectatic lower lobe. **b** Small pleural effusion (subpulmonary height 1.24 cm) in the right recess from the lateral view.

View from the Epigastrium towards the Chest

Longitudinal Section in the Middle of the Epigastrium

The left liver lobe helps for the anatomic orientation. Dorsal of the left lobe appears the caval vein. Its respiratory collapse is investigated in this position. The diameter of the vein is a marker for congestion or volume depletion. The dosage of diuretics can easily be fixed in ventilated patients according to the dimension of the inferior caval vein. The diameter is correctly measured about 2 cm below the diaphragm (online suppl. fig. 1); the caliber should be about 20 mm in expiration and decrease in inspiration.

Left to the caval vein the abdominal aorta appears below the diaphragm. Measuring the aortic diameter (normally less than 25 mm below diaphragm) helps to detect an aneurysm.

In front of and left to the aorta just below the diaphragm the cardia and the inferior part of the esophagus are visible.

In a cranial angulation of the convex transducer following the caval vein the right atrium will be visible. This position allows the typical view into the right atrium to detect a eustachian valve, the Chiari network or thrombi (online suppl. fig. 2; online suppl. video 3a, b). Video

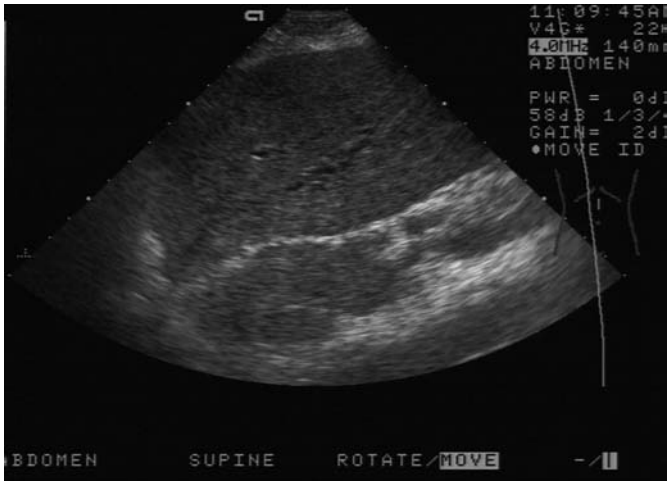

Fig. 5. Enlarged left liver lobe with uneven surface indicative of liver cirrhosis.

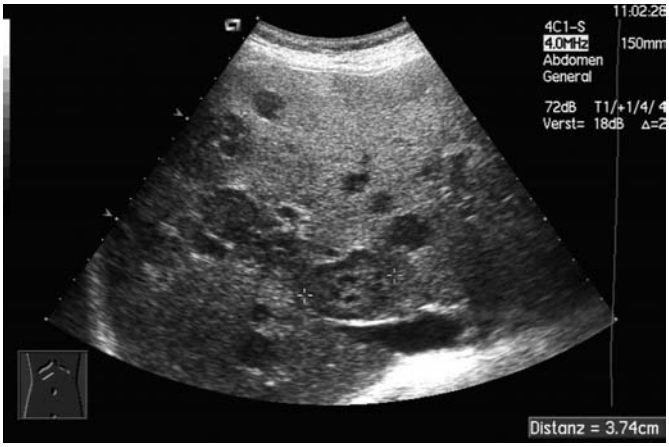

Fig. 6. Oblique subcostal view showing liver metastases in both lobes in a patient with non-small cell carcinoma.

Transverse Section in the Middle of the Epigastrium

The dorsal crura of the diaphragm are situated paravertebrally. In a transversal section in the epigastrium they look like a retroperitoneal tumor near the aorta.

In a cranial angulation of the convex transducer pathologic findings of the pericardium can be found. A pericardial effusion is depicted as a dark surrounding of the right and left ventricle (online suppl. fig. 3a, b).

Tumors infiltrating the right atrium or ventricle are best depicted from this site. An assessment of the cardiac size and the relation of both ventricles are possible as well as the detection of thrombi in the left ventricle. The subcostal view is the best way to display an atrial septal defect in the transthoracic echocardiography.

Pathologic Abdominal Findings of Diagnostic Value in Chest Disease

Abdominal Findings in Pleural Effusion

An abdominal ultrasound examination is mandatory in the diagnosis of pleural effusion. There are several pathologic findings which may explain the cause of an effusion.

Abdominal Signs for Right Heart Failure
A dilated caval vein and dilated liver veins are signs of right heart failure. In case of severe tricuspid insufficiency a systolic reflux can be detected in the liver veins with additional Doppler examination.

Liver Cirrhosis
An enlarged left liver lobe accompanied by an uneven surface (fig. 5) and inhomogeneous parenchyma of the whole organ are signs of cirrhosis. An enlarged spleen in addition to dilated and varicose inlets of the portal vein is a sign of portal hypertension. In case of decompensated liver function ascites and pleural effusion may be present.

Kidney Disease
In kidney disease pleural effusion may occur due to dysproteinemia. In acute nephritis the parenchyma of kidneys is broadened. In chronic renal insufficiency the characteristic finding is a shrinking of the renal parenchyma.

Acute Pancreatitis
Acute pancreatitis causes inflammatory secretion of fluid surrounding the parenchyma. The inflammation may penetrate through the diaphragm mainly on the left side and produce hemorrhagic effusion.

Other Abdominal Manifestations Indicative of a Chest Disease

Liver
Metastasis
At the time of diagnosis about 3% of patients with non-small cell carcinoma present with asymptomatic liver metastasis [13, 14] (fig. 6). In case of small cell carcinoma the number increases to 17% [15]. Extensive metastases may cause diffuse abdominal pain due to tension of the

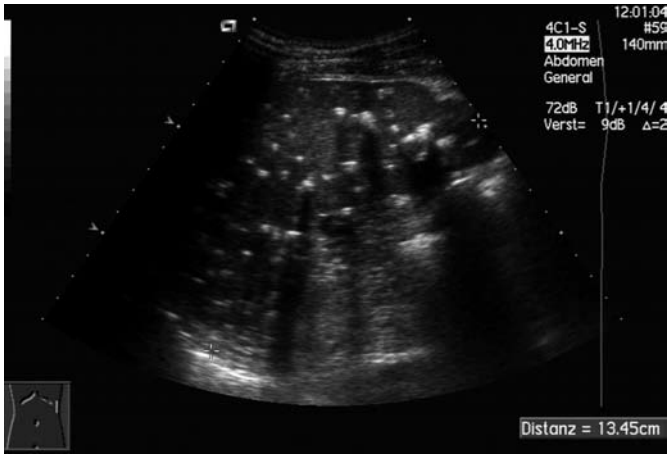

Fig. 7. Multiple calcifications in the slightly enlarged spleen after miliary tuberculosis.

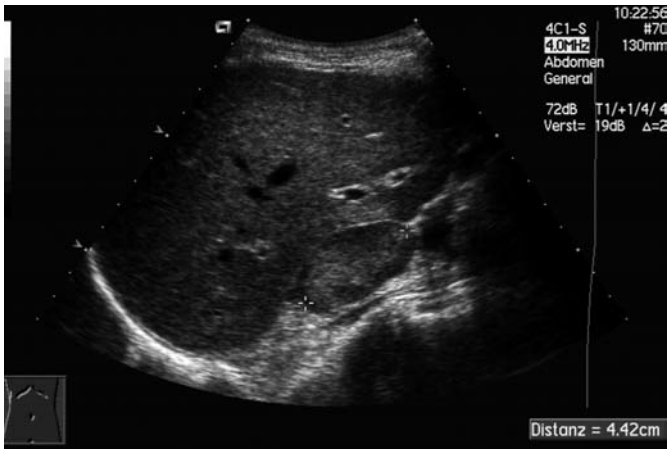

Fig. 9. Enlarged adrenal gland (between crosses) in a patient with known non-small cell carcinoma. On the right side the liver serves as an acoustic window in the lateral view.

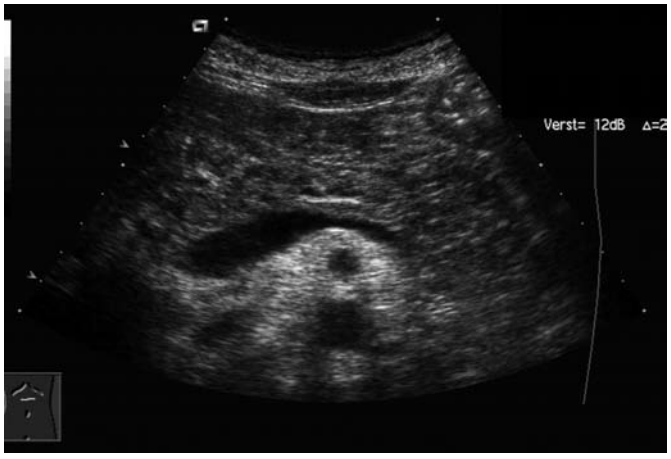

Fig. 8. 35-year-old woman with cystic fibrosis and insufficiency of the pancreas. Sonography shows the inhomogenic parenchyma with disseminated small cysts.

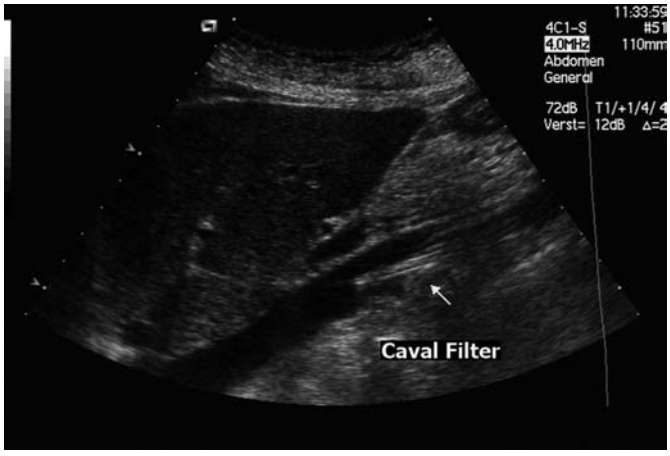

Fig. 10. A caval filter in a patient with recurrent pulmonary thromboembolism due to pelvic venous thrombosis.

liver capsule. Metastases are detected in the liver parenchyma by an echo-poor or less echogenic texture compared to the adjacent normal parenchyma. A typical sign is a surrounding echo-poor line. Sometimes liver metastasis may represent the initial finding of a tumorous disease. A thorough further examination including the chest must follow.

Hereditary Hemorrhagic Telangiectasia

The characteristic manifestation of hereditary hemorrhagic telangiectasia also known as Rendu-Osler-Weber disease is the malformation of arterial and venous vessels. The typical findings in liver and spleen are dilated vessels, aneurysms as well as various arterial and venous shunts. In the course of the disease about 40% of patients with a definite gene mutation develop abnormalities of the vessels in the lung parenchyma [16, 17] (online suppl. fig. 4a–c). Arteriovenous shunts may result in pulmonary hypertension and right heart failure.

Spleen

Infarctions of the spleen are a sudden and painful event. Sonography demonstrates typical triangular echo-poor or even echo-free areas in the parenchyma of the spleen. There

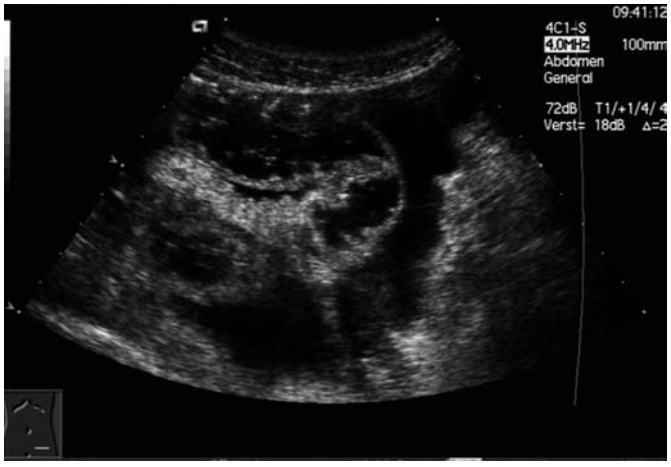

Fig. 11. 46-year-old patient with abdominal pain. Sonography shows fluid between the bowels; in the peritoneal fluid *Mycobacterium tuberculosis* was detected.

will be no vascularization in the lesion. Echo-enhanced sonography is an additional valuable procedure to demonstrate the occlusion of a vessel [18]. A careful examination of the heart is mandatory as endocarditis or thrombi are the main cause of infarctions of the spleen. Sometimes an infarction may develop into an abscess.

In sarcoidosis echo-poor granulomas may be found in the parenchyma (online suppl. fig. 5). The number and size of the granulomas correlate with the activity of the disease.

After miliary tuberculosis multiple calcifications remain in the spleen as a life-long residue (fig. 7).

Pancreas

In patients with cystic fibrosis sonography reveals the typical changes of the parenchyma (fig. 8).

Kidney

Infarctions due to cardiac embolic diseases may also occur in kidney vessels. The leading symptom is a sudden pain in the back extending along the lower ribs. Sonography shows echo-poor areas in the parenchyma. The color Doppler or echo-enhanced sonography leads to the definite diagnosis [18].

A tumor of the kidney may be the source of pulmonary metastases (online suppl. fig. 6a–c).

In lung carcinoma an enlarged adrenal gland is suspicious for metastasis (fig. 9). In autopsy studies adrenal gland metastases were found in 28–44% of patients with lung carcinoma [19]. The probability of a benign or a malignant adrenal mass correlates with the tumor stage and the size of the intrathoracic tumor. For definite staging and prior to the decision for therapy a biopsy of the adrenal tumor may be required [13].

Abdomen

Perforation

Air under the diaphragm is a sign for perforation of the esophagus, stomach or bowels. Sonography shows reverberation artifacts below the diaphragm. Air may spread along the mediastinum to the cervical region.

Caval and Pelvic Venous Thrombosis

In case of pulmonary embolism it is a prerequisite to search for the source of the thrombosis. To examine the large abdominal veins slight pressure might be necessary to push away the gas-containing bowels. Normally the caval vein is oval-shaped. If it is filled with thrombi it appears more rounded. The thrombotic material or a caval filter produce an echogenic pattern in the veins (fig. 10). Additional color Doppler shows a diminished or narrowed flow in the vessels.

Tuberculosis

In peritoneal tuberculous inflammation fluid is to be found between the bowels. The fluid contains floating strings or bands and a lot of small echos due to cellular particles (fig. 11; online suppl. video 4). Video

Metastasis

In case of metastatic peritoneal lesions small nodes on the peritoneum and accompanying fluid can be found. Tumors of the chest may cause metastatic lesions in different parts of the abdomen.

References

1 Lichtenstein DA: Ultrasound in the management of thoracic disease. Crit Care Med 2007;35:S250–S261.
2 Bouhemad B, Zhang M, Lu Q, Rouby JJ: Clinical review: bedside lung ultrasound in critical care practice. Crit Care 2007;11:205.
3 Beckh S, Bölcskei PL, Lessnau K-D: Real-time chest ultrasonography. A comprehensive review for the pulmonologist. Chest 2002;122:1759–1773.
4 Schuler A: Image artifacts and pitfalls; in Mathis G (ed): Chest Sonography. Berlin, Springer, 2008, pp 175–182.
5 Reuss J: The pleura; in Mathis G (ed): Chest Sonography. Berlin, Springer, 2008, pp 41–45.
6 Simpson J, Lobo DN, Shah AB, Rowlands BJ: Traumatic diaphragmatic rupture: associated injuries and outcome. Ann R Coll Surg Engl 2000;82:97–100.
7 Walz M, Muhr G: Sonographische Diagnostik beim stumpfen Thoraxtrauma. Unfallchirurg 1990;93:359–363.
8 Görg C, Görg K, Schwerk WB, Kleinsorge F: Sonographie der Pleura diaphragmatica bei Tumorpatienten. Ultraschall 1988;9:274–278.
9 Vignon P, Chastagner C, Berkane V, Chardac E, François B, Normand S, Bonnivard M, Clavel M, Pichon N, Preux PM, Maubon A, Gastinne H: Quantitative assessment of pleural effusion in critically ill patients by means of ultrasonography. Crit Care Med 2005;33:1757–1763.
10 Chih-Yen T, Wu-Huei H, Te-Chun H, Hung-Jen C, Kuen-Daw T, Chung-Wen H, Chuen-Ming S: Pleural effusions in febrile medical ICU patients. Chest 2004;126:1274–1280.
11 Goerg C, Schwerk W-B, Goerg K, Walters E: Pleural effusion: an 'acoustic window' for sonography of pleural metastases. J Clin Ultrasound 1991;19:93–97.
12 Lichtenstein DA, Menu Y: A bedside ultrasound sign ruling out pneumothorax in the critically ill. Chest 1995;108:1345–1348.
13 Silvestri GA, Gould MK, Margolis ML, Tanoue LT, McCrory D, Toloza E, Detterbeck F: Noninvasive staging of non-small cell lung cancer. ACCP evidenced-based clinical practice guidelines. Chest 2007;132:178S–201S.
14 Hillers T, Sauve M, Guyatt G: Analysis of published studies on the detection of extrathoracic metastases in patients presumed to have operable non-small cell lung cancer. Thorax 1994;49:14–19.
15 Kagohashi K, Satoh H, Ishikawa H, Ohtsuka K, Sekizawa K: Liver metastasis at the time of initial diagnosis of lung cancer. Med Oncol 2003;20:25–28.
16 Sadick H, Sadick M, Götte K, Naim R, Riedel F, Bran G, Hörmann K: Hereditary hemorrhagic telangiectasia: an update on clinical manifestations and diagnostic measures. Wien Klin Wochenschr 2006;118:72–80.
17 Sabbà C, Pasculli G, Lenato GM, Suppressa P, Lastella P, Memeo M, Dicuonzo F, Guant G: Hereditary hemorrhagic telangiectasia: clinical features in ENG and ALK1 mutation carriers. J Thromb Haemost 2007;5:1149–1157.
18 von Herbay A, Schick D, Horger M, Gregor M: Low-MI-sonography with the contrast-agent SonoVue in the diagnosis of infarction of the spleen, kidney, liver and pancreas. Ultraschall Med 2006;27:445–450.
19 Braun B: Nebennieren; in Braun B, Günther R, Schwerk WB (eds): Ultraschalldiagnostik, Lehrbuch und Atlas. München, ecomed, 1990, vol 3, chap 1.10.

Dr. med. Sonja Beckh
Medizinische Klinik 3, Klinikum Nürnberg
Prof. Ernst-Nathan-Strasse 1
DE–90419 Nürnberg (Germany)
Tel. +49 0911 398 2675, Fax +49 0911 398 2441, E-Mail beckh@klinikum-nuernberg.de

Chapter 12

Bolliger CT, Herth FJF, Mayo PH, Miyazawa T, Beamis JF (eds): Clinical Chest Ultrasound: From the ICU to the Bronchoscopy Suite.
Prog Respir Res. Basel, Karger, 2009, vol 37, pp 96–108

Use of Ultrasonography for the Diagnosis of Venous Thromboembolic Disease

Adolfo E. Kaplan[a] · Pierre Kory[b]

[a]Private Practice, Pulmonary, Critical Care and Sleep Medicine, McAllen, Tex., and [b]Attending Physician, Pulmonary, Critical Care and Sleep Division, Beth Israel Medical Center, New York, N.Y., USA

Abstract

The diagnosis of deep venous thrombosis of the upper and lower extremities is an important aspect of critical care ultrasonography. In this chapter, we review the normal venous anatomy of upper and lower limbs, and explain available sonographic modalities and examination techniques. A diagnostic sonographic strategy is proposed. Pitfalls and limitations of vascular ultrasonography, comparison with alternative diagnostic modalities, and review of the literature on clinician-performed examinations are described.

Critically ill patients are at the highest risk for development of deep venous thrombosis (DVT) due to the presence of multiple risk factors such as prolonged immobility, surgery, malignancy, proinflammatory and hypercoagulable states, and high rates of indwelling devices [1–5]. Clinical signs and symptoms are unreliable in the diagnosis of DVT in intensive care unit (ICU) patients who are often unable to relay symptoms, and whose examination is often limited by obesity, edema, and surgical dressings [6, 7]. Consequently, DVT is frequently undertreated which results in an increased mortality in this patient population [8, 9]. Ten to 100% of DVTs in ICU are clinically unsuspected, and pulmonary embolism is the most frequent unsuspected autopsy finding, directly contributing to death in approximately 5% of all cases [10].

Therefore, in the critically ill, prompt and accurate objective testing is necessary for the diagnosis of DVT. Currently, ultrasonography is the primary and oftentimes only modality used to meet this objective. The following is an overview of the strength and limitations, clinical applications, and technical performance of both upper and lower extremity deep venous diagnostic ultrasonography.

DVT of the Lower Extremities

The true incidence and prevalence of lower extremity DVT (LEDVT) in the ICU are unknown. Based on screening studies using ultrasonography for diagnosis, incidence rates vary considerably, likely as a result of differences in the patient population, adequacy of prophylaxis, sonographic technique, and sonographer skills. Reported incidences range from as low as 8% to as high as 18% for proximal LEDVT, with the majority of cases occurring within the first week [1–5]. Of particular concern are the results of Ibrahim et al. [4], noting an 18% incidence of DVT among ICU patients mechanically ventilated for a minimum of 7 days despite receiving standard recommended doses of heparin prophylaxis. A review of published screening studies suggests that, on average, there is a 10% incidence of proximal LEDVT in critically ill patients despite optimal prophylaxis.

Clinically, LEDVT are classified according to their embolic risk. Proximal (popliteal and higher veins) DVTs have a higher risk of embolizing than distal (veins below the popliteal) DVTs. It is estimated that the risk of pulmonary embolism with distal DVTs is approximately 8%, as opposed to the 50% risk associated with proximal DVTs [11, 12]. Since 80% of calf DVTs do not extend proximally, anticoagulation is commonly held to avoid unnecessary complications [10]. Instead, serial sonographic examinations can be performed to identify proximal extension of clots when distal DVT is suspected. In addition, due to the added time required to scan the calf veins and the lower sensitivity of ultrasound for detection of DVTs below the popliteal veins [7, 13–15], we do not routinely examine the

Table 1. Nonsonographic diagnostic modalities for detection of DVT

	Advantages	Disadvantages
Contrast venography	Accuracy	Availability Invasiveness Need for transportation out of ICU Ionizing radiation Ionizing contrast media: kidney injury Allergy to contrast Thrombophlebitis Technical limitations Cost
Impedance plethysmography	Availability Cost Ease of use	Unknown accuracy in ICU population Overall less sensitive than ultrasound Detects venous outflow obstruction alone (cannot differentiate alternative diagnoses: Baker's cyst, etc.)
CT venography	Accuracy (LEDVT only) Performed together with chest CT Assessment of pelvic thrombosis	Ionizing radiation Ionizing contrast media: kidney injury Allergy to contrast Relatively contraindicated in pregnancy Does not assess upper extremities Cost
MR venography with or without gadolinium	Use if allergy or contraindi-cations to contrast media Assessment of pelvic thrombosis	Availability Inability to perform in ventilated patients Risk of kidney injury Cost

distal venous system as part of our examination. Therefore, we will focus our review on the accuracy of diagnostic ultrasonography for proximal DVT only.

Diagnostic Modalities for Detection of DVT

Despite many limitations (table 1), contrast venography is still considered the reference standard for the diagnosis of DVT [7]. Although no longer considered appropriate as the initial diagnostic test when assessing extremities for the presence of acute DVT, we reserve it for situations when noninvasive testing modalities are nondiagnostic and there remains a compelling reason to establish the diagnosis [16–18].

Accuracy of Ultrasound in the Diagnosis of LEDVT

Symptomatic Outpatient Population

A landmark study by Lensing et al. [15] in 1989 compared contrast venography with compression ultrasound (CUS) in 220 clinically symptomatic outpatients and showed ultrasonography to have a sensitivity of 99% (CI: 95–100%) and specificity of 100% (CI: 97–100%) for proximal LEDVT. Multiple other studies in this patient population have shown similar sensitivities ranging from 89 to 100% for proximal LEDVT [19–23]. In addition, Birdwell et al. [24] demonstrated the safety of withholding anticoagulation in a population of 335 symptomatic outpatients with two negative compression studies (follow-up study performed 7 days after the initial one) by reporting a 0.6% rate of DVT at 3 months' follow-up.

Asymptomatic, High-Risk Population

Despite the well-established accuracy of ultrasound in the symptomatic outpatient population, few studies have been performed in high-risk, asymptomatic patients. One study compared the combination of CUS and color Doppler augmentation technique with contrast venography in postoperative hip and knee surgery patients, finding the sensitivity of ultrasound for proximal LEDVT to be 60% with a specificity of 71% [25]. In a meta-analysis of studies assessing the accuracy of ultrasound in asymptomatic postorthopedic surgical patients, the average sensitivity was 65% [26]. Similarly, in a study of asymptomatic hospitalized patients at moderate risk for DVT, sensitivity of ultrasound compared to contrast venography was shown to be 60% with a positive predictive value of 75% [16]. In conclusion, the sensitivity of ultrasound in the high-risk inpatient population is markedly lower than the near perfect sensitivity found in symptomatic outpatients.

Critically Ill Population

There are no studies directly comparing sonography with contrast venography in critically ill patients. Thus, the true accuracy of sonography in this population is unknown. In a recent study, the diagnostic accuracy of CUS was compared with CT venography [27]. Both modalities were found to have a sensitivity of 70% (CI: 41.6–98.4%) for proximal

LEDVT. The reference standard used was documentation of pulmonary emboli combined with a positive CT venography or CUS. This data, combined with the results of studies in other high-risk, inpatient populations [16, 28], suggests that the sensitivity of ultrasound in critically ill patients is considerably lower than in the symptomatic outpatient population. This is due to several factors, including (1) the characteristics of thrombi in this setting are less extensive, less organized, less occlusive, and less echogenic than in symptomatic outpatients, leading to poor visualization and more compressible thrombi, and (2) the inability to perform technically adequate examinations due to patient immobility and frequent limb swelling. Consequently, the incidence of LEDVT in critically ill patients is likely highly underestimated when CUS is used for screening the critically ill.

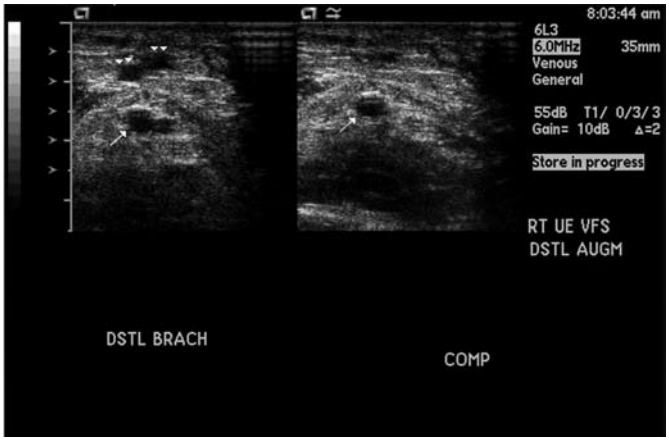

Fig. 1. CUS of brachial veins. There are two superficial brachial veins. They do not usually run contiguously with the deeper artery. When pressure is applied, the lumen of the two veins is completely obliterated, while the arterial lumen remains patent. The anechoic structure behind the artery is the humerus bone.

Ultrasound Modalities for Detection of DVT

There are three sonographic techniques commonly used when evaluating the venous system for the presence of thrombosis: B-mode, spectral Doppler, and color Doppler imaging. The commonly named ultrasound tests ('duplex', 'triplex') differ only in the type and combination of these techniques as follows:

- *Real-time CUS* uses B-mode (brightness modulation) 2-dimensional imaging only and allows direct visualization of the venous segment examinated. Veins are compressed in a sequential manner in transverse section (except for the subclavian vein). Veins are also assessed for intraluminal echogenic material (fig. 1).
- *Duplex ultrasound (CUS plus spectral Doppler analysis)* considered the essential examination mode for peripheral venous testing according to the standards of the Intersocietal Commission for the Accreditation of Vascular Laboratories (ICAVL) in the USA [29] (fig. 2).
- *Triplex ultrasound (CUS, spectral Doppler, and color Doppler analysis):* the addition of color Doppler imaging enables the assessment of the presence and direction of blood flow within the vein [29] (fig. 3). If used, color gain settings must be set in order to avoid oversaturation so that small intraluminal clots or areas of incomplete thrombosis are not obscured.

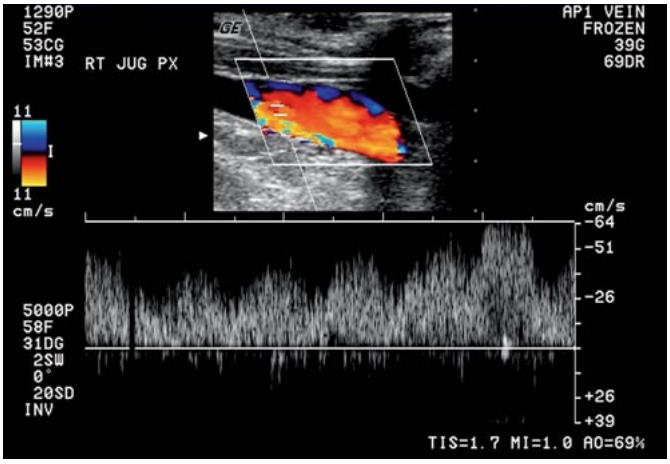

Fig. 2. The upper portion demonstrates the location of the pulsed wave Doppler examination box within the lumen of the proximal internal jugular vein. Color Doppler in the same image demonstrates the presence of flow. The bottom image is the spectral Doppler signal obtained with pulsed wave. It represents phasic flow with respiratory variation at low velocities (0.4 m/s), typical of venous flow velocities.

Diagnostic Sonographic Criteria of DVT

A normal, patent venous system is characterized by four sonographic criteria.

(1) *Compressibility:* Patent veins are fully compressible under light pressure applied with the transducer, with the visible lumen completely disappearing as the opposing venous walls come into full contract (fig. 1, 4). The inability to completely compress the venous lumen is the main criterion for the diagnosis of DVT [30]. Incomplete collapse of the venous lumen with slightly lower pressure than is required to occlude the adjacent artery signifies that a thrombus is present. The amount of pressure required is important to consider since acute thrombi have jelly-like

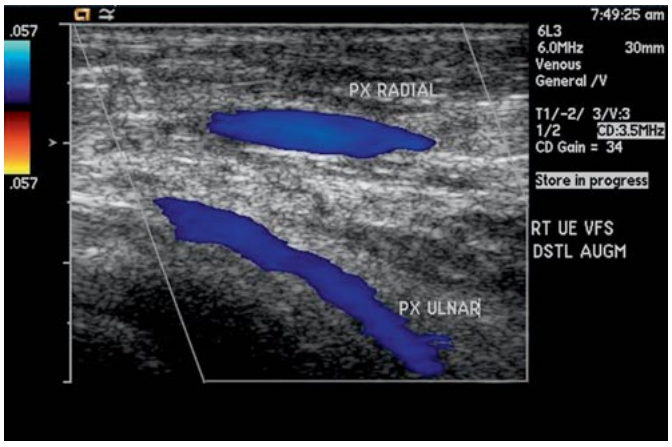

Fig. 3. Color Doppler assists the sonographer to identify these two distinct vessels.

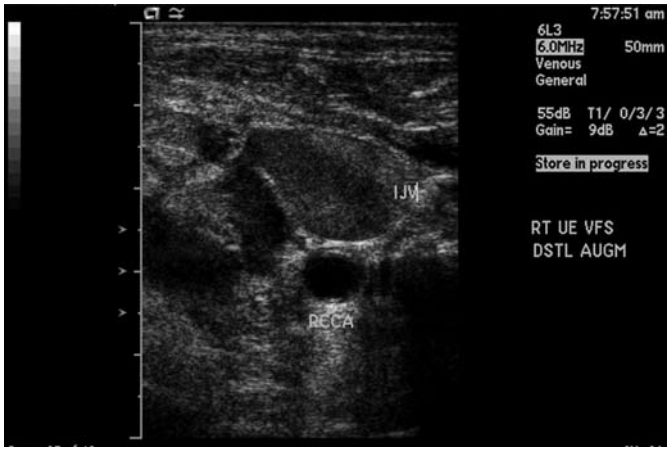

Fig. 5. Transverse image of the right internal jugular vein. Its lumen is filled with spontaneous echoes ('smoke'). In comparison, the lumen of the right common carotid artery is echolucent except for its thickened, calcified walls.

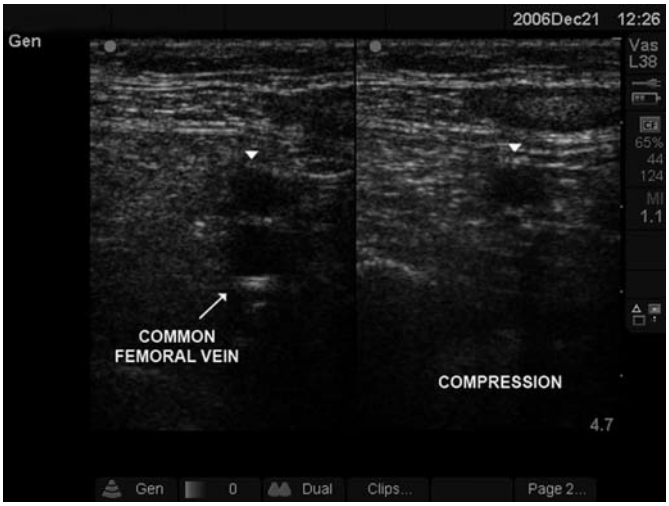

Fig. 4. Normal compression of SFV demonstrating absence of thrombus. A split screen format is utilized. By convention the uncompressed vein image is on the left side of the image and the compressed image is on the right. Note the complete disappearance of the vein lumen under compression.

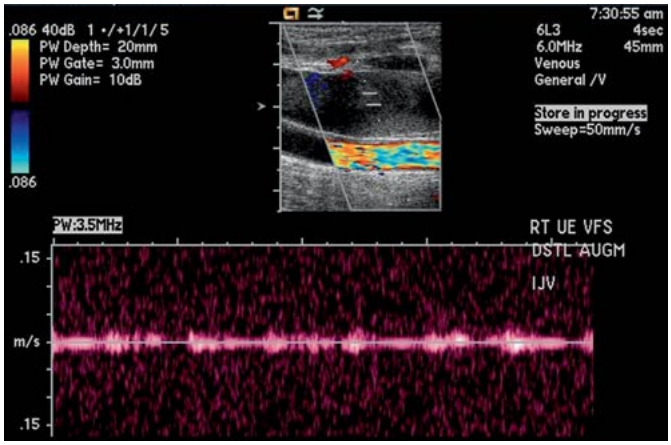

Fig. 6. Notice 'smoke' and lack of color flow in this longitudinal axis view of the internal jugular vein. The bottom spectral Doppler signal reveals almost no flow.

consistency and are frequently partially compressible, potentially resulting in false-negative studies if excess pressure is applied.

(2) *Absence of intraluminal echogenic material:* Normal patent veins are devoid of internal echoes. Acute thrombi are hypoechoic and generally not visible. As thrombi organize, they become progressively more echoic and visible. Visualization of echogenic material within the vein has a high correlation with DVT, but not in isolation (fig. 5). When only this criterion was considered (without assessing for compressibility), Baarslag et al. [31] found that thrombus was absent in 3/27 (11%) of patients when venography was performed.

(3) *Flow pattern:* When using Doppler waveform examination (pulsed-wave or continuous-wave), a patent system demonstrates two normal characteristics: spontaneity (presence of spontaneous, pulsatile flow) and phasicity (flow variation with normal respiration) (fig. 2). Absence of flow and/or monophasic flow findings are only considered suggestive of DVT (fig. 6), particularly if not associated with other diagnostic criteria [18, 32]. A monophasic pattern can also be caused

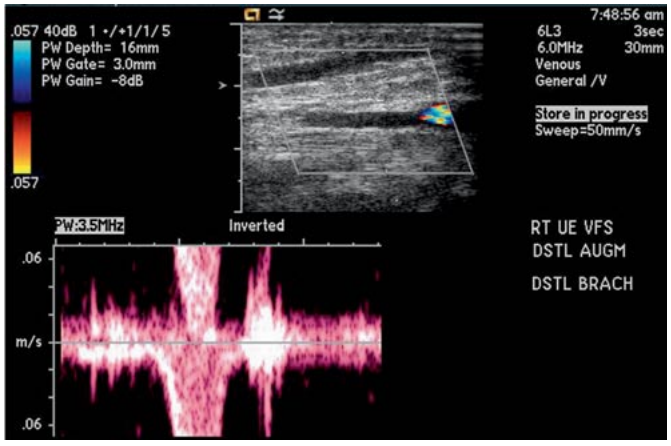

Fig. 7. Normal increase in peak velocity spectral Doppler signal of brachial vein in response to distal compression maneuvers.

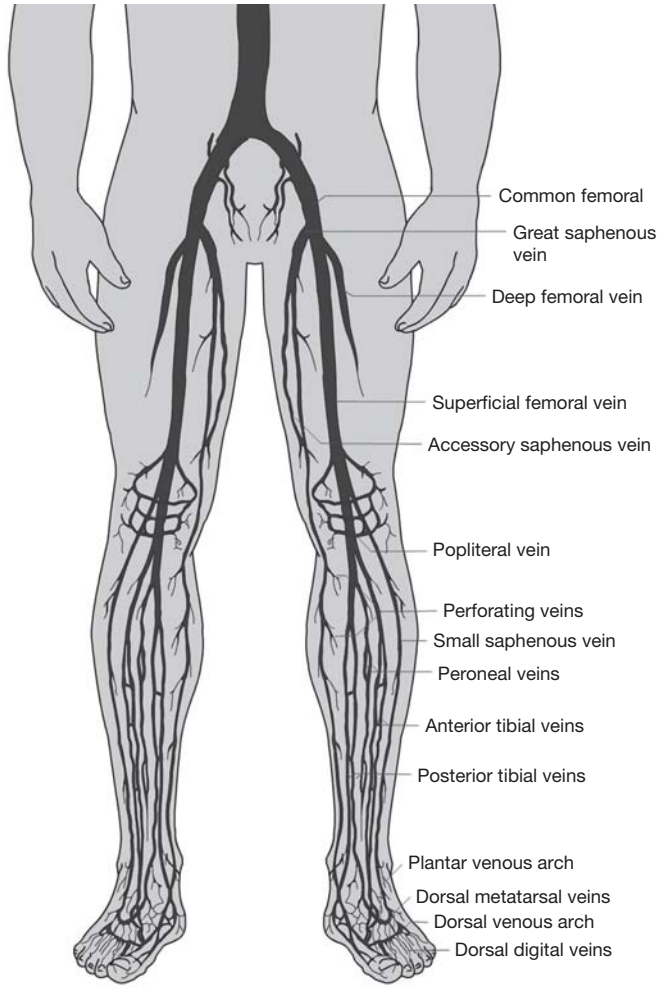

Fig. 8. Lower extremity venous anatomy.

by the presence of external compression on the venous system due to other causes such as lymphadenopathy, hematoma, and extensive swelling.

(4) *Augmentability:* Augmentability refers to increased velocity of flow in the Doppler spectral or color Doppler signals in response to maneuvers such as manual compression of a distal muscle group or Valsalva maneuvers (fig. 7). Augmentation maneuvers can force blood around an area of thrombosis, resulting in falsely negative results if no other sonographic criteria are considered. This finding has been shown to be sufficiently nonspecific [33–35], so that we use it solely to help in the identification of venous segments that are difficult to visualize.

Diagnostic Venous Sonography of the Lower Extremities in Critically Ill Patients

Sonographic Strategy

Although multiple ultrasonographic modalities have been used to diagnose DVT, there is compelling evidence to show that using sonographic techniques in addition to CUS does not increase diagnostic accuracy and as a result, need not be used. In two different patient populations, both Lensing et al. [25] and Blaivas et al. [33] showed that color Doppler findings were too nonspecific to increase accuracy. The addition of an assessment of venous distension during a Valsalva maneuver also did not increase accuracy [15]. Furthermore, several authors found that the value of flow augmentation responses was also insensitive and nonspecific, and did not improve the diagnostic accuracy of CUS [33–37]. Poppiti et al. [38] compared the two-site CUS technique with triplex scan and found that the multimodality test revealed no additional proximal DVT, although it did demonstrate two false-positive popliteal thrombi. As a result of these data, we rely solely on the CUS technique to diagnose DVT. Flow pattern analysis and augmentation maneuvers (by Doppler spectral signal and/or color Doppler) can be used as adjunct techniques, keeping in mind their limitations. As previously noted, we utilize color Doppler to identify venous segments that are difficult to visualize in obese and edematous patients.

The literature divides sonographic examinations of the lower extremities into complete and limited. A complete exam consists of performing sequential compressions every 1–2 cm over the entire proximal venous system from the iliac vein through the trifurcation of the calf veins. A lim-

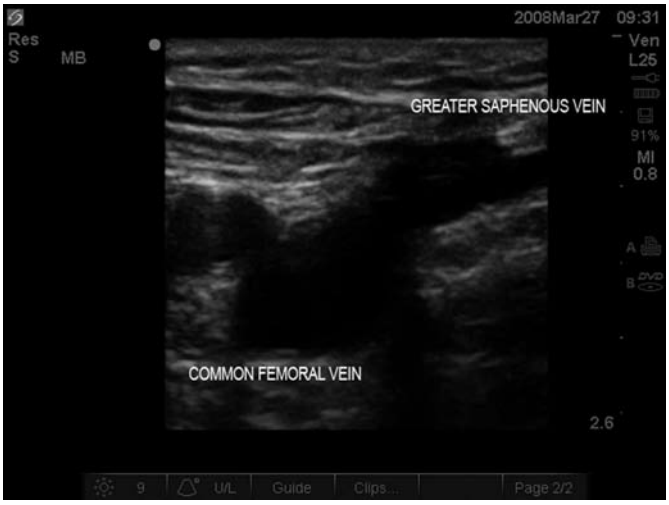

Fig. 9. Right CFV demonstrating with entrance of the GSV on medial aspect.

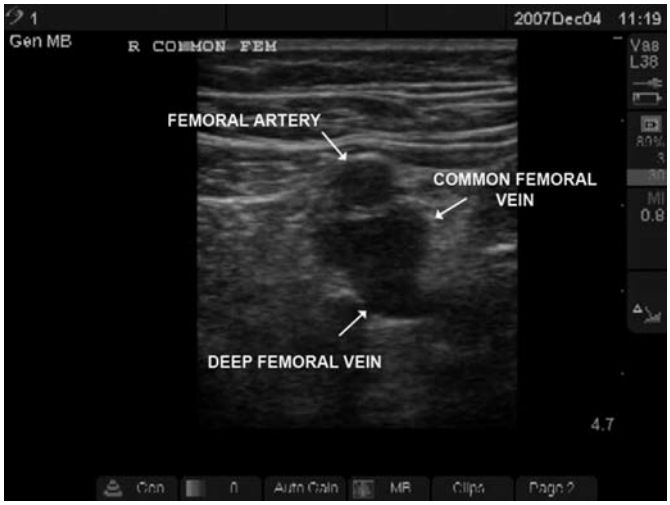

Fig. 10. Right CFV and the DFV posteriorly.

ited or 'two-site' exam consists of performing compressions at two anatomic sites alone, a technique based on data showing that the majority of LEDVTs occur at the two main venous confluences [common femoral vein (CFV)-greater saphenous vein (GSV) junction and the trifurcation of the popliteal into the deep calf veins] and are only rarely isolated to the superficial femoral vein (SFV; 0–6%) [39–43]. In contrast to these studies, Maki et al. [44] reported a 22% rate of DVT isolated to the proximal SFV in their retrospective analysis. Because of this report, we recommend performing a complete study of the common femoral veins and SFV, followed by a full examination of the popliteal vein to the proximal portion of the calf vein trifurcation. To save time, we employ a modified technique: we first scan the two venous confluences, and, if no thrombus is identified, we then examinate the entire length of the SFV down to the adductor canal.

Normal Anatomy of the Lower Extremity Venous System

Prior to scanning the lower extremity, knowledge of venous anatomy is required (fig. 8). Veins are divided into deep (within muscle) and superficial (within fascia). Deep veins are paired and accompany the arteries. Once the external iliac vein crosses the inguinal ligament, it becomes the CFV. The CFV is then joined medially by the GSV. Approximately 1–2 cm beyond this point, the CFV divides into the deep femoral vein (DFV) and the SFV. The DFV can usually be tracked for a short distance before it dives deeper and away from the acoustic window. The SFV runs anteromedially down to the adductor canal, where it then courses posteriorly into the popliteal fossa becoming the popliteal vein (fig. 9, 10).

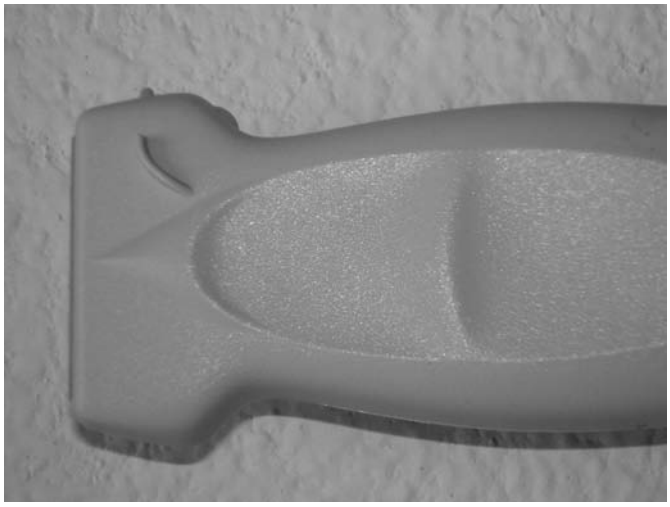

Fig. 11. Standard configuration of a high-frequency transducer used for vascular imaging. Such transducers typically utilize a frequency of 7.5 MHz.

Technique

A linear transducer with a frequency range from 5 to 10 MHz is generally used (fig. 11). The patient is placed supine with the lower extremity fully exposed and externally rotated (fig. 12). Reverse Trendelenburg positioning can be used to better fill the veins. Prior to a compression maneuver, we assess for intraluminal echogenicity (fig. 4). The presence of echoes within the vein (smoke) lacks speci-

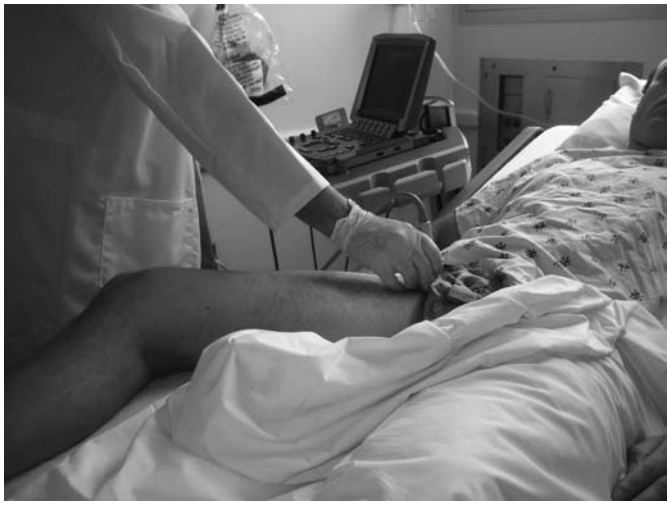

Fig. 12. Demonstration of standard patient and sonographer position during examination of the CFV. The patient leg is externally rotated with the transducer orientation transverse to the vein.

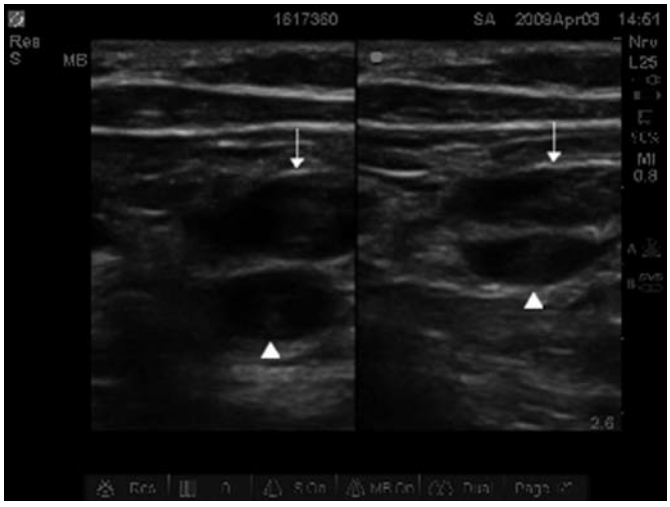

Fig. 13. DVT of the right CFV. Note the lack of disappearance of the vein lumen while under compression (right side of image) (compare to fig. 4).

ficity for thrombus, and most acute thrombi are hypoechoic and not visualized. However, the clinician will encounter situations where an echogenic and well-circumscribed thrombus is found. In those circumstances, we perform longitudinal scanning prior to compressing the vein to avoid the risk of dislodging a mobile, mural clot. Once confident that a mural clot is not present, pressure is applied with the transducer in the transverse axis to the point where the anterior and posterior walls of the vein come into contact and the venous lumen disappears completely. At this point, only slight deformation of the adjacent artery should be seen. The requisite amount of pressure to achieve must be gained from experience as excessive pressure can occlude the artery while inadequate pressure can lead to the erroneous conclusion that a vein is noncompressible. Absence of full compression indicates the presence of venous thrombosis (fig. 13). However, the operator must ensure that the probe is transverse to the vein, with downward pressure applied directly over the vein. If the transducer is angled or positioned incorrectly, pressure is sometimes directed adjacent to the vein or the vein inadvertently slides away from the examination window (more common if the longitudinal axis is used), resulting in a greater likelihood of a false-positive finding.

Storing the digital image or recording of all findings is an important part of the exam, not only for documentation and billing purposes, but also for later interpretation or review if the operator is unclear or inexperienced in interpreting equivocal findings. Compression images are stored in 'split-screen' or 'dual' image format, a common function on portable ultrasound devices. The accepted method is to first 'freeze' a still image with the uncompressed vein of interest in the center of the screen, then the operator switches the monitor to 'dual' screen display, followed by performance of a compression maneuver with the image saved at full compression. The saved image thus shows a side-by-side comparison of the compressed and uncompressed vein. By convention, the uncompressed image is on the left of the screen. Text notation of the vein, extremity, and segment is also required for each image saved. We typically save images at the following junctions: (1) CFV-GSV, (2) CFV-DFV, (3) PV-calf veins and at any point where a thrombus or any other abnormality is visualized.

Common Femoral Vein. The examination begins with the transducer applied in the transverse axis at the origin of the CFV, just below the inguinal ligament and medial to the femoral artery. Sequential compressions are then performed, advancing 2 cm distally along the vein before the next compression. We also examinate the proximal portion of the GSV, as thrombus present at this level is at high risk for extending into the CFV. Continuing distally along the CFV, an unnamed perforator is often seen entering lateral to the CFV just prior to the division into the profunda (or deep) femoral vein and the SFV, and should not be mistaken for the DFV. Following the two-site strategy, we then move to the popliteal fossa.

Popliteal Vein. Ideally, the patient should be prone, an impossible feat in most critically ill individuals. In such patients, we flex the knee to approximately 45° or we position the patient in the contralateral lateral decubitus posi-

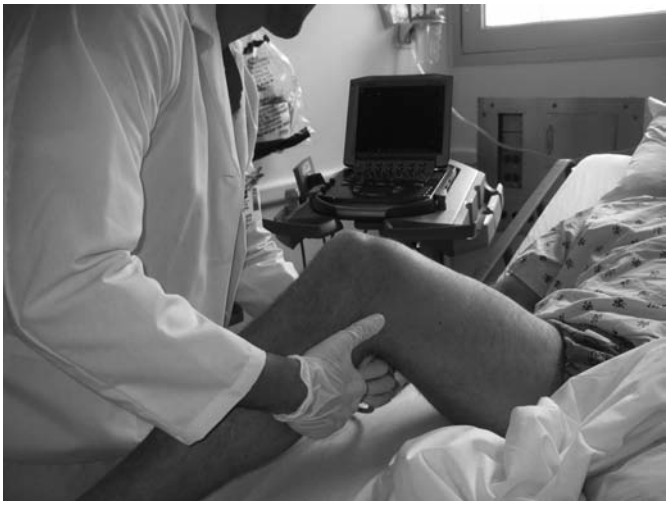

Fig. 14. Demonstration of leg position during examination of the popliteal vein in a supine patient. Leg is raised in a slightly flexed position, the transducer is brought behind the leg and applied to the popliteal fossa in a transverse orientation.

tion, freeing the studied limb for increased mobilization and maneuvering (fig. 14). The latter requires assistance, particularly if airway and other devices need to be secured. The sonographer will find the paired popliteal artery and vein located in a central position (visualization of associated smaller vessels indicates the transducer is positioned too low in the popliteal fossa). Compressions are performed sequentially to a point just distal to the trifurcation of the popliteal vein into the three calf veins.

Superficial Femoral Vein. As previously mentioned, if the two-site technique is negative, we examinate the length of the SFV until it is lost medially in the adductor canal.

Iliac Vein. If no DVT is found within the lower extremity, we attempt to examinate the iliac vein. Reverse Trendelenburg and color Doppler can assist in finding this vein. CUS is generally not feasible here, so we rely on color Doppler results and the presence of a monophasic spectral Doppler pattern with lack of augmentability to diagnose DVT in this area.

Diagnostic Venous Sonography of the Upper Extremities in Critically Ill Patients

As with LEDVT, the true incidence and magnitude of upper extremity deep venous thrombosis (UEDVT) in critically ill patients is not known. Potential fatal pulmonary emboli complicate UEDVT in up to 36% of cases, and probably even more frequently in carriers of central venous catheters [45]. Unfortunately, there are no clinical studies assessing the accuracy of ultrasonography for the diagnosis of UEDVT in the critically ill. We instead rely on indirect information gained from research addressing the risk of DVT associated with venous catheterization or manipulation. For example, the rate of symptomatic UEDVT in patients with central venous catheters was 12–14% in two large series of adults and children [46, 47]. Unfortunately, DVT is frequently asymptomatic in carriers of central venous catheters, and its incidence is unknown in carriers of pacemakers, defibrillators, and hemodialysis catheters commonly found in critically ill patients [48, 49]. Peripherally inserted central catheters, now in widespread use, are associated with an incidence of UEDVT of 1–9%, depending at least partially on the diameter of the catheter [50]. In the largest patients registry to date, the presence of an indwelling central venous catheter was the most powerful independent predictor of UEDVT, with adjusted odds ratio of 9.7 (95% CI: 7.8–12.2) [51]. Compounding the problem, many critically ill patients experience multiple coexistent risk factors associated with an even higher risk of UEDVT: cancer, previous or ongoing LEDVT, surgery, trauma, prolonged immobility and coagulation defects.

As previously mentioned, the accuracy of ultrasonography for the diagnosis of UEDVT in noncritically ill patients is uncertain. Mustafa et al. [52] searched the medical literature from 1980 to 2000 to assess the sensitivity and specificity of this diagnostic methodology. Only 6 prospective studies could be found, and only one study met predefined methodological criteria [53]. Clear methodological differences were noted, and sample sizes ranged between 2 and 58 patients. The authors found ultrasonography to have a sensitivity of 56–100% and a specificity of 77–100%. This significant variability is clearly related to study methodology, patient population, reference standard used and, importantly, the sonographic technique utilized. A more recent, methodologically sound study supports this data. Baarslag et al. [54] found a sensitivity of 82% (95% CI: 70–93%) and specificity of 82% (95% CI: 72–92%) in 126 consecutive non-critically ill patients in both in- and outpatient settings. Even when accounting for the limited data on the accuracy and performance of the test, ultrasonography remains the first, and many times only, test performed to rule out UEDVT. As with the diagnosis of LEDVT, we perform ultrasonographic testing as a first test, with more invasive testing reserved for when clinical suspicion remains high.

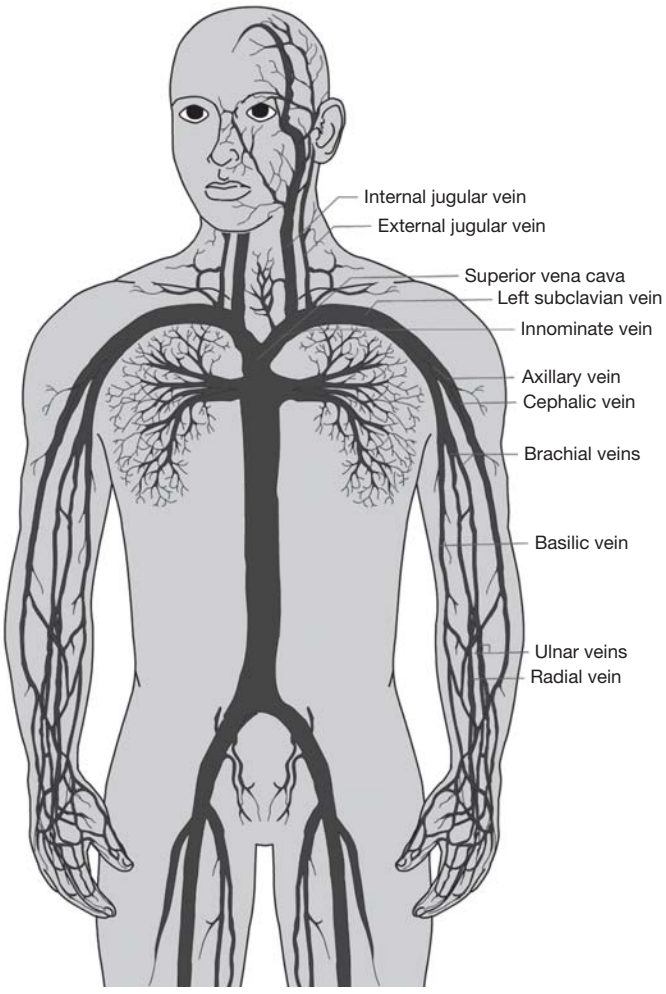

Fig. 15. Upper extremity venous anatomy.

Normal Anatomy of the Upper Extremity Venous System

As previously noted, veins are divided into deep (within muscle) and superficial (within fascia). Deep veins are paired and accompany the arteries: radial, ulnar, brachial and axillary. The latter is commonly single and is only one of the few peripheral veins in the body that does not necessarily run next to its artery. For the purposes of DVT detection, subclavian, internal jugular and innominate (or brachiocephalic) veins are considered part of the upper extremity deep venous system. The superficial veins are single and include the medial basilic and lateral cephalic. They usually communicate at the cubital fossa by way of the median cubital vein (fig. 15).

Technique

A linear transducer with frequency range from 5 to 10 MHz is generally used. The patient is placed supine. Examination begins with the internal jugular vein, from the submandibular area down to the base of the neck. The patient's neck is rotated contra-laterally to expose the area of interest. Trendelenburg positioning can be used to fill the internal jugular and subclavian veins.

Internal Jugular. The internal jugular vein runs anterior and medial to the common carotid artery, and becomes larger as it approaches the thorax. Asymmetry of size is common. Careful attention should be placed on avoiding excess pressure with the transducer, particularly in hypovolemic patients since the vein is often easily compressible and thus may be difficult to identify. A large venous valve can often be identified at the base of the neck.

External Jugular. It is not necessary to routinely assess the external jugular vein although we find it useful to examine this vein when internal jugular thrombosis is suspected. The external jugular vein can be found running parallel to the posterior border of the sternocleidomastoid muscle, without accompanying artery. It is superficial, easily compressible, and smaller than the internal jugular vein unless the internal jugular is occluded, making the external jugular its collateral vein.

Brachiocephalic Vein. The brachiocephalic vein is usually difficult to assess due to overlying bony structures and lung air.

Subclavian Vein. The subclavian vein is inspected from below the clavicle. The transducer is placed longitudinally along the course of the vessel below the clavicle with cephalad angulation (fig. 16). The medial aspect is difficult to assess (left more than right) because of clavicular interposition [55]. The vein can be differentiated from the adjacent artery by its larger size, lack of spontaneous pulsatility, and Doppler venous flow pattern. The phasic respiratory variation of the spectral Doppler signal can also be identified, particularly when the patient is hypovolemic. If the patient can cooperate and the vein is difficult to visualize, he or she should be asked to take in a deep, quick breath through pursed lips, as though sucking on a straw. If the vein collapses with inspiration while performing this maneuver, it can be judged to be free of thrombus. In some subjects, the subclavian vein cannot be visualized despite patient positioning and respiratory maneuvers, particularly on their more medial aspect (left more than right). On these occasions, we use color Doppler to identify vascular structures followed by Doppler waveform examination once the vessel is identified (fig. 17). Attempts are generally made to compress the vein along its longitudinal direction. Support of surrounding

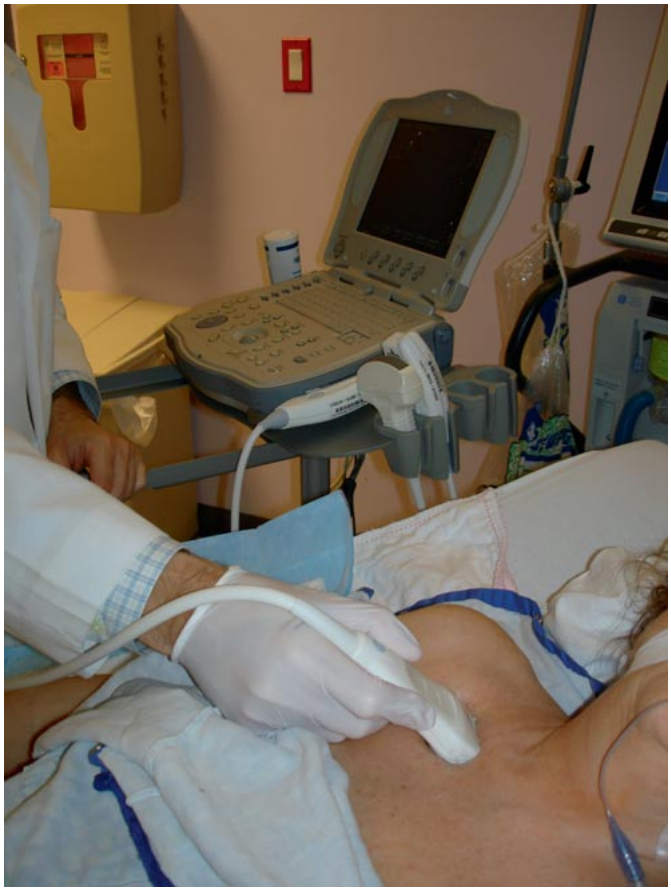

Fig. 16. Demonstration of patient and transducer positioning for subclavian vein examination.

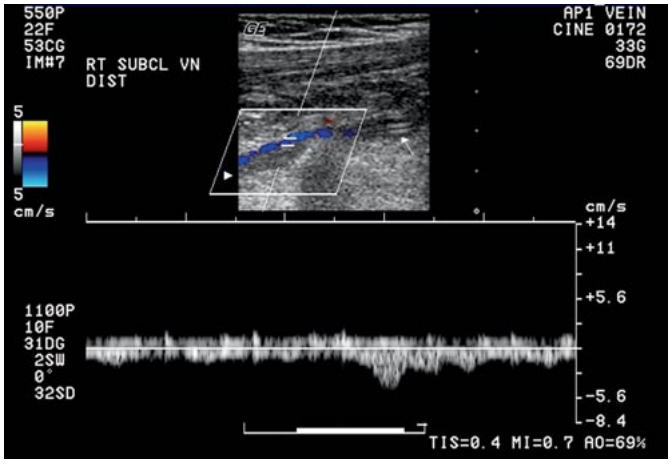

Fig. 17. Examination of distal subclavian vein demonstrates a catheter within its lumen (arrow), and abnormal color flow signal. Pulsed wave Doppler with display of spectral Doppler signal (bottom) reveals no phasicity and decreased velocities.

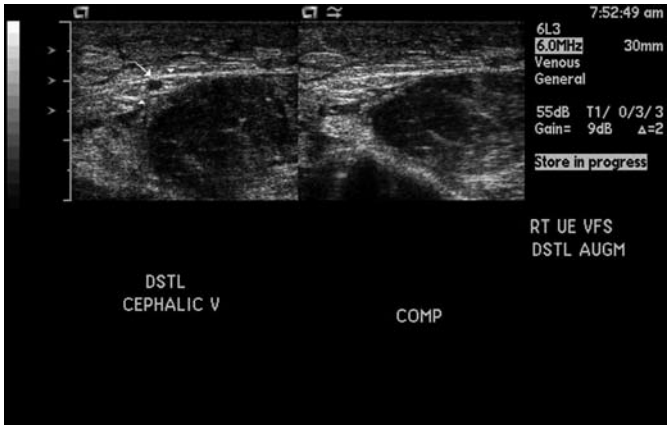

Fig. 18. The small vessel (arrow) within fascia (arrowheads) is the cephalic vein. It does not accompany an artery. It is easily compressible with compression.

tissues and vein can be provided with the examiner's free hand in the supraclavicular area. Unfortunately, compressibility often fails due to the vein slipping away from the area of examination, and the sonographer should not erroneously conclude compressibility unless there is complete certainty. The subclavian vein is followed laterally as far as possible into the deltopectoral cannal.

Cephalic Vein. As we approach the shoulder along the subclavian vein, a small vessel can be observed breaking off: the cephalic vein. This vessel is superficial and does not accompany an artery (fig. 18).

Axillary Vein. After the subclavian-cephalic junction, the subclavian becomes the axillary vein, usually examinated in the axilla. For this purpose, the patient's arm is raised and abducted to 90°. We use a wrist restraint in patients who cannot cooperate because of sedation or who have difficulty keeping the arm elevated (fig. 19). The mostly single axillary vein runs superficially and commonly distant from the artery. Distally, a large single vessel separates and runs toward the skin line: the basilic vein.

Brachial Vein. After giving off the basilic vein, the axillary vein becomes the brachial vein. The patient's arm is then brought back to the patient's side and pronated, exposing the area of interest (fig. 20). The small brachial veins (usually double) are then examinated along the mid arm into the upper portion of the forearm. We do not routinely assess the radial and ulnar veins, unless there are local signs of thrombosis or a specific reason, like the suspicion of a thrombosed dialysis graft. Finally, if thrombosis is discovered, we follow Fraser's recommendations to scan the contralateral neck and proximal upper extremity to assess progression or subsequent recurrence of venous thromboembolic disease [56].

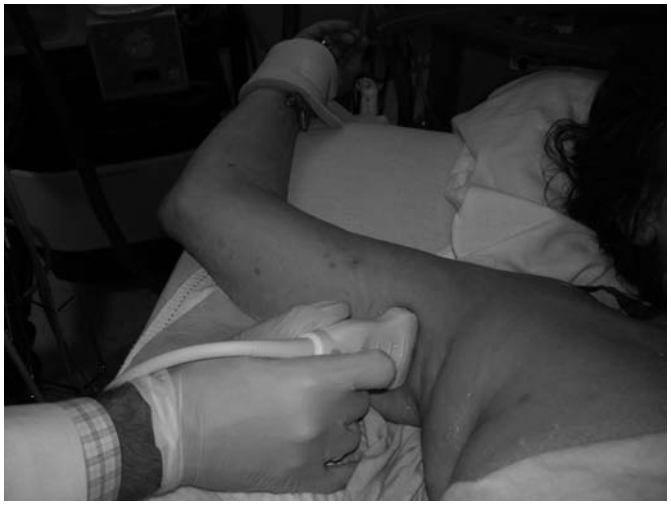

Fig. 19. Demonstration of patient and transducer positioning for examination of axillary vessels.

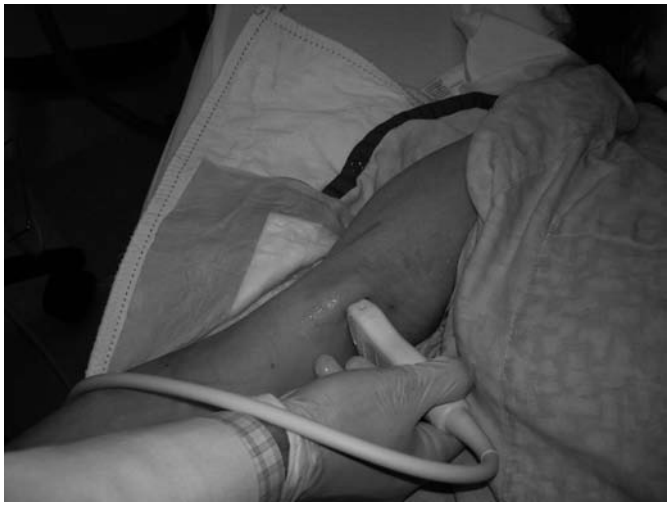

Fig. 20. Demonstration of patient and transducer positioning for examination of brachial vessels.

Pitfalls of Sonography

- Internal echoes ('smoke') are frequently encountered in patent veins in the presence of low-flow states. Smoke is more easily visualized in large veins (i.e., internal jugular and subclavian in the upper extremities, and common, deep femoral, proximal superficial and greater saphenous in the lower extremities). It should not be confused with true thrombi.
- Spontaneous flow and flow augmentation can occur in the presence of incomplete thrombosis, adequate collateralization, and with duplication of deep venous systems.
- Presence of a duplicated venous system can lead the unsuspecting sonographer to miss a thrombosed segment. Conversely, a large collateral system could be mistaken for a patent venous segment while thrombosis is present in an underlying vein.
- Inability to visualize the more proximal, intrathoracic venous system: proximal subclavian, innominate, and superior vena cava in the upper extremities, external iliacs in the lower extremities.
- Presence of local tenderness, obesity, dressings, edema, burn areas and local recent surgery may render the study difficult to perform or altogether nonobtainable.
- Identification of acute on chronic thrombosis: a commonly undiagnosed problem in critically ill patients. The ultrasound appearance of DVT changes over time: thrombi become progressively more echogenic as they organize, and the underlying venous wall in the area of thrombosis gets thicker, more echogenic and resistant to compression. Hence, when DVT is diagnosed, it is important to measure the diameter of the vein at the site of thrombosis. Future thrombosis of lower extremities exists if the compressed venous diameter increases by $\geq$4 mm from the baseline study. Importantly, this criterion was never formally assessed in the upper extremities, but we believe it applies the same.
- Lastly, sonography is undoubtedly operator dependent. Fortunately this skill has a steep learning curve and is relatively easy to perform.

Performance of Diagnostic Venous Ultrasound by Nonradiologists

Given the rapid growth in availability of portable ultrasound units in many ICUs, there are an increasing number of clinicians performing bedside diagnostic venous sonograms. We have no data on the accuracy of these tests when performed under these circumstances. There are, however, several studies assessing the accuracy of such tests performed in the emergency department (ED) setting by ED physicians with variable amounts of ultrasound training (2–30 h). In these studies, CUS results obtained by ED physicians were compared with results obtained by same institution radiology or vascular departments using their standard protocols. Sensitivities ranged from 89 to 100%, with specificities ranging from 76 to 100% [32, 37, 57, 58]. In addition, there is a similar study performed in hospitalized patients assessing the accuracy of CUS performed by a self-trained clinician (had performed 35 practice tests prior to study) with a

vascular access device 'Site Rite™' in a group of 72 hospitalized patients with a moderate risk of DVT. In that study, a sensitivity of 94% and specificity of 99% were reported [59]. These results lend support to the accuracy of bedside CUS examinations performed by clinician sonographers. However, we caution the reader that the diagnostic accuracy of sonography performed by intensivist sonographers in the critically ill has not been formally assessed.

Conclusion

Ultrasonography remains the test of first choice for the diagnosis of DVT of the upper and lower extremities. It is accurate, noninvasive, easy to perform, readily available, relatively inexpensive, and can potentially be repeated without restrictions. It assists in identifying frequently unsuspected diagnoses such as enlarged lymph nodes, hematomas, abscesses, and foreign bodies. Unfortunately, the true accuracy of ultrasound in a heterogeneous critically ill population is not known. Based on the available data, we strongly support the use of compression sonography as the initial test in this patient population to diagnose upper and lower extremity DVT. We emphasize the value of the information obtained by venous compression technique and examination of endoluminal echoes. DVT can be confidently diagnosed when absence of compressibility is present within the context of a clinical situation with a high pretest probability. Assessment of venous flow patterns can assist in confirming the diagnosis, but the significance of isolated abnormalities of spectral Doppler signal analysis should be questioned and alternative diagnostic tests should be considered (venography, CT venogram, MR venography). Color examination and maneuvers to augment flow help identify venous segments that are difficult to visualize with real-time sonography but do not increase diagnostic accuracy.

Acknowledgment

We are indebted to Mrs. Gregorio Garcia Cano and Jorge Aguilar Roman for their assistance with graphic design.

References

1 Hirsch DR, Ingenito EP, Goldhaber SZ: Prevalence of deep venous thrombosis among patients in medical intensive care. JAMA 1995;274:335–337.
2 Marik PE, Andrews L, Maini B: The incidence of deep venous thrombosis in ICU patients. Chest 1997;111:661–664.
3 Kapoor M, Kupfer YY, Tessler S: Subcutaneous heparin prophylaxis significantly reduces the incidence of venous thromboembolic events in the critically ill (poster). SCCM 29th Educational and Scientific Symposium, Orlando, 2000.
4 Ibrahim EH, Iregui M, Prentice D, Sherman G, Kollef MH, Shannon W: Deep vein thrombosis during prolonged mechanical ventilation despite prophylaxis. Crit Care Med 2002;30:771–774.
5 Cook D, Crowther M, Meade M, Rabbat C, Griffith L, Schiff D, Geerts W, Guyatt G: Deep venous thrombosis in medical surgical critically ill patients: prevalence, incidence, and risk factors. Crit Care Med 2005;33:1565–1571.
6 Wheeler HB: Diagnosis of deep venous thrombosis: review of clinical evaluation and impedance plethysmography. Am J Surg 1985;150(suppl):7–13.
7 American Thoracic Society: The diagnostic approach to acute venous thromboembolism: clinical practice guideline. Am J Respir Crit Care Med 1999;160:1043–1066.
8 Stein PD, Henry JW: Prevalence of acute pulmonary embolism among patients in a general hospital and at autopsy. Chest 1995;108:978–981.
9 Twigg SJ, McCrirrick A, Sanderson PM: A comparison of post mortem findings with post hoc estimated clinical diagnoses of patients who die in a United Kingdom intensive care unit. Intensive Care Med 2001;27:706–710.
10 Williams MT, Aravindan N, Wallace MJ, Riedel BJCJ, Shaw ADS: Venous thromboembolism in the intensive care unit. Crit Care Clin 2003;19:185–207.
11 Cogo A, Lensing AW, Prandoni P, Buller HR, Girolami A, ten Cate JW: Comparison of real-time B-mode ultrasonography and Doppler ultrasound with contrast venography in the diagnosis of venous thrombosis in symptomatic outpatients. Thromb Haemost 1993;70:404–407.
12 Huisman MV, Buller HR, ten Cate JW, van Royen EA, Vreeken J, Kersten M, Bakx R: Unexpected high prevalence of silent pulmonary embolism in patients with deep venous thrombosis. Chest 1989;95:498–502.
13 Habscheid W, Hohmann M, Wilhelm T, Epping J: Real-time ultrasound in the diagnosis of acute deep venous thrombosis of the lower extremity. Angiology 1990;41:599–608.
14 Quintavilla R, Larini P, Miselli A, Mandrioli R, Ugolotti U, Pattacini C, Pini M: Duplex ultrasound diagnosis of symptomatic proximal deep vein thrombosis of lower limbs. Eur J Radiol 1992;15:32–36.
15 Lensing AW, Prandoni P, Brandjes D, Huisman PM, Vigo M, Tomasella G, Krekt J, ten Cate JW, Huisman MV, Buller HR: Detection of deep-vein thrombosis by real-time B-mode ultrasonography. N Engl J Med 1989;320:342–345.
16 Tomkowski WZ, Davidson BL, Wisniewska J, Malek G, Kober J, Kuca P, Burakowska B, Oniszh K, Gallus A, Lensing AW: Accuracy of compression ultrasound in screening for deep venous thrombosis in acutely ill medical patients. Thromb Haemost 2007;97:191–194.
17 Baarslag HJ, Koopman MMW, Reekers JA, van Beek EJR: Diagnosis and management of deep vein thrombosis of the upper extremity: a review. Eur Radiol 2004;14:1263–1274.
18 Fraser JD, Anderson DR: Deep venous thrombosis: recent advances and optimal investigation with US. Radiology 1999;211:9–24.
19 Ginsberg JS, Caco CC, Brill-Edwards PA, Panju AA, Bona R, Demers CM, Tuters LM, Nugent P, McGinnis J, Grant BM, Vander Lander Vries MA: Venous thrombosis in patients who have undergone major hip or knee surgery: detection with compression US and impedance plethysmography. Radiology 1991;181:651–654.
20 Cronan JJ, Dorfman GS, Scola FH, Schepps B, Alexander J: Deep venous thrombosis: US assessment using vein compression. Radiology 1987;162:191–194.
21 Appelman PT, De Jong TE, Lampmann LE: Deep venous thrombosis of the leg: ultrasound findings. Radiology 1987;163:743–746.

22 Monreal M, Montserrat E, Salvador R, Bechini J, Donoso L, MaCallejas J, Foz M: Real-time ultrasound for diagnosis of symptomatic venous thrombosis and for screening of patients at risk: correlation with ascending conventional venography. Angiology 1989;40:527–533.
23 Pedersen OM, Aslaksen A, Vik-Mo H, Bassoe AM: Compression ultrasonography in hospitalized patients with suspected deep venous thrombosis. Arch Intern Med 1991;151:2217–2220.
24 Birdwell BG, Raskob GE, Whitsett TL, Durica SS, Comp PC, George JN, Tytle TL, Owen WL, Mckee PA: The clinical validity of normal compression ultrasonography in outpatients suspected of having deep venous thrombosis. Ann Intern Med 1998;128:1–7.
25 Lensing AW, Doris CI, McGrath FP, Cogo A, Sabine MJ, Ginsberg J, Prandoni P, Turpie AG, Hirsh J: A comparison of compression ultrasound with color Doppler ultrasound for the diagnosis of symptomless postoperative deep vein thrombosis. Arch Intern Med 1997;157:765–768.
26 Kassai B, Boissel JP, Cucherat M, Sonie S, Shah NR, Leizorovicz A: A systematic review of the accuracy of ultrasound in the diagnosis of deep venous thrombosis in asymptomatic patients. Thromb Haemost 2004;91:655–666.
27 Taffoni MJ, Revenel JG, Ackerman SJ: Prospective comparison of indirect CT venography versus venous sonography in ICU patients. AJR Am J Roentgenol 2005;185:457–462.
28 Agnelli G, Volpato R, Radicchia S, Veschi F, Di Filippo P, Lupattelli L, Nenci GG: Detection of asymptomatic deep vein thrombosis by real-time B-mode ultrasonography in hip surgery patients. Thromb Haemost 1992;68:257–260.
29 Intersocietal Accreditation Commission (ICAVL): Essentials and standards for accreditation in noninvasive vascular testing. II. Vascular laboratory operations: peripheral venous testing. 2000;1–8. www.intersocietal.org/intersocietal.htm.
30 Kearon C, Julian JA, Newman TE, Ginsberg JS: Non-invasive diagnosis of deep venous thrombosis. McMaster Diagnostic Imaging Practice Guidelines Initiative. Ann Intern Med 1998;128:663–677.
31 Baarslag HJ, van Beek EJR, Koopman MMW, Reekers JA: Prospective study of color Duplex ultrasonography compared with contrast venography in patients suspected of having deep venous thrombosis of the upper extremities. Ann Intern Med 2002;136:865–872.
32 Lin EP, Bhatt S, Rubens D, Dogra VS: The importance of monophasic Doppler waveforms in the common femoral vein. J Ultrasound Med 2007;26:885–891.
33 Blaivas M, Lambert MJ, Harwood RA, Wood JP, Konicki J: Lower-extremity Doppler for deep venous thrombosis: can emergency physicians be accurate and fast? Acad Emerg Med 2000;7:120–126.
34 Lockhart ME, Sheldon HI, Robbin ML: Augmentation in lower extremity sonography for the detection of deep venous thrombosis. AJR Am J Roentgenol 2005;184:419–422.
35 Appelman PR, De Jong TE, Lampmann LE: Deep venous thrombosis of the leg: US findings. Radiology 1987;163:743–746.
36 Mantoni M: Diagnosis of deep venous thrombosis by duplex ultrasonography. Acta Radiol 1989;30:575–579.
37 Frazee BW, Snoey ER, Levitt A: Emergency department compression ultrasound to diagnose proximal deep venous thrombosis. J Emerg Med 2001;21:444–445.
38 Poppiti R, Papanicolaou G, Perese S, Weaver FA: Limited B-mode venous imaging versus complete color-flow duplex venous scanning for detection of proximal deep venous thrombosis. J Vasc Surg 1995;22:553–557.
39 Frederick MG, Hertzber BS, Kliewer MA, Paulson EK, Bowie JD, Lalouche KJ, Delong DM, Carol BA: Can the US examination for lower extremity deep venous thrombosis be abbreviated? A prospective study of 755 examinations. Radiology 1996;199:45–47.
40 Cogo A, Lensing AW, Prandoni P, Hirsh J: Distribution of thrombosis in patients with symptomatic deep vein thrombosis. Implications for simplifying the diagnostic process with compression ultrasound. Arch Intern Med 1993;153:2777–2780.
41 Markel A: The potential role of thrombolytic therapy in venous thrombosis. Arch Intern Med 1992;152:1265–1267.
42 Pezzullo JA, Perkins AB, Cronan JJ: Symptomatic deep vein thrombosis: diagnosis with limited compression US. Radiology 1996;198:67–70.
43 Badgett DK, Comerota MC, Khan MN, Eid IG, Kerr RP, Comerota AJ: Duplex venous imaging: role for a comprehensive lower extremity examination. Ann Vasc Surg 2000;14:73–76.
44 Maki DD, Kumar N, Nguyen B, Langer JE, Miller WT, Gefter WB: Distribution of thrombi in acute lower extremity deep venous thrombosis: implications for sonography and CT or MR venography. AJR Am J Roentgenol 2000;175:1299–1301.
45 Bernardi E, Pesavento R, Prandoni P: Upper extremity deep venous thrombosis. Semin Thromb Hemost 2006;32:729–736.
46 Martine C, Viviand X, Saux P, Gouin F: Upper extremity deep vein thrombosis after central venous catheterization via the axillary vein. Crit Care Med 1999;27:2626–2629.
47 Van Rooden CJ, Tesslar MET, Osanto S, Rosendaal FR, Huisman MV: Deep vein thrombosis associated with central venous catheters: a review. J Thromb Haemost 2005;3:2409–2419.
48 Hill SL, Berry RE: Subclavian vein thrombosis: a continuing challenge. Surgery 1990;108:1–9.
49 De Cicco M, Matovic M, Balestreri L, Panarello G, Fantin D, Morassut S, Testa V: Central venous thrombosis: an early and frequent complication in cancer patients bearing long-silastic catheters. A prospective study. Thromb Res 1997;86:101–113.
50 Grove JR, Pevec WC: Venous thrombosis related to peripherally inserted central catheters. J Vasc Interv Radiol 2000;11:837–840.
51 Joffe HV, Kucher N, Tapson VF, Goldhaber SZ, Deep Vein Thrombosis FREE Steering Committee: Upper-extremity deep vein thrombosis: a prospective registry of 592 patients. Circulation 2004;110:1605–1611.
52 Mustafa BO, Rathbun SW, Whitsett TL, Taskob GE: Sensitivity and specificity of ultrasonography in the diagnosis of upper extremity deep vein thrombosis. Arch Intern Med 2002;162:401–404.
53 Prandoni P, Polistena P, Bernardi E, Cogo A, Casara D, Verlato F, Angelini F, Simioni P, Signorini GP, Benedetti L, Girolami A: Upper extremity deep vein thrombosis. Arch Intern Med 1997;157:57–62.
54 Baarslag HJ, van Beek EJR, Koopman MMW, Reekers JA: Prospective study of color Duplex ultrasonography compared with contrast venography in patients suspected of having deep venous thrombosis of the upper extremities. Ann Intern Med 2002;136:865–872.
55 Hübsch PJ, Stiglbauer RL, Schwaighofer BA, Kainberger FM, Barton PP: Internal jugular and subclavian vein thrombosis caused by central venous catheters: evaluation using Doppler blood flow imaging. J Ultrasound Med 1988;7:629–636.
56 Fraser JD, Anderson DR: Venous protocols, techniques, and interpretations of the upper and lower extremities. Radiol Clin North Am 2004;42:279–296.
57 Magazzini S, Vanni S, Toccafondi S, Paladini B, Zanobetti M, Giannazzo G, Federico R, Grifoni S: Duplex ultrasound in the emergency department for the diagnostic management of clinically suspected deep vein thrombosis. Acad Emerg Med 2007;14:216–220.
58 Jang T, Docherty M, Aubin C, Polites G: Resident-performed compression ultrasonography for the detection of proximal deep vein thrombosis: fast and accurate. Acad Emerg Med 2004;11:319–322.
59 Trottier SJ, Todi S, Veremakis C: Validation of an inexpensive B-mode ultrasound device for detection of deep vein thrombosis. Chest 1996;110:1547–1550.

Adolfo E. Kaplan, MD
1604 East 8th Street, Suite A
Weslaco, TX 78596 (USA)
Tel. +1 956 447 5557, Fax +1 956 447 5747, E-Mail Akaplan0504@yahoo.com

Endoscopic Ultrasound Applications

Chapter 13

Bolliger CT, Herth FJF, Mayo PH, Miyazawa T, Beamis JF (eds): Clinical Chest Ultrasound: From the ICU to the Bronchoscopy Suite.
Prog Respir Res. Basel, Karger, 2009, vol 37, pp 110–127

Principles and Practice of Endoscopic Ultrasound

Kenichi Nishina[a] · Kenji Hirooka[a] · Jochen Wiegand[b] · Harald Dremel[b]

[a]Olympus Medical Systems Corporation, Tokyo, Japan; [b]Olympus Medical Systems Europa GmbH, Hamburg, Germany

Abstract

Thirty years ago Olympus began developing an ultrasound gastroscope. Since that time advances in signal processing and miniaturization have allowed for an increasing area of application of ultrasound diagnosis and treatment. In 1998 mechanical radial ultrasound probes shrunk to a diameter which ensured compatibility with the instrument channel of a bronchoscope. This made ultrasound diagnosis of bronchial wall layers possible. In 2004 the world's first electronic linear ultrasound bronchoscope was introduced to the market and hence fine needles used for the aspiration of tissue specimens could be reliably monitored. Until now different ultrasound technologies have been used for different diagnostic tasks. Moreover, the outer diameter could constantly be reduced to reach peripheral lung areas. In addition, different ultrasound frequencies for varying penetration depths are available nowadays. Complementary to this is the electric linear technology with higher penetration allowing for endobronchial ultrasound-controlled transbronchial needle aspiration. The principles behind this technology together with the functions and enhancements available in today's practice are summarized in this article and a perspective on future technological development and therapeutic applications is given.

Fig. 1. The first prototype of a mechanical mirror-type ultrasound endoscope.

The first attempt at intraluminal ultrasonography is considered to be a rectal scan performed by Wild and Reid [1] in 1956. However, only the study reported by Hagenmüller and Classen [2] in 1980 can be regarded as the first clinical report on endoscopic ultrasonography, so-called EUS. The device used combined endoscopic and ultrasound functions and was manufactured by Olympus (fig. 1, 2). Research and Development at headquarters in Tokyo, Japan had started the development in 1978, with the target of providing an instrument for the early detection of pancreatic cancer. Since then technical evolution, new materials and improved manufacturing have opened the door for the introduction of a broad line-up of both ultrasound endoscopes and probes.

It took another 10 years to develop a mechanical radial ultrasound miniprobe (UM-1W with 7.5 MHz) capable of passing through the endoscope working channel. The outer diameter of 3.5 mm still did not permit use with a bronchoscope. The next development was an ultrasound probe of 2.5 mm in diameter and 12/20 MHz (UM-2R/3R). Finally in 1990, miniaturization permitted the first use of an ultrasound probe in the airways. Hürther and Hanrath [3] (Germany) were the first to report their experiences, followed by Becker [4] (Germany) and Kurimoto et al. [5] (Japan). A further milestone was reached in 1997 when Olympus developed a new mechanical radial ultrasound

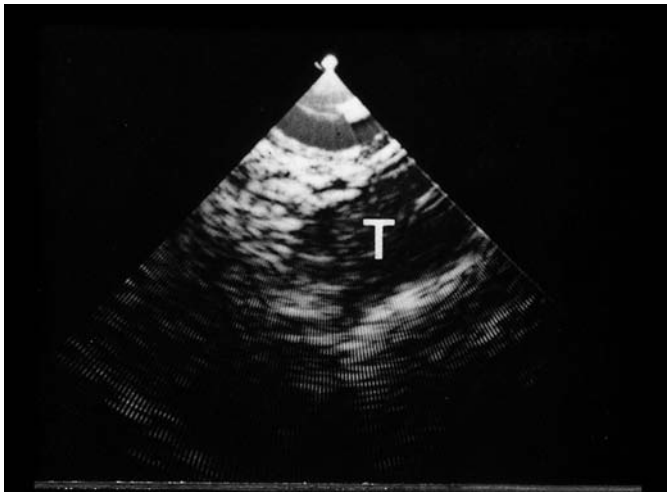

Fig. 2. Ultrasound image of the first prototype with 90° scanning area using 5 MHz.

Fig. 3. UM-BS20-26R, 2.6 mm outer diameter.

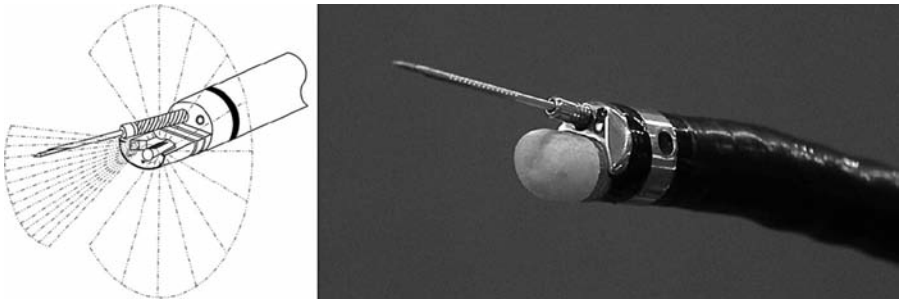

Fig. 4. Mechanical radial scanning EBUS-TBNA scope prototype.

probe with balloon function. In order to observe the central airways, a water-fillable balloon is required for acoustic coupling to the bronchial wall. The outer diameter of the probe and balloon sheath measures 2.6 mm to allow insertion through the flexible bronchoscopes.

This product was released to the market in 1999 (fig. 3) and has been used for tumor staging in the central airway region. Ultrasound probes without a balloon sheath, so-called 'direct contact probes', allow diagnosis of peripheral lesions due to their thin diameter, the thinnest measuring a mere 1.7 mm outer diameter. Furthermore they have been useful in the diagnosis of the layers of the bronchial wall due to their frequency-related (20 or 30 MHz) high resolution. The development of a mechanical linear bronchoscope was under way at the same time. The objective was to provide transbronchial needle aspiration (TBNA) under real-time ultrasound control. The first prototype of the endobronchial ultrasound (EBUS)-TBNA bronchoscope had a reflection mirror placed face-to-face with the ultrasound probe (fig. 4).

As image quality and performance were not meeting the expectations, the focus was modified on the design of a micro-sized electronic convex-type transducer assembled for the first time in 2002. After additional enhancement cycles of the endoscope and the aspiration needle system, the EBUS-TBNA system was finally launched in 2004. The system consists of a dedicated endoscope, aspiration needle and ultrasound processing device (fig. 5–7).

This synopsis of the historical development also illustrates the paradigm shift from transducers with rotating elements to those with electrically driven elements as well as the coexistence of radial and linear transducers. A more in depth description of the development of EBUS follows in chapter 14, see pp. 128–139.

Principles of Endoscopic Ultrasound

Ultrasound: Frequency and Wavelength

Frequency stands for a specific number of vibration cycles per second; it describes the pitch of a sound. Frequencies are measured in units of hertz. In endoscopic ultrasound, usually frequencies between 5 and 30 MHz are used. This

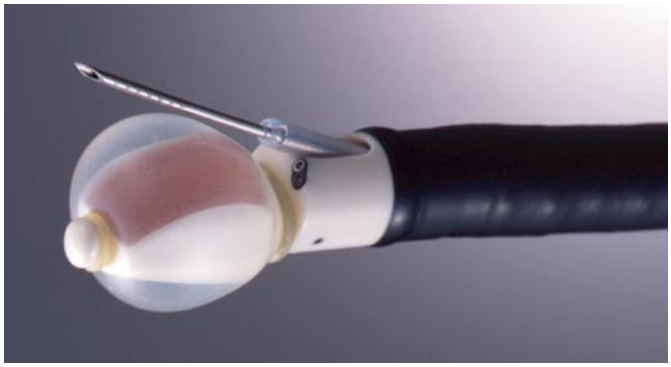

Fig. 5. Ultrasound bronchoscope BF-UC160F-OL5.

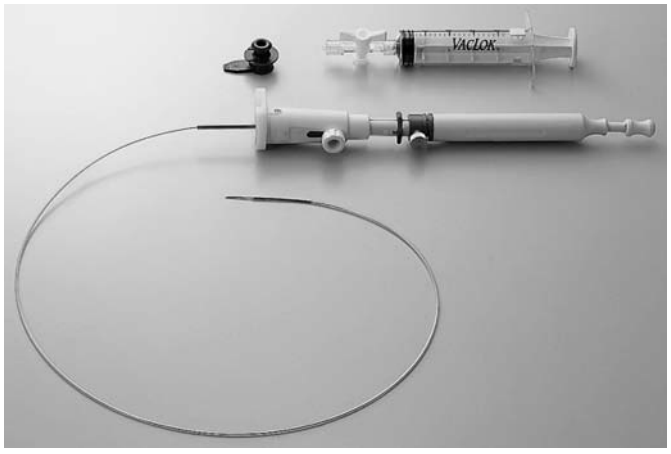

Fig. 6. EBUS-TBNA needle system NA-201SX-4022.

Fig. 7. Ultrasound processing device EU-C60.

high-frequency sound is inaudible to the human ear. The higher the frequency of a given tone the shorter the related wavelength, the lower the frequency of a given tone the longer the wavelength. Frequency and wavelength are inversely proportional to each other.

Propagation and Speed of Sound

Sound advances through various substances (referred to below as the medium) including air and water. This process is called propagation and the advancing speed of a sound wave through the medium is called speed of sound. Ultrasound waves propagate through different media at different speeds of sound.

Reflection and Transmission

When ultrasound waves propagate through the human body, for example, at every border of tissue with a different density (=medium with a different acoustic property) the sound waves are partly reflected. The remaining part transmits further into deeper areas. The 'echo' of a sound wave as a result of the reflection on that tissue border, together with the time from sound emission to reception of the echo, is the information needed for ultrasound image reconstruction. The bigger the difference in acoustic properties between two media the larger the proportion of the reflected ultrasound and the smaller the proportion of transmitted ultrasound. A strong echo results, for example, from bones, typically lung tissue (with high gas concentration) or air (as in the bronchial system). Ultrasound waves are almost completely reflected at the border between body tissue and air. The acoustic properties of both media prevent further transmission.

Attenuation

Ultrasound waves get weaker gradually as they propagate through a medium. This phenomenon is called attenuation. Attenuation is caused by absorption, when the vibration of ultrasound waves is converted to heat due to friction. It can also be due to dispersion as ultrasound waves swerve from their original course when traveling through heterogeneous tissue. Ultrasound wave energy diffuses while traveling through the body tissue, resulting in reduced vibration energy concentration. The level of attenuation depends also on the medium, being much higher in air than in water. Ultrasound attenuation tends to increase with higher frequency.

Resolution

Spatial resolution as the level of detail of an image refers to the capacity of a system to distinguish small objects from others. With regard to the creation of an ultrasound image, resolution can be categorized into two types, axial resolution and lateral resolution.

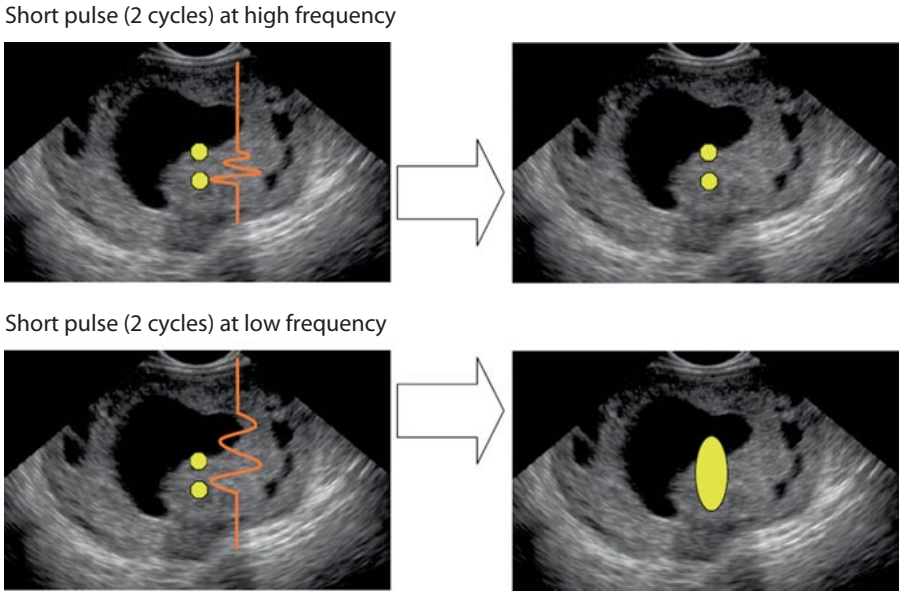

Fig. 8. Axial resolution.

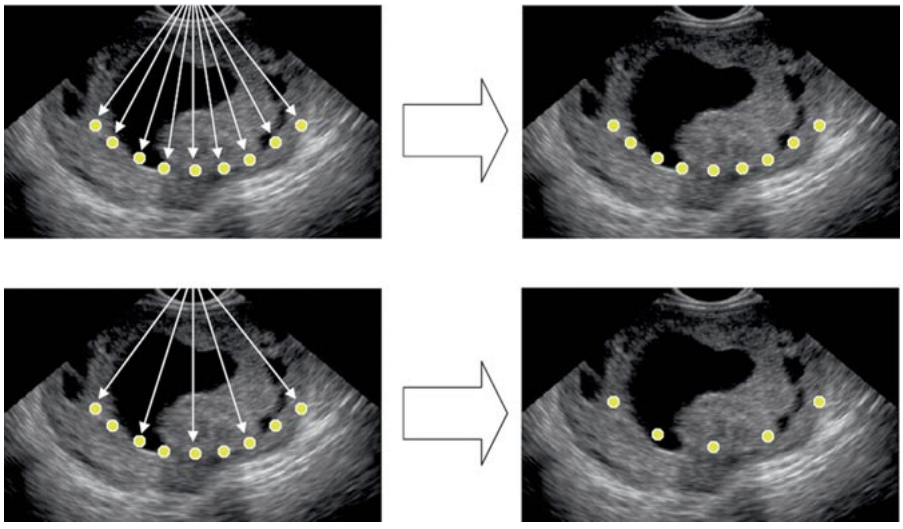

Fig. 9. Ultrasound beam density.

Axial Resolution

Axial resolution depends on the ultrasound pulse duration. If the distance between two targets is larger than half of the ultrasound pulse duration, the ultrasound system can translate the echoes as belonging to two separate targets. If not the two targets become indistinguishable and are displayed as one large structure (fig. 8). Typically, in endoscopic ultrasound two to seven cycles are used. With a fixed number of cycles the dominant factor defining the ultrasound pulse duration is the ultrasound frequency. In daily practice endosonographers experience that the axial resolution increases with higher frequencies; technically this is due to the adjustment of the pulse duration for any chosen frequency by the ultrasound system.

Lateral Resolution

Lateral resolution is the resolution in the ultrasound scanning direction and describes the ability to distinguish small objects placed in parallel to the scanning direction. Lateral resolution depends on the size and number of ultrasound elements and the number of scanning lines used (=ultrasound beam density, (fig. 9) but also on the frequency used (=ultrasound beam width, (fig. 10). The ultrasound beam emitted from each element inside the transducer has a specific width which expands gradually as the beam advances through the medium. Electronic 'beam focusing' is applied to obtain the maximum resolution technically possible. The ultrasound beam width gets smaller as frequency increases; therefore, a higher frequency also results in improved lateral resolution.

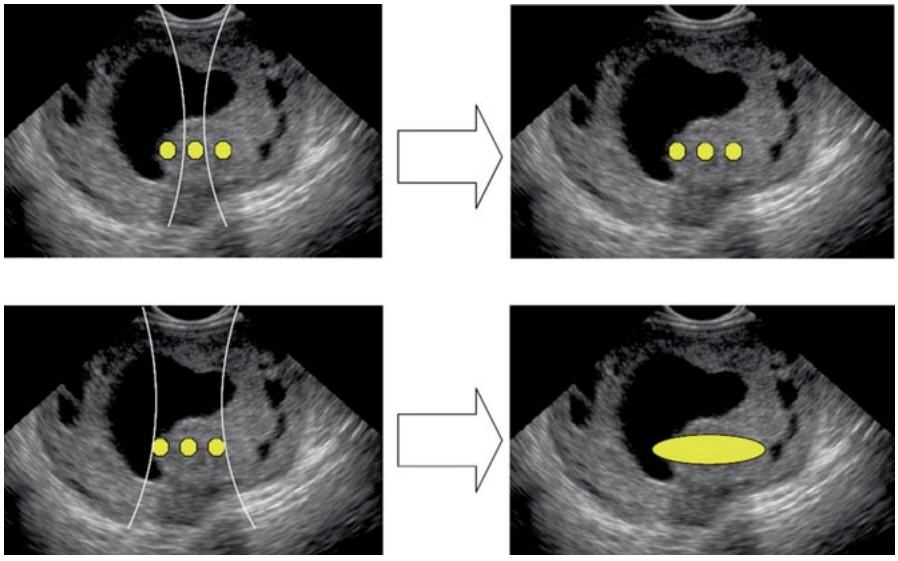

Fig. 10. Ultrasound beam width.

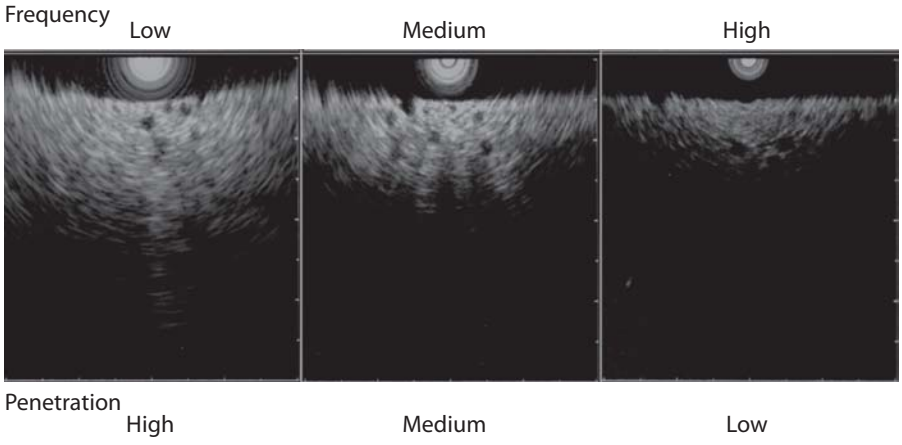

Fig. 11. Dependency between frequency and penetration.

Penetration

Ultrasound images can be acquired only from an area within a limited distance from the ultrasound transducer (see section on Attenuation above). Larger ultrasound transducers are capable of transmitting powerful ultrasound beams and converting weak ultrasound echoes into electrical signals, resulting in increased penetration depth. Due to the limited space available in endoscopic ultrasound, penetration depth is less than in abdominal ultrasonography. The maximum penetration depth depends on the frequency used. In principle, high frequencies (e.g. 20 or 30 MHz) do not penetrate as deep into the tissue as low frequencies (e.g. 5 or 7.5 MHz). This is a principle that is valid for sound in general, such as loud music originating from a room next door. What is noticeable at first is the diffuse, deep hammering sound of the low frequencies. Only when the sound source is approached do the high frequencies become perceptible too and the music becomes more differentiated. This example illustrates the dependency between penetration and frequency (fig. 11).

Scanning Methods

Mechanical Scanning Method

Mechanical radial scanning technology uses a transducer rotating up to 360° around the axis of the endoscope (fig. 12). The transducer is placed inside a cap or a catheter for protection purposes and floats in ultrasound propagation fluid to achieve good acoustic coupling. First introduced in ultrasound gastroscopes, this technology is still unrivaled in ultrasound miniprobes in which a flexible wire connects the transducer with an external motor, thus permitting

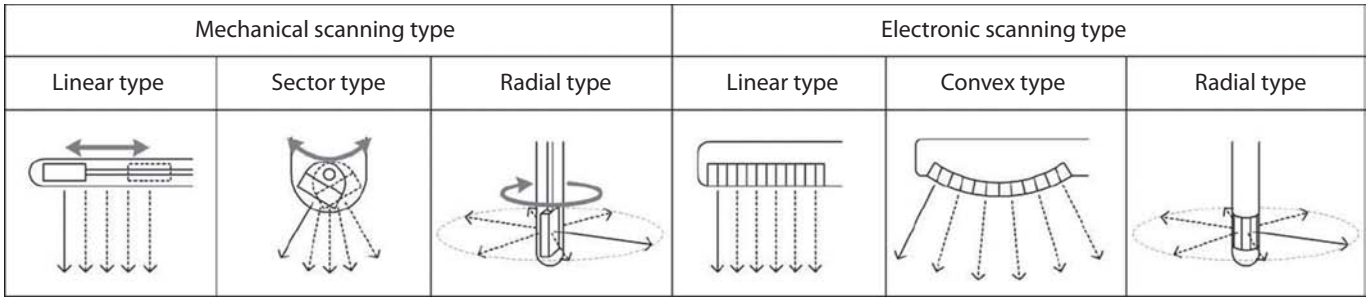

Fig. 12. Ultrasound scanning methods.

Fig. 13. Electronic radial scanning gastroscope GF-UE160-OL5 and mechanical radial scanning miniprobe UM-S20-17S.

diameters down to 1.7 mm. Mechanical radial is the choice for the diagnosis of those cavities in which small instrument diameter is a must, e.g. endoscopic diagnosis of peripheral lung lesions (online suppl. video 1). Due to the high frequencies achievable with radial ultrasound, this technology permits the diagnostic evaluation of, for example, bronchial wall structures to distinguish the ingrowth of tumors from the compression of the airways.

Video

Electronic Scanning Method

Electronic scanning technology uses transducers composed of tens to hundreds of fixed elements that are electronically switched (fig. 12). Mainstream in electronic scanning ultrasound endoscopes are transducers in the form of a curved linear array. The scanning direction of the transducer is parallel to the insertion direction of the endoscope and scans in a 90° angle to the endoscope. This allows full control of the instrument movement within the ultrasound waves in real time. Usually frequencies between 5 and 12 MHz are used for monitoring aspiration needles in e.g. EUS-fine needle aspiration or EBUS-TBNA (online suppl. video 2). Transducers of electronic scanning-type ultrasound endoscopes require dedicated cabling, which limits the possibilities of miniaturization. The advantage of such transducers lies in increased diagnostic options, such as the use of Doppler functions to display flow, multi- or dynamic focus to increase image quality, the use of harmonic waves for image construction and multibeam scanning as the timing, sequence and pairing of ultrasound impulses are managed electronically.

Video

Complementarity of Electronic and Mechanical Scanning

The latest development is the catheter-type ultrasound miniprobe for the airway field, with a distal tip diameter of 1.4 mm and maximum diameter of 1.7 mm in radial mechanical technology. Compared to the first electronic radial gastroscope introduced in 2006 the cross section of the miniprobe is about 50 times smaller despite covering the same 360° scanning area (fig. 13).

Once the transducer is rotated mechanically during the transmission and reception of ultrasound, one scanning line is generated for each transmission/reception. The number of scanning lines in mechanical radial technology has no relation to probe diameter. Based on current technical possibilities, electronic scanning technology in small-diameter devices does not permit the high-quality ultrasound image that mechanical scanning miniprobes provide.

Table 1. Basic components of an ultrasound endoscope

Type	Component	Function
Endoscopic function	lighting lens light guide fiber	emit light into body cavity
	objective lens image-guiding fibers	transmit the endoscopic image
	bending mechanism at distal end angulation wire	bending and straightening of the endoscope
	instrument channel	used for aspiration, delivery of anesthetic fluid and endotherapeutic devices
Ultrasound function	ultrasound transducer	transmitter and receiver unit
	transducer cables	transmit electrical signals to and from the transducer
	balloon attachment mechanism	allow use of a balloon for better acoustic coupling, prevent balloon ruptures
	balloon channel	fill/drain the balloon

Practice of Creating an Ultrasound Image

Limitations of Ultrasound in Endoscopic Devices

The most crucial aspect in constructing an ultrasound endoscope is its compact design (table 1). The right balance between endoscopic functionality, endoscopic image quality, outer diameter of the endoscope and defined requirements with regard to ultrasound diagnosis, i.e. penetration depth, resolution and scanning range, has to be chosen. The complexity increases with the parallel design of a dedicated needle system and the balancing of diameter and stiffness of the needle to achieve the best possible compromise. To accomplish the requirement of minimizing the outer diameter of the endoscope while balancing the components responsible for ultrasound image quality, a compromise was necessary with regard to endoscopic image quality. Olympus decided to move the CCD (charged coupled device or video chip) from the distal tip to the control section of the endoscope. The space that became available permitted more important features for EBUS-TBNA to be implemented. The video image is transmitted via glass fibers from the tip of the endoscope to the endoscope handle. There, a CCD captures the image to be displayed as a video image on a monitor. The adoption of this 'hybrid' optical system helped to achieve specifications allowing access to a maximum area during the EBUS-TBNA diagnostic procedure. Olympus was able to introduce an EBUS-TBNA scope for diagnosis of lesions in the central airways/mediastinum of less than 7 mm in diameter in 2004.

Ultrasound Diagnostic Equipment – An Overview

The Transducer

The transducer consists of anything from a single (radial mechanical) element to several tens to hundreds of (electronic radial or linear) elements. These elements are piezoceramic crystals. Piezo crystals (e.g. polar crystals of barium titanate or lead zirconate) vibrate under high-frequency voltage and are thus used as an ultrasound source. Piezo crystals, if subject to pressure (e.g. impact of an ultrasound echo), generate an electrical voltage. With these properties piezo crystals serve as both sound source and, in the inactive intervals, as receiver. A typical cycle within a transducer element starts with an electrical pulse to generate a few oscillations and then the crystal is switched to reception mode. Typically, more than 99% of the time of one cycle is used to capture ultrasound echoes.

Equation for run time: $t = 2 \cdot s/v$

where t = time, f = frequency, s = penetration depth in m, v = average speed of sound in meters per second.

Depending on the penetration depth and the speed of sound, one cycle will last less than 0.1 ms at 7 cm penetration or 0.05 ms at 4 cm penetration depth (at an average speed of sound through human tissue of 1,540 ms).

The Ultrasound System

Figure 14 illustrates the basic components of an ultrasound system. The system will increase in complexity depending upon additional features such as tissue harmonics or Doppler features.

The transmitter excites the transducer elements with short electrical pulses so that a burst of ultrasound is generated. The returning echoes are then processed in an amplifier known as a 'sensitivity time control' (STC) amplifier. This amplifier increases gain (see section on Gain below) depending on time, thus compensating for attenuation in the deeper regions of the target area. In a consecutive step the compensated echo is converted from an analog to a digital signal. The digital beam-former combines the outputs of the individual

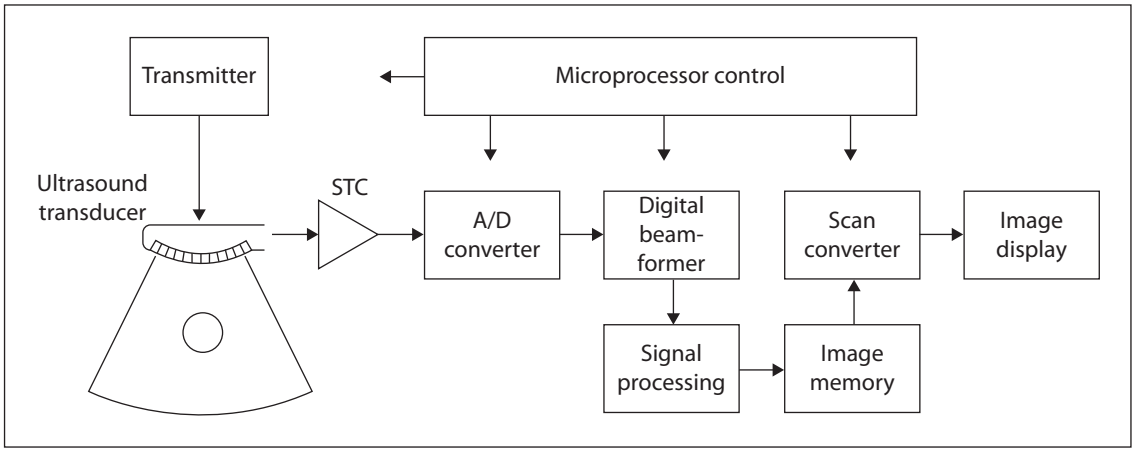

Fig. 14. Basic ultrasound system components.

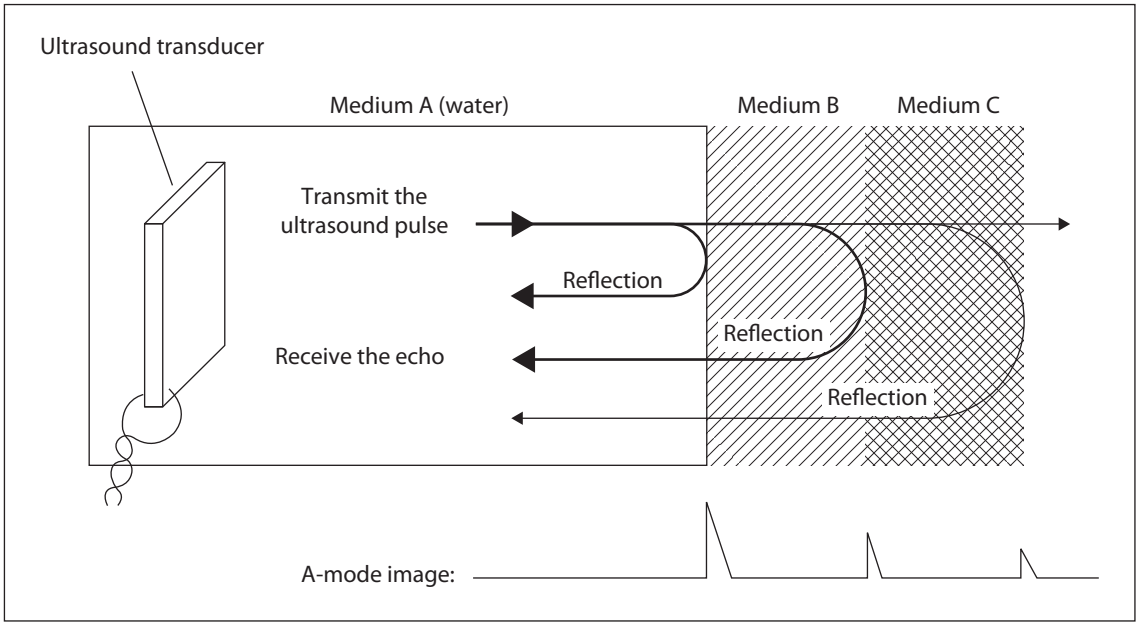

Fig. 15. A-mode imaging.

receiver channels by using variable time delay and phase adjustment to bring the received signals into concurrence and hence bring an object into focus. Due to the wide dynamic range of echo signals, the signal processing stage uses signal level compression. This compressed signal is stored in the memory where it is picked up by the scan converter and constructed into an image frame compatible with a monitor.

Basic Imaging Modes

Amplitude Mode (A-Mode)

In A-mode the ultrasound system calculates and displays the distance to a target based on the time a single reflected ultrasound pulse wave needs to return to the receiver. The strengths of reflections are displayed in the form of amplitude waveforms (fig. 15). This form of ultrasound imaging is confined to the measurement of distances and is applied nowadays in a number of diagnostic fields (ear, nose and throat, eyes, brain).

Brightness Mode (B-Mode)

The most common form of ultrasound image display is brightness mode where multiple single echo data of the fixed transducer elements (linear, convex or radial array) or from a moving single element transducer are combined. After interpolation of the data for the areas between the

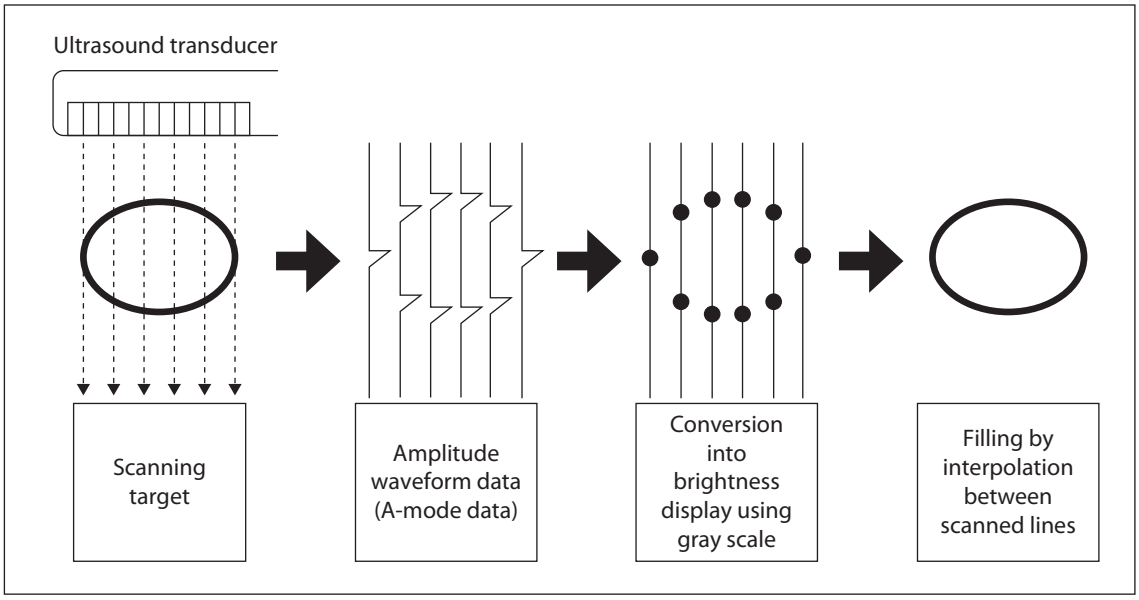

Fig. 16. B-mode imaging.

scanning lines, an image can be displayed on a monitor (fig. 16) using a graduation of 64–256 gray scales (brightness levels). B-mode is the most common imaging mode in endoscopic ultrasound.

Motion Mode (M-Mode)

In M-mode echo data of a single fixed transducer element are displayed over time. It is a common form of ultrasound information display in cardiology, especially to monitor real-time movement of structures (e.g. heart valves), but not in EUS.

Artifacts

A Positive Approach towards Artifacts

Ultrasound imaging is not free of distortions caused by the ultrasound wave energy and the density of tissue. Although the artifacts from e.g. refraction, reflection and attenuation interfere with diagnosis, they also help to describe tissue properties.

Reverberation Artifacts

When a highly reflective tissue surface exists parallel to the transducer, sound waves are repeatedly reflected between the tissue surface and the transducer surface (fig. 17). As a result, strong false echoes appear as multiple equally spaced lines on the ultrasound image. In tissue containing two highly reflective surfaces (e.g. bubbles, calculus), this reverberation artifact can also be seen if the structures are small enough (i.e. the reflective borders are close to each other). In this case an artifact appears distally to the structure like a comet tail (fig. 18).

Mirror Image Artifact

Mirror reflection happens when ultrasound waves propagate through tissue with strong impedance mismatch.

At the border surface the ultrasound beam is reflected almost completely. In consequence it continues to travel back towards proximal structures, producing mirror echoes. As ultrasound systems generate images depending on the time between sound emission and echo, figure 19 illustrates the prolonged run time of the reflected beam that causes the false image (mirror image).

Side Lobe Artifacts

Ultrasound beams are emitted not only in a 90° direction to the central axis direction of the transducer (main lobe), but also in obliquely emitted side lobes (surrounding the main lobe). Side lobes appear due to the vibration of the piezo crystal that is not limited to the central axis. Particularly with electronic scanning-type transducers, the interference of spherical waves can create side lobes (grating artifacts). As the ultrasound system cannot discriminate between echoes resulting from the main lobe and side lobes, a false image is created when a highly reflective object exists in the direction of the side lobe (fig. 20). Repositioning the transducer will help to provide conclusions on the authenticity of the structure displayed.

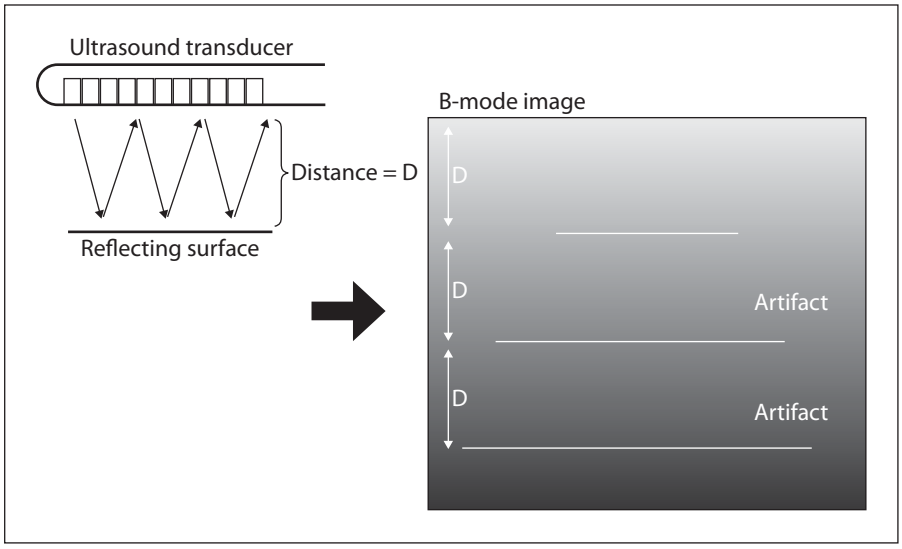

Fig. 17. Reverberation artifact.

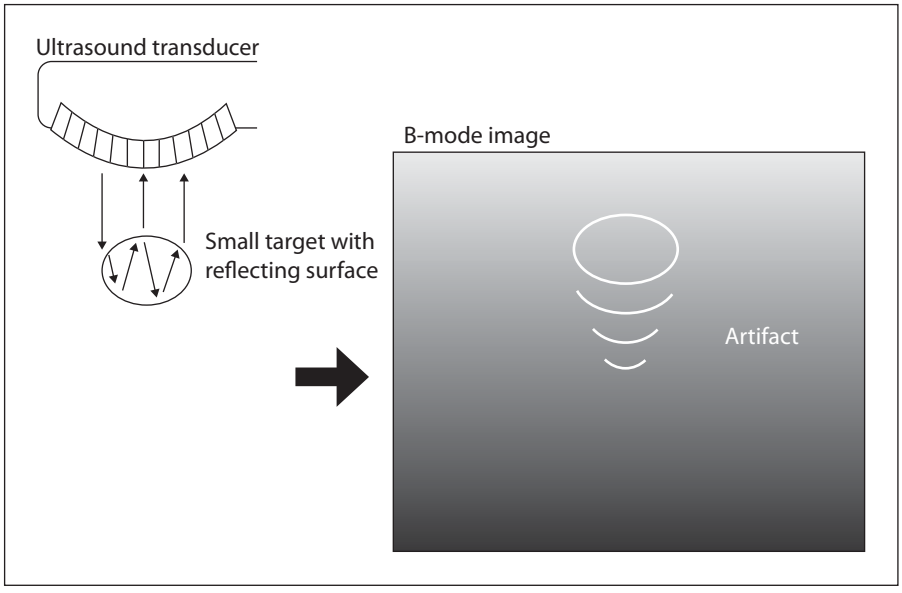

Fig. 18. Comet tail artifact.

Attenuation Artifacts

Artifacts caused by ultrasound attenuation include a tadpole tail sign and acoustic shadow (fig. 21, 22). Tissues with low acoustic impedance result in lower attenuation than tissues with higher impedance. In a diagnostic situation with a central 'low impedance' structure (A), the ultrasound wave (B) propagating through this tissue is less attenuated than corresponding waves (C) from other transducer elements that propagate through higher impedance tissue (D). In conclusion the energy level and echo at the distal border of the low impedance structure (A) will be higher than the energy level of wave C. The ultrasound system will therefore

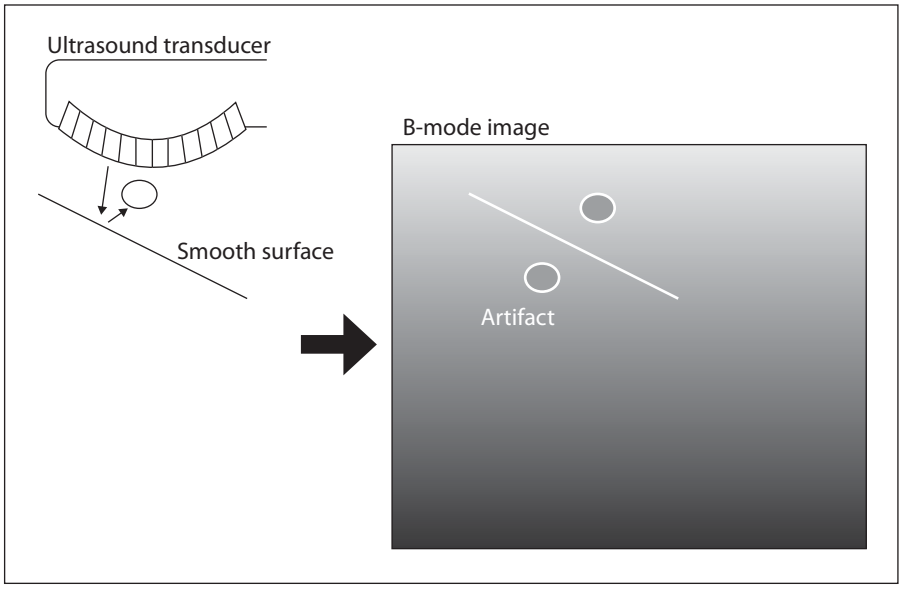

Fig. 19. Mirror image artifact.

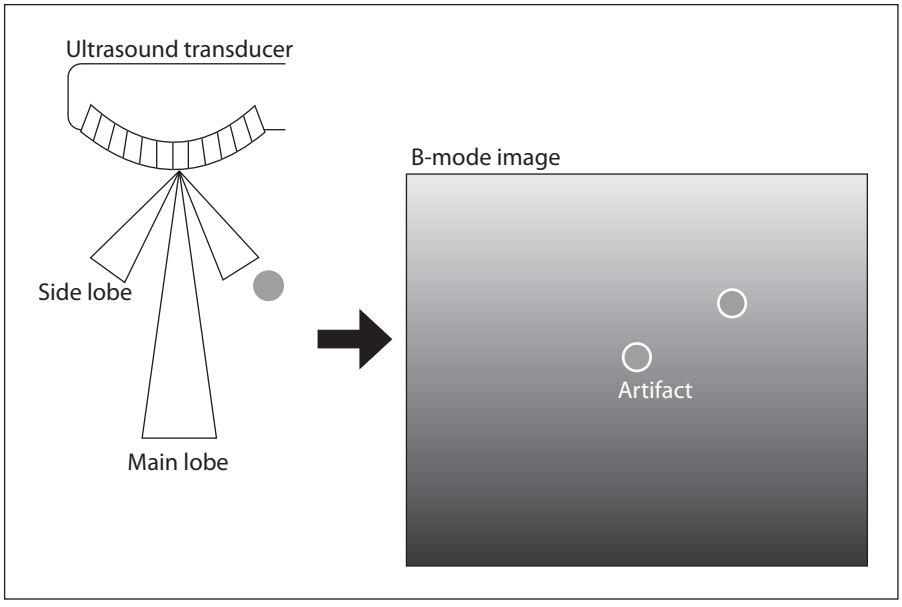

Fig. 20. Side lobe artifacts.

display the area distal to A more brightly compared to surrounding tissue. This phenomenon is called tadpole tail (fig. 21).

The 'acoustic shadow' artifact (fig. 22) is the reverse effect of the tadpole tail, as the area behind a high impedance structure is displayed with lower brightness than the circumference. As the ultrasound beam is almost completely reflected at the border and/or attenuated within the high impedance structure, the posterior area does not receive ultrasound waves or only receives them at a very low energy level. This phenomenon can be studied with, for example, bone and calculus.

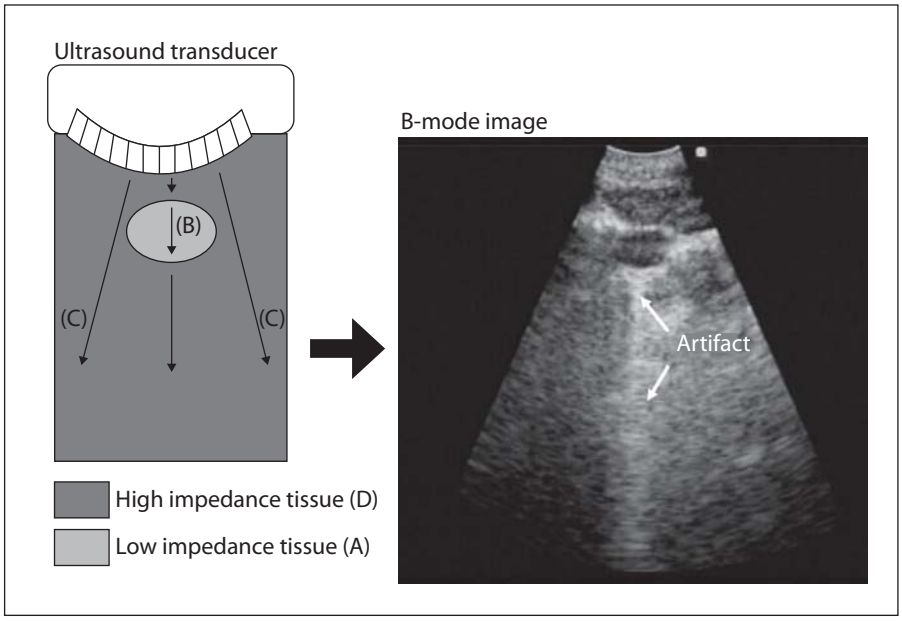

Fig. 21. Tadpole tail attenuation artifact.

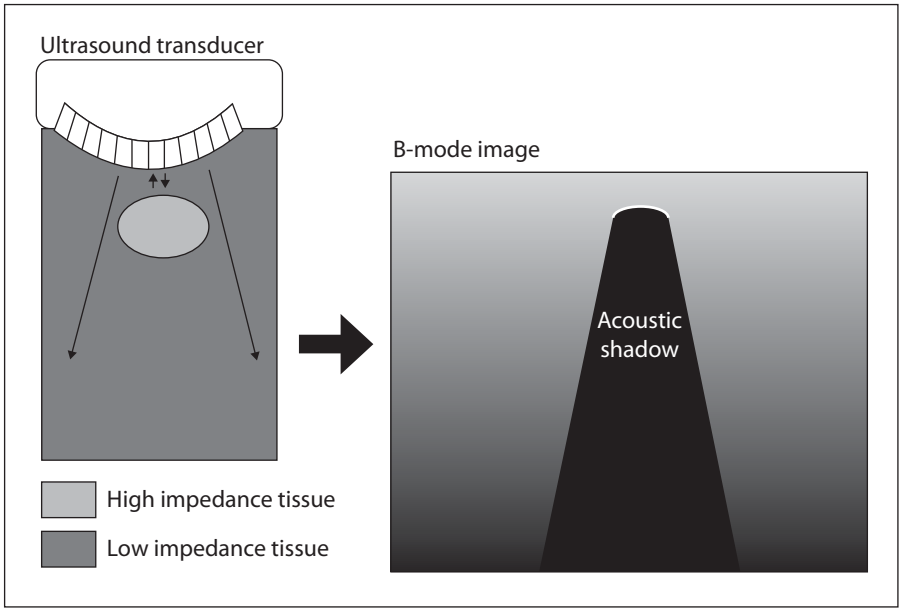

Fig. 22. Acoustic shadow attenuation artifact.

Practice of Enhancing an Ultrasound Image

Basic Features

Gain

Gain is a function for adjusting the brightness of the complete image. Changing gain makes the whole image brighter or darker, but the difference in brightness between light and dark areas on the image does not change.

Contrast

Contrast is a function for adjusting the brightness between light and dark areas of the image. This is especially useful in ultrasound images of echo-poor structures, as the relatively low echo signal can be increased considerably using contrast.

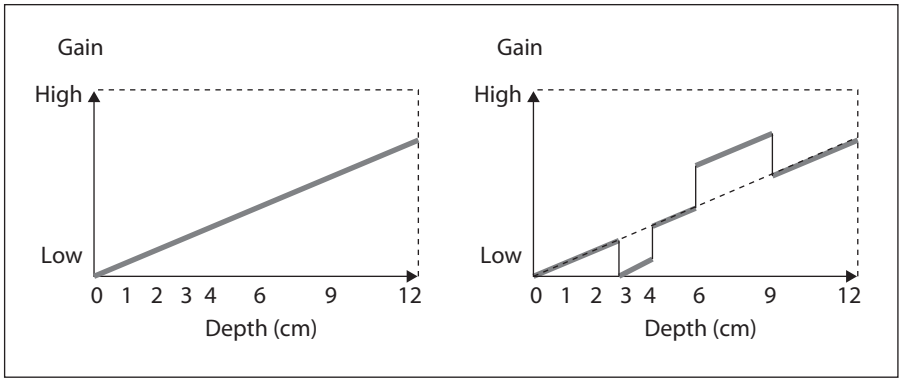

Fig. 23. Default setting of STC and adjusted STC.

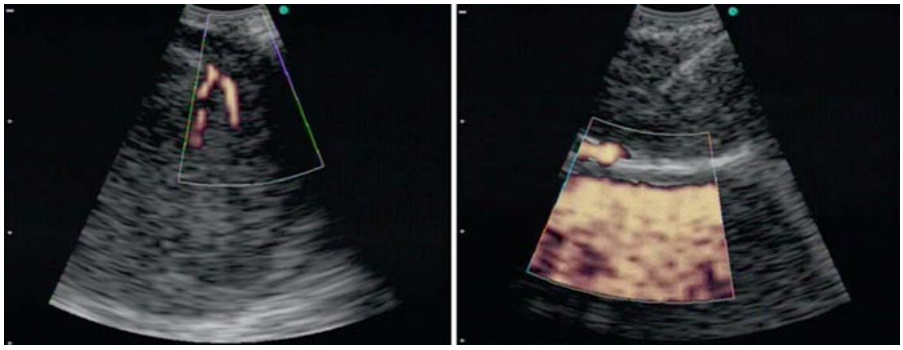

Fig. 24. Power Doppler in B-mode image.

Sensitivity Time Control

STC is also called time gain control and refers to the function for adjusting gain depending on the run time of an echo. As ultrasound waves are attenuated while propagating through the tissue, the brightness of echo signals in the far field is lower compared to areas close to the transducer. In order to correct the brightness and obtain an even brightness across the image, the amplitude ratio of the echo signal is increased in the ultrasound system depending on distance (fig. 23).

Advanced Features

Doppler

Doppler Shift. The Doppler function of the ultrasound processor is named after the Austrian physicist Christian Andreas Doppler who first described in 1842 how the observed frequency of light and sound waves was affected by motion. The phenomenon became known as the Doppler effect. In tissue analysis this effect can be observed as ultrasound waves emitted from the transducer are reflected by moving red blood cells. Depending on the flow direction of the blood cells the original ultrasound frequency is shifted, hence the effect is also called the Doppler shift. From everyday life we know the sound frequency of an approaching and then passing car changes. The number of sound waves reaching the ear in a given amount of time determines the tone; it is stable if the sender and receiver maintain the same distance from each other. The frequency increases when objects move towards each other and decreases when objects move apart. For diagnostics this implies that red blood cells flowing towards the transducer reflect a higher frequency, whilst blood cells flowing away from the transducer reflect a lower frequency. In blood vessels parallel to the transducer (stable distance of the blood cells to the transducer) the Doppler shift frequency becomes 'zero' and hence does not change the original frequency. In endoscopic ultrasound systems pulsed-wave Doppler technology is used to generate depth information of the frequency shift and is most commonly combined in a B-mode image (duplex scanning).

Power Doppler. Power Doppler mode (fig. 24) permits the detection of slow flow movement. It is more sensitive than color Doppler (see section below) as the returning echoes from the blood cells are analyzed by their power spectrum instead of by frequency shift information or

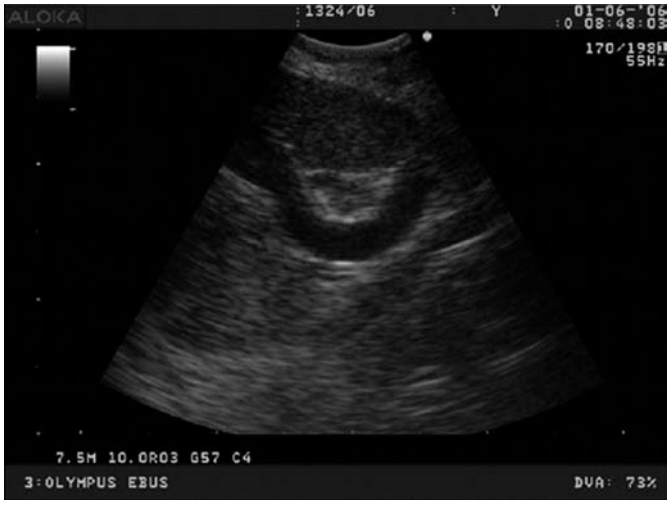

Fig. 25. B-mode image.

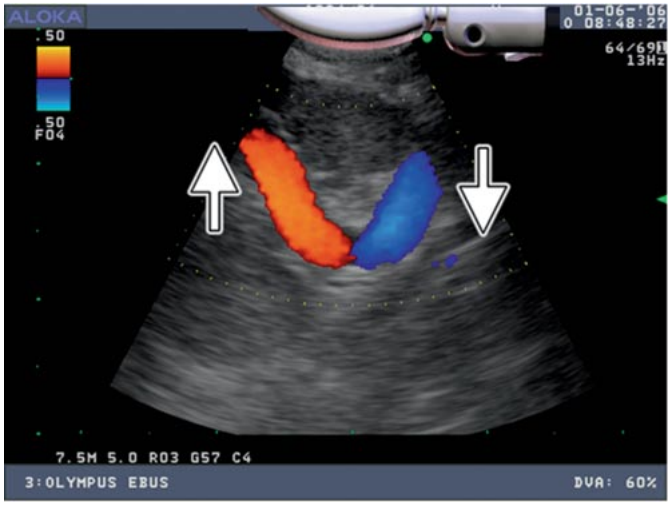

Fig. 27. Blood flow direction.

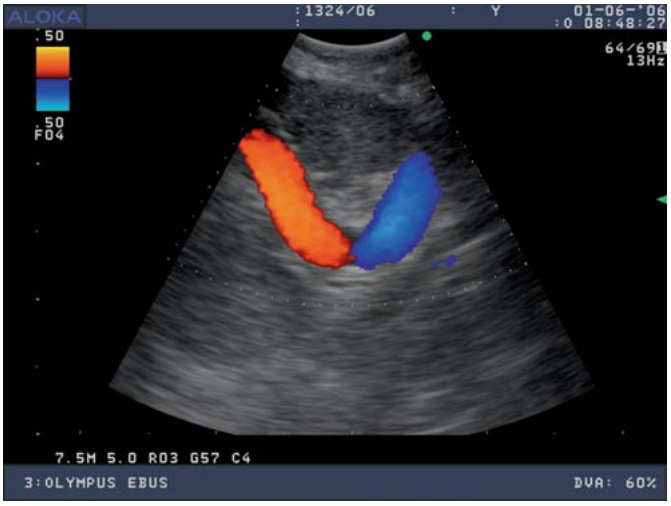

Fig. 26. Color Doppler in B-mode image.

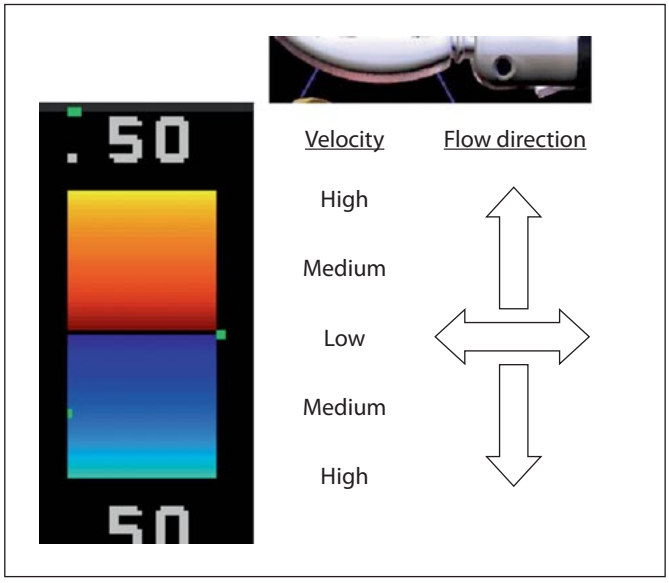

Fig. 28. Explanation of color code bar.

velocity only. Power Doppler is used whenever small blood vessels need to be detected reliably and measurement of speed or direction of flow is not required.

Color Doppler (Duplex Scanning). In color Doppler mode information on frequency shift and blood flow direction is measured. The ultrasound image (fig. 25) shows the location and size of the vessel. With the help of the color Doppler, information on blood flow direction and velocity is added to the image (fig. 26). Figure 27 shows that in this instance blood is flowing from right to left: first away from the transducer then towards the transducer. For the indication of flow direction and velocity a color code is used (fig. 26–28). Here, blood flowing away from the transducer is rendered in blue color shades, blood flowing towards the transducer is rendered in red color shades. The color bar (fig. 28) also includes information on velocity: the color most distal to the central black color stands for fast movement (yellow and turquoise), the black color itself stands for no (measurable) velocity.

Spectral Doppler. Spectral Doppler further enhances the color Doppler information. Using spectral Doppler mode (fig. 29) the flow properties are measured within a small array. The examiner moves the range marker (cursor) onto the vessel under examination. The flow properties of the red blood cells within the gate marked are then calculated

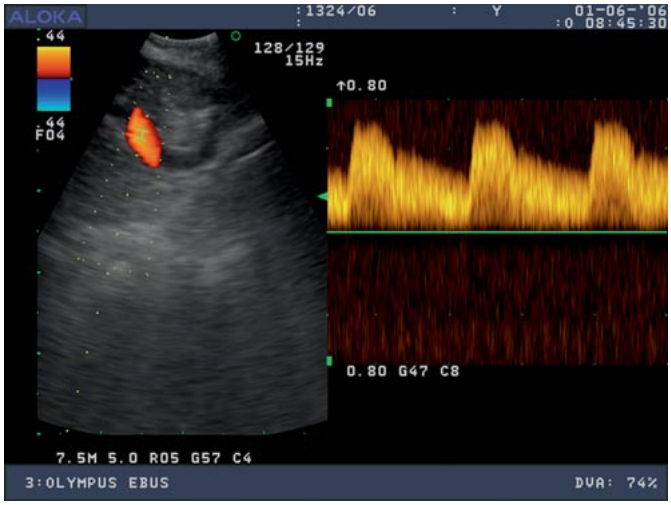

Fig. 29. Spectral Doppler.

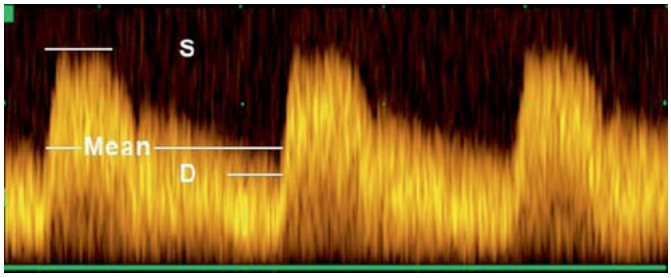

Fig. 30. Spectral Doppler flow velocities. S = Maximum systolic Doppler frequency; D = maximum end diastolic Doppler frequency; mean = mean frequency during one pulse cycle.

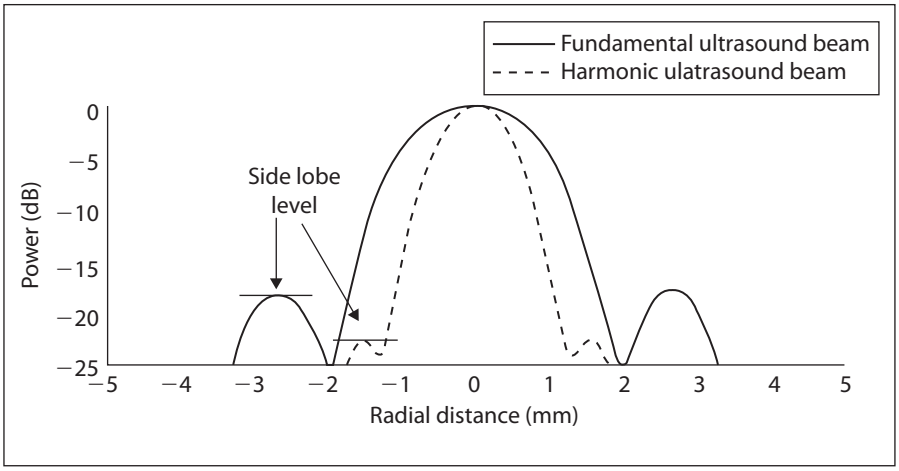

Fig. 31. Beam profile of a fundamental and harmonic frequency.

by the ultrasound system. The output of this information is an audible flow sound and a graph showing the flow velocities (fig. 30) in relation to time (x axis). Systoles and diastoles can thus be easily recognized. Based on the spectrum of frequencies measured, a pulsativity index (PI; Gosling) and a resistance index (RI; Pourcelot) can be calculated.

$$PI = (S - D)/mean$$
$$RI = (S - D)/S$$

Harmonic Imaging

Introduction. In conventional ultrasound, the ultrasound system transmits and receives the sound pulse of a specific frequency. The difference between the transmitted and received signal is intensity, as the signal propagates through tissue. In 'harmonic imaging', the reflected signal includes not only the transmitted 'fundamental' frequency but also 'harmonic' frequencies which are integral multiples of the fundamental frequency.

The ultrasound system receives both signals but further processes only the harmonic components.

Tissue Harmonic Imaging. In tissue harmonic imaging, higher harmonics generated through the propagation of ultrasound are used to improve the lateral resolution in B-mode images. The ultrasound wave acts as pressure wave. This pressure compresses and relaxes the tissue alternately. Where tissue is compressed, the density and therefore also the speed of sound becomes higher. The distal part of the wave runs faster than the rest of the wave. When the tissue relaxes the speed of sound is reduced accordingly. Since the

Fig. 32. Convex EUS gastroscope.

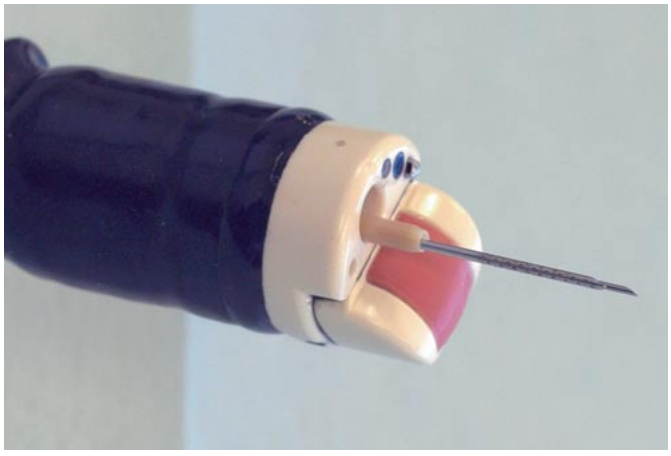

Fig. 33. Forward-viewing convex-type ultrasound endoscope.

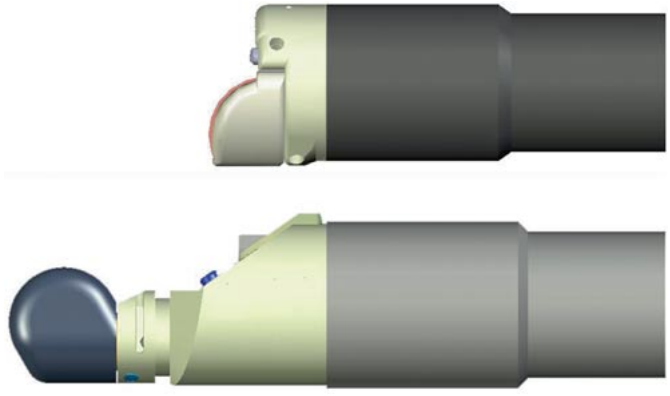

Fig. 34. Comparison of distal tips.

speed of sound varies at different parts of the waveform, the transmitted wave is distorted. This distortion of the waveform produces harmonics. This phenomenon occurs in varying degrees throughout the ultrasound field of view. Due to the run time of the wave, the area close to the transducer is less affected, due to attenuation the far field is not affected; it is only in the midfield that distortion in the wave starts to create harmonics. As a result, the generation of harmonics by tissue will only be observed in the midfield of the ultrasound image. One of the main properties of a harmonic ultrasound beam is a narrow main beam with a low side lobe level compared to a fundamental wave (fig. 31), which permits significantly better gray-scale contrast resolution.

Contrast Harmonic Imaging. Contrast harmonic imaging can be provoked by injecting dedicated contrast agents into the blood cycle during the ultrasound examination. A visible reaction enhances the tissue structure. To generate harmonic signals a contrast agent consisting of microbubbles that are slightly smaller than red blood cells is used. When the transmitted pulse wave hits a bubble, it is partly reflected. More importantly, the impact of the ultrasound pulse makes the bubble vibrate. At high amplitudes the contrast medium shows stronger resistance to compression than to expansion and resulting vibrations become asymmetrical, producing the harmonic echo. This kind of imaging benefits from strong harmonic components being created only in areas with bubbles. By further processing only the harmonic components, the ultrasound system can generate very high contrast images that are relatively free from interference as compared to conventional ultrasound imaging.

Future Perspectives in Endoscopic Ultrasound

Forward-Viewing Ultrasound Endoscope

Ultrasound endoscopy continues to develop from a purely diagnostic into an indispensable therapeutic modality. Therapeutic treatments using EUS-fine needle aspiration are being carried out including pancreatic pseudocyst drainage, celiac plexus neurolysis and drug injection against tumors. In order to perform these advanced interventional procedures, not only suitable endotherapy devices but also improved ultrasound endoscopes are necessary. The current convex-type ultrasound endoscope con-

Fig. 35. Biplane-type ultrasound endoscope.

sists of a transducer placed on the tip, and behind it the oblique optical system and instrument channel open aslant (fig. 32).

This has features that are inconvenient for therapeutic approaches: the rigid part of the endoscope tip is relatively long. All protruding endotherapy devices are bent at the distal end of the working channel, resulting in resistance/friction between the instrument and the endoscope. Figure 33 shows a study of a forward-viewing convex-type ultrasound endoscope. A small size transducer is placed on the tip, which performs linear forward scanning. This allows for a forward-viewing endoscopic optic and a straight instrument channel. The working channel size is 3.7 mm and a water jet function is provided to ensure a permanent optimal endoscopic and ultrasound view. These improved specifications (fig. 34) allow better maneuverability of the distal end of the endoscope and better control of endotherapy devices.

Biplane Ultrasound Endoscope

Despite the strong requests for an improved therapeutic ultrasound endoscope, endosonographers continue to demand an ultrasound endoscope that combines diagnostic and therapeutic specifications, allowing them to switch from diagnostics to therapy with the same scope. A potential solution may be provided by the biplane-type ultrasound endoscope with two scanning planes, radial and convex (fig. 35), resulting in an increase in the distal end of the endoscope in terms of size and length. Consequently the aim is to advance from the biplane-type to a multiplane-type ultrasound endoscope capable of obtaining an arbitrary scanning plane.

So far, due to less strict dimensional requirements and the high level of EUS use, ultrasound endoscopy in gastroenterology allows for the earlier adoption of technologies than bronchoscopy. Today's concepts for improved ultrasound gastroscopes will pave the way for further improvements and the adoption of new concepts in the respiratory field.

Therapeutic Endoscopic Ultrasound

Therapeutic ultrasound-guided procedures such as percutaneous ethanol injection therapy and radiofrequency thermal therapy are already being performed for the treatment of hepatic cancer. Few reports exist on ultrasound-guided therapies in the airway field, but studies are expected to emerge in the future. With regard to interventional EUS procedures reported in recent years, some of them have already been performed clinically, including pancreatic pseudocyst drainage, celiac plexus neurolysis/block (pain relief for advanced pancreatic cancer), choledochoduodenostomy for jaundice treatment and endoscopic necrosectomy. Others are in the animal experiment stage, including gastrojejunostomy. The advantage of interventional ultrasound-controlled therapies is the ability to approach the target organ to be treated, delineate the real-time cross-sectional image of the lesion, confirm the lesion and surrounding organs on the cross-sectional image and perform the treatment (stent delivery, drug injection and so forth) safely and reliably. With regard to pancreatic cancer, some remarkable studies are being performed on ethanol injection into pancreatic cyst tumors [6], anticancer drug injection, and gene injection (TNFerade). Studies of great interest for the future include transesophageal mediastinoscopy [7] and EBUS-guided implantation of a fiducial marker for intensity-modulated radiation therapy [8]. Natural orifice transluminal endoscopic surgery is taking a growing interest in the field of the digestive system. There may exist some potential applications in the mediastinum for which the natural orifice transluminal endoscopic surgery approach is thought to be useful. Ultrasound would be able to assist in showing a safe route towards the mediastinum. Not only marker implantation, but also radiation seed implantation (as performed in the treatment of prostate cancer), may be carried out safely and reliably under ultrasound control. The need for ultrasound guidance and control will further increase with the development not only of markers and radiation sources but also of devices and drugs effective in the local therapy of localized diseases. We believe there is also a high potential for therapeutic ultrasound in the respiratory field.

References

1 Wild J, Reid J: Ultrasonic rectal endoscope for tumor location. Am Inst Ultrasonics Med 1955;4:59.

2 Hagenmüller F, Classen M: Ultrasonic tomography by means of an ultrasonic fiberendoscope. Endoscopy 1980;12:241–244.

3 Hürther TH, Hanrath P: Endobronchiale Songraphie zur Diagnostik pulmonaler und mediastinaler Tumoren. Dtsch Med Wochenschr 1990;115:1899–1905.

4 Becker HD: Endobronchialer Ultraschall – Eine neue Perspektive in der Bronchologie. Ultraschall Med 1996;17:106–112.

5 Kurimoto N, Murayama M, Yoshioka S, Nishisaka T, Inai K, Dohi K: Assessment of usefulness of endobronchial ultrasonography in determination of depth of tracheobronchial tumor invasion. Chest 1999;115:1500–1506.

6 Dewitt JM, Mcgreevy K, Schmidt CM, Collier K, Brugge WR: Ethanol pancreatic injection of cysts (EPIC): preliminary results of a prospective multicenter, randomized, double blinded study. Gastrointest Endosc 2007;65/5:AB106.

7 Fritscher-Ravens A, Patel K, Ghanbari A, Kahle E, von Herbay A, Fritscher T, Niemann H, Koehler P: Natural orifice transluminal endoscopic surgery (NOTES) in the mediastinum: long-term survival animal experiments in transesophageal access, including minor surgical procedures. Endoscopy 2007;39:870–875.

8 McGuire FR, Liming J, Ochran T, Michael Kerley J, McLemore TL: Real-time endobronchial ultrasound-guided implantation of radiotherapy monitoring devices. J Bronchol 2007;14:59–62.

Jochen Wiegand
Olympus Medical Systems Europa GmbH
Wendenstrasse 14–18
DE–20097 Hamburg (Germany)
Tel. +49 40 23773 4849, Fax +49 40 23773 3243, E-Mail jochen.wiegand@olympus-europa.com

Chapter 14

Bolliger CT, Herth FJF, Mayo PH, Miyazawa T, Beamis JF (eds): Clinical Chest Ultrasound: From the ICU to the Bronchoscopy Suite.
Prog Respir Res. Basel, Karger, 2009, vol 37, pp 128–139

Short History of the Development of Endobronchial Ultrasound – A Story of Success

Heinrich D. Becker

Department of Interdisciplinary Endoscopy, Thoraxklinik Heidelberg, Heidelberg, Germany

Abstract

In this article the need for endobronchial ultrasound (EBUS) to expand the bronchoscopist's view beyond the airways is explained. The development of suitable instruments for application in the airways was based on experiences with gastrointestinal endosonography. But special requirements for devices that could be applied within the airways prolonged the development of dedicated devices. First, radial miniaturized catheters had to be fitted with balloon catheters to provide circular contact within the airways. The development of these probes took almost 10 years before coming on the market in 1999. As their application is somewhat complicated, EBUS gained more interest within the pulmonological society since integrated ultrasonographic bronchoscopes were developed and perfected for routine use. Since then ultrasound has become almost a routine procedure and is currently beginning to replace conventional methods. On the basis of the recent increase in speed of the development in EBUS it can be assumed that there is a potential for future development.

EBUS remains the highest impact technology for this year.
Kevin Kovitz, President, American Association for Bronchology
[CHEST, Chicago, Ill., 2007]

Everything we see hides another thing, we always want to see what is hidden by what we see. There is an interest in that which is hidden and which the visible doesn't show us.

Rene Magritte [quoted in Sylvester: Magritte, the Silence of the World. Huston, Menil Foundation, 1992, p 24]

In an editorial published in 2006 in *Respiration*, the author described the development of endobronchial ultrasound (EBUS) as a paradigm for the introduction of innovative technologies in general [1]. This is a complex process from the first idea to the technical development, to studies of feasibility and safety, to evidence-based data and convincing the community, to implementation as standard procedure and reimbursement; processes that were described in detail by Rogers [2] and which the author experienced in the development of other technologies such as the Ultraflex® stent, electromagnetic navigation or currently Vibration Response Imaging (VRI). In this contribution about the history of the development of EBUS the main focus is on the steps in the development of the technology. Not all its indications and results will be described and also, as the literature about EBUS has become so vast [3], references are only made to a few pioneering key note articles. As the nomenclature that the companies created for the different devices has become so complex, mainly common descriptive terms are used and for the more interested reader occasionally the classification type is explained in parentheses. Finally, a large number of engineers and of physicians have been involved and have contributed their ideas and experience to this enterprise. It was time consuming and sometimes difficult to find the exact chronology within the files which during the complex process over almost the last 20 years have become dispersed in different compartments of the archive. Thus when certain names are mentioned, this is also the result of personal memory and judgment and does not imply that any person who should have been given due credit was deliberately omitted; we apologize here to anybody who may not be mentioned. Also, as memories can be treacherous and may fail occasionally, correction of any mistakes that may flaw the undertaking would be appreciated. Having said this why should we need EBUS after all?

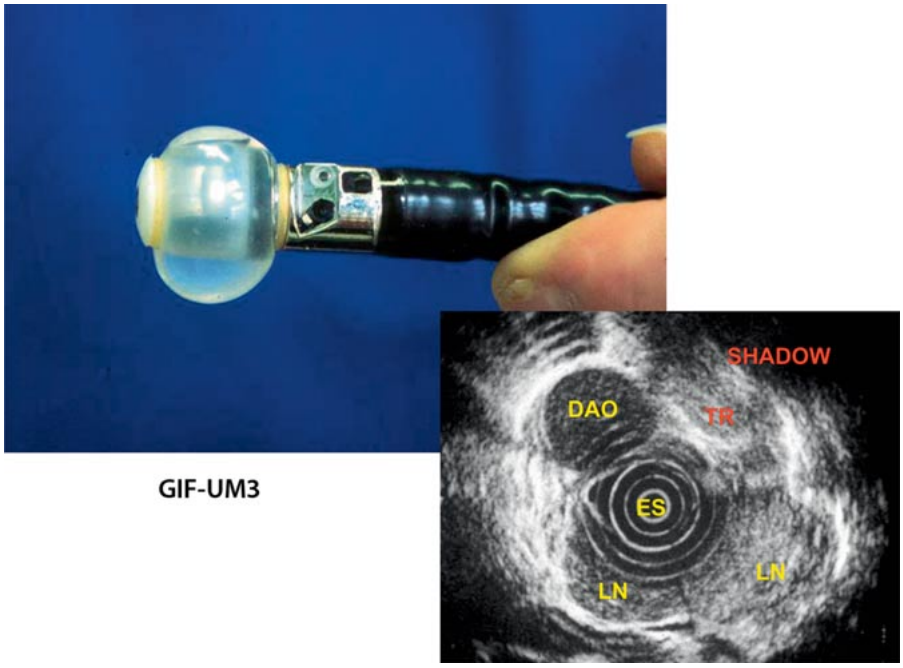

Fig. 1. Tip of the ultrasonic gastroscope type GIF-UM3 with instrumentation channel, port of light guide and lens optic to the right, proximally to the mechanical radial transducer at the tip, which is covered by the dedicated balloon for better surround contact to the esophageal wall. The transesophageal (ES) EUS image shows the descending aorta (DAO), several lymph nodes (LN) and the dorsal wall of the trachea (TR) while the air causes a large shadow, preventing the view to the anterior mediastinum and part of the paratracheal region (Olympus Co).

Why There Was a Need for EBUS

Within the central airways, the endoscopist's view is restricted to the lumen and to the internal surface. Intramural processes and those adjacent to the airways as well as mediastinal structures can only be assessed from indirect signs, including discoloration, displacement and destruction of anatomical structures [4]. In the 1980s, despite early enthusiasm with the broader application of CT, clinical staging of lung cancer corresponded to pTNM in only 60% of cases [5]. After its introduction CT imaging became and still largely is state of the art for preoperative staging of lung cancer. However, whereas CT proved useful for evaluation of primary tumors and metastases, its reliability in diagnosis of lymph node involvement proved disappointing and especially for the diagnosis of airway wall infiltration it is completely insufficient. When an interface between a mediastinal mass and the wall is missing, differentiation is impossible as both structures are of water density. In many cases of such masses our surgeon found no invasion at explorative thoracotomy; thus, there was a demand for a new preoperative imaging technology because from the interior aspect bronchoscopy was also unable to detect invasion. This is why we began to see endoscopic ultrasound (EUS) as a potentially useful technology for the airways [6].

How EBUS Was 'in the Air'

My personal experience with ultrasound in medicine began in the mid 1970s. Trained primarily as a gastroenterologist and having been exposed to abdominal ultrasound from its very beginning in the early 1970s, I started to apply A-mode devices mainly for intra-abdominal lesions as used by neurologists and in obstetrics and later B-mode devices (the first lecture on ultrasound was on the comparison of ultrasound to laparoscopy in diffuse liver disease at the DEGUM congress in Graz in 1979). The transthoracic vision into the mediastinum was very limited even with advanced ultrasound probes [7]. In the late 1980s transesophageal EUS became increasingly established in gastroenterology [8], especially for the exploration of the esophagus with radial scanning endoscopes. Thus a gastrointestinal EUS (Olympus GIF-UM3) was also installed at our hospital in 1989. However, it soon became obvious that visibility of mediastinal structures by EUS was limited due to interference of the airways and also to inaccessibility of important lymph node stations due to their anatomical position (fig. 1). Thus a transfer of the technique to endobronchial application 'was in the air'. However, the large diameter of these instruments was prohibitive for use within the airways. Thus smaller devices had to be found.

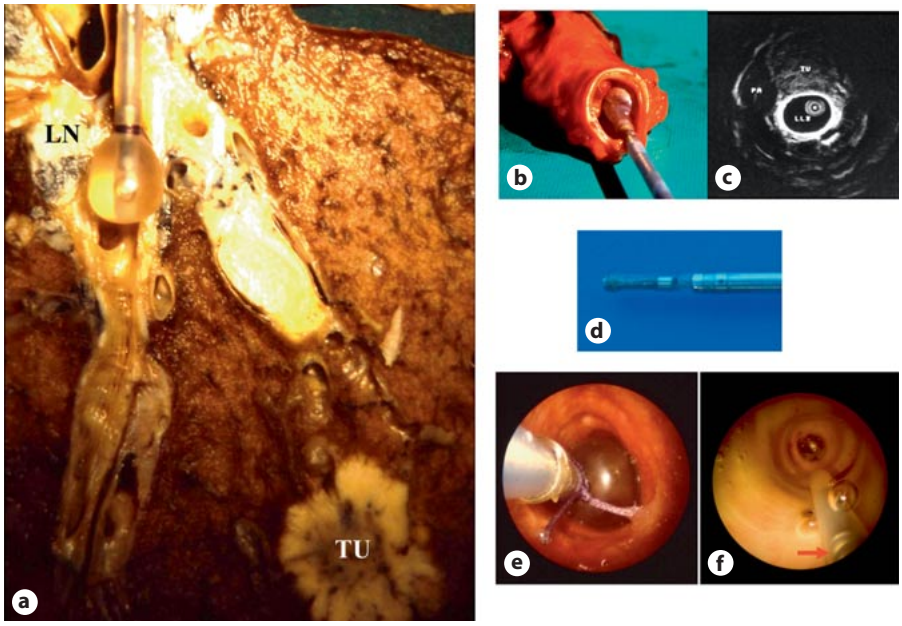

Fig. 2. First radial ultrasound probe Olympus UM-1W. **d** The tip of the probe is seen just outside the metallic catheter (for further details see fig. 5). On a resected specimen of a middle lobe the probe fitted with a balloon attached to its tip is inserted into the lumen (**b**). The ultrasound image shows the tumor in anterior position (TU) with the filled corresponding pulmonary artery (PA) to its left, which is compressed by the tumor at its crossing towards the front (**c**). LLE = Lower lobe bronchus. **e** The endoscopic view of the probe with the balloon tied to its tip inside the intermediate bronchus. **f** The view inside the balloon by direct contact with the lens of the bronchoscope shows the transducer close to the edge of the image (arrow), two air bubbles attached to the probe and the balloon extending well down into the lower lobe bronchus. This shows the problem we had with this balloon as it sometimes was not getting enough contact sideways with the airway wall. The contact technique is always necessary for getting the anatomical orientation and for exact localization of a lesion or lymph node in relation to the airways. **a** The anatomical resection specimen demonstrates the setting schematically with the rigid catheter and probe with the balloon introduced into the intermediate bronchus adjacent to a lymph node (LN) with metastasis from a tumor in the lower lobe (TU).

The Development of the First EBUS Probes (1990–1994)

For this purpose on the occasion of the World Congress for Bronchology, in Tokyo in 1989, we approached Olympus Co., which by that time had developed an ultrasonic radial probe (UM-1W) for application in gastroeneterology for small ducts; this came on the market in 1990. The frequency was 7.5 MHz, the transducer rotated 360° and the outer diameter was 3.4 mm. This probe could only be applied via the rigid bronchoscope as no flexible biopsy channel was large enough. However, it became soon apparent that with this probe the contact was so limited that only a small sector could be visualized and orientation was very difficult. In other applications organs could be filled with water, which is an ideal conductive medium and allowed a complete circular view. As this is not possible within the central airways unless the patient is in danger of suffocation, a metallic catheter was devised with an entrance port for insertion of the probe and a side port for instillation of sterile water. At the tip of this catheter a commercial latex balloon (International Medical Co.) could be fixed by a thread and the water in the balloon provided variable circular contact according to the corresponding bronchial lumen. We tested the device in self-made phantoms, in resected surgical specimens and in animal specimens for safety and image quality before the first application in humans (fig. 2).

At the same time Thomas Hürther in Aachen, Germany cooperated with a cardiologist (Prof. Hanrath) who applied miniature probes inside the blood vessels and thus he developed the idea of using these in the airways, too. He used Boston SC Sonicath® probes of 6.2 and 6.9 french that rotated at 10–15 rpm and had a frequency of 20 MHz with 360° surround view. The depth of penetration was 1.75 cm with a spatial resolution of 200 μm. For visualization of the pulmonary artery he injected 10 ml of oxypolygelatine as contrast medium. He was the first to publish clinical results in 1990 [9] and already described the indication for central tumors,

analysis of the wall, lymph nodes and peripheral lesions. In his paper he also described the need for a balloon catheter and was hoping for a 3-dimensional imaging device. From June 1990 to February 1991 he examined 100 patients with an improved probe of 4.8 french with a balloon sheath of 6.2 french that he introduced via an Olympus BF1T20D Scope. For peripheral lesions he used the probe with an open catheter via which he performed the biopsies after successful placement and could achieve a definite diagnosis in 19/26 cases. In his paper of 1992 [10] he already suggested further studies for the precise role of EBUS as compared to mediastinal, esophageal and endovascular ultrasound. Thus, he has to be considered the first pioneer in EBUS. Unfortunately he left Aachen University in 1991 and afterwards did not work in an environment that allowed him to pursue his studies and, moreover, nobody continued his work at Aachen, so his knowledge was in danger of being lost.

The third pioneer, Ryosuke Ono at the National Cancer Center Hospital Tokyo, Japan together with Aloka Co. developed an ultrasonic bronchoscope for diagnosis and lymph node staging in the hilum and mediastium. The instrument comprised an echo camera, SSD-630 and a transbronchial ultrasonic probe similar to the currently used videobronchoscope. The scope was equipped with an ultrasonic transducer in its tip. The maximum diameter of the probe head was 6.3 mm and that of the transducer was 5.0 mm. The frequency employed was 7.5 MHz and the direction of scanning was parallel to the bronchoscopic axis. With the device, 25 patients, who had given their consent for the ultrasonographic study beforehand, were examined during the 2-month period, January and February 1992. Vessels such as the thoracic aorta, pulmonary artery and brachiocephalic trunk were good landmarks for diagnosis. Lung cancer was detected in 5 patients by biopsy, three malignant lesions in the hilum were diagnosed by videobronchoscopy while two malignant lesions in the periphery were confirmed by bronchoscopic ultrasonography as anterior mediastinal lymph node swellings [11]. I am not aware whether Ono continued his research in EBUS as it was impossible to find relevant information.

For several years the author met Hürther at scientific meetings and we exchanged experiences, especially with respect to the lack of acceptance of the new technique by the scientific community. In a personal letter about the history of the development of EBUS, dated September 25, 2001, he wrote after having received our CD about the radial probe: 'Your consequent work finally confirmed what I imagined and developed some years ago. Back then endobronchial ultrasound was either ridiculed or neglected. I am very happy that my ideas of those days have been confirmed today by your work.' Thus the development of EBUS is another example for success of the motto by Shigeto Ikeda, inventor of the flexible bronchoscope and one of my mentors: 'Never give up!'

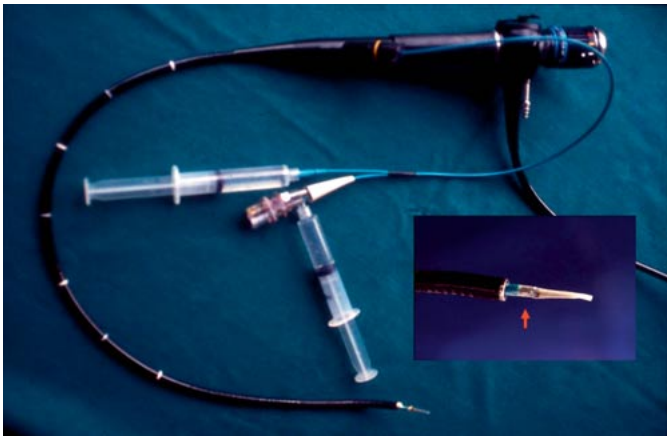

Fig. 3. The CVIS Sonotron catheter system. The catheter is introduced via a bronchofiberscope with its tip protruding outside the biopsy channel. The syringes at the two proximal ports are used for flushing the catheter and the airways with sterile water during the procedure in order to provide better contact. The arrow is pointing to the transducer at the catheter tip.

During our experiences that we presented at several meetings from 1992 on, we soon realized that the application with the rigid tube had to be abandoned and smaller probes for insertion via biopsy channels of regular flexible bronchoscopes had to be found. As in those days Olympus could not provide us with probes of a smaller diameter and after evaluation of several devices of different companies, we bought a CVIS® System of Cardiovascular Imaging Systems Inc. distributed and supported by Diasonics Sonotron (fig. 3). The CVIS catheters had an outer diameter of 8 french (12 MHz) and 10 french (20 MHz). The axial resolution was 0.12 mm, the lateral resolution 0.23 mm. This system could be inserted into fiberoptic endoscopes with a working channel of 2.8 mm. The images were comparable to those generated by the Olympus probe with even a higher resolution as the frequency of 20 MHz proved superior. But, despite repeated attempts, we were not able to find or develop an appropriate balloon catheter sheath for this device.

However, by 1994, when Olympus finally decided to study EBUS research 'in real earnest', we had gained enough experience in the application of EBUS in more than 300 patients to know that the major 5 tasks were solved or about to be solved: (1) to find appropriate systems, (2) to solve the

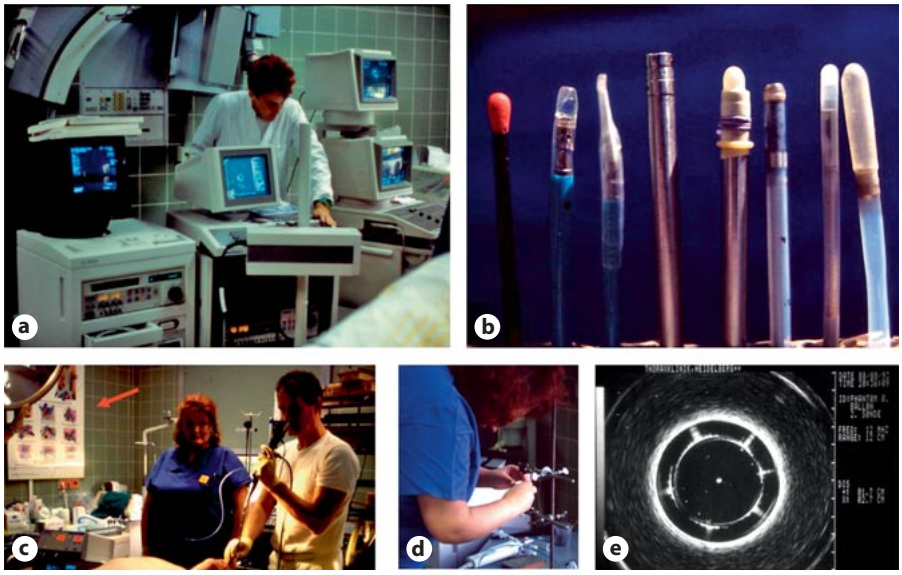

Fig. 4. At the beginning we were exploring and comparing several endoluminal ultrasound devices (**a**) that were equipped with a variety of ultrasound catheter probes with regard to image quality (**b**), of which only the Olympus probe and the CVIS catheter provided satisfactory results. In order to establish an endosonographic anatomy of the mediastinum we could always compare the ultrasound image and the position of the endoscope inside the airways with Dumon's map close to the examination table on the wall (**c**). The former head nurse, Mrs. Messerschmidt, was always enthusiastic and helpful in arranging the phantoms for control of the ultrasound image (**d**). **e** In this case the markers on the periphery of the model, which have been set at regular distances from the center and on the circumference, show identical distances from the core of the probe, but different distances on the circumference, which will also influence measures on images of the airways.

problems of application within the airways, (3) to establish a sonographic anatomy of the airways and of the mediastinum, (4) to check the feasibility of clinical application and (5) to investigate the cost effectiveness.

To this purpose we developed phantoms to evaluate whether the images of the probes were stable and reproducible. Markers where installed at regular intervals around a circular wall with an identical radial distance from the center of the probe that was fixed exactly in the center of the phantom on a stand. Whereas the radial distance from the center of the probe was stable from the beginning and corresponded exactly to the measurements, in the early devices the distances from marker to marker on the circumference could differ considerably. In later devices this was no longer the case (fig. 4).

It was more tedious to establish a dedicated sonographic anatomy of the airways and of the mediastinum. In order to study the layers of the tracheobronchial wall we examined resection specimens, unfixed postmortem specimens and animal specimens of all parts of the airways from the trachea to the peripheral bronchi and also isolated cartilages. This led us to conclude that up to the segmental bronchi the wall comprises seven layers which gradually taper away towards the periphery [12]. The sonographic anatomy of the mediastinal structures is very complex and unusual. The radial image is perpendicular to the axis of the probe and we have to follow the course of the airways, after advancing beyond the bifurcation, up to where the images correspond to CT sections. From there the images are tilting more and more towards a coronary view and finally can be inverse horizontal within the apical segments of the upper lobes. This is why we had Dumon's diagrams of the mediastinal anatomy, edited by the American College of Chest Physicians (ACCP), hanging on the wall adjacent to the examination table and constantly compared what we saw by EBUS with the diagrams [13]. Thus finally we could establish the sonographic anatomy that was edited on an interactive CD in 2000, which can be obtained from Olympus. On it one can compare the endoscopic, ultrasonic and anatomical corresponding structures that can be viewed simultaneously from different angles in an interactive mode.

Development of Dedicated EBUS Systems – The Radial Scanning or Miniprobe 1994–1999

From 1994 the history of EBUS is mainly a history of the success of Olympus, which for many years to come would

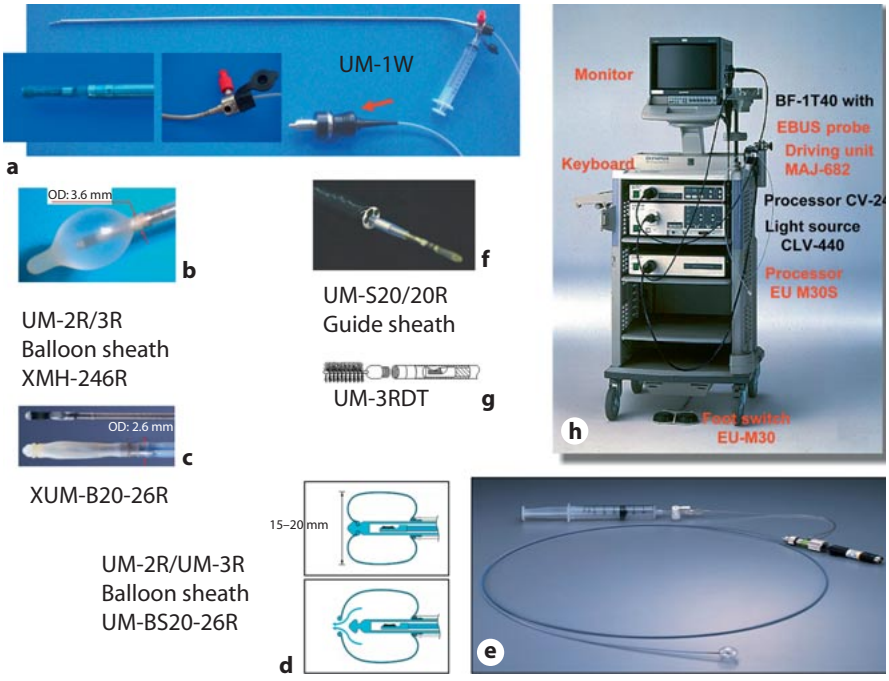

Fig. 5. Evolution of the radial scanning probe. **a** The rigid metal catheter can be seen with the probe inserted and its tip protruding at the distal end, which is shown at closer view as well as the proximal end with ports for inserting the probe and for attaching the syringe with sterile water for filling once the balloon is attached. The arrow points to the connector for the driving unit. **b** The tip of the first prototype UM-2R/3R can be seen, mounted into the balloon catheter. The tip of the balloon (XMH-246R) is not fixed at the tip of the catheter, which caused problems as by filling it always had a tendency to expand more towards the front than towards the sides and then contact with the wall for good image quality was difficult. This was solved by a new model (**c**) and in the final product model, the UM-BS20-26R with balloon sheath MAJ-643R. As seen in the sketch (**d**), the catheter has a notch at its tip, into which an o-ring at the tip of the balloon fits snugly. As a safety feature for prevention of rupture of the balloon with a risk of latex particles dislodging into the lung, this o-ring slips off the notch, when the balloon is overinflated or too much pressure is exerted during coughing and a few milliliters of water can escape into the airways. **e** The catheter is seen completely mounted with the connector to the driving unit and the syringe with a stop cock and a connection catheter. EBUS probe with dedicated catheter for biopsy of peripheral lesions (**f**) and peripheral probe with integrated cytology brush (**g**). Finally the connector is hooked to the driving unit and the probe is introduced via the biopsy channel of the endoscope and the system is ready for use (**h**) with processor, keyboard, monitor and footswitch, which are combined with the regular endoscopic equipment.

be without competition and is still the leader in the field. After evaluating the results of the preliminary studies and after experience with the miniature probes in gastrointestinal endoscopy, the first radial probes for gastrointestinal use were launched in Japan (UM-2R and UM-3R with first 12, later 20 MHz), with which we had gained experience from 1992 on. The first balloon sheath prototype (XMH-246R) was developed for EBUS application with a 3.7-mm channel bronchoscope (XBF-STD30) that we could evaluate in Heidelberg (fig. 5). On August 19, 1994, Noriaki Kurimoto in Hiroshima began studying EBUS as well. In the same year Dr. Takahashi at the Sendai University also received a system for evaluation. In 1995 the balloon sheath was launched in Japan for gastrointestinal use. In the meantime the study groups could confirm the clinical usefulness of EBUS, especially for analysis of tumor invasion in early and more advanced cancer, involvement of the bronchial wall by mediastinal lesions, vessels, lymph nodes and peripheral lesions within the lungs and more physicians joined the group in Japan. On October 14, 1995, EBUS received the first official recognition by the medical profession in Germany, when the author received the DEGUM abstract award by the German Society for Ultrasound in Medicine (at the 19th Meeting of the Societies for Ultrasound in Medicine of Germany, Austria and Switzerland) for presenting my experience in 400 applications, years before the pulmonologists began to realize the impact of EBUS on pulmonary medicine [13].

The current balloon probe had two drawbacks: the diameter was too large for regular bronchoscope channels and the

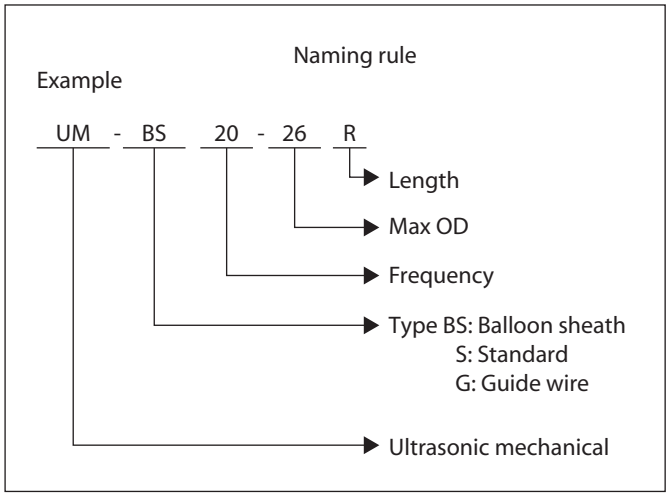

Fig. 6. Example of the complex terminology of the devices, which is not always easy to memorize, but is important to know, when assorting the equipment.

balloon frequently bulged out towards the front before solid contact with the wall could be established. This is why in 1996 development of a new device was started that could go through a biopsy channel of 2.8 mm. In parallel a peripheral probe with an integrated cytology brush was produced as a prototype for diagnosing peripheral lesions. In 1997 the catheters for gastrointestinal use were also launched for endobronchial application and the first prototype of a dedicated EBUS probe (XUM-B20-26R, 2.6 mm) with balloon sheath (XUM-S20-20R7 guide sheath for 3.7 mm) was developed. In parallel, on the request of Dr. Kurimoto to diagnose peripheral lesions more reliably, an even smaller probe of 2 mm was produced that could be inserted via a catheter through a regular bronchoscope [14]. The catheter served as an 'extended working channel' after reaching the lesion by EBUS and a biopsy forceps could be inserted instead of the probe, thus significantly improving the diagnostic results. In 1998 this probe was launched together with the catheter (UM-S20-20R w. guide sheath for 2.8 mm) for peripheral use and a second prototype of the balloon probe was presented with an outer diameter of 2.6 mm. In 1999, finally the dedicated EBUS balloon sheath probe (UM-BS20-26R w. balloon sheath MAJ-643R) could be launched worldwide on the market together with the MH-240 driving unit and the EU-M20 and 30 processors, 10 years after the first request for such a device (fig. 6)! In 2000 we presented its application in a first joint live transmission from Heidelberg and Mayo Clinic, Rochester, Minn. to the congress venue in Yokohama at the 11th World Congress of Bronchology and Bronchoesophagology, which was under the motto: 'Bronchoscopy in the Computer Age'. Since then it has been constantly in use and has proved its reliability and usefulness in thousands of applications worldwide. This is documented in a first monograph on EBUS (in Japanese), which was edited by the Japanese multicenter study group, inaugurated in 1997 and led by Prof. S. Hitomi of the Kyoto University (fig. 7). Further developments in the radial probe were mainly concerned with miniaturization of the probe and sheath for easier application in the periphery and in 1999 we started investigating a prototype of an ultrasonic probe that by simultaneous rotation and movement along its longitudinal axis could produce 3-dimensional images. This was a promising device for the future but needed simplification in its use for spatial reconstruction of the anatomy and pathologies, which might increase the understanding of ultrasound images and enhance discussion with other specialists. Especially in combination with image fusion with endoscopic images and Doppler function it might become useful for planning and monitoring bronchoscopic interventions [15]. In the same year the first request for an integrated ultrasonic endoscope for EBUS-controlled transbronchial needle biopsy of mediastinal lymph nodes was made by Dr. Krasnik from Copenhagen, Denmark.

Development of a Dedicated EBUS Bronchoscope – The So-Called 'Puncture Scope' 1999–2008

As mentioned before, the radial probe was not so easily accepted by the medical community. This was due to the relatively complicated handling of an instrument up to then unfamiliar to pulmonologists, although Falcone et al. [16], member of the European Study group, could show that the method was not too difficult to learn. Also from experience in gastrointestinal ultrasonic endoscopy there was a feeling that real-time ultrasound-controlled needle biopsy would be necessary. For transesophageal needle aspiration this is true. The esophagus is an elastic longitudinal tube without any significant landmarks that is stretched and folded by moving the esophagoscope up and down, whereas the paraesophageal lymph nodes remain in a fixed position. Thus their position cannot be assumed by measuring the distance of the tip of the endoscope to the teeth and real-time control of the needle is necessary. In contrast, the airways are comparatively rigid and do not move inside the mediastinum in relation to the lymph nodes. Also, in the airways it is possible to get orientation according to the

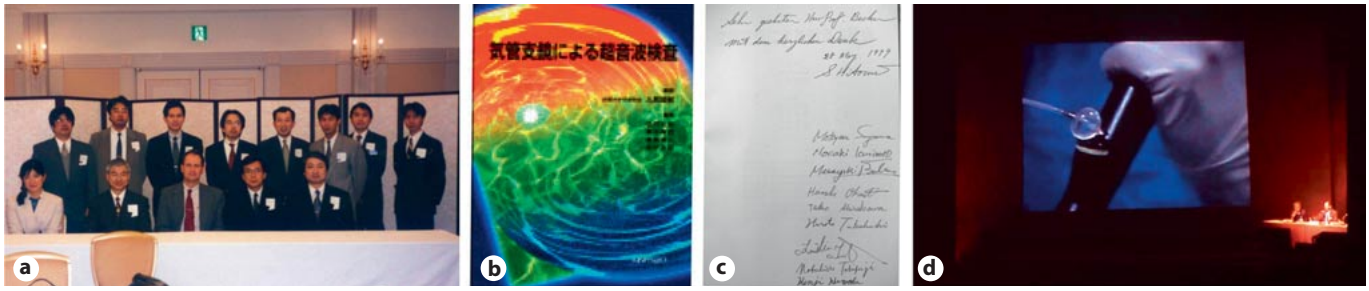

Fig. 7. On the photo of the members of the Japan Multi Center Study Group, taken at the meeting in February 1998 in Osaka, Japan, among others the chair, Prof. S. Hitomi (second from the left), can be seen sitting in the front row between Dr. Shirakawa and the author. Behind Dr. Shirakawa, the Japanese pioneer in EBUS, Dr. Kurimoto is standing in the second row and in this row there are Kenji Hirooka, now General Manager of the Ultrasound Technology Department, Olympus, Tokyo (4th from the right) and Kenichi Nishina, Assistant Manager and Senior Product Engineer of the EUS Scope Group (1st from the right) (**a**). My copy of the first monograph on EBUS published by the group in 1999 (**b**) has a dedication and signatures of all the members in commemoration of the event (**c**). EBUS was the main topic of the first long-distance live transmission from our endoscopy unit in Heidelberg to the congress venue in Yokohama at the 11th WCB/WCBE on June 9, 2000. On the big screen Dr. Herth's hand can be seen holding the bronchoscope while demonstrating how the balloon of the radial EBUS probe is inflated with water while the author is sitting next to Dr. Arai on stage and comments the images (**d**).

clear landmarks of cartilage rings, spurs and ramifications that do not change their position. Thus localization of a lymph node by the radial probe is sufficient for successful transbronchial needle aspiration (TBNA) after withdrawal of the probe as we could show in prospective studies [17, 18] (online suppl. video 1). After preliminary experience with introducing the needle via the flexible endoscope while controlling its position by parallel insertion of the radial probe via the rigid bronchoscope, we had a double-lumen endoscope for simultaneous insertion for evaluation. However, application was pretty clumsy and only a cross section of the needle could be observed as a bright spot within the lymph node, but one could never be certain about the localization of the path and of the tip of the needle (fig. 8).

Video

Then, as the request was there and basically the technology was known from gastrointestinal endoscopy, Olympus started production of the first prototypes of EBUS fiberscopes in 1999. The first one had a radial transducer built into the bronchoscope that was located proximally to the tip with the optical system and the opening of the biopsy channel (XBF-UM30). In addition a balloon could be slipped over the transducer to enhance contact with the wall (XUM-BS30-26R, first prototype of BF-UM40). With 30 MHz the resolution with the larger transducer was better than that of the radial probe, but penetration was insufficient. Therefore, already by 2000 the second prototype was presented (XBF-UM40, second prototype of BF-UM40) with improved image and diameter of the insertion section. However, orientation was not good enough and especially, as the opening of the biopsy channel was still distal to the transducer, optical and ultrasonic images were not congruent and the insertion of the needle could not be followed by ultrasound. Furthermore, the needle could only be seen in cross section as a bright dot. Still this device was launched as BF-UM40 in 2002, but never really caught on with the market for this reason (fig. 9).

In a subsequent model produced in 1999 Olympus tried to overcome these draw backs by moving the transducer distally to the optical lens system and opening the biopsy channel. The ultrasound signal was partially reflected forward by a mirror that was attached in front of the transducer [1st prototype of the so-called 'BUMP' scopes (XBF-UM30P with 7.7 mm diameter)]. This was a certain improvement, but the ultrasound image was poor. Thus in the next prototype of 2000 the mirror became larger and to improve insertion, which was not so easy at the vocal chords under local anesthesia (2nd prototype of 'BUMP' scopes, XBF-UM30P), the rigid part was shorter. Still the ultrasound image was somewhat poor as the distal cap produced multiple echoes. This was overcome by placing the mirror outside the distal cap in the 3rd prototype (XBF-UM40P) in 2001, but then the penetration was not good enough to follow the path of the needle. Finally, production of the 'BUMP'-type scopes was abandoned and the development of the BF-convex systems began. The first prototype of this generation of ultrasonic bronchoscopes (XBF-UC40P) had a curvilinear electronic array at the tip in front of the fiber-optic and the opening of the biopsy channel and an insertion section of less than

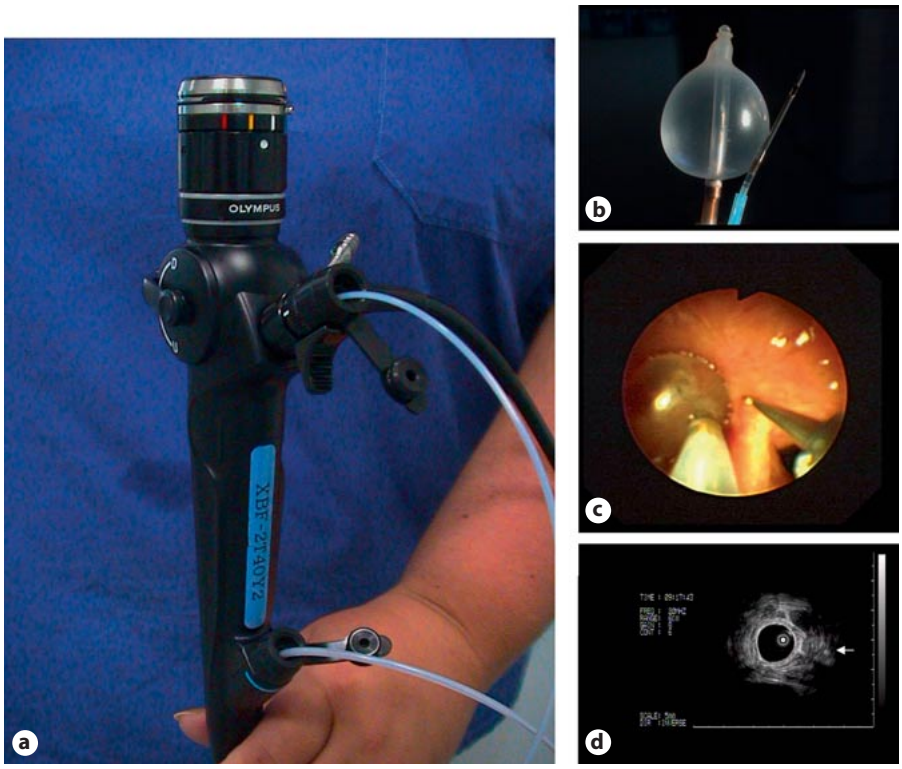

Fig. 8. The intermediate solution between – as we call it – ultrasound-guided TBNA after localization of a lymph node with the radial probe and after withdrawing inserting the needle was ultrasound-controlled TBNA by visualizing the needle real time during the procedure by using a double-channel bronchoscope (XBF-2T 40YZ) (**a**). Once the needle was passed through bronchial wall, the balloon was inflated and the needle could be observed. The setting is shown in vitro (**b**) and the probe (**c**) has been inserted into the left main bronchus with the balloon already inflated, while the needle is just advancing through the wall into the No. 7 subcranial lymph node. The problem with this technique was that as the radial probe provides an image perpendicular to the axis of the needle, only a cross section of the needle was visible as a bright dot, but never the whole needle in its relation to the anatomical structures (arrow in **d**).

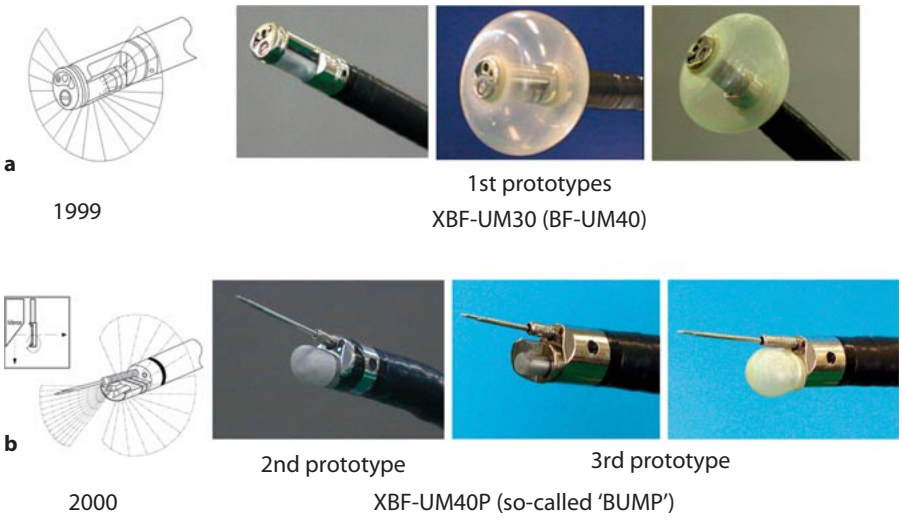

Fig. 9. Evolution of the radial-type ultrasonic bronchoscope, the so-called 'puncture scope'. As the double lumen endoscope was difficult to handle and had a large diameter, in the first versions the radial scanner was placed within the tip of the endoscope to which a balloon could be attached [XBF-UM30 (BF-UM40)] (**a**). The disadvantages, even to the double lumen endoscope, are obvious: the image of the needle is still a dot, but in addition the exact position cannot be seen endoscopically as the distal lens is far in front of the transducer. Therefore, in the next generation a mirror was mounted in front of the transducer that partially reflected the ultrasound in anterior direction and also the optical system was now behind the ultrasound transducers (so-called 'BUMB' scopes) (**b**). But these prototypes had a lot of problems with noise and imaging and so were finally abandoned.

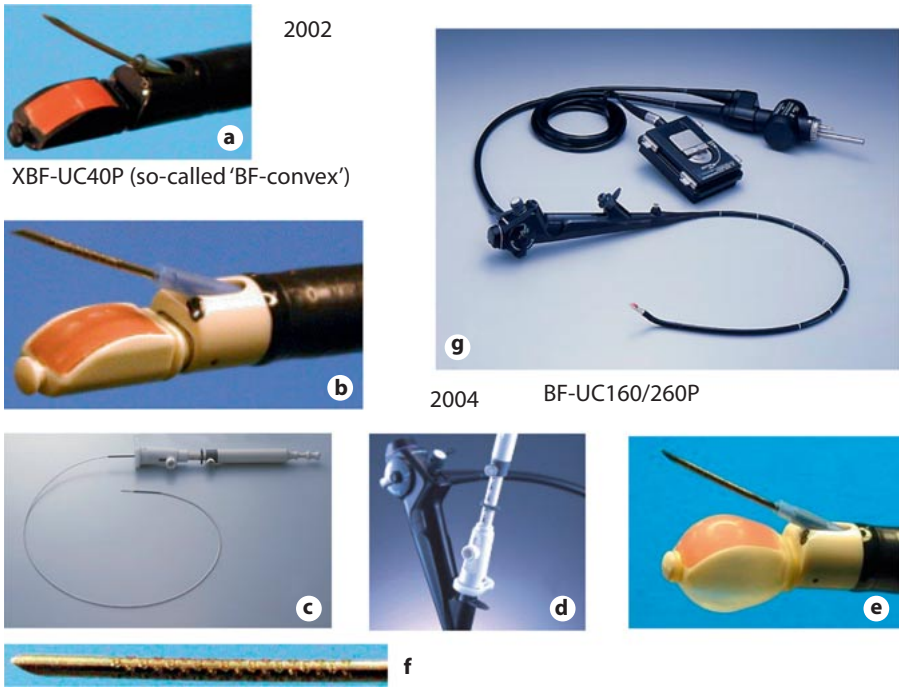

Fig. 10. Evolution of the convex-type ultrasonic bronchoscope. **a** The tip of the first convex-type bronchoscope can be seen with the red electronic transducer and the needle exiting the biopsy channel beside the lens optic. The tip has a notch for the fixation of the balloon that can be attached. The final version (**b**) has a slimmer and more flexible tip. The dedicated needle (**c**) has a few safety features to prevent inadvertent damage to the endoscope by puncturing the biopsy channel. Thus it is fixed at the entrance port of the biopsy channel by a special lever and the tip of the protecting catheter is adjusted to the end of the channel by a screw at the proximal end, already outside the patient as shown in **e**, where for demonstration purposes the balloon is attached and somewhat inflated and the needle is advanced outside the catheter. The needle has a lot of dimples close to its tip to make it more reflecting for the ultrasound, and with this roughness it frequently also provides histological material (**f**). **g** The complete system (BF-UC160/260P) with the connector to the processor and to the light source.

7 mm diameter (fig. 10). Basically this construction proved satisfactory; however, the endoscopic image was comparatively poor and insertion through the vocal chords and penetration with the needle could be difficult. In the following model, the 2nd prototype (XBF-UC160F-OLB/XBF-UC260F-OL8), the image quality was better as a digital camera transferred the fiber-optic image to the processor (so-called hybrid technology). Insertion and penetration became easier by reducing the diameter and making the distal end more stable. The device was already good for routine application, as stated by the European and Japanese study groups and the instrument was launched on the market in 2004 together with a dedicated needle system (NA-201SX-4022) for real-time TBNA of mediastinal lymph nodes (online Video suppl. video 2). This caused a tremendous increase in the interest of pulmonologists and was the real 'kickoff' spreading EBUS worldwide. Further improvements were realized in the next generation prototypes of convex-type ultrasonic bronchoscopes (XFB-UC180F-DT8/XFB-UC280F-DT8, BF180F/BFUC260FW), with detachable cable and compatibility with both Olympus EU-C60 and ALOKA processors provided in 2006. Suction besides the needle is made possible by increasing the channel from 2.0 to 2.2 mm in diameter and in a following 2nd prototype model of 2007 in addition the noise was reduced by altering some electronic parts. With this version another preliminary endpoint seems to be reached and the device will be launched this year as BF180F/BF-UC260FW.

Conclusions and Outlook

As has been shown, EBUS is a fascinating technology that took a very long time to mature, but has subsequently had an impressive history. It has had a tremendous impact on patient management and physicians' work and it is a source of great joy and satisfaction for us to observe how, after its sluggish start and after all the apprehension, skepticism and sarcasm that we encountered at the very beginning, many colleagues worldwide now appreciate its value and find ever new ways and indications for its application. This is due to the perseverance of a few enthusiasts among physicians and engineers and would not have been possible without the commitment of a large company that had the patience, the resources and financial means to overcome the many obstacles encountered during almost 20 years of research and development.

EBUS is still far from reaching the end of its development potential. It is possible that we have only seen the beginning. We are sure that we will see a lot more in the near future with regard to image processing and the com-

puterized analysis of tissues [19, 20]. Image fusion has been successfully combined with interventional technologies such as in electromagnetic navigation and brachytherapy of inoperable peripheral lesions of the lung [21] and the successful treatment of early lung cancer by photodynamic therapy after early detection with autofluorescence and narrow band imaging [22]. Ultrasound in its focused, high-intensified, form might itself become useful for tissue destruction. Refinements of the man-machine interface and robotic instruments could make ultrasound a valuable tool for steering and noninvasively controlling the effects that follow interventional procedures. To facilitate the complimentary application of both devices, the radial mechanical probe and the digital linear probe, an integrated processor would be desirable and would help in spreading the technology worldwide and would eliminate the need to choose between the two devices.

Acknowledgment

An undertaking like the development of EBUS is unthinkable without a lot of support by a great many people. On this occasion the author would like to take the opportunity to thank some of the most important partners for their unstinting cooperation throughout the past 20 years.

First, I would like to thank the engineers of Olympus with whom I have enjoyed discussing and exchanging concepts and ideas and particularly Kenji Hirooka, now General Manager of the Ultrasound Technology Department, whose career I have followed with joy during the years that passed while developing the EBUS. I would also like to thank Mr. Kenichi Nishina, Assistant Manager and Senior Product Engineer of the EUS Scope Group, for his support in documenting all the historical details of the development of the EBUS.

Second, I would like to thank all my colleagues who encouraged me to carry on and who freely shared their ideas and experiences with me and who never ceased to inspire me with ever new ideas, especially those in the study groups with whom I shared many happy hours.

Then, I would like to express my special thanks to my coworkers who spent long hours preparing, improving and evaluating devices and patiently provided all the support that was needed. Two people in particular should be mentioned: the former head nurse Elke Messerschmidt who was very enthusiastic and often worked overtime preparing all the phantoms and animal specimens during the very early stage and also a former coworker, Felix Herth, who took up our ideas and meticulously assembled and systemized them and the preliminary results of the early studies and placed them on an evidence-based foundation, thereby contributing immensely to getting EBUS off the ground.

Last but not least I would like to thank my wife, Simone, who recognized the beauty of EBUS from the beginning and encouraged me to persist, when others were still skeptical.

References

1 Becker HD: EBUS: a new dimension in bronchoscopy (editorial). Respiration 2006;73:583–586.
2 Rogers E: Diffusion of Innovation, ed 5. New York, Free Press, Simon & Schuster, 2005, p 170.
3 http://www.google.de/search?hl=de&q=endobronchial+ultrasound&btnG=Suche&meta=.
4 Becker HD: Bronchoscopy for airway lesions; in Wang KP, Mehta AC (eds): Flexible Bronchoscopy. Oxford, Blackwell Scientific Publications, 1995, pp 136–159.
5 Bülzebruck H, Bopp R, Drings P, Bauer E, Krysa S, Probst G, van Kaick G, Müller K-M, Vogt-Moykopf I: New aspects in the staging of lung cancer. Cancer 1992;70:1102–1110.
6 Herth F, Ernst A, Schulz M, Becker HD: Endobronchial ultrasound reliably differentiates between airway infiltration and compression by tumor. Chest 2003;123:458–462.
7 Werneke K, Vasallo P, Pötter R, Lückener HG, Peters PE: Mediastinal tumors: sensitivity of detection with sonography compared with CT and radiography. Radiology 1985;155:451–465.
8 Tio TL, Coene O, Schouink MH, Tytgat TN: Esophgogastric carcinoma. Preoperative TNM classification with endosonography. Radiology 1989;173:411.
9 Huerther T, Hanrath P: Endobronchiale Sonographie zur Diagnostik pulmonaler und mediastinaler Tumoren. Dtsch Med Wochenschr 1990;115:1899–1905.
10 Hürther T, Hanrath P: Endobronchial sonography: feasibility and preliminary results. Thorax 1992;47:565–567.
11 Ono R, Suemasu K, Matsunaka T: Bronchoscopic ultrasonography for diagnosis of lung cancer. Jpn J Clin Oncol 1993;23:34–40.
12 Shirakawa T, Miyazawa T, Becker HD: The layer structure of central airways as described by endobronchial ultrasonography (EBUS). J Bronchol 2008;15:129–133.
13 Becker HD: Endobronchial ultrasound: a new perspective in bronchology. J Ultraschall Med 1996;17:106–112.
14 Kurimoto N, Murayama M, Yoshioka S, Nishisaka T: Analysis of the internal structure of peripheral pulmonary lesions using endobronchial ultrasonography. Chest 2002;122:1887–1894.
15 Becker HD: Endobronchial ultrasound with miniprobe radial scanning; in Dietrich CF (ed): Endoscopic Ultrasound – an Introductory Manual and Atlas. Stuttgart, Thieme, 2006, pp 334–351.
16 Falcone F, Fois F, Grosso D: Endobronchial ultrasound. Respiration 2003;70:179–194.
17 Herth FJ, Becker HD, Ernst A: Ultrasound-guided transbronchial needle aspiration: an experience in 242 patients. Chest 2003;123:604–607.
18 Herth F, Lunn W, Eberhardt R, Becker HD, Ernst A: Transbronchial versus transesophageal ultrasound-guided aspiration of enlarged lymph nodes. Am J Respir Crit Care Med 2005;171:1164–1167.
19 Becker HD: Bronchoscopy and computer technology; in Simoff M, Sterman H, Ernst A (eds): Thoracic Endoscopy. Advances in Interventional Pulmonology. Oxford, Blackwell, 2006, pp 88–118.

20 Säftiou A, Vilmann P, Hassan H, Gorunescu F: Analysis of endoscopic ultrasound elastography used for characterisation and differentiation of benign and malignant lymph nodes. Ultraschall Med 2006;27:535–542.

21 Harms W, Krempien R, Grehn C, Hensley F, Debus J, Becker HD: Electromagnetically navigated brachytherapy as a new treatment option for peripheral pulmonary tumors. Strahlenther Onkol 2005;2:108–111.

22 Miyazu Y, Miyazawa T, Kurimoto N, Iwamoto Y, Kanoh K, Kohno N: Endobronchial ultrasonography in the assessment of centrally located early-stage lung cancer before photodynamic therapy. Am J Respir Crit Care Med 2002;165:832–837.

Heinrich D. Becker, MD, FCCP
Department of Interdisciplinary Endoscopy, Thoraxklinik Heidelberg
Amalienstrasse 5
DE–69126 Heidelberg (Germany)
Tel. +49 6221 396 302, Fax +49 6221 396 246, E-Mail hdb@bronchology.org

Chapter 15

Bolliger CT, Herth FJF, Mayo PH, Miyazawa T, Beamis JF (eds): Clinical Chest Ultrasound: From the ICU to the Bronchoscopy Suite.
Prog Respir Res. Basel, Karger, 2009, vol 37, pp 140–146

State-of-the-Art Equipment and Procedures

Noriaki Kurimoto[a] · Hiroaki Osada[a] · Teruomi Miyazawa[b]

Departments of [a]Chest Surgery and [b]Pulmonary and Infectious Disease, St. Marianna University, Kawasaki, Japan

Abstract

The development of a balloon-tipped ultrasound probe designed to fit through the working channel of a bronchoscope has been studied. Beyond the sub-sub segmental bronchus, the surface of the radial probe without the balloon attaches to the inner surface of the bronchial lumen. The currently available 20-MHz probes can scan up to about 3 cm deep into the surrounding tissues. Endobronchial ultrasonography (EBUS) can be performed using either the balloon (the probe contacts the object through a balloon filled with medium) or direct contact method (the probe makes direct contact with the object). The method is usually selected according to whether the object of study is centrally or peripherally situated, and probe selection is also made according to the region being examined. The relationship between each tissue layer of the central airways and its ultrasonographic appearance has been established. As the ultrasound frequency increases, resolution is higher and the length of penetration of ultrasound is decreased. The radial probe with 30 MHz shows a differentiated 2nd layer and 4th layer compared to the radial probe with 20 MHz. The use of EBUS is also getting established in other interventional procedures. EBUS using a guide sheath (EBUS-GS) provides the pathway to peripheral pulmonary lesions. The guide sheath covering the miniature radial probe is then advanced through the working channel of a therapeutic bronchoscope with the probe tip outside the sheath until the lesion is visualized. Under fluoroscopy, the sheath is held in place while the EBUS probe is withdrawn. An instrument such as a brush, needle, or biopsy forceps is then inserted through the sheath and the lesion is sampled. One advantage of EBUS-GS lies in the repeatability of access to the bronchial lesion for sampling. Another advantage of EBUS-GS lies in its ability to protect against bleeding into proximal bronchus from the biopsy site. The final advantage of EBUS-GS is the ability to obtain short-axis bronchial views of peripheral pulmonary lesions. The success of EBUS-transbronchial needle aspiration depends on the correct technique being used. It is important not to puncture the bronchial cartilage with the needle. The stylet is the most important part of the needle with regard to obtaining adequate specimens. While the needle is inserted into the lesion, the stylet is pushed and repositioned before it is withdrawn, in order to push out of the needle the primary tissue plug containing superficial layers and bronchial cartilage. After the needle has been removed from the bronchoscope, the stylet is inserted into the needle once again to push out the specimens onto the filter paper. The power Doppler mode of this bronchoscope visualizes major vessels, bronchial arteries outside the bronchial wall, and vessels in the lymph nodes. Vessels in metastatic lymph nodes wind irregularly and vessels in sarcoidosis run in a straight line in the lymph nodes. Vessels are rare in necrotic tissue and the bronchoscopist should, therefore, puncture the hypervascular area in the target lymph node.

Intraluminal ultrasound scanning permits scanning of intrathoracic organs and deep abdominal organs. The use of high-frequency ultrasound yields images with excellent resolution. Endobronchial ultrasonography (EBUS) is an emerging diagnostic modality that gives the bronchoscopist visual and thus diagnostic access to the majority of intrathoracic structures.

Wild and Reid [1] first described the sonographic characteristics of the rectal wall in 1956. Wild and Foderick [2] published a description of their first experiences with a rotating probe on a rigid and flexible endoscope. In 1980, intraluminal ultrasonography was combined with endoscopy, and endoscopic ultrasound instruments were developed by Olympus-Aloka and the Science Research Institute. Endoscopic ultrasound was first used in clinical practice in 1982. The first reported clinical use of a narrow-gauge ultrasonic probe by Pandian et al. [3] in 1988 was for intravascular ultrasonography. The history of EBUS began with the report by Hürter and Hanarath [4] of EBUS of the lung and mediastinum in 1990. Since then, development and research have been carried out mainly in Germany and Japan.

Balloon EBUS (EBUS using a Balloon-Tipped Ultrasound Probe)

The development of a balloon-tipped ultrasound probe designed to fit through the working channel of a bronchoscope by Becker [5] in 1996 vastly improved the efficacy and accuracy of the technique. In Japan, the balloon with the radial probe was used in the duodenum in the duodenum for evaluating the surrounding tissue. We applied this balloon to evaluate tracheobronchial lesions with the bronchoscope. Beyond the sub-sub segmental bronchus, the surface of the radial probe without the balloon attaches to the inner surface of the bronchial lumen. The currently available 20-MHz probes can scan up to about 3 cm deep into the surrounding tissues. Since the resolution and depth penetration of an ultrasonic probe are dependent on the frequency and size of the transducer (as the outer diameter of the probe increases, the size of the ultrasonic transducer also increases), the probe needs to be selected to suit the aim of the procedure.

EBUS can be performed using either the balloon (the probe contacts the object through a balloon filled with medium) or direct contact method (the probe makes direct contact with the object). The method is usually selected according to whether the object of study is centrally or peripherally situated, and probe selection is also made according to the region being examined. When the balloon method is used, the UM-BS20-26R ultrasonic probe (which can be inserted in a bronchoscope instrument channel with a diameter of at least 2.8 mm) in combination with the balloon sheath (MH-676R, Olympus) is generally used. Ultrasound images are obtained by attaching the endoscopic ultrasound probe to the Endoscopic Ultrasound Center (EU-M2000, EU-M30) via the Probe Driving Unit (MH-240).

Many studies on the different uses of EBUS have been done over the last few years. The initial work established the basic correlations among the histological structure, anatomic relationships and ultrasonographic appearance of normal and abnormal airways. We were able to establish the relationship between each tissue layer of the central airways and its ultrasonographic appearance [6] (fig. 1).

Using the balloon probe, there are some tips for getting good ultrasound images. The balloon probe was inserted into the working channel of the bronchoscope, advanced beyond the lesion, and then inflated with a small amount of saline to obtain an EBUS image of the entire circumference of the bronchial wall. Orientation of the 12 o'clock position did not correspond to the bronchoscopic 12 o'clock orientation. The comparison between the bronchoscopic findings and the EBUS image while making up angle by bronchoscopy shows us how to rotate the EBUS image. The anatomy around the bronchus reveals the accurate angle in which to rotate the EBUS image. The EBUS image, therefore, was rotated to the same view as shown by bronchoscopic findings (fig. 2).

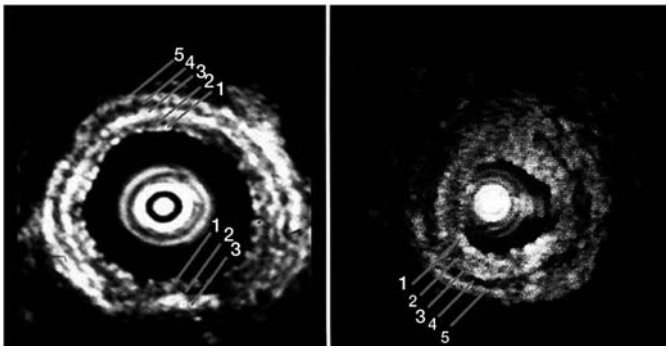

Fig. 1. Normal layers of the bronchus. **a** Extrapulmonary bronchi. **b** Intrapulmonary bronchi. Using a 20-MHz probe, the cartilaginous portion of the extrapulmonary bronchi and the intrapulmonary bronchi is visualized as five layers. The first layer (hyperechoic) is a marginal echo, the second layer (hypoechoic) is submucosal tissue, the third layer (hyperechoic) is the marginal echo on the inside of the bronchial cartilage, the fourth layer (hypoechoic) is bronchial cartilage, and the fifth layer (hyperechoic) is the marginal echo on the outside of the bronchial cartilage. In the membranous portion, the first layer (hyperechoic) is a marginal echo, the second layer (hypoechoic) is submucosal tissue, and the third layer (hyperechoic) is the adventitia.

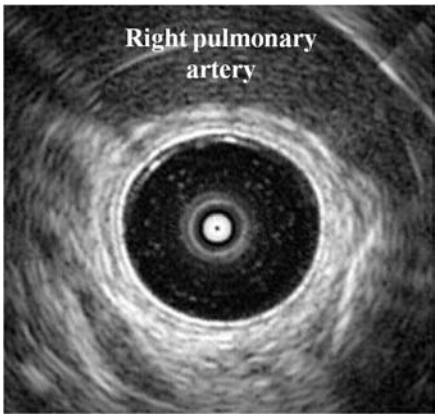

Fig. 2. Anatomy around the bronchus. The right main pulmonary artery is located in front of the intermediate trunk. The anatomy around the bronchus reveals the accurate angle to rotate the EBUS image. The EBUS image therefore was rotated to the same view shown by bronchoscopic findings. The location of the probe at the center of the balloon makes the ultrasound wave advance to the bronchial wall perpendicularly. The bronchial wall where the 1st layer is a thick hyperechoic layer, because the ultrasound wave advances to the bronchial wall perpendicularly, can be visualized as clear layers.

The balloon probe was withdrawn gradually to acquire of EBUS images in the short axis of the lesion and tracheobronchial wall. To get excellent layers of the tracheobronchial wall, the bronchoscopist should control the location of the probe at the center of the balloon and assess the depth of the central tumor in the area where the 1st layer is a thick hyperechoic layer. The location of the probe at the center of the balloon makes the ultrasound wave advance perpendicularly to the bronchial wall. The bronchial wall where the 1st layer is a thick hyperechoic layer, because the ultrasound wave advances to the bronchial wall perpendicularly, can be visualized as clear layers of the bronchial wall (fig. 2).

With increasing ultrasound frequency, resolution is higher and the length of penetration of ultrasound decreases. The radial probe with 30 MHz shows a differentiated 2nd layer and 4th layer compared to the radial probe with 20 MHz. Nakamura et al. [7] compared these two types of probe using Profile of the Image Analysis Software NIH Image. A normal bronchial wall image consists of five layers, and the plot profile shows a W-shaped curve. In order to recognize the laminar structures of the bronchial wall, the 30-MHz probe was found to be more useful than the 20-MHz probe (fig. 3).

EBUS reveals layer structures corresponding to histopathological layers of the tracheobronchial tree. For inflammatory bronchial diseases (relapsing polychondritis, tracheobronchomalacia, Wegener's granulomatosis, etc.), EBUS provides information about ultrasonographic luminar structures of the tracheobronchial wall. Most of these inflammatory bronchial diseases have a thickened 2nd hypoechoic layer corresponding to submucosal tissue of both the cartilaginous and membranous portion. But in relapsing polychondritis there is a thickened 2nd hypoechoic layer of the cartilaginous portion and normal membranous portion. EBUS also shows the thickness of the bronchial cartilage. In inflammatory bronchial diseases, inflammation thickens or destroys the bronchial cartilage.

EBUS has been employed with increasing frequency in therapeutic bronchoscopy as well. It has been used to identify major vascular structures [8] before and during debulking procedures in the airway. In patients with centrally located early-stage lung cancer, and before photodynamic therapy, it can assess the depth of tumor invasion and thus potentially improve the rate of complete remissions [6, 9]. EBUS appears significantly more accurate in determining the depth of tumor invasion when compared with both visual inspection and current imaging standard, high-resolution CT [10].

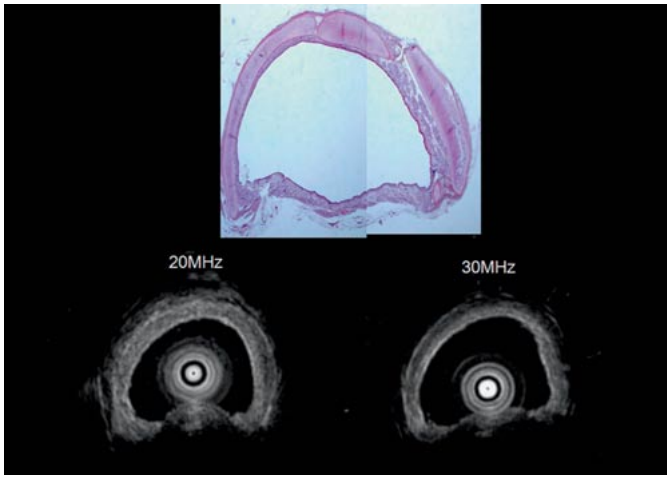

Fig. 3. 20 versus 30 MHz. With increasing ultrasound frequency, resolution is higher and the length of the penetration of ultrasound is decreased. The radial probe with 30 MHz shows a differentiated 2nd layer and 4th layer compared to the radial probe with 20 MHz.

The utility of EBUS is also being established in other interventional procedures. A recent paper [8] evaluated the ability of EBUS to alter, guide, or change therapeutic bronchoscopic procedure in real time. Over a 3-year period, EBUS was employed in 1,174 interventional bronchoscopies. The authors found that as a result therapy was recommended roughly 43% (505/1,174) of the time. We believe that the accumulated evidence suggests that EBUS should be considered as part of any interventional bronchoscopy.

EBUS is sometimes used to evaluate whether central intrathoracic tumors invaded the bronchial tree or not. Herth et al. [11] studied the utility of EBUS in differentiating between airway infiltration and compression by tumor. Sensitivity, specificity, and an accuracy using EBUS were 89, 100 and 94%, respectively. Sensitivity, specificity, and accuracy using CT were 75, 28 and 51%, respectively. EBUS is a highly accurate diagnostic tool and superior to chest CT in evaluating airway involvement by central intrathoracic tumors.

Direct Contact Method (EBUS without the Balloon Sheath)

Apart from surgical exploration, 2 diagnostic modalities currently exist to evaluate solitary pulmonary nodules: transbronchial biopsy (TBB) with fluoroscopic guidance and CT/fluoroscopic-guided transthoracic needle aspiration. EBUS in conjunction with bronchoscopy should be added to this list as a means of evaluating these same

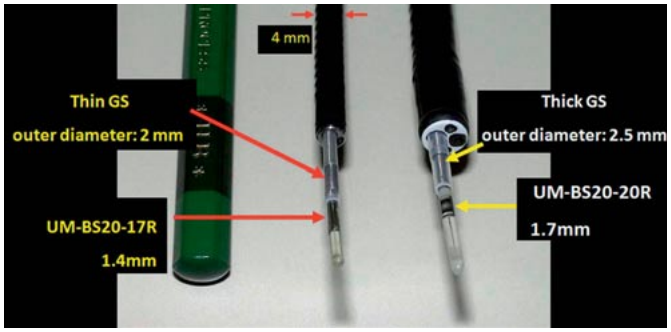

Fig. 4. Equipment of EBUS-GS. A miniature ultrasound probe (UM-S20-20R, UM-S20-17R; 20 MHz, mechanical radial, Olympus Optical Co.) was usually used.

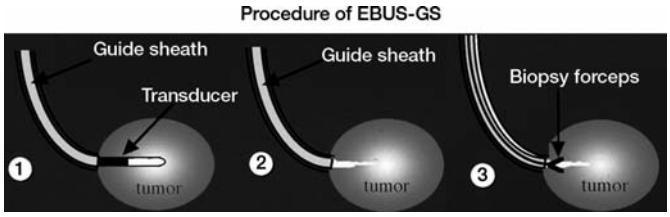

Fig. 5. Procedure of EBUS-GS. The guide sheath covering the miniature radial probe is advanced through the working channel of a therapeutic bronchoscope with the probe tip outside the sheath until the lesion is visualized. Under fluoroscopy, the sheath is held in place while the EBUS probe is withdrawn. An instrument such as a brush, needle, or biopsy forceps is then inserted through the sheath and the lesion is sampled.

lesions. When inserting the probe without balloon and reaching the peripheral lesion, the ultrasonic probe provides a cross-sectional image of the target lesion. In the initial phase, after visualizing the target lesion, the bronchoscopist should pull back the probe and once again insert biopsy forceps. To resolve this demerit, Kurimoto started to use the guide sheath covering the miniature radial probe.

A miniature ultrasound probe (UM-S20-20R, UM-S20-17R; 20 MHz, mechanical radial, Olympus Optical Co., Tokyo, Japan) with an outer diameter of 1.7 mm was usually used (fig. 4). The probe was connected to an Endoscopic Ultrasound System (EU-M30, EU-M2000, Olympus Optical Co.). A guide sheath (Olympus Optical Co.) was manufactured as Guide Sheath Kit (Olympus).

EBUS using a guide sheath (EBUS-GS) provides the pathway to peripheral pulmonary lesions (PPLs) (fig. 5; Video online suppl. video 1). The guide sheath covering the miniature radial probe is then advanced through the working channel of a therapeutic bronchoscope with the probe tip outside the sheath until the lesion is visualized. Under fluoroscopy, the sheath is held in place while the EBUS probe is withdrawn. An instrument such as a brush, needle, or biopsy forceps is then inserted through the sheath and the lesion is sampled. We recommend the use of on-site cytology in conjunction with this method as a way to further expedite and improve the efficacy of this technique. The overall yield of EBUS-GS was 77% and the diagnostic yield of EBUS-GS in malignant and benign lesions was 81 and 73%, respectively [12]. EBUS-GS increases the reliability of specimen collection via bronchoscopy. Diagnostic yields of bronchoscopy for PPLs less than 2 cm in published reports have varied from 5 to 28% [13–22]. The diagnostic yield in this study was far superior and was similar to the overall yield, even when the lesion was undetectable under fluoroscopy. When a lesion undetectable by fluoroscopy is in contact with the probe inserted inside the bronchus, the lesion is visualized by EBUS, and EBUS-GS is particularly useful for lesions ≤20 mm that are undetectable by fluoroscopy.

EBUS-GS was most successful when the probe could be placed within the lesion [12] (fig. 6). The yield of TBB when the probe was adjacent to the lesion was very low. This suggests that the lesions visualized as adjacent to the probe may only be in contact with the outer surface of the bronchus, and therefore sampling is unlikely to be diagnostic. In these circumstances, the operator should attempt to identify the lesion via another bronchial branch (online suppl. video 2). Video

Chechani [23] reported that fluoroscopic localization is most difficult when the lesion is small (<2 cm) and located in the lower lobe basal segment or the upper lobe apical segment. The diagnostic yield for lesions in these two segments (58%) was lower than yields from all other locations (83%). Fletcher and Lewin [24] reported the worst yields were from the lower lobe basal segment (2/7, 28%) and the superior segment (5/19, 26%). In our EBUS-GS study, the worst yield was noted for lesions in the left upper lobe apical posterior segment (6/15, 40%) when compared with yields from all other locations (103/135, 76%). The reason for a lower diagnostic yield in the left upper lobe apical posterior segment is thought to be due to the difficulty in inserting the probe into B1 + 2.

One advantage of EBUS-GS lies in the repeatability of access to the bronchial lesion for sampling. Without a guide sheath, it can be difficult at times to be certain that the forceps are being inserted into the same bronchial branch for the second biopsy. Further, the bronchial mucosa becomes edematous after several attempts at manipulation, and it can be difficult to insert the forceps into the bronchus.

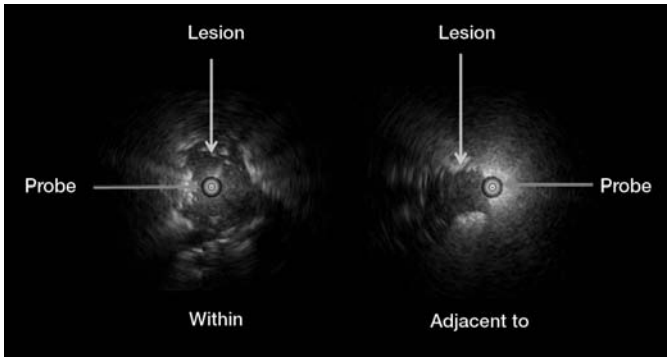

Fig. 6. Location of the ultrasonic probe. EBUS-GS was most successful when the probe could be placed within the lesion. The yield of TBB when the probe was adjacent to the lesion was very low. This suggests that the lesions visualized as adjacent to the probe may only be in contact with the outer surface of the bronchus, and therefore sampling is unlikely to be diagnostic.

Another advantage of EBUS-GS lies in its ability to protect against bleeding into proximal bronchus from the biopsy site. Although massive hemorrhage following TBB is not frequent (<2%) [25, 26] in the bronchus, excessive bleeding may require hemostasis by wedging the tip of the bronchoscope. If bleeding occurs during EBUS-GS, blood drains through the sheath, because the outer surface of the sheath is snug against the internal surface of the bronchus.

The final advantage of EBUS-GS is its ability to obtain short-axis bronchial views of PPLs. Several investigators have reported the use of a miniature probe. Hürter et al. [27] were able to image a peripheral lesion in 19 of 26 patients. Goldberg et al. [28] visualized peripheral lung lesions in 6 patients and hilar lesions in 19 patients. They reported that EBUS provided information that could not be obtained by other diagnostic imaging modalities in 18 of 25 patients. Our method of EBUS using a 20-MHz probe allowed visualization of the inner structures of peripheral lesions, including vessels, bronchi, calcifications, necrosis, hemorrhage, and bronchial dilatation [29]. In most cases of proliferative solid tumors, EBUS revealed avascularity and slightly linear or patchy hyperechogenicity. The internal echoes were heterogeneous, with mixed high echoes. These findings identified the lesion as a proliferative solid tumor of high cell density.

Yoshikawa et al. [30] reported the feasibility and efficacy of TBB and bronchial brushing by EBUS-GS as a guide for diagnosing PPLs without radiographic fluoroscopy. Seventy-six of 123 PPLs (61.8%) were diagnosed by EBUS-GS guidance without fluoroscopy.

Yamada et al. [31] reported factors predicting the diagnostic yield of TBB using EBUS-GS in small PPLs ≤30 mm in mean diameter. In the multivariate analysis, only the position of the probe (within or adjacent to the PPL when judged against outside the PPL) was determined to be a significant factor predicting the diagnostic yield. A pathologic diagnosis was established with the first, second, third, fourth and fifth biopsy specimens in 65, 80, 87, 91 and 97% of PPLs, respectively.

In recent years, two new methods of navigation for PPLs have been developed. The electromagnetic navigation system is a localization device that assists in placing endobronchial accessories (e.g., forceps, brush, or needle) in the desired areas of the lung. This system uses low-frequency electromagnetic waves, which are emitted from an electromagnetic board placed under the bronchoscopy table mattress [32]. Harms et al. [33] introduced a new approach for the treatment of inoperable peripheral lung tumors by combining the electromagnetic navigation system and EBUS with 3-dimensional planned endobronchial brachytherapy. Asano et al. [34] studied the usefulness of another navigation system to approach the PPL. This navigation system is a novel CT-based imaging technique of virtual bronchoscopy that allows a noninvasive intraluminal route to the target lesion. For small PPLs, the combination of EBUS-GS and the navigation system is the most effective for making diagnoses [35, 36]. The system automatically produced virtual images to median of fifth-order bronchi. EBUS visualized 93.8% of cases successfully, and 84.4% could be pathologically diagnosed. To clarify the efficacy the cost/benefit ratio of this procedure needs to be established.

EBUS-Guided Transbronchial Needle Aspiration

EBUS enables the bronchoscopist to visualize the mediastinal lymph nodes and surrounding mediastinal structures. Recently several studies in both EBUS-transbronchial needle aspiration (TBNA) scope-guided TBNA and EBUS probe-guided TBNA have shown a significant increase in yield and a decrease in the number of punctures required to make a diagnosis.

A convex bronchoscope (BF-UC260F, 7.5 MHz, convex type, Olympus Optical Co.) with an outer diameter of 6.9 mm is available on commercial base. The bronchoscope with the convex probe is connected to an Endoscopic Ultrasound System (EU-C6000, Olympus Optical Co.). The needle available on commercial base is 22 gauge (NA-201SX, Olympus Optical Co.)

The success of TBNA depends on the correct technique being used. It is important not to puncture the bronchial cartilage with the needle. The angle of the needle outside of the bronchoscope is oblique toward the tracheobronchial tree, and then the space between bronchial cartilages is very narrow. After the needle has been inserted into the working channel of the bronchoscope, we watch the edge of the outer sheath just as it juts out of the bronchoscope. The outer sheath is pushed toward the bronchial wall and is located at the membranous part between bronchial cartilages. Then the needle is pushed against the tracheobronchial wall and containing the partially withdrawn stylet, it is advanced into the target lesion under constant ultrasound guidance.

The stylet is an important part of the needle to obtain adequate specimens. While the needle is inserted into the lesion, the stylet is pushed and repositioned before it is withdrawn, in order to push out of the needle the primary tissue plug containing superficial layers and bronchial cartilage. After the needle has been removed from the bronchoscope, the stylet is inserted into the needle once again to push out the specimens onto the filter paper.

The suction is then equilibrated while the tip of the needle is still in the lesion. If the needle is withdrawn with suction, bronchial epithelium and submucosal tissue are pulled into the needle and will be contaminated.

The power Doppler mode of this bronchoscope visualizes major vessels, bronchial arteries outside the bronchial wall, and vessels in the lymph nodes. The power Doppler mode reduces complications due to puncturing vessels. Because the internal echo of the lymph node on the B-mode is hypoechoic, the differentiation between major vessels and lymph nodes is sometimes difficult to make. The bronchoscopists should avoid puncturing major vessels and bronchial arteries outside lymph nodes. Vessels in metastatic lymph nodes wind irregularly and vessels in sarcoidosis run in a straight line in lymph nodes. On ultrasonographic B-mode images, necrotic tissue in the lymph node is difficult to differentiate from the viable area of the lymph node. Vessels are rare in the necrotic tissue and so the bronchoscopist should puncture the hypervascular area in the target lymph node.

Future Direction

Technologies are rapidly being developed that will make the transbronchial ultrasound scanning procedure using electronic scanning endoscopic ultrasonography a routine procedure. The main obstacles to this becoming a reality are that the power of the probe is still too weak and the long-awaited software is still not robust enough for practical use. Technology and zeal, however, will resolve these problems in the near future. In the next generation, we hope that electronic scanning endoscopic ultrasonography, harmonic imaging, pulse Doppler and FFT analysis will become available.

Acknowledgment

The authors thank Dr. Fumihiro Asano for his help in the preparation of the videos.

References

1 Wild JJ, Reid JM: Diagnostic use of ultrasound. Br J Phys Med 1956;19:248–257.
2 Wild JJ, Foderick JW: The feasibility of echometric detection of cancer in the lower gastrointestinal tract. Am J Proctol Gastroenterol Colon Rectal Surg 1978;29:16–25.
3 Pandian NG, Kreis A, Brockway B, et al: Ultrsound angioscopy: real-time, two dimensional, intraluminal ultrasound imaging of blood vessels. Am J Cardiol 1988;62:493–494.
4 Hürter T, Hanarath P: Endobronchiale Sonographie zur Diagnostik pulmonaler und mediastinaler Tumoren. Dtsch Med Wochenschr 1990;115:1899–1905.
5 Becker H: Endobronchialer Ultraschall – Eine neue Perspektive in der Bronchologie. Ultraschall Med 1996;17:106–112.
6 Kurimoto N, Murayama M, Yoshioka S, Nishisaka T, Inai K, Dohi K: Assessment of the usefulness of endobronchial ultrasonography in tracheobronchial depth diagnosis. Chest 1999;115:1500–1506.
7 Nakamura Y, Endo C, Sato M, et al: A new technique for endobronchial ultrasonography and comparison of two ultrasonic probes. Analysis with a plot profile of the image analysis software NIH image. Chest 2004;126:192–197.
8 Herth F, Becker H, LoCiero J, et al: Endobronchial ultrasound in therapeutic bronchoscopy. Eur Respir J 2002;20:118–121.
9 Miyazu Y, Miyazawa T, Kurimoto N, et al: Endobronchial ultrasonography in the assessment of centrally located early-stage lung cancer before photodynamic therapy. Am J Respir Crit Care Med 2002;165:832–837.
10 van Boxem TJ, Golding RP, Venmans BJ, et al: High resolution CT in patients with intraluminal typical bronchial carcinoid tumors treated with bronchoscopic therapy. Chest 2000;117:125–128.
11 Herth FJ, Ernst A, Schulz M, et al: Endobronchial ultrasound reliably differentiates between airway infiltration and compression by tumor. Chest 2003;123:458–462.

12 Kurimoto N, Miyazawa T, Okimasa S, et al: Endobronchial ultrasonography using a guide sheath increases the ability to diagnose peripheral pulmonary lesions endoscopically. Chest 2004;126:959–965.
13 Mori K, Yanase N, Kaneko M, et al: Diagnosis of peripheral lung cancer in cases of tumors 2 cm or less in size. Chest 1989;95:304–308.
14 Popvich J Jr, Kvale PA, Eichenhorn MS, et al: Diagnostic accuracy of multiple biopsies from flexible fiberoptic bronchoscopy – a comparison of central versus peripheral carcinoma. Am Rev Respir Dis 1982;125:521–523.
15 Fletcher EC, Levin DC: Flexible fiberoptic bronchoscopy and fluoroscopically guided transbronchial biopsy in management of solitary pulmonary nodules. West J Med 1982;135:477–483.
16 Stringfield JT, Mrkowitz DJ, Bentz RR, et al: The effect of tumor size and location on diagnosis by fiberoptic bronchoscopy. Chest 1977;72:474–476.
17 Radke JR, Conway WA, Eyler WR, et al: Diagnostic accuracy in peripheral lung lesions: factors predicting success with flexible fiberoptic bronchoscopy. Chest 1976;76:176–179.
18 Wallace JM, Deutch AL: Flexible fiberoptic bronchoscopy and percutaneous lung aspiration for evaluating the solitary pulmonary nodule. Chest 1982;81:665–671.
19 Hadson RR, Zavala DC, Rhodes ML, et al: Transbronchial biopsy via flexible fiberoptic bronchoscope; results in 164 patients. Am Rev Respir Dis 1976;114:67–72.
20 Kvale PA, Bode FR, Kini S: Diagnostic accuracy in lung cancer; comparison of techniques used in association with flexible fiberoptic bronchoscopy. Chest 1976;69:752–757.
21 Shiner RJ, Rosenman J, Katz I, et al: Bronchoscopic evaluation of peripheral lung tumors. Thorax 1988;43:887–889.
22 Torrington KC, Kern JD: The utility of fiberoptic bronchoscopy in the evaluation of the solitary pulmonary nodule. Chest 1993;104:1021–1024.
23 Chechani V: Bronchoscopic diagnosis of solitary pulmonary nodules and lung masses in the absence of endobronchial abnormality. Chest 1996;109:620–625.
24 Fletcher EC, Levin DC: Flexible fiberoptic bronchoscopy and fluoroscopically guided transbronchial biopsy in management of solitary pulmonary nodules. West J Med 1982;135:477–483.
25 Blasco LH, Hernandez IMS, Garrido VV, et al: Safety of transbronchial biopsy in outpatients. Chest 1991;99:562.
26 Ahmad M, Livingston DR, Golish JA, et al: The safety of outpatient transbronchial biopsy. Chest 1986;90:403.
27 Hürtur T, Hanrath P: Endobronchial sonography: feasibility and preliminary results. Thorax 1992;47:565–567.
28 Goldberg B, Steiner R, Liu J, et al: US-assisted bronchoscopy with use of miniature transducer-containing catheters. Radiology 1994;190:233–237.
29 Kurimoto N, Murayama M, Yoshioka S, et al: Analysis of the internal structure of peripheral pulmonary lesions using endobronchial ultrasonography. Chest 2002;122:1877–1894.
30 Yoshikawa M, Sukoh N, Yamazaki K, et al: Diagnostic value of endobronchial ultrasonography with a guide sheath for peripheral pulmonary lesions without X-ray fluoroscopy. Chest 2007;131:1788–1793.
31 Yamada N, Yamazaki K, Kurimoto N, et al: Factors related to diagnostic yield of transbronchial biopsy using endobronchial ultrasonography with a guide sheath in small peripheral pulmonary lesions. Chest 2007;132:603–608.
32 Schwarz Y, Mehta AC, Ernst A, et al: Electromagnetic navigation during flexible bronchoscopy. Respiration 2003;70:516–522.
33 Harms W, Krempien R, Grehn C, et al: Electromagetically navigated brachytherapy as a new treatment option for peripheral pulmonary tumors. Strahlenther Onkol 2006;182:108–111.
34 Asano F, Matsuno Y, Matsushita T, Kondo H, Saito Y, Seko A, Ishihara Y: Transbronchial diagnosis of a pulmonary peripheral small lesion using an ultrathin bronchoscope with virtual bronchoscopic navigation. J Bronchol 2002;9:108–111.
35 Asahina H, Yamazaki K, Onodera Y, et al: Transbronchial biopsy using endobronchial ultrasonography with a guide sheath and virtual bronchoscopic navigation. Chest 2005;128:1761–1765.
36 Asano F, Matsuno Y, Tsuzuku A, et al: Diagnosis of peripheral pulmonary lesions using a bronchoscope insertion guidance system combined with endobronchial ultrasonography with a guide sheath. Lung Cancer 2008;60:366–373.

Noriaki Kurimoto, MD
2-16-1, Sugao, Miyamae-ku
Kawasaki, Kanagawa 216-8511 (Japan)
Tel. +81 44 977 8111, Fax +81 44 976 5792, E-Mail n.kurimoto@do7.enjoy.ne.jp

Chapter 16

Bolliger CT, Herth FJF, Mayo PH, Miyazawa T, Beamis JF (eds): Clinical Chest Ultrasound: From the ICU to the Bronchoscopy Suite.
Prog Respir Res. Basel, Karger, 2009, vol 37, pp 147–152

Convex Probe Endobronchial Ultrasound

Kazuhiro Yasufuku[a] · Takahiro Nakajima[b]

[a]Division of Thoracic Surgery, Toronto General Hospital, University Health Network, Toronto, Ont., Canada, [b]Department of Thoracic Surgery, Graduate School of Medicine, Chiba University, Chiba, Japan

Abstract

Endobronchial ultrasound (EBUS) is a promising new modality first introduced in the early 1990s. The radial probe EBUS was initially developed in the search for high resolution imaging of processes within the airway wall and also outside the airways. The structure of special importance was lymph nodes, walls of the central airways and the mediastinum. After the development of miniaturized radial probes with flexible catheters with a balloon at the tip, it has been applied to aid bronchoscopists during biopsy in respiratory diseases. In particular, the role of EBUS in transbronchial needle aspiration (TBNA) has been established by many authors. The radial probe EBUS-guided TBNA has increased the yield of TBNA of mediastinal lymph nodes. However it was still not a real-time procedure with target visualization. To overcome these problems, a new convex probe endobronchial ultrasound (CP-EBUS) with ability to perform real-time EBUS-guided TBNA (EBUS-TBNA) was developed in 2002. EBUS-TBNA can be used for (1) lymph node staging in lung cancer patients; (2) diagnosis of intrapulmonary tumors; (3) diagnosis of unknown hilar and/or mediastinal lymphadenopathy, and (4) diagnosis of mediastinal tumors. Case series using EBUS-TBNA for mediastinal lymph node staging in lung cancer have reported a high yield ranging from 89 to 98%. To date, there are no reports of major complications related to EBUS-TBNA. EBUS-TBNA is a novel approach which can be safely performed in an ambulatory setting with a high diagnostic yield. CP-EBUS has an excellent potential in assisting safe and accurate diagnostic interventional bronchoscopy in respiratory diseases.

The endobronchial application of ultrasound was first described in 1992 [1]. After solving technical difficulties for the application of the ultrasound in bronchoscopic practice, the radial probe endobronchial ultrasound (EBUS) has been commercially introduced in 1992. Currently, EBUS has gradually been introduced into the field of respiratory diseases, which has broadened the diagnostic possibilities for bronchial and mediastinal pathology.

For optimal imaging, the miniaturized 20-MHz radial probe fitted with a catheter that carries a water-inflatable balloon at the tip allows visualization of detailed images of the surrounding structures as well as the bronchial wall structure [2]. By visualization of mediastinal and hilar lymph nodes, EBUS guidance has increased the yield of transbronchial needle aspiration (TBNA) for lymph node staging of lung cancer [3]. However due to the nature of the probe, it was not a real-time procedure with target visualization.

The use of the convex probe endobronchial ultrasound (CP-EBUS) with the ability to perform real-time EBUS-guided TBNA (EBUS-TBNA) under direct US guidance was first reported in preliminary studies on surgical specimens using CP-EBUS [4]. Multiple studies have shown the usefulness of EBUS-TBNA in the assessment of mediastinal and/or hilar lymph nodes, especially for staging of lung cancer [5–10]. EBUS-TBNA has changed the practice of interventional bronchoscopy. In particular, bronchoscopic biopsy of the mediastinum has become minimally invasive with a high yield. Pulmonologists as well as thoracic surgeons have begun to develop an interest in the procedure. In this chapter, the utility of the CP-EBUS and the different usefulness in the assessment of respiratory diseases will be explained in detail.

Instrument

Convex Probe Endobronchial Ultrasound

The currently available CP-EBUS is an ultrasound puncture bronchoscope with a 7.5-MHz convex transducer placed at the tip of a flexible bronchoscope (BF-UC160F-OL8, Olympus, Tokyo, Japan) (see chapter 13, fig. 5). The CP-

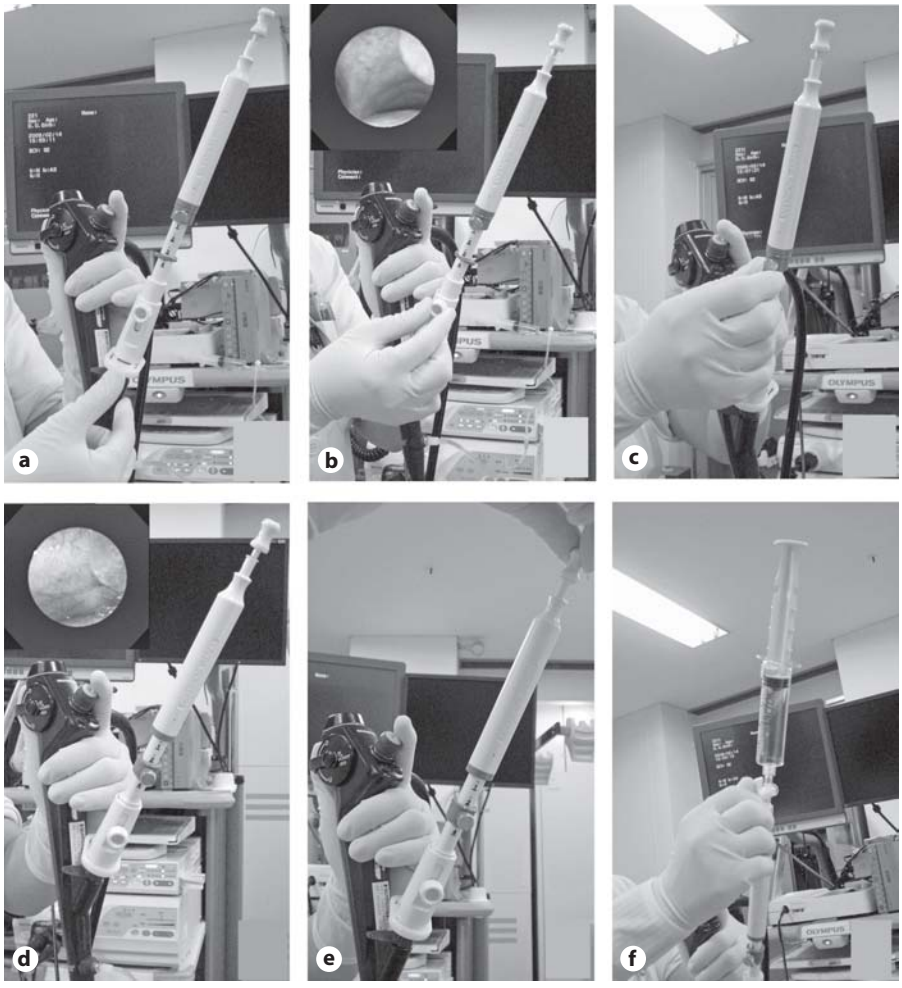

Fig. 1. Dedicated 22-gauge needle (NA-201SX-4022, Olympus). **a** The needle is fastened onto the working channel. **b** The sheath adjuster knob is loosened and the length adjusted. **c** The needle adjuster knob is loosened. **d** EBUS-TBNA is performed. **e** After the initial puncture, the internal stylet is used to clear out the internal lumen. **f** Negative pressure is applied with the Vaclok syringe.

EBUS is a linear curved array transducer that scans parallel to the insertion direction of the bronchoscope. Images can be obtained by direct contact with the probe or by attaching a balloon to the tip and inflating it with saline. The outer diameter of the insertion tube of the CP-EBUS is 6.2 mm and that of the tip is 6.9 mm. The angle of view is 80° and the direction of view is 35° forward oblique. The unique optical system exploits both video and fiberoptic technologies. With the built-in CCD in the control section, it allows sharp images similar to those of regular video bronchoscopes. The inner diameter of the instrument channel is 2.0 mm. A dedicated 22-gauge needle is used to perform EBUS-TBNA.

Ultrasound Processor

The ultrasound image is processed in a dedicated ultrasound processor (EU-C60/EU-C2000, Olympus) (see chapter 13, fig. 7). The display mode includes the B-mode as well as the color power Doppler mode. The display range covers 2–24 cm. The ultrasound images can be frozen and the size of lesions can be measured in two dimensions by the placement of cursors. The area and the circumference enclosed by calliper tracking can be measured as well.

Dedicated 22-Gauge Needle

A dedicated 22-gauge needle (NA-201SX-4022, Olympus) is used to perform EBUS-TBNA (fig. 1). This needle has various adjuster knobs which work as a safety device to prevent damage of the channel. The maximum extruding stroke is 40 mm and to prevent excessive protrusion, a safety mechanism stops the needle at the stroke of 20 mm. The needle is also equipped with an internal sheath which is withdrawn after passing the bronchial wall, avoiding contamination during TBNA. This internal sheath is also used to clear out the tip of the needle after passing the bronchial

wall. The exit of the needle is at 20° with respect to the outer covering of the insertion tube. The needle can be visualized through the optics and on the ultrasound image.

Procedural Technique

Anesthesia

EBUS-TBNA can be performed on an outpatient basis under conscious sedation. The bronchoscope is usually inserted orally, since the ultrasound probe on the tip will limit nasal insertion. Some investigators prefer the use of the endotracheal tube or rigid bronchoscopy under general anesthesia. An endotracheal tube larger than or equal to size 8 is required due to the size of the EBUS-TBNA scope. Cough reflex is minimal under general anesthesia which may be an advantage during the procedure. However, operators should be careful not to put excessive pressure onto the airway with the probe. The disadvantage of the endotracheal tube is that it causes the bronchoscope to lie in the central position within the airway which makes it difficult to bring its tip into close proximity to the trachea or bronchus. The use of the laryngeal mask airway has been shown to be useful during EBUS-TBNA [11].

Insertion to Visualization of Lymph Nodes

Since the linear curved array transducer is on the tip of the flexible bronchoscope, the optic located proximal to the ultrasound probe is set at a 35° forward oblique angle. Therefore, in order to obtain a straight view, the tip of the bronchoscope needs to be slightly flexed down. The bronchoscopist also needs to be aware that the 7.5-MHz ultrasound probe attached to the tip of the bronchoscope is not visible without the inflation of the balloon. Careful attention should be given to advancing the scope atraumatically.

Under local anesthesia and conscious sedation, the CP-EBUS is inserted orally into the trachea. The scope is passed through the vocal cords by visualizing the anterior angle of the glottis (fig. 2a). Once the bronchoscope has been introduced into the airway until the desired position is reached for EBUS imaging, the balloon is inflated with normal saline to achieve maximum contact with the tissue of interest (fig. 2b). The tip of the CP-EBUS is flexed and gently pressed onto the airway (fig. 2c). Ultrasonically visible vascular landmarks are used to identify the specific lymph node stations according to the Mountain classification system [12]. The Doppler mode is used to confirm and identify surrounding vessels as well as the blood flow within lymph nodes [13]. Lymph nodes larger than 1 cm in short axis, round-shaped, and with distinct margins without the presence of central hilar structures are suspicious for malignancy and need to be biopsied.

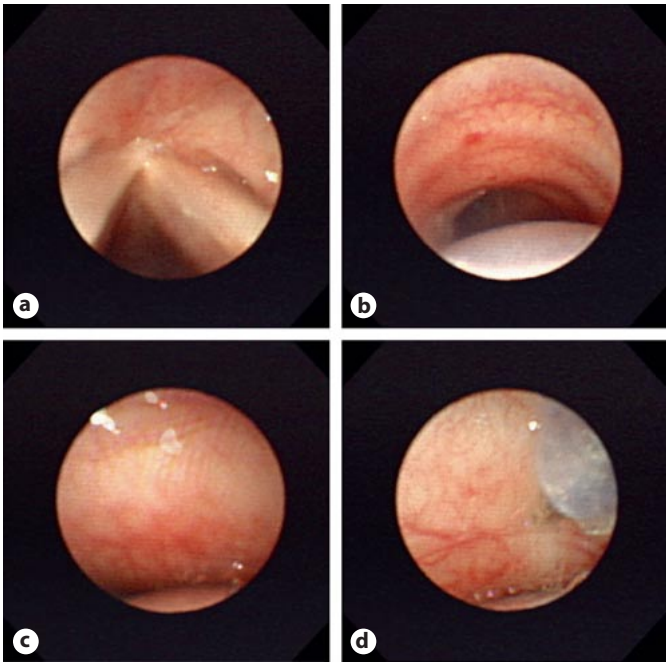

Fig. 2. Endobronchial images of the EBUS-TBNA procedure. **a** The bronchoscope is passed through the vocal cords by visualizing the anterior angle of the glottis. **b** The balloon is inflated with normal saline for maximum contact. **c** The tip is gently pressed onto the airway. **d** The needle is passed through the intercartilage space.

Endobronchial Ultrasound-Guided Transbronchial Needle Aspiration

After identifying the lesion of interest with the CP-EBUS, the bronchoscopic image of the airway is simultaneously visualized to localize the insertion point of the needle. Once the point of entry is decided upon using small landmarks on the airway, the dedicated 22-gauge TBNA needle is fastened onto the working channel of the bronchoscope. The manipulation of the needle is a very important element of performing EBUS-TBNA and is shown in figure 1. The sheath adjuster knob is loosened and the length of the sheath is adjusted so that the sheath can be visualized on an endoscopic image (fig. 2d). The tip of the bronchoscope is flexed up for contact and the lymph node is visualized again on the ultrasound image. After the needle adjuster knob is loosened, real-time EBUS-TBNA can be performed. In case a cartilage ring is encountered during TBNA, the broncho-

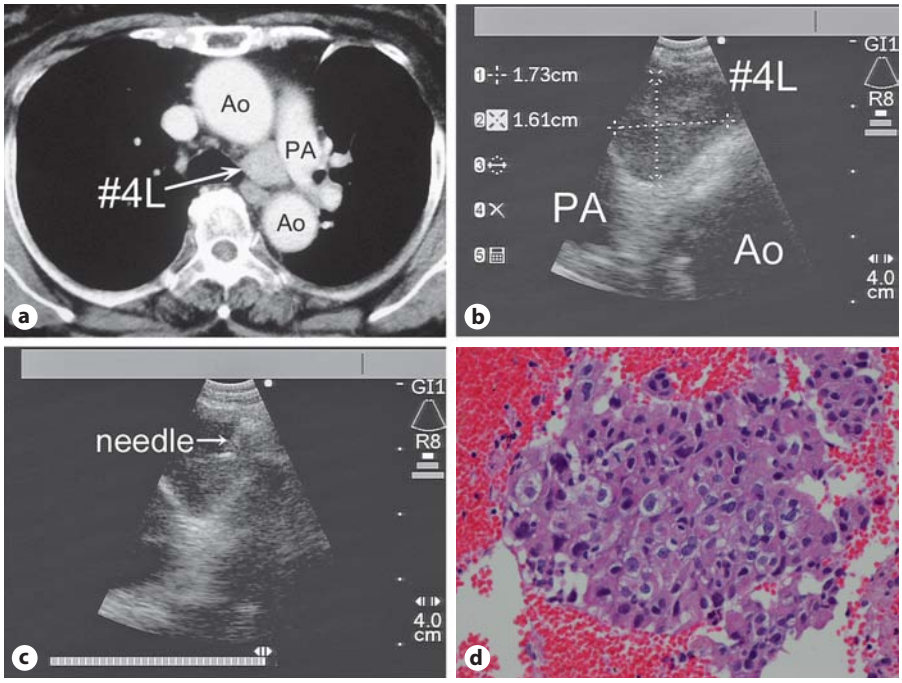

Fig. 3. A representative case of EBUS-TBNA. **a** Chest CT scan image of the enlarged left lower paratracheal lymph node (#4L) between the aorta (Ao) and pulmonary artery (PA). **b** EBUS scan demonstrates station #4L, aorta and the pulmonary artery. **c** EBUS-TBNA of lymph node station #4L with the needle inside the lymph node. **d** Histological examination demonstrated large cell carcinoma.

scope is moved a little bit up or down so that the needle will go through the intercartilage space. After the initial puncture, the internal stylet is used to clear out the internal lumen, which may become clogged with bronchial membrane. The internal sheath is then removed and negative pressure is applied with the Vaclok syringe. After the needle is moved back and forth inside the lymph node, the needle is retrieved and the internal sheath is used once again to push out the histological core. With this method, histological cores as well as cytological specimens can be obtained. The aspirated material is smeared onto glass slides, and the smears are air-dried and immediately stained using Diff-Quik for interpretation by an on-site cytopathologist to confirm adequate cell material. Furthermore, Papanicolaou staining and light microscopy are performed. Histological cores are fixed with formalin and stained with hematoxylin and eosin. Immunohistochemistry can also be performed if needed.

Indication

Indications for EBUS-TBNA are the assessment of mediastinal and hilar lymph nodes, diagnosis of lung tumors and diagnosis of mediastinal tumors. All of the mediastinal lymph nodes except for the subaortic and paraesophageal lymph nodes (stations 5, 6, 8 and 9) are assessable by EBUS-TBNA. Since the outer diameter of the tip of the CP-EBUS is 6.2 mm, stations 10 and 11 are approachable. However, part of station 12 is not accessible [14].

Lymph Node Staging by EBUS-TBNA

EBUS-TBNA is a minimally invasive lymph node staging modality in patients with lung cancer and has been introduced as one of the new technologies and as evidence-based practice for invasive staging [15]. Mediastinal and hilar lymph nodes should be assessed in a systematic way so that all lymph nodes are identified and characterized. The basic principle is to identify the specific lymph node stations according to the Mountain classification system [12]. To avoid contamination and upstaging, EBUS-TBNA should be performed from the N3 nodes, followed by N2 nodes and N1 nodes.

Case series looking at the use of EBUS-TBNA for lymph node staging in lung cancer have reported a high yield ranging from 89 to 98% [5–10]. It is clearly being used more by pulmonologists and thoracic surgeons in clinical practice. Although the reported yield of EBUS-TBNA is high and similar to the 'gold standard' mediastinoscopy, there have been no studies directly comparing the medi-

astinoscopy and EBUS-TBNA for lymph node staging. There is an ongoing prospective trial comparing the yield of mediastinoscopy and EBUS-TBNA for mediastinal lymph node staging in patients with confirmed or suspected lung cancer [16]. Patients with resectable lung cancer who require a mediastinoscopy for mediastinal staging underwent EBUS-TBNA followed by mediastinoscopy under general anesthesia in the same setting. The diagnostic yield was compared between the two procedures. Out of 45 patients enrolled in the study, the diagnostic accuracy of EBUS-TBNA and mediastinoscopy for analysis of each lymph node stations were 95.6 and 96.6%. The sensitivity, specificity, and diagnostic accuracy for the correct mediastinal lymph node staging for EBUS-TBNA and mediastinoscopy were 76.9, 100 and 90.9%, and 84.6, 100 and 93.9% respectively. These preliminary results show that EBUS-TBNA may reduce the number of mediastinoscopy needed for the staging of the mediastinum in NSCLC. However, due to the possibility of false-negative EBUS-TBNA results, it is not clear that EBUS-TBNA will completely replace mediastinoscopy for mediastinal staging.

Similar to mediastinoscopy, the subaortic (5, 6) and paraesophageal lymph nodes are not accessible by CP-EBUS. By combining EBUS-TBNA and EUS-FNA, most of the mediastinum can be evaluated [17]. EBUS-TBNA has better access to anterior and superior mediastinal lymph nodes, whereas EUS has better access to posterior and inferior mediastinal lymph nodes. However, lymph node stations 5 and 6 need to be evaluated by video-assisted thorascoscopy, anterior mediastinotomy, or extended mediastinoscopy [18].

EBUS-TBNA for Mediastinal Lymphadenopathy of Unknown Origin

Although introduced as an invasive staging tool for mediastinal and hilar lymph nodes in lung cancer, EBUS-TBNA can be used for the diagnosis of other mediastinal lymphadenopathies of unknown origin as well as other mediastinal processes [5, 19, 20]. Since EBUS-TBNA can directly sample lymph nodes in the mediastinum or the hilum, it has been shown to be useful in the diagnosis of sarcoidosis [21, 22]. There is also evidence for the utility of EBUS-TBNA for the diagnosis of lymphoma [23]. Other than lung cancer, EBUS-TBNA can be used for the detection of mediastinal lymph node involvement in metastatic lung tumors [24]. Immunohistochemistry is especially helpful to correlate the histology of the metastatic lymph nodes to the primary tumor.

The availability of multiple histological cores from the present 22-gauge needle has raised the possibility of molecular diagnosis from EBUS-TBNA-obtained specimens [25]. In lung cancer patients with N2 or N3 disease proven by EBUS-TBNA, DNA extracted from paraffin-embedded samples was used to detect EGFR mutations. The ability to perform biological analysis using nonsurgical biopsy samples obtained by EBUS-TBNA will become very important for the future of lung cancer treatment.

Complications

Complications related to the procedure are similar to those of conventional TBNA including bleeding from major vessels, pneumomediastinum, mediastinitis, pneumothorax, bronchospam and laryngospasm. The authors have not encountered complications related to EBUS-TBNA and to date no major complications have been reported in the literature. Although EBUS has enabled the bronchoscopist to see beyond the airway, one must be aware of the possible complications related to the procedure.

Conclusion

The CP-EBUS has made a safe and precise evaluation of the mediastinum as well as the hilum possible. It has an excellent potential in assisting safe and accurate diagnostic interventional bronchoscopy in respiratory diseases. From our current experience, EBUS-TBNA should be used as the first test for patients with undiagnosed mediastinal lymphadenopathy if available. It is an attractive procedure allowing simultaneous lymph node staging as well as diagnosis.

References

1 Hurter T, Hanrath P: Endobronchial sonography: feasibility and preliminary results. Thorax 1992;47:565–567.
2 Baba M, Sekine Y, Suzuki M, Yoshida S, Shibuya K, Iizasa T, Saitoh Y, Onuma EK, Ohwada H, Fujisawa T: Correlation between endobronchial ultrasonography (EBUS) images and histologic findings in normal and tumor-invaded bronchial wall. Lung Cancer 2002;35:65–71.
3 Herth F, Becker HD, Ernst A: Conventional vs endobronchial ultrasound-guided transbronchial needle aspiration: a randomized trial. Chest 2004;125:322–325.
4 Yasufuku K, Chhajed PN, Sekine Y, Nakajima T, Chiyo M, Iyoda A, Yoshida S, Otsuji M, Shibuya K, Iizasa T, Saitoh Y, Fujisawa T: Endobronchial ultrasound using a new convex probe: a preliminary study on surgically resected specimens. Oncol Rep 2004;11:293–296.
5 Yasufuku K, Chiyo M, Sekine Y, Chhajed PN, Shibuya K, Iizasa T, Fujisawa T: Real-time endobronchial ultrasound guided transbronchial needle aspiration of mediastinal and hilar lymph nodes. Chest 2004;126:122–128.
6 Krasnik M, Vilman P, Larsen SS, Jacobsen GK: Preliminary experience with a new method of endoscopic transbronchial real time ultrasound guided biopsy for diagnosis of mediastinal and hilar lesions. Thorax 2003;58:1083–1086.
7 Yasufuku K, Chiyo M, Koh E, Moriya Y, Iyoda A, Sekine Y, Shibuya K, Iizasa T, Fujisawa T: Endobronchial ultrasound guided transbronchial needle aspiration for staging of lung cancer. Lung Cancer 2005;50:347–354.
8 Yasufuku K, Nakajima T, Motoori K, Sekine Y, Shibuya K, Hiroshima K, Fujisawa T: Comparison of endobronchial ultrasound, positron emission tomography, and computed tomography for lymph node staging of lung cancer. Chest 2006;130:710–718.
9 Herth FJ, Eberhardt R, Vilmann P, Krasnik M, Ernst A: Real-time endobronchial ultrasound guided transbronchial needle aspiration for sampling mediastinal lymph nodes. Thorax 2006;61:795–798.
10 Vincent BD, El-Bayoumi E, Hoffman B, Doelken P, DeRosimo J, Reed C, Silvestri GA: Real-time endobronchial ultrasound-guided transbronchial lymph node aspiration. Ann Thorac Surg 2008;85:224–230.
11 Sarkiss M, Kennedy M, Riedel B, Norman P, Morice R, Jimenez C, Eapen G: Anesthesia technique for endobronchial ultrasound-guided fine needle aspiration of mediastinal lymph nodes. J Cardiothorac Vasc Anesth 2007;21:892–896.
12 Mountain CF, Dresler CM: Regional lymph node classification for lung cancer staging. Chest 1997;111:1718–1723.
13 Herth F, Krasnik M, Yasufuku K, Rintoul R, Ernst A: Endobronchial ultrasound-guided transbronchial needle aspiration – how I do it. J Bronchol 2006;13:84–91.
14 Yasufuku K, Nakajima T, Chiyo M, Sekine Y, Shibuya K, Fujisawa T: Endobronchial ultrasound: current status and future directions. J Thorac Oncol 2007;2:970–979.
15 Detterbeck FC, Jantz MA, Wallace M, Vansteenkiste J, Silvestri GA: Invasive mediastinal staging of lung cancer: ACCP evidence-based clinical practice guidelines, ed 2. Chest 2007;132:202S–220S.
16 Yasufuku K, Quadri M, dePerrot M, Pierre A, Waddell T, Darling G, Johnston M, Geddie W, Boerner S, Fujisawa T, Keshavjee S: A prospective controlled trial of endobronchial ultrasound guided transbronchial needle aspiration compared to mediastinoscopy for mediastinal lymph node staging of lung cancer (abstract). Western Thoracic Surgical Association 33rd Annual Meeting, Santa Ana Pueblo, 2007.
17 Wallace MB, Pascual JM, Raimondo M, Woodward TA, McComb BL, Crook JE, Johnson MM, Al-Haddad MA, Gross SA, Pungpapong S, Hardee JN, Odell JA: Minimally invasive endoscopic staging of suspected lung cancer. JAMA 2008;299:540–546.
18 Yasufuku K, Fujisawa T: Staging and diagnosis of non-small lung cancer: invasive modalities. Respirology 2007;12:173–183.
19 Nakajima T, Yasufuku K, Suzuki M, Sekine Y, Shibuya K, Hiroshima K, Fujisawa T: Histological diagnosis of spinal chondrosarcoma by endobronchial ultrasound-guided transbronchial needle aspiration. Respirology 2007;12:308–310.
20 Nakajima T, Yasufuku K, Shibuya K, Fujisawa T: Endobronchial ultrasound-guided transbronchial needle aspiration for the treatment of central airway stenosis caused by a mediastinal cyst. Eur J Cardiothorac Surg 2007;32:538–540.
21 Wong M, Yasufuku K, Nakajima T, Herth F, Sekine Y, Shibuya K, Iizasa T, Hiroshima K, Lam WK, Fujisawa T: Endobronchial ultrasound: new insight for the diagnosis of sarcoidosis. Eur Respir J 2007;29:1–6.
22 Garwood S, Judson MA, Silvestri G, Hoda R, Fraig M, Doelken P: Endobronchial ultrasound for the diagnosis of pulmonary sarcoidosis. Chest 2007;132:1298–1304.
23 Kennedy MP, Jimenez CA, Bruzzi JF, Mhatre AD, Lei X, Giles FJ, Flanning T, Morice RC, Eapen GA: Endobronchial ultrasound guided transbronchial needle aspiration in the diagnosis of lymphoma. Thorax 2008;63:360–365.
24 Nakajima T, Yasufuku K, Iyoda A, Yoshida S, Suzuki M, Sekine Y, Shibuya K, Hiroshima K, Nakatani Y, Fujisawa T: The evaluation of lymph node metastasis by endobronchial ultrasound-guided transbronchial needle aspiration: crucial for selection of surgical candidates with metastatic lung tumors. J Thorac Cardiovasc Surg 2007;134:1485–1490.
25 Nakajima T, Yasufuku K, Suzuki M, Hiroshima K, Kubo R, Mohamed S, Miyagi Y, Matsukuma S, Sekine Y, Fujisawa T: Assessment of epidural growth factor receptor mutation by endobronchial ultrasound-guided transbronchial needle aspiration. Chest 2007;132:597–602..

Kazuhiro Yasufuku, MD, PhD
Assistant Professor, University of Toronto
Division of Thoracic Surgery, Toronto General Hospital, University Health Network
200 Elizabeth St 9N–957, Toronto, ON M5G 2C4 (Canada)
Tel. +1 416 340 4290, Fax +1 416 340 3660, E-Mail kazuhiro.yasufuku@uhn.on.ca

Chapter 17

Bolliger CT, Herth FJF, Mayo PH, Miyazawa T, Beamis JF (eds): Clinical Chest Ultrasound: From the ICU to the Bronchoscopy Suite.
Prog Respir Res. Basel, Karger, 2009, vol 37, pp 153–159

Endobronchial Ultrasound for Staging of Lung Cancer

Felix J.F. Herth

Department of Pneumology and Critical Care Medicine, Thoraxklinik, University of Heidelberg, Germany

Abstract

Accurate preoperative staging in patients with non-small cell lung cancer is of paramount importance. It will guide choices of treatment and determine prognosis and outcome. Over the last years, different techniques have become available. For primary staging of the mediastinum and also in PET-positive mediastinal lesions, the findings should always be cyto- or histologically confirmed. Endobronchial ultrasound (EBUS) is a relatively new technique that provides a better view into the mediastinum. EBUS-guided transbronchial needle aspiration is an additional ultrasound technique, which allows a real-time ultrasound-controlled needle aspiration. Its specificity is high but the negative predictive value is limited. Because of this, if it yields negative results, an invasive surgical technique is indicated. However, if fine needle aspiration is positive, this may be valid as proof of N2 or N3 disease. For staging of early cancer lesions as carcinoma in situ and also for the differentiation of tumor ingrowths in central mediastinal structures, the radial EBUS system is an excellent technique to improve T staging.

The staging of lung cancer [1, 2] not only provides important prognostic information with regard to survival but also guides treatment. For patients whose disease has metastasized to mediastinal lymph nodes (stage III) or with tumors that have invaded mediastinal structures, the benefit of surgery as primary therapy is questionable. Combined chemoradiotherapy is most appropriate, although chemoradiotherapy followed by surgery may be considered [2]. Mediastinal lymph nodes are found in 26% of newly diagnosed lung cancer patients, and extrathoracic metastases are found in 49% [2]. Thus, reliable staging of mediastinal lymph nodes and the mediastinum is essential for choosing an appropriate therapy.

In most centers, computed tomography (CT) is the initial method for staging of mediastinal nodes. Nodes detectable by CT that are considered abnormal, generally have a short-axis diameter greater than 1 cm. Smaller lymph nodes can harbor metastatic foci and enlarged nodes may be benign, especially when central tumors are accompanied by inflammation. The accuracy of CT for diagnosing mediastinal disease is low. In a recent meta-analysis of 20 studies and 3,829 patients [3], the pooled sensitivity was 57%; the pooled specificity was 82%, and the pooled negative predictive value was 82% (range 63–85%). Therefore, surgical mediastinal staging is commonly performed in patients with a radiologically normal mediastinum before a planned cancer resection, to rule out unexpected N2 or N3 disease. However, approximately 18% (range 15–37%) of patients with a negative CT scan who undergo surgical mediastinal staging are found to have metastatic disease.

Mediastinoscopy remains the reference standard for evaluating nodal disease. It has a sensitivity of 90–95% [4]. However, only certain mediastinal lymph node stations are accessible (levels 2, 4 and anterior level 7). For sampling levels 5 and 6, thoracoscopy, anterior mediastinotomy (the Chamberlain procedure), or extended mediastinoscopy can be performed. The inferior mediastinum is evaluated by thoracoscopy. However, all these more aggressive staging procedures require general anesthesia, surgical incision, and therefore high costs [5, 6]. Positron emission tomography (PET) was expected to increase the accuracy of mediastinal staging in non-small cell lung cancer (NSCLC), and indeed, a meta-analysis confirmed its superiority [7]. However, more recent reports have tempered enthusiasm for using PET as the sole tool for evaluating the mediastinum [8].

Endobronchial ultrasound (EBUS) is especially useful in diagnosing mediastinal tumors involving the great vessels (e.g., aorta, vena cava, and main pulmonary arteries), the

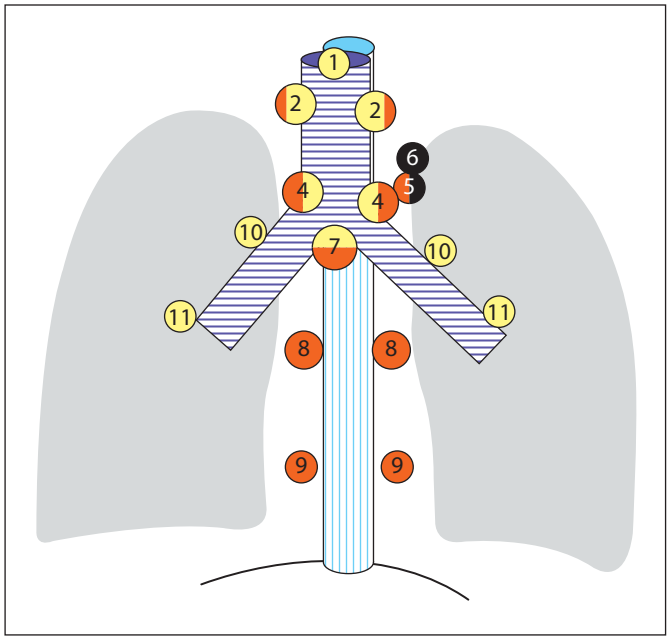

Fig. 1. Lymph node map of the mediastinum and their reachability with different techniques. Red = EUS; yellow = TBNA or EBUS-TBNA; half/half = mediastinoscopy; black = extended mediastinoscopy.

central airways and the esophageal wall, which is frequently impossible with conventional radiology. Also for the local staging of esophageal cancer radial EBUS provides important information.

A further area where EBUS is helpful is the evaluation of early cancer lesions without nodal involvement. In small, radiologically invisible tumors, the decision to use local endoscopic therapeutic intervention depends on the intraluminal and intramural extent of the tumor within the different layers of the bronchial wall. In contrast to radiological imaging, radial EBUS allows even very small tumors of a few millimeters to be analyzed. As Kurimoto et al. [9] demonstrated EBUS is a very reliable tool for analyzing the extent of these small lesions. During preoperative staging, radial EBUS allows detailed analysis of intraluminal, submucosal, and intramural tumor spread, which can be essential for decisions on resection margins.

In the following sections the results of radial and linear EBUS will be described and the value for staging will be discussed.

Mediastinal Lymph Node Staging

Although a complete workup for metastases is important for staging, the presence of lymph node metastases remains one of the most adverse factors for prognosis in NSCLC. The presence of mediastinal lymph node involvement indicates the presence of stage IIIA or IIIB, which suggests inoperability and/or the need for treatment with chemotherapy and/or radiotherapy [10].

Despite the advancement in the latest imaging techniques, while noninvasive tests can identify nodes suspicious for malignancy, they do not provide definitive tissue diagnosis. Cytological or histological confirmation of suspected metastases is required. Possible endoscopic techniques are needle biopsy techniques which include transbronchial needle aspiration (TBNA), endoesophageal ultrasound-guided fine needle aspiration (EUS-FNA) and, most recently, EBUS-guided TBNA (EBUS-TBNA) [11, 12] (fig. 1).

TBNA for mediastinal staging is performed through the bronchoscope under local anesthesia. It can be performed as an outpatient procedure with no significant morbidity [12–14]. TBNA can be readily performed on the hilar and mediastinal lymph nodes adjacent to the tracheobronchial wall. Rapid on-site cytological evaluation of the aspirates improves the yield, is cost-effective and eliminates unnecessary passes during the procedure [15, 16]. However, conventional TBNA is a blind procedure preventing target visualization and therefore the yield for TBNA varies widely (14–91%) [12]. A meta-analysis of 12 studies in 910 evaluable patients showed a sensitivity of 76% [17].

EBUS-TBNA has access to all the mediastinal lymph node stations accessible by mediastinoscopy as well as N1 nodes. Lymph node stations accessible are the highest mediastinal (station 1), the upper paratracheal (station 2R, 2L), the lower paratracheal (station 4R, 4L), the subcarinal (station 7), as well the hilar (station 10), the interlobar (station 11) and the lobar (station 12) lymph nodes (fig. 2, 3) [18]. The convex probe EBUS was first reported to be useful in the visualization and TBNA of hilar lymph nodes in surgically resected lung cancer specimens before its clinical use [19]. After 4 years of clinical use, a growing number of studies have shown its usefulness and accuracy for mediastinal lymph node sampling [20–22].

More recently, a multicenter study of a larger number of patients showed the effectiveness and accuracy of EBUS-TBNA for the evaluation of mediastinal lymph nodes [23]. In 502 patients, 572 lymph nodes were punctured using EBUS-TBNA, resulting in a successful diagnoses in 535 lymph nodes (94%). The sensitivity was 94% and the specificity was 100%.

Although recent advances in imaging, such as PET with ^{18}F-fluorodeoxyglucose, have been shown to be more accurate for the evaluation of the mediastinum compared with

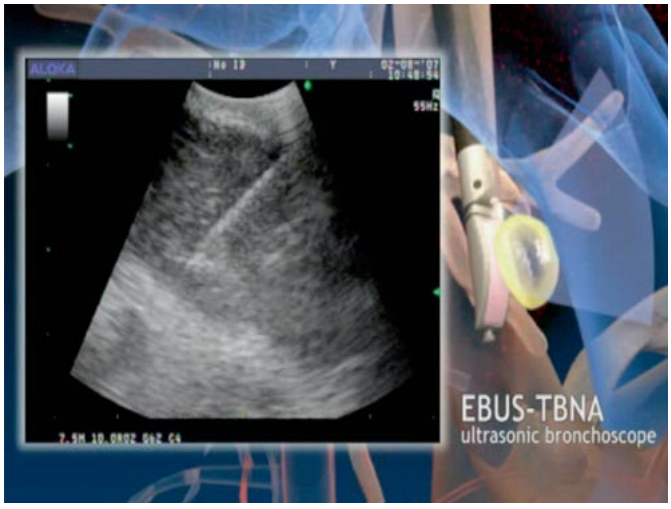

Fig. 2. EBUS-TBNA in position 4 left in the animation. In the ultrasound image the needle is visible in the lymph node.

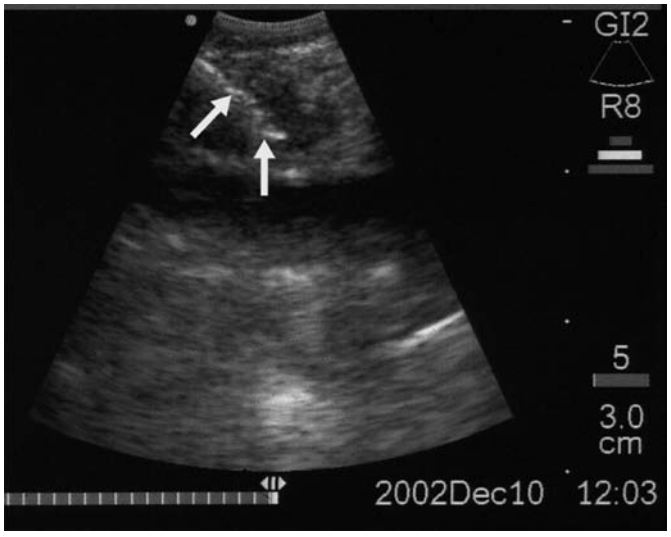

Fig. 3. EBUS-TBNA of an 8-mm lymph node in position 11l.

CT, tissue confirmation of PET-positive lesions is recommended to prove that the lesions are truly malignant [24]. A more recent study comparing EBUS-TBNA, CT and PET for lymph node staging of lung cancer showed a higher yield in favor of EBUS-TBNA [25]. A total of 102 potentially operable patients with lung cancer were included. The sensitivities of CT, PET and EBUS-TBNA for the correct diagnosis of mediastinal and hilar lymph node staging were 76.9, 80.0 and 92.3%, respectively. The specificities were 55.3, 70.1 and 100%. The diagnostic accuracies were 60.8, 72.5 and 98.0%. EBUS-TBNA was proven to have a higher sensitivity as well as specificity compared with CT or PET for mediastinal staging.

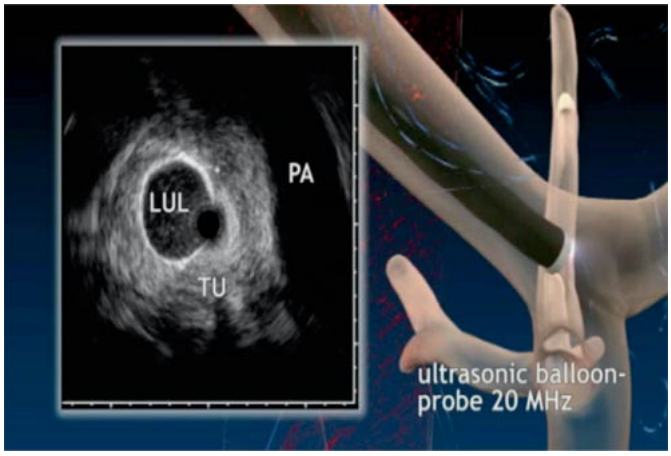

Fig. 4. Small early cancer lesion (TU), which destroys the bronchial wall. LUL = Left upper lobe; PA = pulmonary artery.

Linear EBUS also allows for guidance of biopsies of lymph nodes in regions inaccessible to mediastinoscopy, such as posterior subcarinal and hilar nodes [17] (fig. 4). Though prospective data examining the influence of EBUS on clinical outcomes such as the need for surgery are not available at this time, it is expected that the impact could be significant. Current data suggest that almost 30% of patients undergoing TBNA biopsy of mediastinal and hilar lymph nodes for the staging of bronchogenic carcinoma are found to have unresectable disease [10].

Another study examined the accuracy of EBUS-TBNA in sampling nodes <1 cm in diameter [26]. Of 100 patients, 119 lymph nodes between 4 and 10 mm were detected and sampled. Malignancy was detected in 19 patients but missed in 2 others; all diagnoses were confirmed by surgical biopsy or exploration. The mean (SD) diameter of the sampled lymph nodes was 8.1 mm. The sensitivity of EBUS-TBNA for detecting malignancy was 92.3%; the specificity was 100%, and the negative predictive value was 96.3%.

Even in a completely negative mediastinum assessed by imaging techniques EBUS-TBNA increases the quality of staging. Herth et al. [27] published their experience of EBUS-TBNA in sampling mediastinal lymph nodes in patients with lung cancer and a radiographically normal mediastinum and no PET activity. Patients in whom NSCLC was highly suspected on the basis of CT scans showing no enlarged lymph nodes (no node >1 cm) and a negative PET of the mediastinum underwent EBUS-TBNA.

Identifiable lymph nodes at locations 2r, 2l, 4r, 4l, 7, 10r, 10l, 11r and 11l were aspirated. All patients underwent subsequent surgical staging. In 97 patients 156 lymph nodes of ranging 5–10 mm in size were detected and sampled. Malignancy was detected in 9 patients but missed in 1. The mean diameter of the punctured lymph nodes was 7.9 mm. The sensitivity of EBUS-TBNA for detecting malignancy was 89%, specificity was 100%, and the negative predictive value was 98.9%. No complications occurred.

It seems, therefore, that EBUS-TBNA can be used to accurately sample and stage patients with clinical stage 1 lung cancer and no evidence of mediastinal involvement on CT and PET. Potentially operable patients with no signs of mediastinal involvement may benefit from presurgical staging with EBUS-TBNA.

At present, the optimal treatment for stage IIIA-N2 NSCLC is being evaluated. There may be a role for surgical resection in patients who have been successfully downstaged with induction chemotherapy or chemoradiotherapy [28–30]. However, this treatment option is still under debate, as current guidelines do not recommend surgery in this subgroup [31, 32]. Accurate restaging of the mediastinum in these patients will be of increasing importance in order to identify those patients who have been successfully downstaged and who may benefit from subsequent surgical resection. The most effective approach to restaging is controversial and currently the subject of much debate [33]. Up until now, surgical approaches such as cervical mediastinoscopy and anterior mediastinotomy have been used for restaging [34, 35]. However, it is recognized that remediastinoscopy is technically more difficult to perform on account of adhesions and fibrotic change induced by the initial procedure and the induction treatment [36]. As a result the reported sensitivity and accuracy of repeat procedures are lower than those of the initial procedure. Data from studies examining the role of CT and PET imaging techniques for restaging have produced conflicting results [37–39]. The low sensitivity and specificity of imaging techniques for mediastinal restaging makes tissue sampling necessary for accurate assessment.

In a recently published trial the accuracy of EBUS-TBNA for restaging the mediastinum following induction chemotherapy in patients with NSCLC was investigated [40]. One hundred and twenty-four patients with tissue-proven IIIA-N2 disease that were treated with induction chemotherapy underwent mediastinal restaging with EBUS-TBNA. Based on CT, 58 patients were classified as stable disease and 66 were judged to have had a partial response. All patients subsequently underwent thoracotomy with attempted curative resection and a lymph node dissection regardless of EBUS-TBNA findings. Persistent nodal metastases were detected using EBUS-TBNA in 89 patients (72%). Of the 35 patients, in whom no metastases were assessed with EBUS-TBNA, 28 were found to have residual IIIA-N2 disease at thoracotomy. Sensitivity, specificity, positive predictive value, negative predictive value and diagnostic accuracy of EBUS-TBNA for mediastinal restaging following induction chemotherapy were 76, 100, 100, 20 and 77%, respectively.

Therefore, it seems that EBUS–TBNA is also a highly specific, accurate and minimally invasive test for mediastinal restaging of patients with NSCLC. However, due to the low negative predictive value, tumor-negative findings should be confirmed by surgical restaging.

EBUS-TBNA in Combination with EUS-FNA for Lymph Node Staging

The paraesophageal nodes in particular are not all reachable with the EBUS-TBNA scope. So a possible solution could be a combined EUS-FNA and EBUS-TBNA procedure.

Two papers have been published about the combined approach. Herth et al. [41] showed that the sensitivity and the specificity of the two techniques are comparable to routine mediastinoscopy. A total of 160 patients with enlarged lymph nodes in one of eight mediastinal lymph node stations underwent transbronchial and transesophageal biopsies in a crossover design. Transbronchial aspiration was successful in 85%, and transesophageal aspiration was successful in 78%. Combining both approaches produced successful biopsies in 97% and diagnoses in 94% of patients.

A second study [42] also had promising results regarding the combination. A comparison of EUS-FNA and EBUS-TBNA was performed in 33 patients, i.e. lung cancer staging in patients with an established diagnosis of NSCLC (20 patients) or diagnosis of a lesion in the mediastinum suspected of malignancy in patients suspected of lung cancer (13 patients). The diagnoses could be verified in 28 of 31 patients either by thoracotomy (n = 9) or by clinical follow-up (n = 18). A total of 119 lesions were sampled by EUS-FNA (n = 59) and EBUS-TBNA (n = 60). EUS-FNA and EBUS-TBNA demonstrated cancer in 26 and 28 lesions, respectively, and benign cytology in 30 and 28 lesions, respectively. Suspicious cells were found in 3 and 4 lesions by EUS-FNA and EBUS-TBNA, respectively. When looking at the results of the combined approach (EUS-FNA + EBUS-TBNA) in 28 of 31 patients in whom a final diagnosis could be obtained, regarding evaluation of cancer

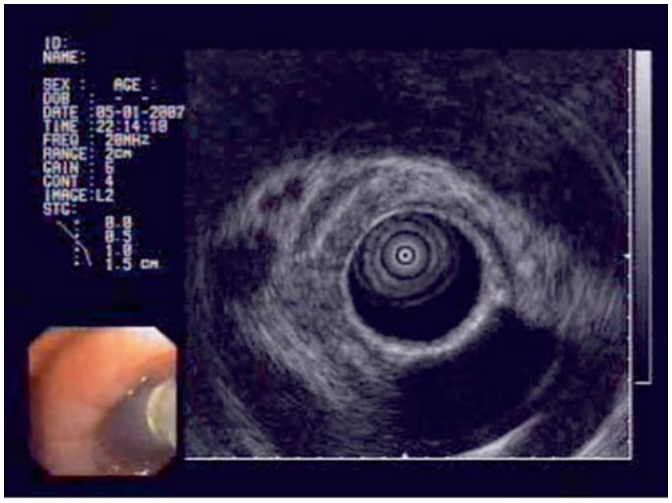

Fig. 5. Small early cancer lesion which destroys the bronchial wall.

involving the mediastinum, 20 patients were found to have mediastinal involvement whereas no mediastinal metastases were found in 8 patients. The accuracy of combined EUS-FNA and EBUS-TBNA for the diagnosis of mediastinal cancer was 95%. All authors concluded that EUS-FNA and EBUS-TBNA seem to be complementary methods.

Staging of Advanced Cancer

In preoperative staging EBUS allows detailed analysis of intraluminal, submucosal and intramural tumor spread which can be essential when deciding on resection margins. EBUS proved especially useful in the diagnosis of mediastinal tumor involvement of, for example, the great vessels such as aorta, vena cava, main pulmonary arteries and of the esophageal wall which by conventional radiology is frequently impossible [43]. In a trial [44] it was shown that differentiation of external tumor invasion from impression of the tracheobronchial wall by EBUS is highly reliable (94%) in contrast to CT imaging (51%) (fig. 5). One hundred and four patients with central tumor were examined with EBUS and CT and classified into invasion or impression. All patients underwent surgery, and the findings were compared to the initial classification. The sensitivity (89–25%) and also the specificity (100–89%) show the superiority of the ultrasound technique in the differentiation between airway infiltration and compression by tumor. Thus many patients considered to be nonresectable by the radiologist due to supposed T4 tumors could be operated on in a curative approach after EBUS.

Takemoto et al. [45] compared the sensitivity of EBUS and CT in detecting bronchial wall or great vessel invasion by tumor. The authors also concluded that EBUS was more sensitive than CT for assessing bronchial wall invasion.

Assessment of preoperative tracheobronchial invasion is also important for the selection of the best treatment, including surgery and radiochemotherapy, and for prediction of prognosis in patients with thyroid or esophageal cancer. For surgical planning, the choice of the procedure is dependent on several variables, including patient age, histological type, and depth and extent of invasion. It is important to establish the extent of tumor spread to determine whether thyroid or esophageal cancer has invaded beyond the tracheal adventitia [46].

Wakamatsu et al. [47] performed a trial to compare the usefulness of CT, MRI and EBUS for the assessment of invasion of thyroid or esophageal cancer in cases with suspected tracheobronchial invasion. In cases with suspected contact between the tumor and tracheobronchial wall, CT, MRI and EBUS indicated deformity of the tracheobronchial wall due to the adjacent mass. The final diagnosis was based on surgical and histological results and/or clinical follow-up. Fifty-four patients were included in this study.

The sensitivity and specificity of CT, MRI and EBUS for invasion were 59 and 56, 75 and 73, and 92 and 83%. The accuracy of EBUS was significantly greater than that of CT and MRI. Also it seems that EBUS is the most useful technique for determining the depth and extent of tumor invasion into the airway wall. CT and MRI are useful imaging techniques; a combination of these procedures will be beneficial for surgical planning for patients with lung cancer, but also for esophageal and thyroid cancer.

Early Cancer Staging

Centrally located, radiologically occult 'early-stage' NSCLC that has not invaded through the airway or carcinoma in situ can be treated with surgery or endobronchial therapy [48]. Kurimoto et al. [9] who used radial EBUS to examine resected airway specimens, 45 of which were normal and 24 involved lung cancers, described the membranous and cartilaginous airways as three-echo and five-echo layers, respectively. In addition, the degree of tumor involvement of the airway was correctly identified in 23 of the 24 lung cancer cases (96%). Tanaka et al. [49] correctly identified the degree of tumor invasion of the airway in 14 of 15 patients (93%). Herth et al. [50] demonstrated that with EBUS in small autofluorescence-positive lesions that were negative in white light bronchoscopy they could improve specificity (predicting malignancy) from 50 to 90%. The

combination of EBUS with autofluorescence has been proven to be efficient in prospective studies and today has become the basis for curative endobronchial treatment of malignancies in some institutions [51].

The most important paper on this was published by Miyazu et al. [52]. They used the findings of EBUS for the treatment decision in patients with early cancer lesions. Among 18 patients they found 9 with a tumor border to the bronchial wall. These patients were treated with photodynamic therapy. All other patients had extracartilaginous tumor growth and were treated nonendoscopically (surgery, radiation and chemotherapy). Using this finding as a decision maker they achieved a 100% complete remission rate in the endoluminally treated group. In a mean follow-up time of 32 months none of the patients developed a recurrence. Compared to trials published earlier using endoluminal techniques in early cancer lesions, they could show that with the help of EBUS endoluminally treatable patients could be identified.

Limitations

The linear EBUS has an outer diameter of almost 7 mm, a 30° view, and a suboptimal-quality white-light image that limits its use in general inspection of the airways; hence, frequently standard fiberoptic bronchoscopy is also used if the airway has not been previously inspected. This leads to additional time, labor, and thus cost.

The chest physician learning the technique of EBUS must be well versed with TBNA and trained in how to interpret ultrasound images. As is usually the case with new techniques, learning from an experienced mentor is ideal. Attending courses that utilize simulators, models, or live animals are additional learning methods. Subsequently spending time with an experienced mentor rounds off the training. Approximately from 20 up to 50 procedures are necessary for the bronchoscopist and his assistant to become comfortable with most aspects of the technique. Interpretation of the ultrasound image was the most difficult aspect to master.

Conclusion

EBUS provides an accurate and safe means of evaluating patients with a variety of lung lesions. It has been widely available for more than 5 years. A growing body of good-quality literature supports its significant role in airway assessment and procedure guidance. With the EBUS-TBNA scope the next step of development is available.

The results of the trials demonstrated a high diagnostic rate in the correct prediction of lymph node staging in lung cancer patients compared to other modalities.

Moreover, with EBUS-TBNA many invasive procedures could be avoided. There were also no complications during all the procedures. EBUS-TBNA is a minimally invasive procedure with a high diagnostic rate, from which many patients will benefit. It should be considered for staging of mediastinal lymph nodes as well as diagnosis of lung cancer.

The combined approach of EUS-FNA and EBUS-TBNA may replace more invasive methods in the evaluation of lung cancer patients suspected of hilar or mediastinal metastases as well as in the evaluation of unknown mediastinal or hilar lesions.

Radial EBUS can facilitate identification of peripheral or central lesions and assessment of depth-of-airway involvement with the tumor, but it does not offer real-time biopsy capability.

References

1 Sihoe AD, Yim AP: Lung cancer staging. J Surg Res 2004;117:92–106.
2 Spira A, Ettinger DS: Multidisciplinary management of lung cancer. N Engl J Med 2004;350:379–392.
3 Toloza EM, Harpole L, Detterbeck F, McCrory DC: Invasive staging of non-small cell lung cancer: a review of the current evidence. Chest 2003;123:157–166.
4 Hoffmann H: Invasive staging of lung cancer by mediastinoscopy and video-assisted thoracoscopy. Lung Cancer 2001;34:3–5.
5 Luke WP, Pearson FG, Todd TR, Patterson GA, Cooper JD: Prospective evaluation of mediastinoscopy for assessment of carcinoma of the lung. J Thorac Cardiovasc Surg 1986;91:53–56.
6 Coughlin M, Deslauriers J, Beaulieu M, Fournier B, Piraux M, Rouleau J, Tardif A: Role of mediastinoscopy in pretreatment staging of patients with primary lung cancer. Ann Thorac Surg 1985;40:556–560.
7 Toloza EM, Harpole L, McCrory DC: Noninvasive staging of non-small cell lung cancer. Chest 2003;123:137–146.
8 Birim O, Kappetein AP, Goorden T, van Klaveren RJ, Bogers AJ: Proper treatment selection may improve survival in patients with clinical early-stage nonsmall cell lung cancer. Ann Thorac Surg 2005;80:1021–1026.
9 Kurimoto N, Murayama M, Yoshioka S, et al: Assessment of usefulness of endobronchial ultrasonography in determination of depth of tracheobronchial tumor invasion. Chest 1999;115:1500–1506.
10 Yasufuku K, Fujisawa T: Staging and diagnosis of non-small cell lung cancer: invasive modalities. Respirology 2007;12:173–183.
11 Silvestri GA, Gould MK, Margolis ML, Tanoue LT, McCrory D, Toloza E, Detterbeck F: Noninvasive staging of non-small cell lung cancer: ACCP evidenced-based clinical practice guidelines, ed 2. Chest 2007;132:178S–201S.

12 Herth FJ, Rabe KF, Gasparini S, Annema JT: Transbronchial and transoesophageal (ultrasound-guided) needle aspirations for the analysis of mediastinal lesions. Eur Respir J 2006;28:1264–1275.
13 Wang KP, Brower R, Haponik EF, Siegelman S: Flexible transbronchial needle aspiration for staging of bronchogenic carcinoma. Chest 1983;84:571–576.
14 Mehta AC, Kavuru MS, Meeker DP, Gephardt GN, Nunez C: Transbronchial needle aspiration for histology specimens. Chest 1989;96:1228–1232.
15 Diacon AH, Schuurmans MM, Theron J, Louw M, Wright CA, Brundyn K, Bolliger CT: Utility of rapid on-site evaluation of transbronchial needle aspirates. Respiration 2005;72:182–188.
16 Baram D, Garcia RB, Richman PS: Impact of rapid onsite cytologic evaluation during transbronchial needle aspiration. Chest 2005;128:869–875.
17 Toloza EM, Harpole L, Detterbeck F, McCrory DC: Invasive staging of non-small cell lung cancer: a review of the current evidence. Chest 2003;123:157–166.
18 Herth FJF, Krasnik M, Yasufuku K, et al: Endobronchial ultrasound guided transbronchial needle biopsy. J Bronchol 2006;13:84–91.
19 Krasnik M, Vilman P, Larsen SS, Jacobsen GK: Preliminary experience with a new method of endoesophageal transbronchial real time ultrasound guided biopsy for diagnosis of mediastinal and hilar lesions. Thorax 2003;58:1083–1086.
20 Yasufuku K, Chhajed PN, Sekine Y, Nakajima T, Chiyo M, et al: Endobronchial ultrasound using a new convex probe – a preliminary study on surgically resected specimens. Oncol Rep 2004;11:293–296.
21 Yasufuku K, Chiyo M, Sekine Y, Chhajed PN, Shibuya K, et al: Real-time endobronchial ultrasound-guided transbronchial needle aspiration of mediastinal and hilar lymph nodes. Chest 2004;126:122–128.
22 Rintoul RC, Skwarski KM, Murchison JT, et al: Endobronchial and endoesophageal ultrasound-guided real-time fine-needle aspiration for mediastinal staging. Eur Respir J 2005;25:416–421.
23 Herth FJ, Eberhardt R, Vilmann P, Krasnik M, Ernst A: Real-time endobronchial ultrasound guided transbronchial needle aspiration for sampling mediastinal lymph nodes. Thorax 2006;61:795–798.
24 Kramer H, Groen HJM: Current concepts in the mediastinal lymph node staging of nonsmall cell lung cancer. Ann Surg 2003;238:180–188.
25 Yasufuku K, Nakajima T, Motoori K, Sekine Y, Shibuya K, et al: Comparison of endobronchial ultrasound, positron emission tomography, and CT for lymph node staging of lung cancer. Chest 2006;130:710–718.
26 Herth FJ, Ernst A, Eberhardt R, Vilmann P, Dienemann H, et al: Endobronchial ultrasound-guided transbronchial needle aspiration of lymph nodes in the radiologically normal mediastinum. Eur Respir J 2006;28:910–914.
27 Herth FJ, Eberhardt R, Krasnik M, Ernst A: Endobronchial ultrasound-guided transbronchial needle aspiration of lymph nodes in the radiologically and positron emission tomography-normal mediastinum in patients with lung cancer. Chest 2008;133:887–891.
28 Bueno R, Richards WG, Swanson SJ, et al: Nodal stage after induction therapy for stage IIIA lung cancer determines patient survival. Ann Thorac Surg 2000;70:1826–1831.
29 Betticher DC, Hsu Schmitz SF, Totsch M, et al: Mediastinal lymph node clearance after docetaxel-cisplatin neoadjuvant chemotherapy is prognostic of survival in patients with stage IIIA pN2 non-small-cell lung cancer: a multicenter phase II trial. J Clin Oncol 2003;21:1752–1759.
30 Lorent N, De Leyn P, Lievens Y, et al: Long-term survival of surgically staged IIIA-N2 non-small-cell lung cancer treated with surgical combined modality approach: analysis of a 7-year prospective experience. Ann Oncol 2004;15:1645–1653.
31 Robinson LA, Ruckdeschel JC, Wagner H Jr, Stevens CW, American College of Chest Physicians: Treatment of non-small cell lung cancer-stage IIIA: ACCP evidence-based clinical practice guidelines, ed 2. Chest 2007;132 (3 suppl):243S–265S.
32 NICE clinical guidelines. Lung cancer: diagnosis and treatment, 2006. http://www.nice.org.uk/guidance/index.jsp?action=download&o=29675.
33 Goldstraw P: Selection of patients for surgery after induction chemotherapy for N2 non-small cell lung cancer. J Clin Oncol 2006;24:3317–3318.
34 Mateu-Navarro M, Rami-Porta R, Bastus-Piulats R, et al: Remediastinoscopy after induction chemotherapy in non-small cell lung cancer. Ann Thorac Surg 2000;70:391–395.
35 Van Schil P, van der Schoot J, Poniewierski J, et al: Remediastinoscopy after neoadjuvant therapy for non-small cell lung cancer. Lung Cancer 2002;37:281–285.
36 De Waele M, Hendriks J, Lauwers P, et al: Nodal status at repeat mediastinoscopy determines survival in non-small cell lung cancer with mediastinal nodal involvement, treated by induction therapy. Eur J Cardiothorac Surg 2006;29:240–243.
37 De Leyn P, Stroobants S, De Wever W, et al: Prospective comparative study of integrated positron emission tomography-computed tomography scan compared with remediastinoscopy in the assessment of residual mediastinal lymph node disease after induction chemotherapy for mediastinoscopy-proven stage IIIA-N2 Non-small-cell lung cancer: a Leuven Lung Cancer Group Study. J Clin Oncol 2006;24:3333–3339.
38 Akhurst T, Downey RJ, Ginsberg MS, et al: An initial experience with FDG-PET in the imaging of residual disease after induction therapy for lung cancer. Ann Thorac Surg 2002;3:259–264.
39 Cerfolio RJ, Ojha B, Mukherjee S, et al: Positron emission tomography scanning with 2-fluoro-2-deoxy-d-glucose as a predictor of response of neoadjuvant treatment for non-small cell carcinoma. J Thorac Cardiovasc Surg 2003;25:938–944.
40 Herth FJF, Annema JT, Eberhardt R, Yasufuku K, Ernst A, Krasnik M, Rintoul RC: Endobronchial ultrasound with transbronchial needle aspiration for restaging the mediastinum in lung cancer. J Clin Oncol 2008;26:3346–3350.
41 Herth FJ, Lunn W, Eberhardt R, Becker HD, Ernst A: Transbronchial vs. transesophageal ultrasound-guided aspiration of enlarged mediastinal lymph nodes. Am J Respir Crit Care Med 2005;171:1164–1167.
42 Vilmann P, Krasnik M, Larsen SS, Jacobsen GK, Clementsen P: Endoesophageal trans-esophageal and endoesophageal-ultrasound guided biopsy: a combined approach in the evaluation of mediastinal lesions. Endoscopy 2005;37:833–839.
43 Herth FJ, Eberhardt R, Ernst A: The future of bronchoscopy in diagnosing, staging and treatment of lung cancer. Respiration 2006;73:399–409.
44 Herth FJ, Ernst A, Schulz M, Becker HD: Endobronchial ultrasound reliably differentiates between airway infiltration and compression by tumor. Chest 2003;123:458–462.
45 Takemoto Y, Kawahara M, Ogura Y, et al: Ultrasound guided flexible bronchoscopy for the diagnosis of tumor invasion to the bronchial wall and mediastinum. J Bronchol 2000;7:127–132.
46 Law S, Wong J: The current management of esophageal cancer. Adv Surg 2007;41:93–119.
47 Wakamatsu T, Tsushima K, Yasuo M, Yamazaki Y, Yoshikawa S, Koide N, Fujimori M, Koizumi T: Usefulness of preoperative endobronchial ultrasound for airway invasion around the trachea: esophageal cancer and thyroid cancer. Respiration 2006;73:651–657.
48 Sheski FD, Mathur PN: Endoesophageal treatment of early stage lung cancer. Cancer Control 2000;7:35–44.
49 Tanaka F, Muro K, Yamasaki S, et al: Evaluation of tracheobronchial wall invasion using transbronchial ultrasonography (TBUS). Eur J Cardiothorac Surg 2000;17:570–574.
50 Herth F, Becker HD: EBUS for early cancer detection. J Bronchol 2003;10:249–253.
51 Herth FJ, Eberhardt R: Actual role of endobronchial ultrasound (EBUS). Eur Radiol 2007;17:1806–1812.
52 Miyazu Y, Miyazawa T, Kurimoto N, et al: Endobronchial ultrasonography in the assessment of centrally located early stage lung cancer before photodynamic therapy. Am J Respir Crit Care Med 2002;165:832–837.

Prof. Felix J.F. Herth, MD, PhD, FCCP
Department of Pneumology and Critical Care Medicine
Thoraxklinik, University of Heidelberg
Amalienstrasse 5, DE–69126 Heidelberg (Germany)
Tel. +49 6221 396 1200, Fax +49 6221 396 1202, E-Mail Felix.Herth@thoraxklinik-heidelberg.de

Chapter 18

Bolliger CT, Herth FJF, Mayo PH, Miyazawa T, Beamis JF (eds): Clinical Chest Ultrasound: From the ICU to the Bronchoscopy Suite.
Prog Respir Res. Basel, Karger, 2009, vol 37, pp 160–165

Endobronchial Ultrasonography for Peripheral Pulmonary Lesions

Noriaki Kurimoto[a] · Hiroaki Osada[a] · Teruomi Miyazawa[b]

Department of [a]Chest Surgery and [b]Pulmonary and Infectious Disease, St. Marianna University, Kawasaki, Japan

Abstract

Since the 1990s, endobronchial ultrasonography (EBUS) has been employed for the diagnosis of peripheral pulmonary lesions. Pulmonary lesions have an echogenic texture and a sharply defined border due to a strong reflective interface between the aerated lung and the lesion. EBUS for peripheral pulmonary lesions has two main impacts in the bronchoscopic diagnosis. One is to analyze the internal structures of peripheral pulmonary lesions, and the other is to detect the location of peripheral pulmonary lesions during bronchoscopy. Internal structures of peripheral pulmonary lesions as visualized by EBUS correlated these findings with the histopathology. The lesions were typed based on the internal echoes (whether homogeneous or heterogeneous), vascular patency, and the morphology of the hyperechoic areas (reflecting the presence of air and the state of the bronchi). EBUS can be used to assist transbronchial biopsy (TBB) of peripheral pulmonary lesions. Because the air content of the lung parenchyma completely reflects the ultrasound signal, pulmonary masses can be precisely located by EBUS. More recently, studies have shown the efficacy of a new procedure, EBUS using a guide sheath (EBUS-GS), for sampling peripheral lesions to increase the diagnostic yield of TBB under EBUS guidance. EBUS-GS increases the reliability of specimen collection via bronchoscopy.

Transbronchial biopsy (TBB) is often performed for the diagnosis of peripheral pulmonary lesions (PPLs). Although the complication rate is generally low, there is radiation exposure and the diagnostic yield varies widely [1, 2]. Since the 1990s, endobronchial ultrasonography (EBUS) was employed for the diagnosis of PPLs. EBUS uses a miniature probe inserted through the working channel of a flexible bronchoscope to scan from the bronchial lumen. EBUS can be used to assist TBB of PPLs. Because the air content of the lung parenchyma completely reflects the ultrasound signal, pulmonary masses can be precisely located by EBUS. Pulmonary lesions have an echogenic texture and a sharply defined border due to a strong reflective interface between the aerated lung and the lesion. When you look at the EBUS image of a PPL, you will be fascinated by the excellent quality of EBUS images. EBUS for PPLs has two main impacts in bronchoscopic diagnosis. One is to analyze the internal structures of PPLs, and the other is to detect the location of PPLs during bronchoscopy.

Internal Structures of PPLs by EBUS

Endoscopic ultrasonography has been used to examine the internal structure of pancreatic, and the results have been correlated with histopathology in cases of cystic tumor, calcifications, and pancreatic stones [3, 4]. Internal structures of PPLs as visualized by EBUS correlated these findings with the histopathology [5]. The lesions in well-differentiated adenocarcinoma had homogeneous internal echoes overall, but some hyperechoic dots (<1 mm in size) were also observed reflecting residual air in invaded alveoli. The distribution of the hyperechoic dots was irregular, and the margins of the lesions were also irregular. Blood vessels could be seen coursing through the lesion (fig. 1). In most cases of moderately differentiated adenocarcinoma and squamous cell carcinoma, the EBUS images showed obstruction of blood vessels within the lesion, obstruction of bronchi, heterogeneous internal echoes, and irregular margins (fig. 2). In several cases of squamous cell carcinoma, numerous echo-free areas of various sizes were noted, and their distribution corresponded to areas of necrosis. In cases of poorly differentiated adenocarcinoma, EBUS revealed few patent blood vessels or bronchi, heterogeneous internal echoes, and irregular margins. In some cases of small cell carcinoma, the tumor had directly

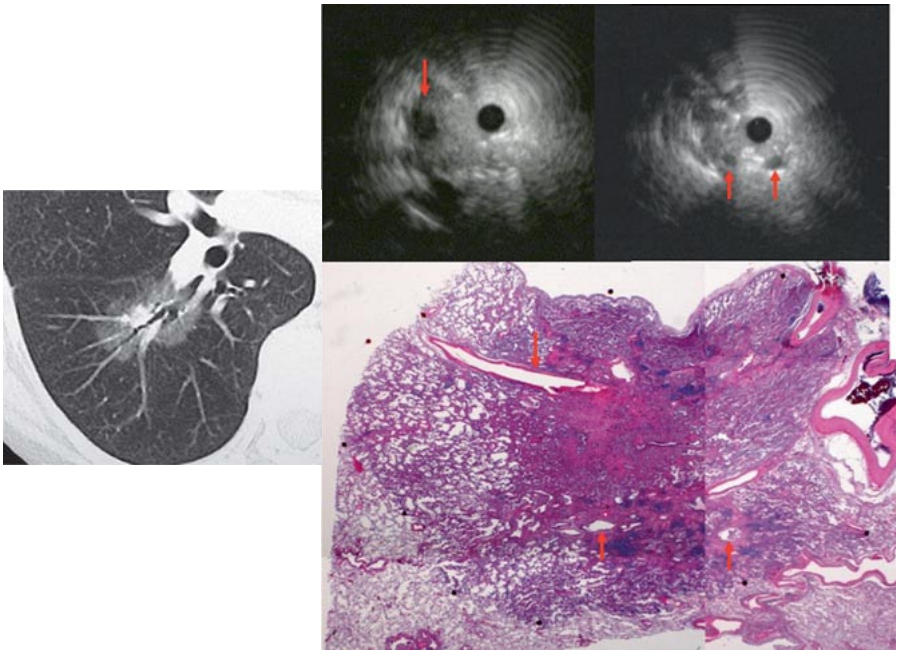

Fig. 1. A representative case of well-differentiated adenocarcinoma. The lesions in well-differentiated adenocarcinoma had homogeneous internal echoes overall, but some hyperechoic dots (<1 mm in size) were also observed reflecting residual air in invaded alveoli. The distribution of the hyperechoic dots was irregular, and the margins of the lesions also were irregular. Blood vessels could be seen coursing through the lesion (arrow).

invaded the pulmonary artery adjacent to the affected bronchus, resulting in stenosis of the pulmonary artery within the lesion. Comparing EBUS images and histopathological findings, EBUS shows bronchioles, vessels, calcifications, bleeding, mucus plug in the bronchus, necrosis, and air in well-differentiated adenocarcinoma (fig. 3). Hürter et al. [6] reported successful visualization of peripheral lung lesions in 19 of 26 cases, and Goldberg et al. [7] reported that EBUS provided unique information that exceeded other diagnostic modalities in 18 of 25 cases (including 6 peripheral lesions and 19 hilar tumors).

Hosokawa et al. [8] reported that a typical EBUS pattern of neoplastic disease was (1) a continuous marginal echo, (2) a rough internal echo, and (3) no hyperechoic spots standing for bronchi, or if there were any, there was no longitudinal continuity. Kuo et al. [9] assessed the feasibility of EBUS in differential diagnosis between malignant and benign lesions by the following three characteristic echoic features indicating malignancy: continuous margin, absence of a linear-discrete air bronchogram, and heterogeneous echogenicity. The negative predictive value for malignancy of a lesion with none of three echoic features is 93.7%. The positive predictive value for malignancy of a lesion with any two of three echoic features is 89.2%. Kurimoto et al. [5] reported a classification system with the aim of distinguishing between benign and malignant diseases, identifying the type of lung carcinoma and determining the degree of differentiation. The lesions were typed based on the internal echoes (whether homogeneous or heterogeneous), vascular patency, and the morphology of the hyperechoic areas (reflecting the presence of air and the state of the bronchi). Factors indicating malignancy were heterogeneous internal echo, obstructive vessels, and obstructive bronchi. A homogeneous pattern (type I) was overwhelmingly benign (92%), whereas hyperechoic dots or a heterogeneous pattern (types II and III, respectively) portended malignancy in 98 of 99 cases (99%) (fig. 4).

Detection of the Location of PPL

EBUS can be used to assist TBB of PPLs. Because the air content of the lung parenchyma completely reflects the ultrasound signal, pulmonary masses can be precisely located by EBUS. EBUS-guided TBB of PPLs has been shown to yield a success rate similar to fluoroscopy guidance [10]. A large-scale, prospective, randomized study to compare EBUS-guided TBB with TBB in patients with lesions <3 cm has been performed with good results [11]. In lesions >3 cm, there were no significant differences in the diagnostic ability between the two procedures. However, in lesions <3 and <2 cm, a considerable decrease in TBB sensitivity (31 and 23%) was seen, whereas EBUS-guided TBB provided its sensitivity (75 and 71%).

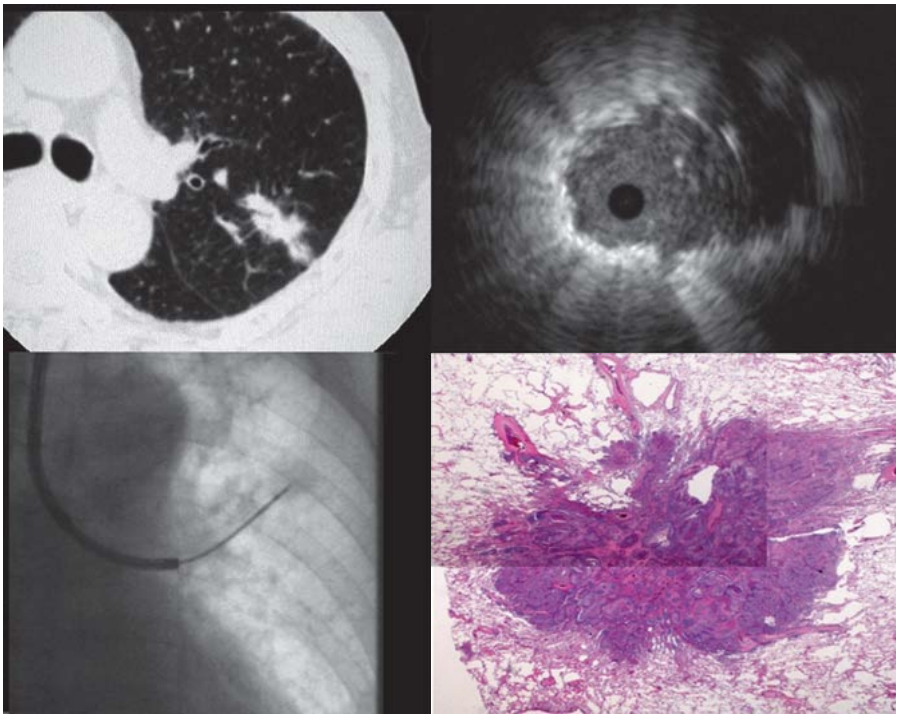

Fig. 2. A representative case of moderately differentiated adenocarcinoma. EBUS images showed obstruction of blood vessels within the lesion, obstruction of bronchi, heterogeneous internal echoes, and irregular margins.

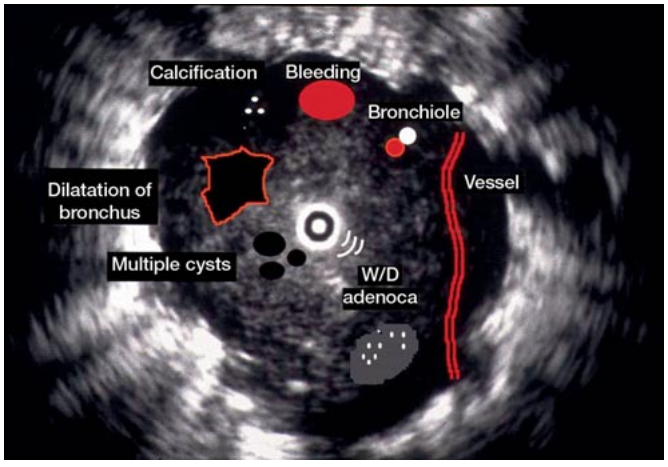

Fig. 3. Internal structures visualized by EBUS. Comparing EBUS images and histopathological findings, EBUS shows bronchioles, vessels, calcifications, bleeding, mucus in the bronchus, necrosis, and air in well-differentiated adenocarcinoma (W/D adenoca).

More recently, studies have shown the efficacy of a new procedure, EBUS using a guide sheath (EBUS-GS), for sampling of peripheral lesions to increase the diagnostic yield of TBB under EBUS guidance [12] (see fig. 5 in chapter 15). A guide sheath covering the miniature radial probe is advanced through the working channel of a therapeutic bronchoscope with the probe tip outside the sheath until the lesion is visualized. Under fluoroscopy, the sheath is held in place while the EBUS probe is withdrawn. An instrument such as a brush, needle, or biopsy forceps is then inserted through the sheath and the lesion is sampled. EBUS-GS increases the reliability of specimen collection via bronchoscopy. Diagnostic yields of bronchoscopy for PPLs of <2 cm in published reports have varied from 5 to 28% [13–21]. When an undetectable lesion under fluoroscopy is in contact with the probe inserted inside the bronchus, the lesion is visualized by EBUS, and EBUS-GS is particularly useful for lesions ≤ 20 mm that are undetectable by fluoroscopy. EBUS-GS was most successful when the probe could be placed within the lesion (fig. 5; online suppl. video 1). The yield of TBB when the probe was adjacent to the lesion was very low. This suggests that the lesions visualized as adjacent to the probe may only be in contact with the outer surface of the bronchus, and therefore sampling is unlikely to be diagnostic.

Video

At the first approach to the target lesion, the probe did not reach the target lesion in about 10% of all cases of EBUS-GS. To resolve this problem, the bronchoscopist withdrew the probe and inserted the curette into the guide sheath. The tip of the curette is able to be angulated and search the correct bronchus (online suppl. video 2).

Video

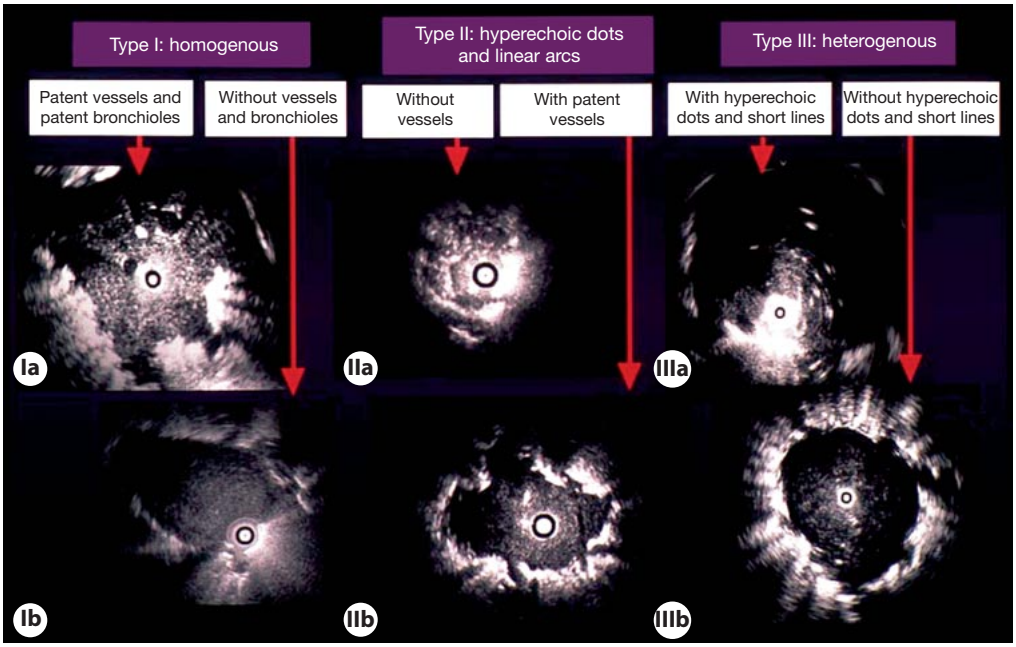

Fig. 4. Classification of PPLs by EBUS. Type I: Homogeneous pattern; type Ia: homogeneous pattern with patent vessels and patent bronchioles; type Ib: homogeneous pattern without vessels and bronchioles. Type II: Hyperechoic dots and linear arc pattern; type IIa: hyperechoic dots and linear arcs without vessels; type IIb: hyperechoic dots and linear arcs with patent vessels. Type III: Heterogeneous pattern; type IIIa: heterogeneous pattern with hyperechoic dots and short lines; type IIIb: heterogeneous pattern without hyperechoic dots and short lines.

One advantage of EBUS-GS lies in the repeatability of access to the bronchial lesion for sampling. Without a guide sheath, it can at times be difficult to be certain that the forceps are being inserted into the same bronchial branch for the second biopsy. Further, the bronchial mucosa becomes edematous after several attempts at manipulation, and it can be difficult to insert the forceps into the bronchus. Another advantage of EBUS-GS lies in its ability to protect against bleeding into the proximal bronchus from the biopsy site. Although massive hemorrhage into the bronchus following TBB is not frequent (<2%) [20–23], excessive bleeding may require hemostasis by wedging the tip of the bronchoscope. If bleeding occurs during EBUS-GS, blood drains through the sheath, because the outer surface of the sheath is snug against the internal surface of the bronchus. Our method of EBUS using a 20-MHz probe allowed visualization of the inner structures of peripheral lesions, including vessels, bronchi, calcifications, necrosis, hemorrhage, and bronchial dilatation [22].

Many reports have been published recently. Yang et al. [24] evaluated whether EBUS may improve the diagnostic yield of TBB in peripheral lung cancer. The diagnostic accuracy of transbronchial lung biopsy was significantly increased under EBUS guidance for small cell carcinoma (88.9%) and for non-small cell carcinoma (67.7%) compared to without EBUS for small cell carcinoma (22.2%) and for non-small cell carcinoma (50.0%). Under EBUS guidance, the diagnostic yield of transbronchial lung biopsy in peripheral lung cancer was significantly improved without EBUS.

Yoshikawa et al. [25] evaluated the feasibility and efficacy of TBB and bronchial brushing by EBUS-GS as a guide for diagnosing PPLs without radiographic fluoroscopy. Seventy-six of 123 PPLs (61.8%) were diagnosed by EBUS-GS guidance without fluoroscopy. The diagnostic yield for PPLs >20 mm in diameter (75.6%) was significantly higher than that for those ≤20 mm in diameter. The PPLs located in the middle lobe and the lingular segment had significantly higher diagnostic yields ($p < 0.05$). Multivariate analysis revealed that the diameter and location of the PPL were independent predictors of diagnostic sensitivity by EBUS-GS-guided bronchoscopy.

Fielding et al. [26] compared the diagnostic yields and pneumothorax rate of EBUS-GS and CT-guided fine-needle aspiration (CT-FNA) in terms of the location of the lesion to be biopsied, in particular whether the lesion is

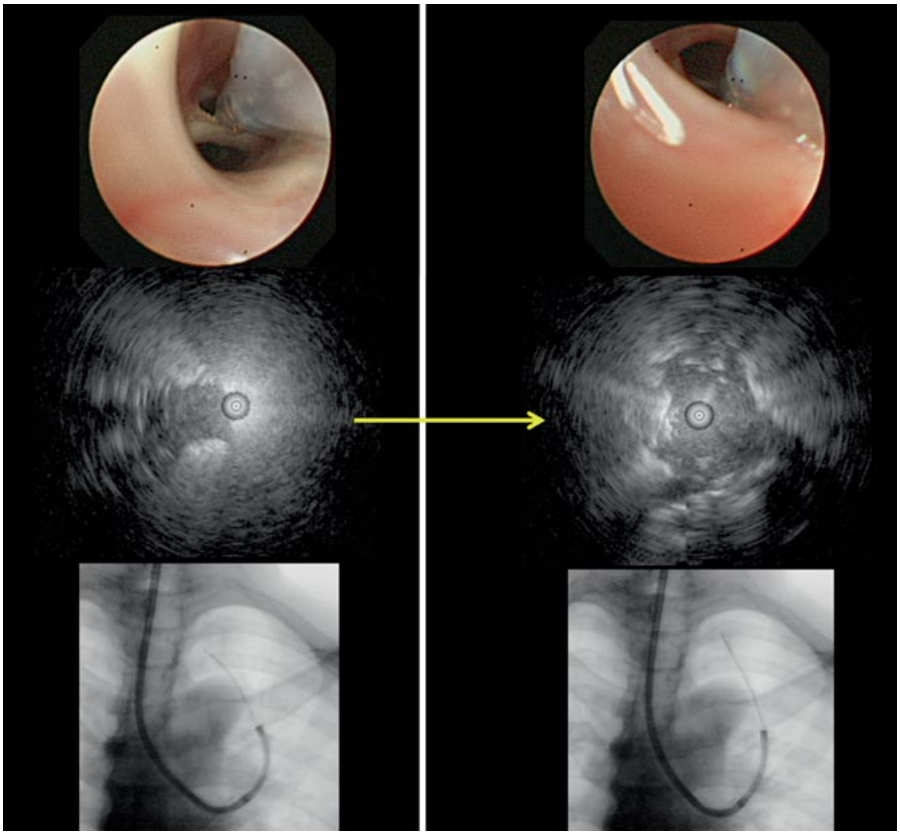

Fig. 5. Technique using EBUS-GS. Once the location of the lesion had been identified precisely by EBUS (middle row, left: adjacent to; right: within), the probe was withdrawn, leaving the guide sheath in place (bottom row). A biopsy forceps or bronchial brush was introduced into the sheath.

touching the pleura. For EBUS-GS 140 cases were performed with a mean lesion size of 29 mm. Overall diagnostic sensitivity was 66%. For lesions not touching the visceral pleura it was 74 compared with 35% where it was on the pleura. For CT-FNA 121 cases were performed with a mean size of 37 mm. Overall diagnostic sensitivity was 64%. The rate of pneumothorax and intercostal catheter (ICC) placement in EBUS-GS was 1 and 0% and in CT-FNA it was 28 and 6%, with $p < 0.001$ for both. Lesion location, in particular, connection to the visceral pleura, can improve decision-making with regard to referral for either CT-FNA or EBUS-GS to maximize diagnostic yield and minimize pneumothorax rate.

In recent years, two methods of navigation for PPLs have been developed. The electromagnetic navigation system is a localization device that assists in placing endobronchial accessories in the desired areas of the lung. This system uses low-frequency electromagnetic waves, which are emitted from an electromagnetic board placed under the bronchoscopy table mattress [27]. Harms et al. [28] in a technical note introduced a new approach for the treatment of inoperable peripheral lung tumors by combining the electromagnetic navigation system and EBUS with 3-D-planned endobronchial brachytherapy. Asano et al. [29–32] developed a bronchoscope insertion guidance system that produces virtual images by extracting the bronchi by automatic threshold adjustment, and searching for the bronchial route to the determined target. They used this system in combination with a thin bronchoscope and EBUS-GS. The system automatically produced virtual images to median of fifth-order bronchi. EBUS visualized 93.8% of cases successfully, and 84.4% could be pathologically diagnosed. Using the bronchoscope insertion guidance system, virtual images can be readily produced, and the bronchoscope can be successfully guided to the target. This method is promising as a routine examination method in the biopsy of PPLs.

Conclusions

EBUS assesses internal structures of PPLs. EBUS-GS provides high diagnostic yields of PPLs.

References

1 Torrington KC, Kern JD: The utility of fiberoptic bronchoscopy in the evaluation of the solitary pulmonary nodule. Chest 1993;104:1021–1024.
2 Baaklini WA, Reinoso MA, Gorin AB, et al. Diagnostic yield of fiberoptic bronchoscopy in evaluating solitary pulmonary nodules. Chest 2000;117:1049–1054.
3 Yasuda K, Mukai H, Nakajima M, et al: Staging of pancreatic carcinoma by endoscopic ultrasonography. Endoscopy 1993;25:151–155.
4 Rosch T, Braig C, Gain T, et al: Staging of pancreatic and ampullary carcinoma by endoscopic ultrasonography. Gastroenterology 1992;102:188–199.
5 Kurimoto N, Murayama M, Yoshioka S, et al: Analysis of the internal structure of peripheral pulmonary lesions using endobronchial ultrasonography. Chest 2002;122:1877–1894.
6 Hürter T, Hanrath P: Endobronchial sonography: feasibility and preliminary results. Thorax 1992;47:565–567.
7 Goldberg B, Steiner R, Liu J, et al: US-assisted bronchoscopy with use of miniature transducer-containing catheters. Radiology 1994;190:233–237.
8 Hosokawa S, Matsuo K, Watanabe Y, et al: Two cases of nodular lesions in the peripheral lung field, successfully diagnosed by endobronchial ultrasonography (EBUS). Kokyuu 2004;23:57–60.
9 Kuo C, Lin S, Chen H, et al: Diagnosis of peripheral lung cancer with three echoic features via endobronchial ultrasound. Chest 2007;132:922–929.
10 Herth FJ, Ernst A, Becker HD: Endobronchial ultrasound-guided transbronchial lung biopsy in solitary pulmonary nodules and peripheral lesions. Eur Respir J 2002;20:972–974.
11 Paone G, Nicastri E, Lucantoni G, et al: Endobronchial ultrasound-driven biopsy in the diagnosis of peripheral lung lesions. Chest 2005;128:3551–3557.
12 Kurimoto N, Miyazawa T, Okimasa S, Maeda A, Oiwa H, Miyazu Y, Murayama M: Endobronchial ultrasonography using a guide sheath increases the ability to diagnose peripheral pulmonary lesions endoscopically. Chest 2004;126:959–965.
13 Mori K, Yanase N, Kaneko M, et al: Diagnosis of peripheral lung cancer in cases of tumors 2 cm or less in size. Chest 1989;95:304–308.
14 Popvich J Jr, Kvale PA, Eichenhorn MS, et al: Diagnostic accuracy of multiple biopsies from flexible fiberoptic bronchoscopy – a comparison of central versus peripheral carcinoma. Am Rev Respir Dis 1982;125:521–523.
15 Fletcher EC, Levin DC: Flexible fiberoptic bronchoscopy and fluoroscopically guided transbronchial biopsy in management of solitary pulmonary nodules. West J Med 1982;135:477–483.
16 Stringfield JT, Mrkowitz DJ, Bentz RR, et al: The effect of tumor size and location on diagnosis by fiberoptic bronchoscopy. Chest 1977;72:474–476.
17 Radke JR, Conway WA, Eyler WR, et al: Diagnostic accuracy in peripheral lung lesions: factors predicting success with flexible fiberoptic bronchoscopy. Chest 1976;76:176–179.
18 Wallace JM, Deutch AL: Flexible fiberoptic bronchoscopy and percutaneous lung aspiration for evaluating the solitary pulmonary nodule. Chest 1982;81:665–671.
19 Hadson RR, Zavala DC, Rhodes ML, et al: Transbronchial biopsy via flexible fiberoptic bronchoscope; results in 164 patients. Am Rev Respir Dis 1976;114:67–72.
20 Kvale PA, Bode FR, Kini S: Diagnostic accuracy in lung cancer; comparison of techniques used in association with flexible fiberoptic bronchoscopy. Chest 1976;69:752–757.
21 Shiner RJ, Rosenman J, Katz I, et al: Bronchoscopic evaluation of peripheral lung tumors. Thorax 1988;43:887–889.
22 Chechani V: Bronchoscopic diagnosis of solitary pulmonary nodules and lung masses in the absence of endobronchial abnormality. Chest 1996;109:620–625.
23 Blasco LH, Hernandez IMS, Garrido VV, et al: Safety of transbronchial biopsy in outpatients. Chest 1991;99:562.
24 Ahmad M, Livingston DR, Golish JA, et al: The safety of outpatient transbronchial biopsy. Chest 1986;90:403.
25 Yang M, Liu W, Wang C, et al: Diagnostic value of endobronchial ultrasound-guided transbronchial lung biopsy in peripheral lung cancers. J Formos Med Assoc 2004;103:124–129.
26 Yoshikawa M, Sukoh N, Yamazaki K, et al: Diagnostic value of endobronchial ultrasonography with a guide sheath for peripheral pulmonary lesions without X-ray fluoroscopy. Chest 2007;131:1788–1793.
27 Fielding DI, Robinson PJ, Kurimoto N: Biopsy site selection for endobronchial ultrasound guide-sheath transbronchial biopsy of peripheral lung lesions. Intern Med J 2008;38:75–76.
28 Schwarz Y, Mehta AC, Ernst A, et al: Electromagnetic navigation during flexible bronchoscopy. Respiration 2003;70:516–522.
29 Harms W, Krempien R, Grehn C, et al: Electromagetically navigated brachytherapy as a new treatment option for peripheral pulmonary tumors. Strahlenther Onkol 2006;182:108–111.
30 Asano F, Matsuno Y, Matsushita T, et al: Transbronchial diagnosis of a pulmonary peripheral small lesion using an ultrathin bronchoscope with virtual bronchoscopic navigation. J Bronchol 2002;9:108–111.
31 Asano F, Matsuno Y, Shinagawa N, et al: A virtual bronchoscopic navigation system for pulmonary peripheral lesions. Chest 2006;130:559–566.
32 Asano F, Matsuno Y, Tsuzuku A, et al: Diagnosis of peripheral pulmonary lesions using a bronchoscope insertion guidance system combined with endobronchial ultrasonography with a guide sheath. Lung Cancer 2008;60:366–373.

Noriaki Kurimoto, MD
Department of Chest Surgery, Department of Pulmonary, St. Marianna University
2-16-1, Sugao, Miyamae-ku
Kawasaki, Kanagawa 216-8511 (Japan)
Tel. +81 44 977 8111, Fax +81 44 976 5792, E-Mail n.kurimoto@do7.enjoy.ne.jp

Chapter 19

Bolliger CT, Herth FJF, Mayo PH, Miyazawa T, Beamis JF (eds): Clinical Chest Ultrasound: From the ICU to the Bronchoscopy Suite.
Prog Respir Res. Basel, Karger, 2009, vol 37, pp 166–170

Esophageal Ultrasound

J.T. Annema · K.F. Rabe

Division of Pulmonary Medicine, Leiden University Medical Center, Leiden, The Netherlands

Abstract

Transesophageal ultrasound-guided fine needle aspiration (EUS-FNA) is a minimally invasive method by which mediastinal nodes and centrally located lung tumors located adjacent to the esophagus can be biopsied. In patients with (suspected) lung cancer and enlarged or PET-positive mediastinal lymph nodes, EUS prevents surgical staging procedures in the majority of cases due to the assessment of lymph node metastases. In numerous studies, EUS-FNA has proven to be a valuable method for the diagnosis and staging of lung cancer and is therefore suggested in recent guidelines as an alternative for surgical staging. However, in case no metastases are found by EUS-FNA, surgical staging still has to be performed due to limitations in the negative predictive value of endoscopic staging. EUS can also be used for the diagnosis of sarcoidosis. EUS has a higher yield in assessing noncaseating granulomas compared to fiberbronchoscopy with transbronchial lung biopsies. In addition, EUS is very safe and complications such as hemoptysis and pneumothorax that can occur after transbronchial biopsies have not been reported. The EUS method needs to be implemented so that it can be made more widely available. With a rather concise but dedicated implementation strategy including on-site training, (chest) physicians without prior (endo)sonography experience can learn mediastinal EUS and achieve results similar to experts.

Transesophageal Ultrasound Procedure and Diagnostic Reach

Endosonography in pulmonary medicine is performed with linear probes that allow real-time ultrasound-guided aspiration. Evaluation of the mediastinum is relatively straightforward but requires a structured systematic approach. Due to its central position in the chest, a considerable part of the middle and posterior mediastinum can be visualized by transesophageal ultrasound (EUS). The various mediastinal lymph nodes that can be visualized from the esophagus are described in relation to vascular structures such as right and left atrium, aorta and pulmonary artery and then given a number according to the Mountain/Dressler classification [1]. EUS can particularly detect mediastinal lymph nodes located in the lower mediastinum, station 9 (pulmonary ligament), station 8 (lower paraesophageal) and station 7 (subcarinal region). Nodes in the aortopulmonary window (station 5) can be seen but not always biopsied due to interposition of vascular structures. The para-aortal nodes (station 6) can be visualized well by EUS but obtaining tissue from such lesions may require a transaortal approach. The paratracheal nodes on the left (station 4L) are also accessible by EUS. Several mediastinal nodal stations cannot regularly be detected by EUS due to the intervening air in the trachea and main bronchi, such as the upper paratracheal nodes on the left (station 2L) and those located paratracheally on the right (station 2R and 4R).

EUS-fine needle aspiration (FNA) in pulmonary medicine is performed in an outpatient setting using a low dose of midazolam. At an EUS examination, all mediastinal nodal regions that can be detected from the esophagus will be checked routinely. Mediastinal nodes with a short axis lager than 1 cm, with sharp borders and a hypoechoic ultrasound pattern are more likely to contain metastases. For accurate assessment of nodal status, tissue verification is needed. Aspirates are first performed in those stations located in a contralateral (N3) position before analyzing nodes in N2 locations. They are usually performed with 22-gauge needles (19- and 25-gauge needles are also available). EUS aspirates can, in addition to evaluation by conventional light microscopy, be processed in paraformaldehyde-fixed cell blocks enabling immunohistochemistry.

EUS and Lung Cancer

In pulmonary medicine, EUS is most often indicated for the diagnosis and staging of lung cancer. In patients suspected of lung cancer, establishing a tissue diagnosis is mandatory to confirm the disease. At bronchoscopy, in only around two thirds of patients is the diagnosis established. Under several clinical conditions EUS can be used as the next diagnostic procedure in the diagnosis and staging of lung cancer (table 1).

Diagnosing and (Re)Staging of Lung Cancer

In those patients in whom the lung mass is located immediately adjacent to the esophagus, the lesion can be visualized by EUS and biopsied in order to secure a diagnosis [2, 3]. Additionally, endosonography can be used to assess the presence or absence of tumor invasion in the mediastinum (T4, stage IIIB). For assessing aortic invasion of the lung tumors (fig. 1), EUS has an accuracy of 92% and is far superior to CT [4].

Those patients with suspected lung cancer after a non-diagnostic bronchoscopy that present with enlarged (short axis >10 mm) mediastinal nodes on computed tomography scan of the chest are good candidates for evaluation by EUS. By demonstration of mediastinal nodal metastases, both a definitive diagnosis and locoregional staging can be achieved in a single test [5]. For this reason, it has even been hypothesized to consider EUS as the first test – before bronchoscopy – in patients with suspected lung cancer. In a study on diagnosing lung cancer where EUS was performed as the first test after CT, EUS not only established a diagnosis in 70% of patients but also provided tissue proof of locally or advanced disease by assessing mediastinal, left adrenal or celiac metastases [6].

The accuracy of EUS in mediastinal staging is dependent on nodal size and has a sensitivity of 90% and a specificity of 97% in patients with mediastinal nodes with a short axis >10 mm. In smaller nodes (fig. 2), however, sensitivity drops to 58% [7–11]. Despite the lower sensitivity, EUS findings can result in a change of patient management in 25–52% of patients without mediastinal nodal enlargement on CT [9–12].

Regarding mediastinal restaging after neoadjuvant chemo(radiation) therapy, a sensitivity of 75% [13] and an accuracy of 86% [14] have been reported. For this indication EUS-FNA is useful to demonstrate persistent mediastinal nodal metastatic involvement. It should be realized, however, that EUS has limitations in excluding persistent malignant nodal involvement.

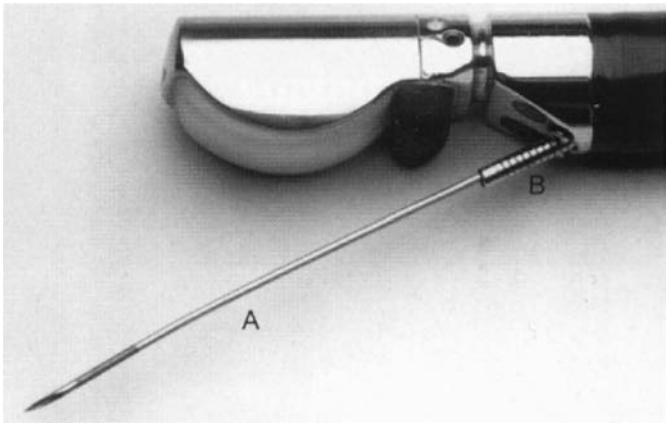

Fig. 1. Linear EUS-FNA scoop (Pentax). A = 22-gauge needle; B = shaft.

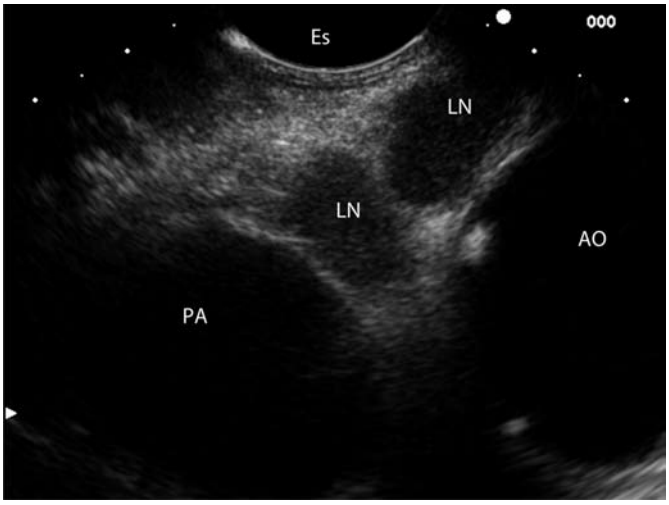

Fig. 2. Lower paratracheal lymph nodes (LN) on the left (station 4L) located between the esophagus (Es), aorta (AO) and pulmonary artery (PA).

Table 1. Indications for EUS-FNA in pulmonary medicine

Suspected lung cancer
Enlarged or PET-positive mediastinal lymph nodes
Primary tumor located adjacent to the esophagus
Staging of non-small cell lung cancer
Mediastinal staging (regardless of nodal size on CT)
Mediastinal involvement on FDG-PET
Mediastinal restaging after induction chemotherapy
Suspected mediastinal tumor invasion (T4)
Suspected left adrenal metastasis
Suspected sarcoidosis

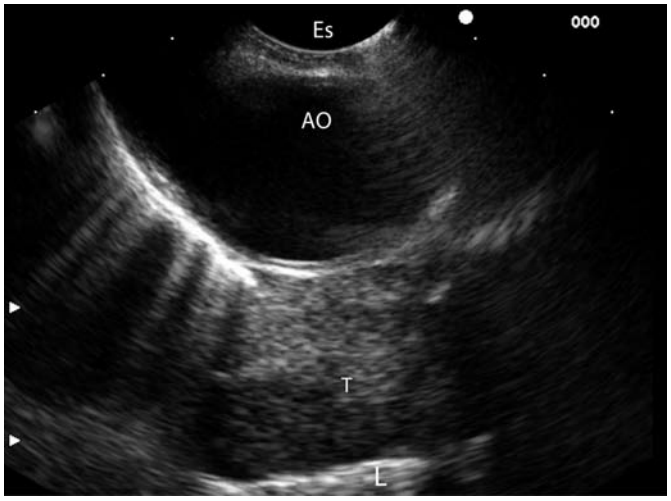

Fig. 3. Centrally located left upper lobe tumor (T) located directly adjacent to the aortic arch (AO). Sonograpically, there are no signs of invasion of the tumor into the aorta. L = Compromised lung tissue; Es = esophagus.

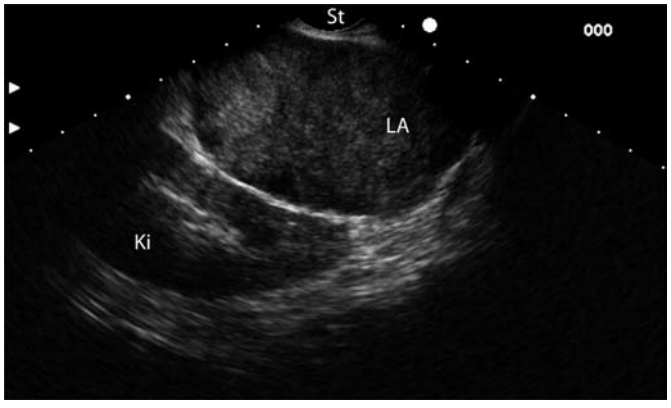

Fig. 4. Transgastric endosonographic view of a left adrenal metastasis (LA) in a patient with squamous cell carcinoma of the lung. St = Stomach; Ki = kidney.

May be surprisingly, EUS can also be used to detect distant metastases as the left adrenal gland (fig. 4) and lymph nodes around the celiac axis can be well visualized from the stomach. By biopsying these sites, EUS has turned out to be a useful method to prove distant metastasis in the left adrenal gland (fig. 3) [15, 16] as well as in celiac nodes [6].

Position of EUS in Lung Cancer Staging Algorithms

How does the EUS method compare to other staging methods [fiberbronchoscopy, transbronchial needle aspiration (TBNA), endobronchial ultrasound (EBUS)-TBNA and surgical staging] and how is EUS best positioned in lung cancer staging algorithms (table 2)? First of all, it is difficult to compare staging studies as patient populations often differ considerably in their clinical presentation and inclusion criteria. Patients who present with bulky mediastinal disease (with a very high likelihood of mediastinal metastases) are largely different from patients with a centrally located lung tumor without nodal enlargement on chest CT, in whom mediastinal spread cannot be excluded. The EUS method is primarily suitable for providing a tissue diagnosis or confirming mediastinal tumor spread in a minimally invasive way rather than excluding it as demonstrated by the relatively low negative predictive value. It should be realized that only part of the mediastinum can be investigated with EUS. Where an EUS investigation is best positioned in lung cancer staging algorithms depends also on the available imaging.

Table 2. EUS-FNA advantages

Diagnostic reach complementary to EBUS/mediastinoscopy Lower mediastinum: stations 7 (also dorsal part), 8 and 9 Aortopulmonary window: station 5 (only in selected cases) Para-aortal region: station 6 (transaortal approach)
Suitable method for on-site cytology during the procedure
Well tolerated by patients
Safe

EUS in a Setting with CT

Due to its complementary reach to mediastinoscopy in assessing different mediastinal nodal stations, staging with EUS in addition to mediastinoscopy significantly improves locoregional staging [17] and reduces futile thoracotomies [18]. In patients with (suspected) lung cancer, EUS-FNA has been shown to prevent surgical staging in up to 70% of patients [5, 19]. In a randomized controlled trial it has been shown that EUS significantly reduces surgical staging [20]. In recent guidelines, EUS has been suggested to be a minimally invasive alternative for surgical staging [21, 22]. It should be noticed that in those cases where EUS does not find advanced disease surgical staging is indicated.

EUS in a Setting with CT-PET

Combined CT-PET imaging is increasingly performed early in the diagnostic workup of patients with lung cancer. Integrated CT-PET imaging has a high accuracy in excluding mediastinal metastases; it has, however, severe limitations in confirming malignancy due to its high false-positive rate. EUS, on the other hand, has a high accuracy in confirming mediastinal metastases and is less accurate in excluding it.

Using EUS-FNA to confirm mediastinal spread based on PET-CT combines the best of both methods. Analyzing PET-positive mediastinal abnormalities suspected of mediastinal nodal involvement by EUS-FNA has been proven to be an accurate (>94%) [23, 24], minimally invasive and cost-effective [25] staging strategy.

EUS and Sarcoidosis

Sarcoidosis is the most common interstitial lung disease and frequently presents with hilar and mediastinal lymphadenopathy. In several studies, EUS-FNA has been shown to be a method with a yield >82% in assessing non-caseating granulomas [26–28]. The yield of EUS is higher than that reported for transbronchial lung biopsies, 65% (range 40–90%), a method that is still advised in current standards, but which carries the risk of hemoptysis and pneumothorax in around 7% of cases. EBUS-TBNA shows an accuracy similar to EUS. With the increasing clinical availability of endosonography, mediastinoscopy has become obsolete for the diagnosis of sarcoidosis.

Training and Implementation

The evidence that EUS is an important method for the analysis of mediastinal lesions is convincing and therefore EUS has been recommended in recent guidelines [21, 22]. The challenge the pulmonary community is faced with is to implement and distribute this method to ensure clinical accessibility. Chest physicians might qualify best to perform EUS for the pulmonary indications. They are the specialists for thoracic diseases and are trained to choose the optimal (set of) diagnostic/ staging tests. Additionally chest physicians are the experts on lung cancer and other pulmonary diseases and are best qualified to integrate all available clinical information [29]. Regarding training, it has been demonstrated that a dedicated EUS implementation strategy for lung cancer staging including on-site training in 45 patients seems adequate to achieve competence in mediastinal staging of lung cancer [30].

Conclusion

EUS-FNA of mediastinal nodes or centrally located tumors has proven to be an accurate, minimally invasive and safe diagnostic method with a large impact on patient management. EUS is complementary in its diagnostic reach to both EBUS and mediastinoscopy and provides in particular good access to the lower mediastinum. The position of EUS in local lung cancer staging algorithms depends on other methods available such as PET, EBUS and surgical staging. Whether the combination of EUS and EBUS can obtain 'complete mediastinal staging' and can be regarded as an alternative to surgical staging is under investigation.

References

1 Mountain CF, Dresler CM: Regional lymph node classification for lung cancer staging. Chest 1997;111:1718–1723.
2 Annema JT, Veselic M, Rabe KF: EUS-guided FNA of centrally located lung tumours following a non-diagnostic bronchoscopy. Lung Cancer 2005;48:357–361.
3 Varadarajulu S, Hoffman BJ, Hawes RH, Eloubeidi MA: EUS-guided FNA of lung masses adjacent to or abutting the esophagus after unrevealing CT-guided biopsy or bronchoscopy. Gastrointest Endosc 2004;60:293–297.
4 Schroder C, Schonhofer B, Vogel B: Transesophageal echographic determination of aortic invasion by lung cancer. Chest 2005;127:438–442.
5 Annema JT, Versteegh MI, Veselic M, Voigt P, Rabe KF: Endoscopic ultrasound-guided fine-needle aspiration in the diagnosis and staging of lung cancer and its impact on surgical staging. J Clin Oncol 2005;23:8357–8361.
6 Singh P, Camazine B, Jadhav Y, Gupta R, Mukhopadhyay P, Khan A, et al: Endoscopic ultrasound as a first test for diagnosis and staging of lung cancer: a prospective study. Am J Respir Crit Care Med 2007;175:345–354.
7 Micames CG, McCrory DC, Pavey DA, Jowell PS, Gress FG: Endoscopic ultrasound-guided fine-needle aspiration for non-small cell lung cancer staging: a systematic review and metaanalysis. Chest 2007;131:539–548.
8 Hernandez LV, Geenen JE, Schmalz MJ, Catalano MF: The underutilization of EUS-guided FNA in the lymph-node staging of non-small-cell lung cancer: perceptions of chest physicians in Wisconsin. Gastrointest Endosc 2005;62:517–520.
9 Leblanc JK, Devereaux BM, Imperiale TF, Kesler K, Dewitt JM, Cummings O, et al: Endoscopic ultrasound in non-small cell lung cancer and negative mediastinum on computed tomography. Am J Respir Crit Care Med 2005;171:177–182.
10 Tournoy KG, Ryck FD, Vanwalleghem L, Praet M, Vermassen F, Maele GV, et al: The yield of endoscopic ultrasound in lung cancer staging: does lymph node size matter? J Thorac Oncol 2008;3:245–249.
11 Wallace MB, Ravenel J, Block MI, Fraig M, Silvestri G, Wildi S, et al: Endoscopic ultrasound in lung cancer patients with a normal mediastinum on computed tomography. Ann Thorac Surg 2004;77:1763–1768.
12 Annema JT, Rabe KF: Lung cancer patients with small nodes on CT – what's the next step? Endoscopy 2006;38(suppl 1):S77–S80.
13 Annema JT, Veselic M, Versteegh MI, Willems LN, Rabe KF: Mediastinal restaging: EUS-FNA offers a new perspective. Lung Cancer 2003;42:311–318.
14 Varadarajulu S, Eloubeidi M: Can endoscopic ultrasonography-guided fine-needle aspiration predict response to chemoradiation in non-small cell lung cancer? A pilot study. Respiration 2006;73:213–220.

15 Eloubeidi MA, Seewald S, Tamhane A, Brand B, Chen VK, Yasuda I, et al: EUS-guided FNA of the left adrenal gland in patients with thoracic or GI malignancies. Gastrointest Endosc 2004;59:627–633.
16 Jhala NC, Jhala D, Eloubeidi MA, Chhieng DC, Crowe DR, Roberson J, et al: Endoscopic ultrasound-guided fine-needle aspiration biopsy of the adrenal glands: analysis of 24 patients. Cancer 2004;102:308–314.
17 Annema JT, Versteegh MI, Veselic M, Welker L, Mauad T, Sont JK, et al: Endoscopic ultrasound added to mediastinoscopy for preoperative staging of patients with lung cancer. JAMA 2005;294:931–936.
18 Larsen SS, Vilmann P, Krasnik M, Dirksen A, Clementsen P, Maltbaek N, et al: Endoscopic ultrasound guided biopsy performed routinely in lung cancer staging spares futile thoracotomies: preliminary results from a randomised clinical trial. Lung Cancer 2005;49:377–385.
19 Larsen SS, Krasnik M, Vilmann P, Jacobsen GK, Pedersen JH, Faurschou P, et al: Endoscopic ultrasound guided biopsy of mediastinal lesions has a major impact on patient management. Thorax 2002;57:98–103.
20 Tournoy KG, De Ryck F, Vanwalleghem LR, Vermassen F, Praet M, Aerts JG, et al: Endoscopic ultrasound reduces surgical mediastinal staging in lung cancer: a randomized trial. Am J Respir Crit Care Med 2008;177:531–535.
21 De Leyn P, Lardinois D, Van Schil PE, Rami-Porta R, Passlick B, Zielinski M, et al: ESTS guidelines for preoperative lymph node staging for non-small cell lung cancer. Eur J Cardiothorac Surg 2007;32:1–8.
22 Detterbeck FC, Jantz MA, Wallace M, Vansteenkiste J, Silvestri GA: Invasive mediastinal staging of lung cancer: ACCP evidence-based clinical practice guidelines, ed 2. Chest 2007;132(3 suppl):202S–220S.
23 Annema JT, Hoekstra OS, Smit EF, Veselic M, Versteegh MI, Rabe KF: Towards a minimally invasive staging strategy in NSCLC: analysis of PET positive mediastinal lesions by EUS-FNA. Lung Cancer 2004;44:53–60.
24 Eloubeidi MA, Cerfolio RJ, Chen VK, Desmond R, Syed S, Ojha B: Endoscopic ultrasound-guided fine needle aspiration of mediastinal lymph node in patients with suspected lung cancer after positron emission tomography and computed tomography scans. Ann Thorac Surg 2005;79:263–268.
25 Kramer H, van Putten JW, Post WJ, van Dullemen HM, Bongaerts AH, Pruim J, et al: Oesophageal endoscopic ultrasound with fine needle aspiration improves and simplifies the staging of lung cancer. Thorax 2004;59:596–601.
26 Annema JT, Veselic M, Rabe KF: Endoscopic ultrasound-guided fine-needle aspiration for the diagnosis of sarcoidosis. Eur Respir J 2005;25:405–409.
27 Fritscher-Ravens A, Sriram PV, Topalidis T, Hauber HP, Meyer A, Soehendra N, et al: Diagnosing sarcoidosis using endosonography-guided fine-needle aspiration. Chest 2000;118:928–935.
28 Wildi SM, Judson MA, Fraig M, Fickling WE, Schmulewitz N, Varadarajulu S, et al: Is endosonography guided fine needle aspiration (EUS-FNA) for sarcoidosis as good as we think? Thorax 2004;59:794–799.
29 Annema JT, Rabe KF: Why respiratory physicians should learn and implement EUS-FNA. Am J Respir Crit Care Med 2007;176:99.
30 Annema JT, Burgers S, Rabe KF: Implementation of EUS-FNA for lung cancer staging. ATS, abstract 1809, 2008.

Jouke Annema, MD, PhD
Department of Pulmonology C3 P, Leiden University Medical Center
Albinusdreef 2, PO Box 9600
NL–2300 RC Leiden (The Netherlands)
Tel. +31 71 5262 950, Fax +31 71 5266 927, E-Mail j.t.annema@lumc.nl

Chapter 20

Bolliger CT, Herth FJF, Mayo PH, Miyazawa T, Beamis JF (eds): Clinical Chest Ultrasound: From the ICU to the Bronchoscopy Suite.
Prog Respir Res. Basel, Karger, 2009, vol 37, pp 171–180

Competing Technologies: Ultrasound, Navigational Bronchoscopy, Optical Coherence Tomography, etc. – Who Will Win Out?

Pyng Lee[a] · J.F. Beamis[b]

[a]Department of Respiratory and Critical Care Medicine, Singapore General Hospital, Singapore, Singapore;
[b]Interventional Pulmonology, Lahey Clinic Medical Center, Burlington, Mass., USA

Abstract

Bronchoscopy in the new millennium spells an exciting time for the pulmonologist, which likens to Alice peering through the looking glass into a wonderland of miniaturized probes, superior optics and technology that are advancing at a maddening pace. Whilst scientists continue to push the envelope using nanotechnology where nanoparticles each measuring one billionth of a meter may facilitate further miniaturization of probes to allow imaging at the cellular or molecular level as well as for targeted drug or gene delivery in the near future, it is opportune to evaluate the strengths and weaknesses of available technologies in thoracic imaging, for the diagnosis and staging of lung cancer as well as in its early detection. This chapter critically appraises the current status of available technologies and what they hold for the future.

Nothing is certain except taxes and death.
Franklin Roosevelt

The freedom to choose exists in all other aspects of morality. As physicians, we witnessed the insemination of evidence-based medicine, which arrived contemporaneously with computers, to transform the art of medical decision making into a science. The primary force driving evidence-based medicine forward has been the perception that clinicians make medical decisions in an idiosyncratic manner that sometimes compromises quality of care or wastes medical resources [1]. To the chagrin of physicians who perceive the practice of medicine as an art guided by experience, today's problem-solving strategies are largely algorithm-driven. Similarly, to convince health authorities to invest in new technology, results derived from research that focuses on prospective data collection, subject randomization, placebo-controlled, and with blinding of both investigators and study subjects are entrusted with the most weight, the very components that are lacking in interventional pulmonology trials. Moreover, different technologies under evaluation are not compared directly. Each piece of equipment is expensive and together with disposables drives up the cost per procedure. There are problems with reimbursement as well as the need for training to overcome the learning curve in order to attain comparable results achieved by expert centers. These often leave the clinicians with a huge dilemma of choosing between technologies and deciding which equipment to purchase.

This chapter reviews the current status of thoracic imaging: endobronchial ultrasound (EBUS) and navigational bronchoscopy for more precise targeting and staging of lung cancer, and improved optics to facilitate early lung cancer detection as well as the understanding of carcinogenesis by means of optical biopsy with optical coherence tomography (OCT) and confocal microendoscopy. It compares the strengths and weaknesses of available technologies as well as evaluates the potential each technique holds for the future.

Thoracic Imaging

Intensive Care Unit

The pleural cavity is easily accessible to ultrasound. Thoracic ultrasound can not only detect pleural effusion, it

is also able to elucidate its nature, for example the finding of septations in purulent pleurisy, it aids in the selection of suitable entry site for thoracentesis and tube placement, which can be performed safely in a ventilated patient. Bedside thoracic ultrasound is used to diagnose pneumothorax quickly and with higher accuracy than bedside chest x-ray (CXR). This is particularly important to patients who are mechanically ventilated, as it is a complication that requires immediate intervention since an alarming half progress to tension pneumothoraces [2]. A normal bedside CXR does not rule out pneumothorax since as much as 30% can be occult; moreover, tension pneumothorax can remain unclear on CXR and may require confirmation with computed tomography (CT). Although CT is the gold standard, its role in the intensive care unit is limited, and thoracic ultrasound performed at the bedside is a viable alternative that offers a quick solution [3].

Central Airway Disorders

The advent of multidetector CT scanners significantly impacts the care of patients with airway disorders by allowing reformation of axial images of the entire thorax acquired during a single breath-hold into 2-dimensional and 3-dimensional (virtual bronchoscopy) images. These allow accurate assessment of the length of the airway lesion, patency of the airway distal to stenosis, and its relationship to surrounding mediastinal structures. In addition, it can serve as a noninvasive imaging modality for follow-up of treated airway pathology [4].

Thoracic Oncology

In the further evaluation of lung cancer, CT is the standard imaging technique for most centers. The T descriptor refers to the characteristics of the tumor, and CT is excellent in defining the location and anatomic size of the primary mass as well as its relationship to surrounding structures such as the mediastinum, fissures and chest wall. Although varying sensitivities (38–90%) and specificities (40–90%) have been reported regarding accuracy of CT in deciding parietal pleura or chest wall invasion (T3 disease) [5, 6], recent studies have concluded that multiplanar reformatting using multidetector CT images has led to an increased confidence in the determination of tumor involvement of the pleura and diaphragm [7, 8].

Of equal importance in the staging of lung cancer is whether there is mediastinal invasion by tumor (T4 disease), and variable sensitivities 40–84% and specificities 57–94% have been reported using conventional CT. Although multidetector CT results in a more accurate assessment of mediastinal fat planes given its quicker imaging times and thus is less prone to respiratory and cardiac artifacts, it is still unable to reliably distinguish simple tumor contact from invasion of the mediastinal structures [9].

In the evaluation of the lung, magnetic resonance imaging (MRI) plays a limited role due to poor spatial resolution, low proton density, magnetic susceptibility-induced signal loss and long imaging times that lead to physiologic motion artifacts. MRI is, however, excellent for assessing extension of intrathoracic masses to the chest wall (superior sulcus tumors) or diaphragm because of its superior tissue contrast, increased sensitivity to blood flow and multiplanar imaging capability [10, 11]. MRI is particularly useful for the evaluation of primary chest wall tumors since imaging in the sagittal and coronal planes demonstrates tumor extension into the chest wall, diaphragm and mediastinum clearly, and therefore plays a significant role in deciding on the operability of malignant mesothelioma [12, 13]. In addition, MRI can differentiate exudative from transudative effusions as well as hemothoraces [14], and although cortical destruction may be better demonstrated by CT, bone marrow involvement by tumor is better visualized on MRI [15].

Staging of the Mediastinum

Staging of lymph nodes by CT or MRI is dependent on size, and a short axis diameter greater than 10 mm is suggestive of metastatic disease. However, 2 meta-analyses, which looked at the sensitivities and specificities of CT for lymph node assessment based on 10 mm threshold, reported sobering results of 57, 59, 78 and 82%, respectively [16, 17]. Although CT as an isolated investigation cannot determine the N status reliably, it nevertheless helps to direct mediastinoscopy in the sampling of enlarged lymph nodes.

Positron emission tomography (PET) using fluorodeoxyglucose (FDG), a glucose analogue that is preferentially taken up by tumor and metastases due to high glucose utilization, has partially replaced conventional imaging for mediastinal nodal staging. FDG-PET is not reliant on the size criterion, and therefore confers a higher diagnostic accuracy of 81–96% than CT or MRI for nodal metastasis [18–20]. In fact a recent meta-analysis comparing different imaging modalities reported a sensitivity of 79% and a specificity of 91% using FDG-PET versus 60 and 77%, respectively, with CT [18].

PET/CT which combines functional information of PET with anatomic precision of CT gives higher sensitivity, specificity and diagnostic accuracy of 89, 94 and 93% than

either CT or PET alone [21]. However pathological confirmation is often required as inflammatory lymph nodes due to tuberculosis, histoplasmosis and sarcoidosis can cause false-positive PET resulting in mistaken upstaging of primary tumor [22]. Similarly micrometastases within lymph nodes occurring beyond the limits of PET detectability can lead to a false-negative rate as high as 8% [18, 20].

The other advantage of PET lies in the detection of extrathoracic metastases. Although it is usual practice to image caudally from thoracic inlet to the inferior edge of liver and adrenals as part of a staging CT for lung cancer, routine search for disease beyond the thorax and abdomen (i.e., brain and bone) is rarely undertaken in asymptomatic patients. However data show that about 20% of patients who have undergone curative surgical treatment for lung cancer relapse with metastatic disease, and PET plays a significant role in identifying occult metastases [23]. Some authors have also suggested that the standardized value of FDG uptake of primary tumor can have prognostic value independent of clinical TNM in predicting tumor recurrence after treatment, and can be used to stratify patients to receive adjuvant chemotherapy or radiotherapy after surgery [24].

Lung Cancer

Bronchoscopy is a useful diagnostic tool for lung cancer, and bronchial washing, brushing, endobronchial and transbronchial biopsies are methods routinely performed for patients suspected to have lung cancer. The diagnostic yield for biopsy of endobronchial lesions is 70–100% whilst that of peripheral lesions is 33–62%. The addition of transbronchial needle aspiration (TBNA) improves the overall yield and may be exclusively diagnostic in 20% especially for submucosal and peribronchial lesions as well as in the staging of enlarged mediastinal or hilar lymph nodes [25].

Pulmonary Nodule

With the escalating use of CT in the evaluation of cardiopulmonary diseases, pulmonologists face an increasing number of patients with pulmonary nodules. Although many of these nodules may be benign, the importance of detecting early-stage bronchogenic carcinoma cannot be overstated, and pathological diagnosis can be achieved with flexible bronchoscopy and transbronchial lung biopsy (TBB), CT-guided transthoracic needle biopsy, thoracoscopic surgery and thoracotomy. Notwithstanding that flexible bronchoscopy is the least invasive of these procedures, its diagnostic yield for the pulmonary nodule can be variable between 19 and 68%, and highly dependent on size, location and tumor bronchus relationship [26, 27].

Novel technologies and techniques have been developed to improve the accuracy for targeting nodules <2 cm, and they include CT-guided TBB for fluoroscopically invisible nodules [28], EBUS guide sheath method [29], electromagnetic navigation[30], and virtual bronchoscopic navigation [31]. Although CT is available in most centers, CT-guided TBB involves delicate logistics planning and exposes the patient and healthcare workers to excessive radiation.

Miniaturized EBUS radial probe (UM-S20-20R, Olympus) inserted via a guide sheath into the working channel of the bronchoscope can be used to localize the lesion.

Once the nodule is visualized by a change in the ultrasound image of snowstorm appearance typical of normal lung, the EBUS probe is withdrawn with the guide sheath in place for the application of biopsy instruments. This method can replace fluoroscopic TBB with 80% yield and without pneumothorax. In fact, under expert hands it confers a diagnostic accuracy of 76% for nodules measuring less than 10 mm [29].

Electromagnetic navigation (superDimension; Plymouth, Minn., USA) consists of 4 essential components: (1) computer software that converts CT images into 3-dimensional virtual bronchoscopy reconstruction, (2) electromagnetic board that emits low-dose electromagnetic field, (3) sensor probe with 8-way steering mechanism that can navigate the bronchial tree and is locatable within the electromagnetic field, and (4) extended working channel that carries the sensor probe or bronchoscopic tools to the peripheral lung lesions. Reference anatomic landmarks such as the main and secondary carinae as well as the target lesion are identified on virtual bronchoscopy and preloaded into the system. The patient is then first placed over the electromagnetic board and the locatable sensor probe is inserted through the working channel of the bronchoscope into the airways. The same landmarks are identified by the probe during bronchoscopy, registered and aligned with the data from chest CT. The locatable sensor probe is directed in real time to the target lesion and sampling of tissue conducted through the extended working channel (fig. 1). In addition to its diagnostic applications, it can also allow placement of fiducial markers to localize tumor for stereotactic radiosurgery in patients who are unfit for surgery as well as for direct delivery of radiofrequency ablation in selected patients [32].

EBUS and electromagnetic navigation bronchoscopy have been shown to increase the yield of bronchoscopic

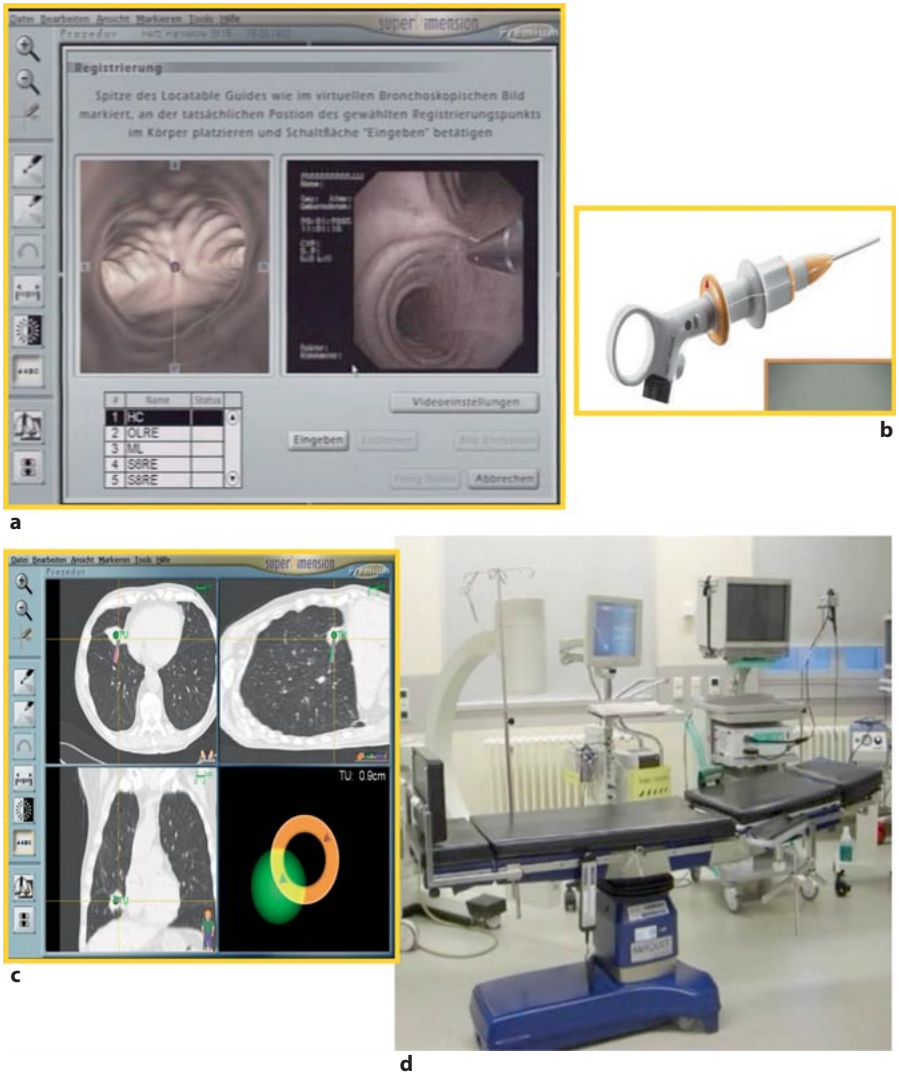

Fig. 1. Electromagnetic navigational bronchoscopy. **a** Computer software that converts CT images into 3-dimensional virtual bronchoscopy. **b** Sensor probe with 8-way steering mechanism. **c** Roadmap to the lesion. **d** Electromagnetic board that emits low-dose electromagnetic field.

biopsy of pulmonary nodules, and sensitivities for EBUS and electromagnetic navigational bronchoscopy range between 58 and 80, and 69 and 74%, respectively. Although both methods seem to be independent of nodule size, electromagnetic navigational bronchoscopy does not allow the operator to confirm the position of forceps within the nodule as it is possible with the EBUS probe prior to biopsy; EBUS, however, lacks navigational guidance and is reliant on the operator to maneuver the bronchoscope and probe to the bronchus that most likely leads to the lesion with the help of preprocedural CT. It was shown in a previous study that up to 24% of nodules could not be localized by EBUS [33]. Thus, by combining both the technology of electromagnetic navigation and EBUS, the diagnostic yield was markedly increased to 88% rather than with EBUS (69%) or electromagnetic navigation (59%) alone [34].

Still under research is virtual bronchoscopic navigation where an ultrathin bronchoscope is guided to the target bronchus by a system that displays a series of virtual bronchoscopic images of increasing order bronchi that ultimately lead to the lesion. Once the bronchoscope is within the target bronchus, a forceps is advanced to the lesion under CT fluoroscopy. Before biopsy is performed, forceps and bronchoscope positions are confirmed on thin section CT images. In a preliminary study of 37 patients with 38 lesions, virtual bronchoscopic images to sixth order bronchi could be produced, the ultrathin bronchoscope advanced into the planned route for 36 of 38 lesions (94.7%), and the forceps into 33 of 38 lesions (86.8%) achieving a diagnostic yield of 81.6% [31]. Although this technique appears promising and obviates the need for a dedicated electromagnetic navigation system as well as additional costs for

single-use disposable electromagnetic sensor probes, success depends not only on the accurate reproduction of virtual bronchoscopic images, which in turn relies on CT software and experience of the technologist but also, there exists a steep learning curve for the operator to navigate the bronchoscope through a myriad of branching smaller order bronchi to access the target bronchus. Notwithstanding that there are weaknesses in each method, rapidly advancing technology in the realm of imaging pushes the envelope to allow greater precision targeting of peripheral pulmonary lesions.

Mediastinal Staging

Accurate staging of the mediastinum is a critical step in the management of lung cancer. It is well established that in non-small cell lung cancer (NSCLC), the stage at presentation is the main determinant of survival [35]. SCLC usually metastasizes via lymphatic system to locoregional lymph nodes (hilar and mediastinal), to distant organs by hematogenous spread, and the degree of spread will impact on the most appropriate and optimal treatment strategy. There are different methods for sampling enlarged or PET-positive mediastinal lymph nodes, which include mediastinoscopy, Chamberlain procedure (anterior mediastinotomy), video-assisted thoracic surgery, transthoracic needle aspiration of the mediastinum, conventional TBNA, CT fluoroscopy-guided TBNA, EBUS-TBNA, and endoscopic ultrasound-guided fine needle aspiration (EUS-FNA).

Although the traditional approach to mediastinal staging is to perform a mediastinoscopy, it is still an invasive procedure that requires general anesthesia and in most instances hospitalization. Whilst a standard cervical mediastinoscopy performed by an experienced thoracic surgeon should allow access to the right and left paratracheal as well as anterior subcarinal nodes, mediastinoscopy is not always a straightforward procedure, and the optimal yield is dependent on the experience of the operator. Moreover, less experienced surgeons may not feel confident about exploring the mediastinum fully for fear of damaging mediastinal structures, and a recent study shows that only 40% of mediastinoscopies are performed adequately [36]. Thus, sensitivity and specificity of mediastinoscopy derived from pooled data are 81 and 100%, respectively [37].

It is important to realize that no one surgical procedure provides access to all mediastinal lymph node stations. A cervical mediastinoscopy allows access to nodal levels 2R, 2L, 4R, 4L and upper anterior part of 7, left anterior mediastinotomy for lymph nodes in the aortopulmonary window and para-aortic area (levels 5, 6), and left video-assisted thoracoscopic procedure for the entire subcarinal area as well as posterior-inferior mediastinum (levels 8, 9), leaving the hilar lymph nodes (levels 10, 11, 12) which are particularly challenging.

Conventional TBNA performed via flexible bronchoscopy permits sampling of nodal levels 2R, 2L, 4R, 4L, 7, 10, 11, 12 in a minimally invasive manner; however, it is by far the most operator-dependent procedure with a variable yield [38]. By incorporating imaging such as CT fluoroscopy, EBUS and EUS where entry of the needle into the lymph node is observed, yield from TBNA is enhanced [39]. Certainly to pulmonologists evaluating these options, CT fluoroscopy-TBNA sounds most attractive since CT is readily available and CT fluoroscopy-TBNA represents an extension of a repertoire of radiographic-guided procedures with which the pulmonologists are already familiar such as fluoroscopic-guided TBB. Even at no additional cost to acquire equipment or in skill training, performance of bronchoscopy at CT scanner holding facility requires considerable logistics planning, and exposes the patient as well as healthcare workers to excessive irradiation.

EUS initially developed for esophageal staging is used increasingly to stage the mediastinum in lung cancer. Curvilinear echoendoscope inserted in the esophagus allows real-time FNA of lymph nodes located in the aortopulmonary window (level 4L), subcarinal area (level 7), paraesophagus (level 8) and inferior pulmonary ligament (level 9). EUS can also be used to examine and biopsy lesions in the left adrenal gland and left lobe of the liver. Sensitivity of EUS-FNA for enlarged lymph nodes measuring more than 10 mm is 90–95%. The procedure also prevented 70% of surgical procedures on account of upstaging [40]. In patients diagnosed with lung cancer but who had 'normal' mediastinum as defined by CT, Wallace et al. [41] found that 25% had unsuspected disease which was detected by EUS-FNA, while LeBlanc et al. [42] showed that when EUS was included in mediastinal staging, it precluded surgery in 12% of patients who were later discovered to have N2 or N3 disease.

EBUS-guided TBNA can be performed using a miniaturized 20-MHz radial probe (UM-BS20-26R, Olympus) fitted with catheter and balloon at the tip or with the convex probe EBUS. Radial EBUS is introduced through the working channel of a flexible bronchoscope; when the balloon is inflated with water it optimizes contact between the probe and bronchial wall and allows visualization of the bronchial wall, mediastinal and hilar lymph nodes. Thus radial EBUS can be used to localize lymph nodes prior to needle aspiration. Although radial EBUS has been shown to increase the

yield of TBNA to 86%, it does not provide real-time visualization of the needle entering the target lymph node unlike convex probe EBUS, which is fitted with a 7.5-MHz transducer at the tip (XBF-UC260F-OL8, Olympus). Reported sensitivity for convex probe EBUS-TBNA ranges between 85 and 95%, and lymph nodes as small as 7 mm at levels 2, 3, 4, 7, 10 and 11 can be sampled using this device [43]. By combining convex probe EBUS-TBNA with EUS-FNA, it is possible to access the mediastinum in a minimally invasive manner, in its entirety except lymph node stations 5 (aortopulmonary window lateral to the arterial ligament) and 6 (para-aortic), which can only be approached via left anterior mediastinotomy [44].

Early Lung Cancer Detection by Autofluorescence Bronchoscopy, Narrow Band Imaging or OCT

When the bronchial surface is illuminated by light, light can be absorbed, reflected, back scattered or induce fluorescence. Reflectance imaging (e.g., white light bronchscopy) defines structural features of the bronchial epithelium to discriminate normal from abnormal while autofluorescence bronchoscopy (AF) depends on the concentration of fluorophores within the bronchial tissue. Normal bronchial epithelium fluoresces in green when illuminated by blue light, but as it transforms through different grades of dysplasia, carcinoma in situ to invasive cancer, a progressive decrease in green fluorescence due to increased epithelial thickness and tumor neovascularization occurs, thereby making these abnormal areas appear red. The spectral differences between 500 and 700 nm for normal, preneoplastic and neoplastic tissues serve as basis for the development of AF reflectance imaging devices such as LIFE (Xilix Technologies, Canada), D-light (Karl Storz, Germany), and SAFE 1000/3000 (Pentax, Japan).

Studies have consistently demonstrated superiority of AF over white light bronchoscopy for the detection of preinvasive lesions and early central airway cancer. Conventional bronchoscopy is highly specific while AF has a high false-positive rate especially if bronchitis or airway inflammation is encountered. Although a high sensitivity is essential to facilitate detection and early diagnosis, low specificity can lead to extensive biopsy and increased procedural time. Efforts have been made to improve AF specificity, which include use of fluorescence (red/green) ratio [45], and simultaneous video- and autofluorescence imaging (fig. 2a, b) [46].

By being a sensitive tool for the detection of airway dysplasia, AF also allows bronchoscopists to monitor progression or regression of these lesions either with or without chemoprevention. However in order to determine progression or regression of airway dysplasia, histological examination is mandatory, and since most of the lesions are superficial (being several cells thick) and small in size, it is plausible that they may be completely removed by biopsy alone, and thus may undermine interpretation of the natural history of carcinogenesis or results of chemoprevention trials [47].

Narrow band imaging [48] that delineates and characterizes microvascular network aims to advance the understanding of angiogenesis and its role in carcinogenesis (fig. 3), while Raman spectroscopy attempts to differentiate preinvasive from benign lesions by measuring the biochemical composition and metabolic state of bronchial tissues. Unlike EBUS, OCT detects backscattered light instead of sound waves, and because light is 200,000 times faster than sound, low coherence interferometry is required to integrate reflectance properties of tissue scanned to produce high-resolution cross-sectional microimages. For the airway, OCT can display structures of the bronchial wall in great detail and allows maximum penetration depth of 2 mm where most endobronchial bronchogenic carcinomas arise and spread, equivalent to the biopsy thickness achieved with standard forceps [49]. Unlike radial EBUS that achieves 4 mm depth and is used primarily to detect tumor invasion into the bronchial wall or enlarged peribronchial lymph nodes, OCT offers high-resolution cross-sectional microimages that allow real-time noninvasive histologic imaging without the performance of biopsy (fig. 4). Confocal microendoscopy [50] provides cellular images, which coupled with OCT may enhance our understanding of the evolution of preinvasive lesions by means of optical biopsy. This is particularly true for minute lesions that are a few millimeters wide and several cells thick where biopsy would interfere in the study of early carcinogenesis and lead to a falsely high rate of 'spontaneous' regression.

Conclusion

In thoracic imaging, ultrasound remains an invaluable tool for quick bedside diagnosis of pneumothorax, and in the careful selection of an entry site for thoracentesis in a mechanically ventilated patient with pleural effusion. Although advancing CT technology has enabled exquisite anatomical detail, it seems unlikely that further refinements will impact on staging accuracy in thoracic oncology. PET and recently PET/CT have shaped the staging algorithm of NSCLC, and help stratify patients treated surgically for

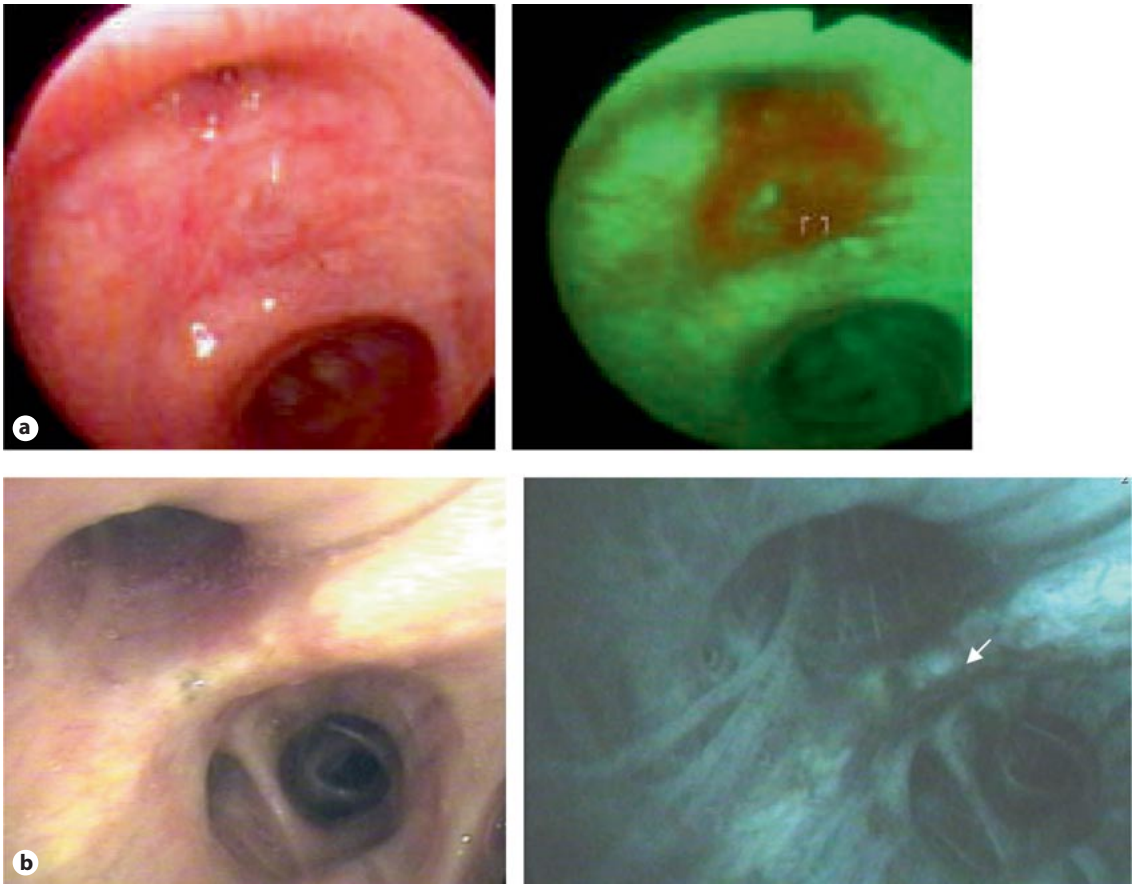

Fig. 2. **a** Quantitative image analysis of carcinoma in situ. White light and AF bronchoscopic images showing carcinoma in situ of LB6. **b** Simultaneous dual digital video-autofluorescence imaging (SAFE 3000). Previous biopsy site over middle lobe carina (arrow) with abnormal fluorescence (right); videobronchoscopy is normal (left), and histology is normal.

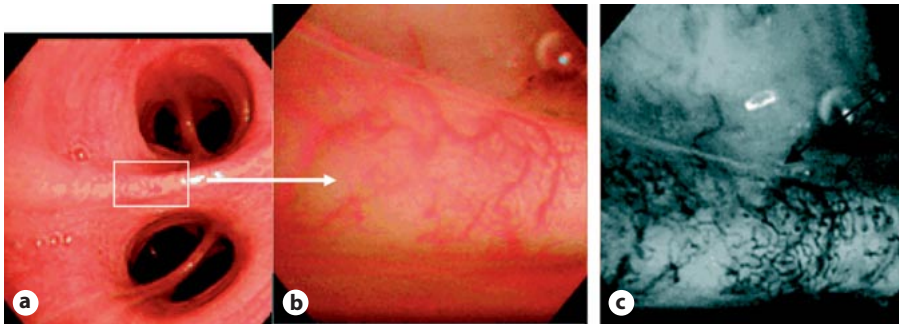

Fig. 3. Angiogenic squamous dysplasia (courtesy of K. Shibuya, Chiba University, Japan). **a** White light bronchoscopy. High magnification bronchovideoscopy (**b**) combined with narrow band imaging (**c**) of the bronchial mucosa. Complex tortuous vessels are clearly visible on narrow band imaging and pathological diagnosis revealed angiogenic squamous dysplasia, a possible precursor of early squamous cell cancer.

early stage lung cancers likely to relapse for adjuvant chemotherapy according to the standardized uptake value score.

In mediastinal staging of lung cancer, PET may have a role in patients with T1 NSCLC by allowing those with PET-negative mediastinum to avoid preoperative mediastinoscopy since nodal metastasis is only found in 5% or less. By combining convex probe EBUS-TBNA and EUS-FNA it is now possible to stage the mediastinum in its entirety, and in a minimally invasive manner.

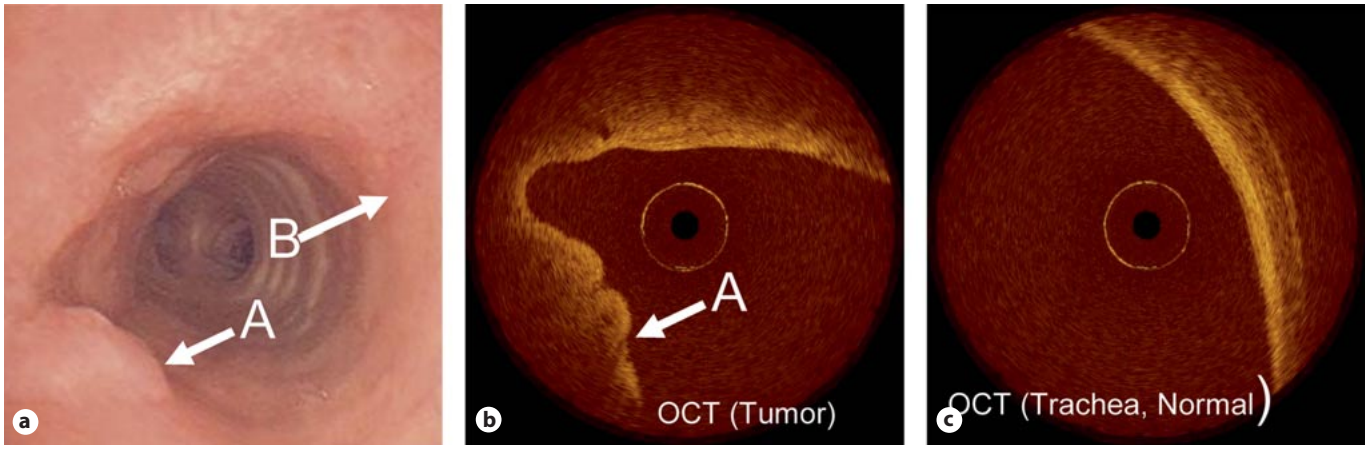

Fig. 4. Squamous cell carcinoma of the trachea (courtesy of N. Ikeda, Tokyo Medical University, Japan). **a** Bronchoscopic image. A = Nodular tumor; B = normal tracheal wall. **b** OCT: tumor (A) infiltrating beyond the cartilage. **c** Normal OCT.

Navigational bronchoscopy coupled with miniaturized radial EBUS probe leads to precision targeting of peripheral pulmonary nodules. Inflating the balloon at the tip of the catheter that houses the radial EBUS probe gives rise to a circumferential display of the layers of the bronchial wall and surrounding structures useful for assessing the extent of tumor invasion as well as for the localization of enlarged peribronchial lymph node before biopsy.

In the study of early lung cancer, AF is a sensitive tool for the detection of airway preneoplasia; however, confirmation with histology mandates biopsy, which can lead to its complete removal, disruption of airway mucosa and thus interference with the natural evolution or carcinogenesis process. As refinements in OCT and confocal microendoscopy continue, superior optical imaging even at a cellular level can enhance our understanding of carcinogenesis by means of optical biopsy.

References

1 Komaroff AL: Algorithms and the 'art' of medicine. Am J Public Health 1982;72:10–12.
2 Lichtenstein DA, Menu Y: A bedside ultrasound sign ruling out pneumothorax in the critically ill. Lung sliding. Chest 1995;108:1345–1348.
3 Lichtenstein DA, Mezière G, Lascols N, Biderman P, Courret JP, Gepner A, Goldstein I, Tenoudji-Cohen M: Ultrasound diagnosis of occult pneumothorax. Crit Care Med 2005;33:1231–1238.
4 Boiselle PM: Imaging of the large airways. Clin Chest Med 2008;29:181–193.
5 Quint LE, Francis IR: Radiologic staging of lung cancer. J Thorac Imaging 1999;14:235–246.
6 Mori K, Hirose T, Machida S, Yokoi K, Tominaga K, Moriyama N, Sasagawa M: Helical computed tomography diagnosis of pleural dissemination in lung cancer: comparison of thick-section and thin-section helical computed tomography. J Thorac Imaging 1998;13:211–218.
7 Higashino T, Ohno Y, Takenaka D, Watanabe H, Nogami M, Ohbayashi C, Yoshimura M, Satouchi M, Nishimura Y, Fujii M, Sugimura K: Thin-section multiplanar reformats from multidetector-row CT data: utility for assessment of regional tumor extent in non-small cell lung cancer. Eur J Radiol 2005;56:48–55.
8 Chooi WK, Matthews S, Bull MJ, Morcos SK: Multislice computed tomography in staging lung cancer: the role of multiplanar image reconstruction. J Comput Assist Tomogr 2005;29:357–360.
9 Munden RF, Swisher SS, Stevens CW, Stewart DJ: Imaging of the patient with non-small cell lung cancer. Radiology 2005;237:803–818.
10 Hatabu H, Stock KW, Sher S, Edinburgh KJ, Levin DL, Garpestad E, Albert MS, Mai VM, Chen Q, Edelman RR: Magnetic resonance imaging of the thorax: past, present, and future. Radiol Clin North Am 2000;38:593–620.
11 Kuhlman JE, Bouchardy L, Fishman EK, Zerhouni EA: CT and MR imaging evaluation of chest wall disorders. Radiographics 1994;14:571–595.
12 Heelan RT, Rusch VW, Begg CB, Panicek DM, Caravelli JF, Eisen C: Staging of malignant pleural mesothelioma: comparison of CT and MR imaging. AJR Am J Roentgenol 1999;172:1039–1047.
13 Wang ZJ, Reddy GP, Gotway MB, Higgins CB, Jablons DM, Ramaswamy M, Hawkins RA, Webb WR: Malignant pleural mesothelioma: evaluation with CT, MR imaging, and PET. Radiographics 2004;24:105–119.
14 Baysal T, Bulut T, Gökirmak M, Kalkan S, Dusak A, Dogan M: Diffusion weighted MR imaging of pleural fluid: differentiation of transudative vs. exudative pleural effusions. Eur Radiol 2004;14:890–896.
15 Verstraete KL, Huysse WC: Health technology assessment of magnetic resonance imaging of the spine and bone marrow. Eur J Radiol 2008;65:201–210.
16 Birim O, Kappetein AP, Stijnen T, Bogers AJ: Meta-analysis of positron emission tomographic and computed tomographic imaging in detecting mediastinal lymph node metastases in non-small cell lung cancer. Ann Thorac Surg 2005;79:375–382.
17 Toloza EM, Harpole L, McCrory DC: Noninvasive staging of nonsmall cell lung cancer: a review of the current evidence. Chest 2003;123(1 suppl):137S–146S.
18 Dwamena BA, Sonnad SS, Angobaldo JO, Wahl RL: Metastases from non-small cell lung cancer: mediastinal staging in the 1990s – meta-analytic comparison of PET and CT. Radiology 1999;213:530–536.

19 Kalff V, Hicks RJ, MacManus MP, Binns DS, McKenzie AF, Ware RE, Hogg A, Ball DL: Clinical impact of (18)F fluorodeoxyglucose positron emission tomography in patients with non-small-cell lung cancer: a prospective study. J Clin Oncol 2001;19:111–118.
20 Dietlein M, Weber K, Gandjour A, Moka D, Theissen P, Lauterbach KW, Schicha H: Cost-effectiveness of FDG-PET for the management of potentially operable non-small cell lung cancer: priority for a PET-based strategy after nodal-negative CT results. Eur J Nucl Med 2000; 27:1598–1609.
21 Antoch G, Stattaus J, Nemat AT, Marnitz S, Beyer T, Kuehl H, Bockisch A, Debatin JF, Freudenberg LS: Non-small cell lung cancer: dual-modality PET/CT in preoperative staging. Radiology 2003;229:526–533.
22 Gould MK, Kuschner WG, Rydzak CE, Maclean CC, Demas AN, Shigemitsu H, Chan JK, Owens DK: Test performance of positron emission tomography and computed tomography for mediastinal staging in patients with non-small-cell lung cancer: a meta-analysis. Ann Intern Med 2003;139:879–892.
23 Weder W, Schmid RA, Bruchhaus H, Hillinger S, von Schulthess GK, Steinert HC: Detection of extrathoracic metastases by positron emission tomography in lung cancer. Ann Thorac Surg 1998;66:886–892.
24 Higashi K, Ueda Y, Arisaka Y, Sakuma T, Nambu Y, Oguchi M, Seki H, Taki S, Tonami H, Yamamoto I: ^{18}F-FDG uptake as a biologic prognostic factor for recurrence in patients with surgically resected non-small cell lung cancer. J Nucl Med 2002;43:39–45.
25 Savage C, Morrison RJ, Zwischenberger JB: Bronchoscopic diagnosis and staging of lung cancer. Chest Surg Clin N Am 2001;11:701–721.
26 Schreiber G, McCrory DC: Performance characteristics of different modalities for diagnosis of suspected lung cancer: summary of published evidence. Chest 2003;123:115S–128S.
27 Baaklini WA, Reinoso MA, Gorin AB, Sharafkaneh A, Manian P: Diagnostic yield of fiberoptic bronchoscopy in evaluating solitary pulmonary nodules. Chest 2000;117:1049–1054.
28 Garpestad E, Goldberg S, Herth F, Garland R, LoCicero J 3rd, Thurer R, Ernst A: CT-fluoroscopy guidance for transbronchial needle aspiration: an experience in 35 patients. Chest 2001;119:329–332.
29 Kurimoto N, MiyazawaT, Okimasa S, Maeda A, Oiwa H, Miyazu Y, Murayama M: Endobronchial ultrasonography using a guide sheath increases the ability to diagnose peripheral pulmonary lesions endoscopically. Chest 2004;126:959–965.
30 Gildea TR, Mazzone PJ, Karnak D, Meziane M, Mehta AC: Electromagnetic navigation diagnostic bronchoscopy: a prospective study. Am J Respir Crit Care Med 2006;174:982–989.
31 Asano F, Matsuno Y, Shinagawa N, Yamazaki K, Suzuki T, Ishida T, Moriya H: A virtual bronchoscopic navigation system for pulmonary peripheral lesions. Chest 2006;130:559–566.
32 Anantham D, Feller Kopman D, Shanmugham LN, Berman SM, DeCamp MM, Gangadharan SP, Eberhardt R, Herth F, Ernst A: Electromagnetic navigation bronchoscopy-guided fiducial placement for robotic stereotactic radiosurgery of lung tumors: a feasibility study. Chest 2007;132:930–935.
33 Herth FJ, Eberhardt R, Becker HD, Ernst A: Endobronchial ultrasound-guided transbronchial lung biopsy in fluoroscopically invisible solitary pulmonary nodules: a prospective trial. Chest 2006;129:147–150.
34 Eberhardt R, Anantham D, Ernst A, Feller Kopman D, Herth F: Multimodality bronchoscopic diagnosis of peripheral lung lesions: a randomized controlled trial. Am J Respir Crit Care Med 2007;176:36–41.
35 Silvestri GA, Gould MK, Margolis ML, Tanoue LT, McCrory D, Toloza E, Detterbeck F: Noninvasive staging of non-small cell lung cancer: ACCP evidenced-based clinical practice guidelines, ed 2. Chest 2007;132:178S–201S.
36 Smulders SA, Smeenk FW, Janssen Heijnen ML, Wielders PL, de Munck DR, Postmus PE: Surgical mediastinal staging in daily practice. Lung Cancer 2005;47:243–251.
37 Detterbeck FC, Jantz MA, Wallace M, Vansteenkiste J, Silvestri GA, American College of Chest Physicians: Invasive mediastinal staging of lung cancer: ACCP evidence-based clinical practice guidelines, ed 2. Chest 2007;132 (3 suppl):202S–220S.
38 Dasgupta A, Mehta AC: Transbronchial needle aspiration. An underused diagnostic technique. Clin Chest Med 1999;20:39–51.
39 Gasparini S: Evolving role of interventional pulmonology in the interdisciplinary approach to the staging and management of lung cancer: bronchoscopic mediastinal staging of lung cancer. Clin Lung Cancer 2006;8:110–115.
40 Annema JT, Versteegh MI, Veseliç M, Voigt P, Rabe KF: Endoscopic ultrasound-guided fine-needle aspiration in the diagnosis and staging of lung cancer and its impact on surgical staging. J Clin Oncol 2005;23:8357–8361.
41 Wallace MB, Ravenel J, Block MI, Fraig M, Silvestri G, Wildi S, Schmulewitz N, Varadarajulu S, Roberts S, Hoffman BJ, Hawes RH, Reed CE: Endoscopic ultrasound in lung cancer patients with a normal mediastinum on computed tomography. Ann Thorac Surg 2004;77:1763–1768.
42 LeBlanc JK, Devereaux BM, Imperiale TF, Kesler K, DeWitt JM, Cummings O, Ciaccia D, Sherman S, Mathur P, Conces D, Brooks J, Chriswell M, Einhorn L, Collins E: Endoscopic ultrasound in non-small cell lung cancer and negative mediastinum on computed tomography. Am J Respir Crit Care Med 2005;171:177–182.
43 Yasufuku K, Nakajima T, Chiyo M, Sekine Y, ShibuyaK, Fujisawa T: Endobronchial ultrasonography: current status and future directions. J Thorac Oncol 2007;2:970–979.
44 Rintoul R: Towards complete endoscopic staging of the mediastinum? Endoscopy 2006;38: S110–S113.
45 Lee P, van den Berg RM, Lam S, Gazdar AF, Grunberg K, McWilliams A, LeRiche J, Postmus PE, Sutedja TG: Quantitative image analysis for bronchial dysplasia and carcinoma in situ. Clin Cancer Res, in press.
46 Lee P, Brokx HA, Postmus PE, Sutedja TG: Dual digital video-autofluorescence imaging for detection of pre-neoplastic lesions. Lung Cancer 2007;58:44–49.
47 Lee P, Sutedja TG: Lung cancer screening: has there been any progress? Computed tomography and autofluorescence bronchoscopy. Curr Opin Pulm Med 2007;13:243–248.
48 Shibuya K, Hoshino H, Chiyo M, Iyoda A, Yoshida S, Sekine YIizasa T, Saitoh Y, Baba M, Hiroshima K, Ohwada H, Fujisawa T: High magnification bronchovideoscopy combined with narrow band imaging could detect capillary loops of angiogenic squamous dysplasia in heavy smokers at high risk for lung cancer. Thorax 2003;58:989–995.
49 Tsuboi M, Hayashi A, Ikeda N, Honda H, Kato Y, Ichinose S, Kato H: Optical coherence tomography in the diagnosis of bronchial lesions. Lung Cancer 2005;49:387–394.
50 Herth FJ, Eberhardt R, Ernst A: The future of bronchoscopy in diagnosing, staging and treatment of lung cancer. Respiration 2006;73: 399–409.

Pyng Lee, MD
Department of Respiratory and Critical Care Medicine
Singapore General Hospital
Outram Road, Singapore169608 (Singapore)
Tel. +65 6321 4700, Fax +65 6227 1736, E-Mail lee.pyng@sgh.com.sg

Ultrasound and Therapeutic Procedures

Chapter 21

Bolliger CT, Herth FJF, Mayo PH, Miyazawa T, Beamis JF (eds): Clinical Chest Ultrasound: From the ICU to the Bronchoscopy Suite.
Prog Respir Res. Basel, Karger, 2009, vol 37, pp 182–188

Ultrasound and Medical Thoracoscopy

Gaëtane Michaud · Armin Ernst

Interventional Pulmonology, Harvard Medical School, Boston, Mass., USA

Abstract

Ultrasound is a very useful adjunct to medical thoracoscopy. It allows a real-time assessment of the complexity of the pleural space at the bedside. This in turn minimizes complications and maximizes safety. Traditionally, the induction of a pneumothorax was necessary prior to beginning the medical thoracoscopy in order to minimize the risk of injury to the lung or adjacent solid organs at the time of insertion of the trocar. Unfortunately, this also required a chest radiograph to confirm that the lung did indeed fall away from the chest wall. The induction and documentation of the pneumothorax incurred unnecessary risk, expense and delays. Ultrasound is useful prior to medical thoracoscopy as it allows the physician to evaluate the pleural space at the time of the procedure in the thoracoscopy position. This facilitates the identification of a safe entry site into the thorax even in more complex cases such as those with multiloculated effusions.

Medical thoracoscopy (MT) is a diagnostic/therapeutic procedure performed to visualize the structures of the pleural space, and perform biopsies and pleurodesis when necessary. It is generally performed by pulmonologists under moderate sedation and does not require endotracheal intubation and single lung ventilation. MT is a sterile procedure; however, it is performed safely by many thoracoscopists in a pulmonary procedure room. Traditionally, this procedure was performed using rigid instruments through a trocar; however, a semirigid thoracoscope has recently been developed using technology similar to flexible bronchoscopy [1].

One of the main indications for MT is the evaluation of patients with undiagnosed exudative effusions despite routine relatively noninvasive testing including diagnostic thoracentesis with cytology specimens. Approximately 25% of patients will have an undiagnosed exudative effusion following thoracentesis and blind pleural biopsy [2]. Worldwide, the most common causes for exudative effusions include malignancy and infection, most particularly tuberculosis. The probability of malignancy versus tuberculosis is strongly dependent on the population studied. Overall, malignancy is thought to account for approximately 45% of all exudative effusions; however, this may not hold true in TB endemic countries [3]. In a large series of patients from TB endemic countries, a diagnosis was possible by MT in 99% compared to 51% with needle biopsy and 61% with pleural fluid analysis plus blind pleural biopsy [4]. With respect to the yield for malignancy, Boutin et al. [5] performed MT in patients with previously negative pleural fluid cytology and blind biopsy. They repeated both the thoracentesis and biopsy the day prior to the MT with a combined yield of only 41%, whereas a diagnosis was made in 97% following MT. MT is clearly superior to either thoracentesis or blind pleural biopsy in the diagnosis of undiagnosed exudative effusions. The improved yield is likely related to the size of specimens that can be obtained using this technique coupled with the ability to biopsy abnormal areas under direct visualization.

Many centers, particularly in Europe, also perform thoracoscopy as part of the management of complicated parapneumonic effusion and empyema [6]. MT is used to breakdown locules of infected fluid and lavage the pleural space under direct vision.

Description of MT and Ultrasound Procedures

Online supplementary video 1 reviews the technique of MT including the preprocedure ultrasound. Patients referred for MT should undergo a comprehensive history and physical examination to ensure there exist no contraindications

Video

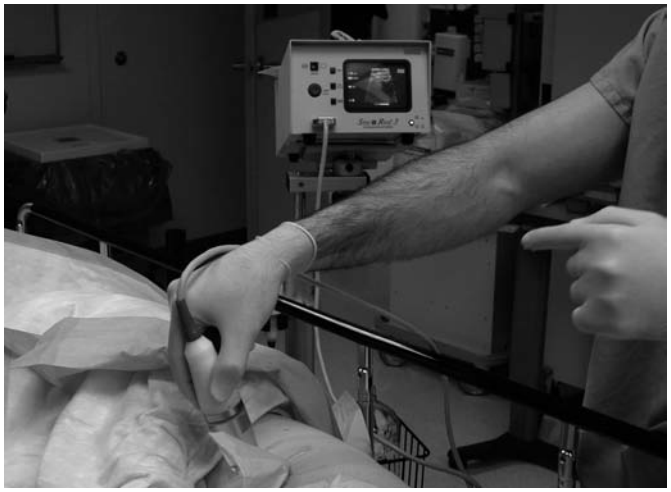

Fig. 1. Transthoracic ultrasound being performed with patient in MT position to localize an insertion site for the thoracoscope.

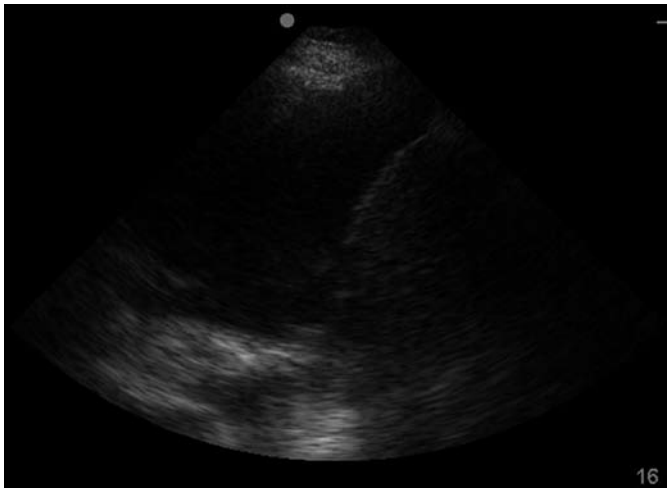

Fig. 2. Ultrasound image showing anechoic pleural fluid with the hemidiaphragm clearly identified above the liver.

to the procedure including uncorrectable bleeding dyscrasias, unstable cardiac or pulmonary disease or inability to tolerate a pneumothorax. Frontal and lateral chest radiographs and thoracic ultrasound to evaluate the pleural space are performed during the initial visit. The patient is placed on respiratory and hemodynamic monitoring throughout the procedure and is positioned in the lateral decubitus position with the healthy lung in the down position. The ipsilateral arm is elevated and abducted while preventing postprocedure plexopathies by supporting and cushioning the elbow and shoulder. A pillow can also be placed under the dependent side to open the intercostal spaces.

Once the patient is positioned, an appropriate entry site is localized using the transthoracic ultrasound (fig. 1). Traditionally, a site in the midaxillary line is selected as there is minimal muscle and adipose tissue. Many physicians use a convex probe with a frequency of 3.5 MHz as this allows an adequate visualization of deeper structures. There is a marker on the probe which corresponds with that on the ultrasound screen to indicate the direction of imaging. By convention the marked probe is oriented in the cephalad direction. The probe is moved along the interspace horizontally and then moved superiorly and inferiorly in adjacent interspaces in order to identify the layers of the chest wall, visceral and parietal pleura, diaphragm, lung and subdiaphragmatic structures (fig. 2). Air within the lung parenchyma causes a scatter of the sound waves and therefore produces a heterogeneous gray artifact. Key structures for orientation include the diaphragm and liver. The liver is considered an echo reference as it is considered isoechoic and structures seen as brighter are considered hyperechoic and those less echogenic are hypoechoic. The liver is readily identified as it is isoechoic and the ducts can often be seen as low echogenicity structures within the organ. The hemdiaphragm is a hyperechoic dome-shaped structure that moves with respiration. The visceral and parietal pleura appear hyperechoic, whereas simple pleural fluid appears anechoic. More viscous fluid such as what might be seen in empyema, blood or more complex or organized pleural fluid will be hypoechoic rather than anechoic. In a healthy pleural space there is only a small amount of fluid separating the thin pleural membranes; therefore, they may be seen as a single bright echo. During the respiratory cycle the lung glides within the pleural cavity producing a phenomenon referred to as the visceral or pleural slide (chapter 3, online suppl. video 5). Adhesions between the pleura can be identified as hyperechoic bands running between the chest wall and lung parenchyma through anechoic or hypoechoic pleural fluid (fig. 3a, b). They may be simple or multiple forming loculations within the pleural space (fig. 4a–c). Pleural symphysis can be recognized by complete absence of pleural slide in combination with the identification of a single bright echo separating the lung parenchyma and chest wall structures. Of note, the preprocedure ultrasound can be suggestive of a nonexpandable lung leading the operator to abort the procedure and consider other therapeutic options (fig. 5a–c).

The skin is cleansed using chlorhexadine and the patient is draped in a sterile fashion. The patient is sedated (many

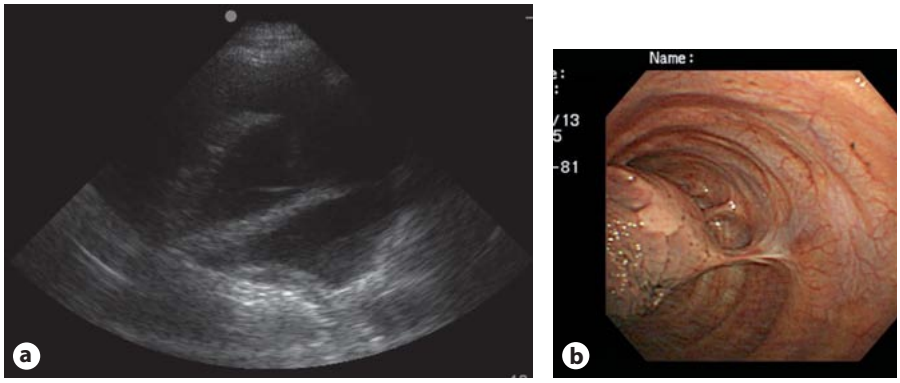

Fig. 3. Thick membraneous pleural adhesion as seen at the time of thoracoscopy (**a**) and the ultrasound correlate (**b**).

centers use a combination of fentanyl and midazolam) with care to maintain spontaneous respiration. Figure 6 demonstrates the equipment necessary to perform the procedure. Approximately 30–40 ml of 1% xylocaine is used for local anesthesia to the intercostal space and periosteum of the rib above and below the selected entry site. Upon puncturing through the parietal pleura, fluid is aspirated back. A 1- to 2-cm incision is made to the skin and the deeper tissues spread using forceps. The trocar is then inserted and a suction catheter passed through it into the pleural space to aspirate excess fluid that will limit inspection of the pleural cavity. The rigid optic or semirigid thoracoscope can then be used to inspect the pleural space, take biopsies and instill a sclerosant if necessary. A second port can be placed under direct visualization for diagnostic or therapeutic purposes, i.e. to pass biopsy forceps or catheter for insufflations of sclerosants, respectively. Upon completion of the procedure, a chest tube is directed posteriorly via the trocar and the optional second entry site sutured. The chest tube is fixed and the drain placed to suction until no further leak exists or no significant quantity of fluid is draining.

MT is generally considered a safe procedure, although the risks do include massive hemorrhage, trauma to the lung with persistent air leak and even death. Colt [7] prospectively evaluated thoracoscopy-related complications and adverse events in a large US center. Of the 52 MTs performed, only 1 patient with scleroderma developed a recurrent effusion with fever and leukocytosis requiring readmission and pleural drainage. There was 1 chest tube site infection and 1 small residual clinically insignificant pneumothorax following chest tube removal. Mortality for this procedure is quoted as $<0.01\%$ and a single case of bleeding requiring conversion to thoracotomy has been reported [8]. It should be noted that the low morbidity and mortality rates quoted are most certainly influenced by patient selection and experience.

The ideal patient for MT has a large uncomplicated pleural effusion. Unfortunately, malignancy and infection are both proinflammatory. Any manipulation of the pleural space can also lead to the production of inflammatory mediators such as tissue growth factor-β, tumor necrosis factor-α, tissue factor and plasminogen activator inhibitors 1 and 2. In short, these proinflammatory mediators serve to increase the intrapleural conversion of fibrinogen to fibrin and then downregulate the fibrinolytic pathway. They also stimulate the mesothelial cells to synthesize and secrete more proinflammatory cytokines. This dysregulation leads initially to the formation of fibrin strands and loculations and eventually to fusion of the visceral and parietal pleurae. This complex cascade of inflammation can result from even minimal disruption of inflamed pleura such as might occur with thoracentesis [9]. As was stated above, thoracoscopy is reserved for patients who despite thoracentesis and pleural biopsy remain as undiagnosed exudative effusions or alternatively for patients with pleural space infections. By definition, the patients being considered for thoracoscopy are at risk of having a complex pleural space running the spectrum from simple loculations, vascular loculations, focal areas of adhesion of the lung to the parietal pleura, to complete fusion of the pleural space (fig. 3, 4).

Traditionally, the selection of patients considered as good candidates for MT was based upon (1) the patient's ability to tolerate an induced pneumothorax and (2) the ability to demonstrate that the lung completely falls away from the chest wall following the induction of a pneumothorax [10]. It is likely that these stringent selection criteria have contributed to a low rate of procedure-related complications. The lung falling away from the chest suggests that

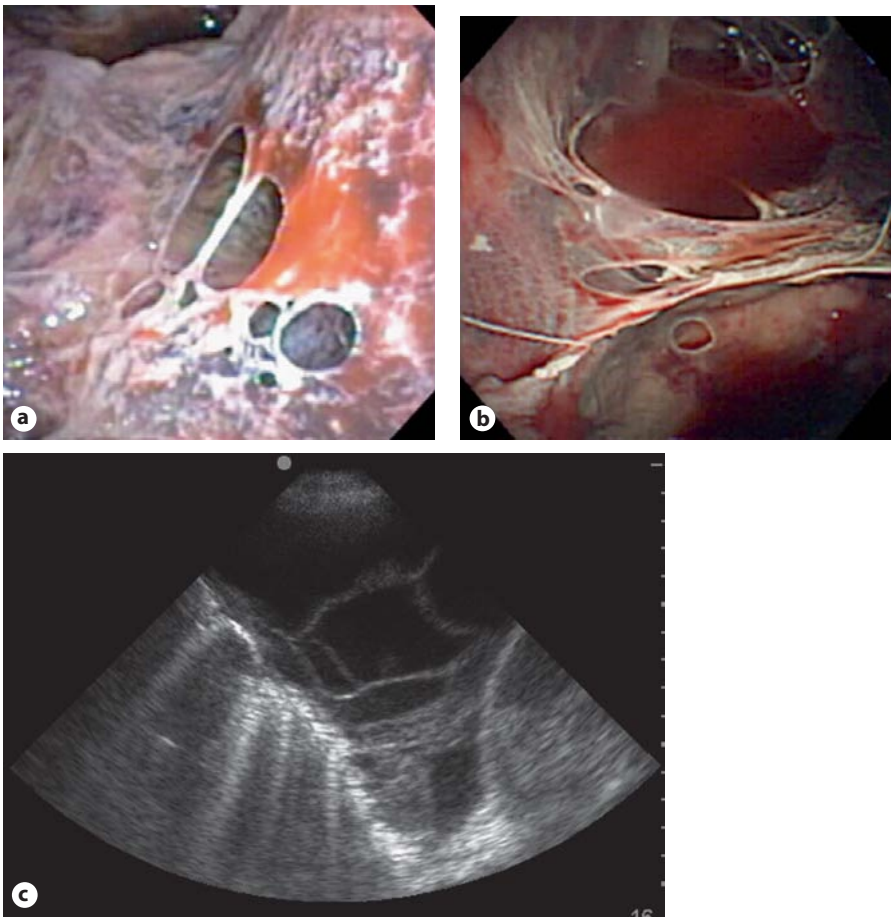

Fig. 4. Multiloculated fibrinous adhesions as seen at thoracoscopy (**a**, **b**) and the ultrasound correlate (**c**).

there are no significant adhesions between the lung and the chest wall and is definitive proof that pleural symphysis has not occurred. The clinical implication of MT is that the lung is a safe distance from the chest wall such that lung perforation or sheering of vascular adhesions by the trocar or thoracoscope at insertion is less likely. The stringent selection unfortunately also means that patients with more complicated pleural pathology, who may benefit as much or more, may not be considered candidates. In addition, the pneumothorax is induced either the day prior to the procedure or a couple of hours before the procedure. It is documented by a standard 2-view chest radiograph. This requires hospital admission the day before the procedure or a 2-phase procedure with a 2 or more hour delay to induce the pneumothorax and perform X-rays.

Knowledge of pulmonary anatomy and pathology by the pulmonologist has historically been guided by clinical examination findings and by chest radiographs. Clinicians localized pleural effusions and identified the most appropriate sites to perform thoracentesis and chest tube placement, by demonstrating dullness to percussion and absence of breath sounds corresponding to areas of complete opacification on the X-ray. Complete atelectasis of a portion of the lung or alternatively elevation of an intra-abdominal structure may manifest in a similar fashion. In fact, a recent study by Diacon et al. [11] clearly showed that ultrasound guidance for thoracentesis not only improved the rate of appropriate site selection by 26%, but also avoided accidental organ puncture in 10%. This study compared the clinical skills of physicians with varying levels of experience to transthoracic ultrasound guidance for the localization of a puncture site for thoracentesis. Of note, they found no relationship between experience and the selection of a potentially erroneous puncture site. In addition, loculation or more complex pleural disease was a risk factor for selection of an inappropriate puncture site. If real-time image guidance is recommended as adjunct to clinical examination for simple thoracentesis, it is certainly important when placing

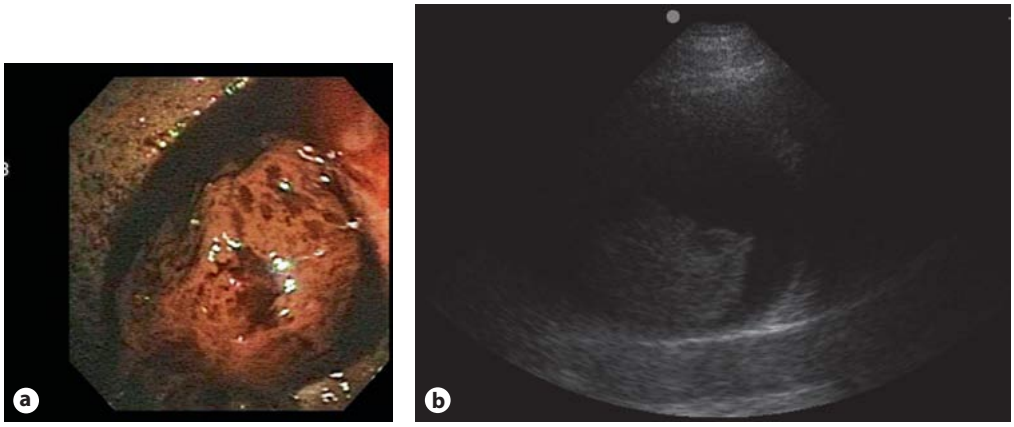

Fig. 5. Nonexpandable lung as seen at thoracoscopy (**a**) and the ultrasound correlate (**b**).

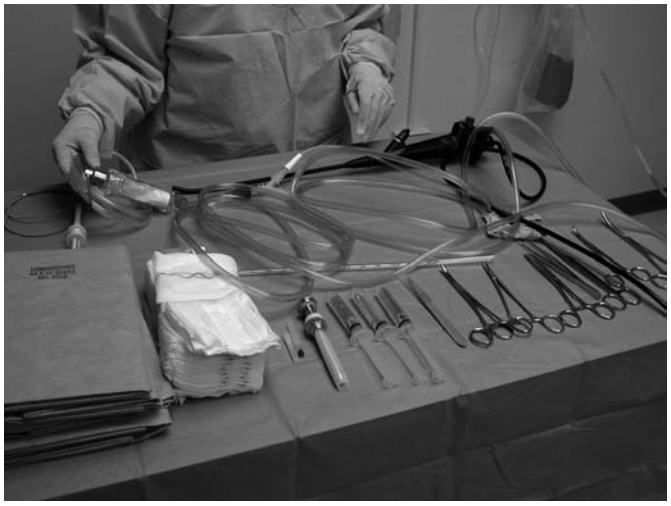

Fig. 6. Table displaying thoracoscopy equipment.

a 7- to 10-mm thoracoscope and trocar into the pleural space.

Image guidance can be performed in advance of MT or in real time. Of course the disadvantage of imaging done in advance is that the patient is unlikely to be in the thoracoscopy position at the time of the study. Also, the patient's position or limitations of the imaging technique itself may render a potential hazard difficult to identify. A chest radiograph, for example, only allows for a frontal, lateral and if requested decubitus view. The resolution is such that even complicated, vascular loculations are not necessarily identified. CT imaging has a much higher resolution and the cross-sectional images render CT a good technique to evaluate the pleura for the presence of disease. Mason et al. [12, 13] evaluated the correlation between pleural thickening on CT and the presence or absence of adhesions present at video-assisted thoracoscopy. It was postulated that the presence of adhesions may be associated with difficulty penetrating the thoracic cavity with the thoracoscopy instruments and an increase in the complication rate. Indeed they found that the presence of pleural plaques was associated with an increased risk of difficulty with the insertion of instruments. Adhesions on the other hand were identified in areas both where there was CT evidence of pleural thickening and in areas where no thickening was seen. There was an absence of adhesions at thoracoscopy in areas of pleural thickening on imaging. Also, CT failed to identify 10 cases of complete symphysis of the pleural space and either missed or wrongly identified 10/11 vascular adhesions as being nonvascular [12, 13]. In short, CT plays a limited role in the preprocedural identification of pleural symphysis and loculations/adhesions prior to video-assisted thoracoscopic surgery (VATS). As MT is sufficiently similar to VATS, it is safe to extrapolate these conclusions to MT.

Transthoracic ultrasound provides several advantages over the other imaging modalities previously described for the preprocedural assessment of the pleura. With the advent of new smaller ultrasound machines, the ultrasound can readily be performed at the bedside with the patient in the MT position. It allows the operator to evaluate the pleural space throughout the respiratory cycle, with the patient spontaneously breathing and not during a breath hold as is the case with CT. A wide variation in the position of the hemidiaphragm may be found during the respiratory cycle. As shown by Diacon et al. [11] for thoracentesis, the identification of the hemidiaphragm is the key to avoiding accidental organ puncture. This is particularly important when

considering an insertion site for the trocar and thoracoscope. Traditionally, a safe entry site was selected at a level most likely to provide a comprehensive evaluation of the pleural space. For pleural fluid the 5th interspace in the midaxillary line was often chosen. Echogenicity of fluid is markedly different from that of solid organs or even pleural thickening. This allows the quantification of pleural fluid and aids in the selection of an appropriate entry site. The fluid serves as a buffer for the lung such that it is protected from the instruments. This is particularly important in the context of a multiloculated fluid collection.

Concern exists regarding the risk of tumor seeding with the chest wall instrumentation for MT in the context of mesothelioma. Ultrasound can readily distinguish between pleural fluid and thickening. In a case suspicious for mesothelioma, it is possible to avoid entry into the hemithorax in an area of pleural thickening with the use of ultrasound. In a series of 687 patients undergoing pre-MT ultrasonography including 79 mesothelioma cases, only 3 patients (approximately 3% of mesotheliomas) developed tumor seeding of the thoracoscopy tract [14]. The incidence of seeding is markedly less than the 30–40% reported by Boutin et al. [15]. It is unclear whether the authors systematically avoided areas of focal thickening when selecting their entry site, although this would be logical.

The preprocedural identification of a fused pleural space or the presence of adhesions is key to minimizing procedural risks of MT. As stated above, CT is only at best of moderate utility in the identification of these predictors of technical difficulties. The ability to identify adhesions with ultrasound is based on the degree of visceral slide, a phenomenon first used in laparoscopic abdominal surgery. It was found that visceral adhesions could be predicted in patients where a less than 2-cm movement of intra-abdominal structures along the abdominal wall was visualized with the ultrasound [16]. Although no studies evaluating the ability of visceral slide to predict pleural symphysis and adhesions prior to MT exist, studies evaluating the benefit of ultrasound in VATS have, however, been published. It was found that the restriction of visceral slide that correlated with pleural adhesions was dependent on the region of the thorax examined. In the upper chest, a restriction of less than 1 cm with exaggerated respiratory effort is indicative of a pleural adhesion, whereas in the lung base restriction is defined as less than 2 cm. Although the sensitivity and specificity are modest 64 and 79% for the upper and 82 and 81% for the lower visceral slide, the negative predictive value is quite good at 88 and 96%, respectively [17]. The ultrasound was actually performed 1 week prior to the VATS and in the sitting position; therefore, the cutoff for a pleural slide performed at the bedside in the MT position cannot be extrapolated. A complete lack of pleural slide would be suggestive of a fused pleural space as might occur following pleurodesis.

The ability to identify adhesions as described above does correlate with the potential localization of a safe site for the thoracoscopy port. Hersh et al. [18] found that even in very complex pleural spaces, i.e. those with multiloculated effusions, a safe entry site for MT was able to be identified. The use of the ultrasound eliminated the need to induce a preprocedure pneumothorax and the requisite chest X-ray to confirm that the lung had indeed collapsed in all 20 cases. There were no procedure-related complications and the use of the ultrasound added very little time to the procedure.

The final advantage of using ultrasound prior to MT is its safety profile. The patients receive no radiation and therefore no radiation precautions are necessary for patient or operator. Ultrasound at the bedside incurs little additional cost as compared to CT or other imaging techniques and does increase the technical as well as the professional fees of the procedure.

References

1 Ernst A, Hersh C, Herth F, et al: A novel instrument for the evaluation of the pleural space: an experience in 34 patients. Chest 2002;122:1530–1534.
2 Lamy P, Canet B, Martinet Y, et al: Evaluation des moyens diagnostiques dans des épanchements pleuraux. Poumon Coeur 1980;36:83–94.
3 Sahn S: Malignant metastases to the pleura. Clin Chest Med 1998;19:351–361.
4 Diacon A, Van de Wal B, Wyser C, et al: Diagnostic tools in tuberculous pleurisy: a direct comparative study. Eur Respir J 2003;22:589–591.
5 Boutin C, Viallat J, Cargnino P, et al: Thoracosopy for malignant effusions. Am Rev Respir Dis 1981;124:588–592.
6 Tassi G, Davies R, Noppen M: Advanced techniques in medical thoracoscopy. Eur Respir J 2006;28:1051–1059.
7 Colt H: Thoracoscopy. A prospective study of safety and outcome. Chest 1995;108:324–329.
8 Blanc F, Atassi K, Bignon J, et al: Diagnostic value of medical thoracoscopy in pleural disease: a 6-year retrospective study. Chest 2002;121:1677–1683.
9 Chung C, Chen Y, Chang S: Effect of repeated thoracentesis on fluid characteristics, cytokines, and fibrinolytic activity in malignant pleural effusion. Chest 2003;123:1188–1195.
10 Mathur P, Astoul P, Boutin C: Medical thoracoscopy. Technical details. Clin Chest Med 1995;16:479–486.
11 Diacon A, Brutsche M, Soler M: Accuracy of pleural puncture sites: a prospective comparison of clinical examination with ultrasound. Chest 2003;123:436–441.

12 Mason A, Krasna M, White C: The role of radiologic imaging in diagnosing complications of video-assisted thoracoscopic surgery. Chest 1998;113:820–825.
13 Mason A, Miller B, Krasna M, et al: Accuracy of CT for the detection of pleural adhesions. Correlation with video-assisted thoracoscopic surgery. Chest 1999;115:423–427.
14 Macha H, Reichle G, von Zwehl D, et al: The role of ultrasound assisted thoracoscopy in the diagnosis of pleural disease. Eur J Cardiothorac Surg 1993;7:19–22.
15 Boutin C, Schlesser M, Frenay C, et al: Malignant pleural mesothelioma. Eur Respir J 1998;12:972–981.
16 Kodama I, Loiacono L, Sigel B, et al: Ultrasonic detection of visceral slide as an indicator of abdominal wall adhesions. J Clin Ultrasound 1992;20:375–380.
17 Sasaki M, Kawabe M, Hirai S, et al: Preoperative detection of pleural adhesions by chest ultrasonography. Ann Thorac Surg 2005;80:439–442.
18 Hersh C, Feller-Kopman D, Wahidi M, et al: Ultrasound guidance for medical thoracoscopy: a novel approach. Respiration 2003;70:299–301.

Dr. Gaëtane Michaud
Interventional Pulmonology
185 Pilgrim Road, Deaconess Suite 116
Boston, MA 02215 (USA)
Tel. +1 617 632 8252, Fax +1 617 632 8090, E-Mail gmichaud@bidmc.harvard.edu

Chapter 22

Bolliger CT, Herth FJF, Mayo PH, Miyazawa T, Beamis JF (eds): Clinical Chest Ultrasound: From the ICU to the Bronchoscopy Suite.
Prog Respir Res. Basel, Karger, 2009, vol 37, pp 189–201

Endobronchial Ultrasound for Difficult Airway Problems

Taeko Shirakawa[a] · Atsuko Ishida[a] · Yuka Miyazu[a] · Noriaki Kurimoto[b] · Yasuo Iwamoto[c] · Seiichi Nobuyama[a] · Teruomi Miyazawa[a]

[a]Division of Respiratory and Infectious Diseases, Department of Internal Medicine and [b]Division of Thoracic Surgery, Department of Surgery, St. Marianna University School of Medicine, Kawasaki, and [c]Department of Pulmonary Medicine, Hiroshima City Hospital, Hiroshima, Japan

Abstract

Radial-type endobronchial ultrasound (EBUS) is useful for a diagnosis based on the depth of invasion of bronchial carcinoma, because it has the ability to analyze the delicate layer structure of the airway wall. EBUS is the most efficient tool to establish candidates for photodynamic therapy. For laser ablation of malignant airway stenosis, EBUS information is very important in order to avoid damage of the peribronchial blood vessels and to prevent fistula formation. Real-time measurement of the airway size using EBUS can provide useful information to help with the decision of stent size, especially in the case of tracheobronchomalacia. Tracheobronchial tuberculosis causes airway stenosis and tracheobronchomalacia. EBUS reveals thickening of the submucosa. When EBUS shows damage of the cartilage of the airway, the airway cannot maintain its patency; therefore, stent placement is necessary. However, if the cartilage looks intact, the airway can be patent without stenting. Thus EBUS information is useful for strategic considerations. In Wegener's granulomatosis, EBUS shows circumferential thickening of the submucosa with intact bronchial cartilage. In relapsing polychondritis, it reveals marked thickening of the cartilage with thickening of the submucosal layer. This is confirmed by histopathology.

Endobronchial ultrasound (EBUS) extends the view of bronchoscopists through the surface of the airway to the airway wall and peribronchial structures. It makes it possible to look at the airway and its surrounding structure to provide useful information for diagnosis and therapeutic strategies. In this chapter, the role of radial-type, 20-MHz EBUS is discussed. Difficult airway problems, such as airway stenosis, airway obstruction and tracheobronchomalacia, will be discussed. At first, we would like to explain the role of EBUS in interventional procedures for treating airway stenosis caused by various diseases. Next, the role of EBUS in several benign diseases will be covered [for malignant diseases, see chapter 23, pp. 202–207].

The Role of EBUS in Airway Interventional Procedures

Airway stenosis and obstruction clinically probably represent the most serious airway problems. These are caused by various circumstances. Malignant causes include bronchial carcinoma itself, extrinsic compression by enlarged lymph nodes of cancer metastasis or malignant lymphoma, mediastinal tumor, or esophageal cancer. Benign causes are attributed to postintubation granuloma, tracheobronchial malacia caused by various situations, or Wegener's granuloma.

Diagnosis Based on Depth of Invasion of Bronchial Carcinoma and Strategic Considerations

When the cause of airway stenosis is bronchial carcinoma, the depth of tumor invasion can be assessed by EBUS [1]. Whether the tumor is restricted inside the bronchial cartilage, invading beyond the cartilage, or infiltrating the peribronchial blood vessels can be clarified. Only EBUS has the advantage of being able to describe the delicate structure of the bronchial wall. To decide on the treatment it is important to evaluate whether the tumor is within the cartilage or invading beyond the cartilage. We assessed the depth of

Table 1. Results of the assessment of bronchoscopy, HR-CT, and EBUS for endobronchial tumor

Case	Histology	Bronchoscopy			HR-CT	EBUS	Therapy	Results	Recurrence	Follow-up (mo)
		detection	Type	Size cm						
1	CIS	AFB	S	0–0.5	IV	intracartilaginous	PDT	CR	no	33
2	CIS	AFB	S	0–0.5	IV	intracartilaginous	PDT	CR	no	21
3	CIS	WLB	S	0–0.5	IV	intracartilaginous	PDT	CR	no	21
4	Sq. ca	WLB	S	0.5–1.0	IV	intracartilaginous	PDT	CR	no	45
5	Sq. ca	WLB	S	0–0.5	IV	intracartilaginous	PDT	CR	no	46
6	Sq. ca	WLB	S	0–0.5	IV	intracartilaginous	PDT	CR	no	10
7	Sq. ca	WLB	S	0–0.5	IV	intracartilaginous	PDT	CR	no	45
8	Sq. ca	WLB	N	0–0.5	IV	intracartilaginous	PDT	CR	no	46
9	Sq. ca	WLB	N	0.5–1.0	IV	intracartilaginous	PDT	CR	no	21
10	Sq. ca	AFB	S	0.5–1.0	IV	extracartilaginous	surgery		no	24
11	Sq. ca	WLB	N	0–0.5	IV	extracartilaginous	surgery		no	18
12	Sq. ca	WLB	S	0.5–1.0	IL	extracartilaginous	surgery		no	48
13	Sq. ca	WLB	P	0.5–1.0	IL	extracartilaginous	surgery		no	7
14	Sq. ca	WLB	P	1.5–2.0	IL	extracartilaginous	PDT + RT	CR	no	45
15	Sq. ca	WLB	S	0.5–1.0	EL	extracartilaginous	PDT + CT + RT	CR	no	11
16	Sq. ca	WLB	P	1.0–1.5	EL	extracartilaginous	surgery		no	21
17	Sq. ca	WLB	P	1.0–1.5	EL	extracartilaginous	PDT + CT	CR	no	18
18	Sq. ca	WLB	P	1.0–1.5	EL	extracartilaginous	surgery		no	16

AFB = Autofluorescence bronchoscopy; CIS = carcinoma in situ; CR = complete response; CT = chemotherapy; EL = sings of extraluminal tumor; extracartilaginous = tumor invasion is beyond the cartilage; IL = strictly intraluminal tumor; intracartilaginous = tumor invasion is within the mucosa and/or submucosa; IV = invisible; N = nodular type; P = polypoid type; PDT = photodynamic therapy; RT = radiotherapy; S = superficial type; Sq. ca = squamous cell carcinoma; WLB = white light bronchoscopy.

invasion of bronchial carcinoma in the central airway by EBUS [2]. We intended to evaluate the use of EBUS in selecting appropriate candidates with centrally located early-stage lung cancer for photodynamic therapy (PDT) with curative intent. We performed EBUS before PDT in 18 biopsy-proven squamous cell carcinomas (including three carcinomas in situ) that had been considered to be appropriate candidates for PDT by conventional bronchoscopy and high-resolution computed tomography (HR-CT). We decided that when the tumor remained inside the cartilage, PDT should be applied and when the tumor extended beyond the cartilage, a surgical procedure should be used. Nine lesions were diagnosed by EBUS as intracartilaginous and subsequently PDT was performed. Long-term complete remission was achieved in these patients with a median follow-up term of 32 months after PDT. This result is much better than that of other reports without a diagnosis by EBUS based on the depth of tumor invasion [3–5]. The remaining nine lesions were diagnosed by EBUS as extracartilaginous and were considered candidates for other therapies such as surgical resection, chemotherapy, and radiotherapy, although two were invisible by HR-CT, three were superficial, and five were <1 cm in diameter on observation by bronchoscopy (table 1; fig. 1). The depth of tumor invasion estimated by EBUS was proven to be accurate by histopathologic findings in six specimens after surgical resection. Whether PDT will achieve complete remission in a patient greatly depends upon accurate patient selection based on the exact assessment of the dimensions of a tumor. The depth of tumor invasion is an important factor for the success of PDT as well as tumor location, size, and lack of nodal involvement. Tumors with extracartilaginous invasion have been reported to have intrapulmonary lymph node and hilar lymph node metastases in 6.4% of cases [6]. On the other hand, if there is no extracartilaginous invasion, there is little likelihood of metastasis [6]. This indicates that it is important to treat tumors by PDT with curative intent only if they remain intracartilaginous, that is limited within the mucosa and submucosa. It is difficult to detect early-stage superficial cancers by conventional white light bronchoscopy because these lesions are only a few mucosal layers thick and a few

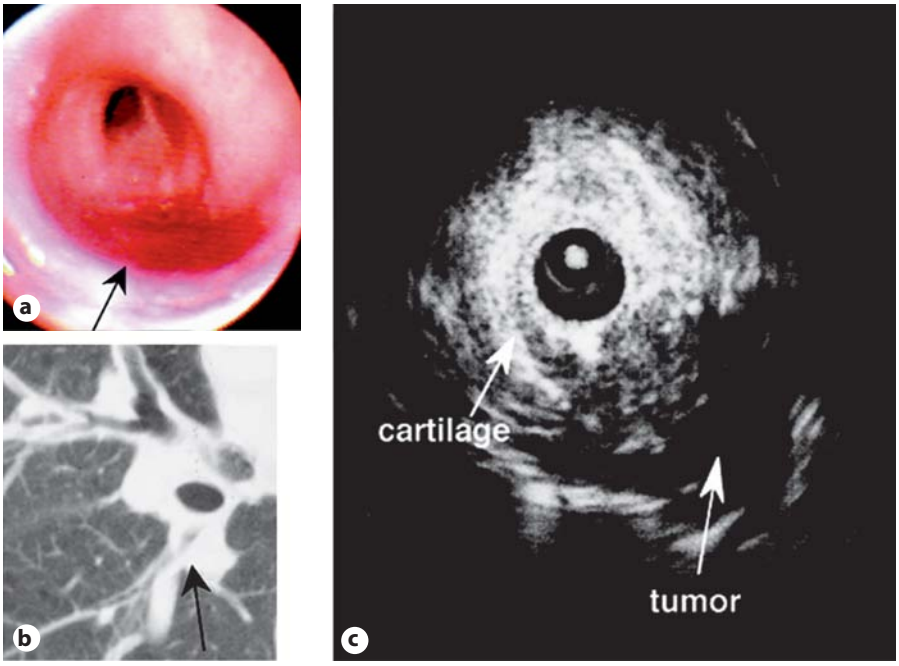

Fig. 1. A case of squamous cell carcinoma at the orifice of the right B6. **a** The bronchoscopic view shows a reddish superficial tumor at the orifice of B6 (arrow) of 0.5–1.0 cm in diameter. **b** HR-CT shows an obscure lesion at the site. Because there was little contrast between it and surrounding mediastinal connective tissue, we diagnosed it as invisible. **c** EBUS can delineate the tumor (arrow) and shows that the cartilage layer is involved and interrupted around the tumor. Therefore, the tumor was diagnosed as extracartilaginous.

millimeters in surface diameter. Autofluorescence bronchoscopy has been used for detecting and localizing early-stage lung cancer and for categorizing the extent of endobronchial spread of lung cancer. However, the view by autofluorescence bronchoscopy is limited to the lumen and the internal surface of the airways [7]. HR-CT has been reported to provide more accurate information about tumor extension than conventional CT scan in patients with early-stage lung cancer who were referred for bronchoscopic treatment [8, 9]. Strictly intraluminal tumors on HR-CT could be achieved with a high rate of complete response after bronchoscopic treatment [8–10]. Therefore, HR-CT might help to estimate the depth of tumor invasion in patients with early-stage lung cancer. However, in this study, EBUS offered more accurate information regarding the depth of tumor invasion than bronchoscopy or HR-CT. For the decision on whether to use PDT, it is necessary to assess the depth of tumor invasion. To date, the most promising way to estimate this depth might be EBUS since other diagnostic imaging techniques do not show it.

Tumor Ablation

In the case of airway stenosis, we frequently perform airway dilatation with Nd-YAG laser or argon plasma coagulation (APC). In such cases, with the help of EBUS we can establish to what extent the ablation should be performed. After detecting bronchial cartilage by EBUS, tumor ablation could be stopped inside the cartilage to avoid injury to the cartilage. Furthermore, EBUS gives us the opportunity to see the peribronchial blood vessels, so that we can avoid damaging them and causing serious complications. Without EBUS guidance, this procedure might cause fistulas and severe bleeding [11, 12]. We experienced several cases of malignant airway stenosis which required airway dilatation by APC ablation. During these procedures, we repeatedly observed airway tumor and peribronchial blood vessels by EBUS and avoided fistula formation and injury of blood vessels. Thereafter, we successfully placed the stent.

Becker and Herth [12] reported a case of complete obstruction of the left main bronchus by exophytic bronchial carcinoma. In this case, they were able to differentiate between the basis and the surface of the tumor, and they could assess the depth of invasion into the bronchial wall and into the mediastinum. By passing the stenosis, they could assess the patency of the distal airways. This information was of importance for endoluminal disobliteration, especially if they could prove simultaneously that the pulmonary artery was not occluded. When occluding a central airway, perfusion of one lung may be completely

shut down due to the Euler-Liljestrand reflex. In this case, the perfusion scan is unable to prove organic occlusion of pulmonary artery, and usually pulmonary angiography has to be performed, because bronchial recanalization in cases of complete occlusion of the pulmnonary artery would only increase dead space ventilation. In some patients, on the other hand, they could demonstrate direct invasion of the pulmonary artery or complete occlusion which could be confirmed by angiography or postoperative pathological examination.

Stent Placement

If the usual size bronchoscope (6 mm) cannot be inserted into the peripheral side of the airway stenosis and bronchoscopic observation is impossible, in many cases an EBUS probe can be inserted to make observation by EBUS possible. According to EBUS findings, we can assess whether the peripheral bronchus is patent or not [12]. This is especially important for stent placement.

Using EBUS, we are able to measure the length and degree of the stenosis. Thus, EBUS can provide useful information for helping to decide on the size of the stent. The size of stent is also estimated by information from three-dimensional (3D)-CT. However, using EBUS, the size of the airway can be measured in real time during the bronchoscopic procedure. When the EBUS probe is retrieved from the distal side of the stenosis to the proximal side with the balloon inflated, the shape of the balloon changes according to the degree of stenosis. Therefore, we can assess the diameter of the airway by measuring the balloon size (fig. 2). Then according to the measurement of the size of the airway, we can decide on the size of the stent. This method is useful for malignant stenosis after laser ablation and balloon dilatation; the size of the airway changes from the measurement by CT taken before the interventional procedure. Especially in long and complicated stenosis, measurement with EBUS is helpful.

For cases of tracheobronchomalacia, stent size should be selected after assessment with EBUS. By inflating the balloon of the sheath applied to the EBUS probe, the collapsed airway could be dilated. Thereafter, by measuring the size of the balloon on the EBUS image, it is possible to establish the suitable size of the stent.

It is an advantage that EBUS describes the delicate layer structure of the airway, so that the airway cartilage can also be clearly observed [1, 12–14]. For the cases of tracheobronchial tuberculosis, it is important to judge whether the cartilage remains intact or damaged. When the cartilage remains intact, it is possible to remove the stent. But when the cartilage is destroyed, the stent is necessary. In such cases, if the stent is removed, the airway may collapse [15].

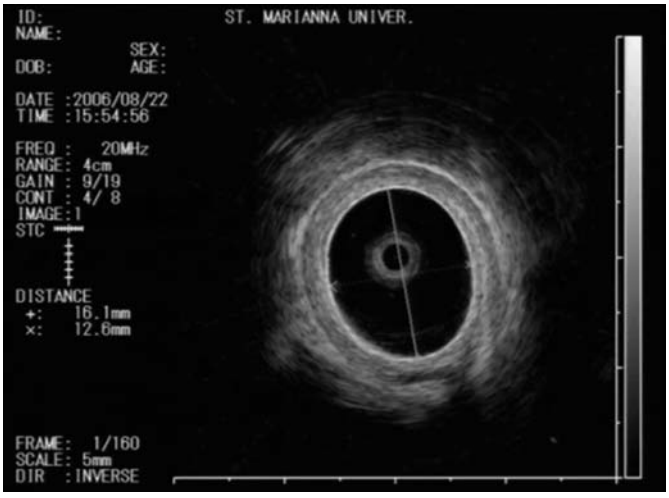

Fig. 2. A case of tracheal stenosis due to malignant lymphoma. The size of the normal portion of the trachea is measured by EBUS (indicated by two arrows). In this way the size of the stent is evaluated.

Airway Problems Caused by Malignant Diseases and EBUS

This topic is discussed in chapter 23, pp. 202– 207.

Airway Problems Caused by Benign Diseases and EBUS

Tracheobronchial Tuberculosis

Tuberculous tracheobronchial stenosis is a serious clinical problem because it can cause obstructive pneumonia and dyspnea on exertion. Surgical resection and bronchoplastic reconstruction have long been the standard treatment. More recently, a variety of interventional bronchoscopic techniques have been developed, including stent placement, laser photoresection, APC, balloon dilatation, and cryotherapy. The development and refinement of various airway stents and increased experience have broadened the indications for these procedures. However, indications of stents for tuberculous tracheobronchial stenosis are difficult to establish as it is a benign disease. When tracheobronchial tuberculosis is observed with EBUS, in some

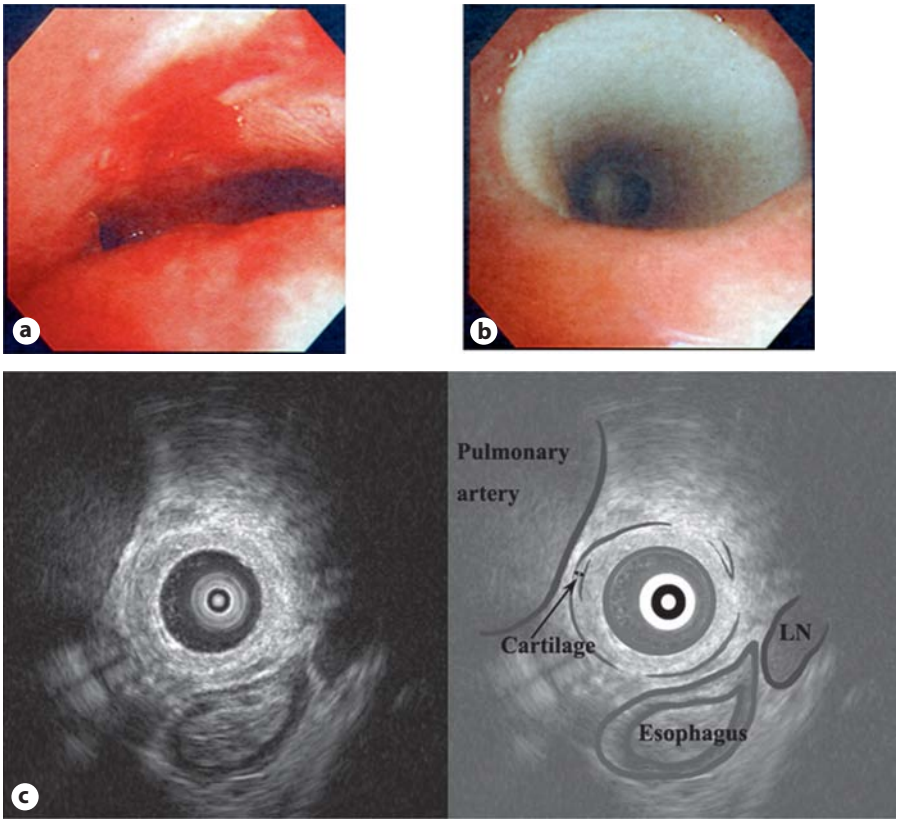

Fig. 3. A case of tracheobronchial tuberculosis. **a** Rigid bronchoscopy revealed a dynamic collapse of the trachea. **b** Bronchoscopic examination after placement of the Dumon Y stent shows restored patency of the trachea. **c** Before stenting, on visualizing the layers of the tracheal wall by EBUS, the normal horseshoe-shaped cartilage could not be seen over a distance of 4 cm from the carina to the main bronchus. EBUS imaging shows the interruption of the tracheal cartilage. LN = Lymph node.

cases mucosa is thick circumferentially. This means the mucosa of the cartilaginous part as well as the membranous part is thick, and the cartilage looks interrupted. We reported 12 cases of tracheobronchial tuberculosis. We performed EBUS in 4 of these cases, in 2 of which we observed an interruption of the cartilage (fig. 3, 4). All cases had severe airway stenosis and tracheobronchomalacia. A Dumon stent was placed in all cases. There were another 2 cases with mucosal thickness, but the cartilage was intact. In 1 of these 2 cases, a Dumon stent was placed. However, it was retrieved 2 months later due to granulation. After the retrieval of the Dumon stent, the airway remained patent, meaning that the cartilage is intact and the airway would not collapse but would remain patent (fig. 5). Therefore, the use of EBUS for the investigation of cartilage makes it possible to assess whether a stent is permanently necessary or whether it can be removed. After the report, we experienced many cases. Now we evaluate the cartilage with EBUS and when it looks intact, we perform only balloon dilatation (fig. 6). When we observe an interruption of cartilage, we place a stent (fig. 7). We find that the study of cartilage with EBUS is mandatory to evaluate whether a stent is necessary or not.

Wegener's Granulomatosis

Wegener's granulomatosis is a disease of unknown etiology characterized by necrotizing granulomatous vasculitis. While it is recognized that the disease can involve any organ in the body, the lungs are usually affected [16]. Up to 60% of patients with Wegener's granulomatosis in whom bronchoscopy was performed may have endobronchial abnormalities of the central airways [17, 18]. We performed EBUS in 2 patients. Bronchoscopy in the first case revealed diffuse, circumferential, irregular edema and erosion of the tracheobronchial tree (fig. 8a). EBUS showed circumferential thickening of the bronchial wall due to submucosal edema. The cartilage layer was intact (fig. 9a, b). The bronchoscopy of the second case revealed annual scarring with stricture of the right main bronchus (fig. 8c). EBUS showed circumferential thickening of the submucosa with intact bronchial cartilage (fig. 9c, d). In both cases, thickening of the tracheobronchial wall included the posterior portion as inflammation took place within the submucosa.

Wegener's granulomatosis along with tracheobronchial tuberculosis, relapsing polychondritis (RP), amyloidosis, and inflammatory bowel disease-related tracheobronchitis

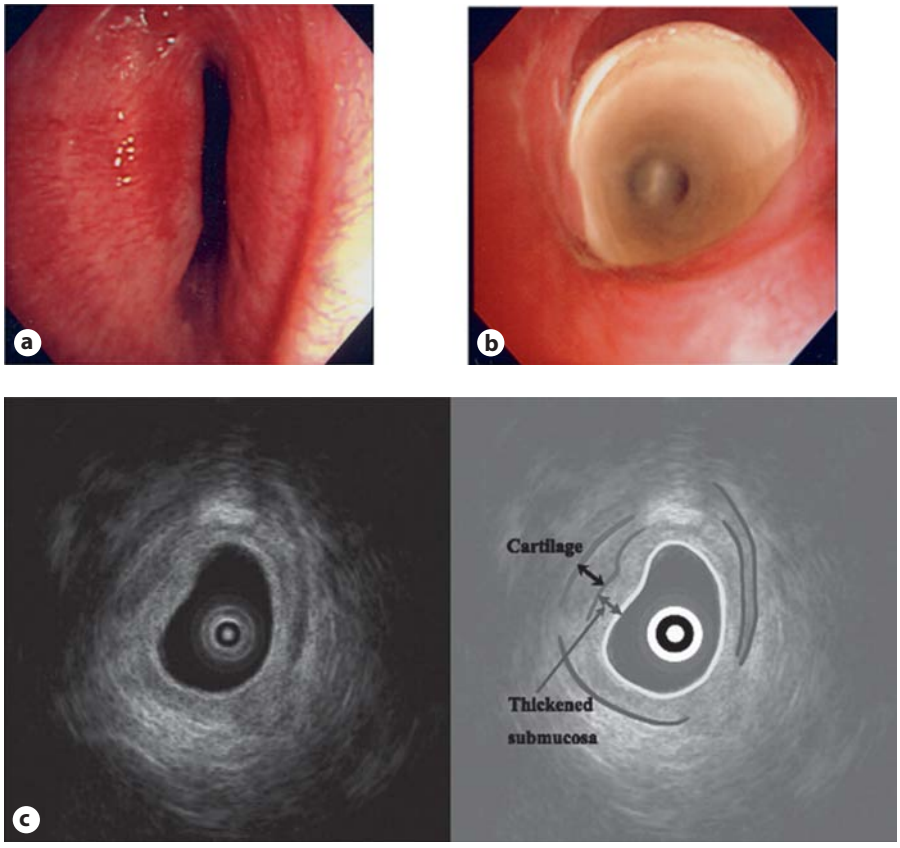

Fig. 4. A case of tracheal tuberculosis. **a** Bronchoscopic examination shows a slit-like tracheal stenosis. **b** To prevent suffocation, we placed a Dumon Y stent. Bronchoscopic examination shows a reestablishment of patency after stenting. **c** EBUS imaging shows an interruption of the cartilage of the trachea and a thickening of the tracheal wall.

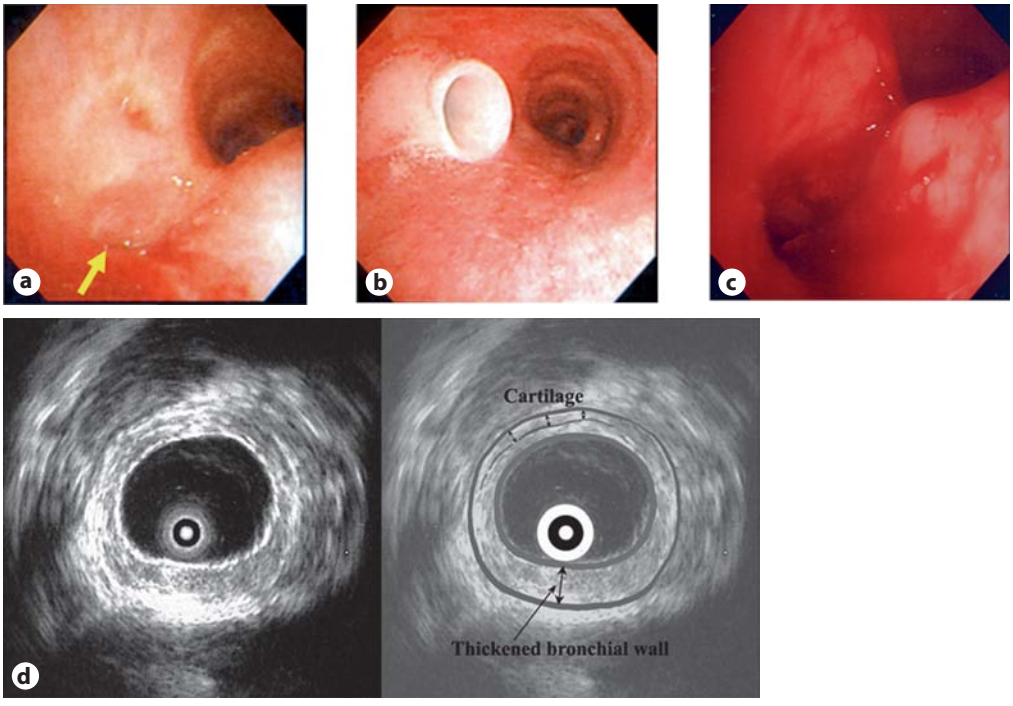

Fig. 5. A case of bronchial tuberculosis with three episodes of obstructive pneumonia. **a** Bronchoscopy revealed a central pin hole stenosis of the left main bronchus. **b** Bronchoscopic examination after the placement of a Dumon stent shows correct positioning of the stent. **c** One year later, we removed the stent, and the patient remained asymptomatic. Bronchoscopic examination after removal of the stent shows restored patency of the left main bronchus. **d** EBUS imaging shows the thickening of the bronchial wall and intact bronchial cartilage.

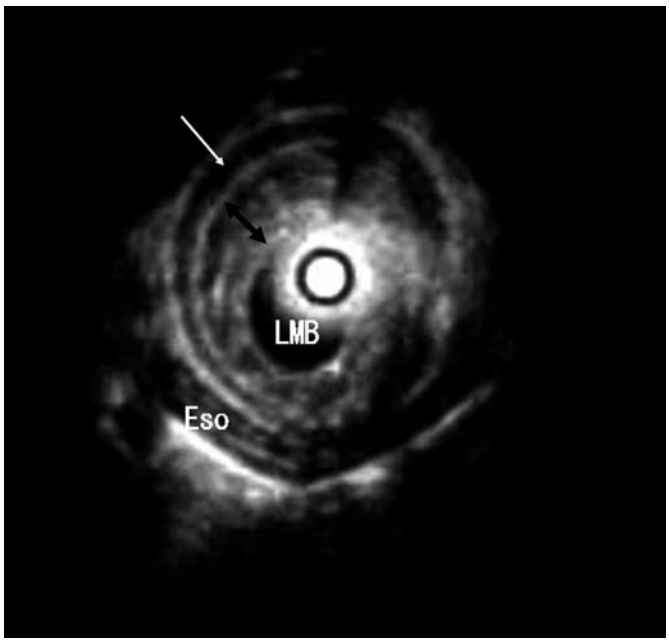

Fig. 6. A case of bronchial tuberculosis. EBUS image of the left main bronchus reveals the stenosis. The mucosa is circumferentially thick (black arrow). However, the cartilage remains intact with a horseshoe-shaped appearance (white arrows). Therefore we only performed balloon dilatation and did not place a stent. LMB = Left main bronchus; Eso = esophagus

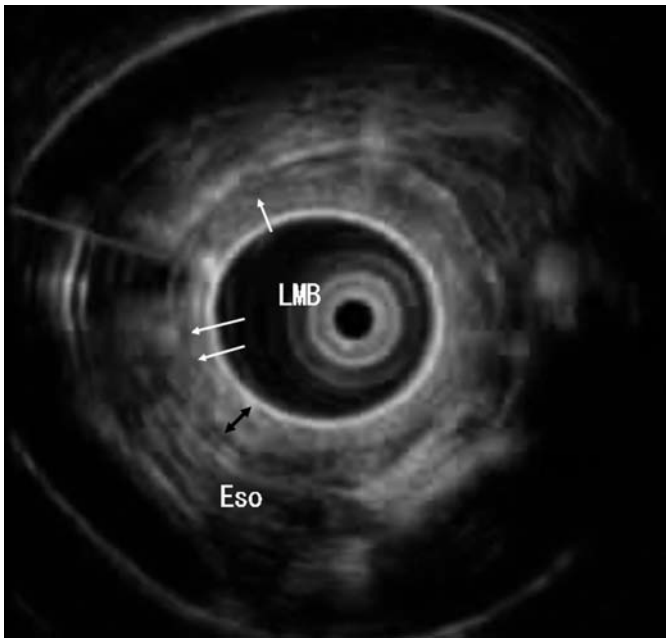

Fig. 7. A case of bronchial tuberculosis. The EBUS image of the left main bronchus shows the cobblestone-like degeneration of the cartilage (white arrow). The submucosa is circumferentially thick, including a membranous portion as well as a cartilaginous portion (black arrow). LMB = Left main bronchus; Eso = esophagus.

can cause diffuse inflammatory changes within the central airways. Diagnosis of these diseases can be suggested by noting the portion of the airway wall that is affected. In RP, for instance, thickening of the tracheobronchial wall is limited to the cartilaginous portion (anterior and lateral walls) while the posterior membranous portion is usually spared because the inflammation occurs mainly within cartilage. In contrast, in Wegener's granulomatosis, EBUS shows circumferential thickening of the tracheobronchial wall including the posterior portion as inflammation occurred within the submucosa.

To assess the condition of the tracheobronchial cartilage and submucosa the use of CT, MRI and EBUS might be considered. Of these, only EBUS shows the tracheobronchial wall as a layered structure, clearly indicating that the second layer is the submucosal layer, and the third and fourth layers are the tracheobronchial cartilage [1]. We consider EBUS to be the best method to assess thickness or other abnormalities of the submucosal layer and cartilage.

In the management of severe tracheobronchial stenosis related to Wegener's granulomatosis, debulking with the tip of a rigid bronchoscope, Nd-YAG laser application, and stent placement have been employed; however, silicone stent placement seems to provide the best results [17]. Mitomycin C is a potent fibroblast inhibitor, and since it prevents granulation response when applied topically, it is considered useful for granulation management in inflammatory tracheobronchial stenosis and may be preferred over airway stents which always carry the risk of complications.

Relapsing Polychondritis

RP is a rare disease of unknown etiology. Cartilage such as ears, nose and respiratory tract is systematically affected. Recurrent chondritis, especially in tracheobronchial cartilage, leads to respiratory failure. RP with tracheobronchial involvement has a poor prognosis, and a delay in diagnosis increases morbidity and mortality; however, it is difficult to make a diagnosis. The diagnosis of RP usually depends on a constellation of clinical and histological features caused by chondritis [19–21]. According to McAdams et al. [19], if patients have at least three of the following six signs the diagnosis is conclusive: bilateral auricular chondritis, nonerosive inflammatory polyarthritis, nasal chondritis, ocular inflammation, laryngotracheobronchial chondritis, and audiovestibular damage. The modified criteria were

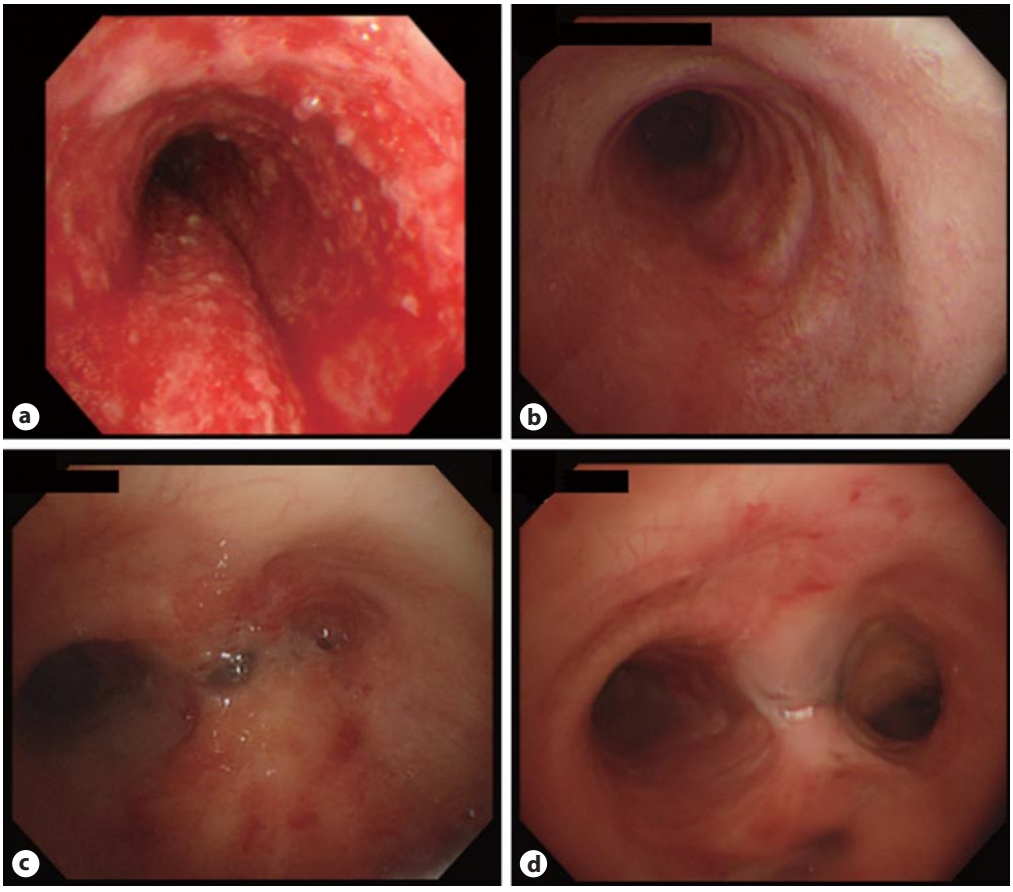

Fig. 8. Two cases of Wegener's granulomatousis. **a** Bronchoscopic view of the left main bronchus of the first case before treatment shows erosive and edematous. **b** After treatment with prednisolone and cyclophosphamide, the first case is almost normal. **c**, **d** Bronchoscopic intervention in the second case. Although the right main bronchus shows a pin hole stenosis on admission, it opens successfully after balloon dilatation and application of mitomycin C.

proposed by Damiani and Levine [20]: one or more of the criteria of McAdams et al. [19] with histologic confirmation or chondritis at least in two distinct locations with therapeutic response.

We would like to briefly outline two cases of RP. The first case is a 72-year-old man. Chest X-ray and 3D-CT revealed stenosis especially of the right intermediate bronchus (fig. 10). We can see on the MRI that T_2 shows airway cartilage much more clearly than T_1. The cartilage seems to have thickened (fig. 11). On CT, the cartilaginous portion of the airway wall is very thick, but the membranous part looks intact. Endoscopy shows that the airway becomes narrow during expiration. EBUS reveals that the right intermediate bronchus is extremely narrow, and compared to normal, the wall, especially the low echoic portion of the cartilage, is very thick. There is thickening of the tracheobronchial cartilage as well as submucosal layer. Its surface is irregular. Some high echoic parts can also be seen. The membranous portion is intact (fig. 12, online suppl. video 1). This EBUS finding of the thickening of the cartilage layer in the trachea was confirmed by histopathology (fig. 13).

The second case is a 37-year-old man. CT reveals that the cartilaginous portions of the central airway look thickened (fig. 14). EBUS also reveals thickening of the airway wall. In the trachea, the hypoechoic cartilage layer is very thick, including some high echoic parts. The membranous portion is intact (fig. 15). The histopathology also shows thickening of the cartilage, indicating degeneration and regeneration (fig. 16).

Therefore, we believe that thickening of the tracheobronchial wall, including submucosal layer and cartilage layer, is characteristic of EBUS of RP. The thickening of the tracheobronchial wall is limited to the cartilaginous portion (anterior and lateral walls) while the posterior membranous portion is usually spared because the inflammation occurs

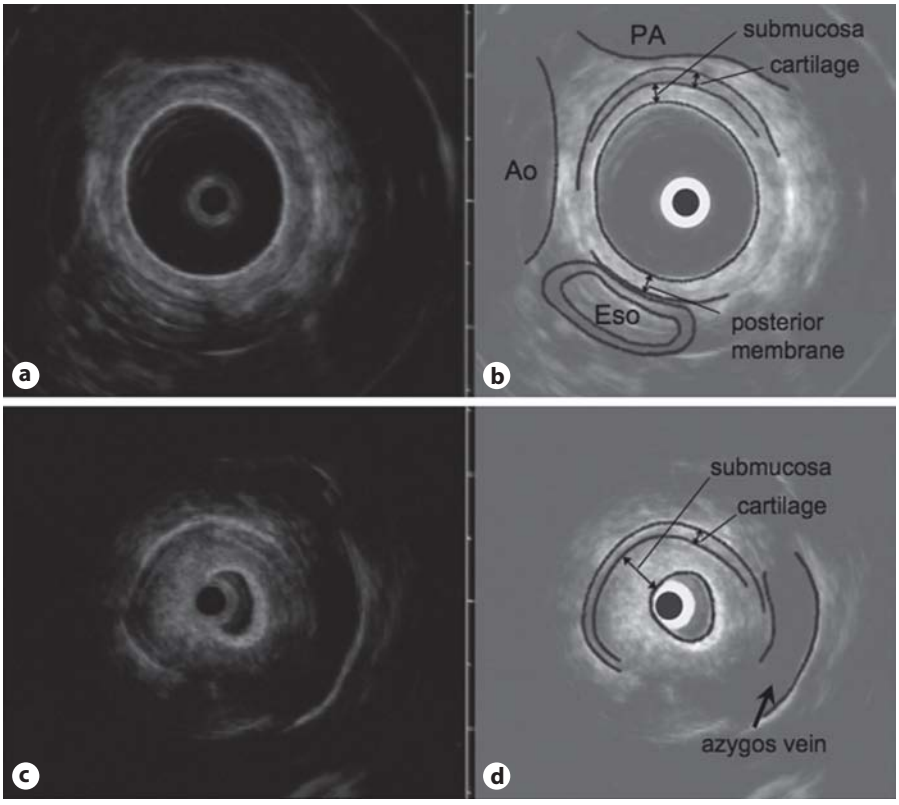

Fig. 9. a EBUS image of the first case. **b** Detail of **a**. EBUS from the left main bronchus shows concentric thickening of the bronchial wall including the posterior portion due to submucosal edema, and the cartilage layer is intact. **c** EBUS image of the second case. **d** Detail of **c**. The right main bronchus shows circumferential thickening of submucosa with the bronchial cartilage intact. PA = Pulmonary artery; Ao = aorta; Eso = esophagus.

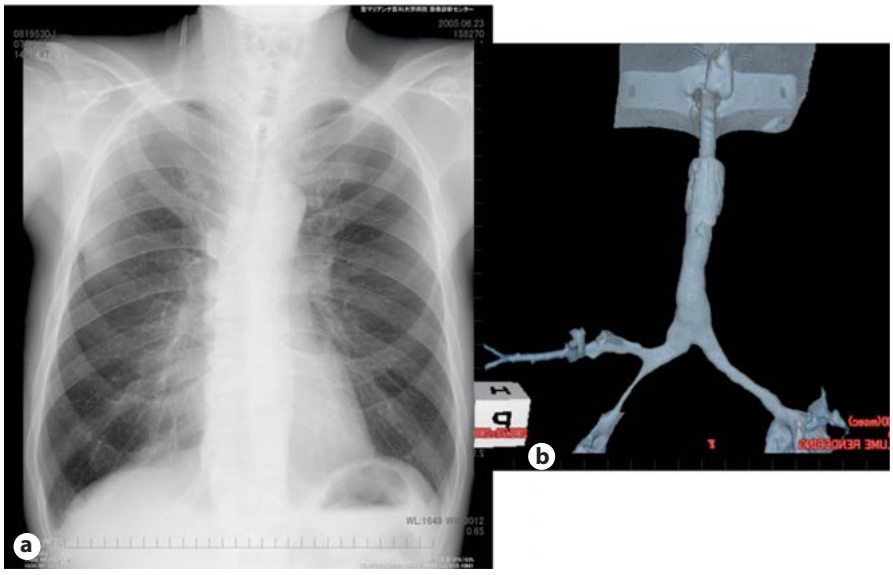

Fig. 10. The first case of RP. **a** Chest X-ray shows the stenosis of the trachea. **b** 3D-CT shows marked stenosis of the central airways, especially of the intermediate bronchus.

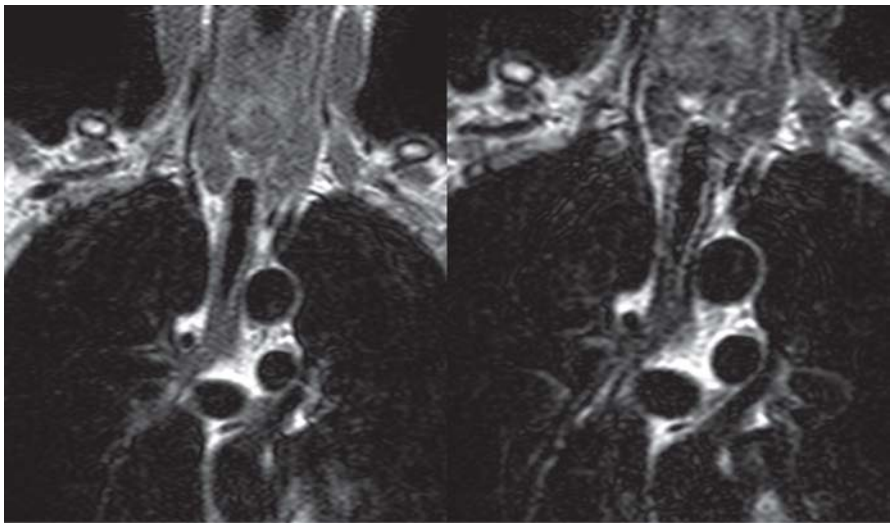

T_1 T_2

Fig. 11. MRI of the first case. On T_2, the cartilage appears much clearer than on T_1. Furthermore, the cartilage appears to be thickened.

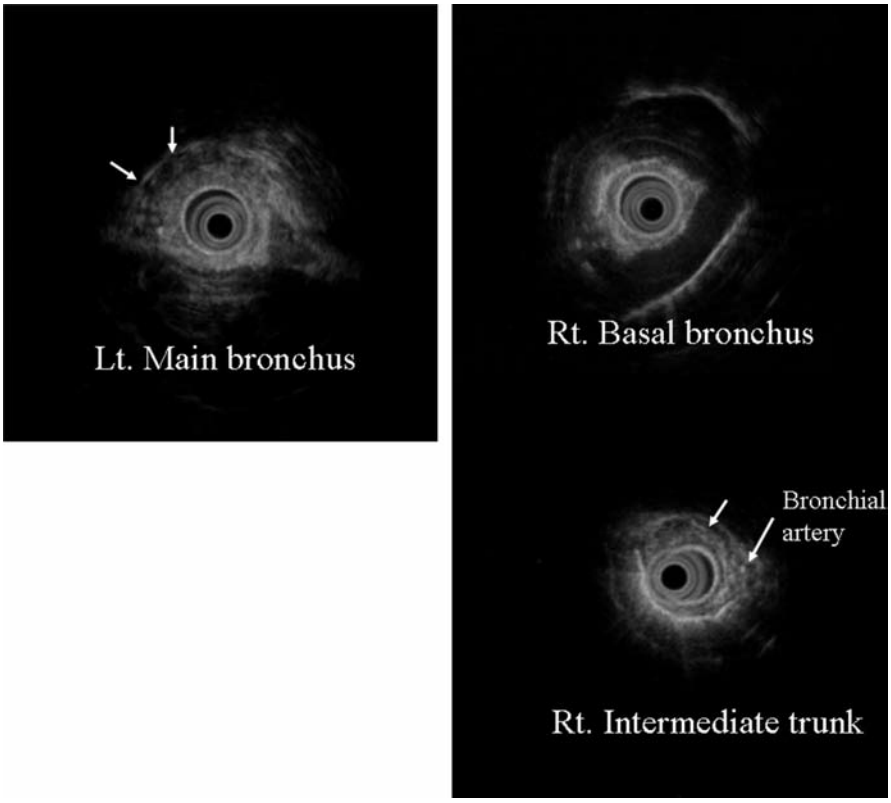

Fig. 12. EBUS of the first case. The right intermediate bronchus and the left main bronchus are extremely stenotic. Compared to the relatively normal right basal bronchus, the cartilage of the intermediate bronchus and the left main bronchus is very thick and its echogenicity is irregularly increased. Its surface is irregular (arrows). The submucosal layer is also thick.

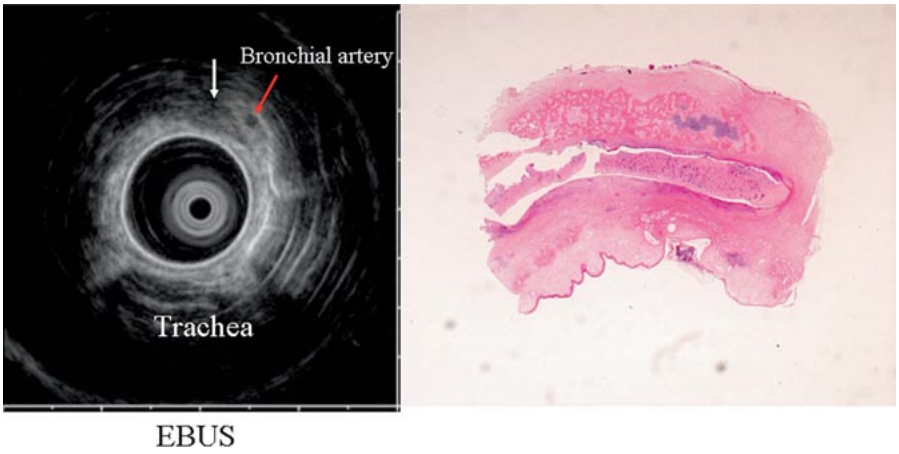

Fig. 13. EBUS (**a**) and histopathology (**b**, HE stain) of the trachea of the first case. EBUS shows that the tracheal cartilage is thick and has an irregular surface. Some high echoic parts are seen in the cartilaginous part. The histopathology reveals inflammation of the cartilage. Around the inflammation, regenerated cartilage can be seen and as a result, the cartilage becomes thick.

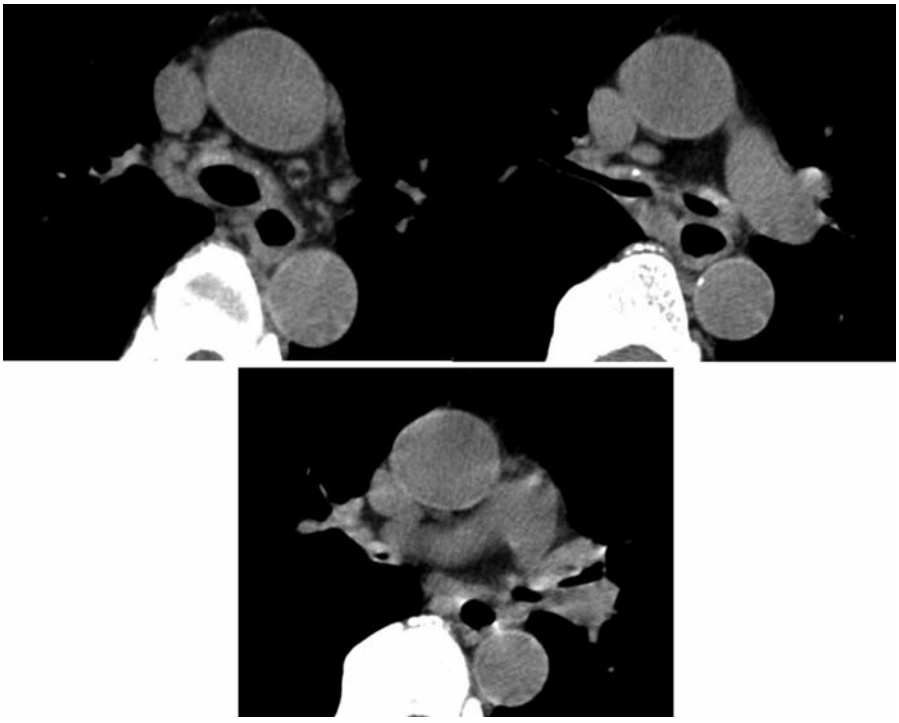

Fig. 14. CT of the second case reveals that the cartilaginous portions of the central airway look thickened; on the other hand, the membranous portions seem to be normal.

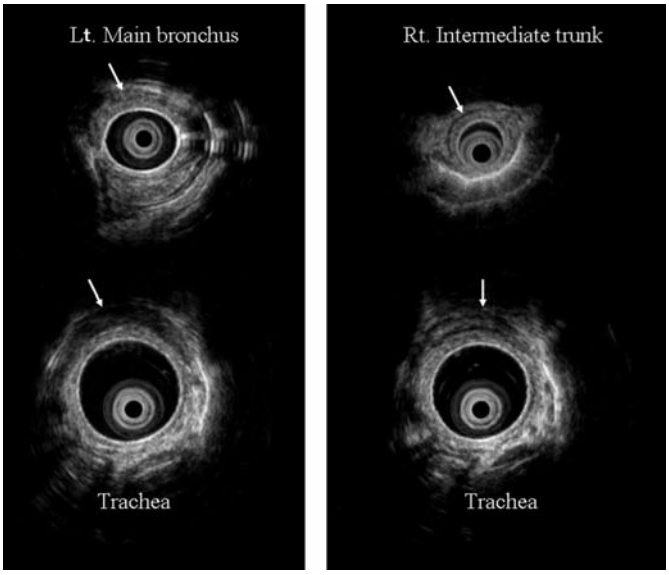

Fig. 15. EBUS of the second case. The left main bronchus and intermediate bronchus are narrow. The hypoechoic cartilage layers are thick (arrows). In the trachea, some high echoic parts are seen in the cartilage layer.

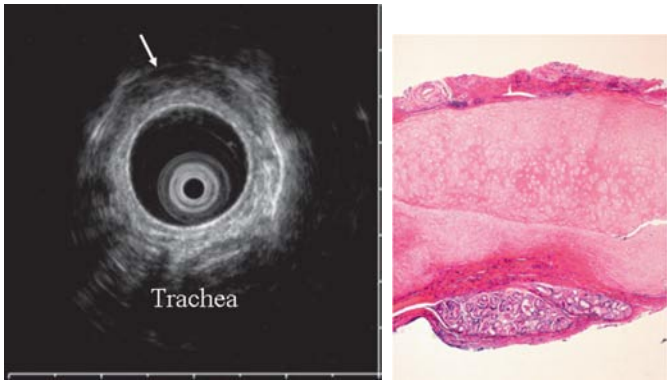

Fig. 16. The histopathology (HE stain) of the second case also shows infiltration of the inflammatory cells and thickening of cartilage, indicating degeneration and regeneration.

mainly within the cartilage. This is the difference between RP and Wegener's granulomatosis which shows circumferential thickening including the membranous portion.

In addition, if degeneration of the cartilage progresses due to repeated inflammation, EBUS shows destruction of the cartilage. The hyperechoic third and fifth layers of the bronchial wall become obscure. When degeneration progresses further, cartilage is completely destroyed, with the result that it is impossible to see the hypoechoic cartilage layer on EBUS.

At present, histological confirmation is necessary for the diagnosis of RP. However, taking a biopsy of tracheobronchial cartilage is an invasive procedure. Therefore, we hope that in future, EBUS findings will be included among the diagnostic criteria. In addition, EBUS findings may provide useful information for the decision on treatment. When degeneration of the cartilage is not so severe, we do not recommend placing a stent. We suggest trying to reduce inflammation by administering steroids. In order to avoid suffocation, tracheotomy may be performed and noninvasive positive pressure ventilation may be introduced. When the inflammation extends toward the main bronchi and more peripheral bronchi, and degeneration of the cartilage appears to be severe, stent placement should be considered in order to avoid suffocation.

References

1 Kurimoto N, Murayama M, Yoshioka S, Nishisaka T, Inai K, Dohi K: Assessment of usefulness of endobronchial ultrasonography in determination of depth of tracheobronchial tumor invasion. Chest 1999;115:1500–1506.

2 Miyazu Y, Miyazawa T, Kurimoto N, Iwamoto Y, Kanoh K, Kohno N: Endobronchial ultrasonography in the assessment of centrally located early-stage lung cancer before photodynamic therapy. Am J Respir Crit Care Med 2002;165:832–837.

3 Edell E, Cortese A: Photodynamic therapy in the management of early superficial squamous cell carcinoma as an alternative to surgical resection. Chest 1992;102:1319–1322.

4 Furuse K, Fukuoka M, Kato H, Horai T, Kubota K, Kodama N, Kusunoki Y, Takifuji N, Okunaka T, Konaka C, Wada H, Hayata Y: A prospective phase II study of photodynamic therapy with photofrin II for centrally located early-stage lung cancer. J Clin Oncol 1993;11:1852–1857.

5 Mathur PN, Edell E, Sutedja T, Vergnon JM: Treatment of early stage non small cell lung cancer. Chest 2003;123:176S–180S.

6 Saito Y, Nagamoto N, Ota S, Sato M, Sagawa M, Kamma K, Takahashi S, Usuda K, Endo C, Imai T: Results of surgical treatment for roentgenographically occult bronchogenic squamous cell carcinoma. J Thorac Cardiovasc Surg 1992;104:401–407.

7 Miyazu Y, Miyazawa T, Iwamoto Y, Kano K, Kurimoto N: The role of endobronchial ultrasonography in choice of appropriate therapy for bronchial cancer. J Bronchol 2001;8:10–16.

8 Sutedja G, Gording RP, Postmus PE: High resolution tomography in patients referred for intraluminal bronchoscopic therapy with curative intent. Eur Respir J 1996;9:1020–1023.

9 van Boxem TJ, Golding RP, Venmans BJ, Postmus PE, Sutedja TG: High-resolution CT in patients with intraluminal typical bronchial carcinoid tumors treated with bronchoscopic therapy. Chest 2000;117:125–128.

10 van Boxem TJ, Venmans BJ, Postmus PE, Sutedja TG: Curative endobronchial therapy in early-stage non-small cell lung cancer. J Bronchol 1999;6:198–206.

11 Herth F, Becker HD, LoCicero J 3rd, Ernst A: Endobronchial ultrasound in the therapeutic bronchoscopy. Eur Respir J 2002;20:118–121.

12 Becker HD, Herth F: Endobronchial ultrasound of the airways and the mediastinum; in Bolliger CT, Mathur PN (eds): Interventional Bronchoscopy. Prog Respir Res. Basel, Karger, 2000, vol 30, pp 80–93.

13 Becker HD, Messerschmidt E, Schindelbeck F: Endobronchial ultrasound. Pneumologie 1997;51:620–629.

14 Shirakawa T, Miyazawa T, Becker HD: The layer structure of the central airways as described by endobronchial ultrasonography (EBUS). J Bronchol 2008;15:129–133.

15 Iwamoto Y, Miyazawa T, Kurimoto N, Miyazu Y, Ishida A, Matsuo K, Watanabe Y: Interventional bronchosocpy in the management of airway stenosis due to tracheobronchial tuberculosis. Chest 2004;126:1344–1352.

16 Hoffman GS, Kerr GS, Leavitt RY, Hallahan CW, Lebovics RS, Travis WD, Rottem M, Fauci AS: Wegener granulomatosis: an analysis of 158 patients. Ann Intern Med 1992;116:488–498.

17 Daum TE, Specks U, Colby TV, Edell ES, Brutinel MW, Prakash UB, DeRemee RA: Tracheobronchial involvement in Wegener's granulomatosis. Am J Respir Crit Care Med 1995;151:522–526.

18 Cordier JF, Valeyre D, Guillervin L, Loire R, Brechot JM: Pulmonary Wegener's granulomatosis. A clinical and imaging study of 77 cases. Chest 1990;97:906–912.

19 McAdams LP, O'Hanlan MA, Bluestone R: Relapsing polychondritis: prospective study of 23 patients and a review of the literature. Medicine 1976;55:193–215.

20 Damiani JM, Levine HL: Relapsing polychondritis: report of ten cases. Laryngoscope 1979;89:929–946.

21 Sarodia BP, Dasgupta MD, Mehta AC: Management of the airway manifestations of relapsing polychondritis. Chest 1999;116:1669–1675.

Dr. Taeko Shirakawa
Division of Respiratory and Infectious Diseases
Department of Internal Medicine
St. Marianna University School of Medicine
2-16-1, Sugao, Miyamae-ku
Kawasaki 216-8511 (Japan)
Tel. +81 44 977 8111, Fax +81 44 977 8361, E-Mail shirakawa@vega.ocn.ne.jp

Chapter 23

Bolliger CT, Herth FJF, Mayo PH, Miyazawa T, Beamis JF (eds): Clinical Chest Ultrasound: From the ICU to the Bronchoscopy Suite.
Prog Respir Res. Basel, Karger, 2009, vol 37, pp 202–207

Ultrasound Guidance for Endoscopic Treatment of Pulmonary Malignancies

Ralf Eberhardt[a] · Antonio Bugalho[b]

[a]Department of Pneumology and Critical Care Medicine, Thoraxklinik, University of Heidelberg, Heidelberg, Germany;
[b]Department of Pneumology, Pulido Valente Hospital, New University of Lisbon, Lisbon, Portugal

Abstract

Radial endobronchial ultrasound (EBUS) improves the sonographic diagnostics of the mediastinum and the staging in patients with lung and non-lung cancer. The use of EBUS allows visualization of the tracheobronchial wall and the immediate surrounding structures in a high resolution. Since it can determine the true thickness and extent of a tumor, this technique already influences the endoscopic treatment of pulmonary malignancies in early and advanced cancers in many centers. Especially in cases with early stage lung cancer EBUS should be considered state of the art and be used as a selection criterion for photodynamic therapy or other local treatments in future. EBUS has increased the yield of flexible bronchoscopy in the diagnosis of solitary pulmonary nodules. The use of this guidance technique in combination with a guide sheath as an extended working channel may provide a means for therapeutic interventions. The ultimate goal of minimally invasive treatment of peripheral lung lesions in inoperable patients now appears feasible.

Endobronchial ultrasound (EBUS) has become a major advance in bronchoscopy. Substantial scientific evidence has confirmed its usefulness in diagnosis and staging of lung cancer as well as in treatment of pulmonary malignancies. It is of increasing importance that endoscopists can perform and interpret this imaging method accurately in order to optimize diagnosis and therapy of their patients [1].

Primary or secondary tumors of the lung often involve the central airways. Dyspnea in patients with malignant disease of the lung occurs in 75% of the patients during the last 6 weeks of their life and one third of the patients with lung cancer will suffer from central airway stenosis [2]. There are now numerous procedures available to treat these tumors of the lung endoscopically. Laser, argon plasma coagulation, electrocautery, cryotherapy, brachytherapy (high-dose rate) and photodynamic therapy (PDT) as well as stenting are different techniques to be used by the interventional bronchoscopist with a palliative intent.

In early lung cancer the endoscopic approaches provide potential cure. All endoscopic treatments have a limited depth of penetration, but in cases with intraepithelial stage disease the results can match those of surgical resection [3].

Therefore, it is important to determine the extent of the disease prior to treatment, as this will directly impact disease management and prognosis. In both, advanced and early lung cancer, it is necessary to expand the view of the endoscopist beyond the confinement of the mucosal wall [4].

One of the challenges in early diagnosis of lung cancer remains the difficulty in reaching single pulmonary nodules. EBUS has increased the yield of flexible bronchoscopy in the diagnosis of these small peripheral lung lesions [5–7]. It may potentially result in minimally invasive endoscopic procedures in the treatment of these suspicious nodules under ultrasound guidance.

As commercial ultrasound devices have been available for a couple of years, this chapter tries to show where experience with radial EBUS may be a benefit and unique adjunct to therapeutic bronchoscopy.

Endoscopic Treatment of Central Tumors

EBUS has opened a window of opportunity since it makes it possible to acquire images and essential information beyond the lumen and mucosa of the tracheobronchial tree as well as to assess extraluminal structures – intramural, paratracheal, parabronchial and mediastinal – with increased detail [1]. EBUS with a standard frequency of 20 MHz permits a

resolution inferior to 1 mm and a depth of penetration of 4 cm. In the EBUS image, the tracheobronchial wall appears as a layered structure with distinct cartilaginous layers [8]. Disruption of this normal multilayer pattern is often an indication of tumor infiltration, making it possible to evaluate the depth of tumor invasion.

It is important to establish the extent of tumor expansion to determine whether cancer has invaded beyond the airway adventitia. In contrast to radiologic imaging, EBUS even makes it possible to analyze very small tumors of a few millimeters in size. In 1999 Kurimoto et al. [9] accurately determined the depth of tumor invasion, comparing ultrasonographic and histopathologic findings in resected lung cancer specimens. In 23 of 24 lesions the depth of invasion was considered the same by the two methods, which is indicative of the reliability of EBUS in the assessment of small tracheobronchial lesions. Herth and Becker [10] demonstrated that the use of EBUS assessment in small autofluorescence-positive lesions that were negative in white light bronchoscopy improved specificity (predicting malignancy), which rose from 50 to 90%. Combining EBUS with autofluorescence has proved efficient in prospective studies and has become the basis for curative endobronchial treatment of malignancies.

These studies verify the evidence that EBUS is superior to conventional computed tomography scan of the lung in evaluating the tracheal and bronchial wall structures and also of the parabronchial space. It could serve as an ideal tool for evaluating airway wall anatomy and related tumor pathology [8–11].

Early Lung Cancer

Precancerous and confined malignant lesions in the respiratory tract are usually accidentally detected in patients who undergo bronchoscopy for other clinical reasons. Early lung cancer is defined to be radiologically occult. In these cases in the early stage it is important to correctly assess pretherapeutically the absence/presence, depth and extent of invasion as well as the length of cancer with tracheobronchial invasion [12].

Because tumors confined to the mucosa and submucosa rarely have lymph node metastases PDT or brachytherapy may be one of the endoscopic approaches for early-stage lung cancer at this time. It has been confirmed that both techniques had curative potential in patients with centrally located early-stage lung cancer [12, 13]. The worldwide data showed that patients with early lung cancer treated with PDT achieve a complete response in approximately 75% of cases, with a recurrence rate of approximately 30% [14]. Laser beams cannot penetrate the exterior wall of the cartilage; for successful endoscopic treatment it is, therefore, important that the tumor is confined to the mucosa and submucosa. Many criteria in selecting the appropriate candidates for curative intent of high-dose rate therapy and PDT have been reported. Bronchoscopic diagnosis is accepted as one of the most important criteria [14], based on statistical data indicating that lesions less than 1.0 cm have a high likelihood of achieving a complete remission after PDT. However, prognostic factors which are probably more important in determining whether a tumor recurs are the thickness, degree of submucosal invasion and possible peribronchial extension.

Miyazu et al. [15] reported the value of EBUS in selecting appropriate candidates with centrally located early-stage lung cancer. In the largest series treatment was planned in selected patients with biopsy-proven confined squamous cell carcinomas based on the evaluation of tumor depth invasion with EBUS.

All patients were considered to be appropriate candidates for PDT by conventional bronchoscopy and high-resolution computed tomography. Miyazu et al. [15] performed radial EBUS before PDT and even when lesions were diagnosed as intracartilaginous by EBUS, PDT was subsequently performed. The remaining lesions were diagnosed as extracartilaginous by EBUS and were considered candidates for other therapies such as surgical resection, chemotherapy, and radiotherapy. The depth of tumor invasion estimated by EBUS was proven to be accurate by histopathologic findings in a couple of specimens after surgical resection. Using the EBUS findings as a decision maker, long-term complete remission had been achieved in the endoluminal group. At a mean follow-up of 32 months, none of the patients had had a recurrence.

Apparently, adding EBUS to the airway assessment in patients with presumed carcinoma in situ significantly increases the likelihood of identifying the patients best treated by endoluminal therapy. The patient selection by radial EBUS may open a new field for other local treatments such as argon plasma coagulation or cryotherapy, which have been proven to be comparably successful treatments for eradicating early lung cancer [16, 17] (fig. 1).

Advanced Cancer

Following histological diagnosis of lung cancer, staging becomes the most important task. The exact location of a central tumor and the invasion of mediastinal organs such as heart, vessels and esophagus most often exclude surgery. One third of presumptive curative thoracotomies for non-

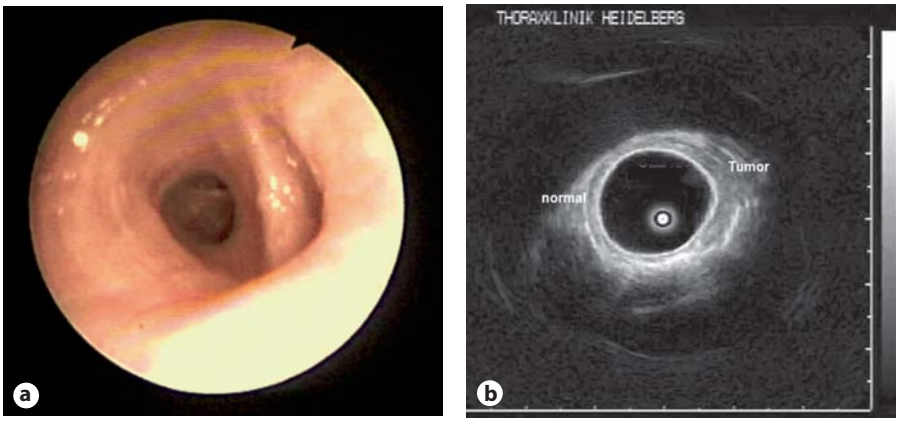

Fig. 1. Typical endoscopic image of a radiologically invisible early stage lung cancer (**a**), but the corresponding EBUS image (**b**) demonstrates an infiltration of the tumor beyond the adventitia.

small cell lung carcinoma (NSCLC) are unnecessary due to the discovery of extensive disease despite preoperative staging procedures [18].

With reference to surgical resection, EBUS can be essential for the decision on resection margins and can be of considerable help in cases of questionable tracheal involvement to prove nonresectability or in questionable main bronchi involvement to guide the extent, feasibility of resection and type of procedure. EBUS makes possible the exact estimation of submucosal and intramural tumor extent, distinguishing between infiltration and compression as well as the assessment of the involvement of mediastinal structures [9, 11, 19].

A prospective trial compared tumor characteristics evaluated by EBUS and CT scan with surgical pathology in 105 patients [11]. In 81 patients (77%), the CT scan was read as consistent with tumor invasion. EBUS only showed invasion in 49 cases (47%). Histology status after surgery revealed a specificity of 100%, a sensitivity of 89%, and an accuracy of 94% for EBUS. Chest CT was far inferior, with a specificity of 28%, a sensitivity of 75%, and an accuracy of 51%. These results confirmed that EBUS has the ability to provide a better staging with subsequent adjustment of therapeutic options and prognosis.

The first recognition of the potential of EBUS to aid endoscopic therapy was made with reference to laser treatment and stent placement in tumor stenosis [20]. EBUS provides a new method to place stents correctly since in most cases the miniaturized probe can evaluate the bronchial lumen distal to the stenosis. EBUS can assess the diameter and length of the stenotic portion more precisely and can examine specific details of the submucosal thickening and cartilage destruction by the tumor, making it possible to choose not only the most suitable stent but also its correct size and diameter [21–23].

Table 1. Frequency in which planned therapeutic approaches were altered or guided by EBUS findings [24]

Indication	n (%)
Mechanical tumor destruction	123/346 (36)
Stent placement	121/235 (51)
Nd:YAG laser resection	56/148 (38)
Argon plasma coagulation	121/262 (46)
Brachytherapy	69/134 (51)
Foreign body removal	3/22 (14)
Abscess drainage	12/27 (42)

Nd:YAG = Neodymium:yttrium aluminium garnet [24].

In a large series the use of EBUS guidance for therapeutic airway procedures was described [24]. In 1,174 cases EBUS was used: 29% mechanical tumor debridement, 20% airway stenting, 13% neodymium:yttrium aluminium gamet laser use, 23% argon plasma coagulation, 11% brachytherapy, 2% foreign body removal and 2% endoscopic abscess drainage. It guided or changed the management of patients in 43% of cases. The changes ranged from altering the sizes of stents to guiding tumor debridement (table 1).

A complication feared by interventionalists when using laser debridement in the airways is bleeding from adjacent vessels or fistula formation. As EBUS allows exact determination of the tumor, penetration through the airway wall and vessels is weIl visualized and debridement can be stopped when approaching critical structures. As a result, neither fistula formation nor fatal bleeding was observed at all in the population of this study [24].

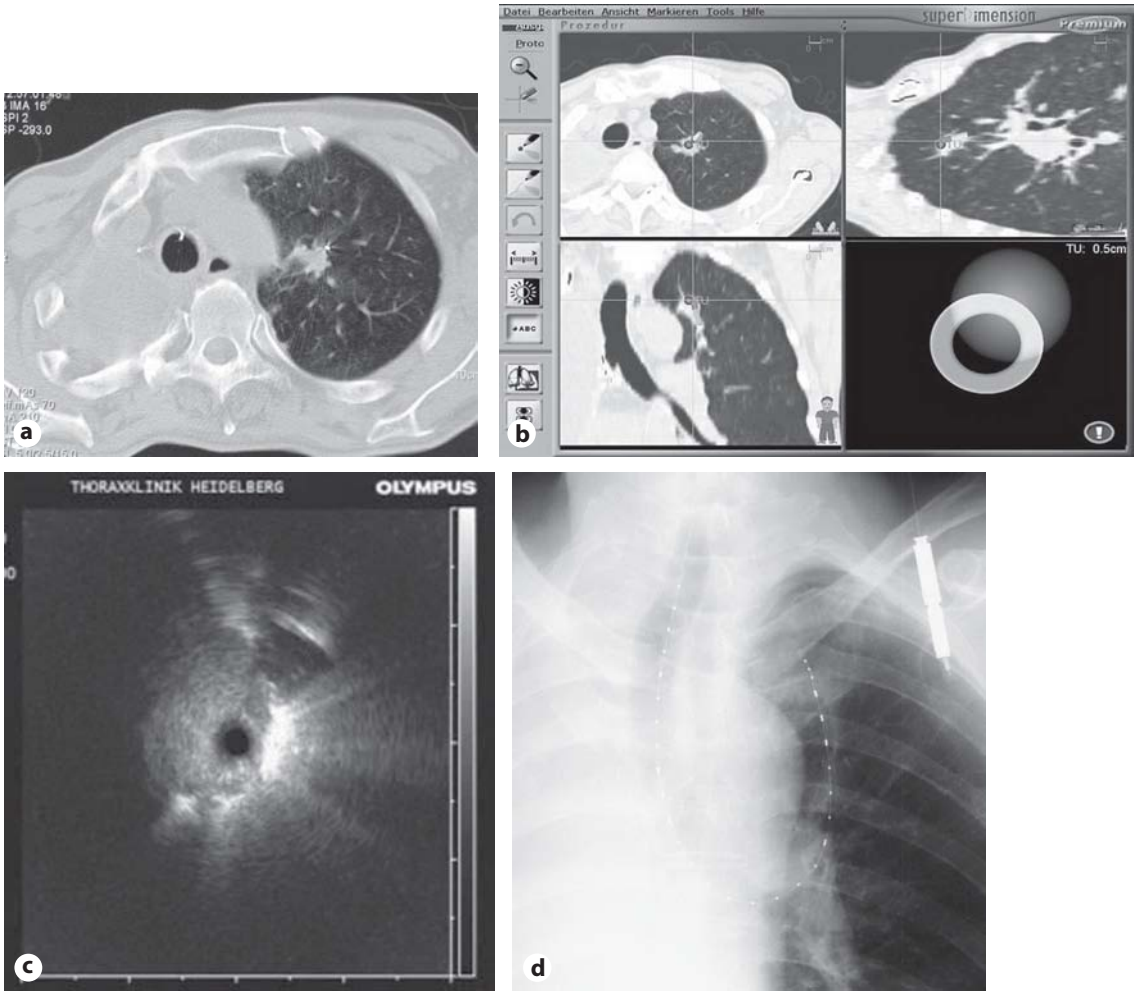

Fig. 2. **a** Small peripheral lesion suspicious of lung cancer recurrence after pneumonectomy 3 years earlier. **b** Typical screen of an electromagnetic navigation system (superDimension, Herzliya, Israel). The locatable guide is navigated to the lesion, the distance from the tip to the marked center (navigation error) is 0.5 cm (see also chapter 20, fig. 1). **c** Confirmation of the position of the extended working channel inside the lesion by EBUS radial probe. **d** Brachytherapy catheter with a dummy probe.

Endoscopic Treatment of Peripheral Tumors

In patients with solitary pulmonary nodules who are surgical candidates and in whom the pretest probability of cancer is high, a biopsy is often not necessary [25]. There are two main reasons to choose an alternative approach for nonsurgical treatment of such a coin lesion. The first is that the patient refuses surgery. The second is that the patient is medically inoperable but a cancer diagnosis has been made based on tissue analysis. There is an increasing demand to provide alternatives to the currently invasive surgical therapy of malignant peripheral pulmonary nodules. Because of comorbidities such as impaired lung capacities or heart disease, many patients are unable to tolerate the highly invasive therapeutic procedures.

EBUS has increased the yield of flexible bronchoscopy in the diagnosis of peripheral lung lesions and single pulmonary nodules. Several studies have reported the efficiency and safety of this guidance technique [5–7, 26–28]. Overall, in the literature yields for EBUS using a radial probe with or without a guide sheath have been reported to be 58.3–80.0% regardless of lesion size when using a sheath. Eleven to 24% of solitary pulmonary nodules could not be localized by EBUS, and all experts agree that lesions smaller than 15 mm are more difficult to reach with the EBUS system.

EBUS enables direct visualization of the target lesion. However, it lacks a navigation system and requires the operator to navigate the bronchoscope blindly to the lesion with the knowledge of prior radiological investigations such as CT scans.

In contrast, electromagnetic navigation-guided bronchoscopy (ENB) allows for real-time navigation of an extended working channel through the tracheobronchial tree to targets in the periphery of the lung [29]. ENB consists of four components: an electromagnetic location board, a locatable sensor probe with a steering mechanism, an extended working channel and computer software that converts CT scans into multiplanar images with three-dimensional virtual bronchoscopy reconstruction. ENB lacks a tool to directly visualize the lesion before biopsy or treatment. Combining EBUS and electromagnetic navigation improves the yield of flexible bronchoscopy in peripheral lung lesions without compromising safety. In a randomized trial it could be demonstrated that combined EBUS and ENB overcome each individual technique's limitation [30]. The diagnostic yield of combined procedures (88%) was greater than either EBUS (69%) or ENB alone (59%, $p = 0.02$). This technology, when fully proven, offers a minimally invasive treatment, and, moreover, has the potential to prevent patients from undergoing unnecessary surgical thoracotomies.

Harms et al. [31] reported on a patient with medically inoperable lung cancer. The patient was treated with external-beam radiotherapy (50 Gy) and electromagnetic-navigated and EBUS-controlled endoluminal brachytherapy (370 GBq iridium 192). Following successful localization of the NSCLC by electromagnetic navigation, EBUS was performed to confirm the exact position in the center of the lesion. A brachytherapy catheter was then placed within the tumor. Primary 3-dimensional planned brachytherapy was applied as a boost 3 times a week (single dose 5 Gy) and provided highly conformal irradiations of the NSCLC, including the draining bronchovascular bundle (fig. 2).

In a feasibility and safety trial this new endoluminal treatment was tolerated without major side effects or complications [32]. Follow-up revealed complete remission in 2 patients and 7 patients achieved partial remission. In future, electromagnetic-navigated and EBUS-controlled brachytherapy could even become a potentially curative treatment for inoperable peripheral lung tumors, preventing major damage to radiosensitive surrounding structures.

Radiofrequency ablation (RFA) has been used in combination with cryotherapy in the treatment of tracheobronchial obstruction [33]. So far there are no reports about bronchoscopic application of RFA in the treatment of pulmonary solitary nodules. In future the image guidance of EBUS may be able to direct a flexible RFA catheter to the exact site of the lesion.

References

1 Bugalho A, Doris MK, Hamacher J, Eberhardt R, Herth FJ: Endobronchial ultrasound: practical aspects and clinical applications. Rev Port Pneumol 2008;14:55–88.

2 Ginsberg RJ, Vokes EE, Ruben A: Non-small cell lung cancer; in DeVita VT, Hellman S, Rosenberg SA (eds): Cancer Principles and Practice of Oncology, ed 5. Philadelphia, Lippincott-Raven, 1997, pp 858–911.

3 Moghissi K: Role of bronchoscopic photodynamic therapy in lung cancer management. Curr Opin Pulm Med 2004;10:256–260.

4 Herth FJF, Eberhardt R: The role of endobronchial ultrasound in diagnosis, staging and treatment. Therapy 2005;2:223–228.

5 Herth FJ, Ernst A, Becker HD: Endobronchial ultrasound-guided transbronchial lung biopsy in solitary pulmonary nodules and peripheral lesions. Eur Respir J 2002;20:972–974.

6 Kurimoto N, Miyazawa T, Okimasa S, Maeda A, Oiwa H, Miyazu Y, Murayama M: Endobronchial ultrasonography using a guide sheath increases the ability to diagnose peripheral pulmonary lesions endoscopically. Chest 2004;126:959–965.

7 Yamada N, Yamazaki K, Kurimoto N, Asahina H, Kikuchi E, Shinagawa N, Oizumi S, Nishimura M: Factors related to diagnostic yield of transbronchial biopsy using endobronchial ultrasonography with a guide sheath in small peripheral pulmonary lesions. Chest 2007;132:603–608.

8 Nakamura H, Kawasaki N, Hagiwara M, Ogawa A, Kato H: Endoscopic evaluation of centrally located early squamous cell carcinoma of the lung. Cancer 2001;15:1142–1147.

9 Kurimoto N, Murayama M, Yoshioka S, Nishisaka T, Dohi K: Assessment of usefulness of endobronchial ultrasonography in determination of depth of tracheobronchial tumor invasion. Chest 1999;115:1500–1506.

10 Herth F, Becker HD: EBUS for early cancer detection. J Bronchol 2003;10:249–253.

11 Herth F, Ernst A, Schulz M, Becker H: Endobronchial ultrasound reliably differentiates between airway infiltration and compression by the tumor. Chest 2003;123:458–462.

12 Vergnon JM, Huber RM, Moghissi K: Place of cryotherapy, brachytherapy and photodynamic therapy in therapeutic bronchoscopy of lung cancers. Eur Respir J 2006;28:200–218.

13 Mathur PN, Edell E, Sutedja T, Vergnon JM, American College of Chest Physicians: Treatment of early stage non-small cell lung cancer. Chest 2003;123(suppl):176S–180S.

14 Moghissi K, Dixon K, Thorpe JA, Stringer M, Oxtoby C: Photodynamic therapy (PDT) in early central lung cancer: a treatment option for patients ineligible for surgical resection. Thorax 2007;62:391–395.
15 Miyazu Y, Miyazawa T, Kurimoto N, Iwamoto Y, Kanoh K, Kohno N: Endobronchial ultrasonography in the assessment of centrally located arly-stage lung cancer before photodynamic therapy. Am J Respir Crit Care Med 2002;165:832–837.
16 Deygas N, Froudarakis M, Ozenne G, Vergnon JM: Cryotherapy in early superficial bronchogenic carcinoma. Chest 2001;120:26–31.
17 van Boxem TJ, Venmans BJ, Schramel FM, van Mourik JC, Golding RP, Postmus PE, Sutedja TG: Radiographically occult lung cancer treated with fibreoptic bronchoscopic electrocautery: a pilot study of a simple and inexpensive technique. Eur Respir J 1998;11:169–172.
18 Herder GJ, Verboom P, Smit EF, van Velthoven PC, van den Bergh JH, Colder CD, van Mansom I, van Mourik JC, Postmus PE, Teule GJ, Hoekstra OS: Practise, efficacy and cost of staging suspected non-small cell lung cancer. A retrospective study in two Dutch hospitals. Thorax 2002;57:11–14.
19 Baba M, Sekine Y, Suzuki M, Yoshida S, Shibuya K, Iizasa T, Saitoh Y, Onuma EK, Ohwada H, Fujisawa T: Correlation between endobronchial ultrasonography (EBUS) images and histologic findings in normal and tumor-invaded bronchial wall. Lung Cancer 2002;35:65–71.
20 Hurter T, Hanrath P: Endobronchial sonography: feasibility and preliminary results. Thorax 1992;47:565–567.
21 Shirakawa T, Imamura F, Hamamoto J, Shirkakusa T: A case of successful airway stent placement guided by endobronchial ultrasonography. J Bronchol 2004;11:45–48.
22 Miyazawa T, Miyazu Y, Iwamoto Y, Ishida A, Kanoh K, Sumiyoshi H, Doi M, Kurimoto N: Stenting at the flow-limiting segment in tracheobronchial stenosis due to lung cancer. Am J Respir Crit Care Med 2004;169:1096–1102.
23 Miyazu Y, Miyazawa T, Kurimoto N, Iwamoto Y, Ishida A, Kanoh K, Kohno N: Endobronchial ultrasonography in the diagnosis and treatment of relapsing polychondritis with tracheobronchial malacia. Chest 2003;124:2393–2395.
24 Herth F, Becker HD, LoCicero J 3rd, Ernst A: Endobronchial ultrasound in therapeutic bronchoscopy. Eur Respir J 2002;20:118–121.
25 Silvestri GA: Boys (and girls) and their toys: a look at new technologies in the bronchoscopy suite. Am J Respir Crit Care Med 2007;176:1–2.
26 Shirakawa T, Imamura F, Hamamoto J, Honda I, Fukushima K, Sugimoto M, Shikakusa T: Usefulness of endobrochial ultrasonography for transbronchial lung biopsies of peripheral lung lesions. Respiration 2004;71:260–268.
27 Kikuchi E, Yamazaki K, Sukoh N, Kikuchi J, Asahina H, Imura M, Onodera Y, Kurimoto N, Kinoshita I, Nishimura M: Endobronchial ultrasonography with guide sheat-sheath for peripheral pulmonary lesions. Eur Respir J 2004;24:533–537.
28 Yang MC, Liu WT, Wang CH, Lin HC, Chen HC, Chou CL, Hsuch S, Kuo HP: Diagnostic value of endobronchial ultrasound-guided transbronchial lung biopsy in peripheral lung cancers. J Formos Med Assoc 2004;103:124–129.
29 Schwarz Y, Greif Y, Becker H, Ernst A, Mehta A: Real-time electromagnetic navigation bronchoscopy to peripheral lung lesions using overlaid CT images: the first human study. Chest 2006;129:988–994.
30 Eberhardt R, Anantham D, Ernst A, Feller-Kopman D, Herth F: Multimodality bronchoscopic diagnosis of peripheral lung lesions: a randomized controlled trial. Am J Respir Crit Care Med 2007;176:36–41.
31 Harms W, Krempien R, Grehn C, Hensley F, Debus J, Becker HD: Electromagnetically navigated brachytherapy as a new treatment option for peripheral pulmonary tumors. Strahlenther Onkol 2006;182:108–111.
32 Becker HD, Harms W: Navigated bronchoscopy and endobronchial ultrasound for brachytherapy of inoperable peripheral lung cancer: a feasibility and safety study. Chest 2006;130(suppl):111S.
33 Marasso A, Bernardi V, Gai R, Gallo E, Massaglia GM, Onoscuri M, Cardaci SB: Radiofrequency resection of bronchial tumors in combination with cryotherapy: evaluation of a new technique. Thorax 1998;53:106–109.

Dr. med. Ralf Eberhardt
Department of Pneumology and Critical Care Medicine
Thoraxklinik at the University of Heidelberg
Amalienstrasse 5
DE–69126 Heidelberg (Germany)
Tel. +49 6221 396 1204, Fax +49 6221 396 1205, E-Mail ralf.eberhardt@thoraxklinik-heidelberg.de

Chapter 24

Bolliger CT, Herth FJF, Mayo PH, Miyazawa T, Beamis JF (eds): Clinical Chest Ultrasound: From the ICU to the Bronchoscopy Suite.
Prog Respir Res. Basel, Karger, 2009, vol 37, pp 208–214

Ultrasound-Guided Drainage Procedures and Biopsies

Jessica S. Wang · Peter Doelken

Division of Pulmonary, Critical Care, Allergy and Sleep Medicine, Medical University of South Carolina, Charleston, S.C., USA

Abstract

The use of ultrasound for guidance in procedures involving the pleural space has become routine and has an excellent safety record. Once understanding of the pleural anatomy as seen on ultrasonography is learned, the techniques for intervention can be easily mastered by the physician operator. Ultrasound guidance is in many cases preferable to CT guidance as transport of the critically ill is avoided and because of the minimal patient discomfort associated with transthoracic procedures in the bronchoscopy suite. Sonography does not subject the patient to the radiation effects of CT and comes at a lower cost. The operator must be familiar with all the possible complications of these procedures and their treatment. The need to understand pleural ultrasonography, especially its role in interventions, will continue to grow and become an important part of the pulmonologist's armamentarium.

Ultrasonography is an integral part of the management of pleural disease. While computed tomography of the chest remains indispensable for overall imaging of the chest in all cases of malignancy and in some nonmalignant conditions, ultrasonography may subsequently be used to guide drainage or biopsy procedures. Ultrasound-guided biopsy can be performed quickly, with low complication rate, with low cost, and without radiation exposure. The basic requirements for a safe procedure are a cooperative patient, availability of equipment and proficiency in chest ultrasonography. In addition to the cognitive and manual skills required for diagnostic pleural sonography, the ability to identify inserted hardware and associated reverberation artifact is essential for the performance of procedures beyond simple thoracentesis and biopsy procedures.

Hardware Issues

The ultrasonographer needs to be familiar with the ultrasound machine, resolution and frequency of the transducer probes, and controls such as gain and depth. By convention, the transducer is oriented with the marker of the probe cephalad. The screen marker corresponding to the mark on the probe is placed at the left upper corner of the screen thus orienting the left side of the screen image cephalad.

Ultrasound probes have various frequencies with higher frequency transducers (7.5–10 MHz) having better resolution but less penetration making them excellent for vascular examination and detailed examination of the pleural surface and chest wall. Lower frequency probes (3.5–5 MHz) lose near field resolution but have superior penetration to evaluate deeper structures. Pleural effusions and other thoracic pathology, as well as adjacent abdominal structures, are better identified with these lower frequency probes and are useful in guiding interventions. The convex array or sector scanning transducers are preferred for chest ultrasound because it facilitates scanning through the intercostal spaces [1]. These same transducers used for diagnostic chest ultrasound can also be used for procedure guidance.

Patient Positioning

Proper patient positioning is essential to visualize the target lesion as well as to facilitate interventional access. Free-flowing pleural effusions collect in the most dependent part of the thoracic cavity with the aerated lung taking a nondependent position. Thus, an effusion will collect in the inferior

and posterior chest in the patient sitting upright, which is ideal for access. In the critically ill patient, hemodynamic instability and support devices may interfere with positioning, and unless the effusion is very large and laterally distributed in the chest, the bed may block visualization of pleural effusions. One option is to place the transducer in the posterior axillary line and then push the bed down while angulating the probe upwards, but this positioning does not give a safe approach for thoracentesis. Another option is to bring the head of the bed, and thus the patient's thorax, near vertical which allows the pleural effusion to collect inferiorly and posteriorly. Adducting the ipsilateral arm across the body elevates the chest wall off the bed. Hemodynamically unstable patients may not tolerate this position, and an assistant is needed to monitor the endotracheal tube and help the patient maintain this position. The patient can also be turned to a full lateral decubitus position with the target hemithorax up exposing a suitable field for thoracentesis. Another option is to slide the patient to the side of the bed with the target hemithorax exposed, but this positioning makes operator positioning more cumbersome. Patient positioning for biopsy of lung or pleural lesions is dictated by the location of the lesion and must be individualized. Particular attention must be placed on the ability of the patient to comfortably maintain position for the duration of the procedure and the position allowing unencumbered access while maintaining sterility [2].

Ultrasound-Guided Thoracentesis

Ultrasound-guided thoracentesis is an easily learned and mastered technique that is especially useful for the pulmonary and critical care physician. It has a low risk of associated pneumothorax, and it can safely be performed in the patient on mechanical ventilation. In these critically ill patients, the positive pressure from the ventilator increases the risk of tension if pneumothorax should develop, and a supine chest radiograph alone does not help determine a safe thoracentesis site. Bedside ultrasound guidance may eliminate the need to transport the critically ill to the interventional radiology suite for CT-guided procedures, thus eliminating the attendant transport risk.

Thoracentesis in general carries various risks including pneumothorax, pain, shortness of breath, cough, and vasovagal reactions. Other less common complications include reexpansion pulmonary edema, inadvertent liver or splenic injury, hemothorax, infection, subcutaneous emphysema, air embolism, and chest wall or subcutaneous hematoma. Compared to clinical exam-guided thoracentesis, ultrasonographic guidance has been noted to carry a lower rate of pneumothorax, approximately 5–18 versus 1–5%, respectively. In nonintubated patients, the risk of pneumothorax from thoracentesis performed by a radiologist has been reported by Jones et al. [3] to be 2.7%, and in a surgical intensive care unit setting the complication rate was found to be 2.4% [4]. Pneumothorax after ultrasound-guided thoracentesis in the spontaneously breathing patient is almost always caused by removal of a large effusion volume in the setting of unexpandable lung [5]. Several studies have looked at the incidence of pneumothoraces in patients who are not intubated versus those on mechanical ventilation. One study by Gervais et al. [6] reported a 5-fold increase in pneumothorax in mechanically ventilated patients, but they had an overall pneumothorax rate of only 2%. Alternately, in a study by Godwin and Sahn [7], the risk of pneumothorax in patients receiving mechanical ventilation was the same as in patients who were spontaneously breathing, which has been supported by several other studies including one by Lichtenstein et al. [8] who reported no pneumothoraces in 45 patients on mechanical ventilation [9, 10]. Another study by Mayo et al. [9] of 232 ultrasound-guided thoracentesis on patients with mechanical ventilation showed a pneumothorax rate of 1.3%. Although no direct comparison between thoracentesis with versus without ultrasound guidance has been done, Diacon et al. [11] found that the use of ultrasonography to locate the most appropriate site for thoracentesis was more accurate than standard physical examination.

Positioning of the patient, of the operator, and of the ultrasound machine is important for successful performance of ultrasound-guided thoracentesis. The field of interest must be free of monitoring and support devices. The operator then must decide on the site, angle, and depth of needle penetration for safe thoracentesis. A suitable site is determined by finding a location with a straight path to the pleural effusion with no lung, bone, vessel, or other obstacle in the needle path. The site on the skin is marked and the appropriate position of the mark is again verified by sonography. After determining the angle of access with the ultrasound probe, the needle is inserted at a similar angle. The safe depth of needle penetration depends on the thickness of the chest wall and the depth of the identified diaphragm or lung. We measure these distances routinely and record the measurements for documentation purposes. Transducer compression artifact must be taken into account. The probe compresses the skin and underlying soft tissues which rebounds when the probe is removed

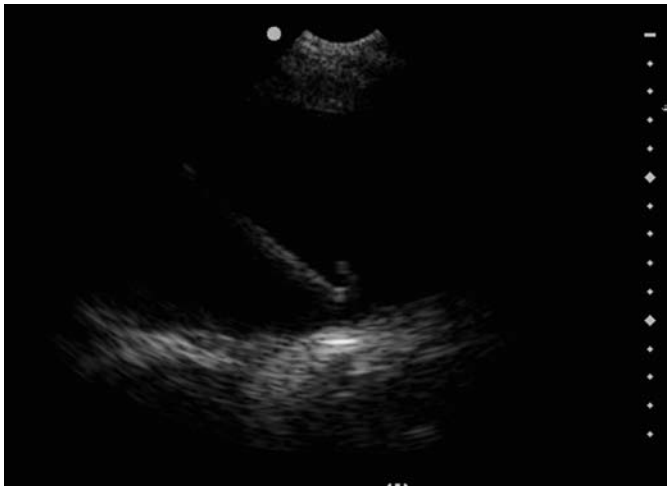

Fig. 1. A J-wire is shown in a large anechoic effusion. We routinely confirm proper placement of the guidewire prior to dilatation and device introduction.

making the actual depth to the effusion greater than measured. This compression artifact is most prominent in the obese and the edematous patient where the indentation can be several centimeters. The thickness of the effusion is not affected due to the rigidity of the chest wall [2]. There is no formal lower limit for the thickness of the effusion below which thoracentesis can be performed, but lung or diaphragm moving into the path of needle insertion prohibit thoracentesis in that location. The patient must maintain their position throughout the procedure as any movement may shift the effusion in relationship to the planned thoracentesis site [12–14].

Unequivocal positive identification of the diaphragm and the underlying liver or spleen is required to avoid puncture of those organs. The inexperienced sonographer may mistake the liver or spleen for an echogenic effusion. The curvilinear line of Morrison's pouch which lies between the liver and kidney must not be falsely identified as the diaphragm. Occasionally a curvilinear structure may also be seen between the spleen and the kidney; again, this line needs to be distinguished from the diaphragm to avoid inadvertent puncture of the spleen. Consequently, the sonographer must be diligent in delineating the diaphragm and the underlying spleen or liver.

Performing thoracentesis with real-time needle visualization unnecessarily complicates the procedure because sterile probe covers and additional assistance are required [15].

Once an appropriate site is located, the upper margin of the rib below that site should be palpated. If the rib cannot be palpated because the patient is obese or edematous, the rib can be identified with a 21-gauge needle. The area should be infiltrated with local anesthetic as the needle is advanced through the soft tissue and over the rib. Once over the rib, intermittent suction should be applied until pleural fluid is withdrawn. A new needle or a catheter-over-needle system should then be inserted along the same path as the smaller gauge needle. While the needle or catheter is within the pleural space, care should be taken to avoid entry of air [16]. If lung sliding is documented anteriorly prior to pleural space interventions and central venous catheter placement and the continued presence of lung sliding is confirmed after the procedure, pneumothorax can be excluded without delay.

Insertion of Chest Drainage Devices

Chest drainage devices include large-bore drains, small-bore catheters, and long-term indwelling drainage systems (online suppl. video 1 and 3). These are placed for complicated pleural effusions due to empyema or complicated paraneumonic effusion, for pneumothoraces either spontaneous or iatrogenic, and for chronic drainage of malignant effusions. Video

Insertion of a chest drainage device employs the same principles as performing an ultrasound-guided thoracentesis. The best site for insertion of device is determined as above taking into account the depth and location of effusion as well as avoiding injury to underlying structures. The difference is that a site for device placement should be more lateral, if possible, to minimize patient discomfort when lying supine. We routinely use real-time ultrasonography to confirm proper position of an inserted guidewire in fluid collections prior to deploying dilatation devices or catheters (fig. 1). However, if the pleural space is filled with air, as in pneumothorax, the device cannot be seen because of the air artifact. In this instance, the ultrasound is used to locate a safe location for placement of the device in reference to the position of the diaphragm. We prefer CT guidance for complex, or loculated, pneumothorax.

General Considerations for Biopsy Procedures

Ultrasound-guided needle biopsy is suitable for peripheral lung lesions, anterior mediastinal masses, and pleural lesions. In some ways it is preferable to CT-guided procedures because the patient does not have to remain in position for extended amounts of time, and there is no radiation

exposure. Critical to the success of performing the biopsy, the operator must be proficient in chest ultrasonography and be able to correlate CT images to ultrasound findings. The same transducers used for diagnostic ultrasonography can be used for biopsy: convex array or sector scanning transducers with a frequency of 2–5 MHz which allows scanning through intercostal spaces. The lesions are better first localized and characterized by CT scan which gives a more accurate determination of the extent of pathology. Once the target is identified, it must be imaged by ultrasound. The presence of an ultrasound window with the absence of bone or air overlying the target and the absence of any vital organs along the needle path are necessary for biopsy. The angle of needle entry and the depth of the lesion can be determined.

Once the needle has been inserted, the location can be confirmed using real-time ultrasound by keeping the needle path parallel to the scanning plane and moving the transducer until the needle is visualized. Transducers with built-in needle guides require less skill because the needle remains in the scanning plane [12–14, 17]. However, routine use of real-time visualization during biopsy of superficial lung lesions or pleural lesions is not needed.

For fine needle aspiration, an 18- or 20-gauge needle is used. Microscopy slides and preservation media should be immediately available. Local anesthetic is given. Once the lesion is entered, suction is applied and to and fro movements in a fan-like pattern are performed. Suction is released before withdrawal of the needle, so as not to contaminate the specimen. The specimen is immediately transferred to microscopy slides and air-dried and/or fixed in alcohol.

Core biopsies of pleural or lung lesions can be performed using standard coaxial cutting needle technique. Commercially available kits usually contain an introducer needle with stylet and a spring-loaded cutting needle with or without adjustable throw. (fig. 2). We use needle sizes of 16, 18 and 20 gauge with the largest used for pleural biopsy.

After local anesthetic has been injected and the introducer assembly advanced into the rib interspace, the patient should hold their breath as the assembly is advanced into the target lesion. Resistance can be encountered when entering the lesion. Whenever the introducer needle is opened to the atmosphere, the patient is again asked to hold breath. The stylet is removed, and the cutting needle is inserted, with throw adjusted to the desired depth if applicable. The cutting needle should be oriented with the cutting aspect directed caudally to avoid laceration of intercostal vessels and nerves. The needle should be immediately discharged after insertion. Core biopsies give a larger amount of tissue which allows for histologic diagnosis in most patients [18–20]. We routinely roll the tissue cylinder on a microscopy slide prior to transfer into fixative. The slides may be air dried and assessed for adequacy by on-site cytopathology.

Absolute contraindications for biopsy are an uncooperative patient, a patient who cannot be maintained in the optimal position for biopsy, and intractable coughing. Mechanical ventilation and severe pulmonary hypertension are relative contraindications. Other relative contraindications are severe coagulopathies, thrombocytopenia with platelet count $<50 \times 10^3$, and uremic platelet dysfunction. Most of these abnormalities can be corrected prior to the procedure. The operator must be prepared for complications of biopsy of lung lesions which are similar to the risks of transbronchial biopsy. The most common complication is pneumothorax with an occurrence rate of about 3%. Since this problem is typically associated with pleuritic chest pain, routine chest radiography after biopsy in an asymptomatic patient may not be necessary. When pneumothorax does occur, the ultrasound image is lost, and the procedure has to be aborted. This need to stop mid-procedure is a disadvantage of using ultrasonography [21, 22]. Underlying lung disease or having only a single lung increases the risk for complications of pneumothorax and immediate treatment may be necessary if it occurs [23–27].

Hemoptysis may occur in 10% of cases when a core biopsy is done but is typically of little consequence. Massive hemoptysis can occur and is associated with mortality. Management of massive hemoptysis is similar to hemoptysis from transbronchial biopsy: tamponade with the bronchocoscope, balloon tamponade, and selective intubation of the contralateral side [26]. Other complications may occur due to coughing such as tearing of the pleura and air embolism, which can also occur without coughing. The risk of air embolism may be lower with ultrasound-guided than with CT-guided biopsy because lesions accessible to ultrasound guidance are typically in the lung periphery. Occluding the introducer cannula between passes of the needle and when excessive bleeding is encountered may reduce the risk of this complication. In the event of air embolism, the patient should be placed in the left lateral decubitus position and given 100% oxygen. Hyperbaric treatment should be considered. Other risks include inadvertent puncture of other vital organs [28].

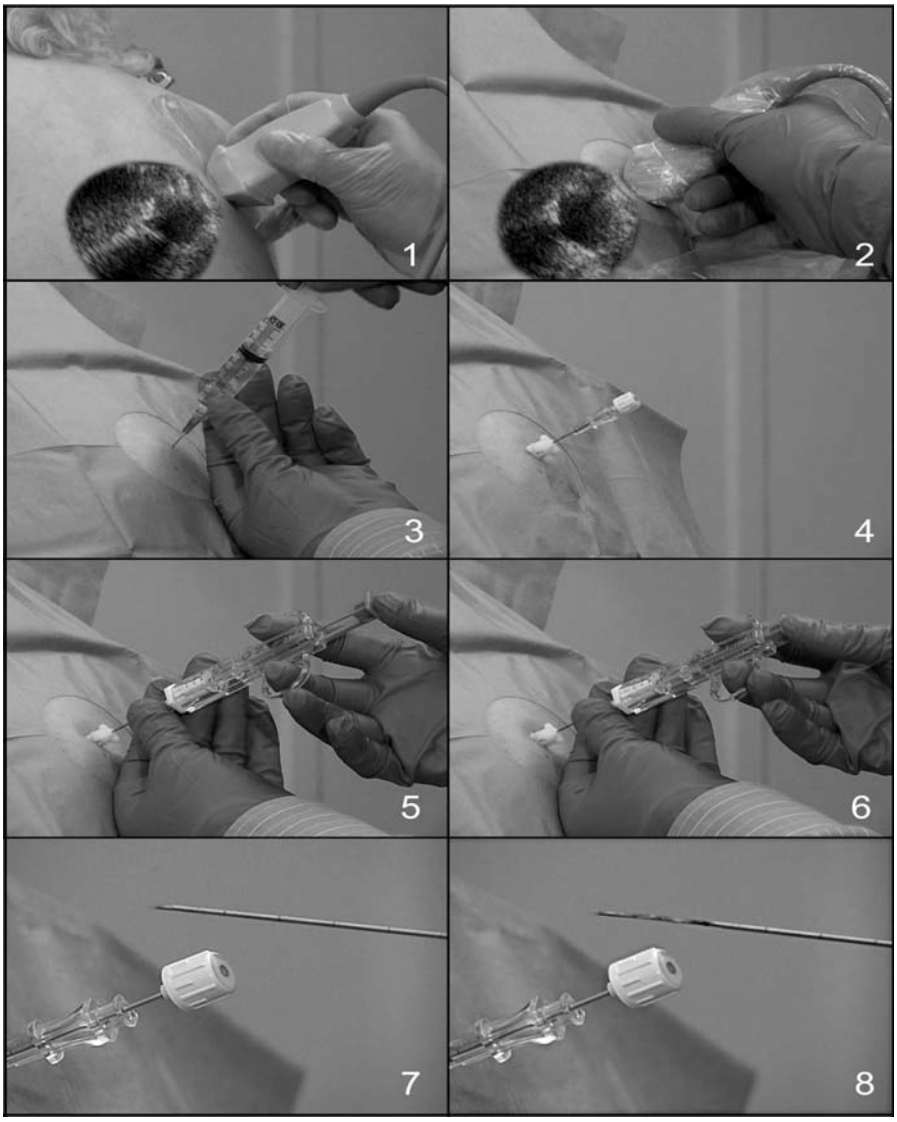

Fig. 2. Coaxial transthoracic needle biopsy of a peripheral lung mass. **a** After review of the CT scan, the lesion is localized with ultrasonography. **b** A sterile field is created and the localization is confirmed with ultrasonography using a sterile sheath over the transducer. **c** Local anesthetic is injected while the needle is advanced over the top of the rib and the lesion is entered. **d** The introducer assembly is advanced into the lesion with the stopper adjusted to match the depth required to enter the lesion with the local anesthesia needle. **e** After removal of the stylet, the charged cutting needle is advanced and locked onto the introducer. **f** The cutting needle is discharged immediately after locking. The cutting side of the needle is oriented caudally and the patient is breath holding. **g** The cutting needle is withdrawn and the introducer immediately occluded with the stylet. **h** The tissue core is shown in the exposed biopsy channel.

Biopsy of Lung Lesions

Any lesion that can be visualized by ultrasonography can be a target for biopsy, and the indications for biopsy are the same as for CT-guided biopsy (online suppl. video 2). The benefit of ultrasound over CT is that it can differentiate between solid and liquid making it preferential in lesions with necrotic centers [29]. Air-filled lesions, though, need to be considered individually. Chronic cavitating or bronchiectatic lesions have a higher risk of bleeding because they are frequently highly vascularized. Of note, the sonographic examination itself can provide staging information by demonstrating presence or absence of movement of the lesion relative to the parietal pleura. If higher frequency transducers are available, interruption of the pleural reflection, invasion of the ribs or chest wall can be visualized. All these findings are strongly associated with chest wall involvement [30].

Video

Pleural Biopsy

Ultrasound-guided pleural biopsy may be indicated in cases where pleural fluid cytology is negative for suspected metastatic disease of pleura or malignant pleural effusion. With ultrasonography, an area of abnormal pleura can be localized which makes yield of this targeted biopsy greater

than random pleural sampling [18, 31]. For malignant pleural mesothelioma, which cannot be diagnosed with cytology alone, a tissue sample needs to be obtained and ultrasound-guided biopsy should be considered as the initial diagnostic procedure. As the diagnosis of malignant mesothelioma requires the demonstration of invasiveness, we use extreme care to include part of the chest wall in the biopsy. This requires careful withdrawal of the introducer assembly into the rib interspace. Again, for safety reasons, it is essential that the cutting apparatus is oriented caudally, away from the neurovascular bundle. The procedure has a reported sensitivity of 77% and a specificity of 88%. If no diagnosis is made, then further evaluation with video-assisted thoracic surgery may be necessary [32].

Anterior Mediastinal Biopsy

In the normal states, the anterior mediastinum is not accessible to ultrasonography because of the overlying aerated lung and bone. When enlarged, though, mediastinal masses can displace the adjacent lung providing a target for ultrasound-guided biopsy. Core biopsy in these instances is necessary because the common diagnoses in the anterior mediastinum require histologic diagnosis. Great care must be employed during biopsy of anterior mediastinal masses to avoid injury to the mammary arteries. Fine needle aspiration has a lower histologic yield but can be performed if carcinoma is highly suspected [33–36].

References

1 Reuss J: Interventional chest sonography; in Mathis G, Lessnau KD (eds): Atlas of Chest Sonography. Berlin, Springer, 2003, pp 147–162.
2 Lichtenstein D: Interventional ultrasound; in General Ultrasound in the Critically Ill. Berlin, Springer, 2005, pp 170–174.
3 Jones PW, Moyers JP, Rogers JT, Rodriguez RM, Lee YC, Light RW: Ultrasound-guided thoracentesis: is it a safer method? Chest 2003;123:418–423.
4 Petersen S, Freitag M, Albert W, Tempel S, Ludwig K: Ultrasound-guided thoracentesis in surgical intensive care patients. Intensive Care Med 1999;25:1029.
5 Heidecker J, Huggins JT, Sahn SA, Doelken P: Pathophysiology of pneumothorax following ultrasound-guided thoracentesis. Chest 2006;130:1173–1184.
6 Gervais DA, Petersein A, Lee MJ, Hahn PF, Saini S, Mueller PR: US-guided thoracentesis: requirement for postprocedure chest radiography in patients who receive mechanical ventilation versus patients who breathe spontaneously. Radiology 1997;204:503–506.
7 Godwin JE, Sahn SA: Thoracentesis: a safe procedure in mechanically ventilated patients. Ann Intern Med 1990;113:800–802.
8 Lichtenstein D, Hulot JS, Rabiller A, Tostivint I, Meziere G: Feasibility and safety of ultrasound-aided thoracentesis in mechanically ventilated patients. Intensive Care Med 1999;25:955–958.
9 Mayo PH, Goltz HR, Tafreshi M, Doelken P: Safety of ultrasound-guided thoracentesis in patients receiving mechanical ventilation. Chest 2004;125:1059–1062.
10 McCartney JP, Adams JW 2nd, Hazard PB: Safety of thoracentesis in mechanically ventilated patients. Chest 1993;103:1920–1921.
11 Diacon AH, Brutsche MH, Soler M: Accuracy of pleural puncture sites: a prospective comparison of clinical examination with ultrasound. Chest 2003;123:436–441.
12 Beckh S, Bolcskei PL, Lessnau KD: Real-time chest ultrasonography: a comprehensive review for the pulmonologist. Chest 2002;122:1759–1773.
13 Dubs-Kunz B: Sonography of the chest wall. Eur J UItrasound 1996;3:103–111.
14 Reuss J: Sonographic imaging of the pleura: nearly 30 years experience. Eur J UItrasound 1996;3:125–139.
15 Tsang TS, Enriquez-Sarano M, Freeman WK, Barnes ME, Sinak LJ, Gersh BJ, Bailey KR, Seward JB: Consecutive 1127 therapeutic echocardiographically guided pericardiocenteses: clinical profile, practice patterns, and outcomes spanning 21 years. Mayo Clin Proc 2002;77:429–436.
16 Doelken P, Sahn SA: Thoracentesis; in Textbook of Critical Care. Philadelphia, Elsevier Saunders, 2005, pp 1845–1848.
17 Matalon TA, Silver B: US guidance of interventional procedures. Radiology 1990;174:43–47.
18 Chang DB, Yang PC, Luh KT, Kuo SH, Yu CJ: Ultrasound-guided pleural biopsy with Tru-Cut needle. Chest 1991;100:1328–1333.
19 McLoud TC: Should cutting needles replace needle aspiration of lung lesions? Radiology 1998;207:569–570.
20 Yang PC, Lee YC, Yu CJ, Chang DB, Wu HD, Lee LN, Kuo SH, Luh KT: Ultrasonographically guided biopsy of thoracic tumors. A comparison of large-bore cutting biopsy with fine-needle aspiration. Cancer 1992;69:2553–2560.
21 Brown KT, Brody LA, Getrajdman GI, Napp TE: Outpatient treatment of iatrogenic pneumothorax after needle biopsy. Radiology 1997;205:249–252.
22 Yankelevitz DF, Davis SD, Henschke CI: Aspiration of a large pneumothorax resulting from transthoracic needle biopsy. Radiology 1996:200:695–697.
23 Charboneau JW, Reading CC, Welch TJ: CT and sonographically guided needle biopsy: current techniques and new innovations. AJR Am J Roentgenol 1990;154:1–10.
24 Heilo A: US-guided transthoracic biopsy. Eur J UItrasound 1996;3:141–151.
25 Klein JS: Interventional techniques in the thorax. Clin Chest Med 1999;20:805–826, ix.
26 Moore EH: Technical aspects of needle aspiration lung biopsy: a personal perspective. Radiology 1998;208:303–318.
27 Weisbrod GL: Transthoracic percutaneous lung biopsy. Radiol Clin North Am 1990;28:647–655.
28 Moore EH, Shepard JA, McLoud TC, Templeton PA, Kosiuk JP: Positional precautions in needle aspiration lung biopsy. Radiology 1990;175:733–735.
29 Pan JF, Yang PC, Chang DB, Lee YC, Kuo SH, Luh KT: Needle aspiration biopsy of malignant lung masses with necrotic centers. Improved sensitivity with ultrasonic guidance. Chest 1993;103:1452–1456.
30 Bandi V, Lunn W, Ernst A, Eberhardt R, Hoffmann H, Herth FJ: Ultrasound vs. computed tomography in detecting chest wall invasion by tumor: a prospective study. Chest 2008;133:881–886.
31 Diacon AH, Theron J, Schubert P, Brundyn K, Louw M, Wright CA, Bolliger CT: Ultrasound-assisted transthoracic biopsy: fine-needle aspiration or cutting-needle biopsy? Eur Respir J 2007;29:357–362.
32 Heilo A, Stenwig AE, Solheim OP: Malignant pleural mesothelioma: US-guided histologic core-needle biopsy. Radiology 1999;211:657–659.

33 Pedersen OM, Aasen TB, Gulsvik A: Fine needle aspiration biopsy of mediastinal and peripheral pulmonary masses guided by real-time sonography. Chest 1986;89:504–508.
34 Saito T, Kobayashi H, Sugama Y, Tamaki S, Kawai T, Kitamura S: Ultrasonically guided needle biopsy in the diagnosis of mediastinal masses. Am Rev Respir Dis 1988;138:679–684.
35 Wernecke K, Vassallo P, Peters PE, von Bassewitz DB: Mediastinal tumors: biopsy under US guidance. Radiology 1989;172:473–476.
36 Yu CJ, Yang PC, Chang DB, Wu HD, Lee LN, Lee YC, Kuo SH, Luh KT: Evaluation of ultrasonically guided biopsies of mediastinal masses. Chest 1991;100:399–405.

Jessica S. Wang, MD
Division of Pulmonary, Critical Care, Allergy and Sleep Medicine
96 Jonathan Lucas Street, Suite 812-CSB
PO Box 250630, Charleston, SC 29425 (USA)
Tel. +1 843 792 3161, Fax +1 843 792 0732, E-Mail wanjs@musc.edu

Author Index

Subject Index